

# **Cold-Formed Steel Frame and Beam-Column Design**

**RESEARCH REPORT RP03-2**

**AUGUST 2003  
REVISION 2006**

Committee on Specifications  
for the Design of Cold-Formed  
Steel Structural Members



**American Iron and Steel Institute**

The material contained herein has been developed by researchers based on their research findings. The material has also been reviewed by the American Iron and Steel Institute Committee on Specifications for the Design of Cold-Formed Steel Structural Members. The Committee acknowledges and is grateful for the contributions of such researchers.

The material herein is for general information only. The information in it should not be used without first securing competent advice with respect to its suitability for any given application. The publication of the information is not intended as a representation or warranty on the part of the American Iron and Steel Institute, or of any other person named herein, that the information is suitable for any general or particular use or of freedom from infringement of any patent or patents. Anyone making use of the information assumes all liability arising from such use.

## PREFACE

This report is based on a thesis presented to the faculty of the Graduate School of Cornell University by Andrew T. Sarawit for the degree of Doctor of Philosophy.

The sponsorship of the Rack Manufacturers Institute and the American Iron and Steel Institute is gratefully acknowledged. The authors are also wish to thank Mr. James Crews, Mr. Daniel Clapp, Mr. John Nofsinger, and Dr. Helen Chen of the sponsoring organizations for their outstanding help through out the duration of the research.

**COLD-FORMED STEEL FRAME  
AND BEAM-COLUMN DESIGN**

by

Andrew T. Sarawit<sup>1</sup>

Teoman Peköz<sup>2</sup>, Project Director

August 2003

Report 03-03

A Research Project Sponsored by  
The American Iron and Steel Institute  
and The Rack Manufacturers Institute

1. Graduate Research Assistant - School of Civil and Environmental Engineering, Cornell University
2. Professor - School of Civil and Environmental Engineering, Cornell

## TABLE OF CONTENTS

<b>1. Introduction</b>	<b>1</b>
1.1. Background	1
1.2. Objectives and Scope	2
1.3. Related Literature	3
<b>2. Column Bases</b>	<b>5</b>
2.1. Introduction	5
2.2. Development of a Base Fixity Equation	13
2.2.1. Contact Stresses Between Base Plate and Floor	13
2.2.2. Normal Loads on the Boundary of Half-Space	19
2.2.3. Base Fixity Charts	29
2.3. Finite Element Analysis Verification	30
2.4. Conclusions	33
<b>3. Beam to Column Connections</b>	<b>34</b>
3.1. Introduction	34
3.2. Beam to Column Connection Tests	35
3.3. Proposed Portal Test	40
3.4. Finite Element Simulation of the Cantilever Test	42
3.5. Conclusions	48
<b>4. Members</b>	<b>49</b>
4.1. Introduction	49
4.2. Elastic Buckling Strength of Perforated Members	50

4.3. Torsional-Flexural Buckling	64
4.4. Effective Lengths	73
4.5. Effective Design Area	81
4.5.1. Stiffened Elements	82
4.5.2. Unperforated Members	86
4.5.3. Perforated Members	95
4.6. Member Design Strength	103
4.7. Effective Section Modulus	113
4.8. Moment Magnification Factor	116
4.9. Conclusions	121
<b>5. Cold-Formed Steel Frames</b>	<b>124</b>
5.1. Introduction	124
5.2. Elastic Buckling Strength of Pallet Racks	125
5.2.1. Effective Length $K_x$	125
5.2.2. Alignment Chart and Torsional-Flexural Buckling Provisions	129
5.3. Plumbness	132
5.4. Moment Magnification Factor	135
5.5. Nonlinear Analysis of Pallet Racks	139
5.6. Effective Length Approach and Notional Load Approach for Cold-Formed Steel Frame and Beam-Column Design	143
5.6.1. Isolated Rotationally Restrained Sway Column	148
5.6.2. Interaction Equation	157
5.6.3. Cold-Formed Steel Frames	160
5.6.4. Development of Approach 2 <i>b</i>	172
5.6.5. Approach 1 <i>a</i> with $K_x = 1.7$	174

5.7. Finite Element Simulation of Pallet Rack Test	174
5.7.1. Beam Model	179
5.7.2. Shell Model	180
5.8. Conclusions	184
<b>6. Results and Conclusions</b>	<b>186</b>
<b>Appendix A Column Bases</b>	<b>191</b>
<b>Appendix B Base Fixity Charts</b>	<b>202</b>
<b>Appendix C Thin-Walled Sections</b>	<b>215</b>
<b>Appendix D Beam-Columns</b>	<b>220</b>
<b>Appendix E Design Results</b>	<b>223</b>
<b>Appendix F Design Examples</b>	<b>290</b>
<b>Appendix G Pallet Rack Drawings</b>	<b>297</b>
<b>Appendix H Computer Programs</b>	<b>300</b>
<b>References</b>	<b>327</b>

## LIST OF TABLES

2.1	Column and Base Plate Dimensions in Study	24
3.1	Beam to Column Connection Test Results	44
4.1	Values of Plate Buckling Coefficients	51
4.2	Section A-LDR Dimensions and Properties	54
4.3	Section A-LDR-2 Dimensions and Properties	55
4.4	Section A-HDR Dimensions and Properties	56
4.5	Centrically Loaded Compression Member Buckling Modes	63
4.6	Flexural Member Buckling Modes	63
4.7	Section Dimensions and Properties	66
4.8	Boundary Conditions of the Open-section Beam Element for Elastic Buckling Problems	67
4.9	Evaluation of the Torsional-Flexural Buckling Equation - Study II	68
4.10	Evaluation of the Torsional-Flexural Buckling Equation - Study III	69
4.11	Evaluation of the Torsional-Flexural Buckling Equation - Study IV	70
4.12	Evaluation of the Torsional-Flexural Buckling Equation - Study V	71
4.13	Values of Column $K_y$ and $K_t$ for Upright Frame A & B	75
4.14	Values of Column $K_y$ and $K_t$ for Upright Frame C & D	76
4.15	Values of Column $K_y$ and $K_t$ for Upright Frame E & F	77
4.16	Values of Column $K_x$ and $P_e$ for Upright Frame A, B, C, and D	79
4.17	Values of Column $K_x$ and $P_e$ for Upright Frame E & F	80
4.18	Comparison Among the AISI Design Approach, the Modified AISI Design Approach, and the Analytical Results	89
4.19	Stub-Column Tests and Analytical Results	96
4.20	Evaluation of Sub-Column Flexural Strength	115



5.1	Different Levels of Structural Analysis	140
5.2	Boundary Conditions in Study	150
5.3	Statistics for the Correlation of Design Procedures with the FEM Results	150
5.4	Beam to Column Connection Stiffnesses in Study	162
5.5	Load Case 1 - Statistics for the Correlation of Design Procedures with the FEM Results	164
5.6	Load Case 2 - Statistics for the correlation of design procedures with the FEM Results	165

## LIST OF FIGURES

2.1	(a) Beam element (b) Equivalent floor beam for rack not braced against sidesway (c) Equivalent floor beam for rack braced against sidesway	7
2.2	Model 1: Concrete springs	10
2.3	Model 2: Concrete beam	10
2.4	Model 3: Deformation shape of the concrete block under the base plate	10
2.5	Model 4	11
2.6	Model 4: Surface deformation under the base plate	12
2.7	Model 5 (a) Square base plate (b) 2 by 1 Rectangular base plate	12
2.8	Column wall section positioned at the edges of the plate	15
2.9	Column wall section positioned at the center of the plate	16
2.10	Column wall section positioned at the edges of the plate: Normal load distribution on the concrete surface	17
2.11	Column wall section positioned at the center of the plate: Normal load distribution on the concrete surface	17
2.12	Relationship between load block intensity factor $\sigma_c/\sigma_w$ and $t_p/t_w$	18
2.13	Base plate configurations	21
2.14	(a) Base plate type A (b) Base plate type B (c) Base plate type C (d) Base plate type D	22
2.15	Base fixity results for base plate type A	25
2.16	Base fixity results for base plate type B	25
2.17	Base fixity results for base plate type C	26
2.18	Base fixity results for base plate type D	26
2.19	(a) Thick base plate (b) Thin base plate	28
2.20	Column base finite element model	31

2.21	Column base finite element analysis results	31
2.22	Column base finite element analysis verification	32
3.1	Cantilever test	36
3.2	Portal test	36
3.3	Beam to column connection stiffness	37
3.4	Proposed portal test	41
3.5	Finite element model of the cantilever test	44
3.6	Details of the joint connection surface-based contact	45
3.7	Details of the connection stud	45
3.8	Finite element simulation of the cantilever test	46
3.9	Four nodes monitored to determine the rotation	46
3.10	Comparison of the cantilever test and the finite element simulation	47
4.1	Perforated plate buckling modes	51
4.2	(a) Section A-LDR (b) Section A-LDR-2 (c) Section A-HDR	53
4.3	Concentrically loaded compression member buckling modes	58
4.4	Flexural member buckling modes	59
4.5	Elastic buckling axial load for Section A-LDR	60
4.6	Elastic buckling moment for Section A-LDR	60
4.7	Elastic buckling axial load for Section A-LDR-2	61
4.8	Elastic buckling moment for Section A-LDR-2	61
4.9	Elastic buckling axial load for Section A-HDR	62
4.10	Elastic buckling moment for Section A-HDR	62
4.11	Convergence study for the simply supported torsional-flexural buckling problem using open-section beam finite element - Study I	67
4.12	Evaluation of the torsional-flexural buckling equation - Study II	68
4.13	Evaluation of the torsional-flexural buckling equation - Study III	69

4.14 Upright frame load cases and beam to column connection stiffness, $K_{\theta}$	74
4.15 Upright frame elastic critical buckling modes	74
4.16 Effect of initial geometric imperfection on effective design width	83
4.17 Stiffened compression elements - Correlation between effective design width equation and analytical results	83
4.18 Stiffened compression elements - Correlation between RMI effective design area equation and analytical results	84
4.19 Stiffened compression elements - Correlation between proposed effective design area equation and analytical results	84
4.20 Comparison between the RMI effective design area equation and the proposed equation	87
4.21 Comparison between the RMI effective design area equation and the proposed equation	87
4.22 Comparison between the AISI effective width approach and the proposed approach	88
4.23 Comparison between the AISI design approach and the modified AISI design approach	88
4.24 Section FS Open Back - Correlation between AISI design approach and analytical results	91
4.25 Section FS Open Back - Correlation between modified AISI design approach and analytical results	91
4.26 Section FS Open Back - Correlation between RMI effective design area equation and analytical results	92
4.27 Section FS Open Back - Correlation between proposed effective design area equation and analytical results	92

4.28	Section FS Closed Tube - Correlation between AISI design approach and analytical results	93
4.29	Section FS Closed Tube - Correlation between modified AISI design approach and analytical results	93
4.30	Section FS Closed Tube - Correlation between RMI effective design area equation and analytical results	94
4.31	Section FS Closed Tube - Correlation between proposed effective design area equation and analytical results	94
4.32	Section TB Open Back - Correlation between RMI effective design area equation and analytical results	97
4.33	Section TB Open Back - Correlation between proposed effective design area equation and analytical results	97
4.34	Section TB Closed Tube - Correlation between RMI effective design area equation and analytical results	98
4.35	Section TB Closed Tube - Correlation between proposed effective design area equation and analytical results	98
4.36	Section IG Open Back - Correlation between RMI effective design area equation and analytical results	99
4.37	Section IG Open Back - Correlation between proposed effective design area equation and analytical results	99
4.38	Section IG Closed Tube - Correlation between RMI effective design area equation and analytical results	100
4.39	Section IG Closed Tube - Correlation between proposed effective design area equation and analytical results	100
4.40	Section Type II Open Back - Correlation between RMI effective design area equation and analytical results	101

4.41	Section Type II Open Back - Correlation between proposed effective design area equation and analytical results	101
4.42	Comparison between the RMI approach for column design and the proposed approach	102
4.43	Comparison between the RMI approach for beam design and the proposed approach	102
4.44	Initial conditions of the finite element model (a) Bending residue stresses (b) Geometric imperfections	104
4.45	Section A-LDR - Comparison between the RMI approach for column design and the proposed approach	107
4.46	Section A-LDR - Comparison between the RMI approach for beam design and the proposed approach	107
4.47	Unperforated Section A-LDR - Comparison between the RMI approach for beam-column design and the proposed approach	108
4.48	Perforated Section A-LDR - Comparison between the RMI approach for beam-column design and the proposed approach	108
4.49	Section A-LDR-2 - Comparison between the RMI approach for column design and the proposed approach	109
4.50	Section A-LDR-2 - Comparison between the RMI approach for beam design and the proposed approach	109
4.51	Unperforated Section A-LDR-2 - Comparison between the RMI approach for beam-column design and the proposed approach	110
4.52	Perforated Section A-LDR-2 - Comparison between the RMI approach for beam-column design and the proposed approach	110
4.53	Section A-HDR - Comparison between the RMI approach for column design and the proposed approach	111

4.54	Section A-HDR - Comparison between the RMI approach for beam design and the proposed approach	111
4.55	Unperforated Section A-HDR - Comparison between the RMI approach for beam-column design and the proposed approach	112
4.56	Perforated Section A-HDR - Comparison between the RMI approach for beam-column design and the proposed approach	112
4.57	Contour plots of the elastic critical axial force $P_e$ , kips	119
4.58	Bending moment about the $x$ -axis	119
4.59	Bending moment about the $y$ -axis	120
4.60	Twisting moment about the $z$ -axis	120
5.1	Parameters that influences the value of $K_x$ for column flexural buckling	126
5.2	Loading sequence in study	128
5.3	Relationship between the frame stability and the loading sequence	128
5.4	Storage rack in study	130
5.5	Evaluation of the Alignment chart	130
5.6	Evaluation of the torsional-flexural buckling equation	131
5.7	Storage rack in study	133
5.8	Different modes of frame initial out-of-plumb	133
5.9	Effect of initial out-of-plumb on the load carrying capacity of the frame	134
5.10	Frame with $K_\theta = 300$ kips-in. - Correlation between second-order elastic analysis and moment magnification factors	137
5.11	Frame with $K_\theta = 600$ kips-in. - Correlation between second-order elastic analysis and moment magnification factors	137
5.12	Frame with $K_\theta = 1200$ kips-in. - Correlation between second-order elastic analysis and moment magnification factors	138

5.13	Frame with $K_{\theta} = \text{Rigid}$ - Correlation between second-order elastic analysis and moment magnification factors	138
5.14	Different levels of structural analysis	140
5.15	Base fixity model (a) Torsional spring (b)-(e) Double axial spring	142
5.16	(a) Effective length approach (b) Notional load Approach	146
5.17	(a) Rotationally restrained sway column (b) out-of-straightness (c) out-of-plumbness	149
5.18	Column sections in study	149
5.19	Correlation between the Effective Length Approach (Approach 1a) and the FEM results	152
5.20	Correlation between the Effective Length Approach (Approach 1b) and the FEM results	152
5.21	Correlation between the Effective Length Approach (Approach 1c) and the FEM results	153
5.22	Correlation between the Effective Length Approach (Approach 1d) and the FEM results	153
5.23	Correlation between the Notional Load Approach (Approach 2a) and the FEM results	154
5.24	Correlation between the Notional Load Approach (Approach 2b) and the FEM results	154
5.25	Correlation between the Notional Load Approach (Approach 2c) and the FEM results	155
5.26	Loading conditions in study	161
5.27	Frame dimensions in study	161
5.28	Upright frame configurations in study	162
5.29	Braces and Shelf beams in Study	162



5.30	Load Case 1 - Correlation between the Effective Length Approach (Approach 1 <i>a</i> ) and the FEM results	166
5.31	Load Case 1 - Correlation between the Effective Length Approach (Approach 1 <i>c</i> ) and the FEM results	166
5.32	Load Case 1 - Correlation between the Notional Load Approach (Approach 3 <i>a</i> ) and the FEM results	167
5.33	Load Case 1 - Correlation between the Notional Load Approach (Approach 2 <i>b</i> ) and the FEM results	167
5.34	Load Case 1 - Correlation between the Notional Load Approach (Approach 2 <i>c</i> ) and the FEM results	168
5.35	Load Case 2 - Correlation between the Effective Length Approach (Approach 1 <i>c</i> ) and the FEM results	170
5.36	Load Case 2 - Correlation between the Notional Load Approach (Approach 2 <i>a</i> ) and the FEM results	170
5.37	Load Case 2 - Correlation between the Notional Load Approach (Approach 3 <i>b</i> ) and the FEM results	171
5.38	Load Case 2 - Correlation between the Notional Load Approach (Approach 3 <i>c</i> ) and the FEM results	171
5.39	Load Case 1 - Frame out-of-plumb or the magnitude of the notional horizontal load required for the notional load approach	173
5.40	Correlation between the Effective Length Approach (Approach 1 <i>a</i> with $K_x = 1.7$ ) and the FEM results	175
5.41	Same plot as Figure 5.40 but with a different y-axis scale	175
5.42	Load Case 1 - Correlation between the Effective Length Approach (Approach 1 <i>a</i> with $K_x = 1.7$ ) and the FEM results	176
5.43	Same plot as Figure 5.42 but with a different y-axis scale	176

5.44 Combined shell and beam finite element frame model	177
5.45 Middle upright frame modeled as shell elements	178
5.46 Finite element frame model: Critical buckling mode	181
5.47 Finite element shell model II Gravity + Horizontal Load Case	181
5.48 Results for Gravity Loads	182
5.49 Results for Gravity + Horizontal Loads	182

---

---

# Chapter 1

## Introduction

---

---

### 1.1 BACKGROUND

The design of industrial steel storage racks presents several challenges to the structural engineer. Presently, the design in the United States is carried out according to the 1997 edition of the Specification published by the Rack Manufacturers' Institute (RMI). The RMI published its first "Minimum Engineering Standards for Industrial Storage Racks" in 1964.

The work that resulted in the first edition of the Specification was initiated by the RMI in 1972 at Cornell University. Several editions of the Specification have been prepared based on the work by the RMI Specification Advisory Committee and the researchers at Cornell University under the supervision of Professors George Winter and Teoman Peköz until 1979 and under the supervision of Teoman Peköz since 1979. The RMI (1997) Specification is tied closely to the AISI (1996) Specification for the provisions on Cold-Formed Steel Design.

## **1.2 OBJECTIVES AND SCOPE**

The design of cold-formed steel frames and beam-columns used in industrial storage racks is complex because of the significant perforations in the columns, and the semi-rigid nature of the beam to column connections and column bases. In addition, the columns usually have open cross-sections, making it vulnerable to torsional-flexural buckling. Many assumptions are made in the current design specification to simplify the design procedures, and as a result the design becomes quite conservative. The objective of this research was to make improvements in the RMI (1997) Specification and the AISI (1996) Specification.

Numerical methods were used to carry out studies at both the component and the frame level, to verify or modify the current design provisions. At the component level, the topics focused upon are the column base fixity, the beam to column connection test procedure, and the design of perforated members. At the frame level, studies were carried out to evaluate the current effective length approach, and to examine the notional load approach as an alternative design procedure; as well as to use numerical methods for structural analysis, such as elastic buckling analysis and second-order elastic analysis considering semi-rigid connections. Studies are presented in this thesis for each of these components, and then followed by a study on cold-formed steel frames.

### 1.3 RELATED LITERATURE

The work presented in this thesis would not be possible without studying previous works of other researchers. The following are some of the works which the author studied and referred to extensively throughout this research project.

Textbooks written by Galambos (1988), Hancock (1998), Peköz (1987), Rhodes (1991), Salmon and Johnson (1996), Timoshenko and Gere (1961), and Yu (2000) provided in depth explanations of the fundamental basis for the design of cold-formed steel and metal structures.

Studies given by Galambos (1960), and Salmon, Schenker and Johnston (1955) were the basis for the column base fixity equation used in the RMI specification. The author referred to the following solid mechanic textbooks: Gurtin (1981), Malvern (1969), Sokolnikoff (1983), Timoshenko and Goodier (1969) to solve column base fixity problems.

Beam-to-column connection test procedures given in the commentary section of the RMI specification were reviewed and used to develop a new alternative test procedure. These beam to column connection tests had been carried out extensively by Markazi, Beale, and Godley (1997), and Harris and Hancock (2002).

Journal papers by Stuto (1993), and White and Clarke (1997) thoroughly give the historical background, philosophies, and comparison between different standards for the design of steel beam-columns. And discussion by Peköz and Winter (1973) provide background information on the development of the RMI specification.

The influence that the semi-rigid nature of the beam to column joints and column bases have on the pallet racks stability were investigated by Baldassino and Bernuzzi (2000), Cheng (1973), and Lewis (1991). Salmon, Welch and Longinow (1973), and Godley (2002) investigated the behavior of drive-in and drive-thru storage racks; Olsson, Sandberg and Austrell (1999) investigated the influence of damage on

the load carrying capacity of storage rack columns; and Teh, Hancock and Clarke (2001) investigated the buckling behavior of high-rise storage rack structures.

Torsional-flexural buckling and moment magnification factor studies carried out in the thesis were based primarily on Peköz (1967), Peköz and Celebi (1969), and Salmon and Johnson (1996).

Comparison between the effective length approach and notional load approach for assessing frame stability has been and is continuously being studied by the ASCE Task Committee on Effective Length. The author has referred to their ASCE (1997) report and is very grateful for their collaboration making the study on Effective Length Approach and Notional Load Approach for Cold-Formed Steel Frame and Beam-Column Design in this research project possible.

Previous researchers at Cornell University have studied the finite element modeling assumptions of cold-formed steel members extensively. The analytical studies carried out in this research project would not be possible without reference to the finite element studies conducted by Schafer and Peköz (1998), and Schafer (1997).

The several computer programs that the author developed for this research project were based on the theory of structural analysis given by Chen and Atsuta (1976), Gattass and Abel (1987), Huebner, Thornton and Byrom (1995), Gotluru (1998), McGuire, Gallagher and Ziemian (2000), Timoshenko and Gere (1961), Yang (1986), as well as the cold-formed steel design approaches given by AISI (1996), Schafer (1997), and Schafer and Peköz (1999).

The author is certain that many more researchers other than those mentioned here contributed to the research and development of cold-formed steel frame and beam-column design. These omissions are either for the sake of brevity or because they were unknown to the author.

---

---

# Chapter 2

## Column Bases

---

---

### 2.1 INTRODUCTION

Storage rack stability depends significantly on the conditions of the column bases. The RMI specification uses the following base fixity expression, for the ratio of the moment with respect to the corresponding rotation of the base to account for the semi-rigid nature of the connection of the column to the floor as

$$\frac{M}{\theta} = \frac{bd^2E_c}{12} \quad (2.1)$$

where  $b$  is the width of the column parallel to the flexural axis,  $d$  is the depth of the column perpendicular to the flexural axis, and  $E_c$  is the modulus of elasticity of the floor, which is assumed to be concrete. The expression above is based on an analytical approximation developed by Salmon, Schenker and Johnston (1955) for the case where the footing does not rotate in soil, which is the case for the storage racks in this study. Rotation takes place between the column ends and the floor due to the deformation of the base plate, the anchor bolts, and the concrete. Salmon, Schenker and Johnston (1955) also developed a method for finding the moment-rotation

relationship by analyzing the behavior of such anchorages in five different stages starting with a trapezoidal stress distribution in the concrete floor under the base plate and ending at the failure of the anchor bolts. The RMI specification considered only the first stage.

The connection between the column and the floor could be represented in an analytic frame model either by a torsional spring or by inserting an equivalent floor beam between the column bases. The stiffness of the equivalent floor beam that would provide the same restraints as Eq. (2.1) could be found from basic structural analysis. Consider a beam element shown in Fig. 2.1a with its two ends identified as  $a$  and  $b$ . The bending moments at the two ends are

$$M_a = \frac{4EI}{L}\theta_a + \frac{2EI}{L}\theta_b + \frac{6EI}{L^2}u_a - \frac{6EI}{L^2}u_b \quad (2.2)$$

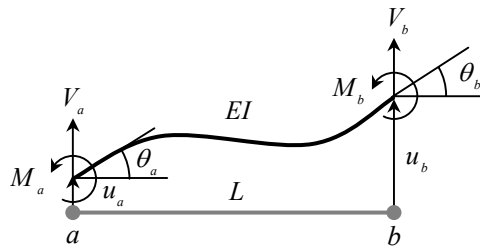
$$M_b = \frac{2EI}{L}\theta_a + \frac{4EI}{L}\theta_b + \frac{6EI}{L^2}u_a - \frac{6EI}{L^2}u_b \quad (2.3)$$

where  $u_a$  and  $u_b$  are the translation degrees of freedom,  $\theta_a$  and  $\theta_b$  are the rotational degrees of freedom,  $L$  is the length,  $I$  is the moment of inertia, and  $E$  is the modulus of elasticity of the beam element. To determine the stiffness of the equivalent floor beam for rack not braced against sidesway, consider a frame that has its column bases rotate equally because of the sidesway as shown in Fig. 2.1b, the boundary conditions of segment  $ab$  in this case are  $M_b = 0$ ,  $u_a = 0$ , and  $u_b = 0$ . Using Eqs. (2.2) and (2.3) with these boundary conditions  $M_a$  is obtained as follows:

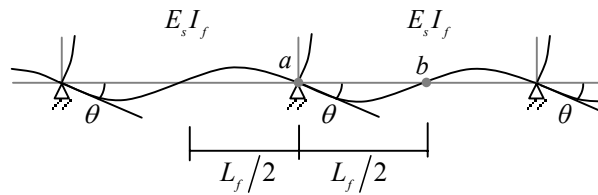
$$M_a = \frac{6E_s I_f}{L_f} \theta_a$$

the resisting moment that is developed in the interior column base from the two ends of the equivalent floor beam is  $M = 2M_a$  that is

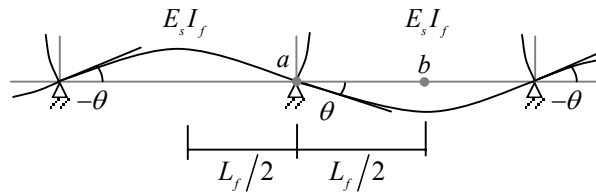




(a)



(b)



(c)

**Figure 2.1** (a) Beam element (b) Equivalent floor beam for rack not braced against sidesway (c) Equivalent floor beam for rack braced against sidesway

$$M = \frac{12E_s I_f}{L_f} \theta \quad (2.4)$$

where  $\theta$  is the angle of rotation of the column base which is equal to  $\theta_a$ . Inserting the above equation in Eq. (2.1) and assuming  $E_s/E_c = 10$  we have the stiffness of the equivalent floor beam for rack not braced against sidesway as given in the RMI specification.

$$\frac{I_f}{L_f} = \frac{bd^2}{1440} \quad (2.5)$$

To determine the stiffness of the equivalent floor beam for a rack braced against sidesway the same procedure is used, however, as shown in Fig. 2.1c the boundary conditions of segment  $ab$  in this case are  $M_b = -M_a$ ,  $u_a = 0$ , and  $\theta_b = 0$ . Using Eqs. (2.2) and (2.3) with these boundary conditions  $M_a$  is obtained as follows:

$$M_a = \frac{2E_s I_f}{L_f} \theta_a$$

the resisting moment that is developed in the interior column base at the two ends of the equivalent floor beam is  $M = 2M_a$  that is

$$M = \frac{4E_s I_f}{L_f} \theta \quad (2.6)$$

Inserting the above equation in Eq. (2.1) and assuming  $E_s/E_c = 10$  we have the stiffness of the equivalent floor beam for rack braced against sidesway as given in the RMI specification.

$$\frac{I_f}{L_f} = \frac{bd^2}{480} \quad (2.7)$$

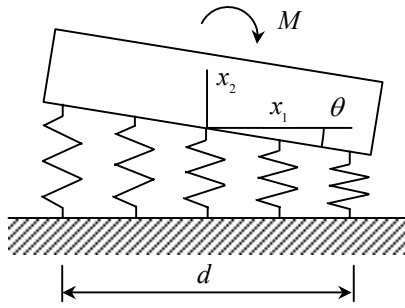
The effective length factor for the portion of the column from the floor to the first beam level could then be found from the alignment chart with the following:

$$G_b = \frac{I_c / L_{c1}}{2 \left( I_f / L_f \right)} \quad (2.8)$$

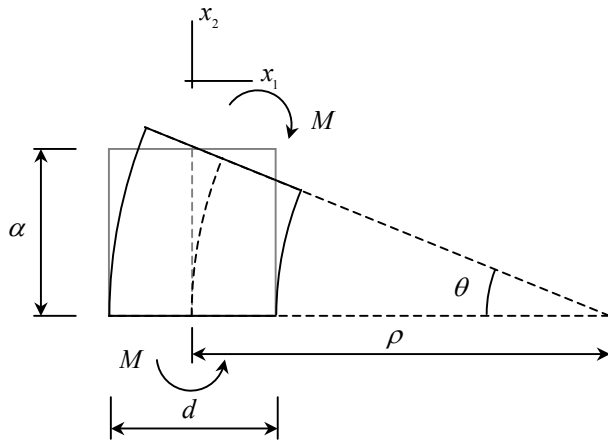
where  $I_c$  is the column moment of inertia and  $L_{c1}$  the distance from the floor to the first beam level.

Several analytical models of the base fixity problem were studied. Details of their derivation can be found in Appendix A. The first model shown in Fig. 2.2 consists of a series of springs to represent the concrete floor. If the stiffness of these springs is set to  $k = E_c/d$  the base fixity is found to be the same as in Eq. (2.1). The second model shown in Fig. 2.3 is similar to the first model, that is considering only the concrete block under the base plate, but instead of springs the second model uses the beam theory approach with the same result obtained if  $\alpha = d$  where  $\alpha$  is the depth of the concrete block. A third model uses a basic solid mechanic approach to understand better how the concrete block in the first two models deforms. Starting from a defined stress field and boundary conditions, the displacement field could be found for the concrete block as shown in Fig. 2.4.

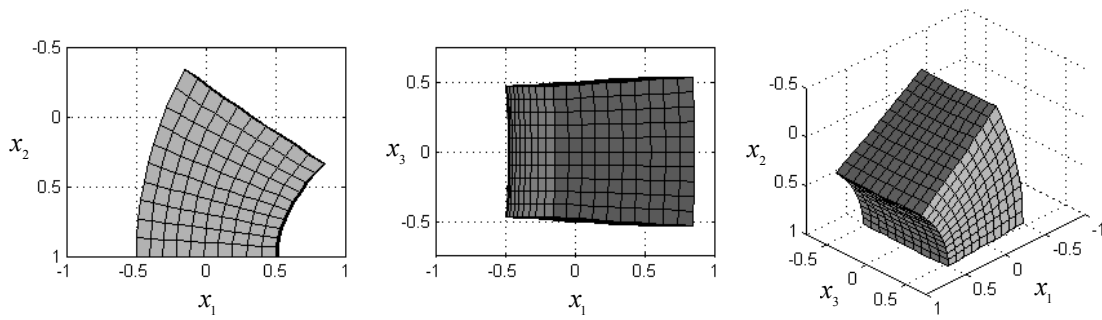
Considering only the concrete block under the base plate, however, results in a lower stiffness than what the actual floor could develop; this is because the confinement from the surrounding material was neglected. The concrete floor should instead be represented with a half-space material. Based on this idea a fourth model was studied where it is a two-dimensional elastostatic problem with normal loads on the boundary of half-space. By superimposing some combinations of Figs. 2.5a and 2.5b, a bending load distribution indicated in Fig. 2.5c can be obtained. Once the applied load is defined the displacement field can be found. The deformation of the concrete surface under the applied load region is shown in Fig. 2.6. Although the fourth model is only a plane strain problem and may not represent the actual three



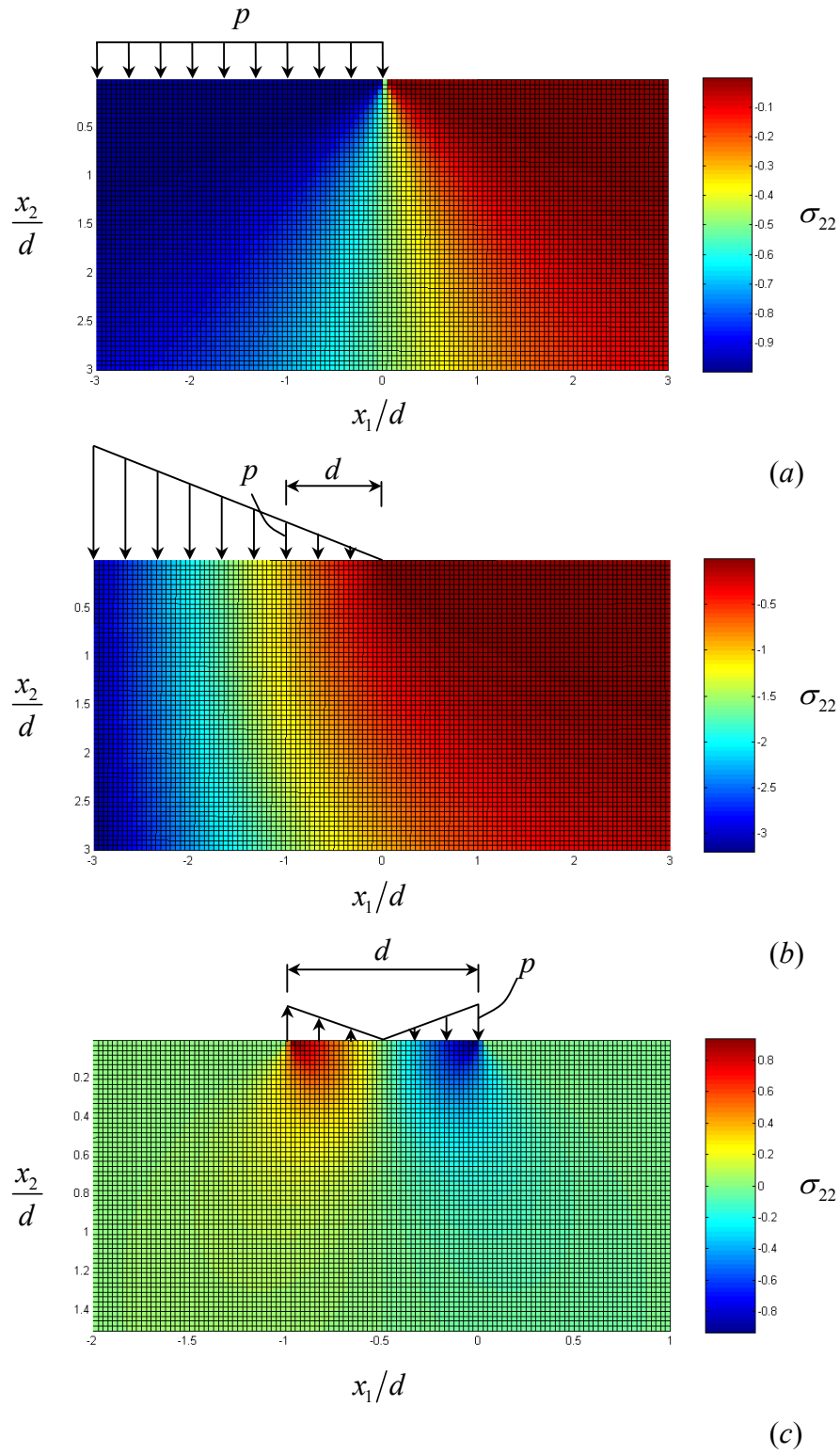
**Figure 2.2** Model 1: Concrete springs



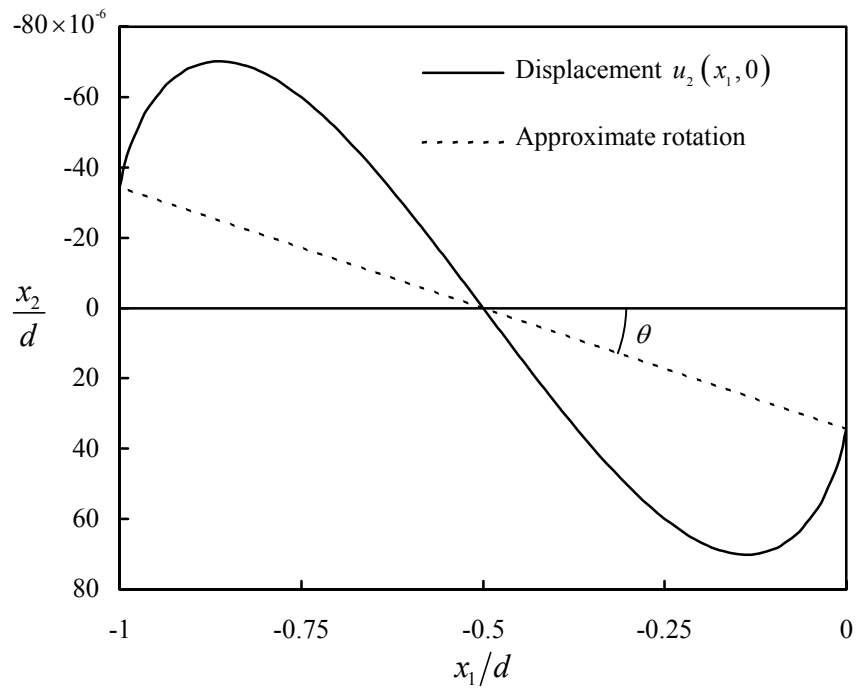
**Figure 2.3** Model 2: Concrete beam



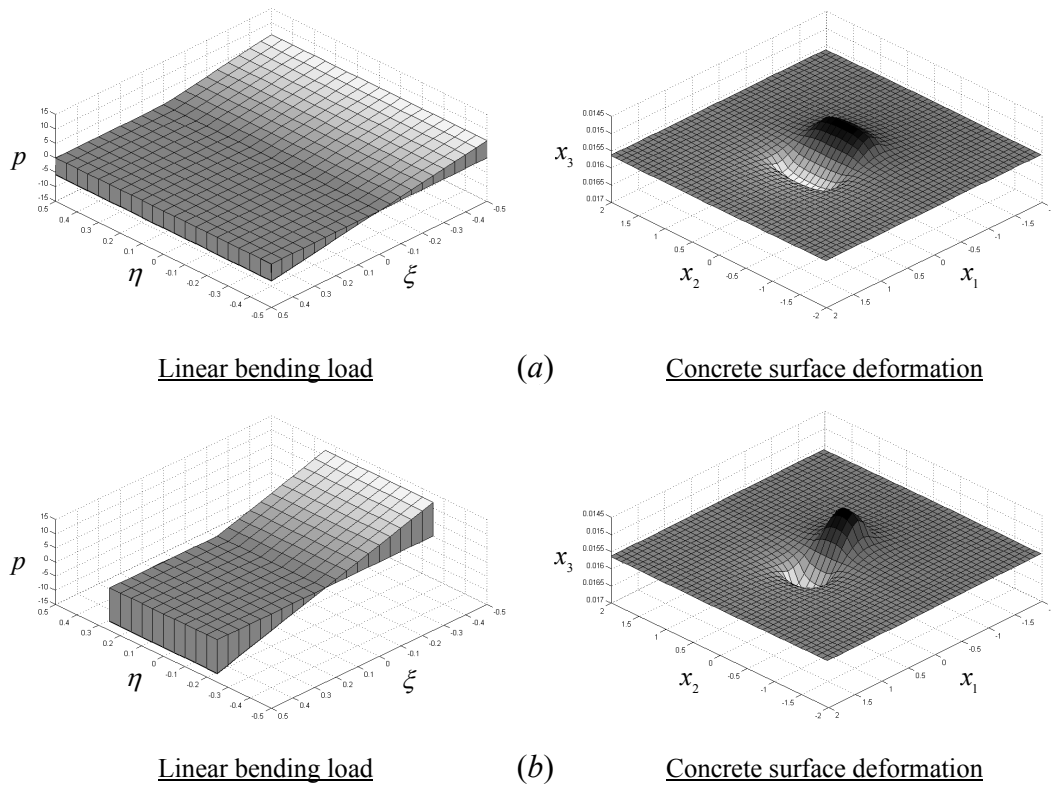
**Figure 2.4** Model 3: Deformation shape of the concrete block under the base plate



**Figure 2.5** Model 4: (a) Load extends indefinitely to the left (b) Linearly increasing load extending indefinitely to the left (c) Linear bending load under the base plate



**Figure 2.6** Model 4: Surface deformation under the base plate



**Figure 2.7** Model 5 (a) Square base plate (b) 2 by 1 Rectangular base plate

dimensional base fixity problem, it can be seen that the surrounding concrete does affect the surface displacement thus differing from the previous models.

Finally, the fifth model not only considered the half-space nature of the floor, but it also considered the three-dimensional aspect of the problem. This model is considered to be better than all the previous models to represent the base fixity problem. Normal loads were applied on the boundary of the concrete floor and the resulting displacement was determined. When a square base plate was considered in this model, normal load distribution  $p$  was applied and the surface deformation was obtained as shown in Fig. 2.7a. The resulting base fixity was 4.05 times higher than Eq. (2.1). For a 2 by 1 rectangular base plate, the results showed that the stiffness was 5.128 times higher than Eq. (2.1). This confirms that the current base fixity equation may be underestimating the actual stiffness. However, defining contact pressure between the base plate and concrete surface as a linear bending load distribution must be justified. This motivated the study described in Section 2.2. By using the fifth model approach but with improvement in defining the normal load, a new base fixity equation was developed.

## **2.2 DEVELOPMENT OF A BASE FIXITY EQUATION**

### **2.2.1 Contact Stresses Between Base Plate and Floor**

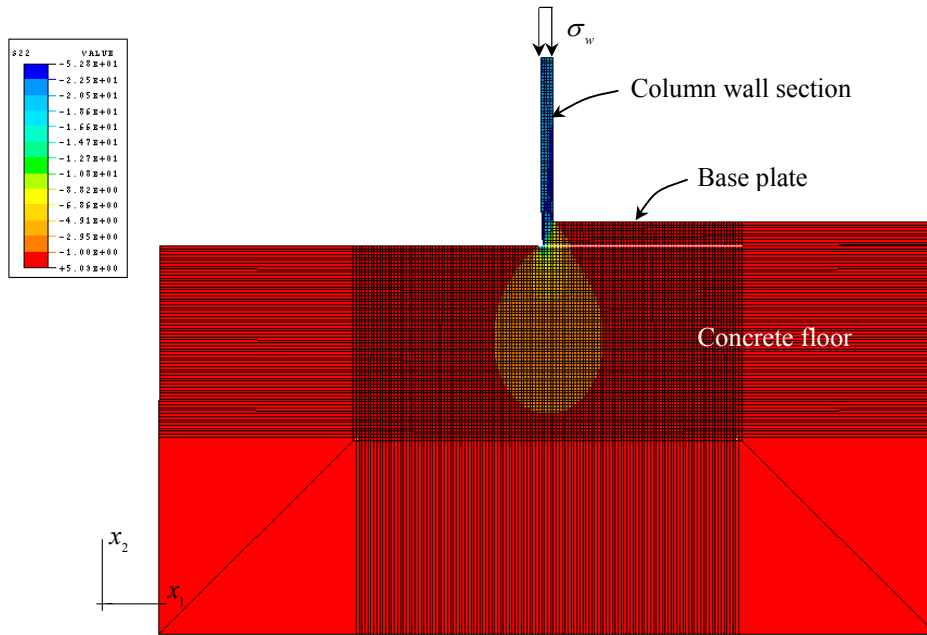
The objective here was to study how the load is transferred from the column to the floor. Once the load distribution on the concrete surface is known, the surface deformation can be found by an approach similar to the fifth model approach and thus the base fixity can be obtained. The load distribution on the concrete surface must be solved from a contact simulation between the base plate and the floor. The finite element method was used to solve this problem. Since the columns in consideration

are thin-walled sections, namely, the column wall thickness  $t_w$  and base plate thickness  $t_p$  both are relatively small compared to the width or depth of the column, the problem was simplified by solving each wall section separately with a plane strain analysis. Two cases were considered, one when the column wall section is positioned at the edges of the base plate as shown in Fig. 2.8 and the other when it is at the center as shown in Fig. 2.9.

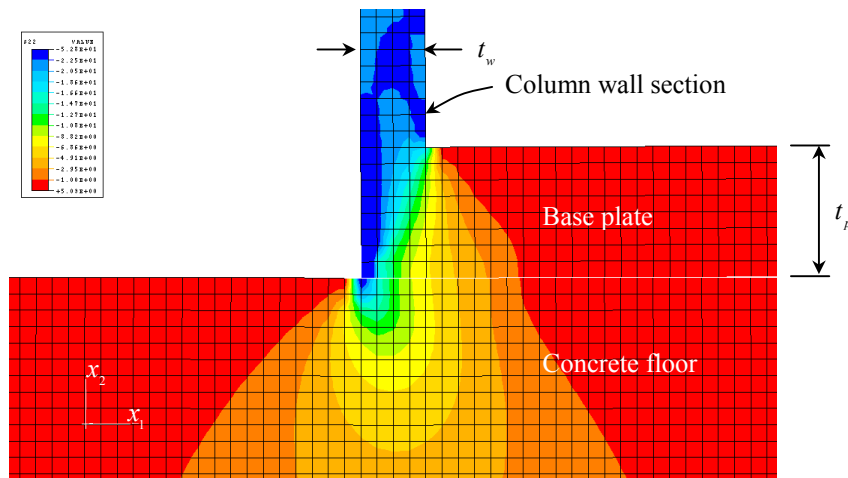
Finite element assumptions are as follows: The four node plane strain elements were used to model. Contact surfaces were defined between the base plate and the concrete to simulate their interaction. However, in this study no friction was considered between the two surfaces. In addition, since the floor was assumed to be a half-space and only a small region of the base plate was considered, plane strain infinite elements were needed to model the far-field region of the concrete and base plate. For the case when the column wall section is positioned at the middle, because it is a symmetric problem only a half model is needed as shown in Fig. 2.9. The material model used for the column wall and base plate was elastic with  $E_s = 29500$  ksi and  $\nu = 0.3$  while the concrete was assumed elastic with  $E_c = 2950$  ksi and  $\nu = 0.2$ . A uniform compression stress was applied at the top of the column wall.

A parametric study was carried out for the two cases to find out how the contact stress distribution changes as the base plate to column wall thickness ratio,  $t_p/t_w$  is varied from 1 to 3. The normal load distribution on the concrete surface was obtained and plotted as shown in Figs. 2.10 and 2.11. The vertical axis represents the stress intensity factor  $\sigma_c/\sigma_w$ , where  $\sigma_c$  is the stress on the concrete surface, and  $\sigma_w$  is the applied stress on the column wall. The horizontal axis represents the normalized position across the concrete surface. As seen in both cases as the  $t_p/t_w$  increases the load distribution expands. The load distribution was then further simplified by representing it with an equivalent load block, which will give the same total force and



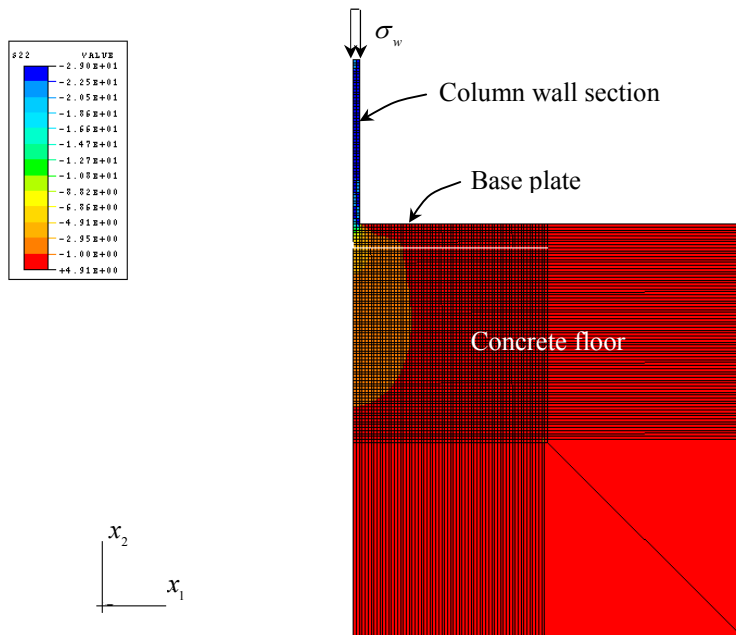


(a)

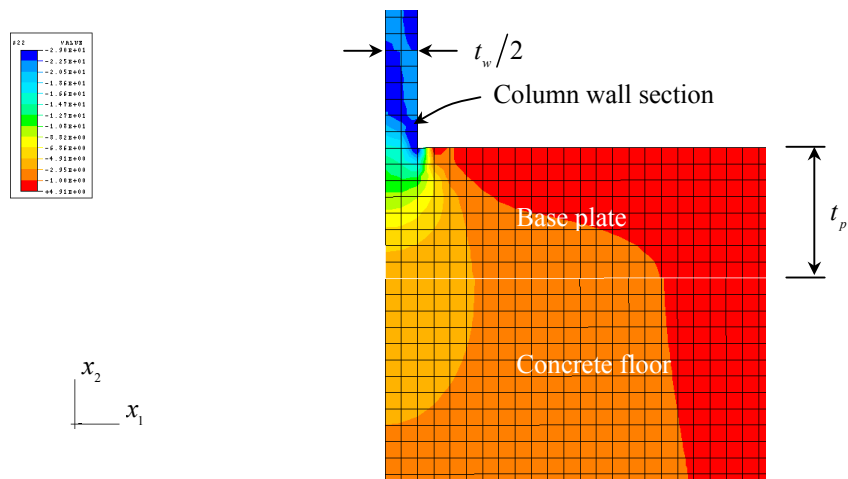


(b)

**Figure 2.8** Column wall section positioned at the edges of the plate: Finite element plane strain analysis  $\sigma_{22}$  contour (a) Entire model (b) At the column wall to base plate connection

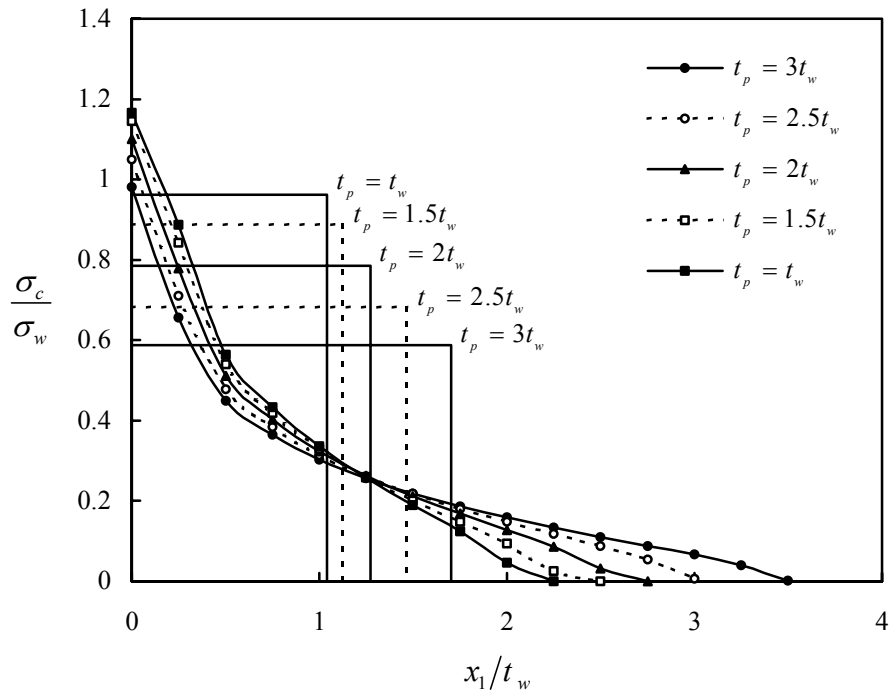


(a)

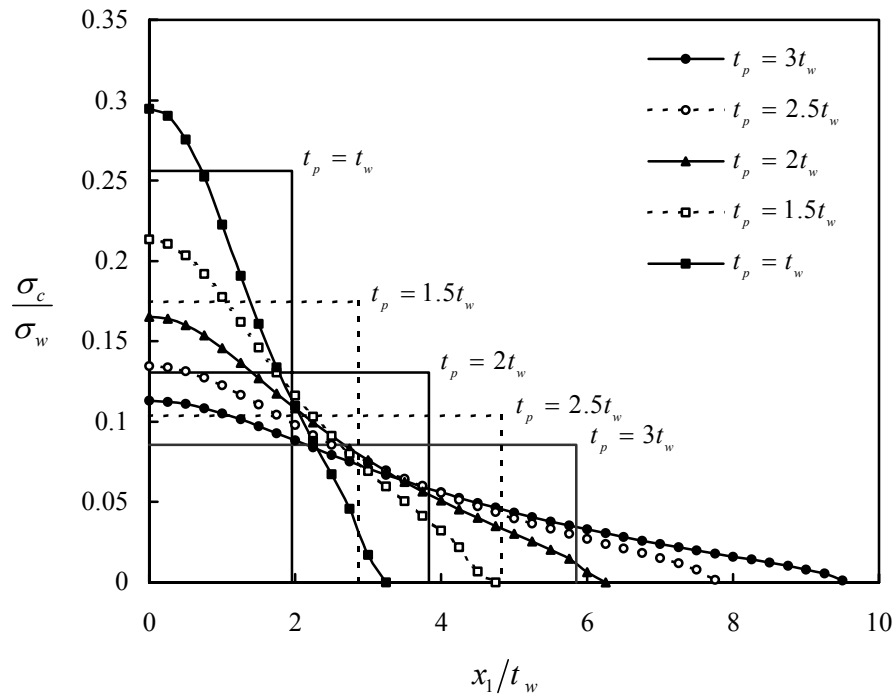


(b)

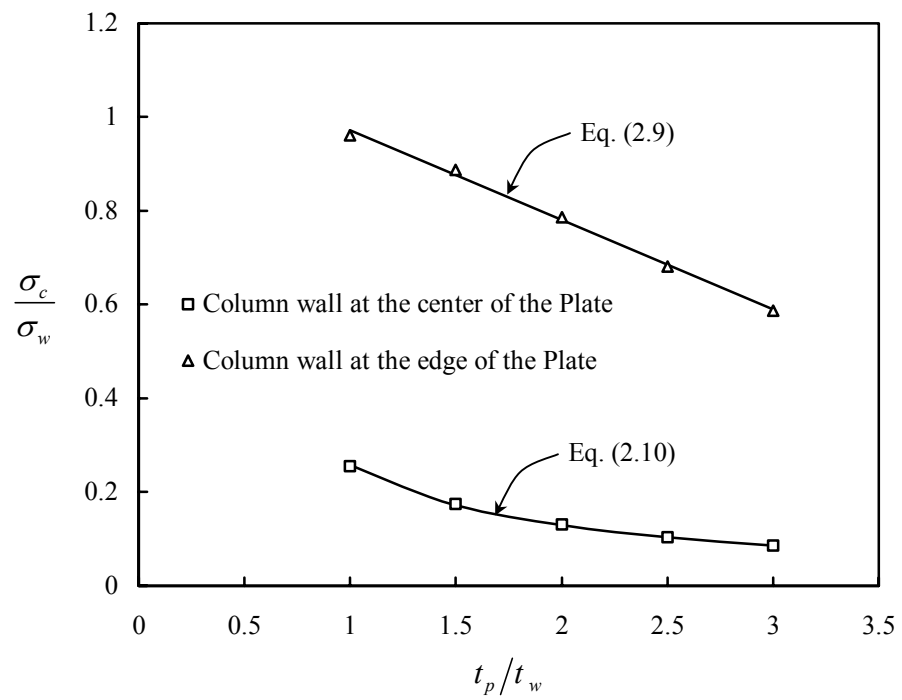
**Figure 2.9** Column wall section positioned at the center of the plate: Finite element plane strain analysis  $\sigma_{22}$  contour (a) Entire model (b) At the column wall to base plate connection



**Figure 2.10** Column wall section positioned at the edges of the plate: Normal load distribution on the concrete surface ( $\sigma_c$  is  $\sigma_{22}$  given Figure 2.8)



**Figure 2.11** Column wall section positioned at the center of the plate: Normal load distribution on the concrete surface ( $\sigma_c$  is  $\sigma_{22}$  given Figure 2.9)



**Figure 2.12** Relationship between load block intensity factor  $\sigma_c/\sigma_w$  and  $t_p/t_w$

moment respect to the vertical axis. The relationship between the load block intensity factor  $\sigma_c/\sigma_w$  and the  $t_p/t_w$  can be plotted as in Fig. 2.12 with the following expression obtained for the case where the column wall section is positioned at the edges of the plate:

$$\frac{\sigma_c}{\sigma_w} = 1.162 - 0.191 \frac{t_p}{t_w} \quad (2.9)$$

and for when the column wall section is positioned at the center of the plate:

$$\frac{\sigma_c}{\sigma_w} = 0.2584 \frac{t_w}{t_p} \quad (2.10)$$

The width of the equivalent load block  $t_c$  was found by imposing the condition that the total force of the equivalent load block is equal to the total force applied on the column wall.

$$\sigma_c t_c = \sigma_w t_w \quad (2.11)$$

### 2.2.2 Normal Loads on the Boundary of Half-Space

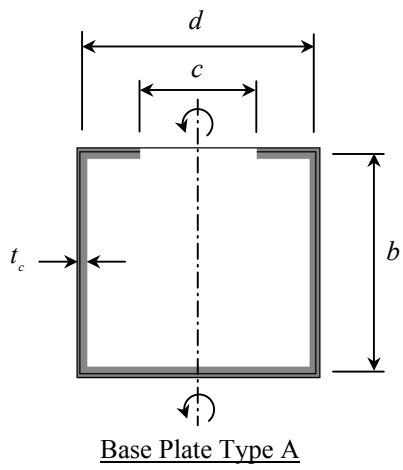
Finite element studies of the base fixity problem, have shown that contact pressures between the base plate and concrete surface, are concentrated around the column wall section, rather than having a linear bending load distribution as assumed in Eq. (2.1). This is because the column wall thickness and base plate thickness in study are relatively thin, compared to the width or depth of the column. The distribution of the normal loads on the concrete surface depends on these thicknesses, and the location of the column wall section on the base plate. Once the normal load distribution on the concrete surface for a certain amount of bending moment is known, deformation can be obtained by solving the problem of normal loads on the boundary of the half-space, using solid mechanic approaches as suggested

in Sokolnikoff (1983). The column base rotation was found from the floor surface deformation, and then the base fixity was computed.

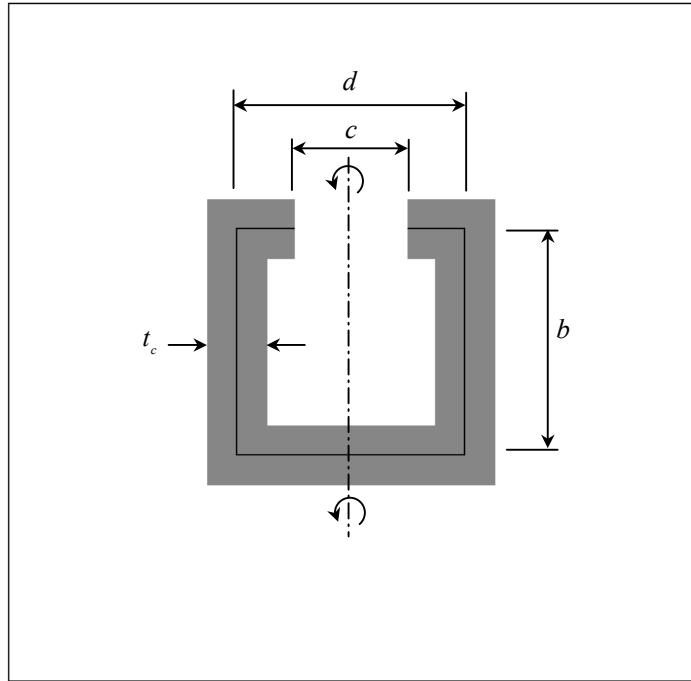
With the relationship between the load block intensity factor  $\sigma_c/\sigma_w$  and  $t_p/t_w$  known, different types of base plate configurations could then be studied. Four types of base plates were considered as shown in Fig. 2.13. The column load was assumed to be a combination of an axial and bending force. However, only the bending force contributes to the rotation of the base. The force in the column is transferred through the base plate and then onto the floor. The intensity of the normal load distribution was found by using either Eq. (2.9) or Eq. (2.10) depending on the location of the column wall section. The width of the load distribution was then found by using Eq. (2.11).

Type A has the base plate the same size as the column. Because all the column wall sections are located at the edges of the base plate, only Eq. (2.9) is needed to approximate the normal load distribution. Type B has the base plate extended out from the opening of the column, thus Eq. (2.10) must be used at the stiffeners. For type C the column is placed on a large base plate so only Eq. (2.10) is needed. For Type D the base plate is extended out from both sides of the flanges. For this base plate type Eq. (2.10) is used for the flanges and Eq. (2.9) is used at the web and stiffeners. Examples of the resulting normal load distribution for a 3 in. square C-section with  $c = d/2$ ,  $t_w = t_p = 0.10$  in., for the different base plate types are shown in Fig. 2.14.

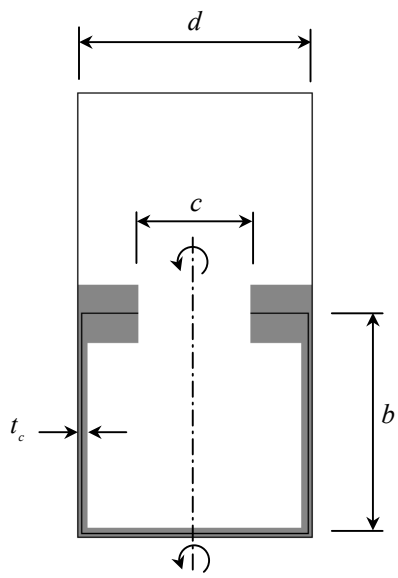
Once the load distribution on the concrete surface for a certain moment force is known, deformation of the concrete can be obtained by solving the problem of normal loads on the boundary of the half-space. Concrete surface deformation for the C-section example is shown in Fig. 2.14. The rotation was then found from the surface deformation, and the base fixity was calculated. A parametric study was carried out for a wide range of column base configurations to develop a new base fixity equation.



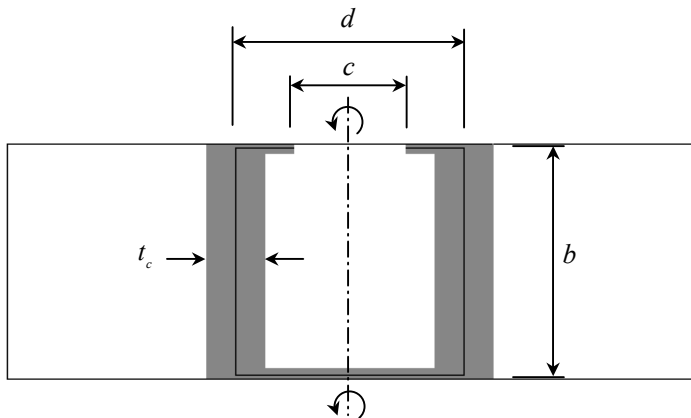
Base Plate Type A



Base Plate Type C

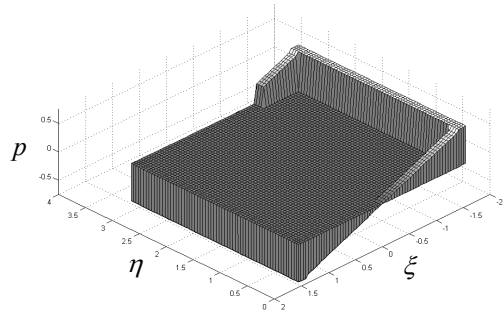


Base Plate Type B

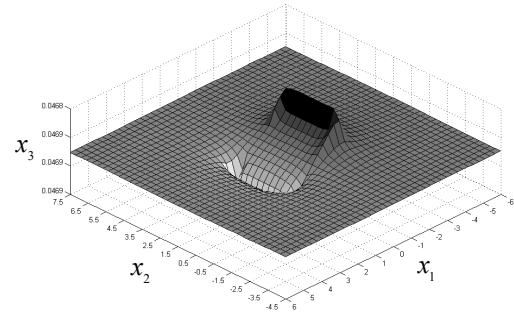


Base Plate Type D

**Figure 2.13** Base plate configurations

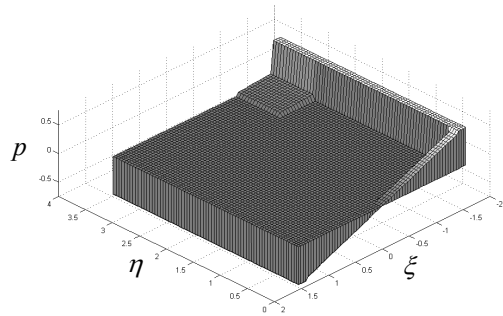


Normal loads distribution



(a)

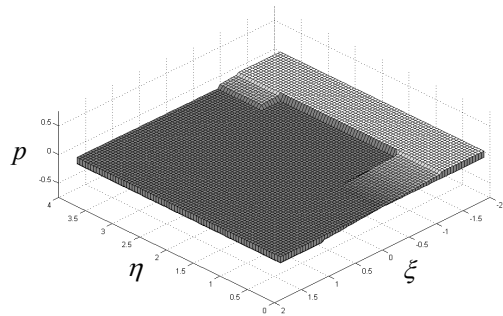
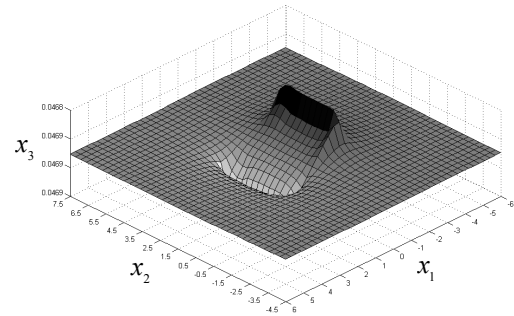
Concrete surface deformation



Normal loads distribution

(b)

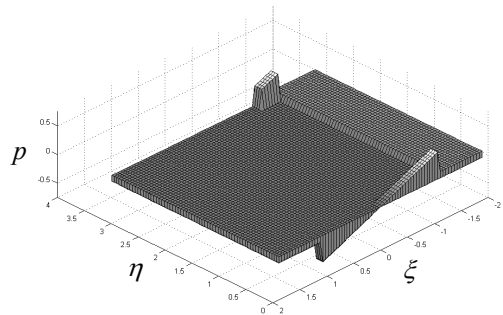
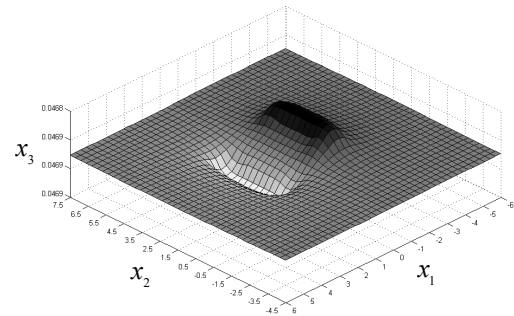
Concrete surface deformation



Normal loads distribution

(c)

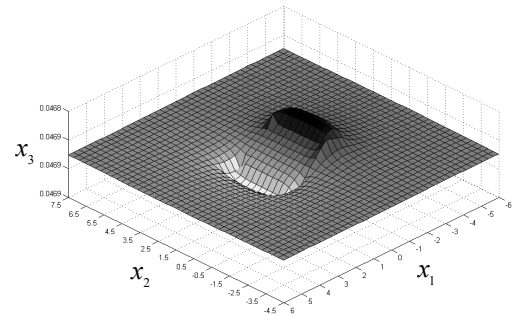
Concrete surface deformation



Normal loads distribution

(d)

Concrete surface deformation



**Figure 2.14** (a) Base plate type A (b) Base plate type B (c) Base plate type C (d) Base plate type D



The parameters included are summarized in Table 2.1. Combinations of these parameters yielded a total of 500 models for each base plate type. Results for the different base plate types are shown in Figs. 2.15 through 2.18. It can be seen that the results of base plate type A are similar to type B while the results of base plate type C are similar to type D. This is mainly because the load at the stiffener and web is rather low. Most of the rotation takes place due to the loads from flanges.

New base fixity equations were obtained by fitting a regression line through the data results. For use with base plate type A or B, the equation is

$$\frac{M}{\theta} = \frac{7}{25}bd^2E_c \quad (2.12)$$

For use with base plate type C or D, the equation is

$$\frac{M}{\theta} = \frac{9}{25}bd^2E_c \quad (2.13)$$

For practical purposes it is recommended that a single base fixity equation, Eq. (2.12), be used for all types of base plates. As can be seen Figs. 2.17 and 2.18, the design will simply be slightly more conservative when Eq. (2.12) is used for base plate type C or D. The stiffness of the equivalent floor beam corresponding to Eq. (2.12) for rack not braced against sidesway is

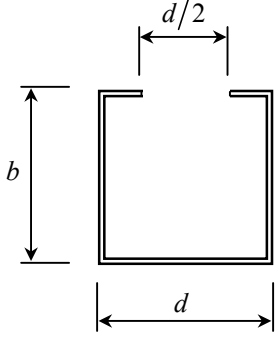
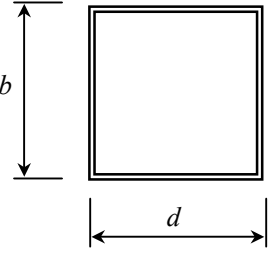
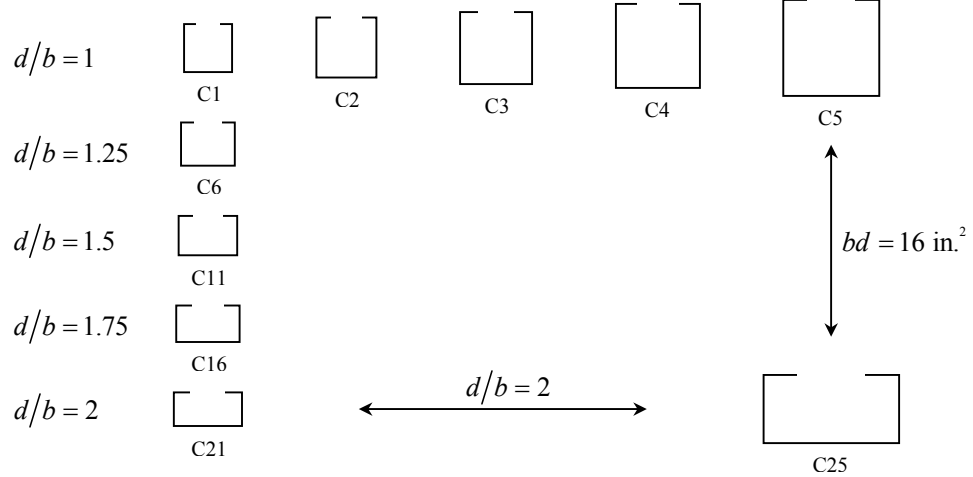

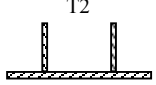
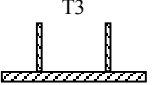
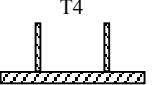
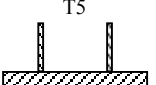
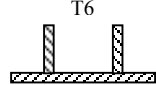
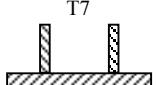

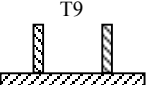
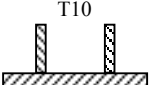
$$\frac{I_f}{L_f} = \frac{7}{3000}bd^2 \quad (2.14)$$

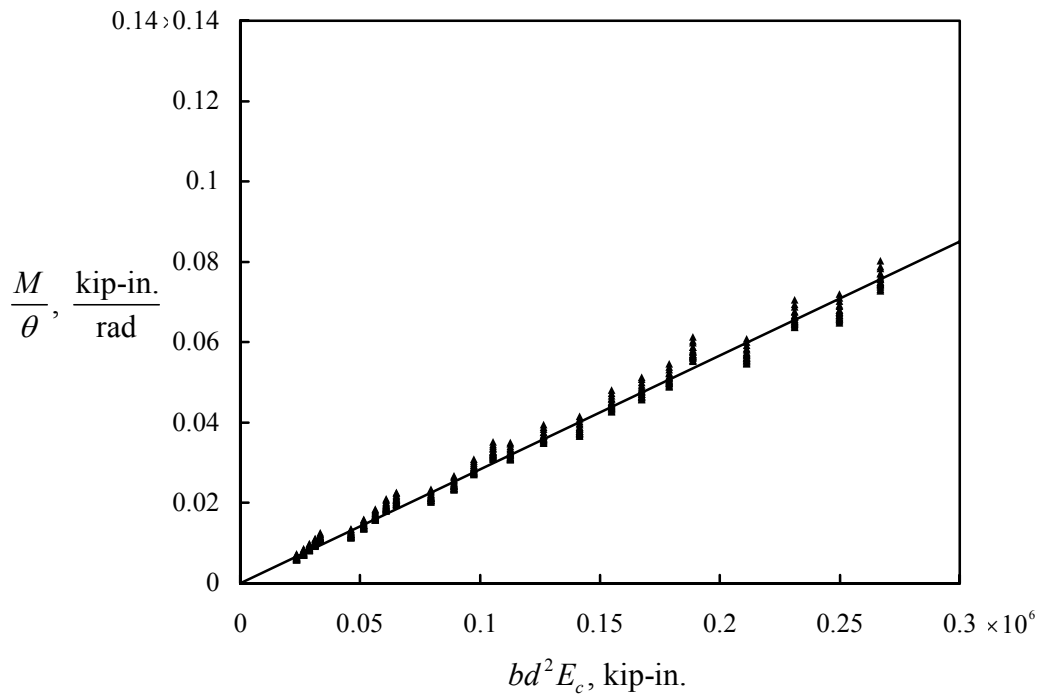
for rack braced against sidesway is

$$\frac{I_f}{L_f} = \frac{7}{1000}bd^2 \quad (2.15)$$

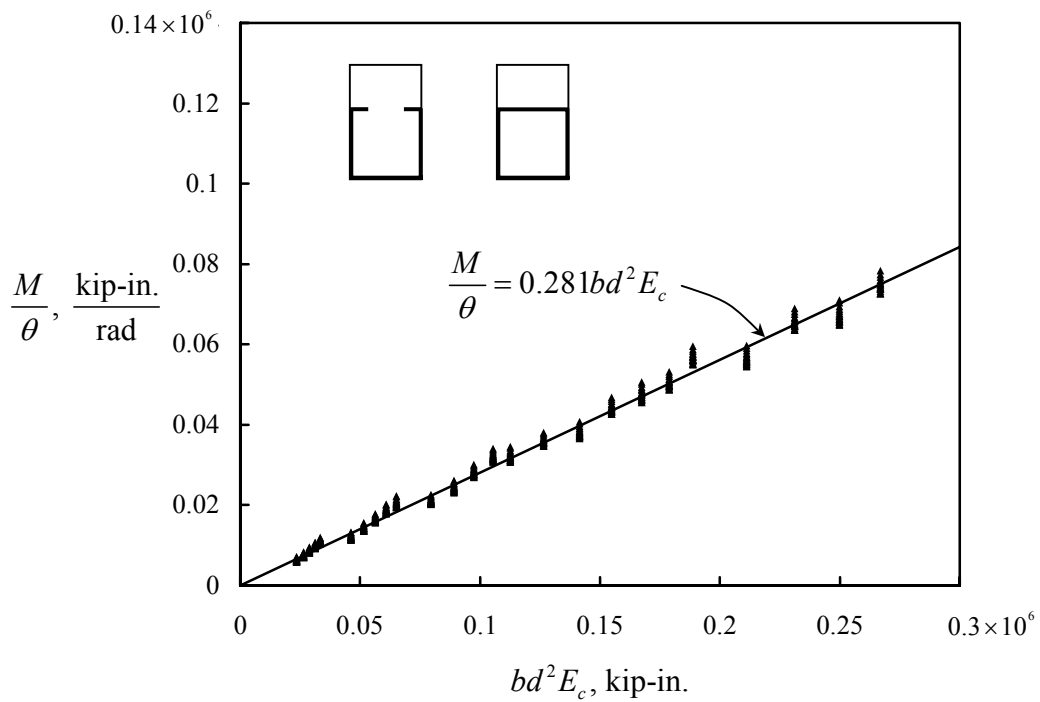
The base fixity equations presented here are suggested only for the initial stiffness of the connection, namely, only the first stage of the behavior as defined by

**Table 2.1** Column and Base Plate Dimensions in Study

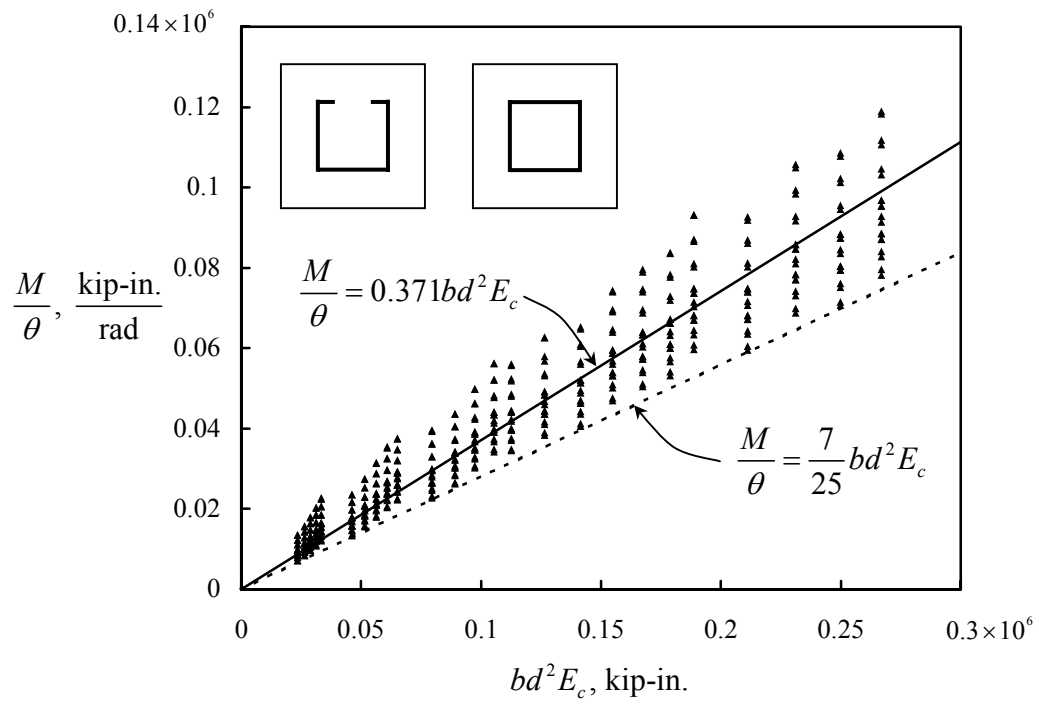
Column Types	
 <p>C-Section</p>	 <p>Closed Tube</p>
Column Dimensions	
$bd = 4 \text{ in.}^2$	$bd = 6.25 \text{ in.}^2$
$bd = 9 \text{ in.}^2$	$bd = 12.25 \text{ in.}^2$
$bd = 16 \text{ in.}^2$	$bd = 16 \text{ in.}^2$
$d/b = 1$	$d/b = 2$
$d/b = 1.25$	
$d/b = 1.5$	
$d/b = 1.75$	
$d/b = 2$	
	
Column and Base Plate Thicknesses	
 <p>T1 <math>t_w = 0.05 \text{ in.}</math> <math>t_p = 0.05 \text{ in.}</math></p>	 <p>T2 <math>t_w = 0.05 \text{ in.}</math> <math>t_p = 0.075 \text{ in.}</math></p>
 <p>T3 <math>t_w = 0.05 \text{ in.}</math> <math>t_p = 0.1 \text{ in.}</math></p>	 <p>T4 <math>t_w = 0.05 \text{ in.}</math> <math>t_p = 0.125 \text{ in.}</math></p>
 <p>T5 <math>t_w = 0.05 \text{ in.}</math> <math>t_p = 0.15 \text{ in.}</math></p>	
 <p>T6 <math>t_w = 0.1 \text{ in.}</math> <math>t_p = 0.1 \text{ in.}</math></p>	 <p>T7 <math>t_w = 0.1 \text{ in.}</math> <math>t_p = 0.15 \text{ in.}</math></p>
 <p>T8 <math>t_w = 0.1 \text{ in.}</math> <math>t_p = 0.2 \text{ in.}</math></p>	 <p>T9 <math>t_w = 0.1 \text{ in.}</math> <math>t_p = 0.25 \text{ in.}</math></p>
 <p>T10 <math>t_w = 0.1 \text{ in.}</math> <math>t_p = 0.3 \text{ in.}</math></p>	



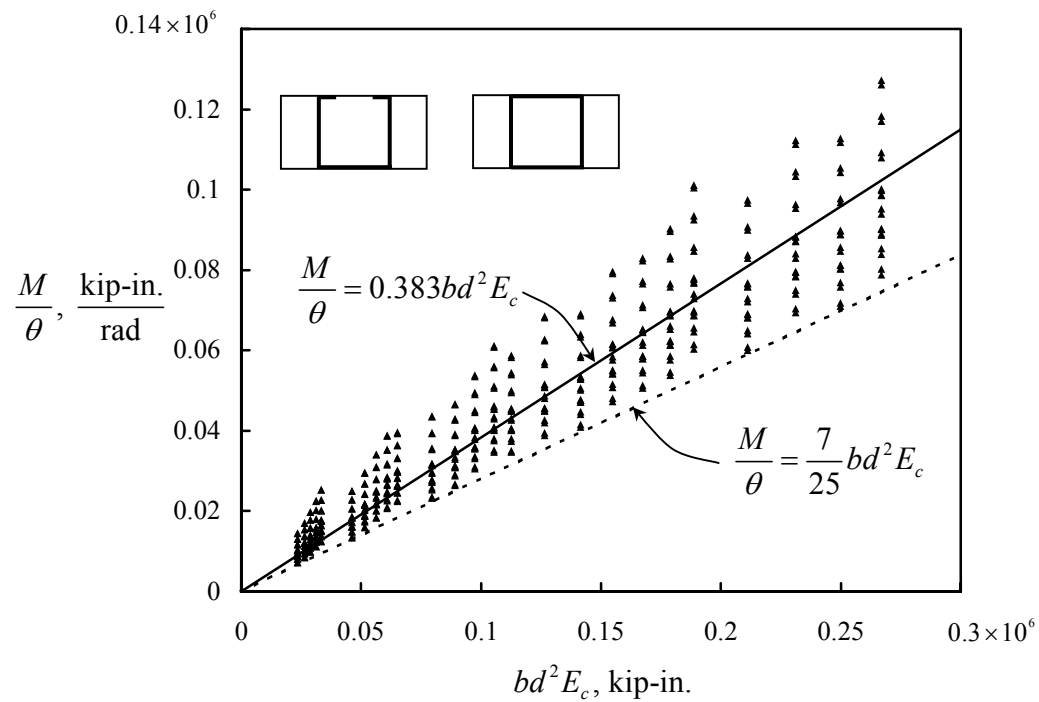
**Figure 2.15** Base fixity results for base plate type A



**Figure 2.16** Base fixity results for base plate type B



**Figure 2.17** Base fixity results for base plate type C



**Figure 2.18** Base fixity results for base plate type D

Salmon, Schenker and Johnston (1955) where the base plate is still in full contact with the concrete surface, having trapezoidal compression stress distribution. By considering the axial force  $P$  and bending moment  $M$ , to prevent tension stresses from occurring on the concrete surface, an upper bound limit of the equations can be found as

$$\frac{M}{P} \leq \frac{S}{A} \quad (2.16)$$

This upper bound limit when used for columns with thick base plates as shown in Fig 2.19a, the contact stress area  $A$ , would be equal to  $bd$ , and  $S$  the elastic section modulus of the rectangular area about the axis of bending would equal to  $bd^2/6$ , therefore Eq. (2.16) becomes

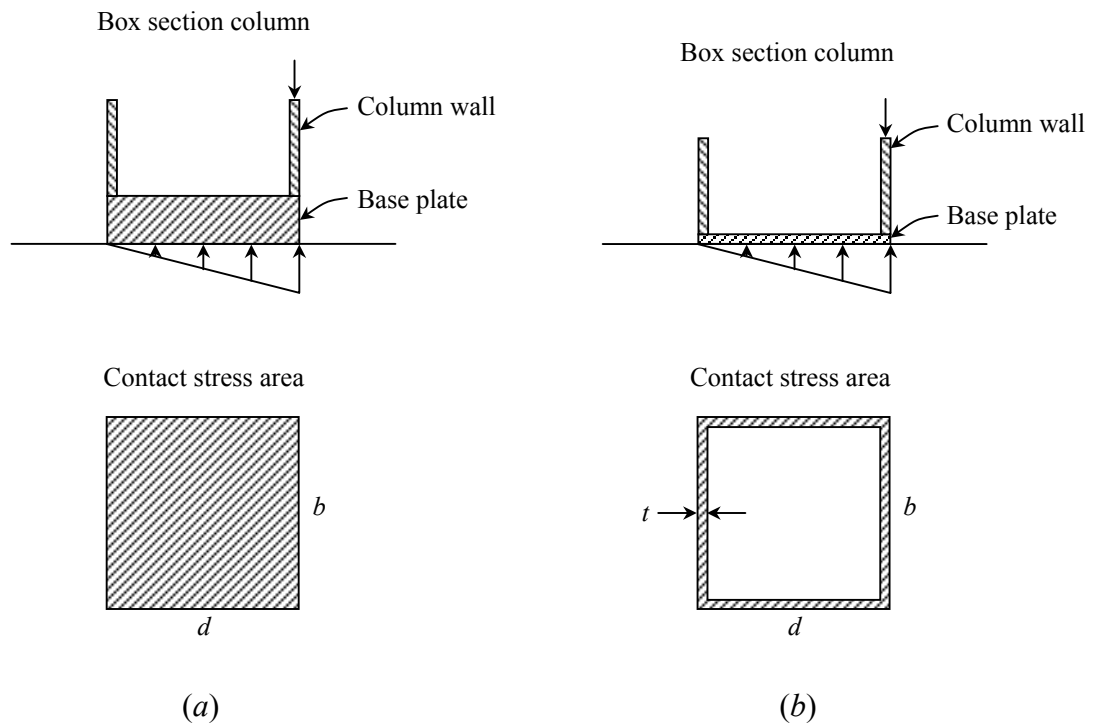
$$\frac{M}{P} \leq \frac{d}{6} \quad (2.17)$$

However, when used for design columns with thin base plates as shown in Fig 2.19b,  $A$  would instead equal to  $2t(d+b)$ , where  $t$  is the thickness of the contact area, and  $S$  would be equal to  $td(d/3+b)$ , therefore in this case Eq. (2.16) becomes

$$\frac{M}{P} \leq \frac{d(d+3b)}{6(d+b)} \quad (2.18)$$

For practical purposes it is recommended that a single upper bound limit, Eq. (2.17), should be used for all types of base plate because it is always more conservative than using Eq. (2.18).

Once the upper bound limitation has been reached, the stiffness of the connection is expected to decrease. The RMI specification does not explicitly give an upper bound limit for its base fixity equation but expects that the limit will not be reached for gravity load design.



**Figure 2.19** (a) Thick base plate (b) Thin base plate

### 2.2.3 Base Fixity Charts

The proposed base fixity equation provides a rough estimate of the connection stiffness approximated from a wide range of column base configurations. To obtain a more accurate value for a particular column base, charts given in Appendix B should be used. The charts were developed by using the data points given in Figs. 2.15 through 2.18, then rearranged and curved to fit them such that the data could be read directly from these charts. The charts are given for all base plate types with box column sections. Two column wall thicknesses were provided,  $t_w = 0.05$  in. and  $t_w = 0.10$  in. with the column dimension ranging from a square section to a 2 by 1 rectangular section. In all cases there are a group of five solid lines where the top line refers to base plate thickness of  $t_p = 3t_w$ , the second line  $t_p = 2.5t_w$ , the third line  $t_p = 2t_w$ , the fourth line  $t_p = 1.5t_w$ , and the bottom line  $t_p = t_w$ .

The base fixity values given here assume the column and base plate material to be  $E_s = 29500$  ksi and  $\nu = 0.3$  while for the concrete floor  $E_c = 2950$  ksi and  $\nu = 0.2$ . For other concrete material properties, assuming that Eq. (2.9) and Eq. (2.10) still hold, the base fixity can be found by modifying the obtained chart value as follows:

$$\frac{M}{\theta} = \frac{G}{G_{chart}} \left( \frac{M}{\theta} \right)_{chart} \quad (2.19)$$

where  $G_{chart}$  is equal to 1229 ksi, and  $G$  is the shear modulus of elasticity of the concrete material of interest.

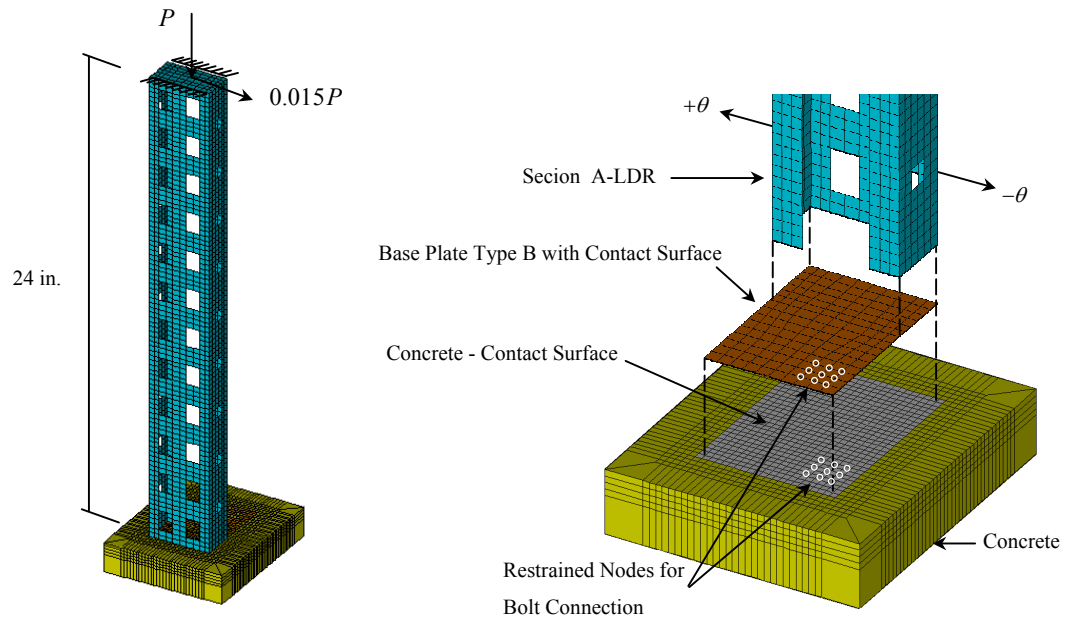
### 2.3 FINITE ELEMENT ANALYSIS VERIFICATION

Non-linear finite element analyses of the column to floor connection were performed using ABAQUS in order to verify the proposed base fixity equation. The geometry and boundary condition of the finite element model were made to best simulate the A-LDR column with base plate type B connection (columns 3CS1.625x90). The finite element model of the column base is shown in Fig. 2.20.

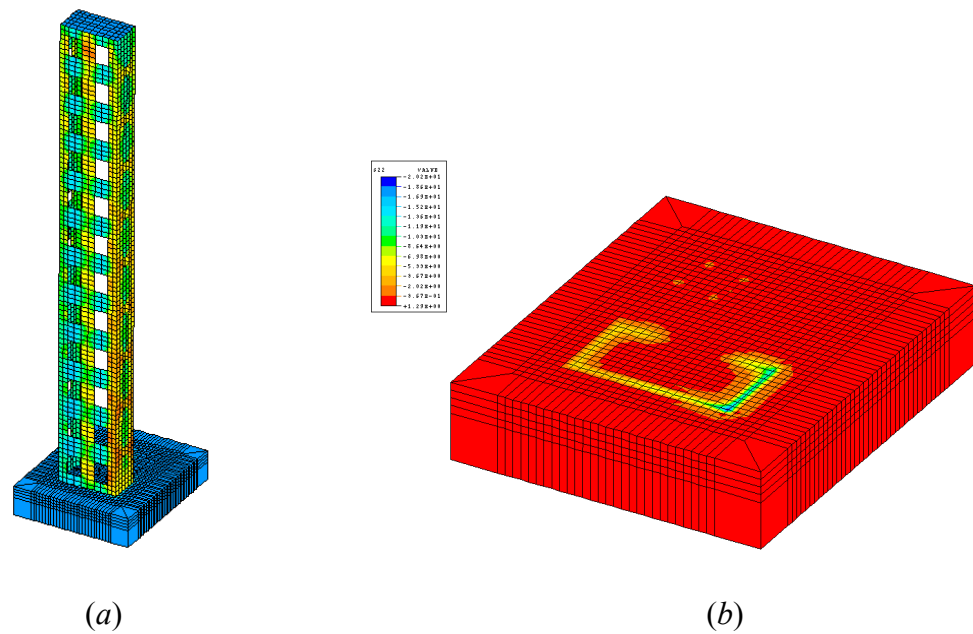
Finite element assumptions are as follows: The vertical and lateral loads transferred from the frame to the isolated column were modeled by nodal forces applied at the centroid of the column on the top plate as shown in Fig. 2.20. The ratio of the lateral load with respect to the vertical load is maintained at 0.015 throughout the analysis. The top plate has been thickened to avoid large deformation and localized failure due to the concentrated loads, and lateral bracing is also provided at the top plate to prevent the column from twisting. In addition, because only one anchorage bolt on the left was chosen for this model, it was expected that the placement of the bolts would affect the behavior of the column. Therefore, both directions of the lateral load were considered. Positive and negative signs of the direction are given in Fig. 2.20. An idealization of the boundary conditions of the anchorage bolts connection was made by the matching displacements of the base plate nodes and the concrete nodes.

The four node general purpose shell element was used to model the column and base plate while an eight node brick element was used to model the concrete floor. Contact surfaces were defined between the base plate and the concrete to simulate their interaction. No friction was considered between the two surfaces. In addition, since the floor was assumed to be a half-space, eight node infinite elements were used to model the far-field region. The material model used for the column and base plate was elastic-plastic with strain hardening  $F_y = 45$  ksi,  $F_u = 59$  ksi,  $E = 29500$  ksi,

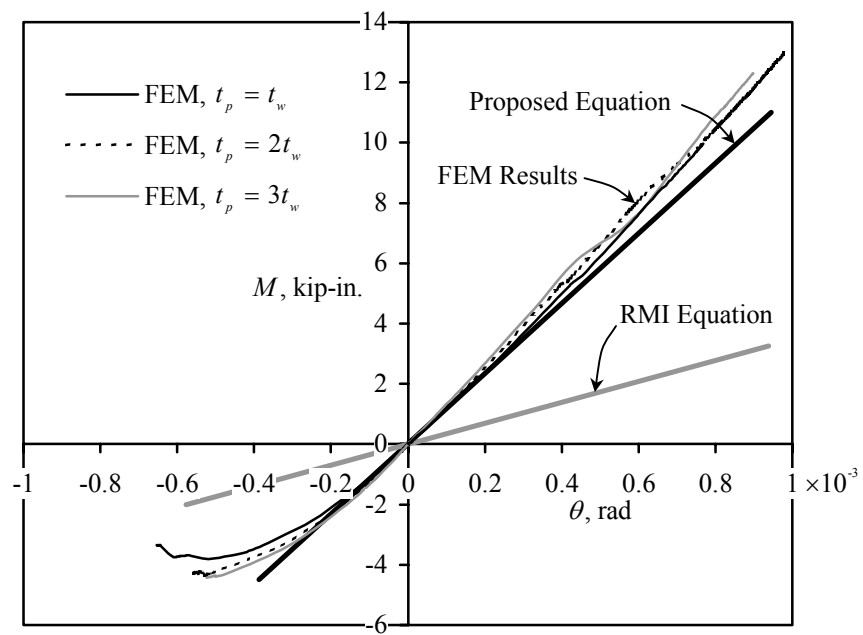




**Figure 2.20** Column base finite element model



**Figure 2.21** Column base finite element analysis results (a) von Mises Stress (b) Normal stress,  $\sigma_{22}$  on the concrete surface



**Figure 2.22** Column base finite element analysis verification

$E_{st} = E/45$ ,  $\nu = 0.3$ , and  $e_{st}$  was 15 times the maximum elastic strain, while the concrete was assumed elastic with  $E_c = 2950$  ksi and  $\nu = 0.2$ . Using these finite element modeling assumptions a parametric study was carried out by varying  $t_p/t_w$  from 1 to 3. Deformation and stress distribution resulted from the finite element analysis for the case of loading in the positive direction is as shown in Fig. 2.21. The rotation of the base plate was obtained and plotted against the applied moment to compare with the RMI and the proposed base fixity equation as shown in Fig. 2.22. As can be seen in this figure the proposed equation agrees better with the finite element results than the RMI equation does.

## 2.4 CONCLUSIONS

It was shown in this chapter that the current RMI base fixity equation underestimates the stiffness. Several analytical models of the column base were studied. The base fixity was found by solving a normal load on the boundary of the half-space problem. With this approach a parametric study was carried out for a wide range of base configurations to develop a new base fixity equation. Unless actual tests are conducted to obtain the base fixity, the proposed base fixity equation, Eq. (2.12), along with the upper bound limits, Eq. (2.17), of the base fixity behavior should be used. Finite element studies were used to verify the proposed equation. The proposed equation agrees well with the finite element solution. Some errors do occur from the assumptions in the approach, such as neglecting the flexibility of the base plate and using an approximate load block for the load distribution on the concrete surface.

---

---

# Chapter 3

## Beam to Column Connections

---

---

### 3.1 INTRODUCTION

In storage racks, beam end connectors are used to make beam to column connections. The semi-rigid nature of this connection is primarily due to the distortion of the column walls, tearing of the column perforation, and distortion of the beam end connector. The storage rack stability depends significantly on the behavior of this connection, thus it is important to have the means for predicting it. Designs of these connections vary widely; making it is impossible to develop a general analytic model. Instead, beam to column connection tests are usually done to determine the relationship of the moment at the joint  $M$  and the change in angle between the column and the connecting beam  $\theta$ .

### 3.2 BEAM TO COLUMN CONNECTION TESTS

The RMI specification recommends the use of a cantilever test or a portal test. Schematics of these test setups are shown in Figs. 3.1 and 3.2. The result from the cantilever test is normally used to design beams and connections; while the result from the portal test is used as connection stiffness in sidesway analyses. The following is a review of these tests. In the cantilever test the constant connection stiffness  $F$  relating the moment to the rotation as

$$F = \frac{M}{\theta} \quad (3.1)$$

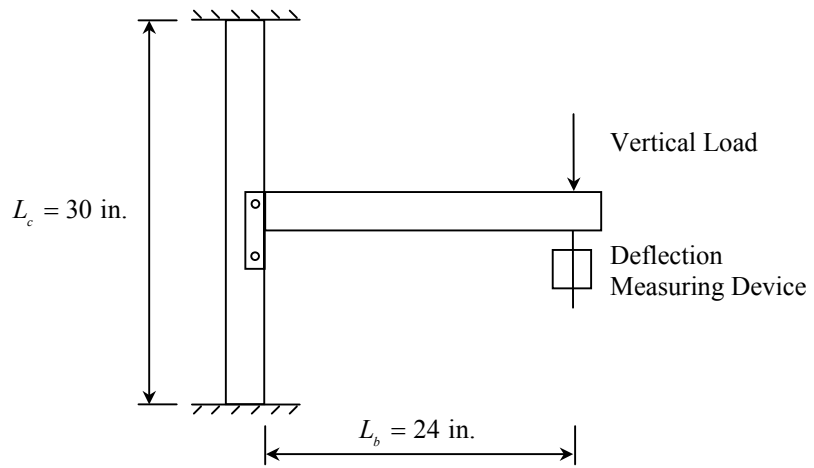
is determined by using the known applied vertical load  $P$  and deflection of the free end of the cantilever  $\delta$  in the following expression

$$\delta = PL_b^2 \left( \frac{L_c}{16EI_c} + \frac{L_b}{3EI_b} + \frac{1}{F} \right) \quad (3.2)$$

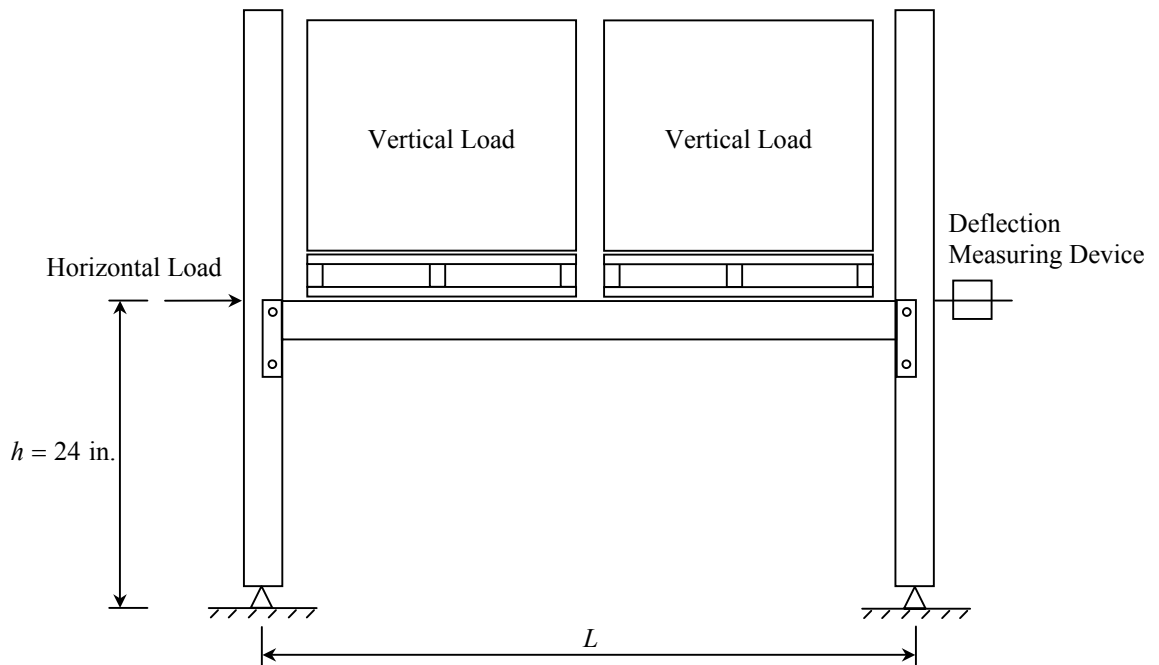
where  $E$  is the modulus of elasticity,  $L_b$  and  $L_c$  are the length of the beam and column segment,  $I_b$  and  $I_c$  are the moments of inertia of the beam and column segment, respectively. Solving Eq. (3.2) for  $F$ , the following is obtained:

$$F = \frac{1}{\frac{\delta}{PL_b^2} - \frac{L_c}{16EI_c} - \frac{L_b}{3EI_b}} \quad (3.3)$$

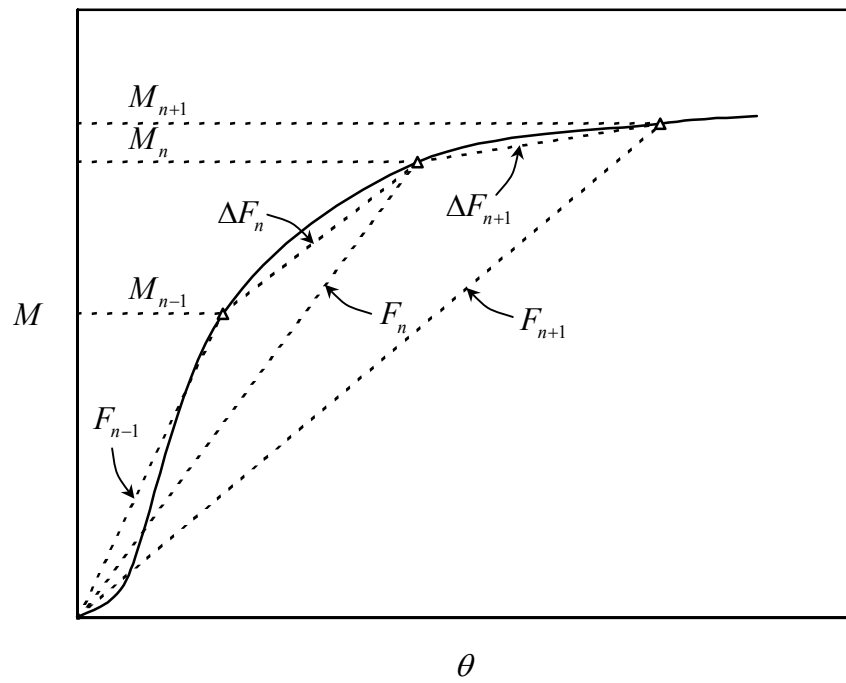
With  $M = PL_b$  and  $F$  known,  $\theta$  can then be determined from Eq. (3.1) for each load step. Plots such as Fig. 3.3 giving the moment and rotation relationship may then be developed. Instantaneous stiffness  $\Delta F$  can be found by connecting the resulting data points or by substituting  $\Delta P$  for  $P$ , and  $\Delta\delta$  for  $\delta$  into Eq. (3.3) where  $\Delta P$  is the load increment, and  $\Delta\delta$  is the deflection increment due to  $\Delta P$ . The RMI specification recommends that the connection stiffness to be used in linear analyses can be given as



**Figure 3.1** Cantilever test



**Figure 3.2** Portal test



**Figure 3.3** Beam to column connection stiffness

the  $F$  determined from Eq. (3.3) with  $P$  equal to 0.85 times the ultimate load and  $\delta$  equal to the deflection at that load.

In the portal test, a certain amount of vertical load is applied before the connection stiffness is determined. By applying an additional horizontal load and measuring the corresponding lateral deflection,  $F$  can be computed from the following expression:

$$\delta = \frac{Hh^2}{2} \left( \frac{h}{3EI_c} + \frac{L}{6EI_b} + \frac{1}{F} \right) \quad (3.4)$$

where  $H$  is the horizontal load per beam. Two beams are required in this test assembly; therefore, a horizontal load of  $2H$  is applied in the test,  $\delta$  is the lateral deflection corresponding to a horizontal load of  $2H$ ,  $h$  is the distance from the floor to top of the beam, and  $L$  is the distance between the centroid of the two columns parallel with the shelf beam. Solving Eq. (3.4) for  $F$ , the following is obtained:

$$F = \frac{1}{\frac{2\delta}{Hh^2} - \frac{h}{3EI_c} - \frac{L}{6EI_b}} \quad (3.5)$$

The RMI specification recommends that  $F$  determined from Eq. (3.5) be used as the connection stiffness in sidesways analyses. Tests for  $F$  with vertical loads at both the design load and the ultimate load levels should be conducted since the behavior at both of these loads are of interest.

If the vertical load is applied such that it is equally distributed over the entire bay then the vertical force on each shelf beam can be assumed to be a uniform distribution load  $w$ , (force per length). The pre-existing moments in the joints due to this load, before the horizontal load is applied can be determined as follows:



$$M = \frac{wL^3}{24EI_b \left( \frac{h}{3EI_c} + \frac{L}{2EI_b} + \frac{1}{F} \right)} \quad (3.6)$$

As the horizontal load is applied to the right as in Fig. 3.2, the left joint will loosen and the right joint will tighten up, meaning the pre-existing moment in the joints from Eq. (3.6) will decrease by  $Hh/2$  in the left joint and increase by  $Hh/2$  in the right joint. This, however, assumes that both joints have the same stiffness, but generally this may not be the case, for example if the pre-existing moment in the joints is equal to  $M_n$  as shown in Fig. 3.3. As the horizontal load is applied, the stiffness of the left and right joints will instead be approximately  $\Delta F_n$  and  $\Delta F_{n+1}$ , respectively. The lateral displacement in this case can be found as:

$$\delta = \frac{Hh^2}{2} \left[ \frac{\left( \frac{h}{3EI_c} + \frac{L}{2EI_b} + \frac{1}{\Delta F_n} \right) \left( \frac{h}{3EI_c} + \frac{L}{2EI_b} + \frac{1}{\Delta F_{n+1}} \right)}{\left( \frac{h}{3EI_c} + \frac{L}{2EI_b} + \frac{\Delta F_n + \Delta F_{n+1}}{2\Delta F_n \Delta F_{n+1}} \right)} - \frac{L}{3EI_b} \right] \quad (3.7)$$

By equating Eq. (3.4) and Eq. (3.7) it can be found that the constant connection stiffness determined from Eq. (3.5) is actually a combination of these different joint stiffnesses  $\Delta F_n$  and  $\Delta F_{n+1}$  as follows:

$$F = \frac{\Delta F_n + \Delta F_{n+1} + 2\Delta F_n \Delta F_{n+1} \left( \frac{h}{3EI_c} + \frac{L}{2EI_b} \right)}{2 + (\Delta F_n + \Delta F_{n+1}) \left( \frac{h}{3EI_c} + \frac{L}{2EI_b} \right)} \quad (3.8)$$

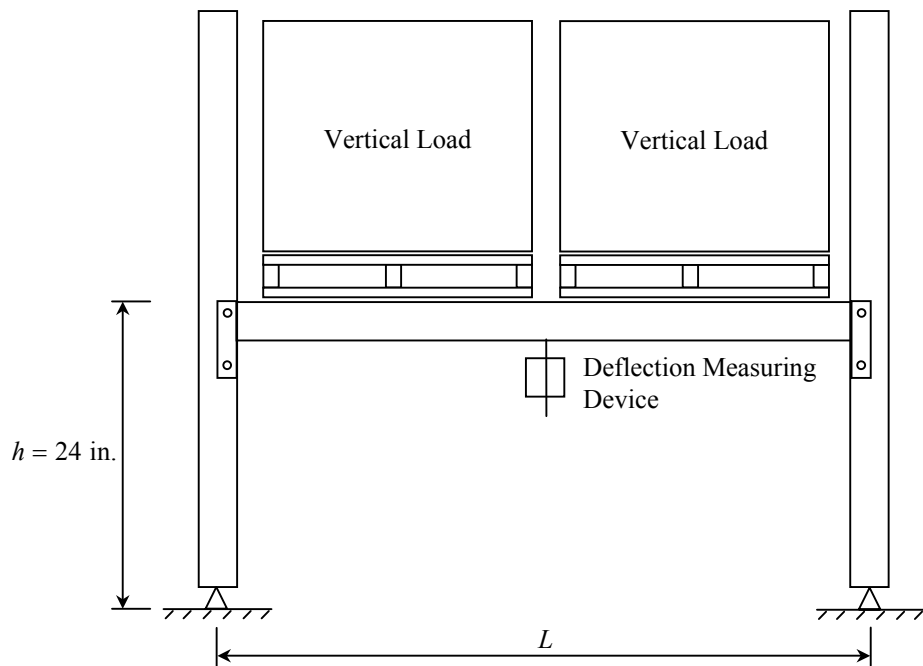
The connection stiffness of the individual joints is not obtained from the portal test but is instead an approximate average value of the connection stiffness as the tightening up and the loosening process is obtained. The loosening process may not be as simple as assumed in the above example where the unloading stiffness is same as the loading stiffness  $\Delta F_n$ . If the connections were loaded beyond the elastic range, permanent

deformation would occur in the joint, resulting in different moment and rotation relationships in the loading and unloading process.

### 3.3 PROPOSED PORTAL TEST

An alternative beam to column test presented here is to be used instead of the cantilever test. In the cantilever test the shear to moment ratio of the actual frames may not be well represented. For some connections the behavior may depend significantly on this ratio. Namely, if the cantilever test is conducted for different  $L_b$  values, the moment and rotation relationships obtained from each of these tests will be different. To solve this problem, a proposed connection test where the entire bay is assembled the same as in the portal test is to be used. This proposed procedure shown in Fig. 3.4 will be referred to in this study as the proposed portal test. This test is similar to the previous portal test but instead of applying the horizontal loads, vertical loads are applied incrementally and the corresponding mid-span beam deflection  $\delta$  is measured. The vertical load applied must be equally distributed over the entire bay so that the vertical force on each shelf beam can be assumed to be a uniformly distribution load  $w$ . The developing moment in each joint will be the same in this test and the expression for the maximum beam deflection at mid-span can be found as follows:

$$\delta = \frac{wL^4}{384EI_b} \left[ 5 - \frac{4}{1 + \frac{2EI_b}{L} \left( \frac{h}{3EI_c} + \frac{1}{F} \right)} \right] + \frac{wLh}{2AE} \quad (3.9)$$



**Figure 3.4** Proposed portal test

Solving Eq. (3.9) for  $F$ , the following is obtained:

$$F = \frac{1}{\frac{L}{2EI_b} \left( \frac{4wL^4}{5wL^4 - 384EI_b \left( \delta - \frac{wLh}{2AE} \right) - 1} \right) - \frac{h}{3EI_c}} \quad (3.10)$$

with  $M$  the same as given in Eq. (3.6) and  $F$  known,  $\theta$  can then be determined from Eq. (3.1) for each vertical load step. Plots such as in Fig. 3.3 giving the moment and rotation relationship may then be developed. The load carrying capacity of the entire bay may also be determined from this test whether failure is due to the connection or the shelf beam. However, if the load carrying capacity is not of interest, the proposed portal test could be conducted prior to the portal test. The mid-span deflection  $\delta$  could be measured in the vertical loading process. The connection stiffness from the proposed portal test can then be used in designing beams while the connection stiffness from the portal test can be used in sidesway analyses.

### 3.4 FINITE ELEMENT SIMULATION OF THE CANTILEVER TEST

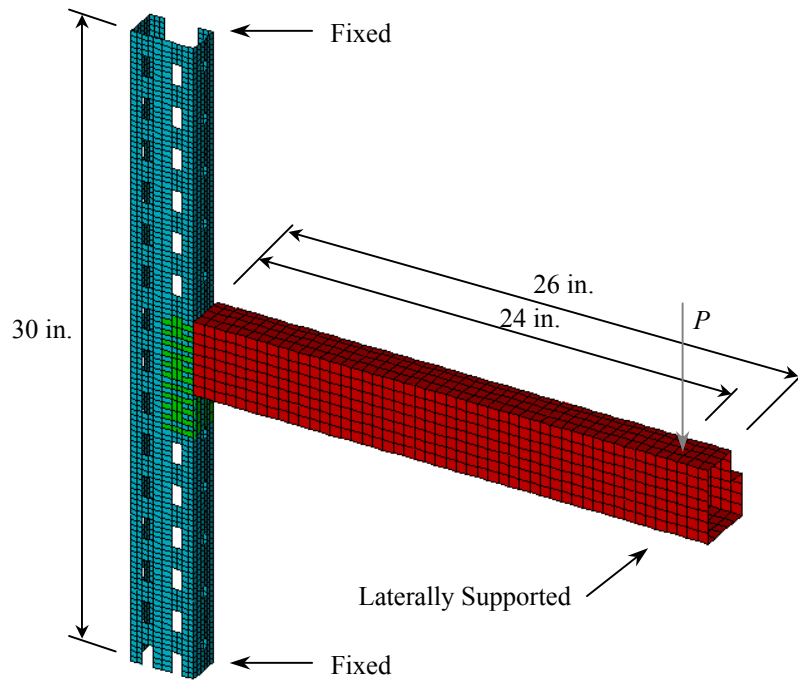
A cantilever test of a light duty rack connection was conducted by Peköz (1975). The vertical load was applied by a jack until failure took place at the connection. Results showed that the failure took place with tearing of the column perforation by the upper hex stud. The load-deflection relationship and the determination of the moment-rotation relationship from the test results are summarized in Table 3.1. A finite element simulation of this test is presented in this study. The objective is to develop a finite element model that best represents the behavior of the connection so that the modeling assumptions can later be implemented into the beam to column connections in the frame analysis study in Chapter 5.

In order to study the behavior of the connection, nonlinear finite element analyses were performed using ABAQUS. The geometry, boundary and loading conditions of the finite element model were made to best simulate the cantilever test as shown in Fig. 3.5. A 30 in. length column was fixed in all degrees of freedom at both ends to represent the ends of the column that were welded to immovable supports. A 26 in. beam with an end plate was connected at mid height of the column. Contact surfaces were defined between the end plate and the column to simulate their interaction as shown in Fig. 3.6. The lower hex stud was modeled by the use of multipoint constraints to provide a pinned joint between the node on the end plate and the column, while the upper hex stud was modeled by the use of multipoint constraints and non-linear axial springs as shown in Fig. 3.7. The non-linear axial spring was used to capture the initial looseness behavior of the joint. The stiffness of the spring was calibrated to best match initial looseness behavior of the test result.

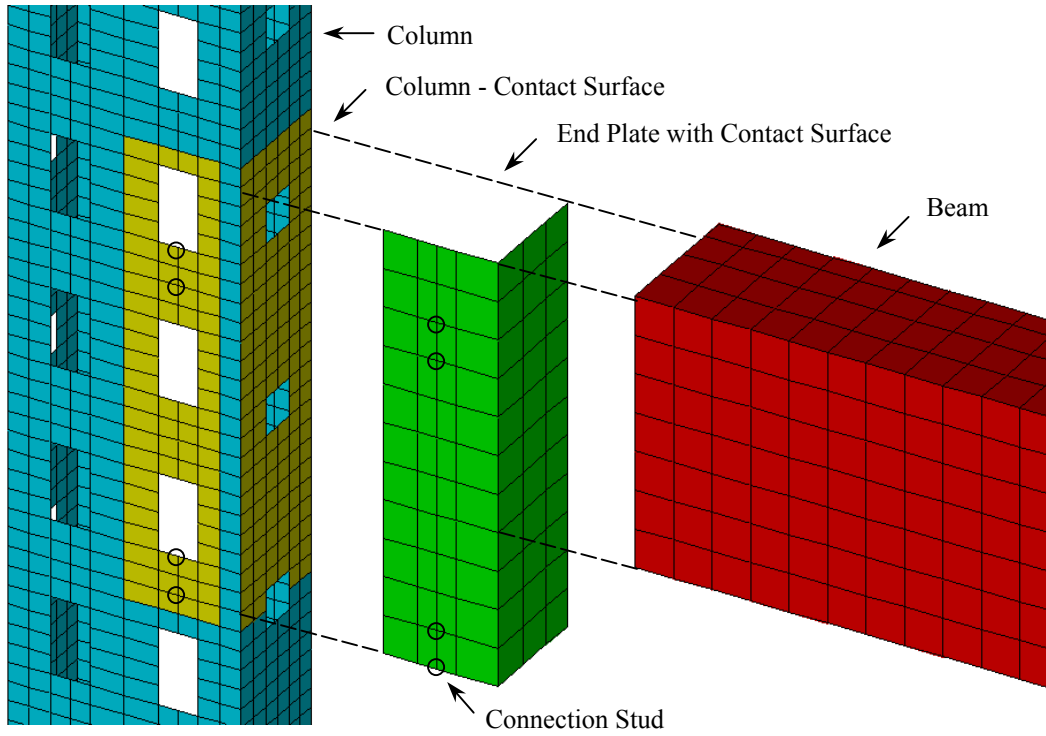
The concentrated load was applied 24 in. from the connection to simulate the jack load. The material model used was elastic-plastic with strain hardening  $F_y = 45$  ksi,  $F_u = 59$  ksi,  $E = 29500$  ksi,  $E_{st} = E/45$ ,  $\nu = 0.3$ , and  $e_{st}$  was 15 times the maximum elastic strain. Failure mode at ultimate load is shown in Fig. 3.8. The connection rotation was determined by monitoring node  $P_3$  and  $P_4$  as shown in Fig. 3.9 to find the angle of rotation of the beam and node  $P_1$  and  $P_2$  to find the movement of the column to correct the connection rotation. A moment-rotation curve resulting from the finite element simulation and the physical test are compared in Fig. 3.10. The beam to column stiffness obtained from 85% of the joint moment capacity as suggested by the RMI specification used in linear frame analyses was also plotted for comparison.

**Table 3.1** Beam to Column Connection Test Results

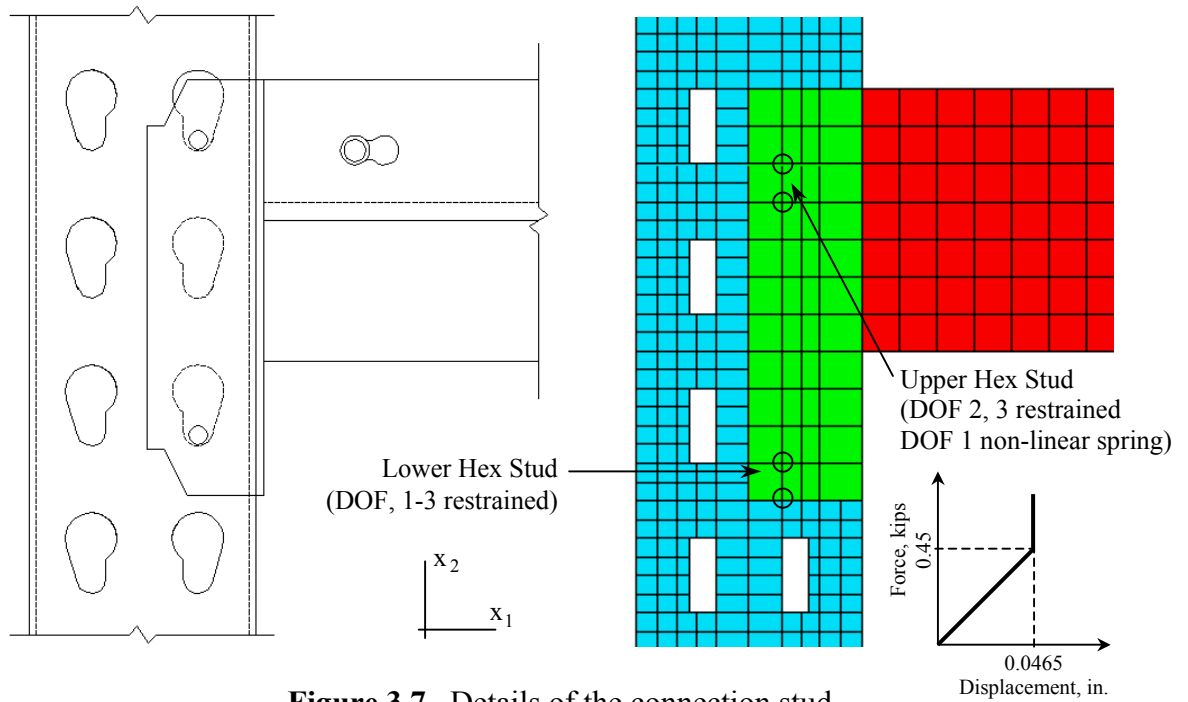
$P$ , kips	$\delta$ , in.	$F$ , kip-in./rad	$M$ , kip-in.	$\theta$ , rad
0.10	0.266	227	2.4	0.0106
0.20	0.406	302	4.8	0.0159
0.30	0.498	374	7.2	0.0192
0.40	0.641	389	9.6	0.0247
0.45	0.71	395	10.8	0.0273
0.50	0.794	393	12.0	0.0306
0.55	0.941	362	13.2	0.0364
0.60	1.063	349	14.4	0.0413
0.65	1.247	320	15.6	0.0487
0.70	1.585	269	16.8	0.0625
0.75	2.033	222	18.0	0.0809
0.80	2.646	181	19.2	0.1062



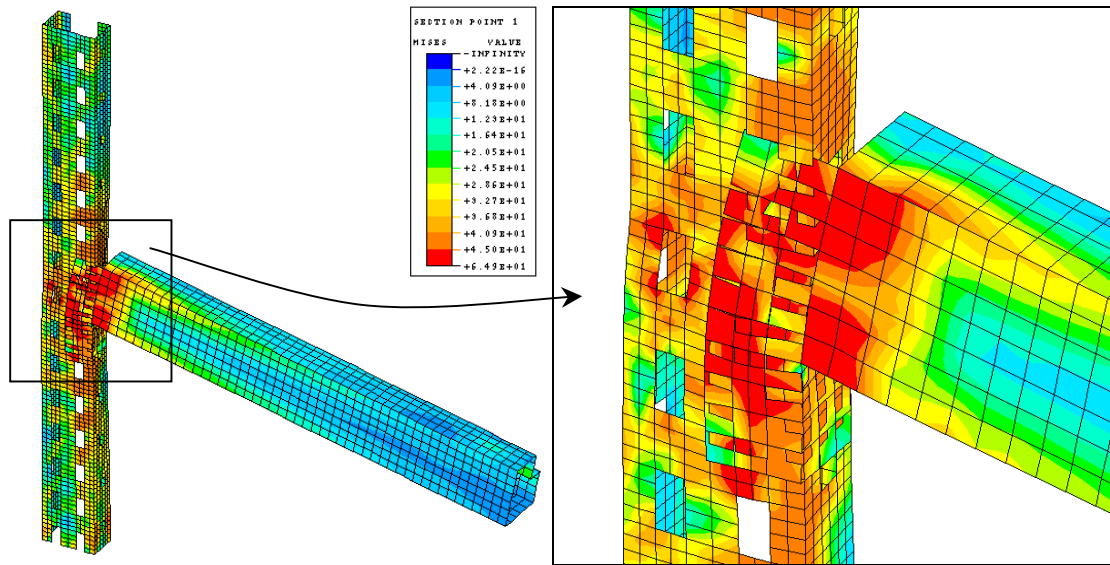
**Figure 3.5** Finite element model of the cantilever test



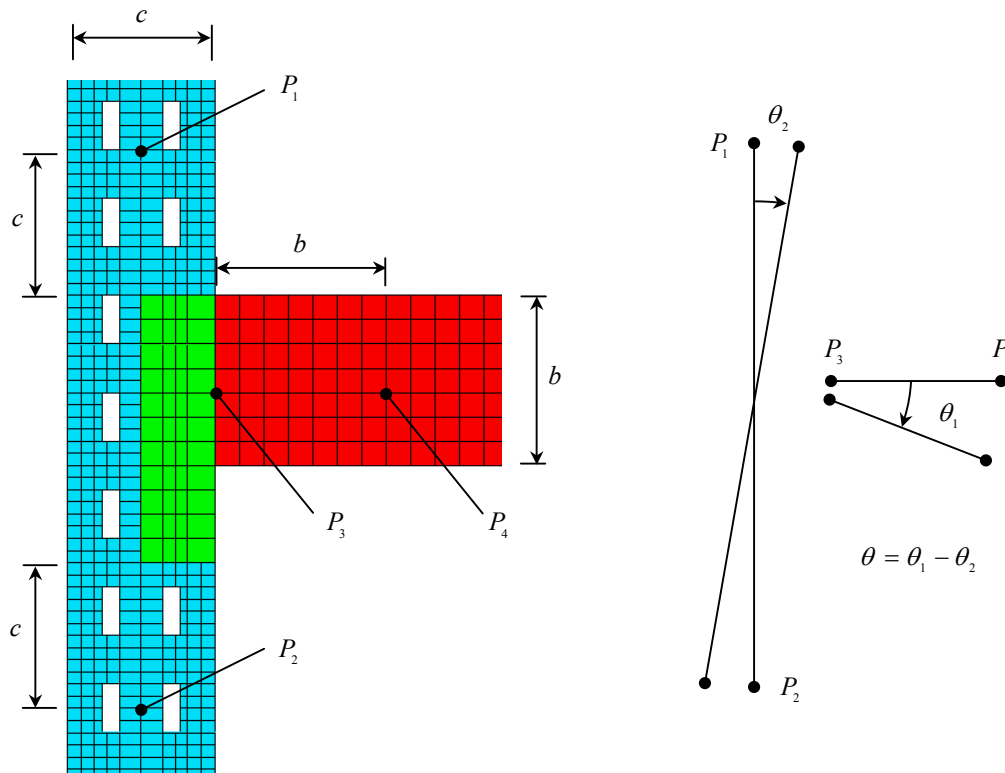
**Figure 3.6** Details of the joint connection surface-based contact



**Figure 3.7** Details of the connection stud

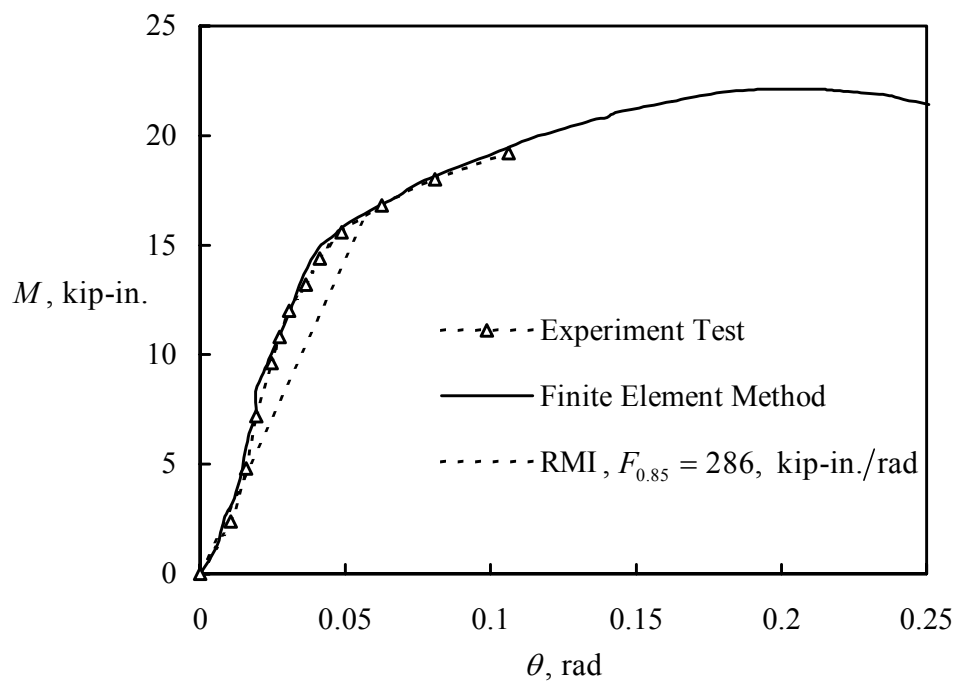


**Figure 3.8** Finite element simulation of the cantilever test: von Mises Stress at ultimate load



**Figure 3.9** Four nodes monitored to determine the rotation





**Figure 3.10** Comparison of the cantilever test and the finite element simulation

### 3.5 CONCLUSIONS

A new beam to column connection test to be used instead of the cantilever test has been presented in this study. The shear to moment ratio in an actual frame is better represented by this proposed portal test than the cantilever test. For some designs, the connection behavior may depend significantly on this ratio. Therefore it is recommended that in addition to current beam to column connection tests, this proposed portal test should be included as a possible means of determining the moment to rotation relationship of the connection.

The beam to column connection stiffness obtained from the finite element cantilever test simulation agrees well with the test results. However, the finite element model was not able to capture the failure mode which was observed in the test. In the test the failure took place with tearing of the column perforation by the upper hex stud. Thus the connection ultimate moment capacity obtained from the finite element model was higher than obtained from the test. Improvement in the finite element result can be made with better modeling details of the connection stud and considering fracture mechanics.

---

---

# Chapter 4

## Members

---

---

### 4.1 INTRODUCTION

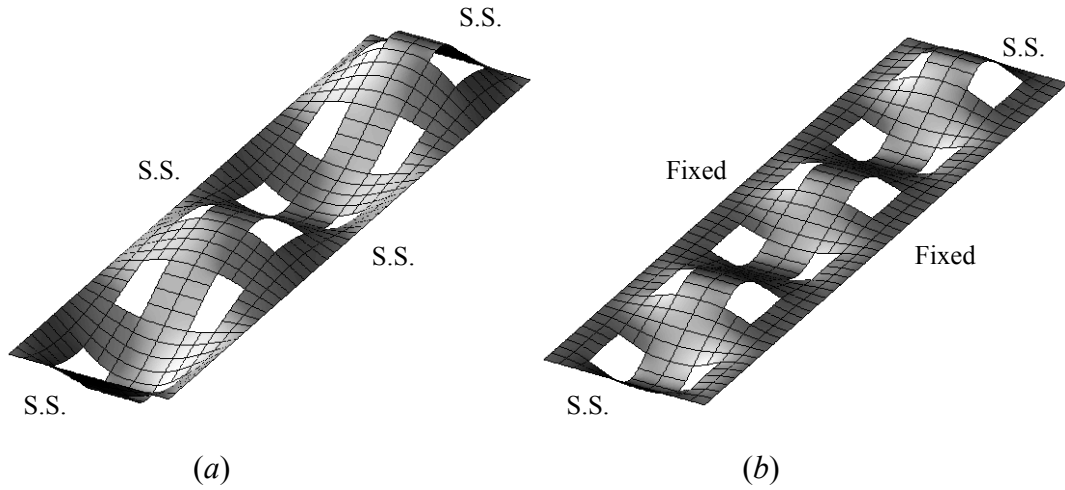
The current RMI design provision for cold-formed steel members is similar to the AISI specification. Both specifications consist of the following general steps. First, the overall stability of the member is considered. Once the overall buckling stress is known, then the design equations are used to determine the nominal failure stress, whether the member will fail from elastic buckling, inelastic buckling, or yielding. With the nominal failure stress known, the corresponding effective section properties can then be computed. Effective section properties are used to account for the local buckling of thin-walled sections. The nominal member strength is determined based on the governing nominal failure stress and the effective section properties. Finally, the design member strength is obtained by multiplying the nominal member strength by a resistance factor in the case of LRFD or dividing it by a safety factor in the case of ASD. However, special considerations must be given to members subject to a combined compressive axial load and bending. Additional steps must also be taken to account for various possible modes of failure and the presence of second-

order moments. Based on the general design steps discussed above, studies were carried out in this chapter to verify or modify the current design provisions for member design.

## **4.2 ELASTIC BUCKLING STRENGTH OF PERFORATED MEMBERS**

The column sections in storage racks are perforated for the purpose of easy assembly of the beam end connector. It is well known that the presence of such perforation reduces the local buckling strength of the individual component element and the overall buckling strength of the section. The significance of this reduction will however depend on the geometry and material properties of the member and the boundary conditions. The RMI specification currently allows the use of unperforated section properties to predict the overall elastic buckling strength of perforated members, thus assuming that the presence of such perforation does not have significant influence on the reduction of the overall elastic buckling strength. The objective of this study is to check this assumption. Two finite element buckling analyses studies were carried out to investigate how the perforations affect the local and overall buckling strength.

The first study considered a rectangular plate with two rows of perforations as shown in Fig. 4.1. The plate was modeled to represent the web of a Section A-LDR shown in Fig. 4.2*a*. The actual holes in the web are irregular shapes. Here they are simplified by an approximate equivalent rectangular hole. The plate is subject to a uniform compression stress in the longitudinal direction. Two boundary condition cases were considered as shown in Fig. 4.1. The actual boundary condition along the longitudinal edges lies between these two extreme cases because the web to flange junction provides some rotational stiffness. The elastic critical buckling stress was



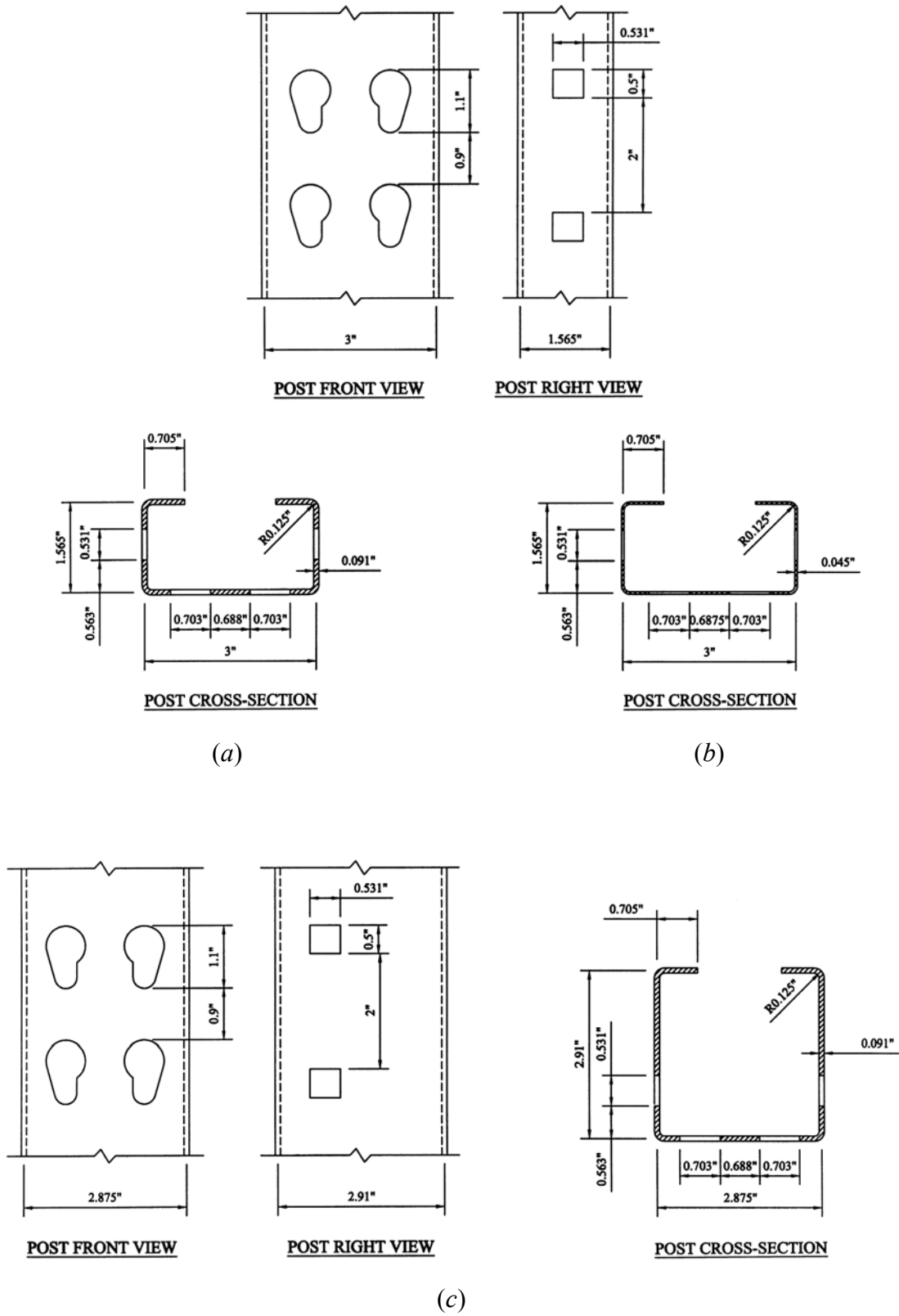
**Figure 4.1** Perforated plate buckling modes (a) Case I (b) Case II

**Table 4.1** Values of Plate Buckling Coefficients

Case	Boundary Condition	Value of $k$	
		Unperforated Plate	Perforated Plate
I		4.0	2.61
II		6.97	4.03

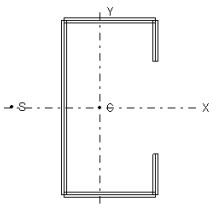
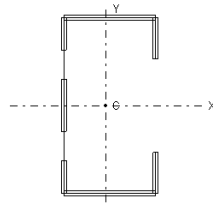
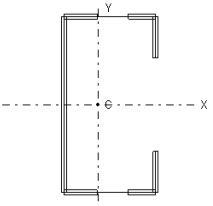
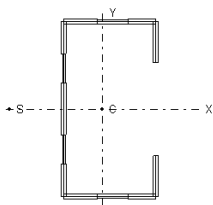
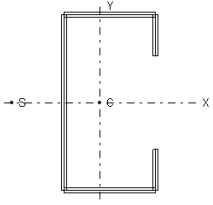
solved by using the computer program CU-PBF shown in Appendix H. The program uses the finite element method with four-node rectangular thin plate elements to solve this eigenvalue problem. With the critical buckling stress known, the plate-buckling coefficient  $k$  was calculated and then compared with the unperforated long plate values given by the AISI specification. Table 4.1 summarizes the results. Results show that the presence of such perforations significantly reduces the  $k$  value in both cases.

The second study was carried out to compare the buckling strengths of perforated and unperforated sections. Three C-sections were considered: A-LDR, A-LDR-2, and A-HDR. Their cross sectional geometry is given in Fig. 4.2 and section properties are summarized in Tables 4.2, 4.3, and 4.4. The cross sectional geometry of Sections A-LDR and A-LDR-2 are similar but their section thicknesses are different. The elements of Section A-LDR are thick making it locally stable, while the elements of Section A-LDR-2 are thin making it locally unstable under uniform compressive yield stress. All three sections were studied as both a concentrically loaded compression member and a flexural member subject to bending about the strong axis. Boundary conditions at the ends of the member for both cases were pinned condition such that the effective length for flexural buckling of both the strong and weak axis and torsion were equal to the length of the member. The critical buckling load was found for different length members. Two approaches were used to solve the buckling problem and then compared: the first approach is using finite element method using the ABAQUS computer program where the four node general purpose shell element was used to model the member, and second approach is using the theoretical overall buckling equations as given in the AISI specification. The theoretical overall buckling equations were solved for arbitrary open thin-walled sections by using the computer program CU-TWP shown in Appendix H. The finite element method is considered to give more accurate results.



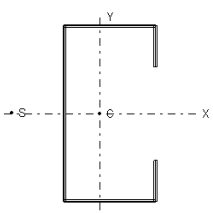
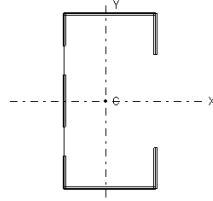
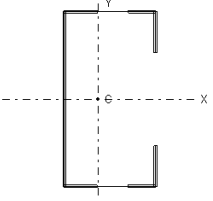
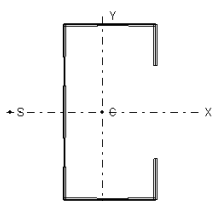
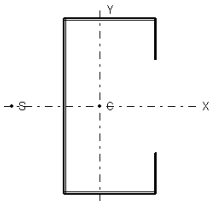
**Figure 4.2** (a) Section A-LDR (b) Section A-LDR-2 (c) Section A-HDR

**Table 4.2 Section A-LDR Dimensions and Properties**

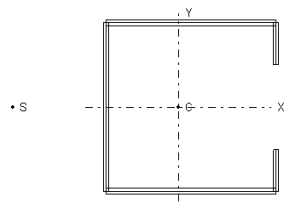
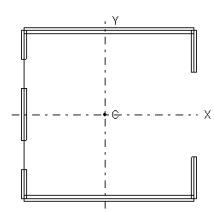
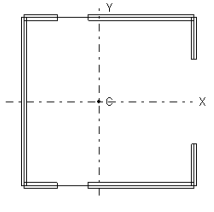
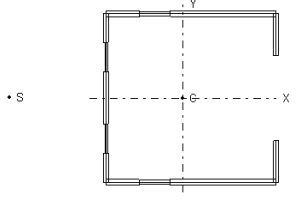
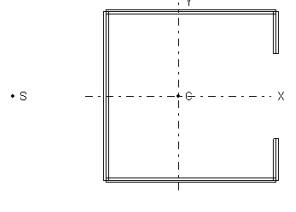
FULL UNREDUCED GROSS SECTION			
	<b>Node Data:</b> x-coord., y-coord.	<b>Segment Data:</b> node-i, -j, thickness	<b>Section Properties</b>
	1.565 0.795 1.565 1.5 0 1.5 0 -1.5 1.565 -1.5 1.565 -0.795	1 2 0.091 2 3 0.091 3 4 0.091 4 5 0.091 5 6 0.091	A = 0.68614 I <sub>x</sub> = 1.01988 I <sub>y</sub> = 0.285177 I <sub>xy</sub> = 0 J = 0.00189398 C.G. = (0.61749, 0) S.C. = (-0.902084, 0) C <sub>w</sub> = 0.784752
NET SECTION I – PERFORATED WEB			
	<b>Node Data:</b> x-coord., y-coord.	<b>Segment Data:</b> node-i, -j, thickness	<b>Section Properties</b>
	1.565 0.795 1.565 1.5 0 1.5 0 0.952 0 0.44 0 -0.44 0 -0.952 0 -1.5 1.565 -1.5 1.565 -0.795	1 2 0.091 2 3 0.091 3 4 0.091 4 5 0 5 6 0.091 6 7 0 7 8 0.091 8 9 0.091 9 10 0.091	A = 0.592956 I <sub>x</sub> = 0.972709 I <sub>y</sub> = 0.244062 I <sub>xy</sub> = 0 C.G. = (0.71453, 0)
NET SECTION II – PERFORATED FLANGES			
	<b>Node Data:</b> x-coord., y-coord.	<b>Segment Data:</b> node-i, -j, thickness	<b>Section Properties</b>
	1.565 0.795 1.565 1.5 1.094 1.5 0.563 1.5 0 1.5 0 -1.5 0.563 -1.5 1.094 -1.5 1.565 -1.5 1.565 -0.795	1 2 0.091 2 3 0.091 3 4 0 4 5 0.091 5 6 0.091 6 7 0.091 7 8 0 8 9 0.091 9 10 0.091	A = 0.589498 I <sub>x</sub> = 0.80244 I <sub>y</sub> = 0.277897 I <sub>xy</sub> = 0 C.G. = (0.582897, 0)
WEIGHTED SECTION			
	<b>Node Data:</b> x-coord., y-coord.	<b>Segment Data:</b> node-i, -j, thickness	<b>Section Properties</b>
	1.565 0.795 1.565 1.5 1.094 1.5 0.563 1.5 0 1.5 0 0.952 0 0.44 0 -0.44 0 -0.952 0 -1.5 0.563 -1.5 1.094 -1.5 1.565 -1.5 1.565 -0.795	1 2 0.091 2 3 0.091 3 4 0.073 4 5 0.091 5 6 0.091 6 7 0.0455 7 8 0.091 8 9 0.0455 9 10 0.091 10 11 0.091 11 12 0.073 12 13 0.091 13 14 0.091	A = 0.620432 I <sub>x</sub> = 0.953286 I <sub>y</sub> = 0.265125 I <sub>xy</sub> = 0 J = 0.00153986 C.G. = (0.65736, 0) S.C. = (-0.927725, 0) C <sub>w</sub> = 0.763688
AVERAGE SECTION			
	<b>Node Data:</b> x-coord., y-coord.	<b>Segment Data:</b> node-i, -j, thickness	<b>Section Properties</b>
	1.565 0.795 1.565 1.5 0 1.5 0 -1.5 1.565 -1.5 1.565 -0.795	1 2 0.0823 2 3 0.0823 3 4 0.0823 4 5 0.0823 5 6 0.0823	A = 0.620542 I <sub>x</sub> = 0.922379 I <sub>y</sub> = 0.257912 I <sub>xy</sub> = 0 J = 0.00140104 C.G. = (0.61749, 0) S.C. = (-0.902084, 0) C <sub>w</sub> = 0.709727



**Table 4.3 Section A-LDR-2 Dimensions and Properties**

FULL UNREDUCED GROSS SECTION			
	Node Data:	Segment Data:	Section Properties
	x-coord., y-coord.	node-i, -j, thickness	
	1.565 0.795 1.565 1.5 0 1.5 0 -1.5 1.565 -1.5 1.565 -0.795	1 2 0.045 2 3 0.045 3 4 0.045 4 5 0.045 5 6 0.045	A = 0.3393 Ix = 0.504339 Iy = 0.141021 Ixy = 0 J = 0.000229027 C.G. = (0.61749, 0) S.C. = (-0.902084, 0) Cw = 0.388064
NET SECTION I – PERFORATED WEB			
	Node Data:	Segment Data:	Section Properties
	x-coord., y-coord.	node-i, -j, thickness	
	1.565 0.795 1.565 1.5 0 1.5 0 0.952 0 0.44 0 -0.44 0 -0.952 0 -1.5 1.565 -1.5 1.565 -0.795	1 2 0.045 2 3 0.045 3 4 0.045 4 5 0 5 6 0.045 6 7 0 7 8 0.045 8 9 0.045 9 10 0.045	A = 0.29322 Ix = 0.48101 Iy = 0.12069 Ixy = 0 C.G. = (0.71453, 0)
NET SECTION II – PERFORATED FLANGES			
	Node Data:	Segment Data:	Section Properties
	x-coord., y-coord.	node-i, -j, thickness	
	1.565 0.795 1.565 1.5 1.094 1.5 0.563 1.5 0 1.5 0 -1.5 0.563 -1.5 1.094 -1.5 1.565 -1.5 1.565 -0.795	1 2 0.045 2 3 0.045 3 4 0 4 5 0.045 5 6 0.045 6 7 0.045 7 8 0 8 9 0.045 9 10 0.045	A = 0.29151 Ix = 0.396811 Iy = 0.137422 Ixy = 0 C.G. = (0.582897, 0)
WEIGHTED SECTION			
	Node Data:	Segment Data:	Section Properties
	x-coord., y-coord.	node-i, -j, thickness	
	1.565 0.795 1.565 1.5 1.094 1.5 0.563 1.5 0 1.5 0 0.952 0 0.44 0 -0.44 0 -0.952 0 -1.5 0.563 -1.5 1.094 -1.5 1.565 -1.5 1.565 -0.795	1 2 0.045 2 3 0.045 3 4 0.0361 4 5 0.045 5 6 0.045 6 7 0.0225 7 8 0.045 8 9 0.0225 9 10 0.045 10 11 0.045 11 12 0.0361 12 13 0.045 13 14 0.045	A = 0.306808 Ix = 0.471408 Iy = 0.131106 Ixy = 0 J = 0.000186207 C.G. = (0.65736, 0) S.C. = (-0.927724, 0) Cw = 0.377648
AVERAGE SECTION			
	Node Data:	Segment Data:	Section Properties
	x-coord., y-coord.	node-i, -j, thickness	
	1.565 0.795 1.565 1.5 0 1.5 0 -1.5 1.565 -1.5 1.565 -0.795	1 2 0.0407 2 3 0.0407 3 4 0.0407 4 5 0.0407 5 6 0.0407	A = 0.306878 Ix = 0.456146 Iy = 0.127546 Ixy = 0 J = 0.000169447 C.G. = (0.61749, 0) S.C. = (-0.902084, 0) Cw = 0.350983

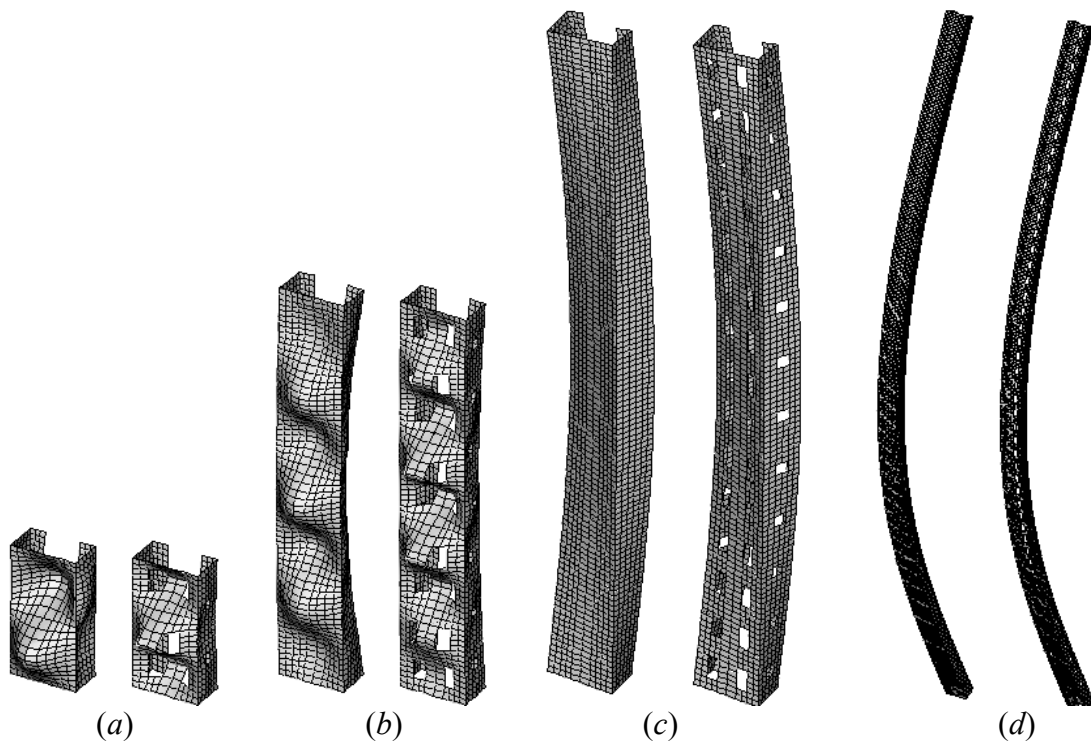
**Table 4.4 Section A-HDR Dimensions and Properties**

FULL UNREDUCED GROSS SECTION			
	Node Data:	Segment Data:	Section Properties
	x-coord., y-coord.	node-i, -j, thickness	
	2.91 0.7325	1 2 0.091	A = 0.919555
	2.91 1.4375	2 3 0.091	Ix = 1.43098
	0 1.4375	3 4 0.091	Iy = 1.15832
	0 -1.4375	4 5 0.091	Ixy = 0
	2.91 -1.4375	5 6 0.091	J = 0.00253828
	2.91 -0.7325		C.G. = (1.24406, 0)
			S.C. = (-1.60873, 0)
			Cw = 2.91218
NET SECTION I – PERFORATED WEB			
	Node Data:	Segment Data:	Section Properties
	x-coord., y-coord.	node-i, -j, thickness	
	2.91 0.7325	1 2 0.091	A = 0.826371
	2.91 1.4375	2 3 0.091	Ix = 1.38381
	0 1.4375	3 4 0.091	Iy = 0.997843
	0 0.952	4 5 0	Ixy = 0
	0 -0.44	5 6 0.091	C.G. = (1.38434, 0)
	0 -0.44	6 7 0	
	0 -0.952	7 8 0.091	
	0 -1.4375	8 9 0.091	
	2.91 -1.4375	9 10 0.091	
	2.91 -0.7325		
NET SECTION II – PERFORATED FLANGES			
	Node Data:	Segment Data:	Section Properties
	x-coord., y-coord.	node-i, -j, thickness	
	2.91 0.7325	1 2 0.091	A = 0.822913
	2.91 1.4375	2 3 0.091	Ix = 1.23128
	1.094 1.4375	3 4 0	Iy = 1.1374
	0.563 1.4375	4 5 0.091	Ixy = 0
	0 1.4375	5 6 0.091	C.G. = (1.29286, 0)
	0 -1.4375	6 7 0.091	
	0.563 -1.4375	7 8 0	
	1.094 -1.4375	8 9 0.091	
	2.91 -1.4375	9 10 0.091	
	2.91 -0.7325		
WEIGHTED SECTION			
	Node Data:	Segment Data:	Section Properties
	x-coord., y-coord.	node-i, -j, thickness	
	2.91 0.7325	1 2 0.091	A = 0.853847
	2.91 1.4375	2 3 0.091	Ix = 1.36789
	1.094 1.4375	3 4 0.073	Iy = 1.07738
	0.563 1.4375	4 5 0.091	Ixy = 0
	0 1.4375	5 6 0.091	J = 0.00218416
	0 0.952	6 7 0.0455	C.G. = (1.32125, 0)
	0 -0.44	7 8 0.091	S.C. = (-1.659, 0)
	0 -0.44	8 9 0.0455	Cw = 2.8227
	0 -0.952	9 10 0.091	
	0 -1.4375	10 11 0.091	
	0.563 -1.4375	11 12 0.073	
	1.094 -1.4375	12 13 0.091	
	2.91 -1.4375	13 14 0.091	
	2.91 -0.7325		
AVERAGE SECTION			
	Node Data:	Segment Data:	Section Properties
	x-coord., y-coord.	node-i, -j, thickness	
	2.91 0.7325	1 2 0.0845	A = 0.853873
	2.91 1.4375	2 3 0.0845	Ix = 1.32877
	0 1.4375	3 4 0.0845	Iy = 1.07559
	0 -1.4375	4 5 0.0845	Ixy = 0
	2.91 -1.4375	5 6 0.0845	J = 0.00203229
	2.91 -0.7325		C.G. = (1.24406, 0)
			S.C. = (-1.60873, 0)
			Cw = 2.70417

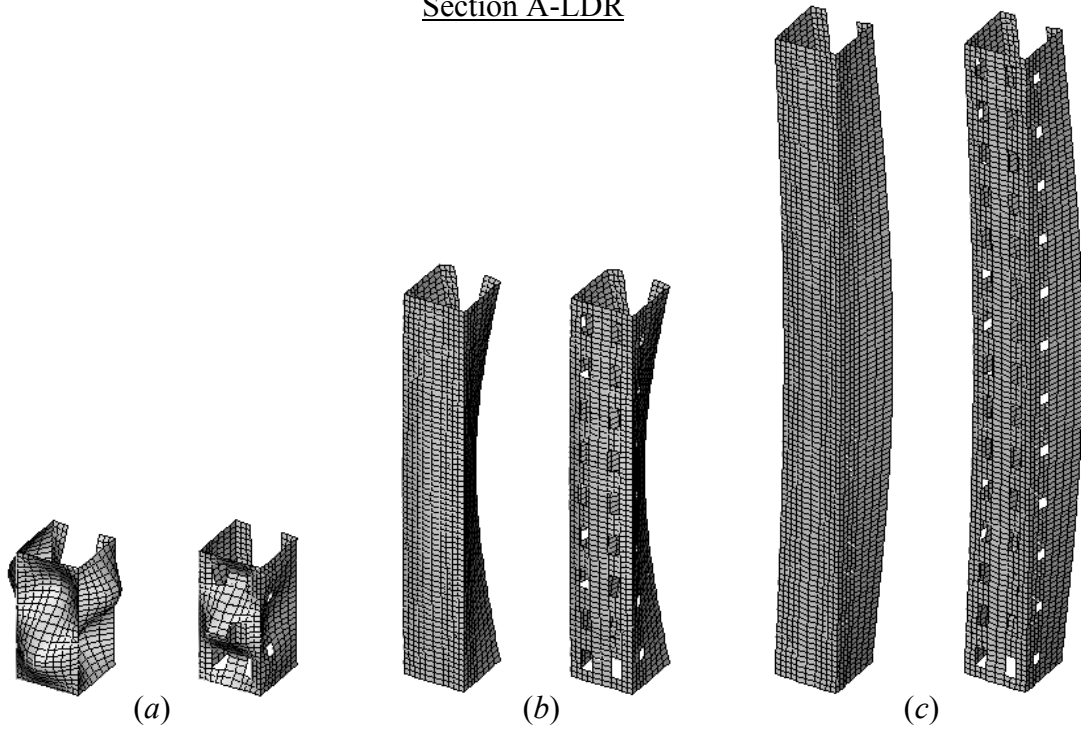
Finite element models range from a member length of 12 to 120 in. with a 6 in. increment between models. The theoretical values were obtained for the unperforated section, weighted section, average section, and in addition the net moment of inertia section for the flexural buckling mode. A weighted section as shown in Tables 4.2, 4.3, and 4.4, refers to a section that uses an average thickness in the perforated segment of the section to account for the absence of the material from the holes along the length of the section. An average section as also shown in Tables 4.2, 4.3, and 4.4, refers to a section that uses a uniform average thickness to account for the absence of the material from the holes in the section. The material volume of the weighted section and the average section is the same, and is equal to the perforated section. The cross sectional area of a weighted section is the same as an average section despite the fact that the weighted section has varying element thicknesses while the average section does not. The different possible overall buckling modes of these open thin-walled sections involve torsional-flexural buckling and flexural buckling for the concentrically loaded compression member, and lateral buckling for the flexural member as shown in Figs. 4.3 and 4.4.

The results are given in Figs. 4.5 and 4.6 for Section A-LDR, Figs. 4.7 and 4.8 for Section A-LDR-2, and Figs. 4.9 and 4.10 for Section A-HDR. The vertical axes in the figures are the elastic axial buckling load  $P_e$  divided by the axial load causing the yield of the full unreduced gross section  $P_y = AF_y$ , and the elastic flexural buckling moment  $M_e$  divided by the moment causing initial yield at the extreme compression fiber of the full unreduced gross section  $M_y = S_f F_y$ .

Results indicated that increasing the presence of perforations in the section will reduce the buckling strength. To take this into account, instead of using the unperforated section properties to predict the buckling strength of perforated sections, as assumed in the current design specification, better results can be obtained by using

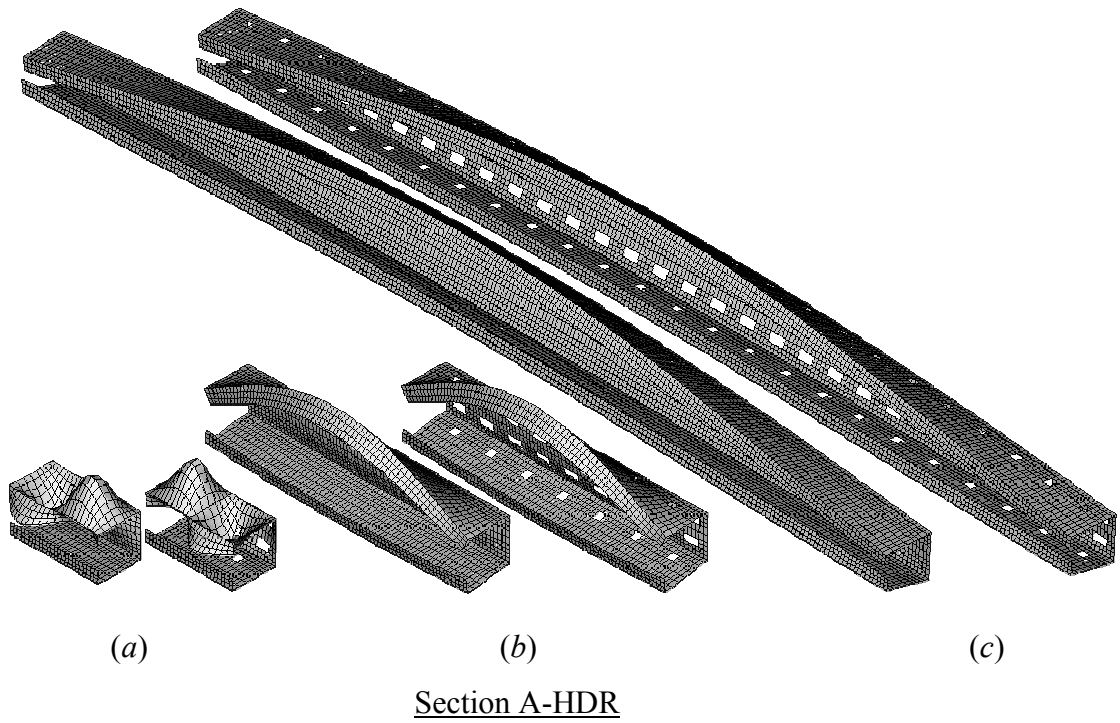
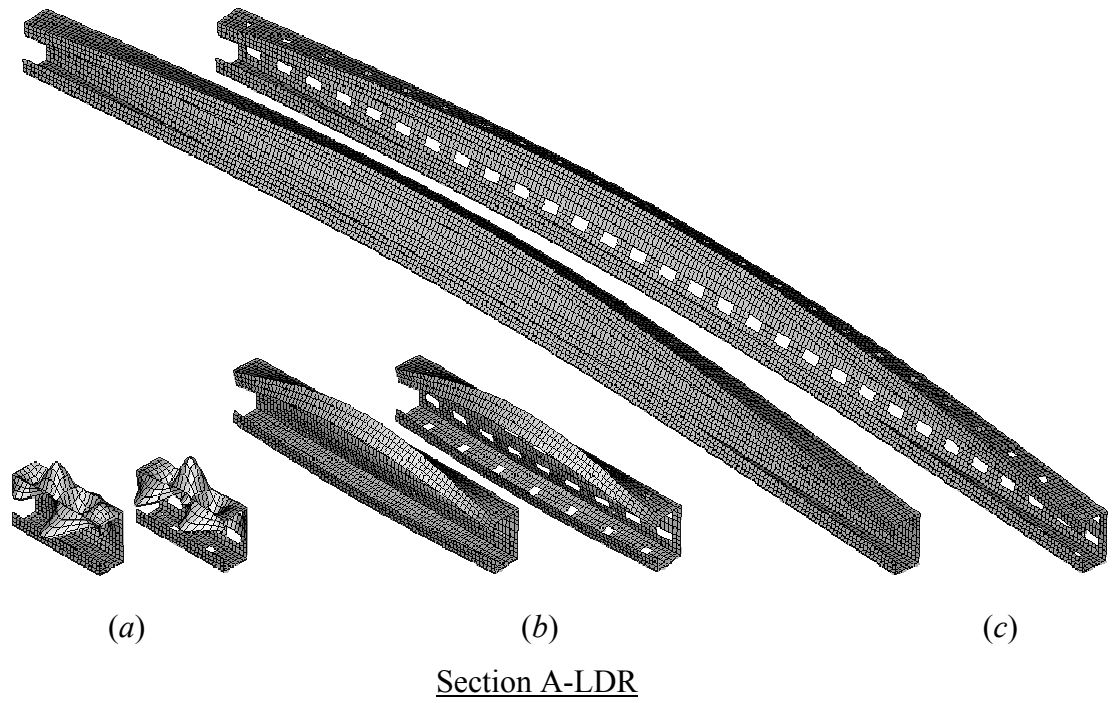


Section A-LDR

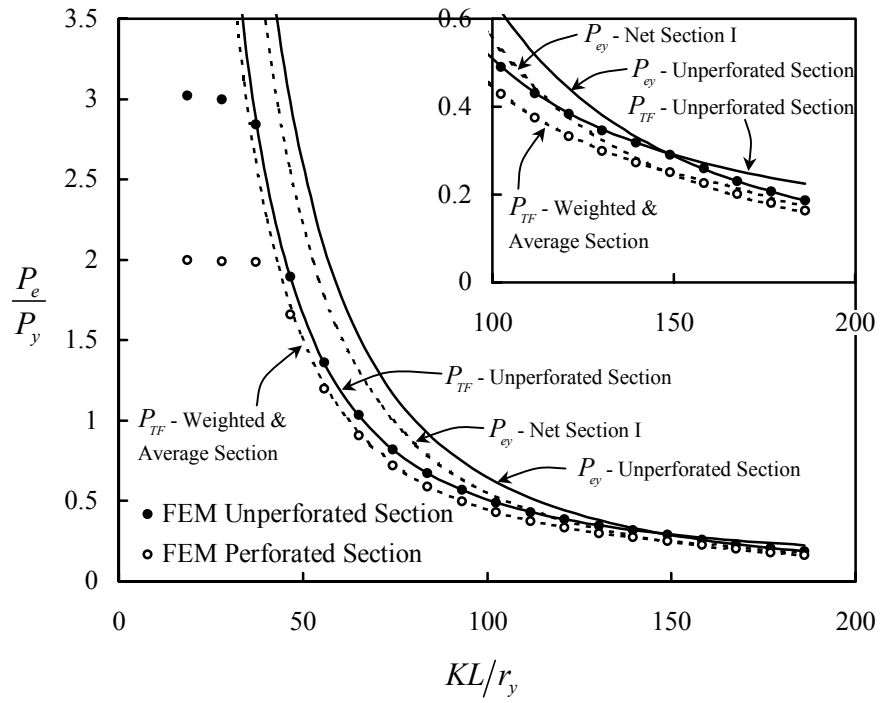


Section A-HDR

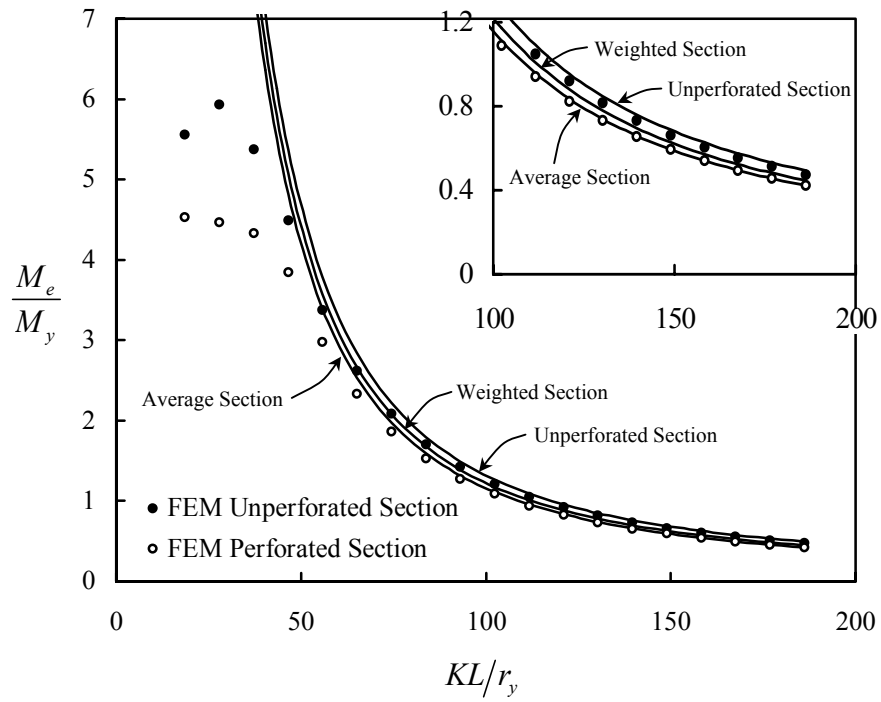
**Figure 4.3** Concentrically loaded compression member buckling modes (a) Local (b) Distortional (c) Torsional-flexural (d) Flexural



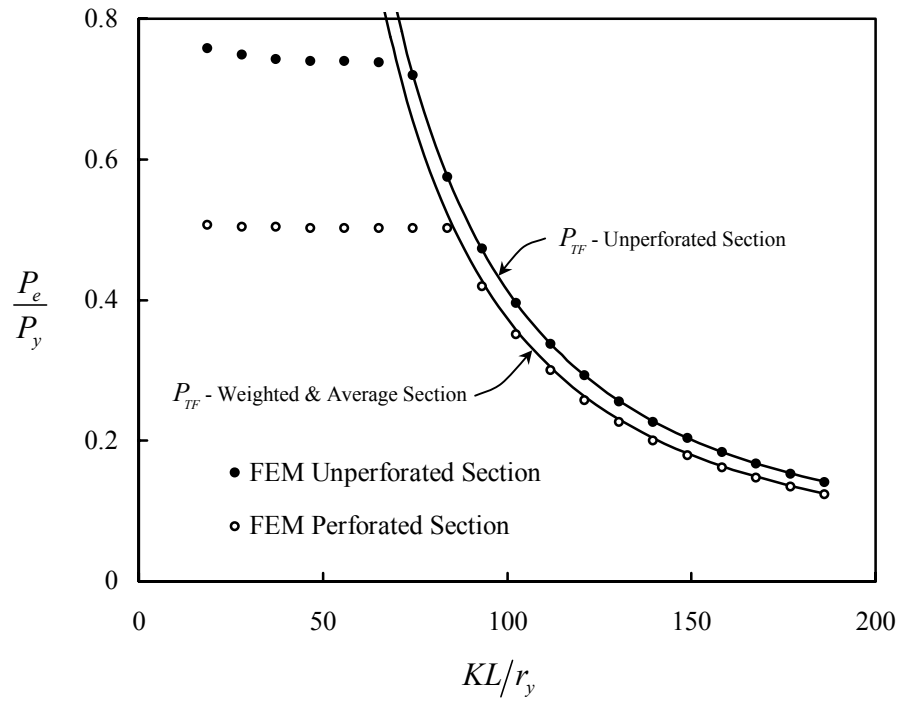
**Figure 4.4** Flexural member buckling modes (a) Local (b) Distortional (c) Lateral



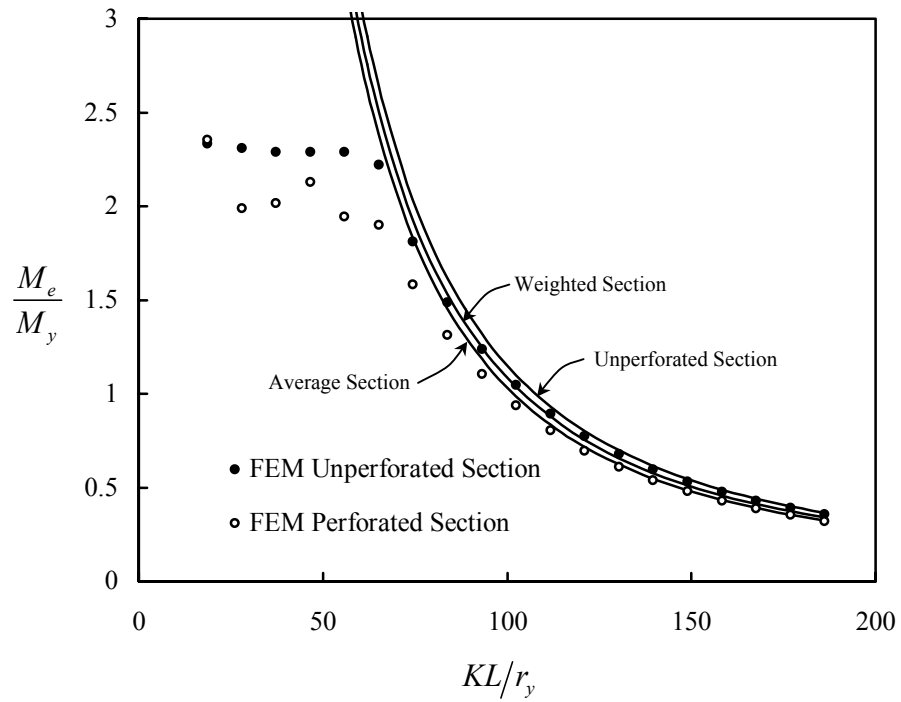
**Figure 4.5** Elastic buckling axial load for Section A-LDR



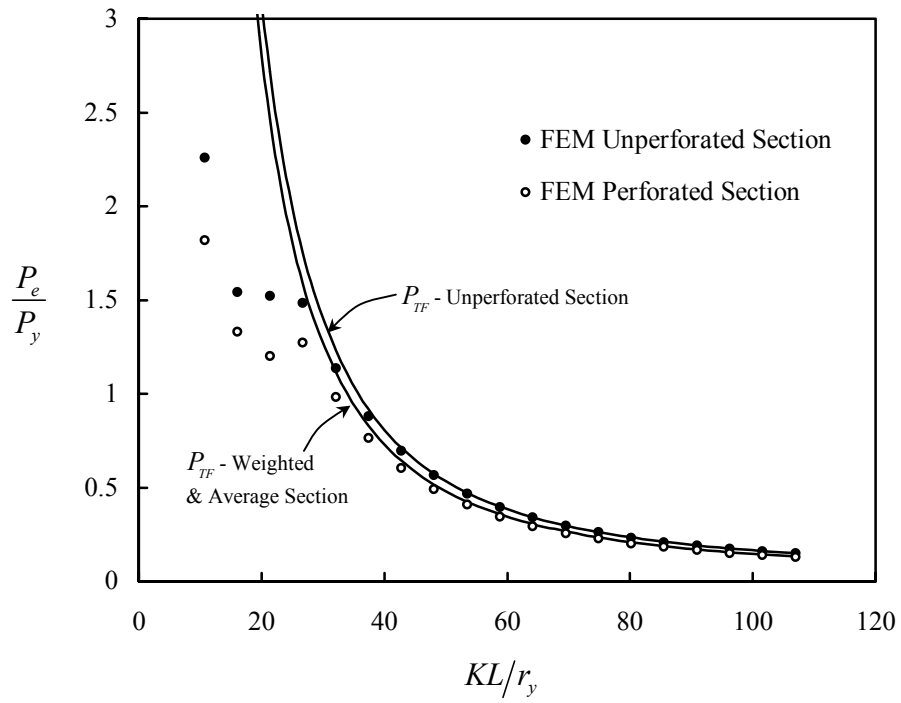
**Figure 4.6** Elastic buckling moment for Section A-LDR



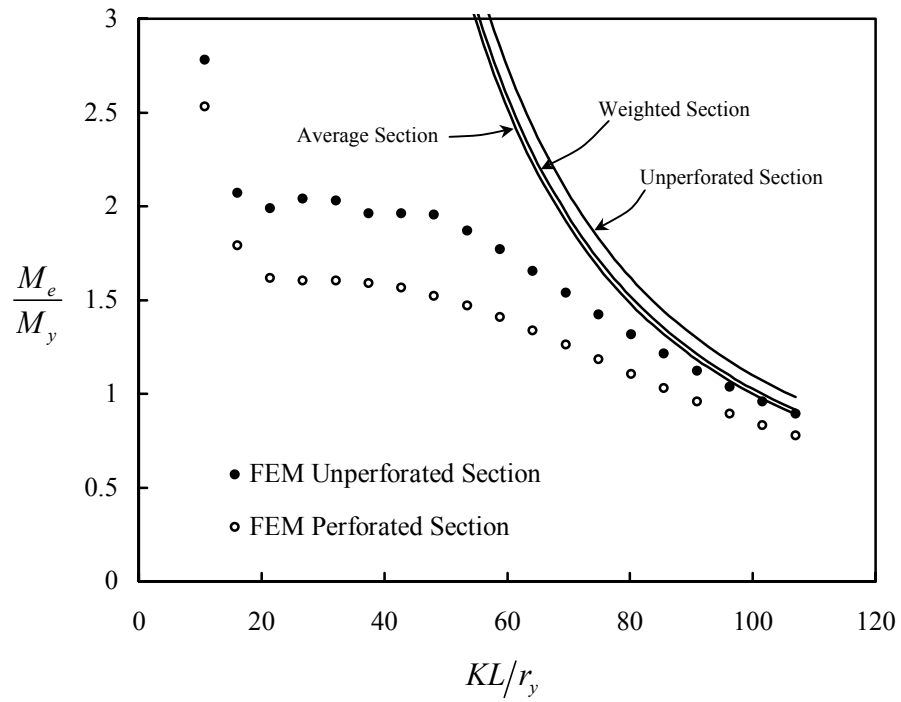
**Figure 4.7** Elastic buckling axial load for Section A-LDR-2



**Figure 4.8** Elastic buckling moment for Section A-LDR-2



**Figure 4.9** Elastic buckling axial load for Section A-HDR



**Figure 4.10** Elastic buckling moment for Section A-HDR



**Table 4.5** Concentrically Loaded Compression Member Buckling Modes

Case	Member Length, in.			
	Local	Distortional	Torsional-Flexural	Flexural
Unperforated Section A-LDR	-	12-18	24-96	102-120
Perforated Section A-LDR	12	18-24	30-96	102-120
Unperforated Section A-LDR-2	12-42	-	48-120	
Perforated Section A-LDR-2	12-54	-	60-120	
Unperforated Section A-HDR	-	12-24	30-120	-
Perforated Section A-HDR	12	18-24	30-120	-

**Table 4.6** Flexural Member Buckling Modes

Case	Member Length, in		
	Local	Distortional	Lateral
Unperforated Section A-LDR	-	12-24	30-120
Perforated Section A-LDR	-	12-24	30-120
Unperforated Section A-LDR-2	12-36	-	42-120
Perforated Section A-LDR-2	12	18-36	42-120
Unperforated Section A-HDR	-	12-48	54-120
Perforated Section A-HDR	12	18-48	54-120

the weighted section, or the average section properties for torsional-flexural buckling, the average section properties for lateral buckling, and the net moment of inertia section properties for flexural buckling. The torsional-flexural buckling could be computed either by using the weighted section or the average section because their results are almost the same. It is however more convenient to use the average section because its section properties are easier to compute.

The critical modes of the finite element models are summarized in Tables 4.5 and 4.6. It should be noted, however, that although some of the models are indicated as having instability by the torsional-flexural buckling or lateral buckling it is possible that the buckling strength may be much lower than the theoretical values. This is because they are still in transition, switching between the different buckling modes, thus the cross section deforms as a combination of distortional and torsional-flexural buckling or distortional and lateral buckling, which contradicts the theoretical buckling equations that assume that the cross section does not deform.

### **4.3 TORSIONAL-FLEXURAL BUCKLING**

Torsional-flexural buckling is usually the governing critical buckling mode for columns having an open-cross section. Generally the torsional-flexural buckling equation of the AISI specification is used to determine the buckling load. This equation, however, imposes several boundary condition assumptions, which often do not represent the actual bracings of the member, making the buckling load prediction sometimes inaccurate. Finite element buckling analysis studies were carried out to evaluate this equation. An open-section 3-node quadratic beam element was used to solve the problem in study. Open-section beam elements have a warping magnitude as an additional degree of freedom at each node. Five studies were carried

out, all of which used the Column Section-C1 shown in Table 4.7, and local axis definitions as shown in Table 4.8.

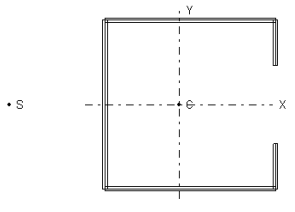
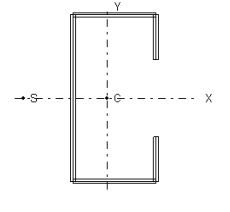
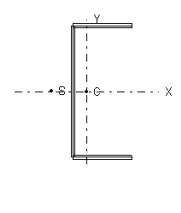
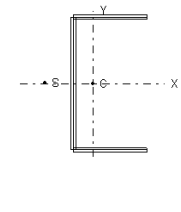
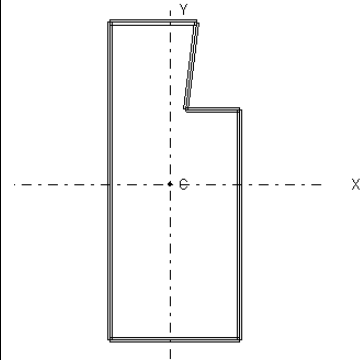
Study I: is a convergence study for a simply supported torsional-flexural buckling problem. As shown in Fig. 4.11 using 2 elements is sufficient to solve this problem. In the following studies, where additional interior braces are given; 30 elements were used to ensure the accuracy of the result.

Study II: is a torsional-flexural buckling problem of a simply supported column with two additional interior braces that constrain the column from twisting as shown in Fig. 4.12. The buckling load was obtained from the finite element analysis and compared to those values calculated from the buckling equation. To use the torsional-flexural buckling equation  $K_x L_x$  and  $K_t L_t$  must be known. In this study  $K_x L_x$  is 60 in. and  $K_t L_t$  was determined using two different approaches, for which their results are also compared in this study. The first approach, which is commonly used in current practice, was to assume the effective length factor  $K_t$  for torsional buckling to be 0.8, and the unbraced length against twisting  $L_t$  to be the maximum distance between adjacent braces. The second approach, which is considered to give a more accurate result than the first approach, was to determine  $K_t L_t$  from a torsional buckling analysis. Torsional buckling or flexural buckling analyses were performed by constraining certain degrees of freedom of the member as given in Table 4.8. As seen in Fig. 4.12 and Table 4.9 the torsional-flexural buckling equation can become quite conservative, in some cases over 25 percent.

Study III: is similar to Study II but with only one interior brace. The results shown in Fig 4.13 and Table 4.10 again suggest that the torsional-flexural buckling equation is conservative.

Study IV: shown in Table 4.11 looks at the torsional-flexural buckling problem for certain effective lengths  $K_x L_x$  and  $K_t L_t$ . For example when the torsional-

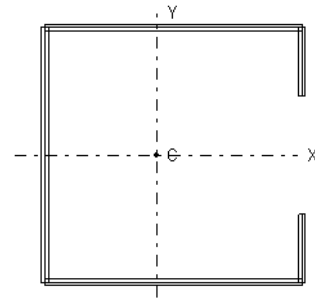
**Table 4.7 Section Dimensions and Properties**

COLUMN SECTION - C1			
	Node Data:	Segment Data:	Section Properties
	x-coord., y-coord.	node-i, -j, thickness	
	2.917 0.663	1 2 0.08	A = 0.81936
	2.917 1.4335	2 3 0.08	Ix = 1.25774
	0 1.4335	3 4 0.08	Iy = 1.05187
	0 -1.4335	4 5 0.08	Ixy = 0
	2.917 -1.4335	5 6 0.08	J = 0.00174797
	2.917 -0.663		C.G. = (1.26967, 0)
			S.C. = (-1.64311, 0)
			Cw = 2.84629
COLUMN SECTION - C2			
	Node Data:	Segment Data:	Section Properties
	x-coord., y-coord.	node-i, -j, thickness	
	1.417 0.663	1 2 0.078	A = 0.564876
	1.417 1.4335	2 3 0.078	Ix = 0.745446
	0 1.4335	3 4 0.078	Iy = 0.200071
	0 -1.4335	4 5 0.078	Ixy = 0
	1.417 -1.4335	5 6 0.078	J = 0.00114557
	1.417 -0.663		C.G. = (0.578775, 0)
			S.C. = (-0.856028, 0)
			Cw = 0.568044
HORIZONTAL AND DIAGONAL BRACES - B1			
	Node Data:	Segment Data:	Section Properties
	x-coord., y-coord.	node-i, -j, thickness	
	1 1.125	1 2 0.064	A = 0.272
	0 1.125	2 3 0.064	Ix = 0.22275
	0 -1.125	3 4 0.064	Iy = 0.0276078
	1 -1.125		Ixy = 0
			J = 0.000371371
			C.G. = (0.235294, 0)
			S.C. = (-0.363636, 0)
			Cw = 0.0245455
HORIZONTAL AND DIAGONAL BRACES - B2			
	Node Data:	Segment Data:	Section Properties
	x-coord., y-coord.	node-i, -j, thickness	
	1.25 1.125	1 2 0.083	A = 0.39425
	0 1.125	2 3 0.083	Ix = 0.341402
	0 -1.125	3 4 0.083	Iy = 0.0654126
	1.25 -1.125		Ixy = 0
			J = 0.000905329
			C.G. = (0.328947, 0)
			S.C. = (-0.480769, 0)
			Cw = 0.0578684
SHELF BEAMS			
	Node Data:	Segment Data:	Section Properties
	x-coord., y-coord.	node-i, -j, thickness	
	0 -2.899	1 2 0.083	A = 1.40106
	2.417 -2.899	2 3 0.083	Ix = 5.94383
	2.417 1.393	3 4 0.083	Iy = 1.43828
	1.417 1.393	4 5 0.083	Ixy = -0.343469
	1.617 3.018	5 6 0.083	I1 = 5.96986
	0 3.018	6 1 0.083	I2 = 1.41224
			theta = 0.0756498
			J = 3.24201
			C.G. = (1.12574, -0)

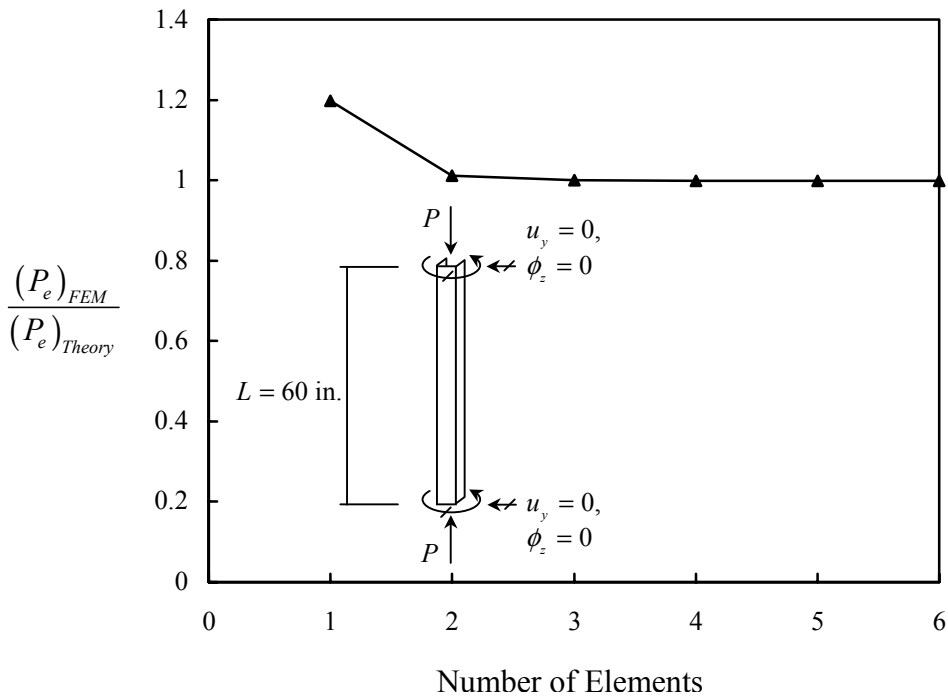
**Table 4.8** Boundary Conditions of the Open-section Beam Element for Elastic Buckling Problems

Buckling Mode	Active degrees of freedom						
	$u_x$	$u_y$	$u_z$	$\phi_x$	$\phi_y$	$\phi_z$	$w$
$P_{ex}$	X	√	√	√	X	X	X
$P_{ey}$	√	X	√	X	√	X	X
$P_{et}$	√	√	√	X	X	√	√
$P_e$	√	√	√	√	√	√	√

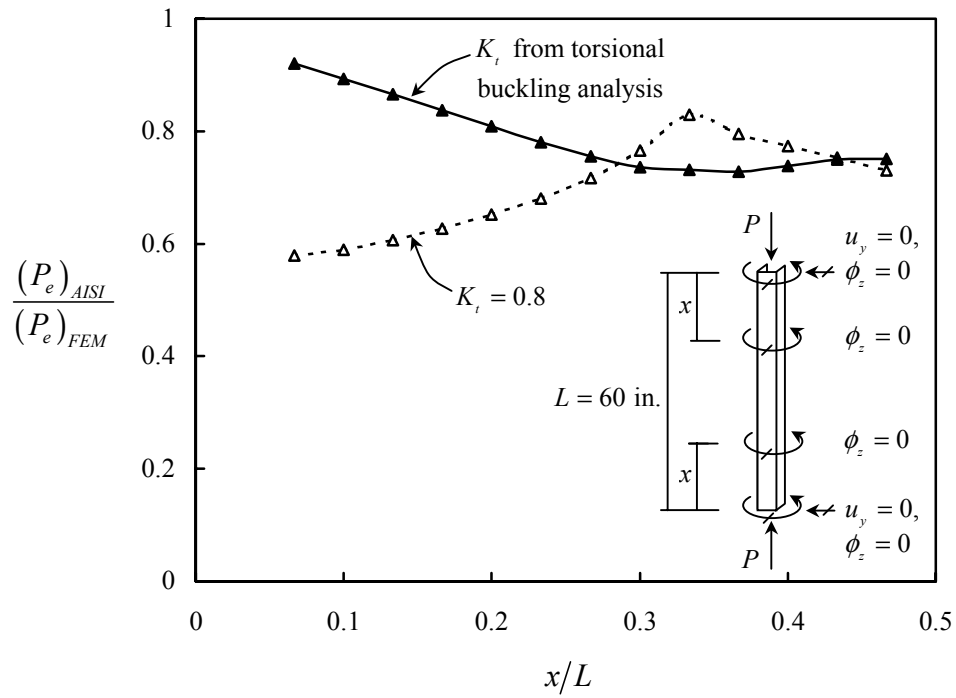
√ - free  
 X - constrained  
 $w$  - warping amplitude



Local axis definition



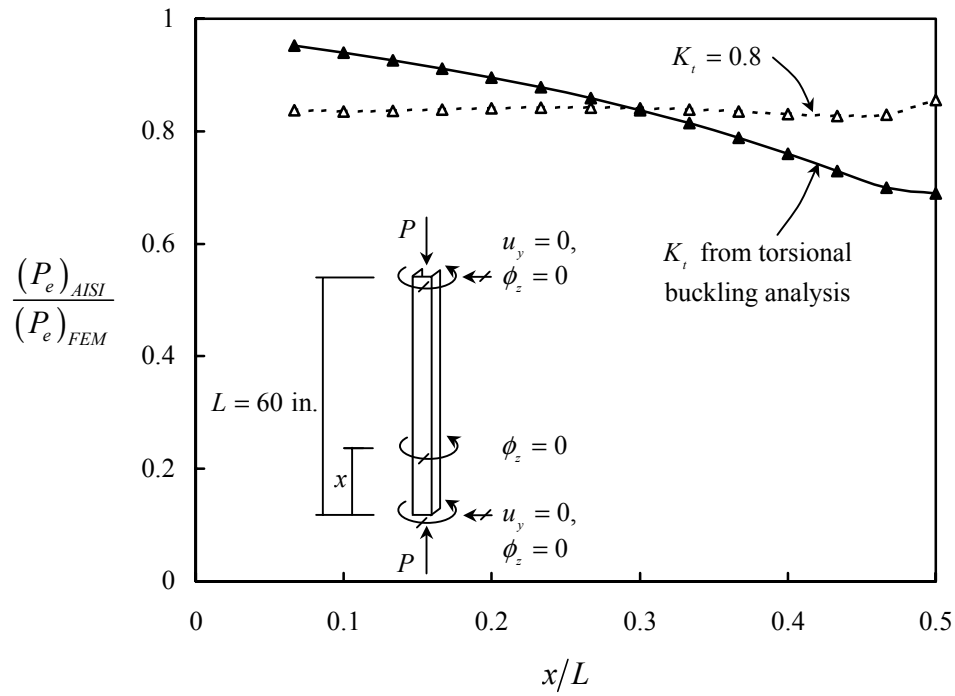
**Figure 4.11** Convergence study for the simply supported torsional-flexural buckling problem using open-section beam finite element - Study I



**Figure 4.12** Evaluation of the torsional-flexural buckling equation - Study II

**Table 4.9** Evaluation of the Torsional-Flexural Buckling Equation - Study II

$x$ (in.)	$L_t$ (in.)	$(P_e)_{FEM}$ (kips)	$K_t = 0.8$		$K_t$ from torsional buckling analysis	
			$K_t$	$\frac{(P_e)_{AIS}}{(P_e)_{FEM}}$	$K_t$	$\frac{(P_e)_{AIS}}{(P_e)_{FEM}}$
4	52	56.29	0.8	0.579	0.548	0.920
6	48	61.61	0.8	0.590	0.559	0.893
8	44	67.00	0.8	0.606	0.577	0.865
10	40	72.68	0.8	0.627	0.601	0.837
12	36	78.58	0.8	0.652	0.633	0.808
14	32	84.47	0.8	0.681	0.679	0.781
16	28	89.81	0.8	0.717	0.746	0.755
18	24	93.77	0.8	0.765	0.849	0.736
20	20	95.48	0.8	0.829	1	0.732
22	22	94.88	0.8	0.796	0.924	0.729
24	24	92.80	0.8	0.773	0.859	0.738
26	26	90.31	0.8	0.753	0.805	0.750
28	28	88.25	0.8	0.730	0.770	0.751

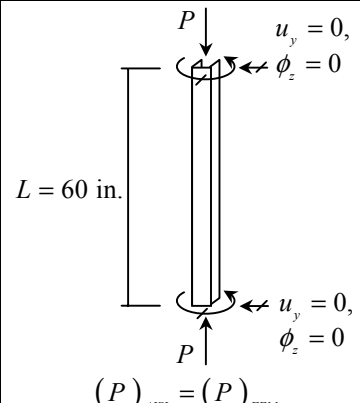
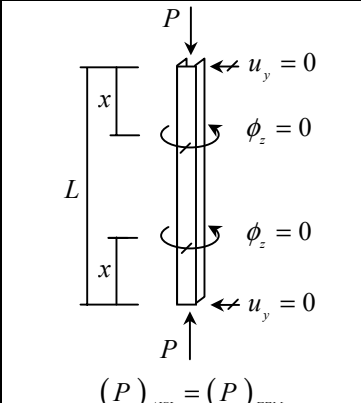
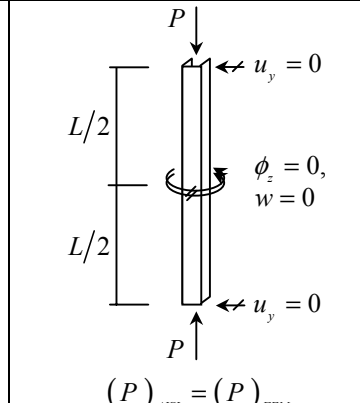
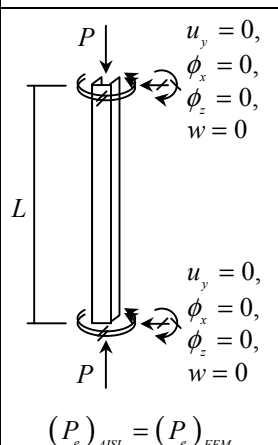
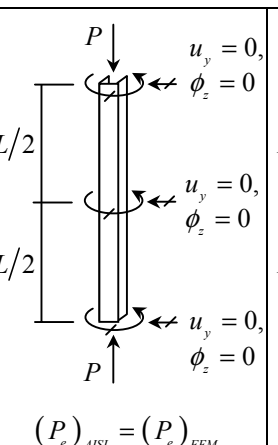
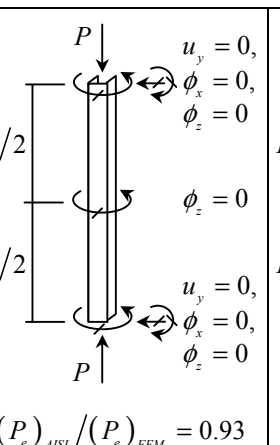
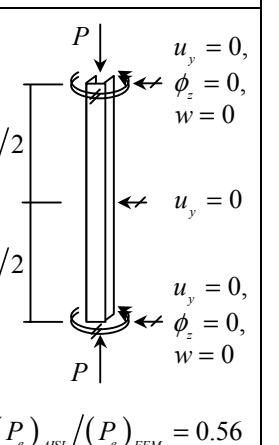
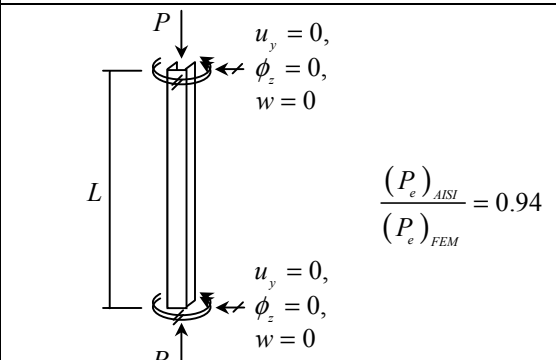
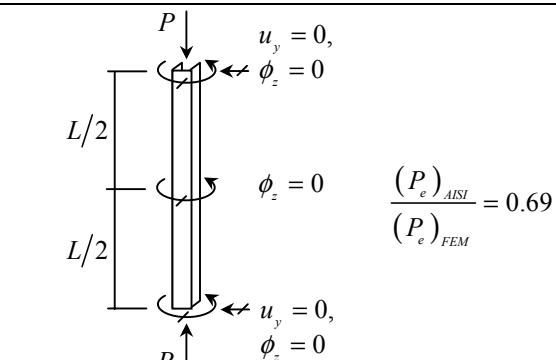


**Figure 4.13** Evaluation of the torsional-flexural buckling equation - Study III

**Table 4.10** Evaluation of the Torsional-Flexural Buckling Equation - Study III

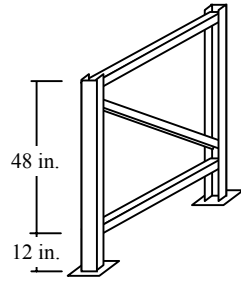
$x$ (in.)	$L_t$ (in.)	$(P_e)_{FEM}$ (kips)	$K_t = 0.8$		$K_t$ from torsional buckling analysis	
			$K_t$	$\frac{(P_e)_{AIS}}{(P_e)_{FEM}}$	$K_t$	$\frac{(P_e)_{AIS}}{(P_e)_{FEM}}$
4	56	35.06	0.8	0.837	0.730	0.952
6	54	37.00	0.8	0.835	0.735	0.939
8	52	38.95	0.8	0.837	0.743	0.926
10	50	41.01	0.8	0.839	0.752	0.911
12	48	43.23	0.8	0.840	0.762	0.895
14	46	45.65	0.8	0.841	0.774	0.878
16	44	48.29	0.8	0.842	0.787	0.859
18	42	51.19	0.8	0.840	0.802	0.838
20	40	54.38	0.8	0.838	0.820	0.814
22	38	57.87	0.8	0.835	0.842	0.788
24	36	61.66	0.8	0.830	0.868	0.760
26	34	65.64	0.8	0.827	0.902	0.729
28	32	69.33	0.8	0.829	0.946	0.700
30	30	71.14	0.8	0.856	1	0.689

**Table 4.11** Evaluation of the Torsional-Flexural Buckling Equation - Study IV

CASE 1: $K_x L_x = 60, K_t L_t = 60$			
 <p style="text-align: center;"><math>(P_e)_{AISI} = (P_e)_{FEM}</math></p> <p style="text-align: center;">A</p>	 <p style="text-align: center;"><math>(P_e)_{AISI} = (P_e)_{FEM}</math></p> <p style="text-align: center;">B</p>	 <p style="text-align: center;"><math>(P_e)_{AISI} = (P_e)_{FEM}</math></p> <p style="text-align: center;">C</p>	
Finite element analysis result: A = B = C			
CASE 2: $K_x L_x = 30, K_t L_t = 30$			
 <p style="text-align: center;"><math>(P_e)_{AISI} = (P_e)_{FEM}</math></p> <p style="text-align: center;">D</p>	 <p style="text-align: center;"><math>(P_e)_{AISI} = (P_e)_{FEM}</math></p> <p style="text-align: center;">E</p>	 <p style="text-align: center;"><math>(P_e)_{AISI} / (P_e)_{FEM} = 0.93</math></p> <p style="text-align: center;">F</p>	 <p style="text-align: center;"><math>(P_e)_{AISI} / (P_e)_{FEM} = 0.56</math></p> <p style="text-align: center;">G</p>
Finite element analysis result: D = E ≠ F ≠ G			
CASE 3: $K_x L_x = 60, K_t L_t = 30$			
 <p style="text-align: center;"><math>\frac{(P_e)_{AISI}}{(P_e)_{FEM}} = 0.94</math></p> <p style="text-align: center;">H</p>	 <p style="text-align: center;"><math>\frac{(P_e)_{AISI}}{(P_e)_{FEM}} = 0.69</math></p> <p style="text-align: center;">I</p>		
Finite element analysis result: H ≠ I			



**Table 4.12** Evaluation of the Torsional-Flexural Buckling Equation - Study V



$$(P_e)_{AISI} / (P_e)_{FEM}$$

Case	A	B	C	D	E	F
I	1	0.998	0.869	0.751	0.763	0.894
II	0.989	0.982	0.900	0.883	0.771	0.660
III	0.913	0.873	0.644	0.751	0.787	0.894
IV	0.426	0.501	0.930	1	0.895	0.808

<p>60 in.</p> <p><math>K_x L_x = 120</math></p> <p>I</p>	<p>60 in.</p> <p><math>K_x L_x = 60</math></p> <p>II</p>	<p>60 in.</p> <p><math>K_x L_x = 120</math></p> <p>III</p>	<p>60 in.</p> <p><math>K_x L_x = 60</math></p> <p>IV</p>
<p>60 in.</p> <p><math>K_t L_t = 120</math></p> <p>A</p>	<p>48 in.</p> <p>12 in.</p> <p><math>K_t L_t = 104.7</math></p> <p>B</p>	<p>12 in.</p> <p>48 in.</p> <p><math>K_t L_t = 63.4</math></p> <p>C</p>	
<p>60 in.</p> <p><math>K_t L_t = 60</math></p> <p>D</p>	<p>48 in.</p> <p>12 in.</p> <p><math>K_t L_t = 36.6</math></p> <p>E</p>	<p>12 in.</p> <p>36 in.</p> <p>12 in.</p> <p><math>K_t L_t = 22.8</math></p> <p>F</p>	

flexural buckling equation is used, the results are obviously  $A = B = C$ ,  $D = E = F = G$ , and  $H = I$ , but finite element results suggested that  $A = B = C$ ,  $D = E \neq F \neq G$ , and  $H \neq I$ . The buckling load determined from the AISI equation for cases F, G, H, and I is conservative compared with finite element results.

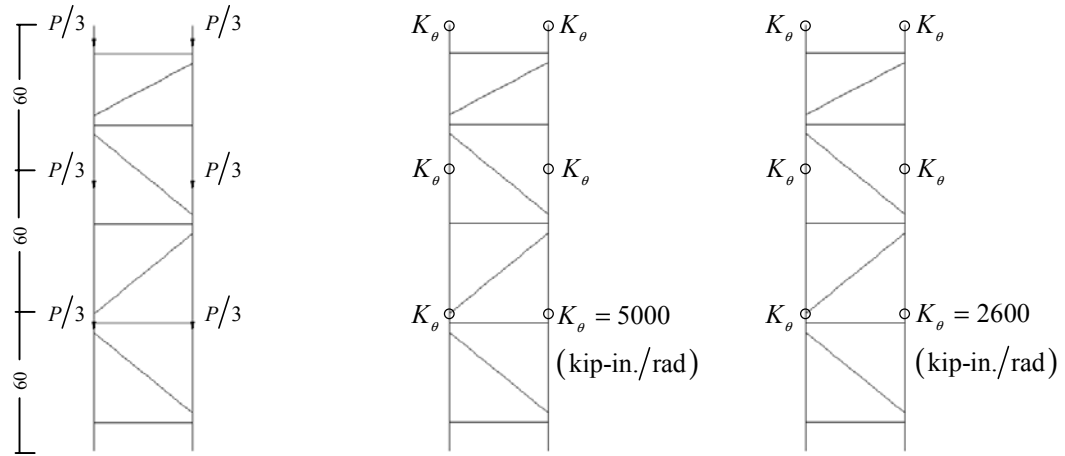
Study V: shown in Table 4.12 looks at the torsional-flexural buckling problem for different combinations of the effective lengths  $K_x L_x$  and  $K_t L_t$ , to represent pallet rack bottom story columns. In this study  $K_t L_t$  was determined from a torsional buckling analysis. For example, case E has the column base, and at elevations 12 and 60 in., constrained against twisting. Combinations such as I + E, II + E, or III + E may represent the columns of a sidesway uninhibited frame. In these cases, the torsional-flexural buckling equation is over 20 percent conservative compared with the finite element results.

Studies II through V have shown that the buckling load obtained from using the AISI torsional-flexural buckling equation can be quite conservative compared to the finite element solution. There are two particular reasons for this. First, the buckling equation assumes that the buckled shape maximum deflection and maximum rotation coincide; however, depending on the boundary conditions of the member this may not always be the case. Second, the buckling equation assumes that the translation support,  $u_y = 0$ , is about the shear center but the finite element analysis boundary conditions are imposed at the cross-section centroid. The AISI torsional-flexural buckling equation has proved to be a source of the conservatism in the current design provisions.

#### 4.4 EFFECTIVE LENGTHS

The AISI, AISC and RMI specifications use the effective length approach for assessing frame stability. The approach relies significantly on the prediction of the effective lengths and critical buckling load of the member. For pallet racks, the value of  $K_x$  for column flexural buckling in the direction perpendicular to the upright frames is usually determined from the alignment charts, elastic buckling analysis, or simply assumed to be 1.7 as suggested by the RMI specification. The RMI specification also recommends that  $K_y$  for column flexural buckling in the plane of the upright frame can be taken as one, and  $K_t$  for column torsional buckling can be taken as 0.8, providing that the upright frame has adequate braces. These recommended  $K$  values, are approximated from numerous typical rack assemblies. Structural frame elastic buckling analysis is needed if the exact  $K$  values are to be computed. The objective of this study was to evaluate the RMI recommended values of  $K_y$  and  $K_t$  for column buckling.

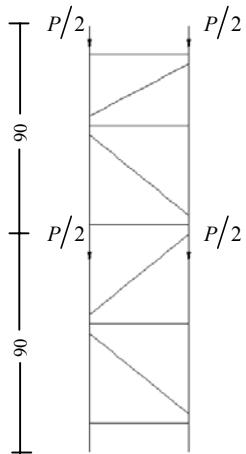
Finite element elastic buckling analyses of upright frames were performed to obtain  $K_y$  and  $K_t$  for column buckling, and evaluate the AISI torsional-flexural buckling equation. A parametric study was carried out for different types of upright frame configurations. The parameters included: two load cases as shown in Fig. 4.14, two types of column sections as shown in Table 4.7, two types of braces also shown in Table 4.7, and six types of bracing patterns as shown in Tables 4.13 through 4.15. The finite element assumptions were as follows: The joint connection between the braces and columns were considered to be continuous except for the warping degree of freedom. The warping degree of freedom was constrained only at the ends of the braces. Column base fixity for both the strong and weak axis bending of the column was modeled by torsional springs with the stiffnesses determined from the proposed



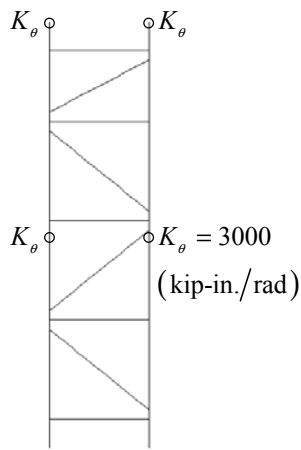
Load Case I

Column Section - C1

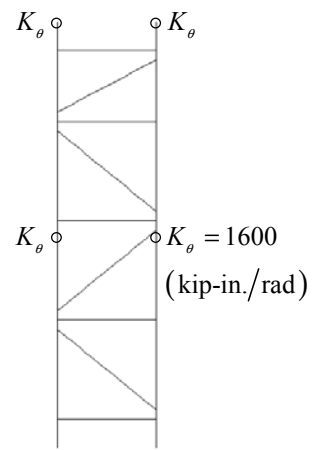
Column Section - C2



Load Case II

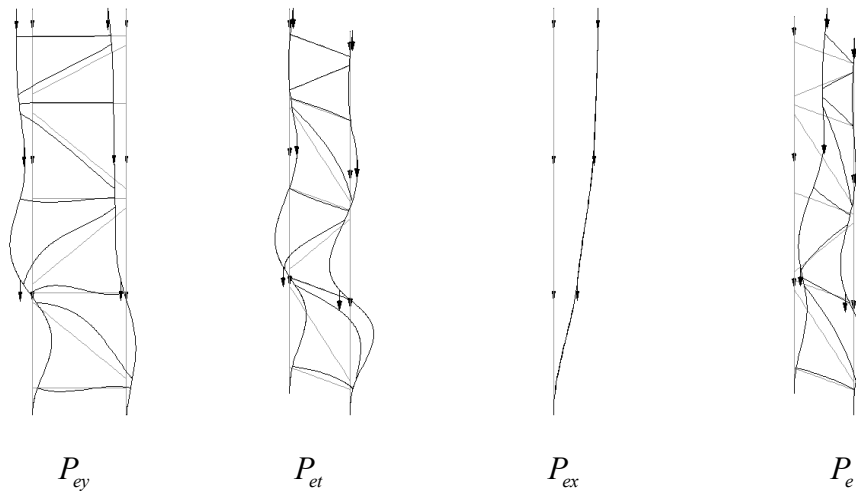


Column Section - C1



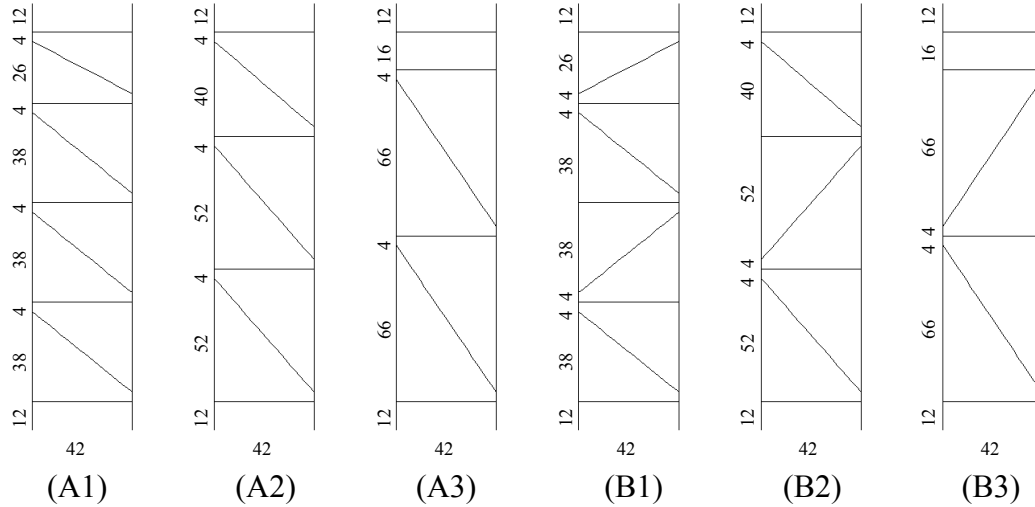
Column Section - C2

**Figure 4.14** Upright frame load cases and beam to column connection stiffness,  $K_\theta$



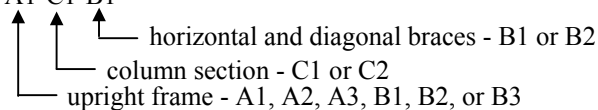
**Figure 4.15** Upright frame elastic critical buckling modes (upright frame B1-C1-B1)

**Table 4.13** Values of Column  $K_y$  and  $K_t$  for Upright Frame A & B

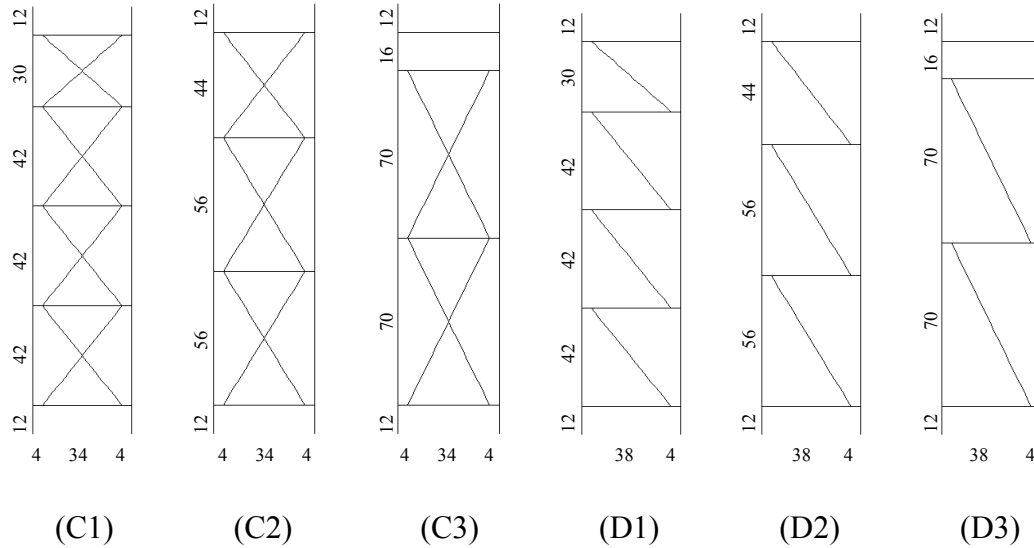


Upright Frame*	Load Case I				Load Case II			
	$P_{ey}$ (kips)	$K_y$	$P_{et}$ (kips)	$K_t$	$P_{ey}$ (kips)	$K_y$	$P_{et}$ (kips)	$K_t$
A1-C1-B1	230.19	0.960	75.51	0.830	212.77	0.998	69.87	0.863
A1-C1-B2	241.29	0.938	80.70	0.802	227.84	0.965	74.29	0.837
A2-C1-B1	166.26	0.825	51.75	0.736	140.53	0.898	43.27	0.808
A2-C1-B2	174.18	0.806	54.58	0.716	148.48	0.873	45.75	0.785
A3-C1-B1	88.02	0.894	40.15	0.662	62.17	1.063	33.21	0.731
A3-C1-B2	105.65	0.816	41.94	0.647	76.04	0.962	34.80	0.714
A1-C2-B1	51.43	0.886	63.96	0.712	48.96	0.908	58.42	0.747
A1-C2-B2	60.47	0.817	70.42	0.677	57.59	0.837	60.38	0.734
A2-C2-B1	36.76	0.766	41.63	0.655	31.86	0.822	36.89	0.700
A2-C2-B2	42.86	0.709	44.83	0.629	38.00	0.753	40.21	0.668
A3-C2-B1	25.63	0.722	31.54	0.602	19.56	0.827	26.71	0.662
A3-C2-B2	32.32	0.643	33.47	0.582	27.02	0.704	28.52	0.637
B1-C1-B1	227.04	0.967	75.32	0.831	207.61	1.011	69.93	0.863
B1-C1-B2	240.03	0.940	79.69	0.807	223.68	0.974	74.01	0.838
B2-C1-B1	165.86	0.826	52.07	0.734	136.40	0.911	43.74	0.804
B2-C1-B2	174.30	0.806	55.38	0.711	145.70	0.882	46.24	0.781
B3-C1-B1	88.13	0.893	40.53	0.659	62.29	1.062	33.86	0.724
B3-C1-B2	105.69	0.816	44.13	0.630	76.14	0.961	35.90	0.702
B1-C2-B1	51.64	0.884	56.89	0.758	49.00	0.907	53.28	0.785
B1-C2-B2	60.70	0.815	59.57	0.740	57.76	0.836	55.94	0.765
B2-C2-B1	36.87	0.764	39.62	0.673	31.84	0.822	34.19	0.730
B2-C2-B2	42.85	0.709	42.14	0.651	38.23	0.751	36.05	0.709
B3-C2-B1	25.64	0.722	30.36	0.615	19.57	0.827	25.41	0.681
B3-C2-B2	32.27	0.644	33.26	0.584	26.92	0.705	26.84	0.660

\*Upright frames are named as: A1-C1-B1

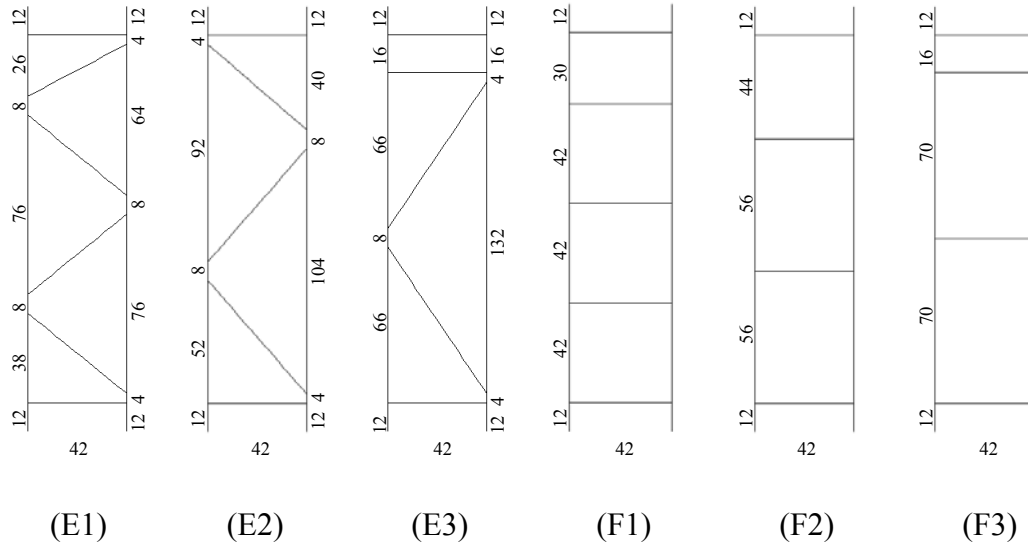


**Table 4.14** Values of Column  $K_y$  and  $K_t$  for Upright Frame C & D



Upright Frame	Load Case I				Load Case II			
	$P_{ey}$ (kips)	$K_y$	$P_{et}$ (kips)	$K_t$	$P_{ey}$ (kips)	$K_y$	$P_{et}$ (kips)	$K_t$
C1-C1-B1	255.56	0.824	71.38	0.773	228.37	0.872	66.14	0.803
C1-C1-B2	280.59	0.787	75.76	0.749	268.41	0.804	69.53	0.783
C2-C1-B1	174.07	0.749	51.47	0.686	152.55	0.800	42.01	0.762
C2-C1-B2	202.60	0.694	55.23	0.661	175.28	0.746	44.37	0.741
C3-C1-B1	97.05	0.803	41.95	0.610	70.28	0.943	33.84	0.683
C3-C1-B2	118.89	0.725	45.68	0.584	86.69	0.849	36.59	0.655
C1-C2-B1	59.28	0.746	49.64	0.738	56.64	0.764	45.77	0.771
C1-C2-B2	72.35	0.676	52.59	0.715	69.51	0.689	48.19	0.750
C2-C2-B1	42.07	0.664	37.21	0.647	37.47	0.704	30.44	0.724
C2-C2-B2	51.49	0.601	40.31	0.619	47.26	0.627	32.46	0.698
C3-C2-B1	28.60	0.645	31.15	0.572	21.82	0.738	25.07	0.647
C3-C2-B2	39.09	0.551	34.24	0.542	32.29	0.607	27.30	0.616
D1-C1-B1	233.75	0.862	66.21	0.803	221.79	0.885	61.35	0.835
D1-C1-B2	247.39	0.838	66.96	0.798	236.11	0.858	61.77	0.832
D2-C1-B1	167.23	0.764	47.05	0.718	140.72	0.833	38.80	0.794
D2-C1-B2	175.67	0.746	47.31	0.716	150.60	0.805	38.90	0.793
D3-C1-B1	90.09	0.833	38.43	0.639	63.99	0.988	31.30	0.712
D3-C1-B2	106.25	0.767	38.62	0.637	78.24	0.894	31.51	0.709
D1-C2-B1	52.12	0.796	44.28	0.785	49.62	0.816	40.82	0.820
D1-C2-B2	59.51	0.745	44.20	0.785	56.50	0.765	40.75	0.821
D2-C2-B1	36.67	0.712	32.41	0.699	31.85	0.764	26.95	0.776
D2-C2-B2	41.82	0.666	32.37	0.699	36.72	0.711	26.88	0.777
D3-C2-B1	25.14	0.688	27.06	0.619	19.54	0.780	22.10	0.697
D3-C2-B2	31.47	0.615	26.86	0.622	26.43	0.671	21.97	0.699

**Table 4.15** Values of Column  $K_y$  and  $K_t$  for Upright Frame E & F



Upright Frame	Load Case I				Load Case II			
	$P_{ey}$ (kips)	$K_y$	$P_{et}$ (kips)	$K_t$	$P_{ey}$ (kips)	$K_y$	$P_{et}$ (kips)	$K_t$
E1-C1-B1	96.95	0.740	40.00	0.576	83.29	0.798	34.81	0.620
E1-C1-B2	104.78	0.711	43.23	0.553	91.11	0.763	37.45	0.596
E2-C1-B1	77.45	0.605	26.55	0.523	59.31	0.691	25.44	0.535
E2-C1-B2	81.17	0.591	27.74	0.511	66.76	0.651	27.45	0.514
E3-C1-B1	52.26	0.580	21.34	0.464	42.36	0.644	21.18	0.465
E3-C1-B2	58.37	0.549	22.12	0.455	50.38	0.591	22.02	0.456
E1-C2-B1	22.75	0.666	32.85	0.511	19.96	0.711	28.13	0.558
E1-C2-B2	27.05	0.611	34.00	0.501	23.71	0.652	29.09	0.547
E2-C2-B1	16.50	0.571	21.29	0.480	15.37	0.592	20.84	0.486
E2-C2-B2	17.89	0.549	22.05	0.470	18.06	0.546	21.49	0.477
E3-C2-B1	12.45	0.518	17.24	0.430	11.62	0.536	17.28	0.429
E3-C2-B2	13.60	0.496	17.91	0.420	13.28	0.502	18.02	0.418
F1-C1-B1	10.85	4.001	66.45	0.801	9.11	4.365	61.81	0.832
F1-C1-B2	17.97	3.109	67.93	0.792	15.36	3.362	62.83	0.825
F2-C1-B1	9.56	3.196	47.37	0.716	8.03	3.488	39.10	0.791
F2-C1-B2	15.16	2.538	48.06	0.711	12.99	2.742	39.51	0.787
F3-C1-B1	9.71	2.537	38.54	0.638	8.24	2.754	31.33	0.711
F3-C1-B2	14.73	2.060	39.26	0.632	12.83	2.207	31.91	0.704
F1-C2-B1	5.75	2.397	45.32	0.775	5.00	2.569	41.81	0.809
F1-C2-B2	9.88	1.828	45.50	0.773	8.66	1.953	41.93	0.808
F2-C2-B1	4.66	1.997	33.14	0.690	4.11	2.126	27.50	0.767
F2-C2-B2	7.52	1.571	33.22	0.689	6.86	1.645	27.56	0.766
F3-C2-B1	4.20	1.683	27.67	0.611	3.75	1.781	22.52	0.689
F3-C2-B2	6.21	1.384	27.75	0.610	5.67	1.449	22.59	0.688

base fixity equation given in Chapter 2. In addition to the torsional springs, the column bases were also constrained against twisting.

The  $K_y$  and  $K_t$  values for columns was determined from flexural buckling and torsional buckling analyses of the upright frame. To perform these analyses without having torsional-flexural buckling certain degrees of freedom of the columns had to be constrained as shown in Table 4.8. The obtained  $K_y$  and  $K_t$  values are given in Tables 4.13 through 4.15 for the different upright frame configurations, and an example of the buckling mode shapes are shown in Fig. 4.15. From these tables it was found that, the RMI recommendation of  $K_y$  taken as one is conservative with the exception of upright frame type F. Upright frame type F has inadequate braces causing the upright frame to be in sidesway buckling mode. It was also found that the recommendation of  $K_t$  taken as 0.8 is in most cases reasonable. Upright frame type E had the load applied between the bracings making the calculation of  $K_t$  very conservative. In this study it was found that it is very important to constrain the column bases from twisting, otherwise  $K_t$  can be more than one. Generally this assumption should be valid because the base plate usually has at least one anchorage bolt, and the friction between the steel base plate and concrete floor should be sufficient to prevent the bases from twisting. The ideal column bases condition to prevent it from twisting is however to have more than one anchorage bolt.

In the following study  $K_x$  for columns was assumed to be 1.2. A certain  $K_x$  value can be defined by providing torsional springs as shown in the Fig. 4.14 to resist the columns from flexural buckling in the direction perpendicular to the upright frame. Elastic buckling analysis of the upright frames was performed to determine the critical buckling load,  $P_e$ . Summaries of the results are given in Tables 4.16 and 4.17. Upright frame type A through E has torsional-flexural as the column critical buckling mode while upright frame type F has flexural buckling about the weak axis.



**Table 4.16** Values of Column  $K_x$  and  $P_e$  for Upright Frame A, B, C, and D

Upright Frame	Load Case I					Load Case II				
	$P_{ex}$ (kips)	$K_x$	$P_e$ (kips)	$\frac{P_{cal}}{P_e}$	$\frac{P_{RMI}}{P_e}$	$P_{ex}$ (kips)	$K_x$	$P_e$ (kips)	$\frac{P_{cal}}{P_e}$	$\frac{P_{RMI}}{P_e}$
A1-C1-B1	70.98	1.197	65.93	0.59	0.61	31.48	1.198	30.30	0.76	0.79
A1-C1-B2	71.11	1.196	67.24	0.60	0.60	31.60	1.196	30.61	0.77	0.78
A2-C1-B1	71.29	1.195	46.46	0.69	0.63	31.59	1.196	28.66	0.68	0.69
A2-C1-B2	71.48	1.193	48.85	0.68	0.60	31.75	1.193	29.24	0.69	0.68
A3-C1-B1	71.10	1.196	34.49	0.79	0.62	31.59	1.196	27.99	0.62	0.57
A3-C1-B2	71.30	1.194	36.11	0.78	0.59	31.76	1.193	28.81	0.62	0.55
A1-C2-B1	41.98	1.198	41.16	0.70	0.64	18.85	1.192	18.61	0.84	0.82
A1-C2-B2	42.10	1.197	41.26	0.73	0.64	18.96	1.189	18.69	0.85	0.82
A2-C2-B1	42.22	1.195	36.71	0.66	0.54	18.94	1.189	18.34	0.77	0.71
A2-C2-B2	42.51	1.191	37.98	0.66	0.52	19.09	1.185	18.47	0.79	0.71
A3-C2-B1	42.10	1.197	25.63	0.80	0.52	18.94	1.189	18.41	0.69	0.60
A3-C2-B2	42.22	1.195	28.58	0.75	0.47	19.09	1.185	18.47	0.71	0.60
B1-C1-B1	71.01	1.197	64.23	0.61	0.63	31.49	1.198	30.08	0.77	0.80
B1-C1-B2	71.15	1.196	65.97	0.61	0.62	31.61	1.196	30.28	0.77	0.79
B2-C1-B1	70.45	1.202	45.61	0.70	0.63	31.56	1.197	28.17	0.70	0.70
B2-C1-B2	71.66	1.191	46.94	0.71	0.62	31.72	1.194	28.48	0.71	0.69
B3-C1-B1	71.78	1.190	33.53	0.82	0.64	31.58	1.197	27.50	0.64	0.58
B3-C1-B2	71.30	1.194	34.21	0.85	0.62	31.76	1.193	28.02	0.64	0.57
B1-C2-B1	42.01	1.198	41.06	0.67	0.65	18.85	1.192	18.39	0.84	0.83
B1-C2-B2	42.13	1.196	41.14	0.69	0.65	18.97	1.188	18.42	0.85	0.83
B2-C2-B1	42.34	1.193	33.23	0.71	0.59	18.92	1.190	17.92	0.77	0.73
B2-C2-B2	42.55	1.190	33.81	0.72	0.58	19.07	1.185	17.97	0.78	0.73
B3-C2-B1	42.11	1.196	24.43	0.83	0.55	18.95	1.189	18.41	0.67	0.60
B3-C2-B2	42.38	1.193	24.77	0.86	0.54	19.09	1.185	18.47	0.69	0.60
C1-C1-B1	71.22	1.195	61.20	0.62	0.60	31.56	1.197	30.01	0.76	0.76
C1-C1-B2	71.57	1.192	64.49	0.61	0.57	31.80	1.192	30.50	0.76	0.75
C2-C1-B1	71.41	1.194	45.00	0.71	0.59	31.61	1.196	28.09	0.69	0.66
C2-C1-B2	71.86	1.190	47.98	0.70	0.55	31.90	1.191	28.93	0.69	0.64
C3-C1-B1	71.45	1.193	34.33	0.82	0.57	31.60	1.196	27.90	0.63	0.54
C3-C1-B2	71.92	1.189	37.02	0.81	0.53	31.86	1.191	29.48	0.62	0.51
C1-C2-B1	42.23	1.195	40.85	0.64	0.60	18.92	1.190	18.49	0.81	0.79
C1-C2-B2	42.56	1.190	41.41	0.65	0.59	19.14	1.183	18.75	0.81	0.79
C2-C2-B1	42.39	1.193	32.19	0.71	0.56	18.97	1.188	18.06	0.74	0.69
C2-C2-B2	42.79	1.187	34.05	0.70	0.53	19.24	1.180	18.40	0.75	0.68
C3-C2-B1	42.42	1.192	25.29	0.81	0.47	18.96	1.189	18.57	0.66	0.56
C3-C2-B2	42.84	1.186	26.98	0.81	0.44	19.20	1.181	18.88	0.68	0.56
D1-C1-B1	70.84	1.198	57.15	0.64	0.64	31.37	1.200	29.48	0.75	0.77
D1-C1-B2	70.96	1.197	58.34	0.63	0.63	31.49	1.198	29.81	0.74	0.76
D2-C1-B1	70.89	1.198	41.70	0.72	0.63	31.37	1.200	27.16	0.68	0.68
D2-C1-B2	71.04	1.197	42.28	0.72	0.63	31.50	1.198	27.55	0.68	0.67
D3-C1-B1	70.91	1.198	31.76	0.84	0.62	31.36	1.201	26.30	0.64	0.57
D3-C1-B2	71.05	1.197	32.31	0.82	0.61	31.46	1.199	26.84	0.63	0.56
D1-C2-B1	41.85	1.200	39.04	0.63	0.62	18.73	1.196	18.21	0.79	0.80
D1-C2-B2	41.97	1.198	39.16	0.63	0.62	18.85	1.192	18.33	0.79	0.80
D2-C2-B1	41.89	1.200	29.25	0.72	0.62	18.73	1.196	17.59	0.72	0.70
D2-C2-B2	42.03	1.198	29.35	0.71	0.62	18.85	1.192	17.71	0.71	0.70
D3-C2-B1	41.90	1.199	22.90	0.82	0.52	18.72	1.197	18.10	0.64	0.58
D3-C2-B2	42.03	1.198	23.02	0.81	0.52	18.82	1.193	18.22	0.64	0.57

**Table 4.17** Values of Column  $K_x$  and  $P_e$  for Upright Frame E & F

Upright Frame	Load Case I					Load Case II				
	$P_{ex}$ (kips)	$K_x$	$P_e$ (kips)	$\frac{P_{cal}}{P_e}$	$\frac{P_{RMI}}{P_e}$	$P_{ex}$ (kips)	$K_x$	$P_e$ (kips)	$\frac{P_{cal}}{P_e}$	$\frac{P_{RMI}}{P_e}$
E1-C1-B1	71.00	1.197	33.12	0.82	0.52	31.48	1.198	27.52	0.64	0.50
E1-C1-B2	71.14	1.196	35.00	0.82	0.50	31.60	1.196	28.23	0.65	0.49
E2-C1-B1	70.44	1.202	22.01	0.92	0.49	31.51	1.198	20.18	0.75	0.46
E2-C1-B2	71.65	1.192	22.64	0.93	0.48	31.62	1.196	20.67	0.76	0.45
E3-C1-B1	71.72	1.191	17.68	0.98	0.43	31.58	1.197	15.46	0.88	0.45
E3-C1-B2	71.22	1.195	17.93	0.99	0.43	31.76	1.193	15.69	0.89	0.44
E1-C2-B1	42.00	1.198	22.75	0.93	0.44	18.85	1.192	17.96	0.72	0.54
E1-C2-B2	42.12	1.196	26.72	0.81	0.38	18.97	1.189	18.03	0.73	0.54
E2-C2-B1	42.33	1.193	16.50	0.97	0.33	18.85	1.192	14.87	0.76	0.36
E2-C2-B2	42.54	1.190	17.62	0.93	0.31	18.95	1.189	15.03	0.77	0.36
E3-C2-B1	42.06	1.197	12.45	1.00	0.27	18.94	1.189	11.62	0.89	0.29
E3-C2-B2	42.34	1.193	13.60	1.00	0.25	19.08	1.185	12.02	0.88	0.28
F1-C1-B1	70.72	1.199	10.85	1.00	1.00	31.25	1.203	9.11	1.00	1.00
F1-C1-B2	70.72	1.199	17.97	1.00	1.00	31.25	1.203	15.36	1.00	1.00
F2-C1-B1	70.72	1.199	9.56	1.00	1.00	31.25	1.203	8.03	1.00	1.00
F2-C1-B2	70.72	1.199	15.16	1.00	1.00	31.25	1.203	12.99	1.00	1.00
F3-C1-B1	70.72	1.199	9.71	1.00	1.00	31.25	1.203	8.24	1.00	1.00
F3-C1-B2	70.72	1.199	14.73	1.00	1.00	31.25	1.203	12.83	1.00	1.00
F1-C2-B1	41.74	1.202	5.75	1.00	1.00	18.62	1.200	5.00	1.00	1.00
F1-C2-B2	41.74	1.202	9.88	1.00	1.00	18.62	1.200	8.66	1.00	1.00
F2-C2-B1	41.74	1.202	4.66	1.00	1.00	18.62	1.200	4.11	1.00	1.00
F2-C2-B2	41.74	1.202	7.52	1.00	1.00	18.62	1.200	6.86	1.00	1.00
F3-C2-B1	41.74	1.202	4.20	1.00	1.00	18.62	1.200	3.75	1.00	1.00
F3-C2-B2	41.74	1.202	6.21	1.00	1.00	18.62	1.200	5.67	1.00	1.00

Calculation of the torsional-flexural buckling load  $P_{cal}$  by using the buckling equation with  $K_t$  from Tables 4.13 through 4.15, and  $K_x$  from Tables 4.16 and 4.17 was carried out. And calculation of the torsional-flexural buckling load  $P_{RMI}$  by using the buckling equation with  $K_t = 0.8$ , and  $K_x$  from Tables 4.16 and 4.17 was also carried out. As shown in Tables 4.16 and 4.17 the torsional-flexural buckling values calculated from the AISI torsional-flexural buckling equation in all cases are conservative compared with the finite element results.

#### 4.5 EFFECTIVE DESIGN AREA

The effective design width equations of the AISI specifications are not applicable for designing rack columns, because of the presence of perforations. Stub-column tests are instead required in the RMI specification to account for the member local behavior. By measuring the axial load and the corresponding axial shortening in the stub-column test, the relationship between the stress on the effective section  $F_n$  and the effective area  $A_e$  can be obtained; however, for tests where only the ultimate strength of the stub-column is measured, the following effective design area equation of the RMI specification must be used

$$\frac{A_e}{A_{net\ min}} = 1 - (1 - Q) \left( \frac{F_n}{F_y} \right)^Q \quad (4.1)$$

where

$$Q = \frac{\text{ultimate strength of stub-column}}{F_y A_{net\ min}}$$

The following studies were carried out to verify or modify this effective design area equation.

#### 4.5.1 Stiffened elements

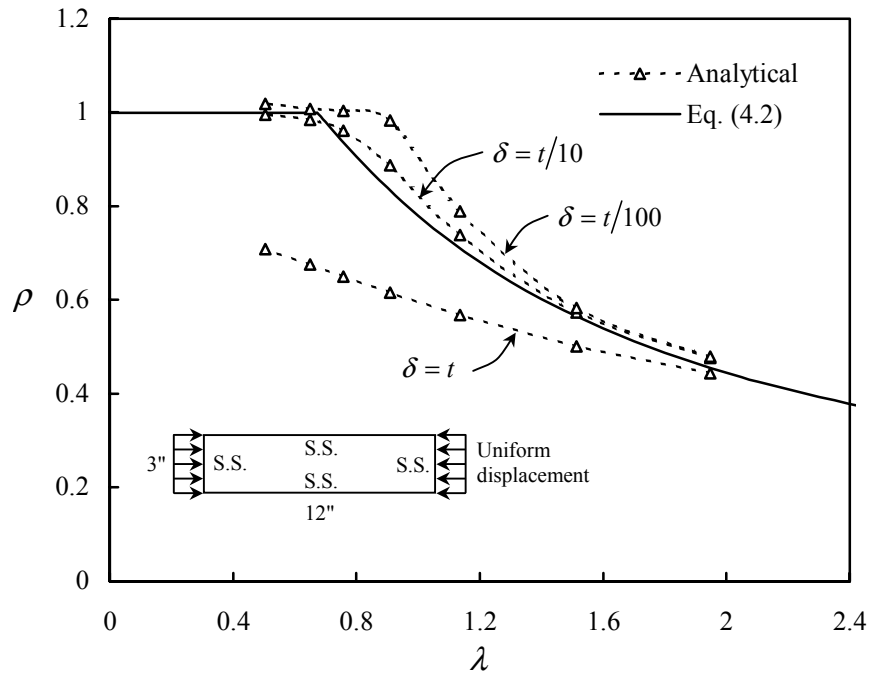
In order to evaluate the effective design area equation, finite element simulations of stub-column tests were carried out to obtain the relationship between  $F_n$  and  $A_e$ . This was then compared to those relationships between  $F_n$  and  $A_e$  suggested by Eq. (4.1). However, before this study was carried out, finite element modeling assumptions, in particularly the initial geometric imperfection assumption, had to first be verified.

Precise data of the distribution on the initial geometric imperfection was not available. Imperfection was therefore introduced by using the critical buckling mode shape obtained from buckling analysis. Finite element studies of a simply supported rectangular plate under uniform compression displacement as shown in Fig. 4.16 has shown that when the maximum magnitude of imperfection  $\delta$  is assumed equal to one tenth of the element thickness, the analytical results tend to agree with the well known effective design width equation

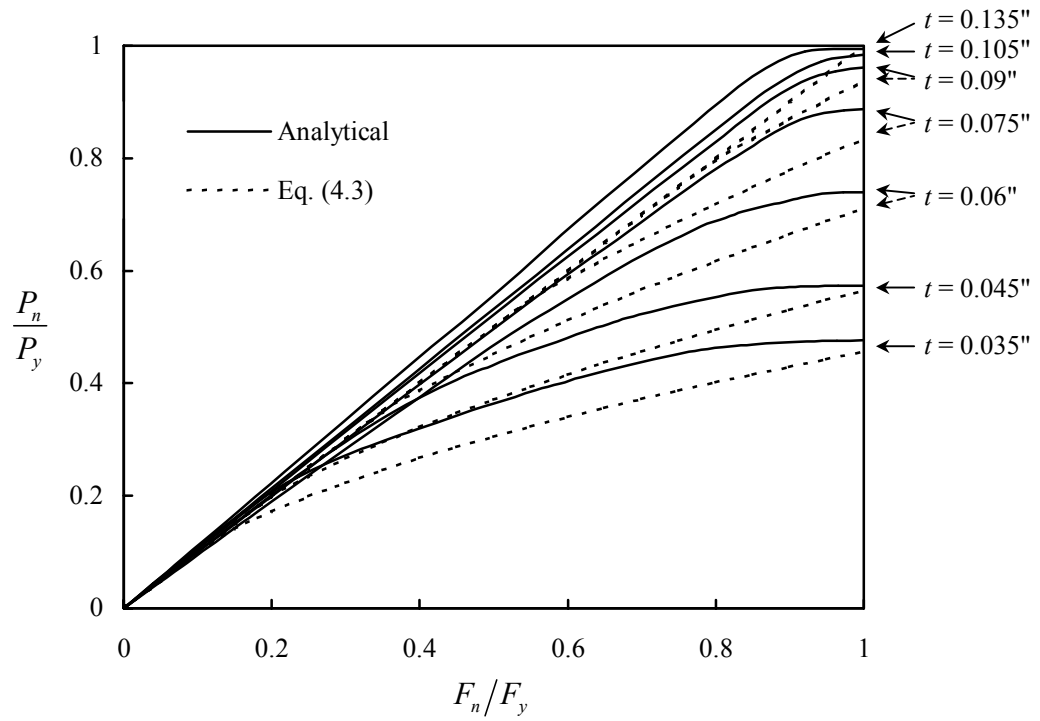
$$\rho = (1 - 0.22/\lambda)/\lambda \text{ for } \lambda > 0.673 \text{ otherwise } \rho = 1 \quad (4.2)$$

This initial geometric imperfection assumption seems reasonable and therefore was used in subsequent finite element studies. The material model used in the above finite element study was elastic-plastic with strain hardening  $F_y = 55$  ksi,  $F_u = 70$  ksi,  $E = 29500$  ksi,  $E_{st} = E/45$ ,  $\nu = 0.3$ , and  $e_{st}$  is 15 times the maximum elastic strain.

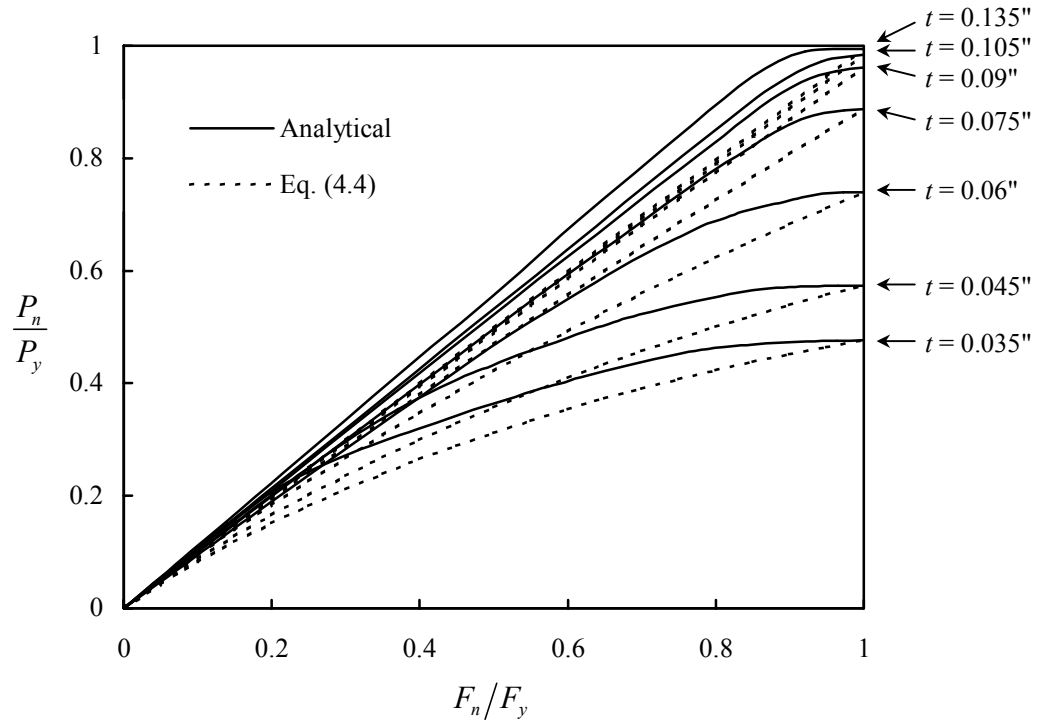
Similar to the stub-column test, by measuring the axial load and the corresponding axial shortening of the stiffened element, the relationship between  $F_n$  and  $A_e$  was obtained. With these values known the relationship between  $P_n/P_y$  and  $F_n/F_y$  could be found. In Fig. 4.17, the analytical results are compared to the following equation



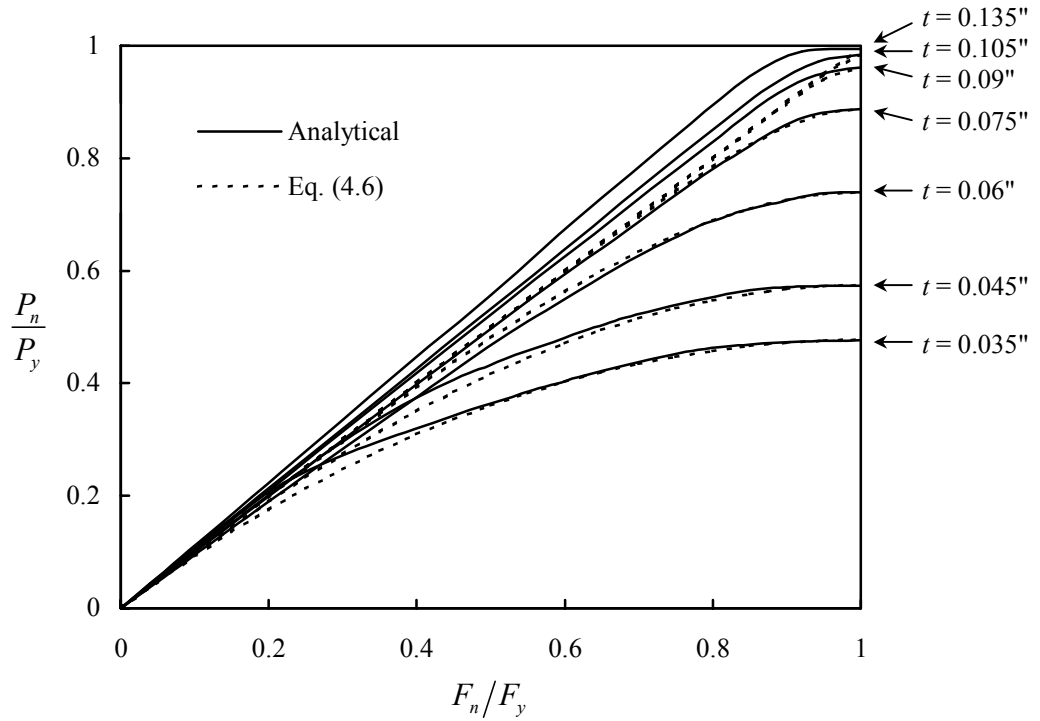
**Figure 4.16** Effect of initial geometric imperfection on effective design width



**Figure 4.17** Stiffened compression elements - Correlation between effective design width equation and analytical results



**Figure 4.18** Stiffened compression elements - Correlation between RMI effective design area equation and analytical results



**Figure 4.19** Stiffened compression elements - Correlation between proposed effective design area equation and analytical results

$$\frac{P_n}{P_y} = \rho \frac{F_n}{F_y} \quad (4.3)$$

where  $\rho$  is computed according to Eq. (4.2). As can be seen in Fig. 4.17, at the ultimate load ( $P_n$  when  $F_n = F_y$ ) the analytical results agree well with the effective design width equation because of the initial geometric imperfection calibration. However it was found that at design loads ( $P_n$  when  $F_n < F_y$ ) the effective design width equation is quite conservative compared to the analytical solution. In Fig. 4.18, the analytical results are compared to the following equation

$$\frac{P_n}{P_y} = \frac{F_n}{F_y} \left( 1 - (1-Q) \left( \frac{F_n}{F_y} \right)^Q \right) \quad (4.4)$$

which is the RMI effective design area equation Eq. (4.1) multiplied by  $F_n/F_y$  to give the relationship between  $P_n/P_y$  and  $F_n/F_y$ . The  $Q$  factor is obtained from the finite element solution; therefore, analytical results and Eq. (4.4) match at the ultimate load. It was found that at design loads the RMI effective design area equation is also quite conservative compared to the analytical solution. The following new effective design area equation is therefore proposed to improve the results.

$$\frac{A_e}{A_{net\ min}} = 1 - (1-Q) \left( \frac{F_n}{F_y} \right)^{\frac{Q}{1-Q}} \quad (4.5)$$

This proposed equation was developed by modifying the exponential term in Eq. (4.1) so that the results will agree better with the analytical solutions. By multiplying this proposed equation with  $F_n/F_y$  the new relationship between  $P_n/P_y$  and  $F_n/F_y$  is obtained as follows

$$\frac{P_n}{P_y} = \frac{F_n}{F_y} \left( 1 - (1-Q) \left( \frac{F_n}{F_y} \right)^{\frac{Q}{1-Q}} \right) \quad (4.6)$$

In Fig. 4.19, the analytical results are compared to the above equation. As can be seen improvement has been made. At the same stress levels Eq. (4.5) simply predicts a larger effective design area than Eq. (4.1) as shown in Fig. 4.20; therefore Eq. (4.6) will give a higher design load than Eq. (4.4) as shown in Fig. 4.21.

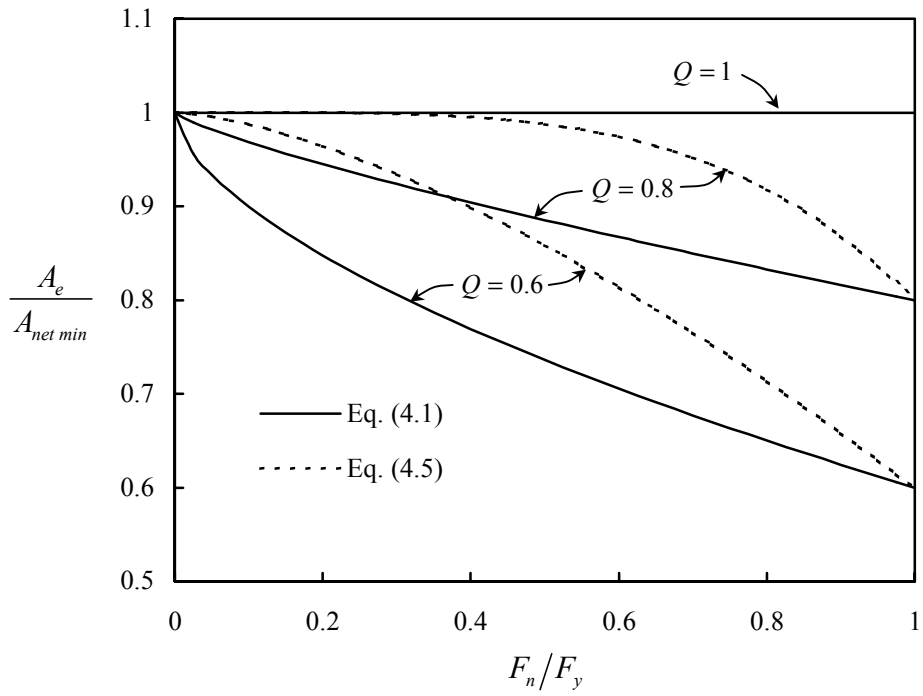
The results in this section indicate that unperforated compression elements should be designed by using Eq. (4.5), where the  $Q$  factor can be easily computed from Eq. (4.2). If this proposed procedure is used the element design curve will be altered from Eq. (4.2) as shown in Fig. 4.22. Unperforated members and perforated members are studied in the next sections.

#### **4.5.2 Unperforated members**

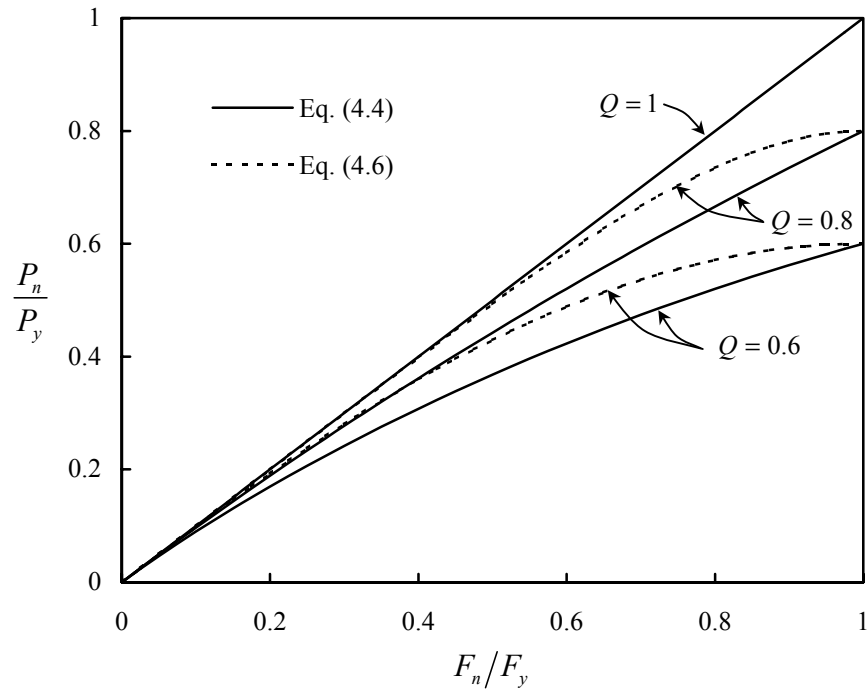
Finite element simulations of stub-column tests for unperforated sections were carried out in this study to evaluate the current AISI column design procedure and the RMI effective design area equation. The finite element analysis considers both geometric and material nonlinearities; residual stresses and geometric imperfections are also included in the model. The  $Q$  factor obtained from the AISI design approach and from the finite element method is compared in Table 4.18. Cold-formed steel member strength designed according to AISI specification was obtained by using the computer program CU-EWA shown in Appendix H.

It was found that when sections are thin, the AISI design approach is unconservative compared to the analytical results. The reason for this is that when the elements are thin and the radius of the corners in the section is large, local buckling calculations based on the element flat width is unconservative. This problem can be corrected by using a modified AISI design approach as shown in Fig. 4.23. In the modified approach the element width is based on the centerline to centerline distance

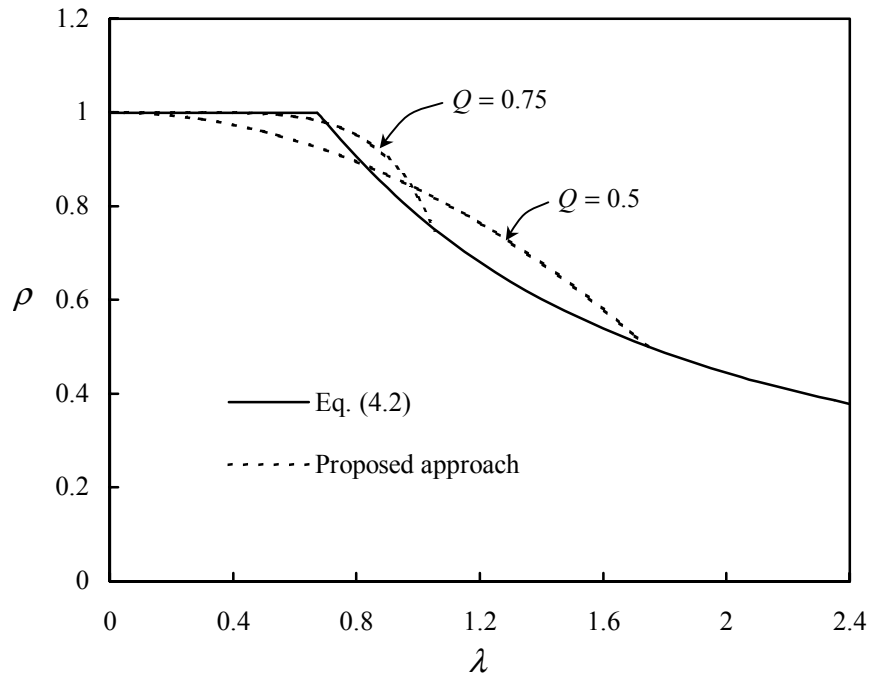




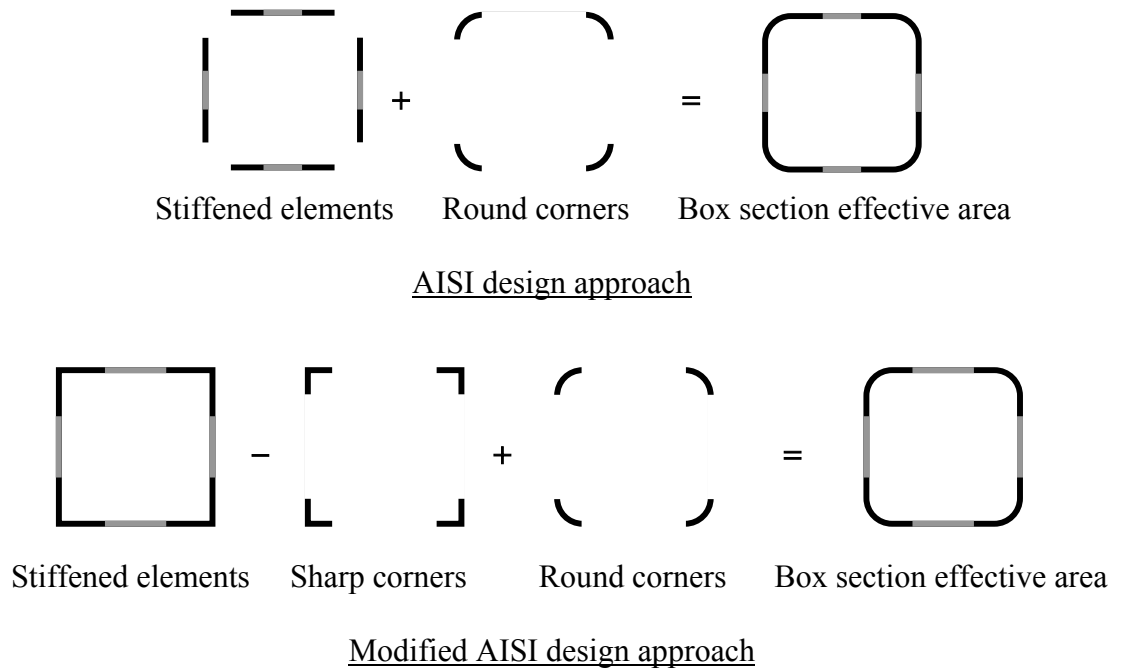
**Figure 4.20** Comparison between the RMI effective design area equation and the proposed equation



**Figure 4.21** Comparison between the RMI effective design area equation and the proposed equation

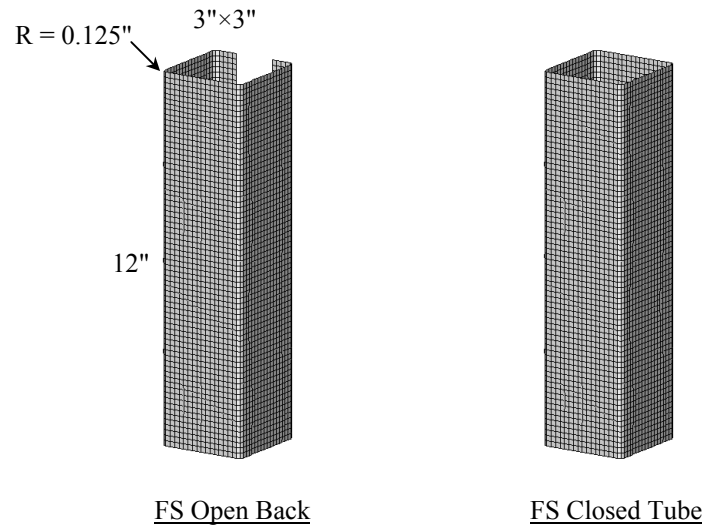


**Figure 4.22** Comparison between the AISI effective width approach and the proposed approach



**Figure 4.23** Comparison between the AISI design approach and the modified AISI design approach

**Table 4.18** Comparison Among the AISI Design Approach, the Modified AISI Design Approach, and the Analytical Results



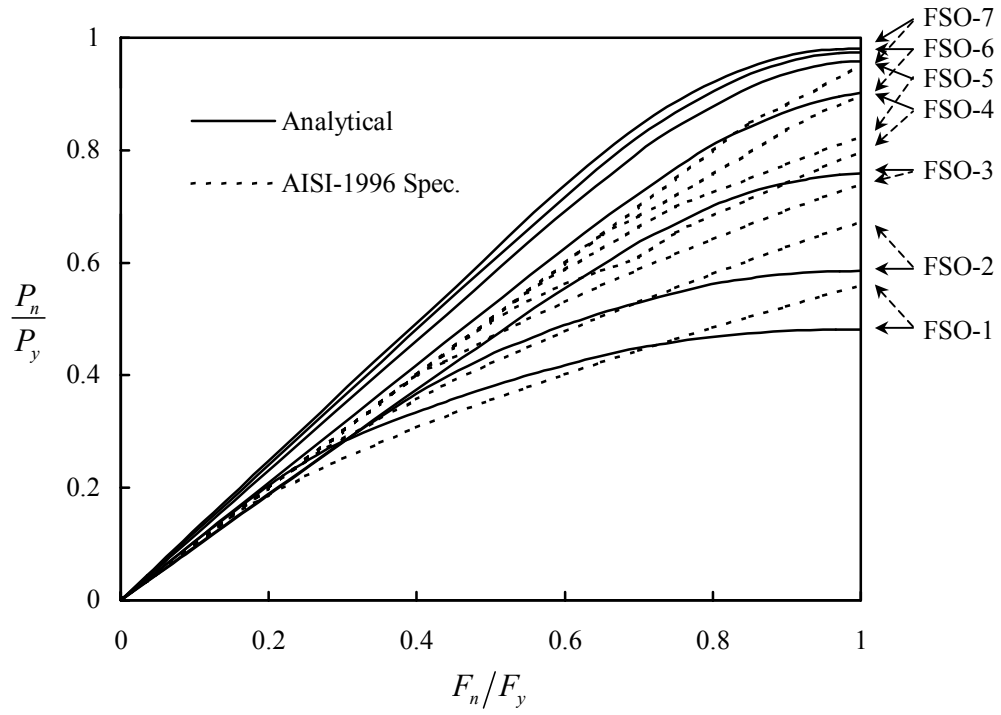
Section		$t$ (in.)	$Q_{\text{AISI}}$	$Q_{\text{modified}}$	$Q_{\text{FEM}}$
FS Open Back	FSO-1	0.035	0.559	0.460	0.482
	FSO-2	0.045	0.673	0.576	0.585
	FSO-3	0.06	0.739	0.722	0.759
	FSO-4	0.075	0.797	0.775	0.902
	FSO-5	0.09	0.823	0.822	0.958
	FSO-6	0.105	0.896	0.852	0.973
	FSO-7	0.135	0.952	0.939	0.981
FS Closed Tube	FSC-1	0.035	0.545	0.452	0.463
	FSC-2	0.045	0.658	0.566	0.564
	FSC-3	0.06	0.806	0.719	0.736
	FSC-4	0.075	0.928	0.850	0.889
	FSC-5	0.09	1	0.957	0.961
	FSC-6	0.105	1	1	0.983
	FSC-7	0.135	1	1	0.995

between the supporting elements and hence will be larger, the section properties are based on the round corners and hence the design will be more conservative agreeing better with the analytical solution as shown in Table 4.18.

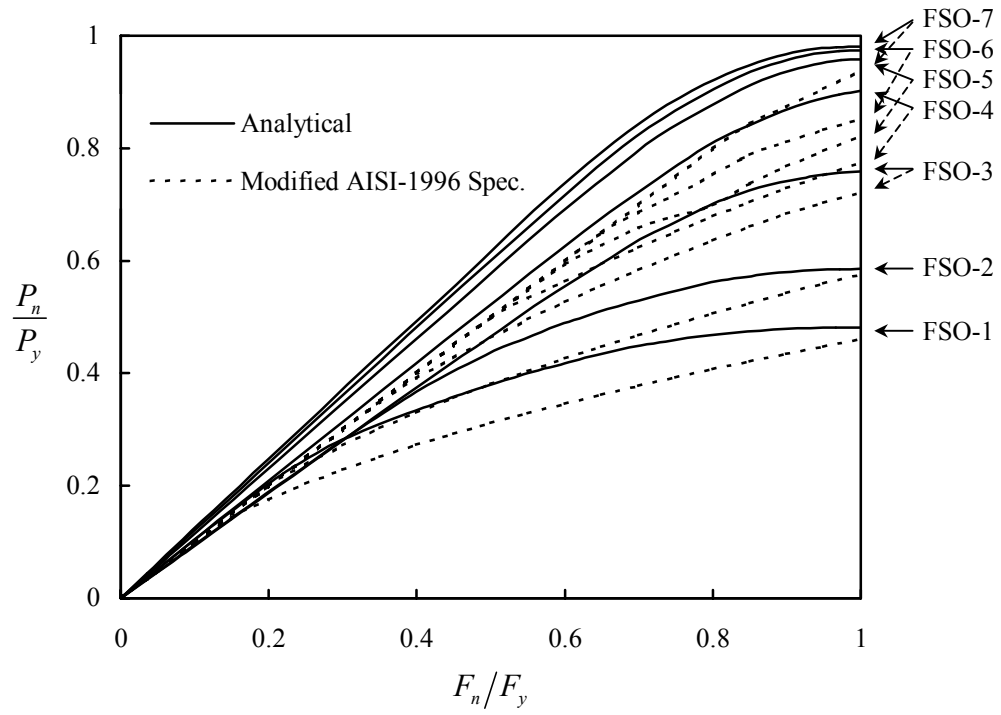
Five methods were used to compute the relationship between  $P_n/P_y$  and  $F_n/F_y$ . The first method uses the finite element simulation of the stub-column test, the second method uses the AISI design approach, the third method uses the modified AISI design approach, the fourth method uses the RMI effective design area equation, and the fifth method uses the proposed effective design area equation.

In Figs. 4.24 and 4.28, the finite element results are compared to the AISI design approach. In Figs. 4.25 and 4.29, the finite element results are compared to the modified AISI design approach. When the modified AISI design approach was used, results similar to the previous stiffened elements study were found; that is, at the ultimate load the analytical results agrees well with the design approach; however at design loads the design approach is quite conservative compared to the analytical solution.

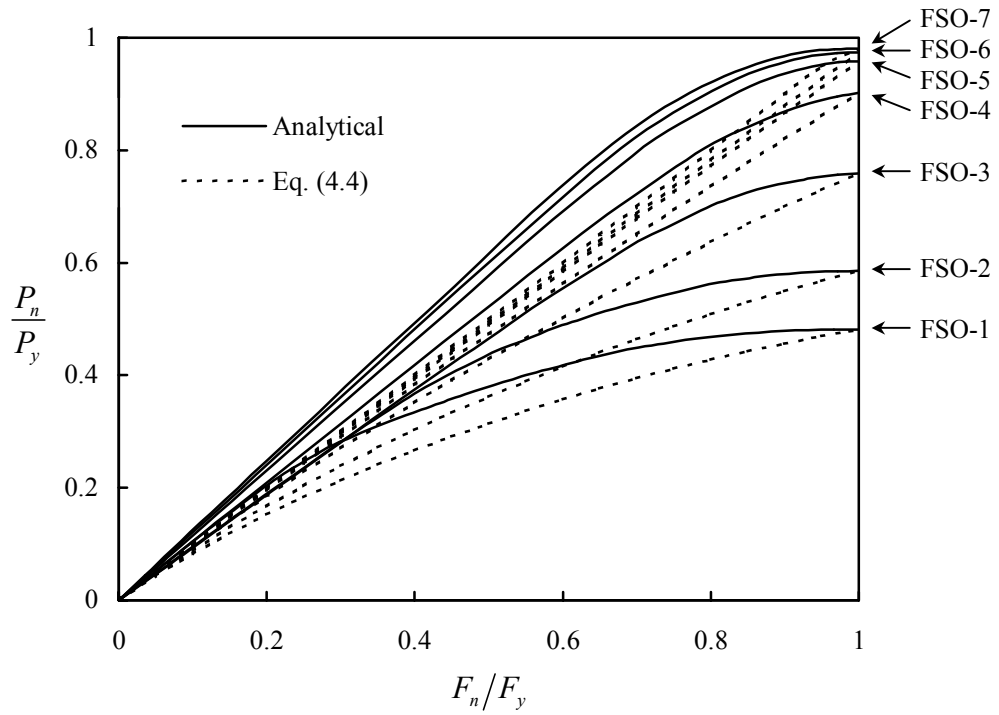
In Figs. 4.26 and 4.30, the finite element results are compared to the RMI effective design area equation. In Figs. 4.27 and 4.31, the finite element results are compared to the proposed effective design area equation. As can be seen from these figures improvement has been made for the case of thin-walled sections. The results are still quite conservative for thick-walled sections because of the material strain hardening, which was included in the finite element model but is not considered in the design since the component elements are not fully effective.



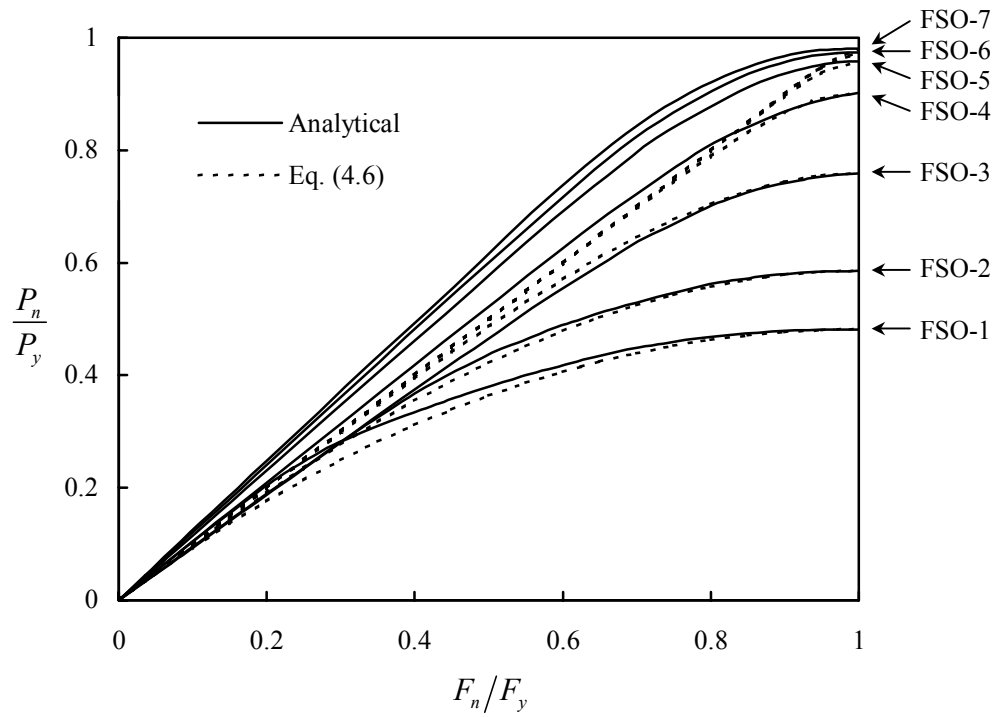
**Figure 4.24** Section FS Open Back - Correlation between AISI design approach and analytical results



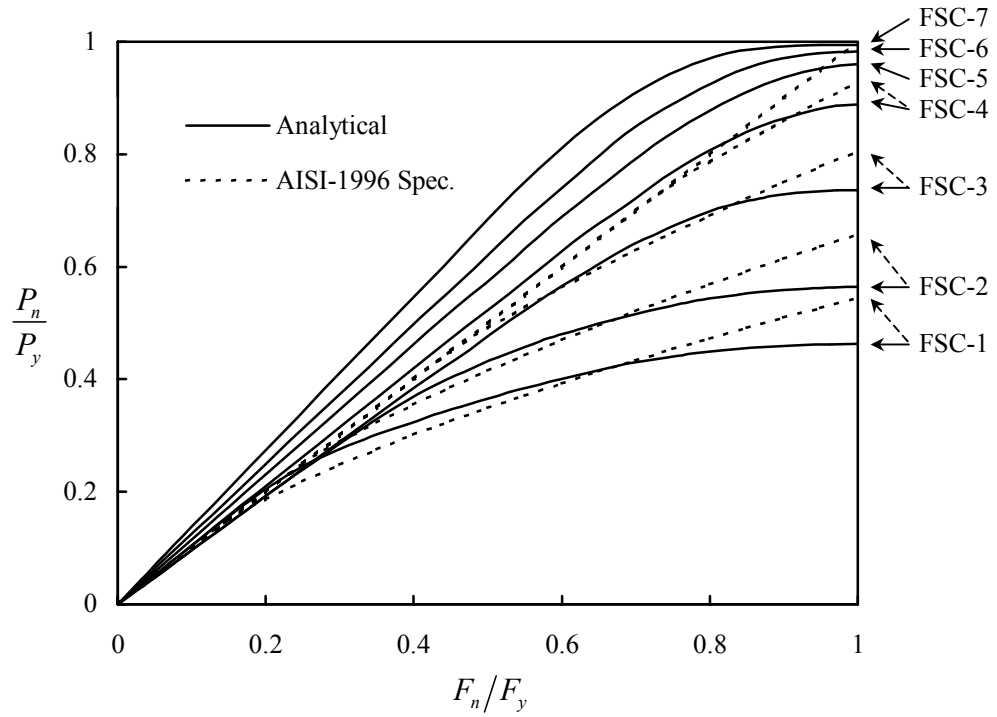
**Figure 4.25** Section FS Open Back - Correlation between modified AISI design approach and analytical results



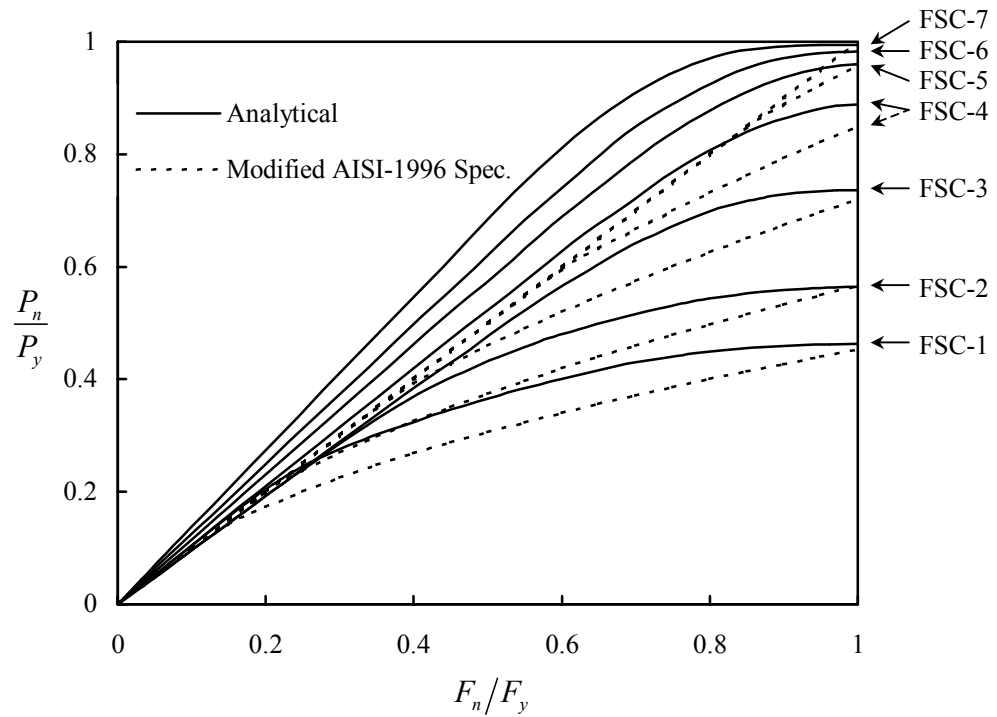
**Figure 4.26** Section FS Open Back - Correlation between RMI effective design area equation and analytical results



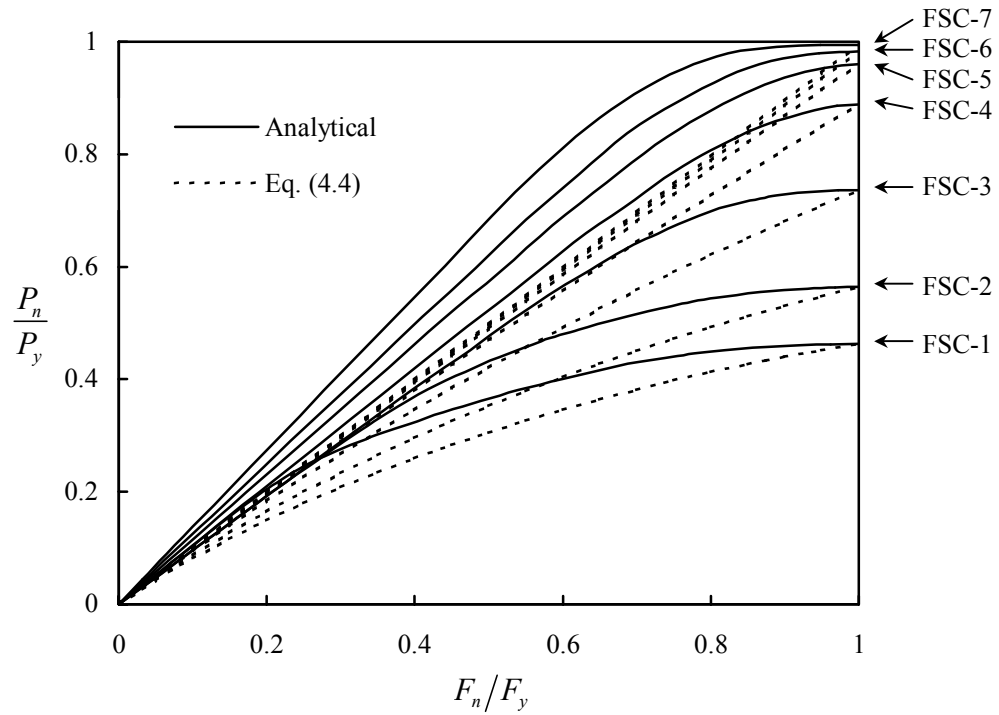
**Figure 4.27** Section FS Open Back - Correlation between proposed effective design area equation and analytical results



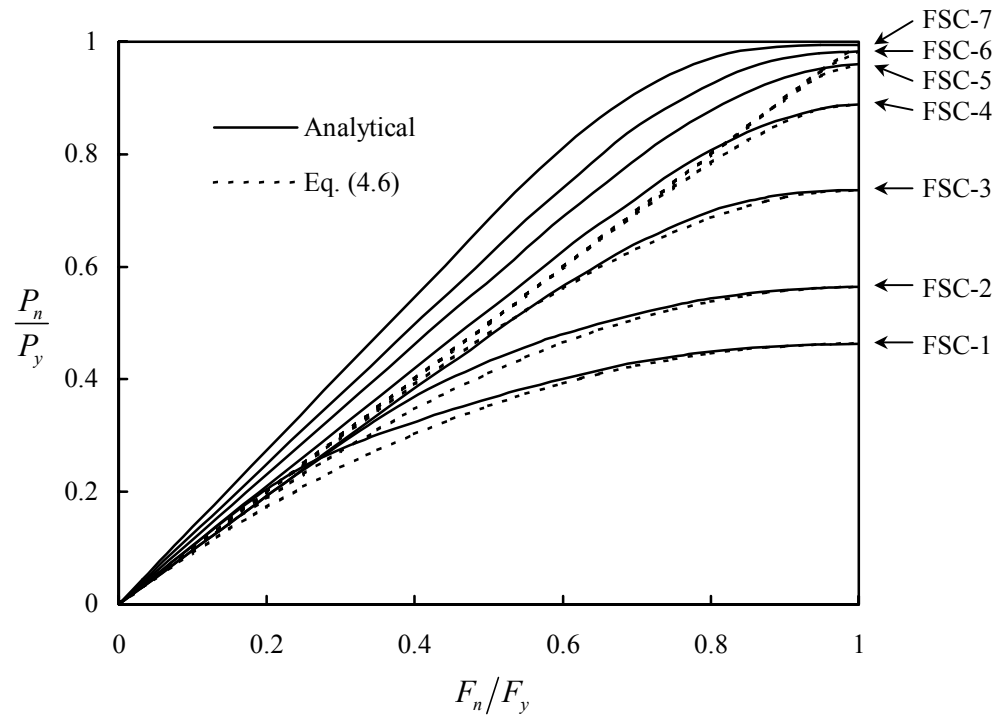
**Figure 4.28** Section FS Closed Tube - Correlation between AISI design approach and analytical results



**Figure 4.29** Section FS Closed Tube - Correlation between modified AISI design approach and analytical results



**Figure 4.30** Section FS Closed Tube - Correlation between RMI effective design area equation and analytical results



**Figure 4.31** Section FS Closed Tube - Correlation between proposed effective design area equation and analytical results



### 4.5.3 Perforated members

Finite element simulations of stub-column tests for perforated sections were carried out in this study to evaluate the RMI effective design area equation. The  $Q$  factor obtained from physical stub-column tests (provided by Unarco Material Handling) and from the finite element method is compared in Table 4.19.

Three methods were used to compute the relationship between  $P_n/P_y$  and  $F_n/F_y$ . The first method uses the finite element simulation of the stub-column test, the second method uses the RMI effective design area equation, and the third method uses the proposed effective design area equation.

In Figs. 4.32, 4.34, 4.36, 4.38, and 4.40, the finite element results are compared to the RMI effective design area equation. In Figs. 4.33, 4.35, 4.37, 4.39, and 4.41, the finite element results are compared to the proposed effective design area equation. As can be seen from these figures, the design is more efficient if the proposed equation is used.

Similar changes are also recommended for the effective section modulus equation, which is used for the determination of the member flexural strength. From the current RMI equation

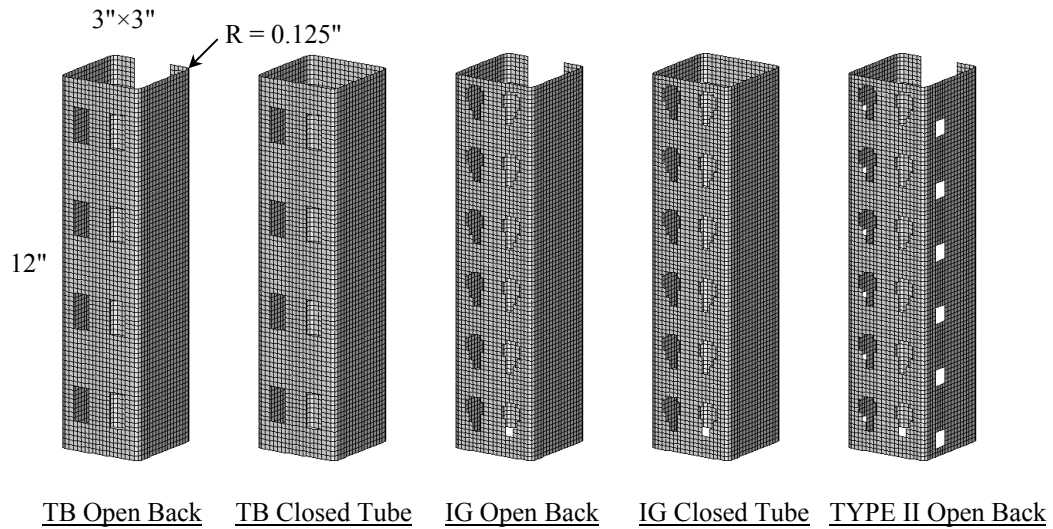
$$\frac{S_c}{S_{net\ min}} = 1 - \frac{(1-Q)}{2} \left( \frac{M_c/S_f}{F_y} \right)^Q \quad (4.7)$$

to the following proposed effective section modulus equation

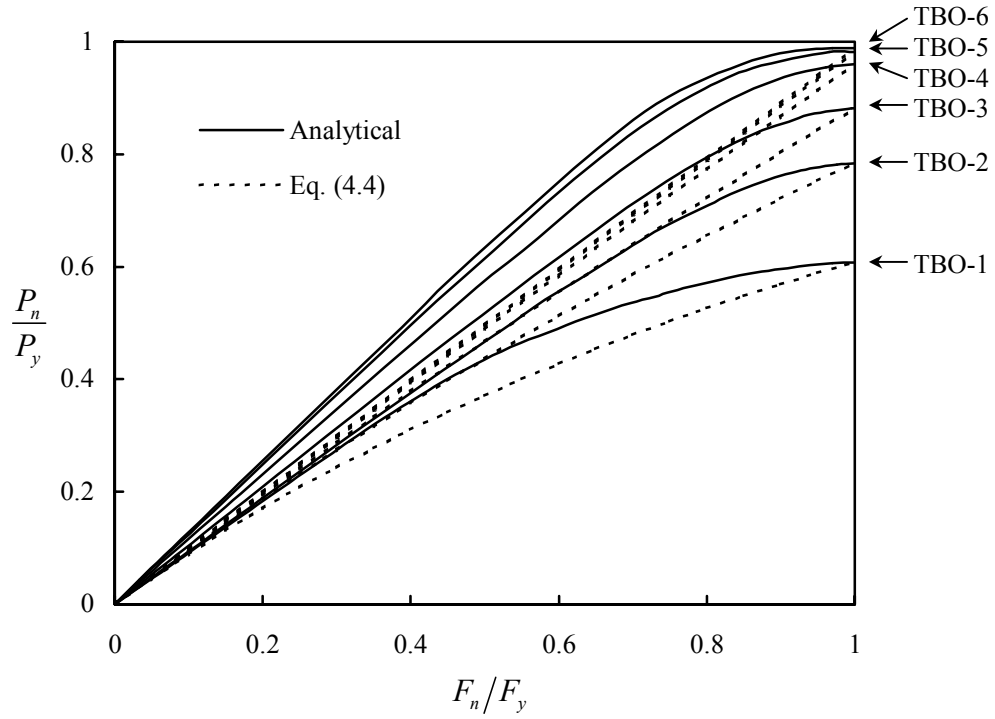
$$\frac{S_c}{S_{net\ min}} = 1 - \frac{(1-Q)}{2} \left( \frac{M_c/S_f}{F_y} \right)^{\frac{Q}{1-Q}} \quad (4.8)$$

By using the proposed equations (Eqs. (4.5) and (4.8)) the member design strength will increase from the current design specification as shown in Figs. 4.42 and 4.43.

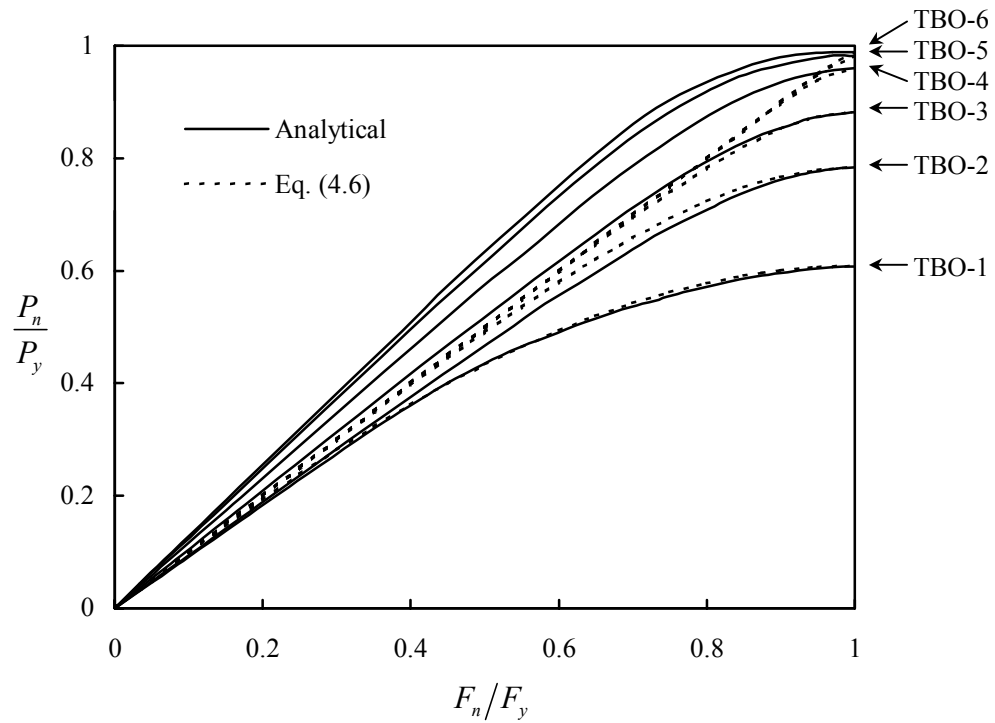
**Table 4.19** Stub-Column Tests and Analytical Results



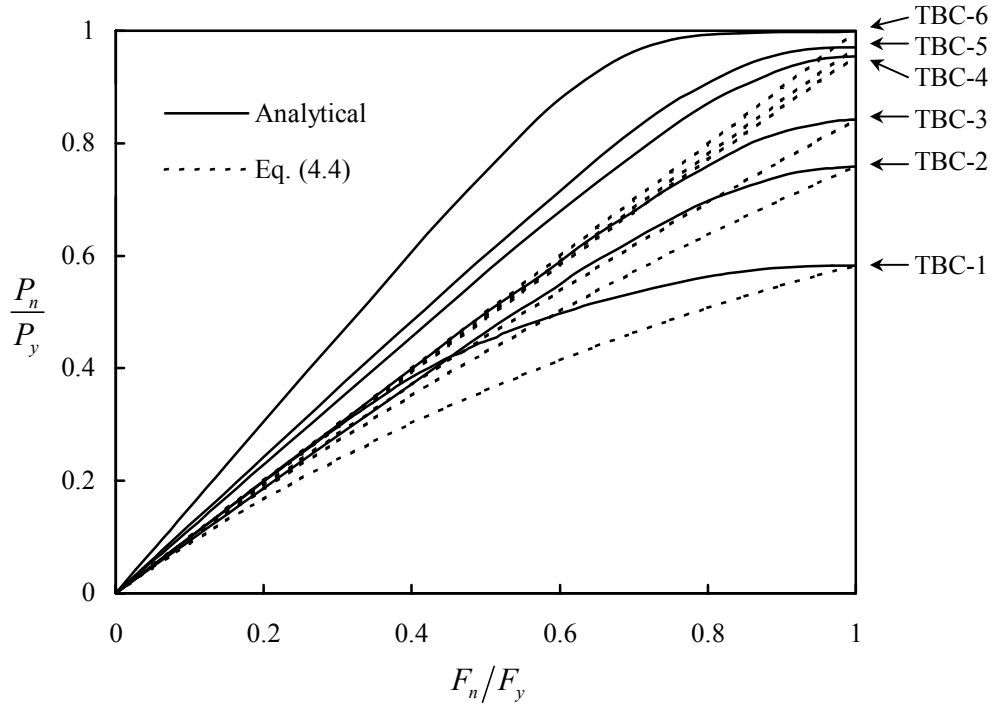
Section		<i>t</i> (in.)	<i>F<sub>y</sub></i> (ksi)	<i>F<sub>u</sub></i> (ksi)	<i>Q<sub>TEST</sub></i>			<i>Q<sub>FEM</sub></i>
					max	min	mean	
TB Open Back	TBO-1	0.045	55	70	-	-	-	0.608
	TBO-2	0.06	55	70	-	-	-	0.784
	TBO-3	0.069	54.9	62.6	0.888	0.776	0.832	0.882
	TBO-4	0.081	51.2	69.5	1.067	0.987	1.035	0.960
	TBO-5	0.1	54.2	64	1.060	0.990	1.030	0.982
	TBO-6	0.123	59.6	78.4	1.169	1.021	1.100	0.989
TB Closed Tube	TBC-1	0.045	55	70	-	-	-	0.583
	TBC-2	0.06	55	70	-	-	-	0.759
	TBC-3	0.067	55	70	-	-	-	0.842
	TBC-4	0.082	53.9	69.2	0.991	0.981	0.986	0.955
	TBC-5	0.09	57.4	63	0.983	0.977	0.981	0.970
	TBC-6	0.122	61.3	68.3	1.081	1.073	1.076	0.998
IG Open Back	IGO-1	0.045	55	70	-	-	-	0.613
	IGO-2	0.06	55	70	-	-	-	0.799
	IGO-3	0.067	55	70	-	-	-	0.873
	IGO-4	0.085	63.8	73.2	1.001	0.818	0.921	0.951
	IGO-5	0.099	56.3	65.4	1.028	0.972	0.997	0.989
	IGO-6	0.126	55	70	-	-	-	0.997
IG Closed Tube	IGC-1	0.045	55	70	-	-	-	0.587
	IGC-2	0.06	55	70	-	-	-	0.765
	IGC-3	0.067	55	70	-	-	-	0.844
	IGC-4	0.082	55.7	75.3	0.933	0.925	0.929	0.952
	IGC-5	0.1	55	70	-	-	-	0.995
	IGC-6	0.124	58.3	68	1.188	1.154	1.173	1.007
TYPE II Open Back	T2O-1	0.045	55	70	-	-	-	0.592
	T2O-2	0.06	55	70	-	-	-	0.752
	T2O-3	0.067	55	70	-	-	-	0.813
	T2O-4	0.083	56.8	75	1.009	0.855	0.918	0.880
	T2O-5	0.1	56.2	62.8	1.044	0.933	0.984	0.896
	T2O-6	0.126	55	70	-	-	-	0.902



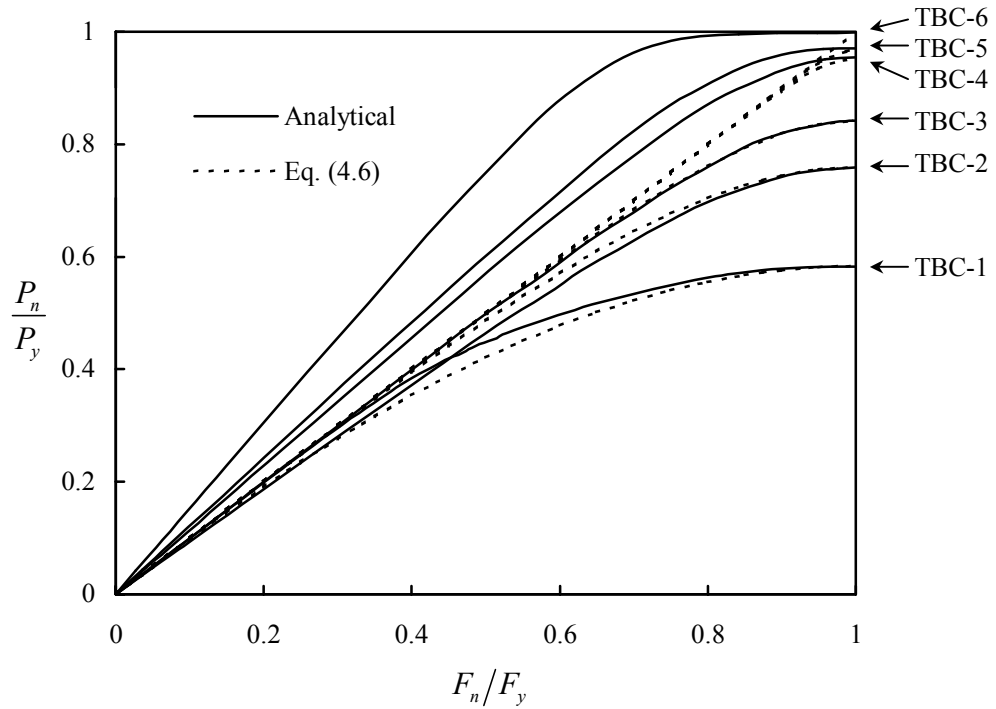
**Figure 4.32** Section TB Open Back - Correlation between RMI effective design area equation and analytical results



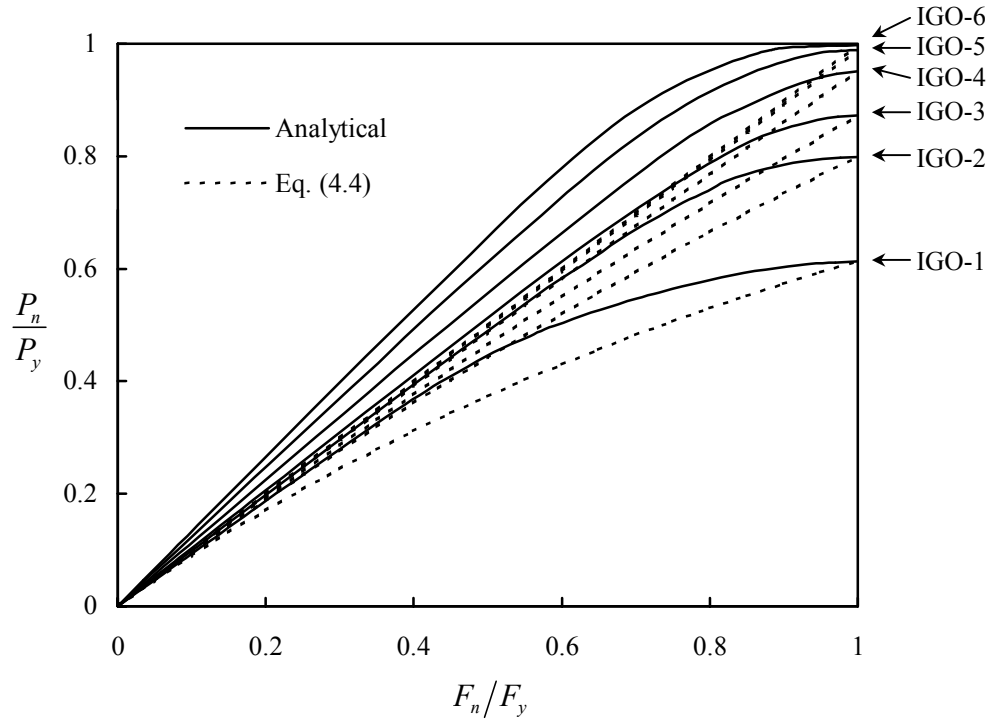
**Figure 4.33** Section TB Open Back - Correlation between proposed effective design area equation and analytical results



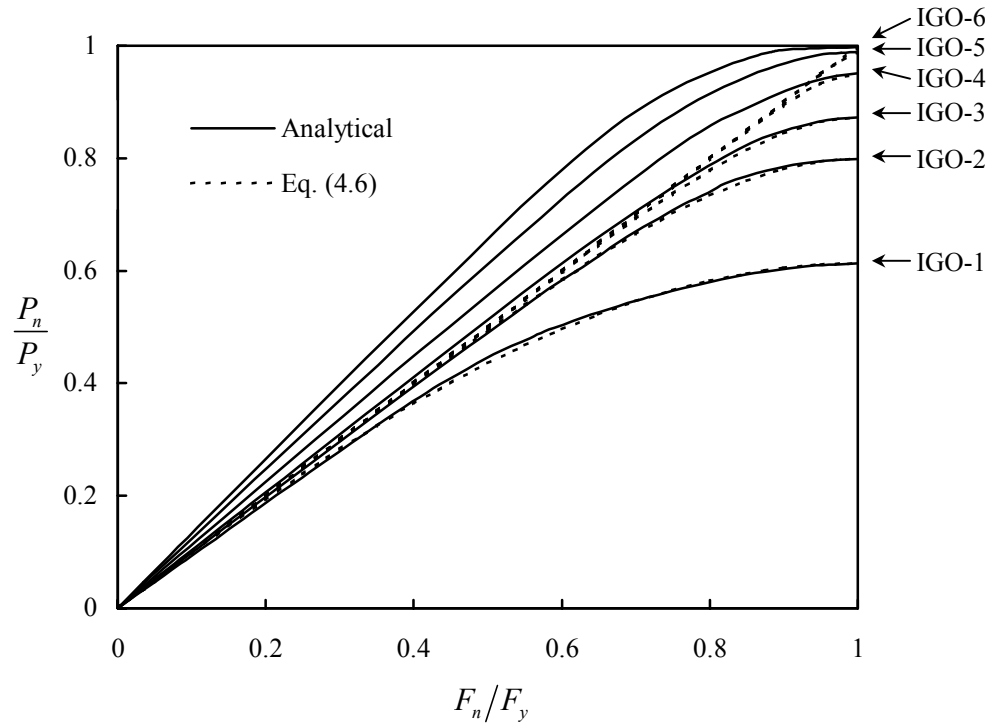
**Figure 4.34** Section TB Closed Tube - Correlation between RMI effective design area equation and analytical results



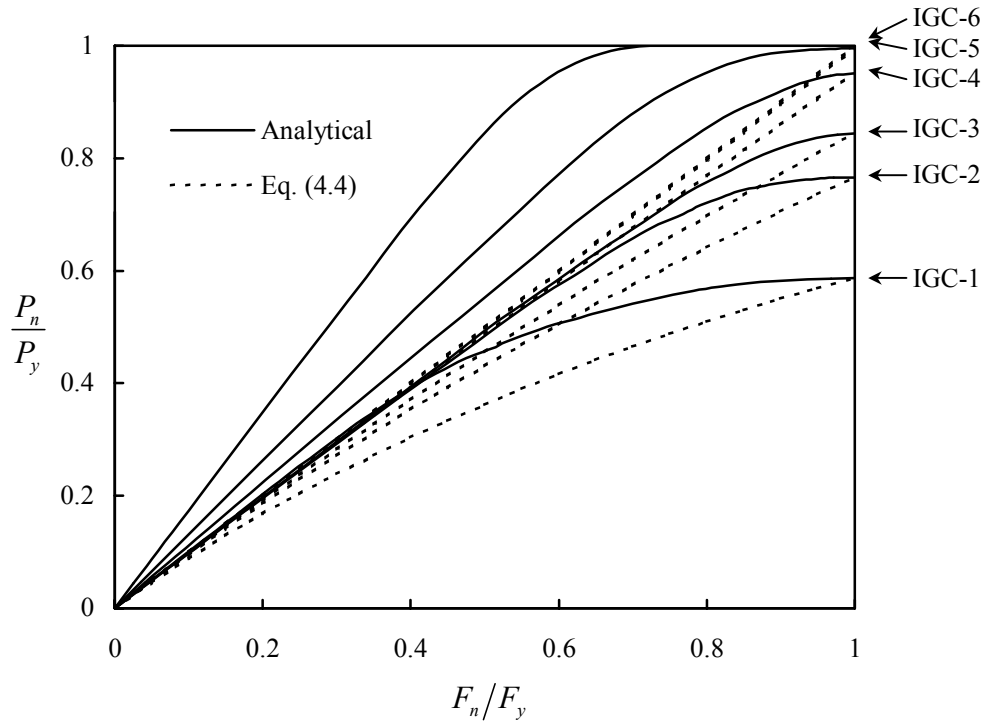
**Figure 4.35** Section TB Closed Tube - Correlation between proposed effective design area equation and analytical results



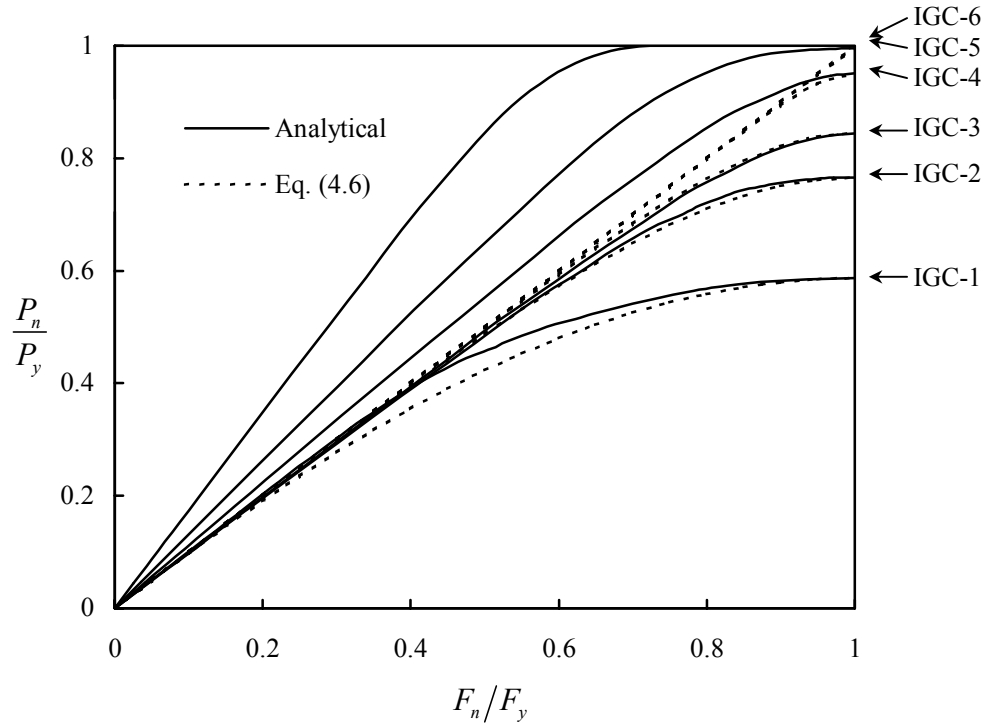
**Figure 4.36** Section IG Open Back - Correlation between RMI effective design area equation and analytical results



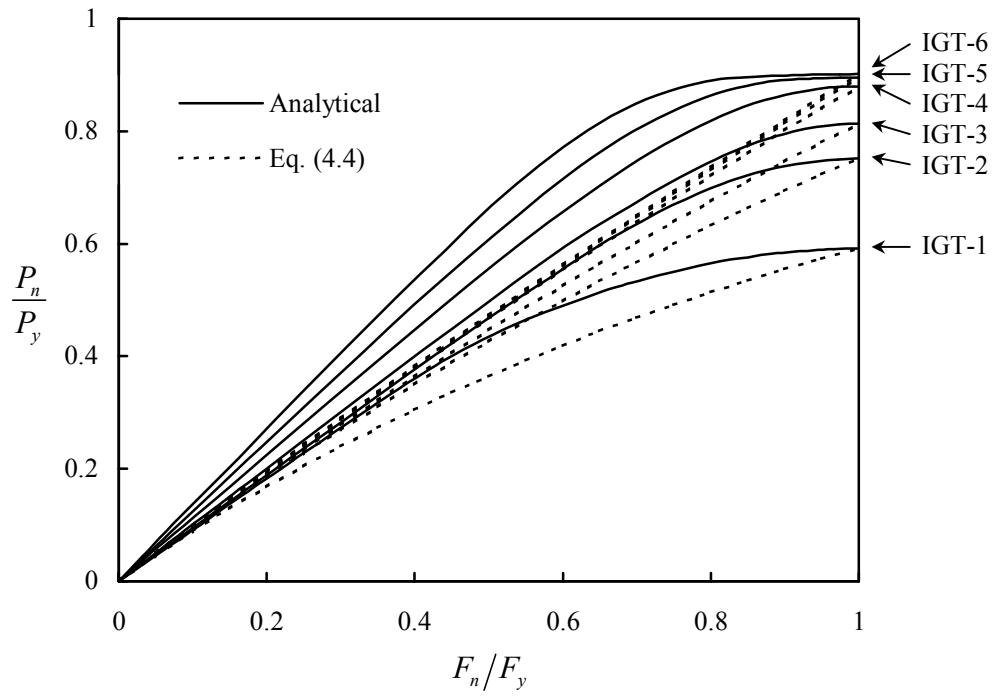
**Figure 4.37** Section IG Open Back - Correlation between proposed effective design area equation and analytical results



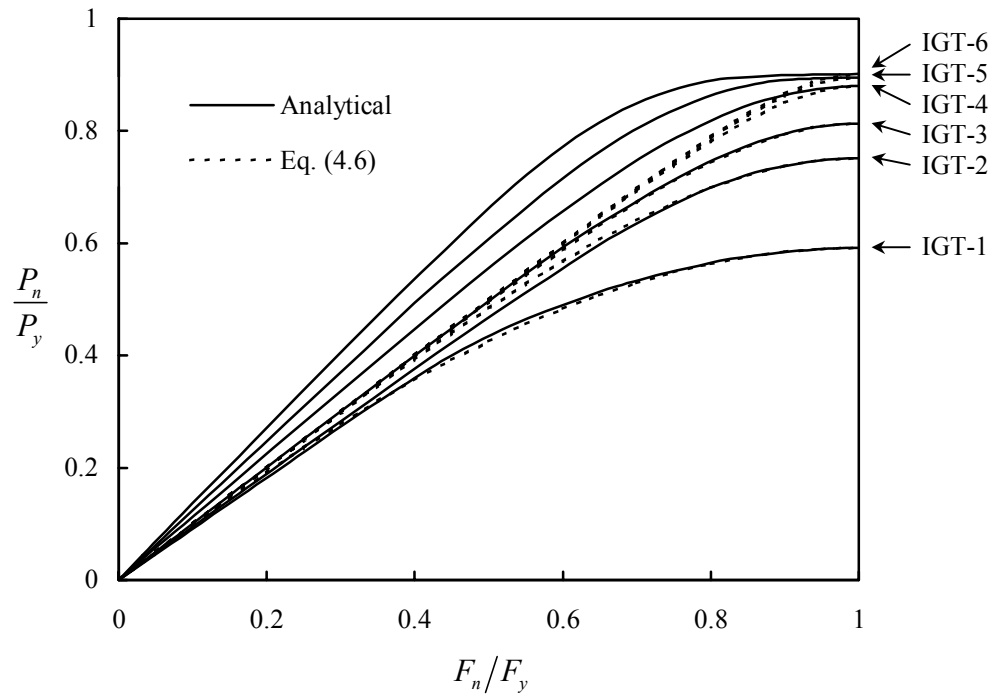
**Figure 4.38** Section IG Closed Tube - Correlation between RMI effective design area equation and analytical results



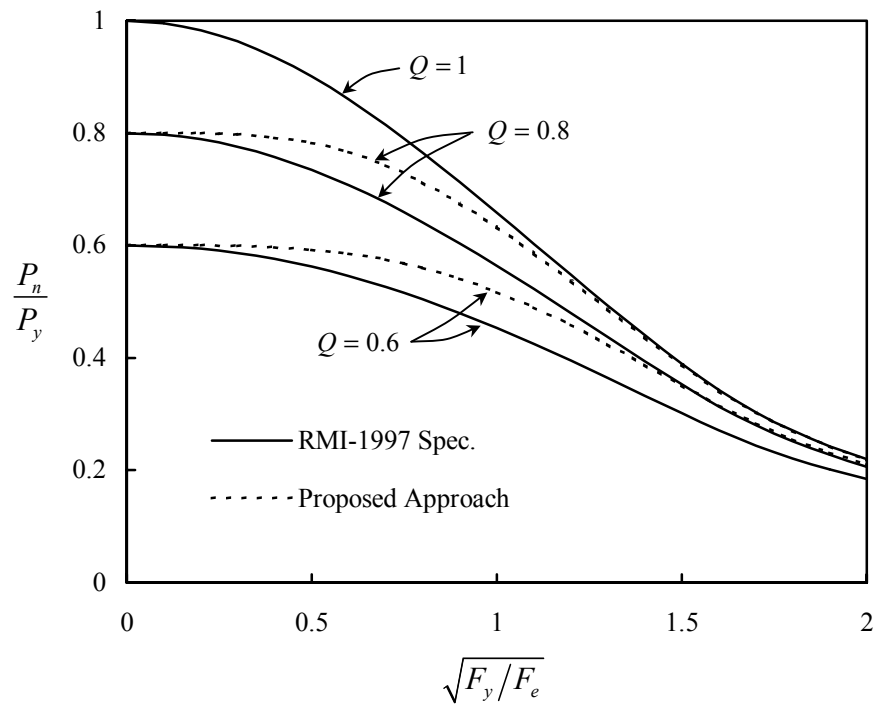
**Figure 4.39** Section IG Closed Tube - Correlation between proposed effective design area equation and analytical results



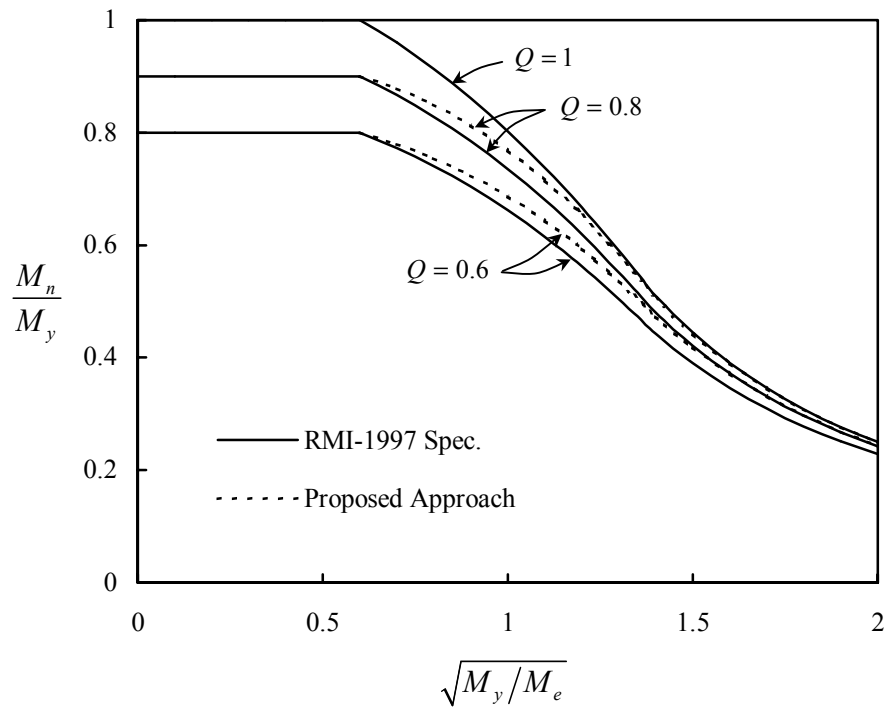
**Figure 4.40** Section Type II Open Back - Correlation between RMI effective design area equation and analytical results



**Figure 4.41** Section Type II Open Back - Correlation between proposed effective design area equation and analytical results



**Figure 4.42** Comparison between the RMI approach for column design and the proposed approach



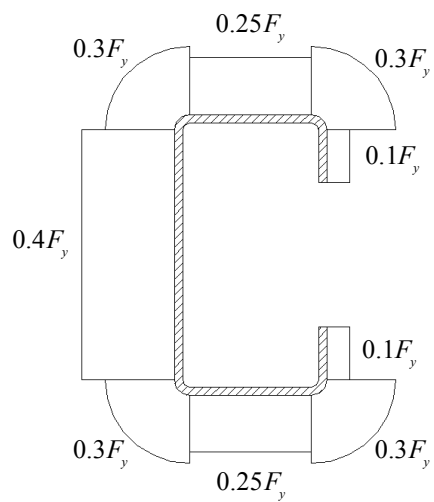
**Figure 4.43** Comparison between the RMI approach for beam design and the proposed approach



## 4.6 MEMBER DESIGN STRENGTH

The proposed equations for determining the effective section properties (Eqs. (4.5) and (4.8)) have altered the member design strength from the current design specification. In this study, unperforated and perforated member strength capacity, under different loading conditions and for various member lengths, were computed using the finite element method, and compared to those values using the RMI specification which uses Eqs. (4.1) and (4.7), and the proposed design approach which uses Eqs. (4.5) and (4.8).

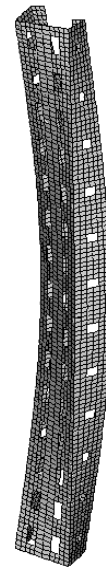
Three C-sections, the same ones used in the previous study *Elastic Buckling Strength of Perforated Members*, were considered: A-LDR, A-LDR-2, and A-HDR. Their cross sectional geometry is given in Fig. 4.2. The finite element analysis considered both geometric and material nonlinearities. Finite element models range from a member length of 12 to 120 in. with a 6 in. increment between models. Initial conditions of the model involved both flexural residual stresses and geometric imperfections. The magnitude of the flexural residual stresses throughout the thickness in the longitudinal direction is given in Fig. 4.44a. These stresses were assumed to have tension on the outside and compression on the inside of the section. Geometric imperfection was introduced by using the buckling mode shape obtained from the buckling analysis. For short members where local or distortional buckling is critical, buckling mode shape with a maximum imperfection magnitude of one tenth of the thickness was used as the geometric imperfection. For long members where overall buckling is critical as shown in Fig. 4.44b, the geometric imperfection was generated by superimposing the overall buckling and the local buckling mode shape together, where the maximum imperfection magnitudes of these modes are one thousandth of the member length and one tenth of the thickness, respectively. An idealization of the material model that is elastic-plastic with strain hardening was assumed. For Sections



(a)



Local Buckling



Overall Buckling

(b)

**Figure 4.44** Initial conditions of the finite element model (a) Bending residue stresses (b) Geometric imperfections

A-LDR and A-LDR-2,  $F_y = 45$  ksi,  $F_u = 59$  ksi,  $E = 29500$  ksi,  $E_{st} = E/45$ ,  $\nu = 0.3$ , and  $e_{st}$  is 15 times the maximum elastic strain. For Section A-HDR the material properties are same but with  $F_y = 47.8$  ksi.

All three sections were studied as a concentrically loaded compression member, a flexural member subject to bending about the strong axis, and a member subject to combined compressive axial load and bending about the strong axis. Boundary conditions at the ends of the member for all cases were pinned condition such that the effective length for flexural buckling of both the strong and weak axis and torsion were equal to the length of the member.

The loads were applied through nodal forces at the ends of the member. To avoid localized failure at the member ends the nodal forces were distributed in to the first three rows of elements. This loading condition is different from the one previously used for the finite simulation of the stub-column test in the *Effective Design Area* study. In the stub-column test simulation model, nodal displacements were used to apply the load. The reason why in this study nodal forces were selected over applying nodal displacements was to assure that the member ends remain pinned condition. Finite element studies of these two loading conditions have shown that the resulting ultimate compression load of the two can be significantly different, especially if the section is locally unstable. The reason for this is that when the uniform displacement is applied, the end surface stresses will not be uniform, and on the other hand when the uniform stresses is applied, the end surface displacement will not be uniform. The ultimate compression load is higher when the uniform displacement is applied rather than when the uniform load is applied. The reason for this is that additional restraints are provided at the ends of the member in the case of applying uniform displacement, preventing the member ends from rotating.

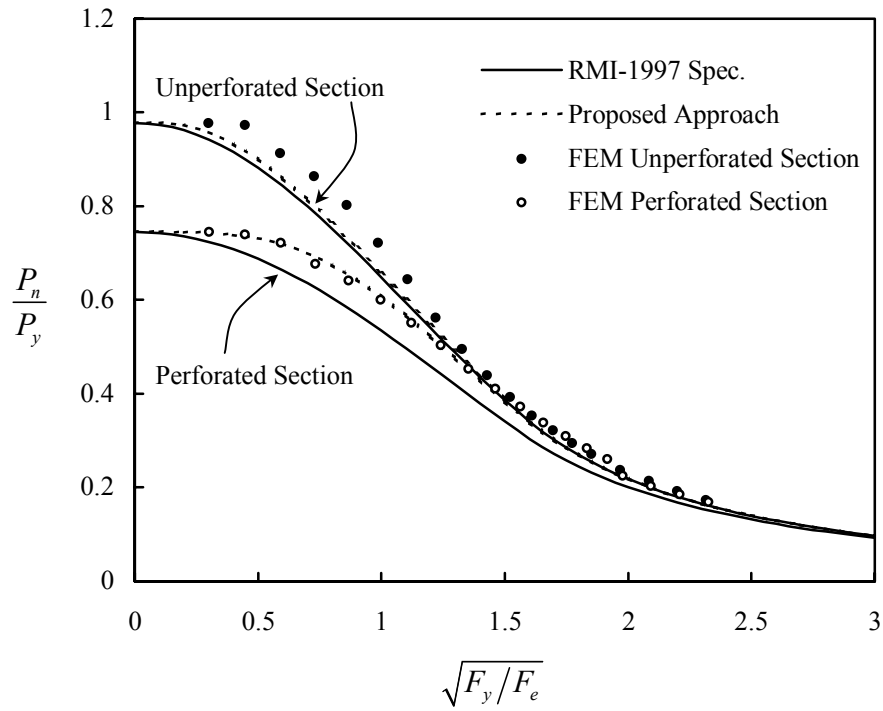
The differences in these two cases are however not significant if the section is locally stable because ultimately the entire section will yield for both cases.

The finite element results are compared with design specifications in Figs. 4.45 through 4.56. The design approach requires the use of the ultimate compression load from a stub-column test to compute the  $Q$  factor. Thus, ultimate compression strength obtained from finite element analysis of the member with the shortest length is used.

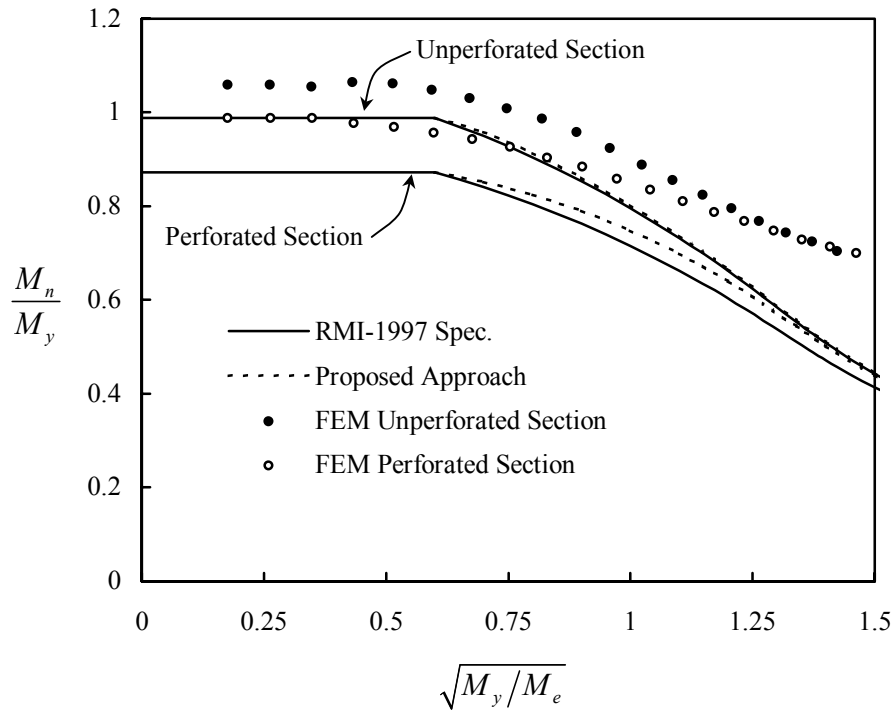
For the case of compressive axial strength shown in Figs. 4.45, 4.49, and 4.53, it can be seen that the proposed design approach agrees well with the analytical solutions, while the current specification is slightly conservative.

For the case of flexural strength for Sections A-LDR and A-LDR-2 shown in Figs. 4.46 and 4.50, it can be seen that both approaches are quite conservative for designing flexural members compared to the finite element solution, especially for the very long members. According to the finite element solution, these members have postbuckling strength. The results are also conservative because of the way in which the effective section modulus is computed according to the RMI specification, further investigation of this is given in the next study on the *Effective Section Modulus*. The conservative results shown in this study can, however, only be obtained if the net section II properties as given Tables 4.2 and 4.3 are used. The reason for this is clear but not explicitly suggested in the specification that the net moment of inertia of the bending axis should be used in the design of the flexural members.

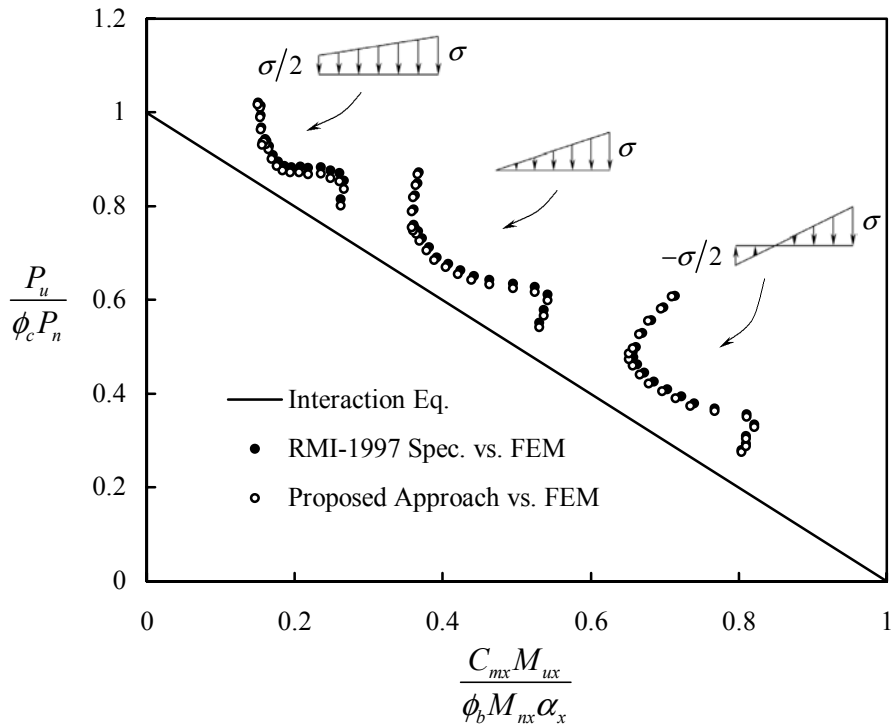
For the case of flexural strength for Section A-HRD shown in Fig. 4.54, even though net moment of inertia is used, both the proposed approach and the RMI approach for this case over estimates the flexural strength. This is because the distortional buckling strength of this section is rather low. The design specification currently does not consider this buckling mode.



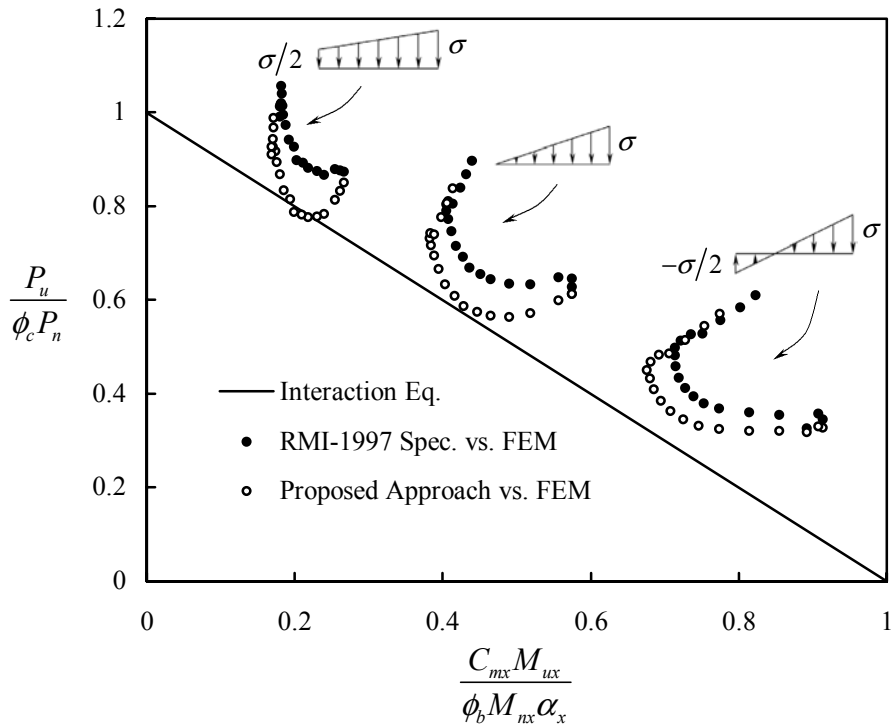
**Figure 4.45** Section A-LDR - Comparison between the RMI approach for column design and the proposed approach



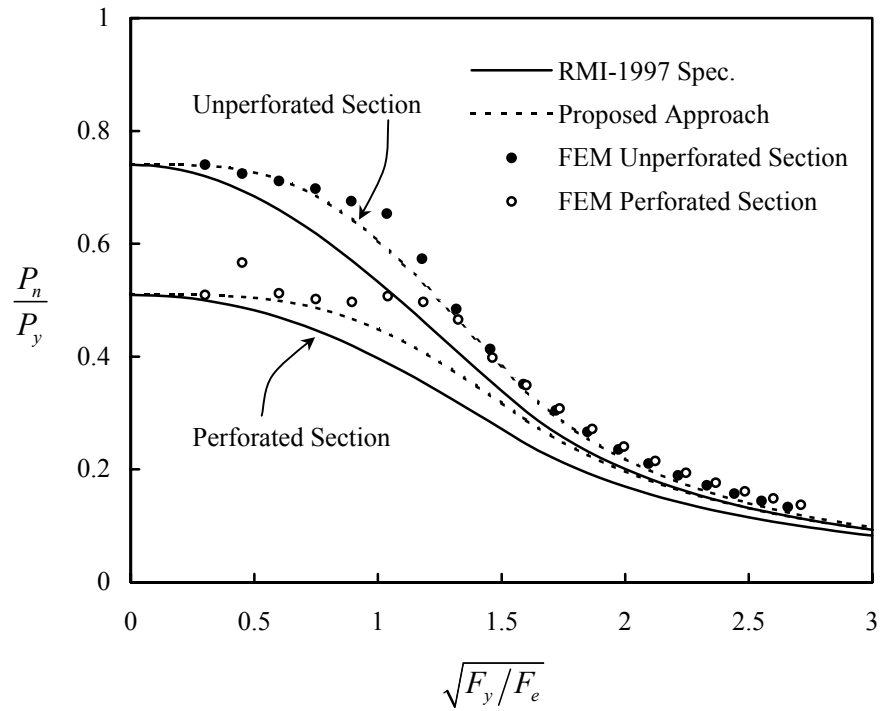
**Figure 4.46** Section A-LDR - Comparison between the RMI approach for beam design and the proposed approach



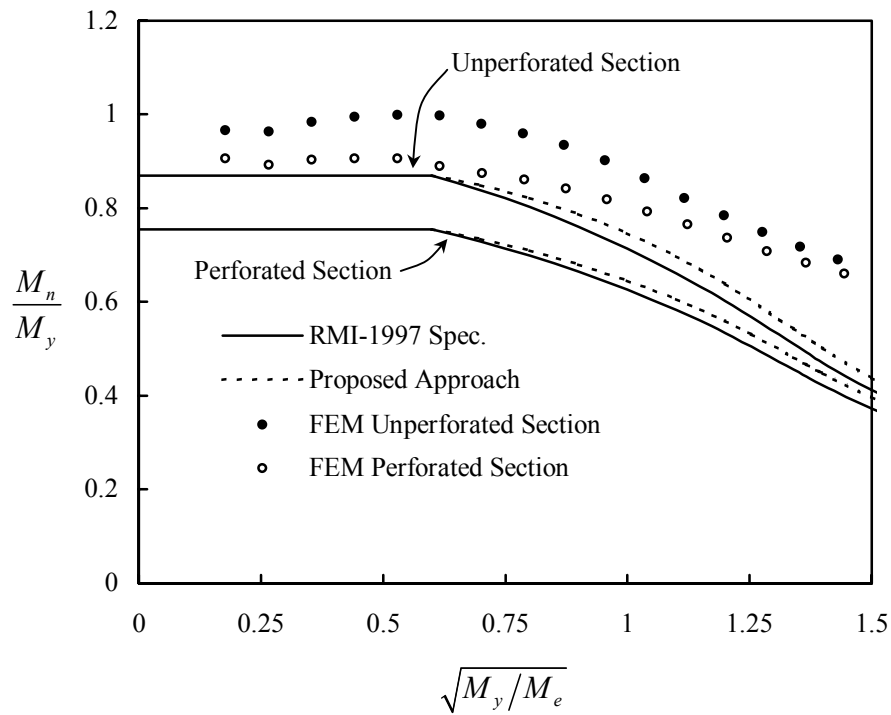
**Figure 4.47** Unperforated Section A-LDR - Comparison between the RMI approach for beam-column design and the proposed approach



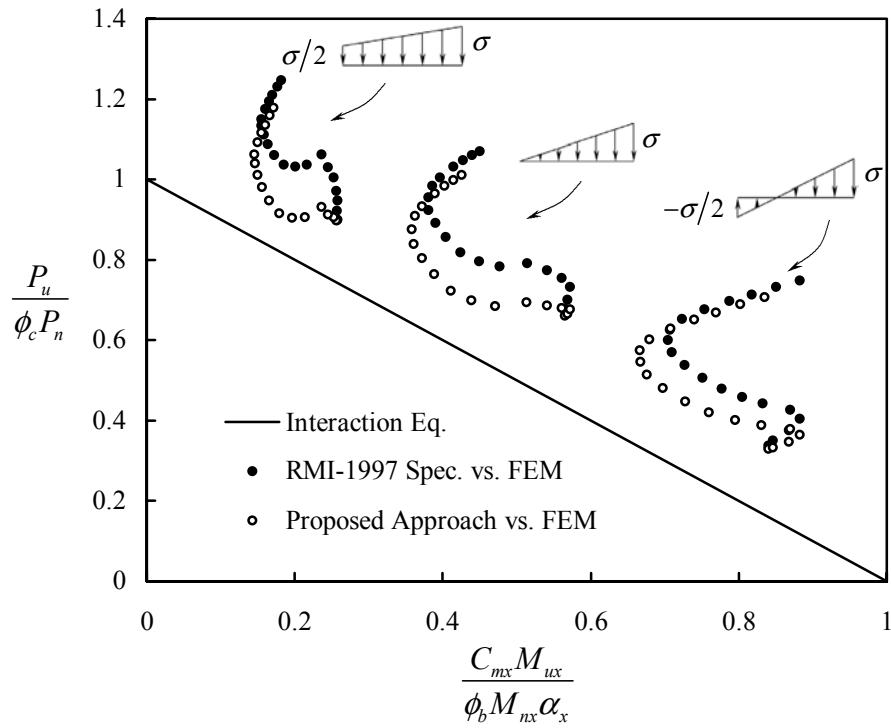
**Figure 4.48** Perforated Section A-LDR - Comparison between the RMI approach for beam-column design and the proposed approach



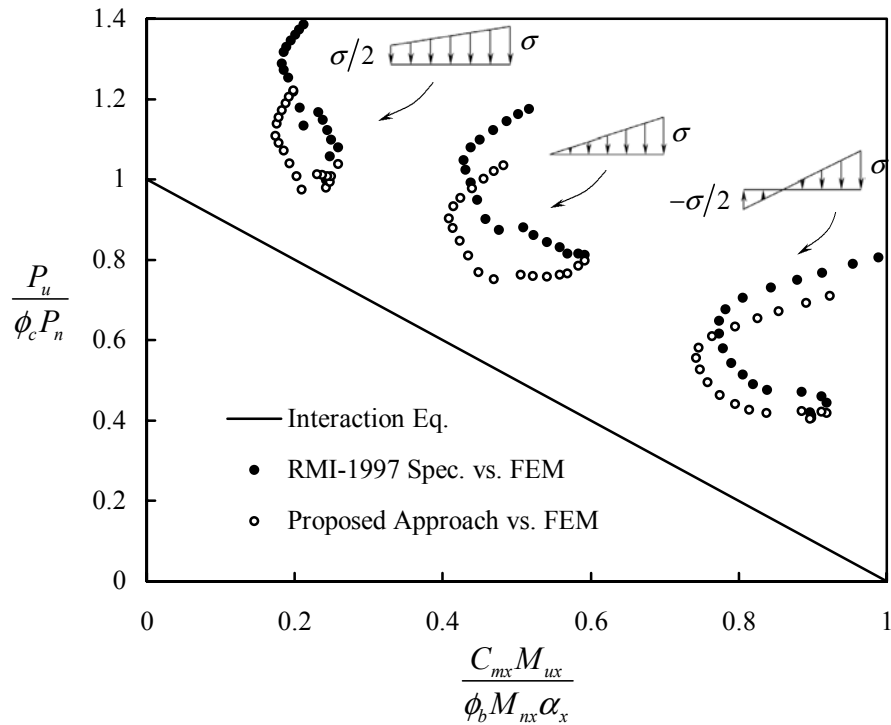
**Figure 4.49** Section A-LDR-2 - Comparison between the RMI approach for column design and the proposed approach



**Figure 4.50** Section A-LDR-2 - Comparison between the RMI approach for beam design and the proposed approach

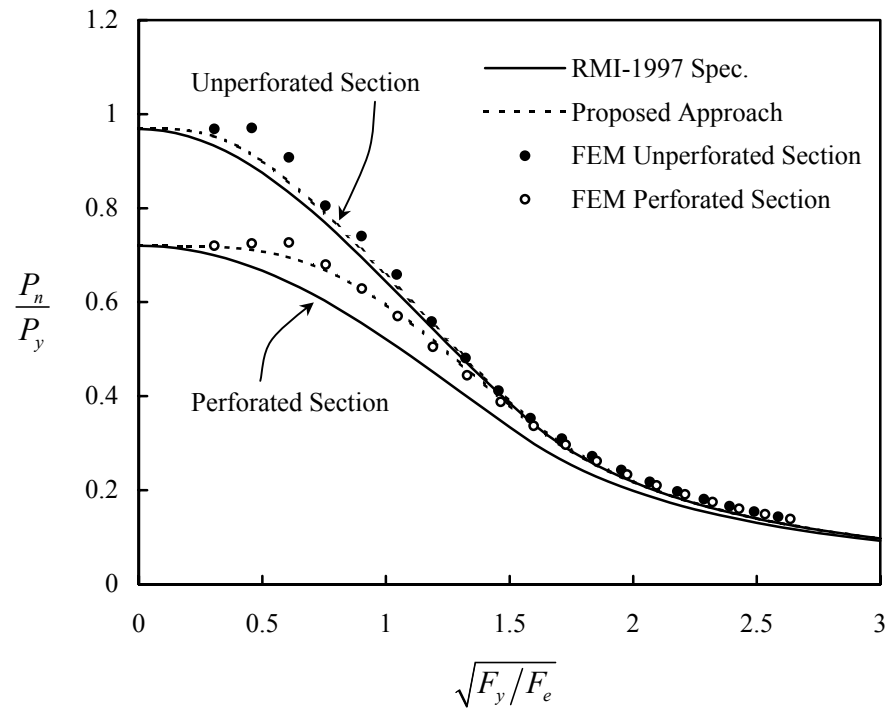


**Figure 4.51** Unperforated Section A-LDR-2 - Comparison between the RMI approach for beam-column design and the proposed approach

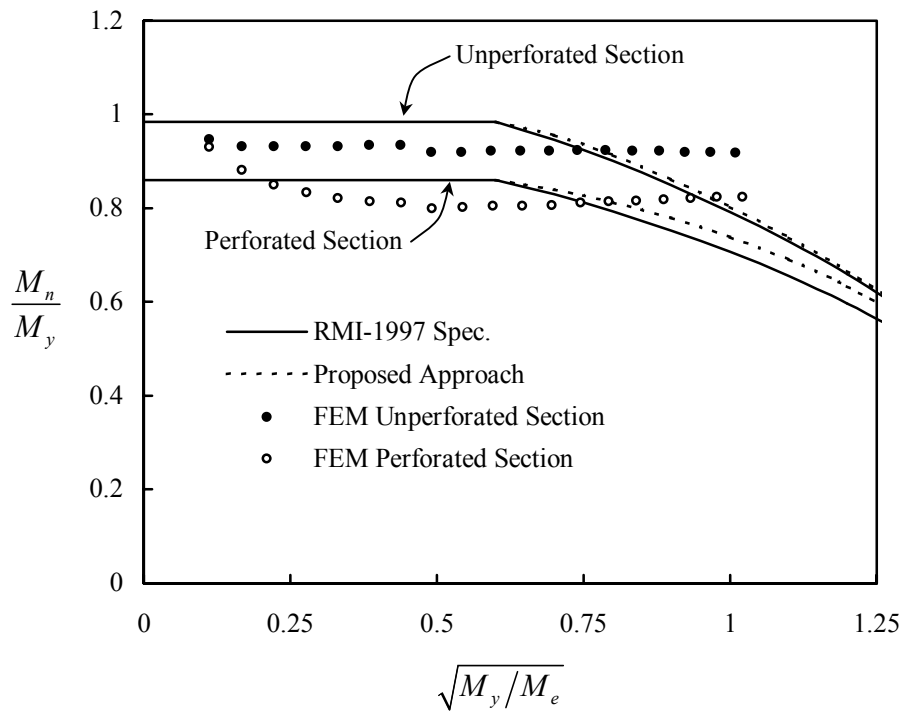


**Figure 4.52** Perforated Section A-LDR-2 - Comparison between the RMI approach for beam-column design and the proposed approach

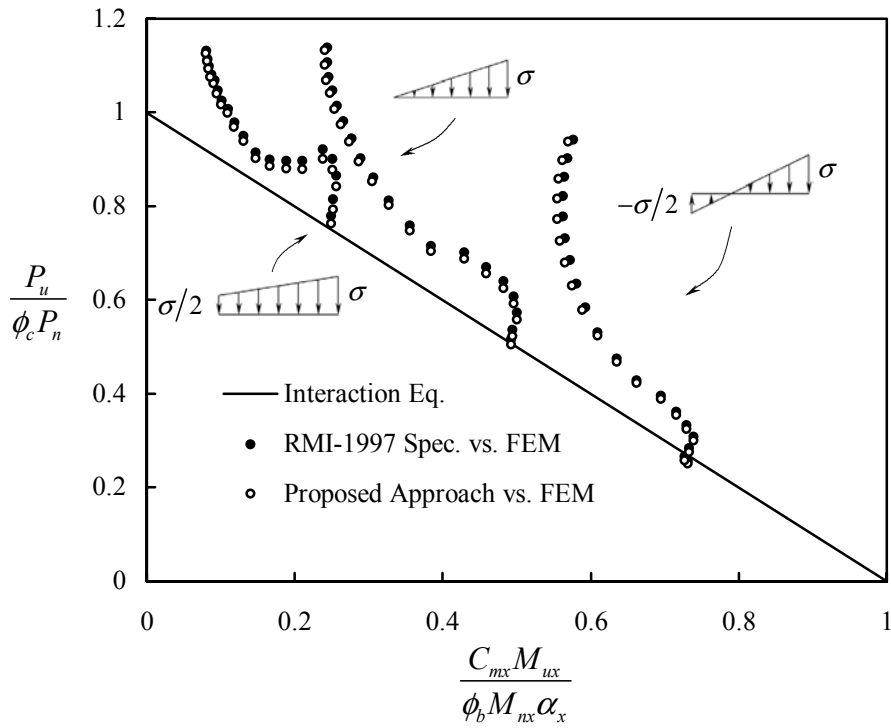




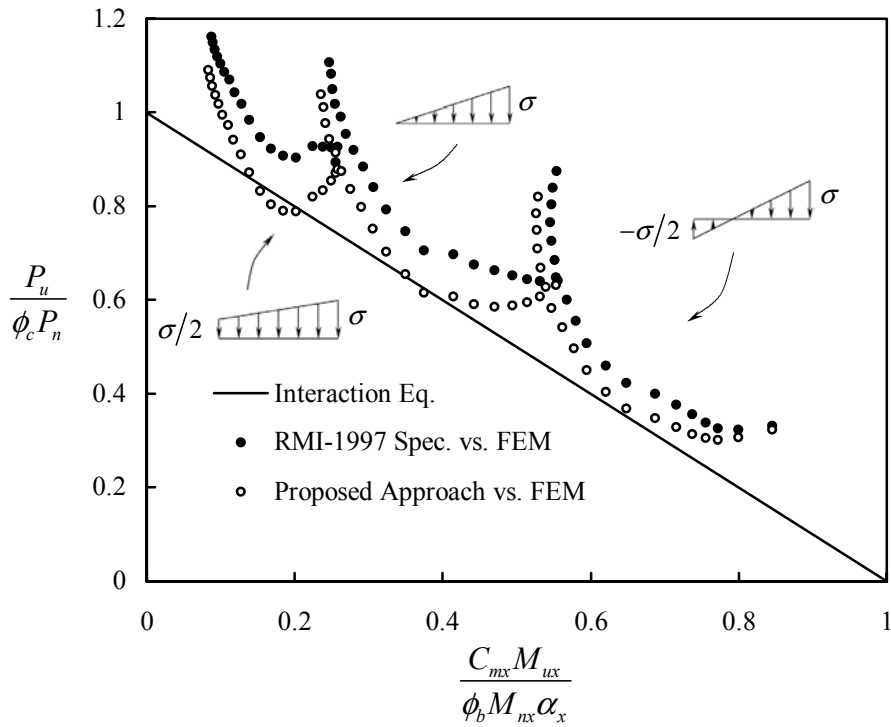
**Figure 4.53** Section A-HDR - Comparison between the RMI approach for column design and the proposed approach



**Figure 4.54** Section A-HDR - Comparison between the RMI approach for beam design and the proposed approach



**Figure 4.55** Unperforated Section A-HDR - Comparison between the RMI approach for beam-column design and the proposed approach



**Figure 4.56** Perforated Section A-HDR - Comparison between the RMI approach for beam-column design and the proposed approach

For the case of combined compression axial load and bending shown in Figs. 4.47, 4.48, 4.51, 4.52, 4.55, and 4.56, correlations between the finite element results and the interaction equation for beam-column design is given. For a given finite element result, the members strength  $P_u$  and  $M_{ux}$  are substituted in the interaction equation and the resulting axial and flexural strength ratio is plotted. Data points that fall outside the triangle indicate that the interaction equation is conservative. Data points of the proposed design approach are closer to the interaction equation line when compared to the current design procedure, indicating that improvement has been made.

#### **4.7 EFFECTIVE SECTION MODULUS**

In order to deal with the presence of perforations in a column section, the RMI specification recommends the use of a stub-column test to establish an effective net section area. The area of the effective section is for an axially loaded member failing due to local behavior. The results are also further used to calculate the elastic section modulus of the effective section for determination of the member flexural strength. The objective of this study was to validate this calculated flexural strength by using the finite element approach.

A finite element parametric study of stub-columns subject to bending moment was carried out. The column sections in study were the same ones used in the previous study *Effective Design Area*, which are given in Table 4.19. The bending moments were applied by applying nodal displacements rotating the end surfaces of the stub-column. The flexural strength was determined for the strong axis bending, weak axis bending with web in tension, and weak axis bending with web in compression as shown in Table 4.20. The analysis in this study considered both geometric and

material nonlinearities. Initial conditions of the model involved both flexural residual stresses and geometric imperfections. Geometric imperfection was introduced by using the buckling mode shape obtained from the buckling analysis with a maximum imperfection magnitude of one tenth of the thickness. An idealization of the material model that is elastic-plastic with strain hardening was assumed.

The RMI specification recommends that nominal flexural strength  $M_n$  for members not subject to lateral buckling, such as the stub-column under end surface rotations in this study, can be determined as follows:

$$M_n = S_e F_y \quad (4.9)$$

where

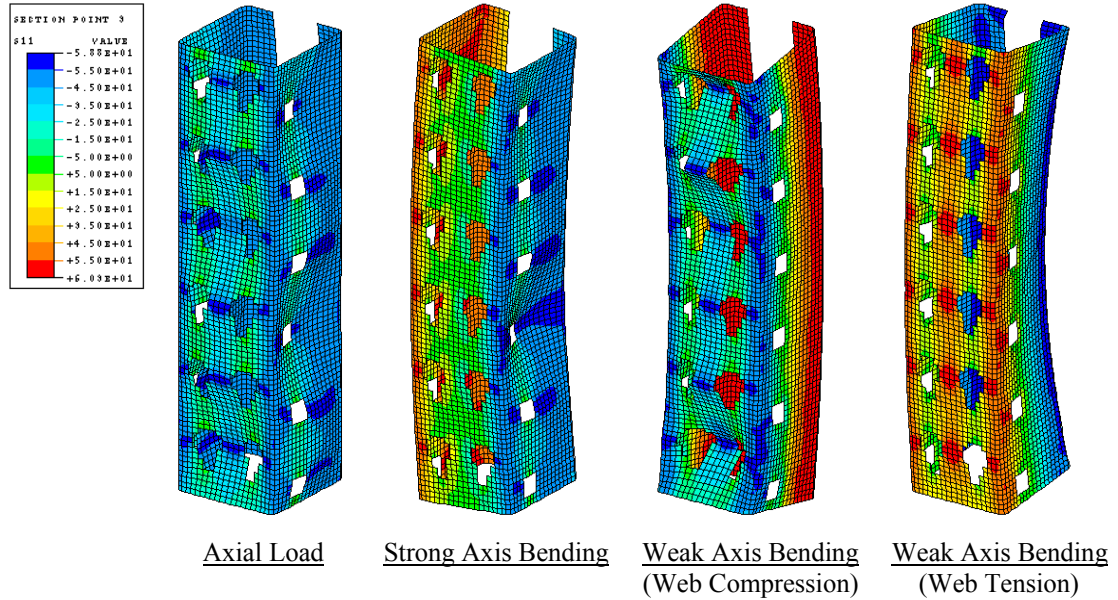
$$S_e = S \left( 0.5 + \frac{Q}{2} \right) \quad (4.10)$$

$S$  is the elastic section modulus of the full unreduced section for the extreme compression or tension fiber at  $F_y$ . The  $Q$  factor determined from the finite element approach given in Table 4.19 is used in the above equation to calculate  $M_n$  and then compared with finite element results of the stub-column under end surface rotations. Results are summarized in Table 4.20. It was found that  $M_n$  agrees well with the finite element results for the case of strong axis bending, but is rather conservative for weak axis bending. Results are conservative because  $M_n$  is calculated on the basis of initiation of yielding. Higher values can be obtained by considering the nominal flexural strength  $M_p$  that is calculated on the basis of inelastic reserve capacity, determined as follows:

$$M_p = Z_e F_y \quad (4.11)$$

where

**Table 4.20** Evaluation of Sub-Column Flexural Strength



Section	Strong Axis Bending			Weak Axis Bending (Web Compression)			Weak Axis Bending (Web Tension)		
	$M_{FEM}$	$\frac{M_n}{M_{FEM}}$	$\frac{M_p}{M_{FEM}}$	$M_{FEM}$	$\frac{M_n}{M_{FEM}}$	$\frac{M_p}{M_{FEM}}$	$M_{FEM}$	$\frac{M_n}{M_{FEM}}$	$\frac{M_p}{M_{FEM}}$
	(kip-in.)			(kip-in.)			(kip-in.)		
TBO-3	37.89	0.941	1.030	30.56	0.807	1.008	29.47	0.837	1.045
TBO-4	42.50	0.942	1.035	33.73	0.819	1.028	33.27	0.831	1.043
TBO-5	55.47	0.932	1.030	44.22	0.804	1.016	43.12	0.824	1.042
TBO-6	73.69	0.924	1.030	59.36	0.785	1.003	57.25	0.814	1.040
TBC-3	37.04	0.931	1.045	36.15	0.745	1.000	33.95	0.793	1.065
TBC-4	47.53	0.907	1.023	43.79	0.768	1.038	43.26	0.777	1.051
TBC-5	55.56	0.905	1.024	51.13	0.767	1.040	51.04	0.768	1.042
TBC-6	80.04	0.886	1.014	74.27	0.742	1.024	73.86	0.747	1.029
IGO-3	35.88	0.954	1.036	29.02	0.786	0.987	27.10	0.842	1.056
IGO-4	54.01	0.950	1.038	42.92	0.794	1.004	40.36	0.844	1.067
IGO-5	55.99	0.943	1.035	44.83	0.780	0.992	42.37	0.825	1.049
IGO-6	68.46	0.930	1.030	55.76	0.751	0.967	52.09	0.804	1.035
IGC-3	36.35	0.940	1.048	35.52	0.696	0.976	32.31	0.765	1.073
IGC-4	46.89	0.938	1.052	44.53	0.714	1.008	42.63	0.745	1.053
IGC-5	57.64	0.918	1.036	54.33	0.702	1.002	52.91	0.721	1.028
IGC-6	75.24	0.902	1.027	71.05	0.687	0.992	69.29	0.704	1.017
T2O-3	30.87	0.948	1.067	27.82	0.794	0.996	26.34	0.839	1.053
T2O-4	40.82	0.931	1.054	35.82	0.799	1.009	34.07	0.840	1.061
T2O-5	48.36	0.924	1.052	43.05	0.779	0.991	40.42	0.830	1.056
T2O-6	58.43	0.913	1.050	53.10	0.751	0.967	49.13	0.812	1.045
mean		0.928	1.038	mean	0.764	1.003	mean	0.798	1.048
st. dev		0.018	0.013	st. dev	0.039	0.020	st. dev	0.043	0.014

$$Z_e = Z \left( 0.5 + \frac{Q}{2} \right) \quad (4.12)$$

$Z$  is the plastic modulus. Overall  $M_p$  agrees better with the finite element approach than  $M_n$  but the results are slightly on the unconservative side; therefore, it is not recommended for design purposes.

#### 4.8 MOMENT MAGNIFICATION FACTOR

In the design of beam-columns, primary bending moments due to lateral loads and end moments are multiplied by moment magnification factors to account for the second order effects and the moment gradient in the member. This factor used in the current AISI specification was developed based on the assumption that failure by instability will be in the plane of bending. Thus, the current moment magnification factor does not consider the torsional-flexural failure mode. Generally this may not be the case. The torsional-flexural failure mode is common in thin-walled sections. If it takes place, the bending moments in the elastic beam-column will be unconservative if computed with the current moment magnification factor.

An alternative approach to determine maximum bending moments in elastic beam-columns for the case where it is simply supported with equal end eccentricities is given in this study. Peköz and Celebi (1969) presented an approximate analysis approach for elastic beam-columns with equal end eccentricities. The problem was solved by assuming the deflection functions to satisfy the geometric boundary conditions but with unknown coefficients. The deflection functions were then used in the beam-column differential equations where their unknown coefficients were solved by applying the Galerkin method. The corresponding bending moments about principal axes and twisting moment in the member were obtained in this study by using the resulting deformation from the approach given by Peköz and Celebi (1969).

For the case of a simply supported beam-column,  $M_{x\max}$  and  $M_{y\max}$  the maximum bending moment about principal  $x$ - and  $y$ -axes occurs at mid-span and  $M_{t\max}$  the maximum twisting moment occurs at the member ends. These moments can be computed as follows:

$$M_{x\max} = M_{x0} \left\{ 1 + \frac{P(P_{ey} - P)[(P_{et} - P)\bar{r}_0^2 + Pa_x^2] - P^3a_y^2}{\Delta} \right\} - \frac{M_{y0}P^2P_{ex}a_xa_y}{\Delta} \quad (4.13)$$

$$M_{y\max} = M_{y0} \left\{ 1 + \frac{P(P_{ex} - P)[(P_{et} - P)\bar{r}_0^2 + Pa_y^2] - P^3a_x^2}{\Delta} \right\} - \frac{M_{x0}P^2P_{ey}a_xa_y}{\Delta} \quad (4.14)$$

$$M_{t\max} = \frac{P}{\Delta} \left( \frac{\pi GJ}{L} + \frac{\pi^3 EC_w}{L^3} \right) [(P_{ey} - P)M_{x0}a_x - (P_{ex} - P)M_{y0}a_y] \quad (4.15)$$

where

$$M_{x0} = Pe_y$$

$$M_{y0} = Pe_x$$

$$\Delta = \frac{\pi}{4} \begin{vmatrix} P_{ey} - P & 0 & -Pa_y \\ 0 & P_{ex} - P & Pa_x \\ -Pa_y & Pa_x & \bar{r}_0^2 (P_{et} - P) \end{vmatrix}$$

$P$  is the applied eccentric load,  $M_{x0}$  and  $M_{y0}$  are the end bending moment about the  $x$ - and  $y$ -axes, respectively. Definitions of the other variables and derivation of Eqs. (4.13) to (4.15) are given in the Appendix C and D.

Consider the case when the beam-column section has one plane of symmetry and  $P$  is applied in that plane. Assume that  $y$ -axis is the axis of symmetry. Then  $a_x = e_x = 0$ , Eqs. (4.14) and (4.15) will give  $M_{y\max} = M_{t\max} = 0$ , and Eq. (4.13) becomes

$$M_{x\max} = \frac{C_{mx}M_{x0}}{(1-\alpha)} \approx M_{x0} \sec\left(\frac{\pi}{2}\sqrt{\alpha}\right) \quad (4.16)$$

where

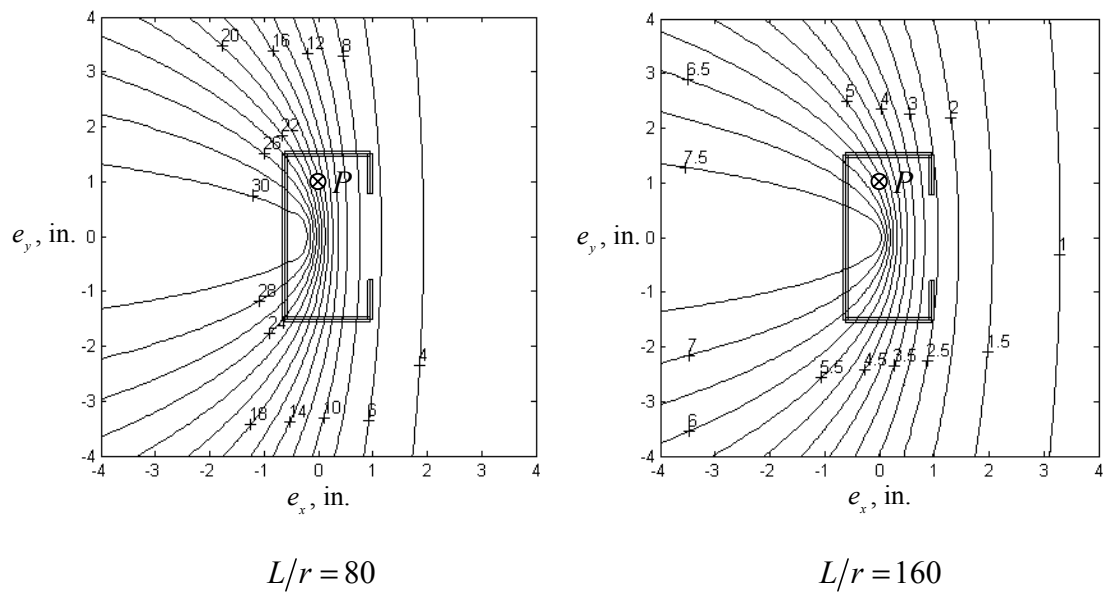
$$C_{mx} = 1 + 0.273\alpha$$

$$\alpha = P/P_{ex}$$

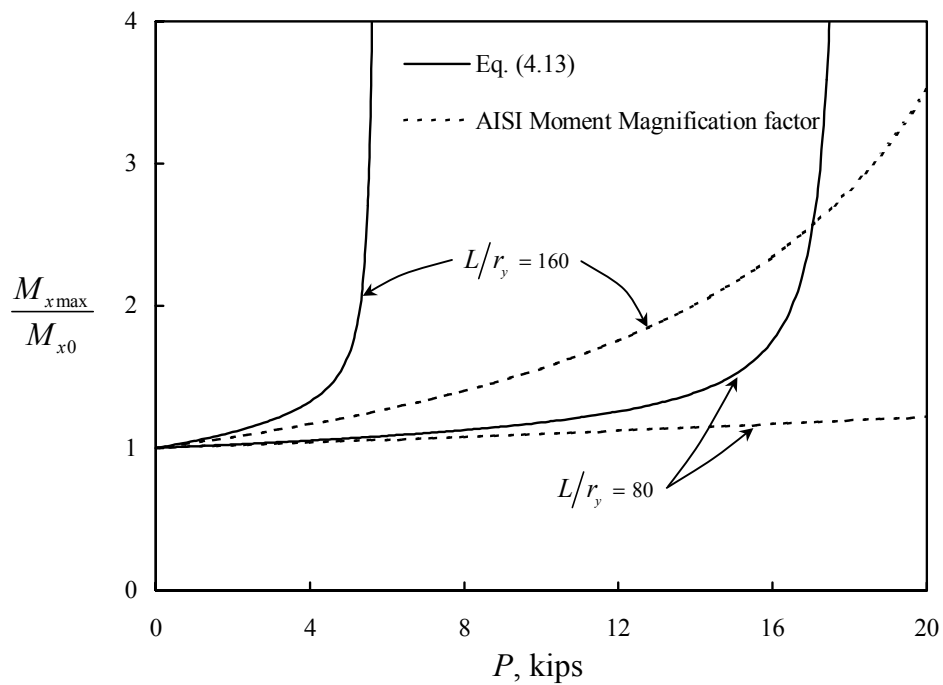
$C_{mx}/(1-\alpha)$  is the moment magnification factor which amplifies the end moment  $M_{x0}$  to account for the second order effects. This is the same moment magnification factor given by the AISI specification but with an approximation of  $C_{mx} = 1$  for the same corresponding boundary conditions.

Consider another case when the Section A-LDR is subjected to a compression load with eccentricities:  $e_x = 0$  and  $e_y = 1$  in. as shown in Fig. 4.57. In this case  $M_{x\max}$  from Eq. (4.13) will not be the same as from using the moment magnification factor given by the AISI specification. Fig. 4.58 compares the results. It can be seen that the AISI approach gives an unconservative  $M_{x\max}$ . This is because Eq. (4.13) has the level of  $P$  limited at the elastic critical axial load  $P_e$ , agreeing with the actual behavior in which the member will buckle by torsional-flexural at this load. But the AISI approach has it limited at the flexural buckling load  $P_{ex}$  instead. Contour plots given in Fig. 4.57 can be used to obtain  $P_e$  for the different load eccentricities. The failure mode for this member is by combined bending and torsion. The cross section between the supports will undergo translation and rotation. Therefore, in addition to the bending moment about the  $x$ -axis directly developing from the applied loads, the bending moment about  $y$ -axis and the twisting moment will also exist. The maximum values of these moments are obtained by using Eqs. (4.14) and (4.15). Results are shown in Figs. 4.59 and 4.60, respectively.

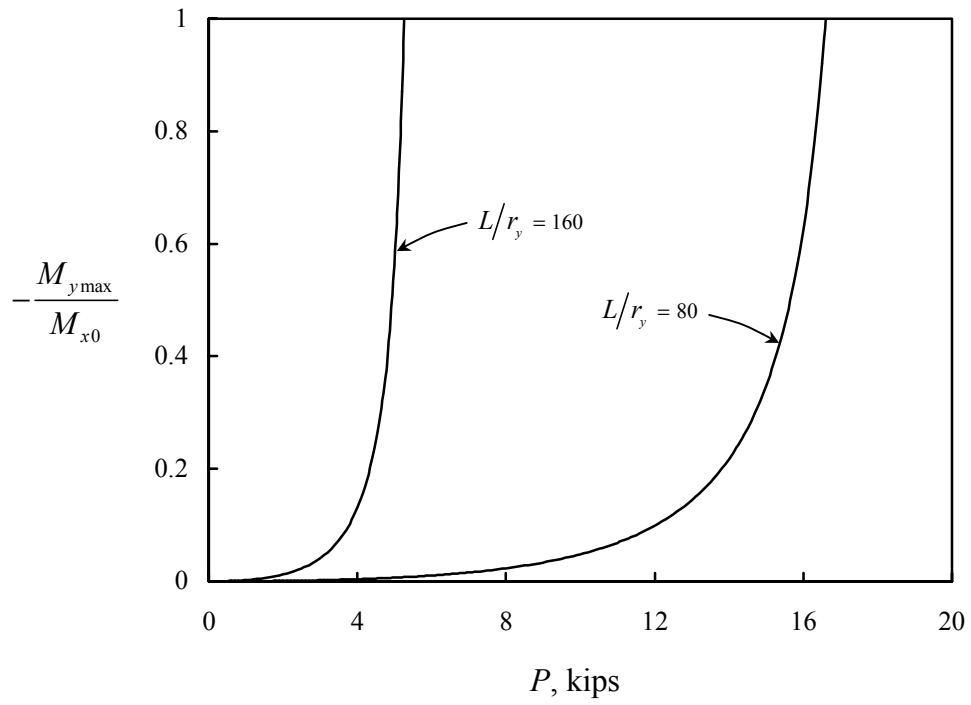




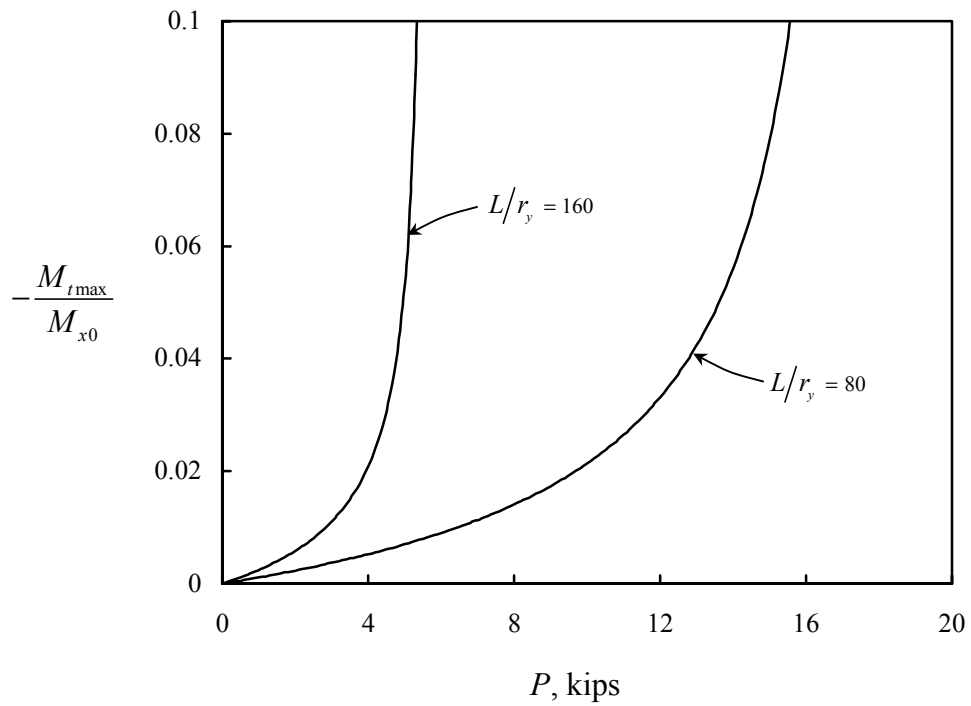
**Figure 4.57** Contour plots of the elastic critical axial force  $P_e$ , kips



**Figure 4.58** Bending moment about the  $x$ -axis



**Figure 4.59** Bending moment about the  $y$ -axis



**Figure 4.60** Twisting moment about the  $z$ -axis

In this study, equations for determining the maximum bending moments in elastic beam-columns for the case where it is simply supported with equal end eccentricities and failure is by torsional-flexural buckling are given. Developing simple means for determining the bending moments in beam-columns with unequal end eccentricities, subject to support translation, and failure is by torsional-flexural buckling would be useful for the design of cold-formed steel frames. However, preliminary studies have shown that the equations become very complicated and may not be practical for the design purpose.

#### 4.9 CONCLUSIONS

A critical review of the RMI specification for member design was carried out in this chapter. A total of seven studies were carried out. In the first study *Elastic Buckling Strength of Perforated Members*, numerous finite element elastic buckling analyses of perforated member were carried out. Results indicate that increasing the presence of perforations in the section will reduce the buckling strength. To take this into account, instead of using the unperforated section properties to predict the buckling strength of perforated sections, as assumed in the current design specification, better results can be obtained by using the weighted section, or the average section properties for torsional-flexural buckling, the average section properties for lateral buckling, and the net moment of inertia section properties for flexural buckling.

In the second study *Torsional-Flexural Buckling*, the torsional-flexural buckling equation used in the current design provision was evaluated by comparing the results with finite element solutions. It was found that the elastic buckling load obtained from using the buckling equation is usually conservative compared to the

finite element results. The reason for this is that the buckled shape assumptions made in the buckling equation are inconsistent with the actual buckled shape. This leads to errors underestimating the elastic buckling load of member and has proven to be a source of the conservatism in the current design provision.

In the third study *Effective Lengths*, the effective length factors used in the current design provision were evaluated by comparing the results with finite element solutions. It was found that the recommended value of  $K_y$ , taken as one is in general conservative while  $K_x$ , taken as 0.8 is in most cases reasonable, providing that the upright frame has adequate braces and the column base is constrained against twisting.

In the fourth study *Effective Design Area*, finite element simulation of stub-column tests were carried out to evaluate the current effective design area equation and effective section modulus equation. Modifications of these equations are suggested. The effective design area equation of the RMI specification, Eq. (4.1), should be modified to the proposed equation, Eq. (4.5). The effective section modulus equation of the RMI specification, Eq. (4.7), should be modified to the proposed equation, Eq. (4.8).

In the fifth study *Member Design Strength*, unperforated and perforated member strength capacity, under different loading conditions and for various member lengths, was computed using the finite element method, and compared to those values using the RMI specification, which uses Eqs. (4.1) and (4.7), and the proposed design approach, which uses Eqs. (4.5) and (4.8). It was found that the compressive axial strength and the beam-columns strength designed according to the proposed design approach agrees better to the finite element results than the current design procedure does. Flexural strength design according to either design approach is quite conservative compared to the finite element results, if distortional buckling failure mode does not take place.

In the sixth study *Effective Section Modulus*, finite element simulation of stub-column tests under bending moments were carried out to evaluate the current RMI procedures for determining the member flexural strength. It was found that current procedure for calculating the nominal flexural strength on the basis of initiation of yielding  $M_n$  for members not subject to lateral buckling is conservative, especially for weak axis bending. Equations for determining the nominal flexural strength on the basis of inelastic reserve capacity  $M_p$  are given in this study and have been shown to agree better with the finite element results than  $M_n$ , but the results are slightly on the unconservative side, therefore it is not recommended for design purposes.

In the seventh study *Moment Magnification Factor*, equations for determining the maximum bending moments in elastic beam-columns for the case where it is simply supported with equal end eccentricities and failure is by torsional-flexural buckling are given. Determining the maximum moments for this boundary condition using the current moment magnification factor suggested by the AISI specification has been shown to give unconservative results if the member failure is by torsional-flexural. This unconservatism in the AISI moment magnification factor by itself, however, does not suggest that current design procedures for beam-columns is unconservative. On the contrary, as to be shown in Chapter 5, in practice when the AISI moment magnification factor is used with the interaction equation to design beam-columns current design procedure is very conservative.

---

---

# Chapter 5

## Cold-Formed Steel Frames

---

---

### 5.1 INTRODUCTION

The behavior of industrial storage racks depends on how the three individual components discussed in the previous chapters: column bases, beam to column connections, and members perform interactively with each other. Thus the frame behavior can become very complex. Many parameters such as semi-rigid nature of connections, presence of significant perforations, and susceptibility to local buckling and torsional-flexural buckling are part of the cause. As to which method of analysis is best to solve this problem will certainly depend on the tools available to the designer. The analysis model can be as simple as using a sub-structure model such as isolating the column and using the alignment chart, or as sophisticated as using numerical methods to analyze the entire frame. With the availability of powerful computers and software, the latter approach has become more attractive, allowing more complex and efficient designs. In this chapter results will be presented from studies which were carried out to evaluate the current effective length approach and to examine the

notional load approach as an alternative design procedure, as well as to review current guidelines for methods of analysis and for using numerical methods for structural analysis, such as elastic buckling analysis and second-order elastic analysis considering semi-rigid connections.

## **5.2 ELASTIC BUCKLING STRENGTH OF PALLET RACKS**

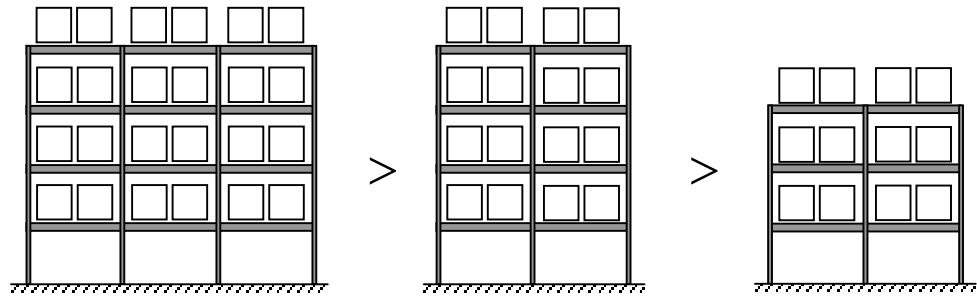
The AISI, AISC, and RMI specifications use the effective length approach for assessing frame stability. It is essential that effective lengths and the elastic buckling load of members are accurately determined in the effective length approach. Parameters that influence the value of  $K_x$  for column flexural buckling were examined in this study. The alignment chart and the AISI torsional-flexural buckling provisions, used to obtain the effective lengths and elastic buckling load of members were also evaluated.

### **5.2.1 Effective Length $K_x$**

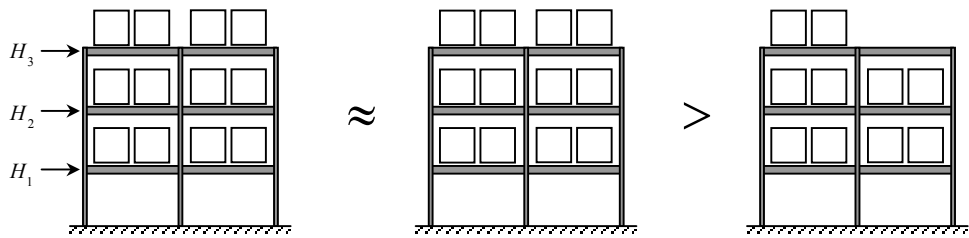
Parameters that influence the value of  $K_x$  for column flexural buckling in the direction perpendicular to the upright frames can be summarized in three categories as shown in Fig. 5.1.

The first category is the number of bays and stories. For fully loaded frames, as the number of bays increases so does the value of  $K_x$  because the supporting action of light loaded end frame columns diminishes, and as the number of stories increases so does the value of  $K_x$  because the difference in loads in the bottom story and the second story columns decreases.

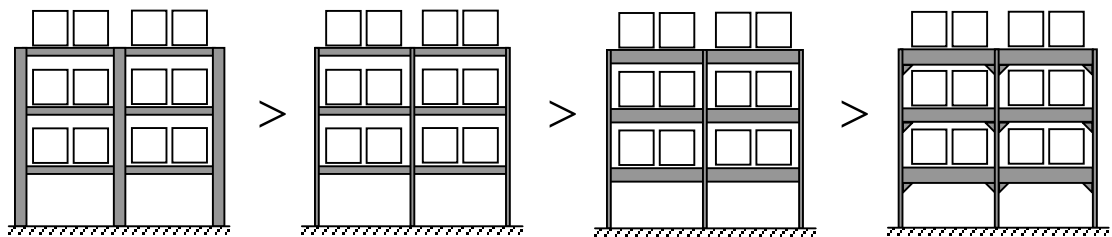
The second category is the loading conditions. Adding horizontal forces on a fully loaded frame makes insignificant changes to the value of  $K_x$  because the



Number of bays and stories



Loading conditions



Section properties and connection stiffness

**Figure 5.1** Parameters that influences the value of  $K_x$  for column flexural buckling

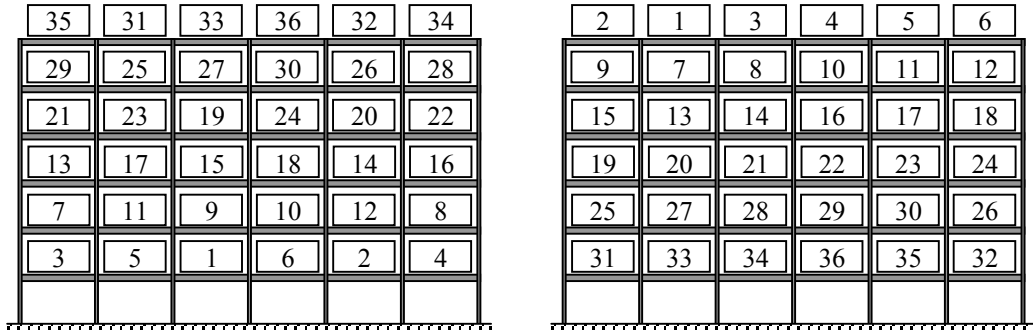


additional horizontal force makes insignificant changes to the level of axial loads on the interior columns. As the number of loaded bays increases so does the value of  $K_x$ ; therefore, a fully loaded frame is always the most critical load case as far as elastic buckling is concerned.

The third category is the section properties and connection stiffness. As the column size increases so does the value of  $K_x$ ; however as the beam size and the connection stiffness increases the value of  $K_x$  will decrease because additional restraint from the beam and connection stiffness helps prevent the frame from sidesway buckling.

A parametric study was carried out to investigate the effects of the loading conditions on the frame stability. Two loading sequences on a 6-bay by 6-story pallet rack shown in Fig. 5.2 were studied. One is the best possible loading sequence which will minimize the frame instability while the other is the worst possible loading sequence which will maximize the frame instability. As can be seen in Fig. 5.2, the best loading sequence is one which starts loading from the lower stories, while the worst loading sequence is one which does the opposite; that is, it starts loading from the upper stories.

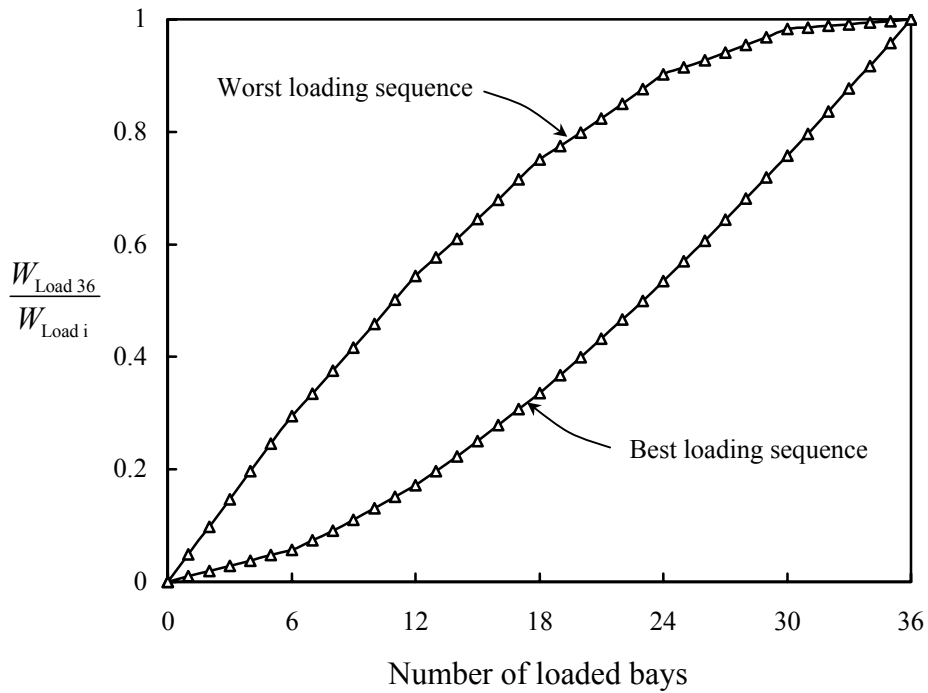
The resulting effects that these two loading sequences have on the frame stability are plotted in Fig. 5.3 where  $W_{\text{Load } i}$  is the elastic buckling gravity load per bay when  $i$  number of bays have been loaded, and  $W_{\text{Load } 36}$  is the elastic buckling gravity load per bay when all bays have been loaded. As can be seen in this figure, it is better to start accessing the products from the upper stories while keeping the lower stories loaded until last.



Best loading sequence

Worst loading sequence

**Figure 5.2** Loading sequence in study



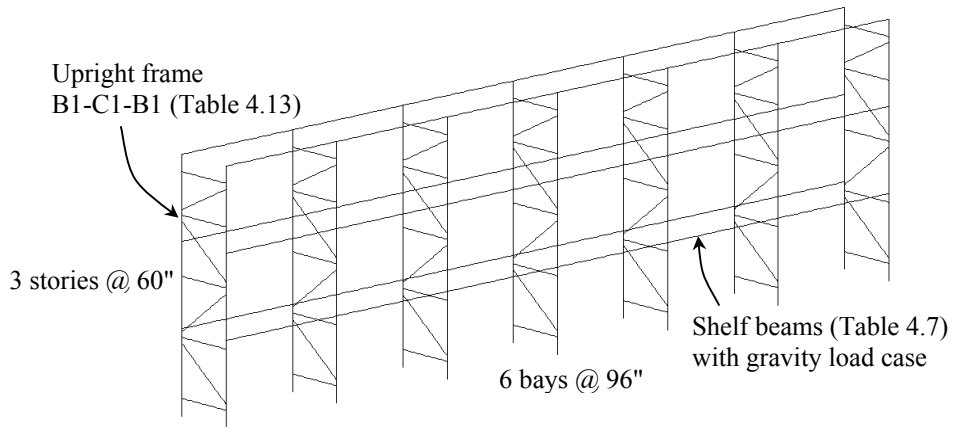
**Figure 5.3** Relationship between the frame stability and the loading sequence

### 5.2.2 Alignment Chart and Torsional-flexural Buckling Provisions

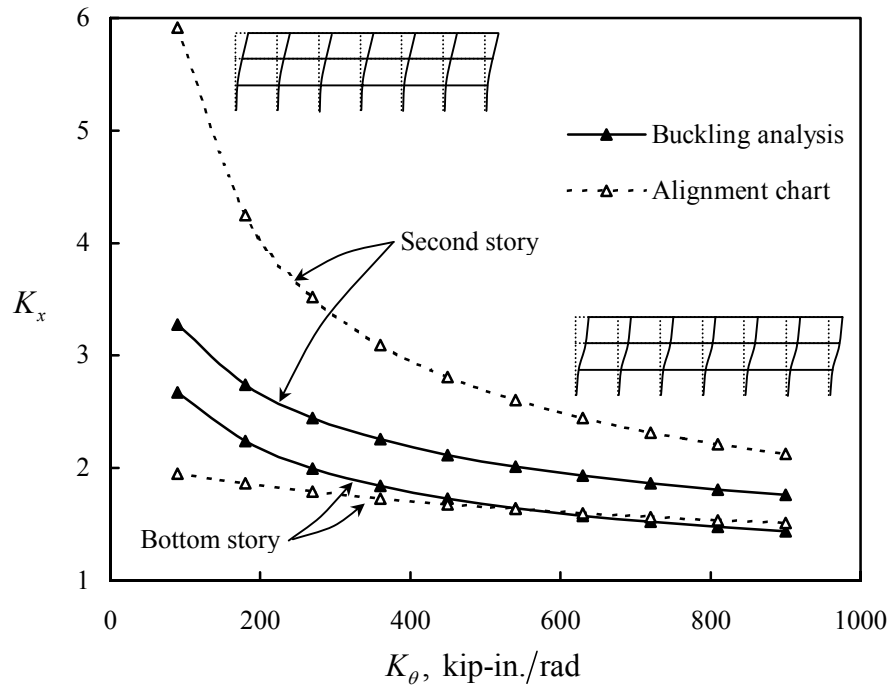
The objective of this study was to evaluate the alignment chart and the AISI torsional-flexural buckling provisions. The 6-bay by 3-story pallet rack as shown in Fig. 5.4 was used as the vehicle for carrying out this study. The value of  $K_x$  was determined from the alignment chart and compared to those values determined more accurately from a finite element flexural buckling analysis. The finite element modeling assumptions are as follows: the column base fixity was modeled by torsional springs with its stiffness determined from the proposed base fixity equation given in Chapter 2 and the beam to column connection stiffness  $K_\theta$  was also modeled by torsional springs.

In this study  $K_\theta$  was varied and the corresponding  $K_x$  was determined for the bottom story and the second story middle column. The results are as shown in Fig. 5.5. It was found that the alignment chart was unconservative when used for the bottom story column with low  $K_\theta$  values, and was always too conservative when used for the second story column. The reason for this is that, in actual practice the alignment chart assumptions are rarely satisfied exactly. Such violations lead to errors making the results unconservative for the bottom story column even when reductions in beam stiffness have already been made to reflect the semi-rigid nature of the connections, and the results are too conservative for the second story column because the high base fixity value was not accounted for in the alignment chart. Thus, the alignment chart is inaccurate when differences between the base fixity and the connection flexibility is high.

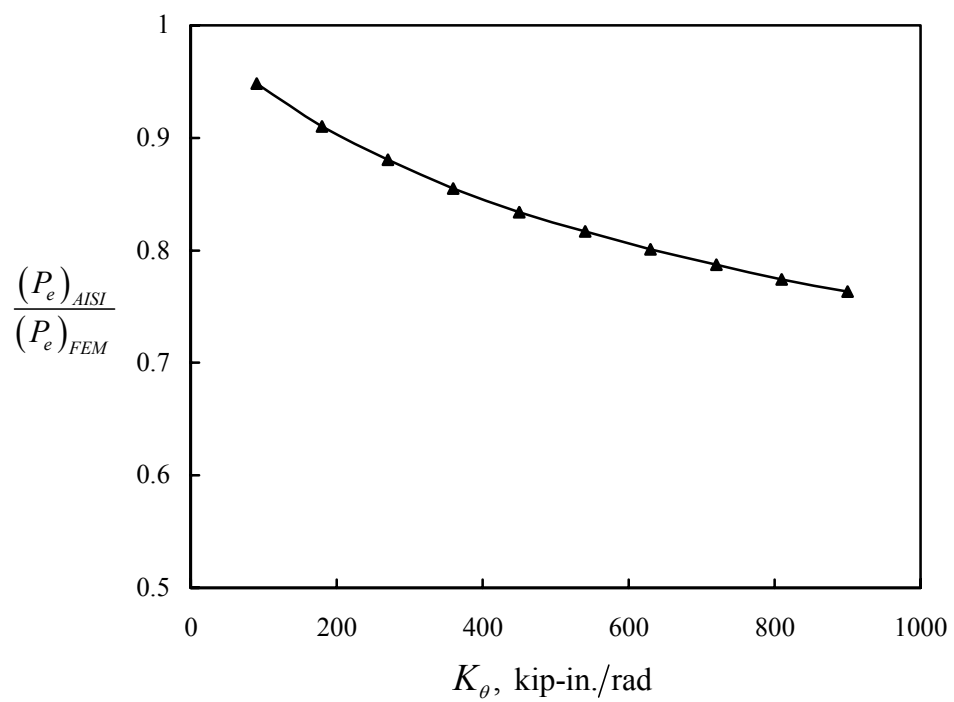
The column section used in the pallet rack shown in Fig. 5.4 was a 3x3 C-section with its axis of symmetry perpendicular to the aisle. Torsional-flexural buckling is normally the critical buckling mode for this section. The buckling load is usually determined by either using the AISI torsional-flexural buckling provisions or



**Figure 5.4** Storage rack in study



**Figure 5.5** Evaluation of the Alignment chart



**Figure 5.6** Evaluation of the torsional-flexural buckling equation

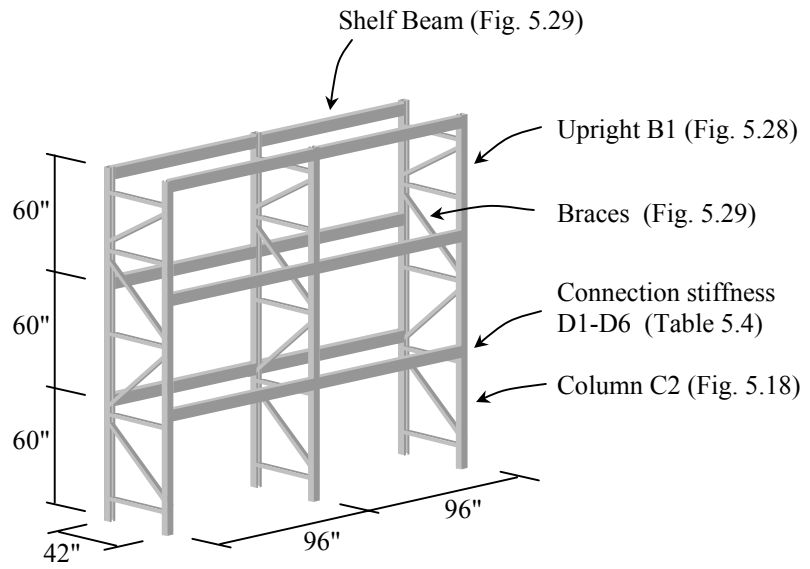
more accurately obtained by performing an elastic buckling analysis of the entire frame. The results of using these two approaches to determine the buckling load of the bottom story middle column are compared in Fig. 5.6. The AISI buckling equation is computed based on the values of  $K_x$  determined from flexural buckling analysis, which were given in Fig. 5.5, and  $K_t = 0.717$  determined from a torsional buckling analysis. It was found that the AISI torsional-flexural buckling provisions become gradually more conservative as the value of  $K_\theta$  increases.

### 5.3 PLUMBNESS

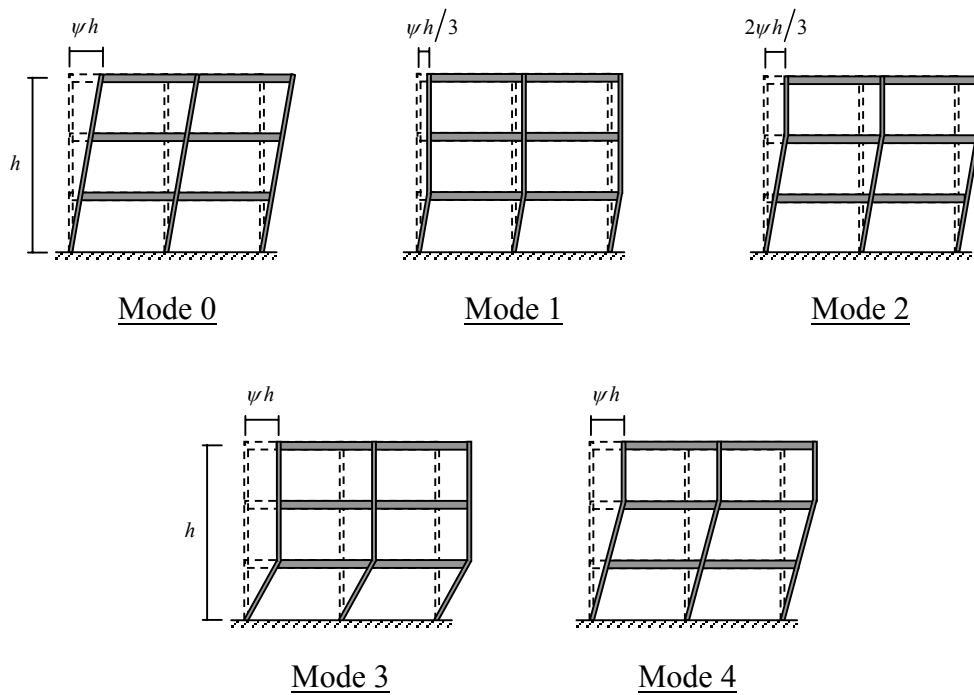
Out-of-plumb installation of frames creates secondary moments in the columns causing frame instability. The RMI specification recommends that the frame initial out-of-plumbness should not be more than 0.5 inches in 10 feet ( $\psi = 1/240$ ). The following study was carried out to investigate different initial out-of-plumb modes and the impact it has on the load carrying capacity of frame.

Five frame initial out-of-plumb modes as shown in Fig. 5.8 were considered. The initial out-of-plumbness of the first three modes are within the RMI guidelines while the last two modes are not because the column imperfection gradient has exceeded 0.5 inches in 10 feet.

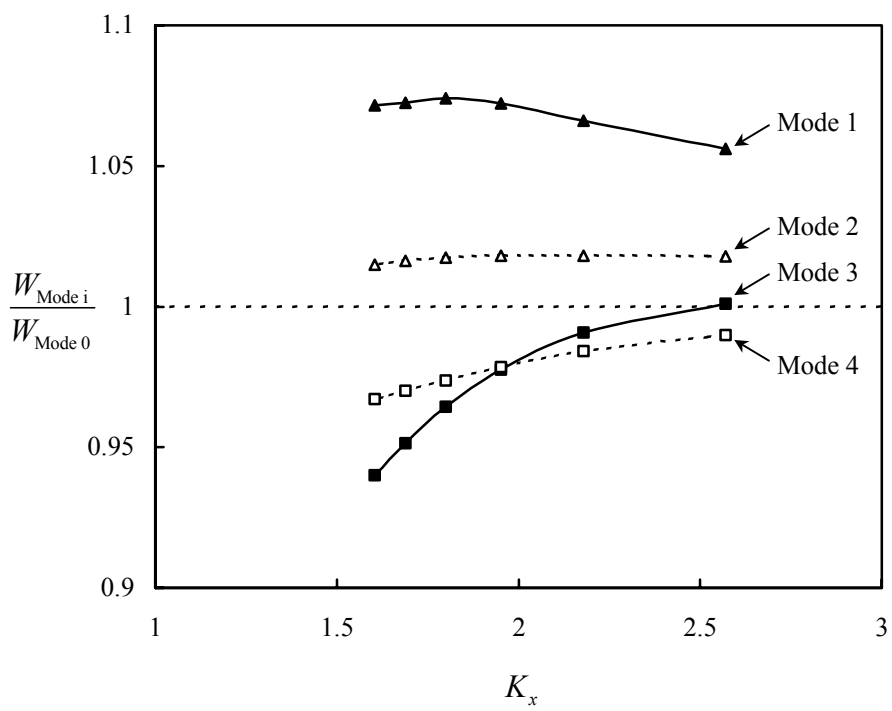
The pallet rack shown in Fig. 5.7 was used as the vehicle for carrying out this study. Finite element analysis was performed to compute the load carrying capacity of the frame for the different initial out-of-plumb modes, and also for the different frame beam to column connection stiffnesses to cover a wide range of column  $K_x$  values. Results are compared with respect to Mode 0 as shown in Fig. 5.9. Finite element modeling assumptions include using a three-dimensional model, using open-section beam elements to model the columns and braces, using linear torsional springs to



**Figure 5.7** Storage rack in study



**Figure 5.8** Different modes of frame initial out-of-plumb



**Figure 5.9** Effect of initial out-of-plumb on the load carrying capacity of the frame



model the connection stiffness, using the proposed base fixity equation given in Chapter 2 to compute the stiffness of the column base, and using an elastic-plastic material model  $F_y = 55$  ksi, and  $E = 29500$  ksi. The finite element analysis considers both geometric and material nonlinearities.

As can be seen in Fig. 5.9, the load carrying capacity of Mode 1 and 2 is always higher than Mode 0; therefore, as long as the actual frame initial out-of-plumbness is within the RMI guideline, it is always conservative to assume Mode 0 in the design analysis. The results of Mode 3 and 4 clearly show why the initial out-of-plumbness of 0.5 inches in 10 feet should be interpreted as restrictions of the imperfection gradient of the column rather than the absolute maximum column imperfection tolerances.

#### 5.4 MOMENT MAGNIFICATION FACTOR

In the design of beam-columns, the relationship between the required axial compression strength  $P_u$  and flexural strength  $M_u$  for the member under consideration could be obtained by performing a second-order elastic analysis, or alternatively approximated by performing a first-order elastic analysis using moment magnification factors as follows:

$$M_u = B_1 M_{nt} + B_2 M_{lt} \quad (5.1)$$

where  $M_{nt}$  and  $M_{lt}$  are the required flexural strength in the member obtained from first-order elastic analysis assuming the frame to have no lateral translation and assuming the frame to have lateral translation, respectively.  $B_1$  and  $B_2$  are moment magnification factors which are needed to account for the second-order effects. The objective of this study was to evaluate the AISI and the AISC recommended

sidesway moment magnification factor  $B_2$ . The AISC specification gives an expression for  $B_2$  as

$$B_2 = \frac{1}{1 - \frac{\sum P_u}{\sum P_{ex}}} \quad (5.2)$$

or

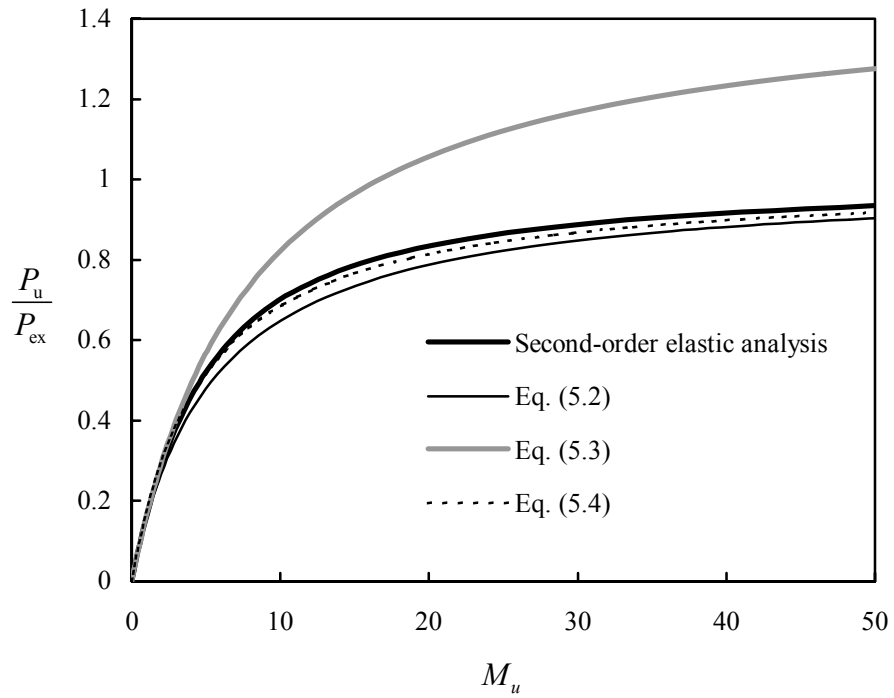
$$B_2 = \frac{1}{1 - \sum P_u \left( \frac{\Delta_{oh}}{\sum HL} \right)} \quad (5.3)$$

where  $\sum P_u$  is the required axial strength of all columns in the a story,  $\Delta_{oh}$  is the lateral inter-story deflection,  $\sum H$  is the sum of all story horizontal forces producing  $\Delta_{oh}$ ,  $L$  is the story height, and  $\sum P_{ex}$  the elastic flexural buckling strength of all columns in the story. The AISI specification accounts for the second-order effects by multiplying the moment term in the interaction equation by  $C_{mx}/\alpha_x$ , where  $C_{mx}$  is 0.85 for sidesway and  $\alpha_x = 1 - P_u/P_{ex}$ , which is equivalent to having  $B_2$  as

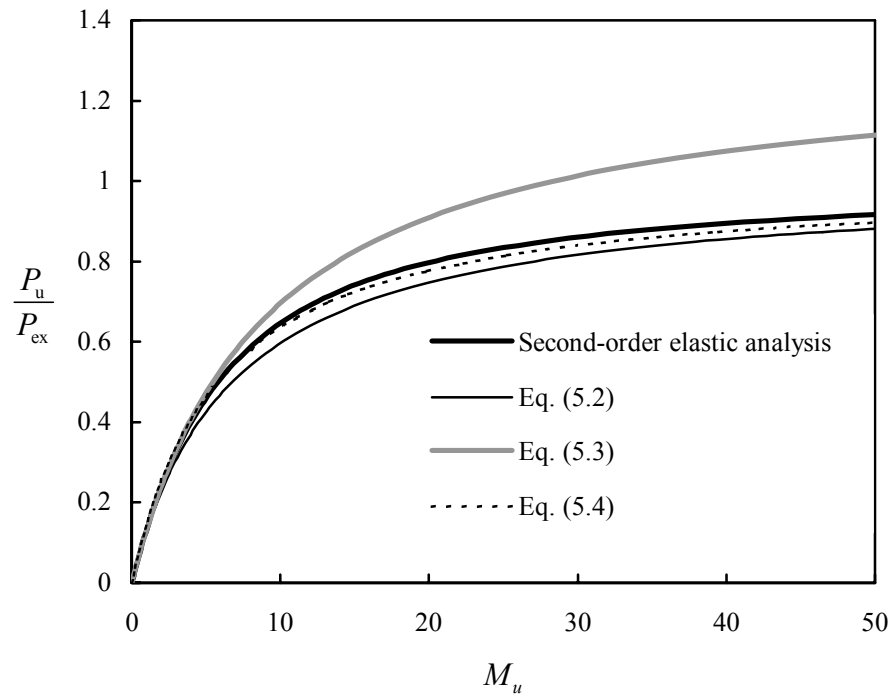
$$B_2 = \frac{0.85}{1 - \frac{P_u}{P_{ex}}} \quad (5.4)$$

the value of  $P_u/P_{ex}$  in the above equation and the value of  $\sum P_u/\sum P_{ex}$  in Eq. (5.2) are the same when their parameters are obtained from performing first-order analysis and elastic buckling analysis, therefore Eq. (5.2) and Eq. (5.4) differ only by a factor of 0.85.

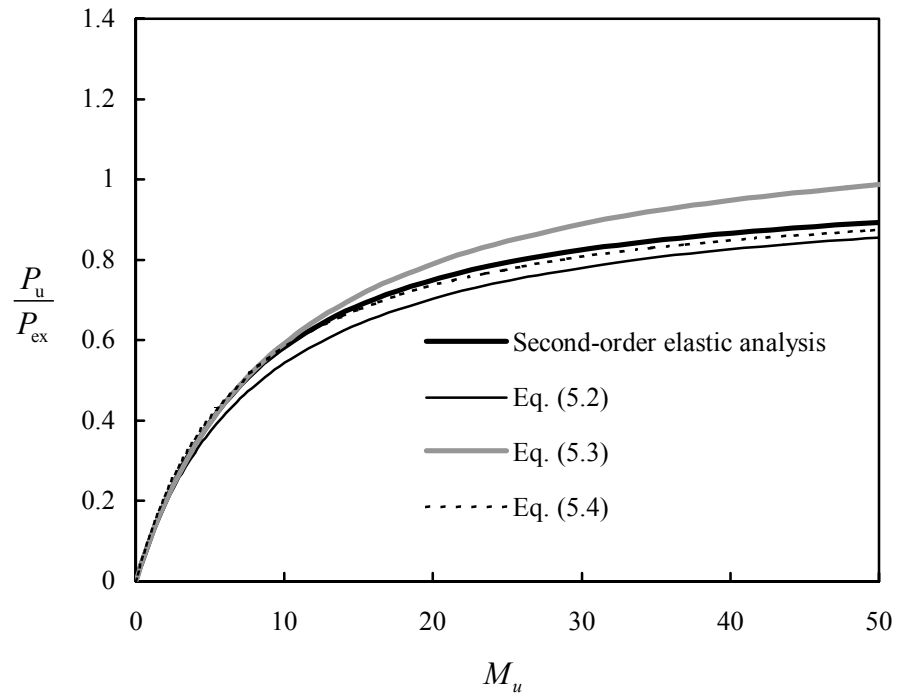
The developing moment at the base of the center column of the pallet rack shown in Fig. 5.7 was investigated. All bays are equally loaded causing zero  $M_m$  in the center column; therefore, the moment magnification factor  $B_1$  is not needed;  $M_u$  arises only from the lateral translation of the frame which is due to the frame initial out-of-plumbness. Frame initial out-of-plumb mode 0 as shown in Fig. 5.8 is



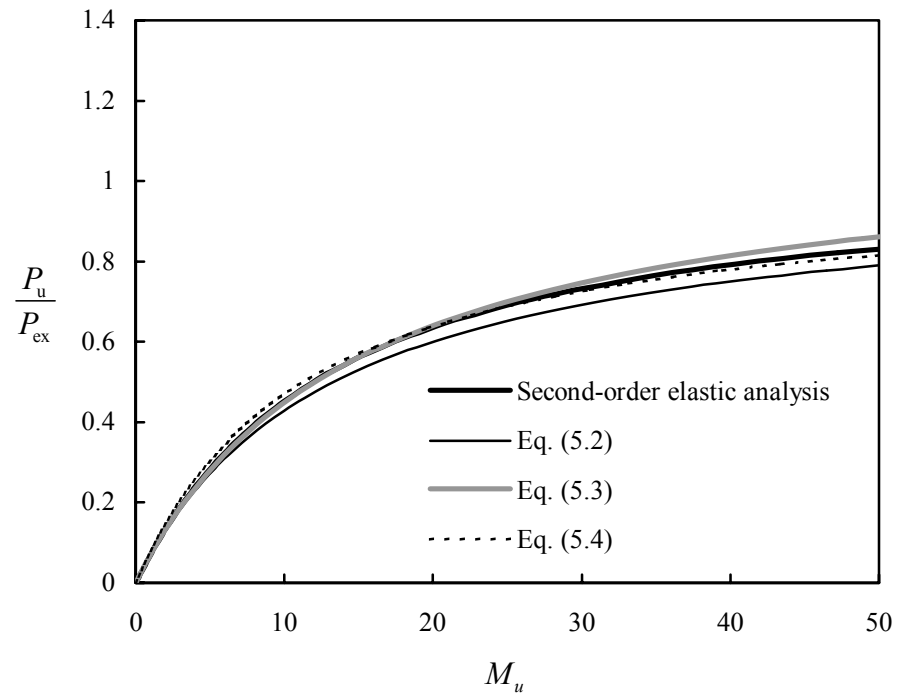
**Figure 5.10** Frame with  $K_\theta = 300$  kips-in. - Correlation between second-order elastic analysis and moment magnification factors



**Figure 5.11** Frame with  $K_\theta = 600$  kips-in. - Correlation between second-order elastic analysis and moment magnification factors



**Figure 5.12** Frame with  $K_\theta = 1200$  kips-in. - Correlation between second-order elastic analysis and moment magnification factors



**Figure 5.13** Frame with  $K_\theta = \text{Rigid}$  - Correlation between second-order elastic analysis and moment magnification factors

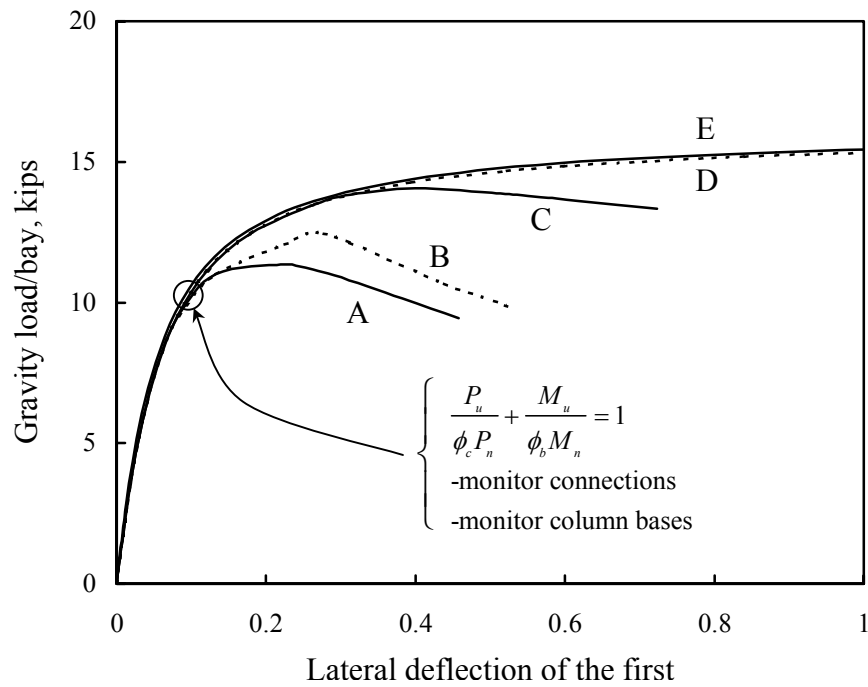
assumed. The relationship between  $P_u$  and  $M_u$  at the base of the center column obtained from second-order elastic analysis is used as a basis for evaluating Eqs. (5.2), (5.3), and (5.4). The results are given for four beam to column connection stiffnesses:  $K_\theta = 300, 600, 1200$  kips-in., and rigid as shown in Figs. 5.10 through 5.13. As can be seen from these figures, Eq. (5.4) agrees better with the second-order elastic analysis than Eqs. (5.2) and (5.3) do. Eq. (5.2) is slightly more conservative than the results from second-order elastic analysis and Eq. (5.4), while Eq. (5.3) is unconservative compared with the results from second-order elastic analysis when used for semi-rigid frames. If the designer does not use second-order elastic analysis to obtain the required member strength, the result from this study suggests that the AISI sidesway moment magnification factor Eq. (5.4) should be used to account for the sidesway second-order effects.

## 5.5 NONLINEAR ANALYSIS OF PALLET RACKS

The behavior of industrial storage racks depends on how the three components: column bases, beam to column connections, and members perform interactively with each other. These components and the slender nature of the structure are sources of nonlinearity, thus the frame behavior can become very complex. Different levels of structural analysis were carried out to investigate four fundamental modeling assumptions: model geometry, material property, column base, and beam to column connection. Five different analysis levels as summarized in Table 5.1, all of which are second-order analyses, were performed on the pallet rack shown in Fig. 5.4 to investigate the different nonlinear responses. Definitions of the four fundamental modeling assumptions are as follows:

**Table 5.1** Different Levels of Structural Analysis

Analysis type	Model geometry	Material property	Column base	Beam to column connection
A	3D	Inelastic	Inelastic	Inelastic
B	3D	Inelastic	Inelastic	Elastic
C	3D	Inelastic	Elastic	Elastic
D	3D	Elastic	Elastic	Elastic
E	2D	Elastic	Elastic	Elastic



**Figure 5.14** Different levels of structural analysis

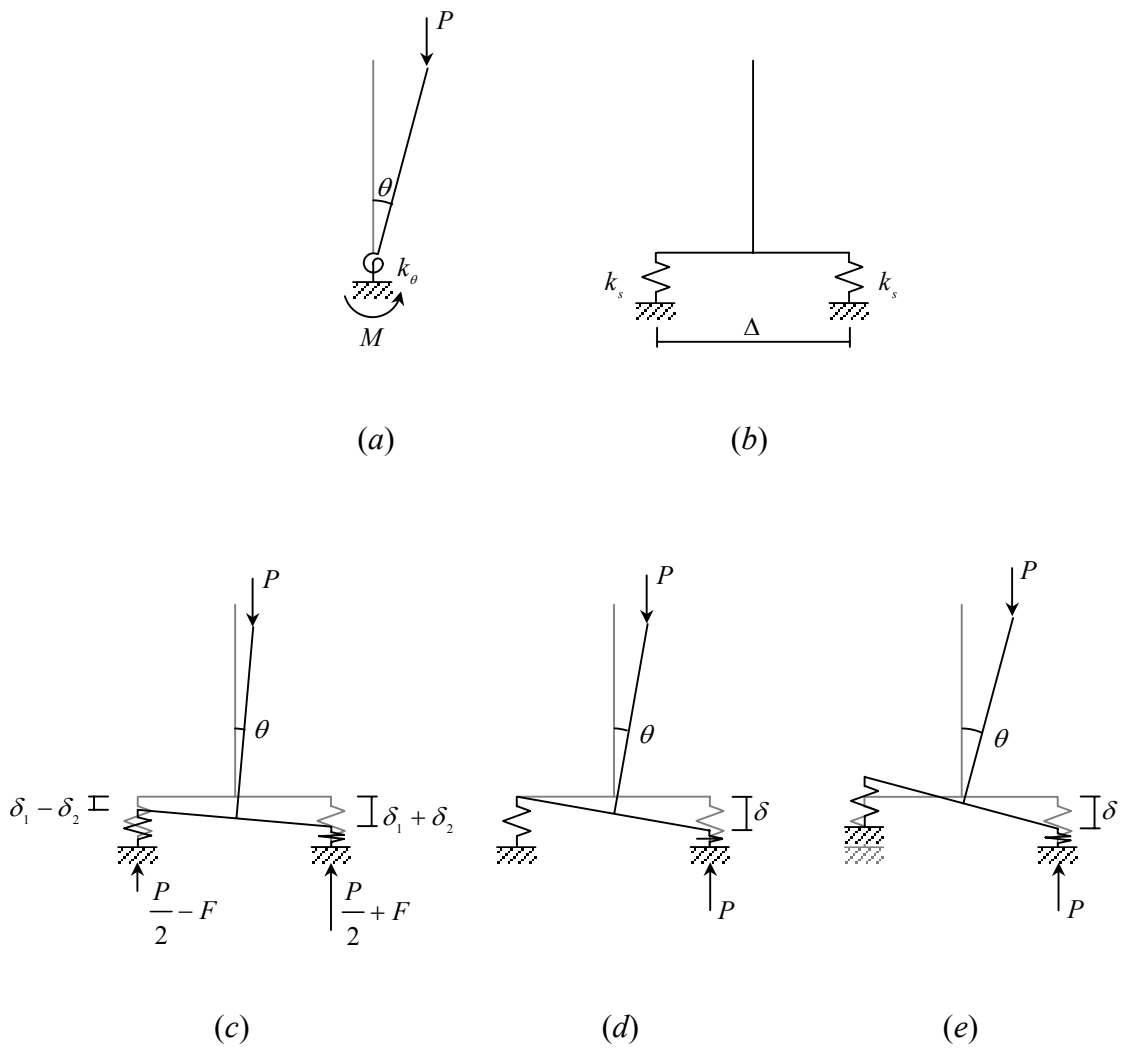
Model geometry: The 3D frame refers to modeling the entire pallet rack as a space frame and open-section beam elements are used to model the columns and braces, while 2D frame refers to modeling the pallet rack as a plane frame with only in-plane beam elements.

Material property: The inelastic material model refers to having all components modeled as elastic-plastic material with strain hardening.  $F_y = 55$  ksi,  $F_u = 70$  ksi,  $E = 29500$  ksi,  $E_{st} = E/45$ ,  $\nu = 0.3$ , and  $e_{st}$  is 15 times the maximum elastic strain.

Column base: The elastic column base refers to using torsional springs to model the base fixity where its stiffness is determined from the proposed base fixity equation given in Chapter 2. The behavior of the column base is generally elastic as long as the base plate remains in full contact with the floor. Once the column base's moment to axial load ratio reaches its upper bound limit, which is when the base plate starts to overturn, the base fixity will decrease dramatically. The inelastic column base in this study refers to modeling the column base with a double axial spring model as shown in Fig. 5.15b. This model not only has the same stiffness as the elastic case but will also capture the upper bound limit of base fixity behavior. Further detail on how the double axial spring model was developed is given in Appendix A.

Beam to column connection: The inelastic beam to column connection means considering the connection to be semi-rigid setting the moment and rotation relationship as elastic-plastic. In this study the connection stiffness  $K_\theta = 270$  kips-in./rad and ultimate connection moment capacity  $M = 6$  kips-in. was assumed.

Results for the different levels of analysis are given in Fig. 5.14. Analysis type A is considered to best represent the actual frame's behavior. As the levels of analysis decrease, higher load carrying capacity of the frame is obtained. This result is as



**Figure 5.15** Base fixity model (a) Torsional spring (b)-(e) Double axial spring



expected; therefore, when simple analytical models such as analysis type E are used for design special considerations are necessary to account for the effects that the analysis is incapable of simulating; for example, calculating the column torsional-flexural buckling load, using the beam-column interaction equation, and monitoring moments at the beam to column connections and column bases.

## **5.6 EFFECTIVE LENGTH APPROACH AND NOTIONAL LOAD APPROACH FOR COLD-FORMED STEEL FRAME AND BEAM-COLUMN DESIGN**

The effective length approach and the notional load approach are used in many specifications and standards for steel frame design. The differences between these two approaches are the way in which the physical nature of the column and frame imperfections are accounted for in the design. For more background information on the philosophy behind these two design approaches, the reader is referred to ASCE (1997). The objective of this study was to compare the effective length approach and the notional load approach for accuracy and appropriateness for cold-formed steel frame and beam-column design. The storage rack industry currently uses the effective length approach. Design procedures of these two approaches are as follows:

### **APPROACH 1 - EFFECTIVE LENGTH APPROACH**

#### **– Centrally Loaded Compression Members**

The column is considered to be a centrally loaded compression member. The axial load carrying capacity of the member is determined according to the effective length approach using the following equation:

$$P_u = \phi_c P_n \quad (5.5)$$

This approach relies significantly on the prediction of the critical buckling load of the member. The critical buckling load is usually determined by using the AISI torsional-flexural buckling provisions, or could be more accurately obtained by performing an elastic buckling analysis. Both procedures were investigated.

**Approach 1a** - the elastic buckling load was computed by using the AISI torsional-flexural buckling provisions with the value of  $K_x$  determined from the alignment chart or more accurately determined from an elastic flexural buckling analysis, and the values of  $K_y$  and  $K_t$  are assumed equal to 1 and 0.8, respectively.

**Approach 1b** - the elastic buckling load was obtained directly from a finite element elastic buckling analysis. This yielded a more accurate design than Approach 1a because as has been illustrated in Chapter 4, the torsional-flexural elastic buckling load obtained from using the AISI buckling provisions can sometimes be quite conservative compared to the more accurate value obtained from performing the elastic buckling analysis.

#### – Combined Compressive Axial Load and Bending

The member is considered to be subject to a combined compressive axial load and bending. The axial compression strength  $P_u$  and flexural strength  $M_u$  for the member is determined according to the effective length approach using the following equation:

$$\frac{P_u}{\phi_c P_n} + \frac{M_u}{\phi_b M_n} \leq 1 \quad (5.6)$$

Moment magnification factors are not included in the above interaction equation because the second-order elastic analysis is used to obtain  $P_u$  and  $M_u$ . Moment

magnification factors are needed if the first-order analysis is used. Second-order elastic analysis is conducted on a frame with story-out-of-plumbness of 0.5 inches in 10 feet ( $\psi = 1/240$ ) as suggested by the RMI Specification. A simple plane frame (2D) model as shown in Fig. 5.16a could be used for the second-order elastic analysis but semi-rigid connections must be considered. Second-order elastic analyses and elastic buckling analyses of semi-rigid frames could be performed by using the computer program CU-SRF shown in Appendix H. This approach relies significantly on the prediction of the critical buckling load of the member. The two different procedures for obtaining critical buckling load as mentioned previously in Approaches 1a and 1b were investigated.

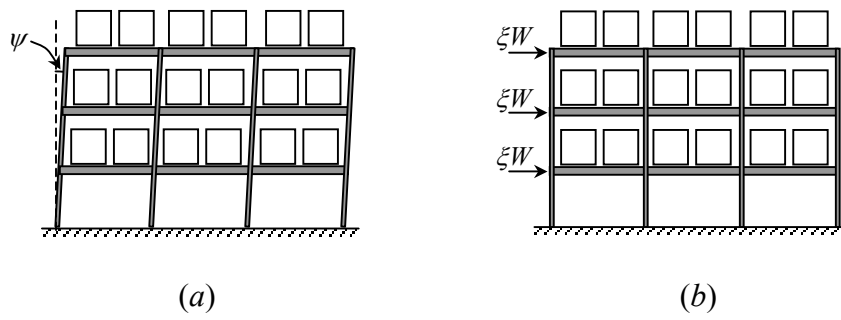
**Approach 1c** - the elastic buckling load was computed by using the AISI torsional-flexural buckling provisions with the value of  $K_x$  determined from the alignment chart or more accurately determined from elastic flexural buckling analysis, and the value of  $K_y$  and  $K_t$  were assumed equal to 1 and 0.8, respectively.

**Approach 1d** - the elastic buckling load was obtained directly from an elastic buckling analysis.

## APPROACH 2 - NOTIONAL LOAD APPROACH

The member is considered to be subject to a combined compressive axial load and bending. The axial compression strength  $P_u$  and flexural strength  $M_u$  for the member is determined according to the notional load approach using the following equation:

$$\frac{P_u}{\phi_c P_{n(L)}} + \frac{M_u}{\phi_b M_n} \leq 1 \quad (5.7)$$



**Figure 5.16** (a) Effective length approach (b) Notional load Approach

where  $P_{n(L)}$  is the axial strength computed based on the values of  $K_x$  and  $K_y$ , both assumed equal to one, and  $K_t$  assumed equal to 0.8. The AISI torsional-flexural buckling provisions are used to compute the elastic buckling load. Moment magnification terms are not included in the above interaction equation because the second-order elastic analysis is used to obtain  $P_u$  and  $M_u$ . Moment magnification factors are needed if the first-order analysis is used. Second-order elastic analysis is conducted on a geometrically perfect frame subject to notional horizontal load  $\xi W_{story}$  at each story, where  $W_{story}$  is the gravity load at that story, and  $\xi$  is the notional load parameter. A simple plane frame (2D) model as shown in Fig. 5.16b could be used for the second-order elastic analysis but semi-rigid connections must be considered. Performing the second-order elastic analysis on a frame with initial out-of-plumbness as shown Fig. 5.16a or on a geometrically perfect frame subject to notional horizontal loads as shown Fig. 5.16b is the same if  $\psi$  is equal to  $\xi$  because they are statically equivalent. Therefore, the only difference between the effective length approach and the notional load approach is the value of the column axial strength used in the interaction equation because it is a function of  $K_x$ . The column flexural strength  $M_n$  is not the function of  $K_x$  when the column is bending in the direction perpendicular to the upright frames.

The notional load approach relies significantly on the selection of the notional horizontal load and the flexural stiffness of the analysis model. Three procedures for selecting the notional horizontal load and the flexural stiffness of the analysis model were investigated.

**Approach 2a** - the notional load parameter  $\xi$  was assumed equal to the frame initial out-of-plumbness. The RMI specification recommends that the frame initial out-of-plumbness should not be more than 0.5 inches in 10 feet, therefore in this approach  $\xi$  was assumed equal to 1/240.

**Approach 2b** - the notional load parameter  $\xi$  was determined from

$$\xi = \begin{cases} (K_x - 1)/168, & 1 < K_x < 1.7 \\ 1/240, & K_x \geq 1.7 \end{cases} \quad (5.8)$$

**Approach 2c** - the notional load parameter  $\xi$  was assumed equal to 1/240 and the second-order elastic analysis was performed on a reduced flexural stiffness model. A 10% reduction in the flexural stiffness was proposed. This was done by using a reduce flexural stiffness  $EI^*$  for all members and connections in the analysis model

$$EI^* = 0.9EI \quad (5.9)$$

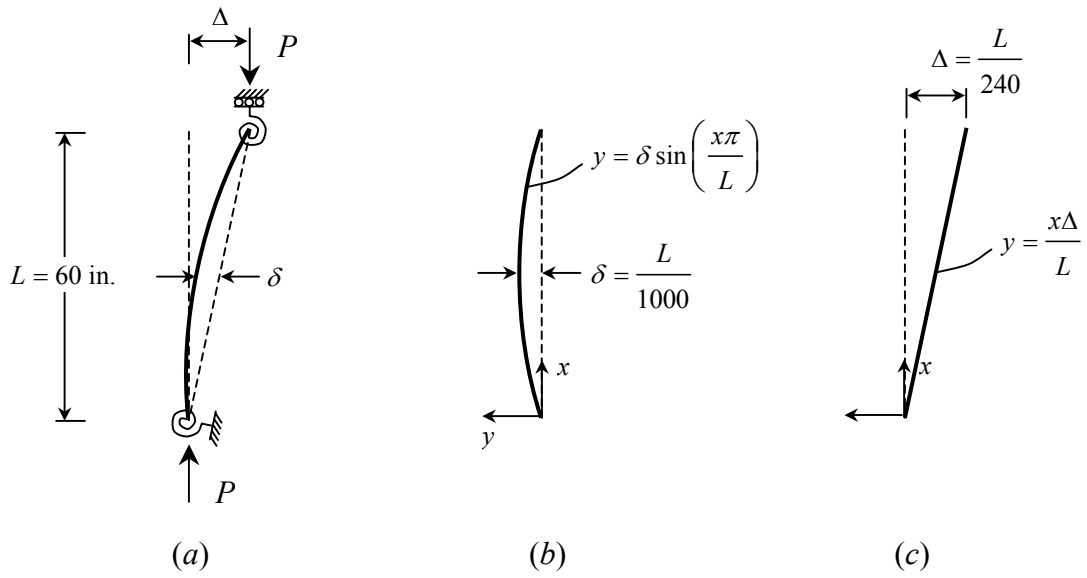
where  $E$  is the modulus of elasticity, and  $I$  is the moment of inertia about the axis of bending. When the moment magnification factors are used to approximate the relationship between  $M_u$  and  $P_u$  from first-order analysis, and the first-order analysis is based on a reduced flexural stiffness model, Eq. (5.7) becomes

$$\frac{P_u}{P_{ex(L)}} + \frac{C_{mx}M_u}{\left(1 - \frac{P_u}{P_{ex}^*}\right)M_n} \leq 1 \quad (5.10)$$

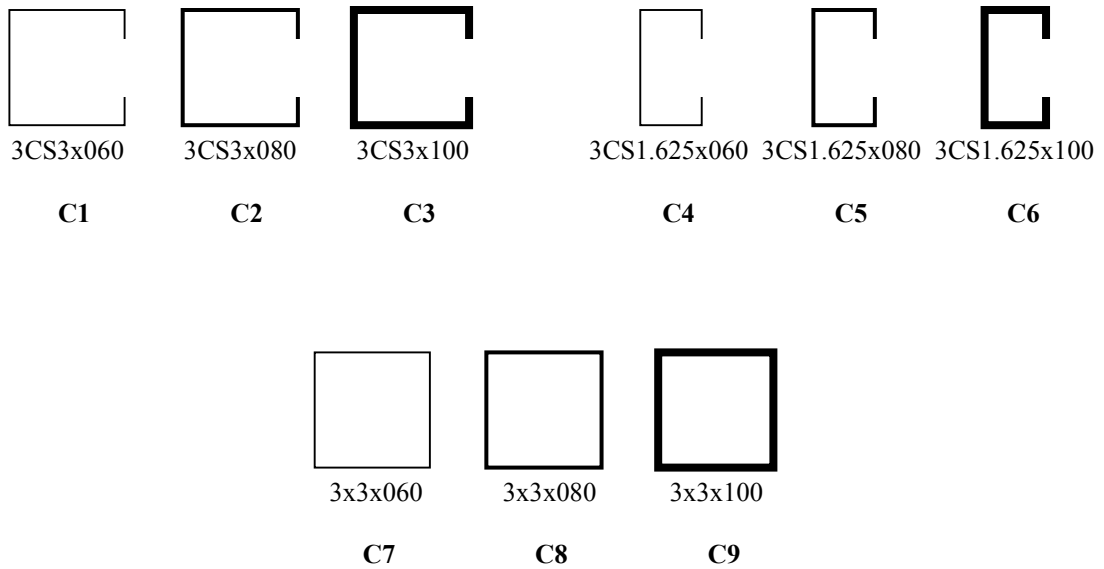
where  $P_{ex}^*$  is the elastic flexural buckling load based on  $EI^*$ , thus  $P_{ex}^* = 0.9P_{ex}$

### 5.6.1 Isolated rotationally restrained sway column

A parametric study was carried out to compare the effective length approach and the notional load approach for accuracy and appropriateness for beam-column design. An isolated rotationally restrained sway column as shown in Fig. 5.17a was used as the vehicle for carrying out the parametric study. The parameters included: nine column sections as shown in Fig. 5.18, three material yield stresses (33, 55, and 70 ksi), and twenty different rotational end-restraints as given in Table 5.2. Combinations of these parameters yielded a total of 540 beam-column configurations.



**Figure 5.17** (a) Rotationally restrained sway column (b) out-of-straightness (c) out-of-plumbness



**Figure 5.18** Column sections in study

**Table 5.2** Boundary Conditions in Study

Boundary Condition	$G_A$	$G_B$	$K_x$
G1	60	$\infty$	10.095
G2	20	$\infty$	6.018
G3	6	$\infty$	3.650
G4	0.6	$\infty$	2.198
G5	0	$\infty$	2
G6	60	60	7.080
G7	20	60	5.106
G8	6	60	3.379
G9	0.6	60	2.108
G10	0	60	1.924
G11	20	20	4.155
G12	6	20	3.009
G13	0.6	20	1.965
G14	0	20	1.804
G15	6	6	2.404
G16	0.6	6	1.675
G17	0	6	1.548
G18	0.6	0.6	1.196
G19	0	0.6	1.097
G20	0	0	1

**Table 5.3** Statistics for the Correlation of Design Procedures with the FEM Results

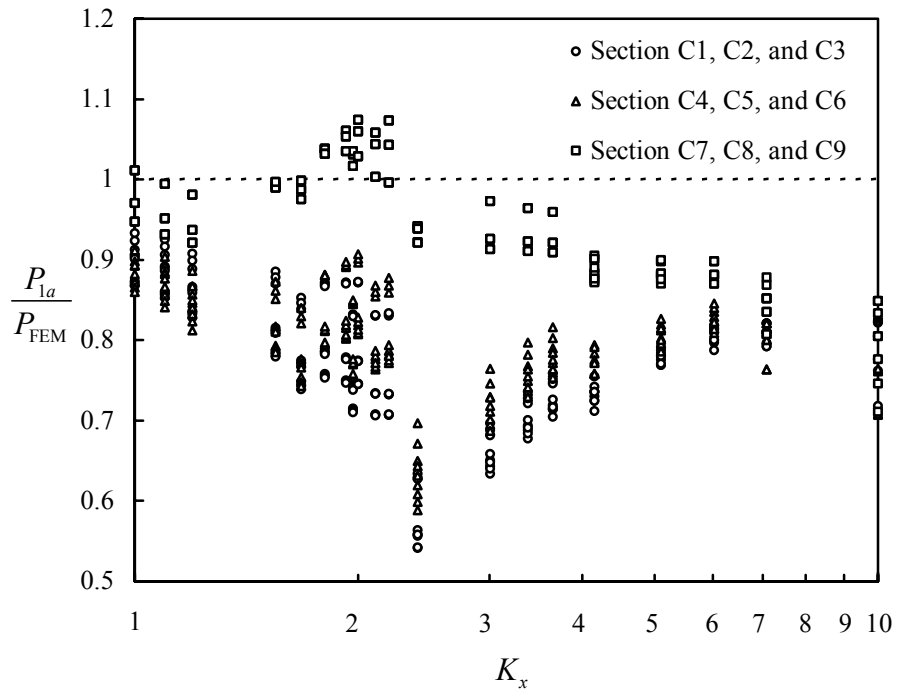
Section	Statistics	$\frac{P_{1a}}{P_{FEM}}$	$\frac{P_{1b}}{P_{FEM}}$	$\frac{P_{1c}}{P_{FEM}}$	$\frac{P_{1d}}{P_{FEM}}$	$\frac{P_{2a}}{P_{FEM}}$	$\frac{P_{2b}}{P_{FEM}}$	$\frac{P_{2c}}{P_{FEM}}$
		C1, C2, and C3	Mean	0.776	0.960	0.715	0.850	0.927
	Max	0.933	1.082	0.872	0.956	0.999	0.999	0.954
	Min	0.541	0.744	0.521	0.629	0.808	0.808	0.762
	Standard Deviation	0.081	0.066	0.073	0.066	0.052	0.044	0.036
	Coefficient of Variation, %	10.4	6.9	10.2	7.7	5.6	4.7	4.1
C4, C5, and C6	Mean	0.800	0.964	0.717	0.826	0.916	0.926	0.871
	Max	0.911	1.107	0.844	0.925	1.000	1.000	0.971
	Min	0.588	0.725	0.556	0.579	0.796	0.816	0.734
	Standard Deviation	0.062	0.083	0.056	0.071	0.060	0.049	0.046
	Coefficient of Variation, %	7.7	8.6	7.8	8.6	6.6	5.3	5.3
C7, C8, and C9	Mean	0.957	0.957	0.796	0.796	0.959	0.979	0.894
	Max	1.074	1.074	0.888	0.888	1.000	1.010	0.941
	Min	0.711	0.711	0.620	0.620	0.820	0.871	0.793
	Standard Deviation	0.074	0.074	0.037	0.037	0.051	0.022	0.030
	Coefficient of Variation, %	7.7	7.7	4.6	4.6	5.3	2.3	3.4
All sections	Mean	0.844	0.960	0.743	0.824	0.934	0.946	0.883
	Max	1.074	1.107	0.888	0.956	1.000	1.010	0.971
	Min	0.541	0.711	0.521	0.579	0.796	0.808	0.734
	Standard Deviation	0.108	0.074	0.068	0.064	0.057	0.046	0.039
	Coefficient of Variation, %	12.8	7.8	9.2	7.7	6.1	4.9	4.4



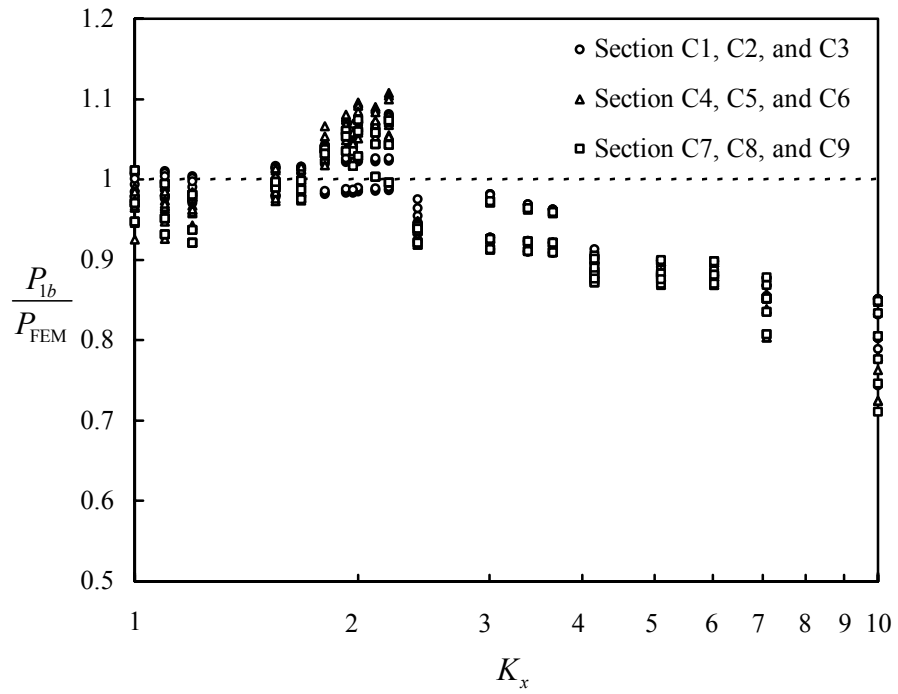
The finite element method, which considers both geometric and material nonlinearities, was used as the basis for evaluating the accuracy of the design approaches. The finite element modeling assumptions included using a three-dimensional model, using open-section beam elements to model the open-section columns, using linear torsional springs to model the rotational end-restraints for bending about the major axis, using pin-ended supports for bending about the minor axis and for twisting, using a combination of the out-of-straightness and the out-of-plumbness as shown in Figs. 5.17*b* and 5.17*c* for the member initial geometric imperfection, and using an elastic-plastic material model.

The correlations between the different design approaches and the finite element results are summarized in Appendix E Table E.1 where  $P_{1a}$ ,  $P_{1b}$ ,  $P_{1c}$ ,  $P_{1d}$ ,  $P_{2a}$ ,  $P_{2b}$ , and  $P_{2c}$  are the axial load carrying capacity of the member obtained by using the Approaches 1*a*, 1*b*, 1*c*, 1*d*, 2*a*, 2*b*, and 2*c*, respectively.  $P_{FEM}$  is the axial load carrying capacity of the member obtained by using the finite element method. In practice, the resistance factor  $\phi_c$  is equal to 0.85, and  $\phi_b$  is equal to 0.90 or 0.95; these values are, however, for research purposes in this study all assumed equal to one. In practice, the value of  $K_t$  for column torsional buckling is assumed equal to 0.8 if braces constrain the column from twisting. This value was, however in this study assumed equal to one, because the column was simply supported for twisting. The statistical summary of Table E.1 is given in Table 5.3. Design examples for the difference approaches are given in the Appendix F.

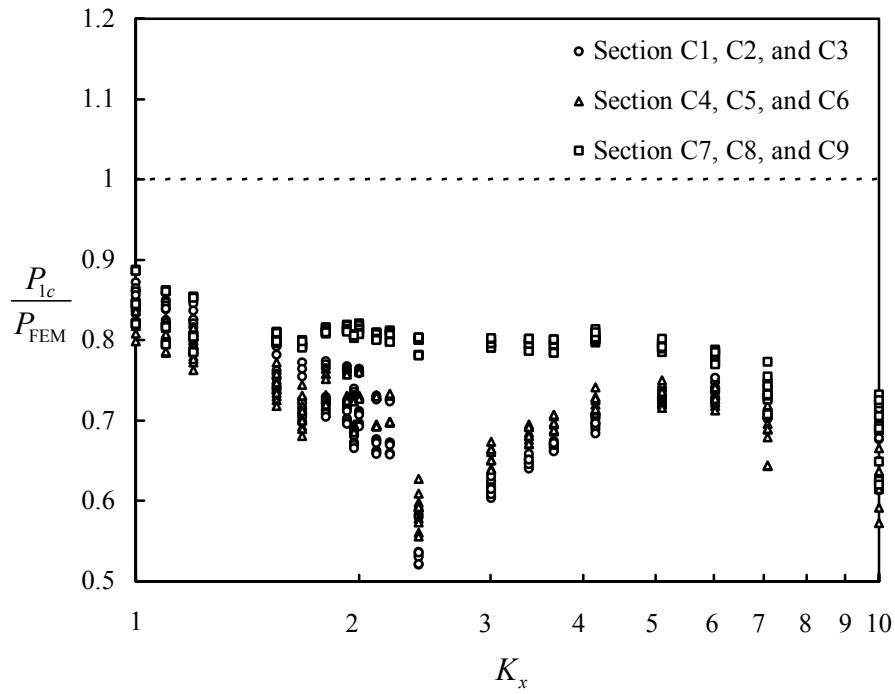
The results, which are given in Appendix E Table E.1, are also plotted in Figs. 5.19 through 5.25 where the finite element analysis was used as the basis for evaluating the accuracy of the different design approaches. As can be seen in these figures, Approaches 1*c*, 1*d*, 2*a*, 2*b*, and 2*c* are conservative compared to the finite element results while the Approaches 1*a* and 1*b* have a few unconservative designs.



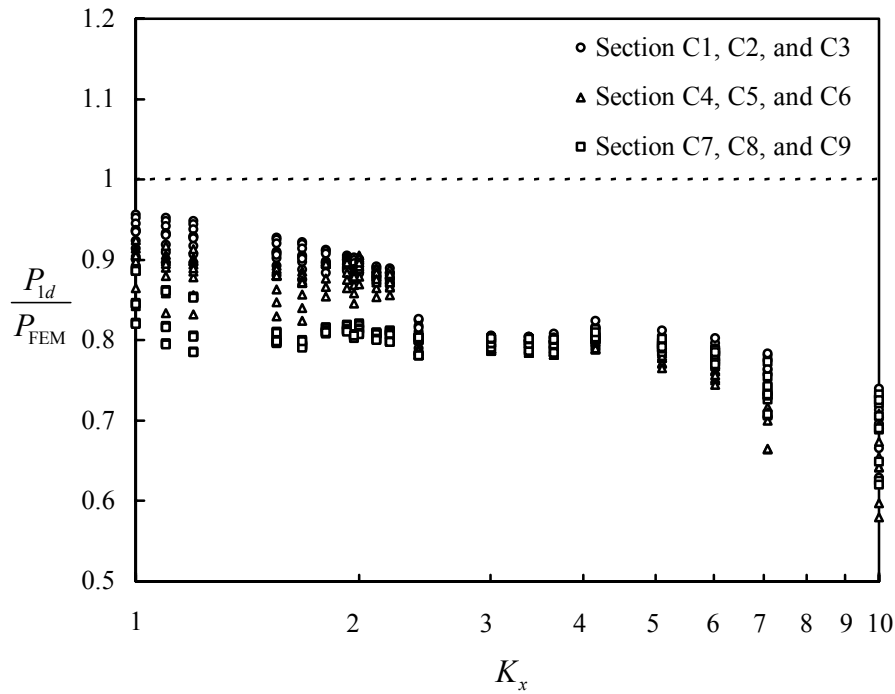
**Figure 5.19** Correlation between the Effective Length Approach (Approach 1a) and the FEM results



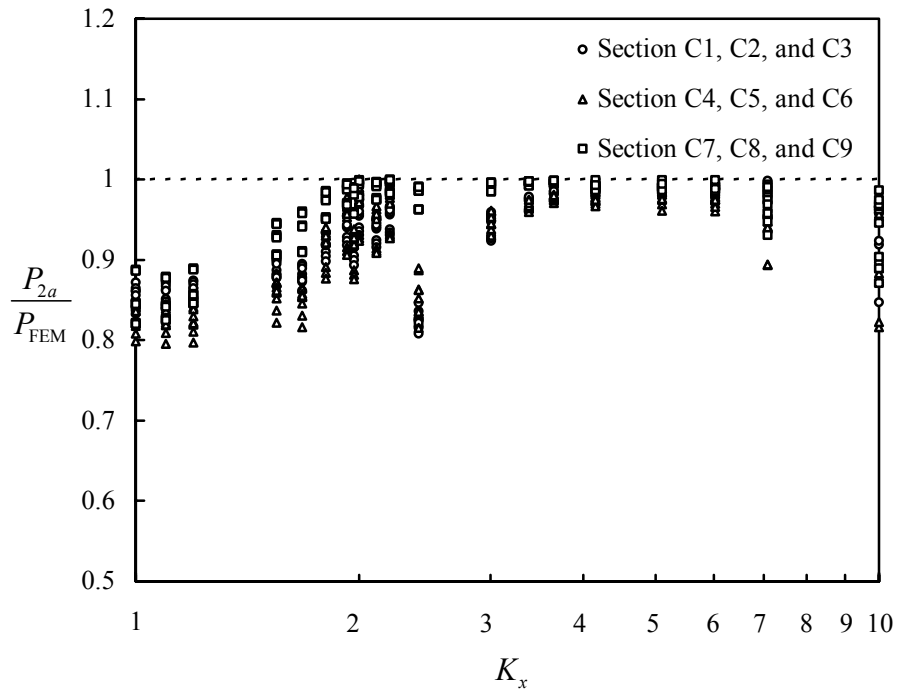
**Figure 5.20** Correlation between the Effective Length Approach (Approach 1b) and the FEM results



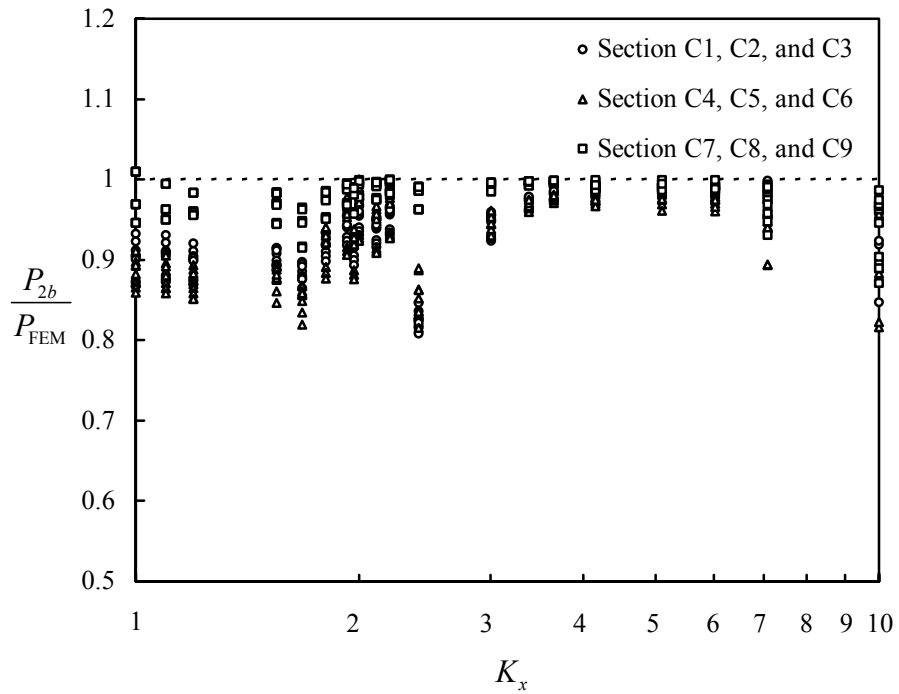
**Figure 5.21** Correlation between the Effective Length Approach (Approach 1c) and the FEM results



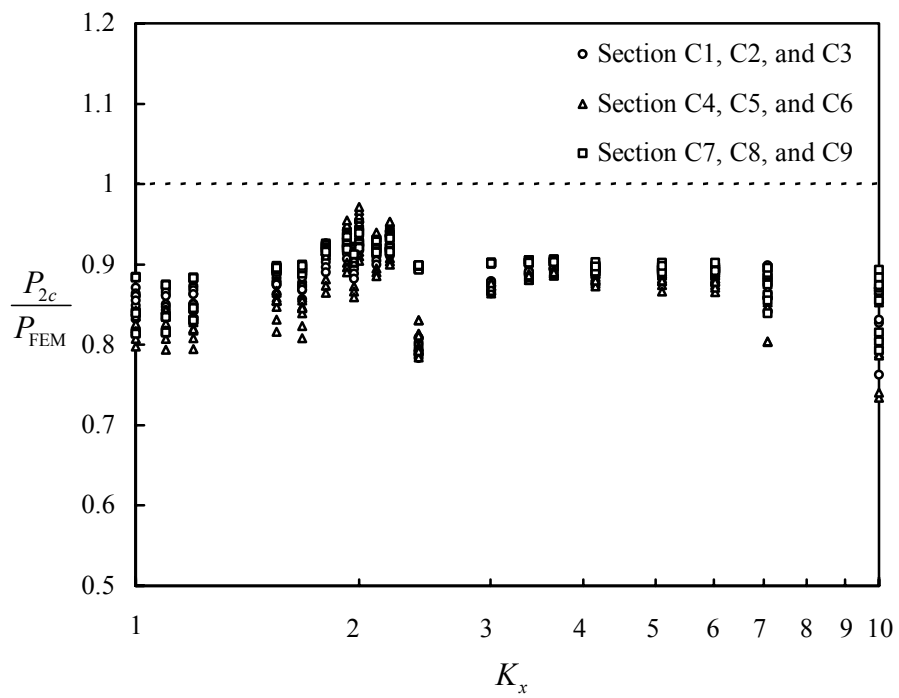
**Figure 5.22** Correlation between the Effective Length Approach (Approach 1d) and the FEM results



**Figure 5.23** Correlation between the Notional Load Approach (Approach 2a) and the FEM results



**Figure 5.24** Correlation between the Notional Load Approach (Approach 2b) and the FEM results



**Figure 5.25** Correlation between the Notional Load Approach (Approach 2c) and the FEM results

Comparison between Approach *1a* and *1b* indicates that *1b* agrees better with the finite element results than *1a* does. Approach *1a* has lower design loads than *1b* because of the conservatism in the AISI torsional-flexural buckling provisions. Both Approaches *1a* and *1b* have a few unconservative designs because the secondary moment coming from the member out-of-plumbness was not considered in the design.

Comparison between Approach *1c* and *1d* indicates that *1d* agrees better with the finite element results than *1c* does. Approach *1c* has lower design loads than *1d* because of the conservatism in the AISI torsional-flexural buckling provisions. Overall both Approaches *1c* and *1d* predict a very conservative design.

Comparison between Approach *1a* and *1c* indicates that even though the overall result of *1a* agrees better with the finite element results than *1c* does, Approach *1c* is still more appropriate for design because it accounts for the secondary moments having no unconservative designs.

Comparison between Approach *2a* and *2b* indicates that *2b* agrees better with the finite element results than *2a* does. When  $K_x$  is less than 1.7, Approach *2b* will have higher design loads than Approach *2a* because it uses less notional horizontal loads according to Eq. (5.8). Implementation of Approach *2b*, however, must be considered carefully, because Eq. (5.8) was developed based on the design calibration of a limit number of frame configurations. Thus, it may not always be applicable.

Comparison between Approach *2a* and *2c* indicates that even though the overall result of *2a* agrees better with the finite element results than *2c* does, Approach *2c* provides a more consistent conservatism in its design across the different  $K_x$  values. In Approach *2c*, a 10% reduction in the flexural stiffness of the analysis model was made; this has an effect mostly on the beam-columns, which have high  $K_x$  values, causing a 10% reduction in the design strength.

Comparison between Approaches 1 and 2 indicates that overall Approach 2, which is the notional load approach, agrees better with the finite element results than Approach 1, which is the effective length approach. Among the three notional load approaches:  $2a$ ,  $2b$ , and  $2c$ , it is recommended that Approach  $2c$  be considered as an alternative means for cold-formed steel frame and beam-column design. Approach  $2c$ , which is the notional load approach with flexural stiffness reduction, provides a reliable consistently conservative design across wide ranges of beam-column configurations. The reason for choosing this approach, even though the overall results of Approaches  $2a$  and  $2b$  agree better with the finite element results, is because the 10% reduction in the flexural stiffness is needed to account for the strength reduction due to member initial crookedness for the same reasons that in the effective length approach the column axial strength is designed according to the following equation  $F_n = 0.877F_e$  for  $\lambda_c \geq 1.5$ . This equation when used in the notional load approach to compute  $P_{n(L)}$  does not account for the structural strength reduction because  $P_{n(L)}$  is computed based on  $K_x$  equal to one.  $P_u$  and  $M_u$ , which are used in the interaction equation, obtained based on a reduced flexural stiffness analysis model do account for the structural strength reduction.

### **5.6.2 Interaction Equation**

The difference between the effective length approach and the notional load approach is the value of the column axial strength used in the interaction equation because it is a function of  $K_x$ . The column flexural strength  $M_n$  is not the function of  $K_x$ . To explain how the interaction equation works differently for these two design approaches one can classify the failure modes for beam-columns into three categories as follows:

The first category is failure by material yielding. The design of stocky columns having this failure mode are independent of the members elastic buckling load. The interaction equation used for this design can be simplified as follows:

$$\frac{P_u}{P_y} + \frac{M_u}{M_n} \leq 1 \quad (5.11)$$

where  $P_y$  is the axial strength at yield stress. The value of  $P_y$  is independent of the elastic buckling load; therefore, the same design load is obtained using the effective length approach or the notional load approach.

The second category is failure by elastic buckling. The load carrying capacity of slender columns having this failure mode is very close to its elastic buckling load. The interaction equation used for this design can be simplified as follows:

$$\frac{P_u}{P_e} + \frac{M_u}{M_n} \leq 1 \quad (5.12)$$

where  $P_e$  is the elastic buckling load. For the case when flexural buckling is the critical buckling mode, and the moment magnification factor is used instead of performing the second-order analysis, further simplification can be made as follows:

$$\frac{P_u}{P_{ex}} + \frac{C_{mx} M_u}{\left(1 - \frac{P_u}{P_{ex}}\right) M_n} \leq 1 \quad (5.13)$$

where  $P_{ex}$  is the elastic flexural buckling load and  $C_{mx}$  is a constant coefficient. The above interaction equation is for designing beam-columns according to the effective length approach. For designing beam-columns according to the notional load approach the following equation is used instead:

$$\frac{P_u}{P_{ex(L)}} + \frac{C_{mx} M_u}{\left(1 - \frac{P_u}{P_{ex}}\right) M_n} \leq 1 \quad (5.14)$$



where  $P_{ex(L)}$  is the elastic flexural buckling load computed based on  $K_x$  being equal to one. As can be readily seen from Eqs. (5.13) and (5.14), the design load  $P_u$  obtained from either of these equations will never exceed  $P_{ex}$  because of the moment magnification factor term. The notional load approach will, however, allow a higher design load than the effective length approach because the value of  $P_{ex(L)}$  is higher than  $P_{ex}$ ; that is,  $P_u$  obtained from the notional load approach will be closer to the estimated value  $P_{ex}$  making it more accurate than the effective length approach. This remark also holds true when member failure is by torsional-flexural buckling as can be seen by comparing the results of Figs. 5.21 and 5.23 for the high  $K_x$  value cases.

The third category is failure by inelastic buckling. By comparing Eq. (5.6) and Eq (5.7), which are the interaction equations used to design beam-columns for this failure mode according to the effective length approach and the notional load approach, respectively; it can be seen that the notional load approach will allow a higher design load than the effective length approach because the value of  $P_{n(L)}$  is higher than  $P_n$ . The discrepancy between these two approaches is small when the value of  $K_x$  is close to one, but as the value of  $K_x$  increases, that is the failure mode changes toward failure by elastic buckling, the differences become apparent as can be seen by comparing the results of Figs. 5.21 and 5.23.

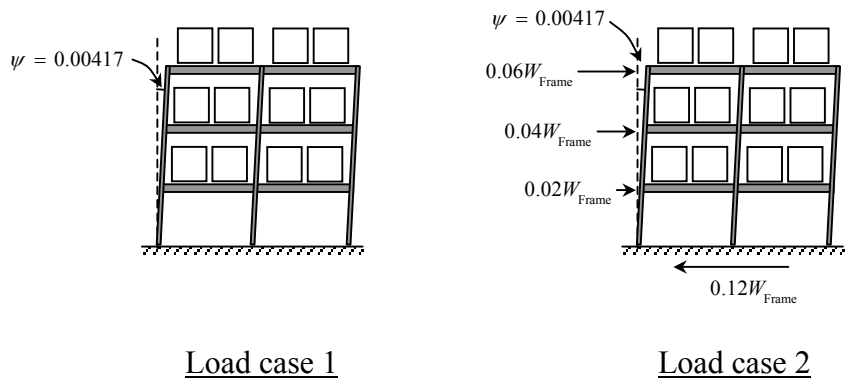
A beam-column designed according to the notional load approach can sometimes have higher design strength than a concentrically loaded compression member designed according to the effective length approach. That is  $P_u$  obtained by using the notional approach can sometimes be higher than  $P_n$ . Even though this seems to be unacceptable according to the current design procedure, the finite element result from this study does support this. In the effective length approach, columns and beam-columns subject to torsional-flexural buckling are designed based on a column curve for an equivalent pin-ended effective length member. This process of simplification

used to design members with boundary conditions other than pin-ended supports such as a rotationally restrained sway column has been shown to be conservative compared to the results obtained from performing a finite element analysis.

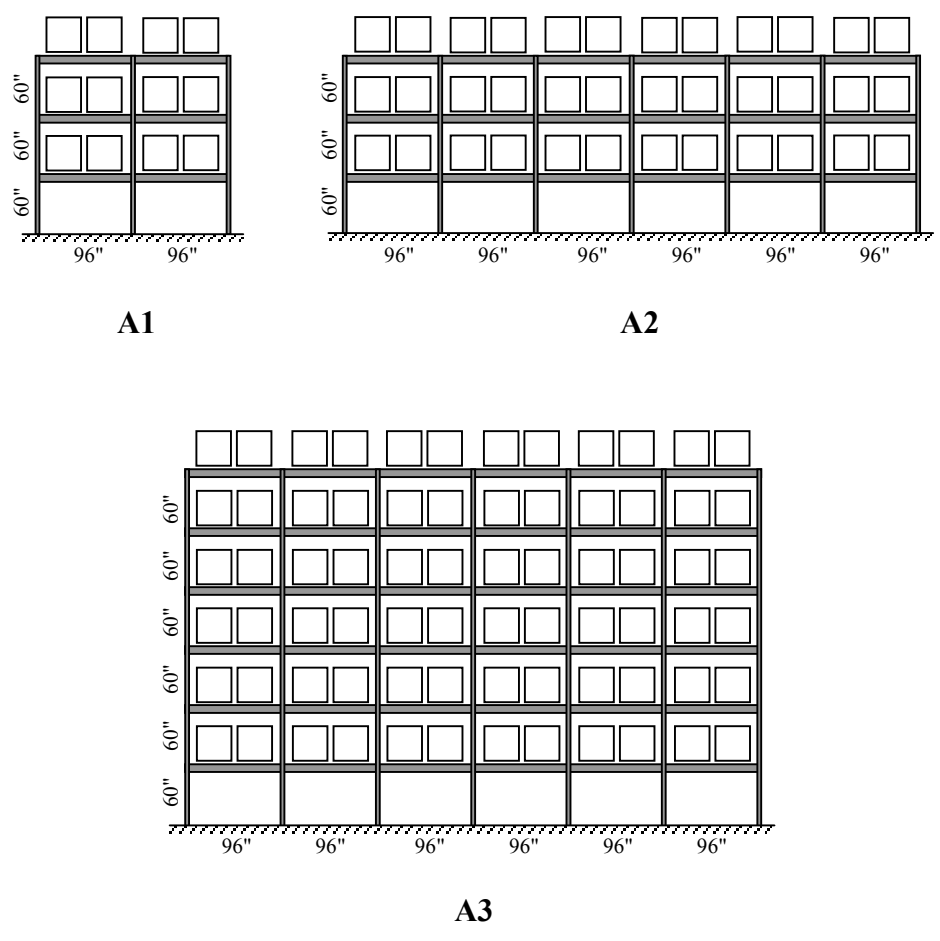
### **5.6.3 Cold-Formed Steel Frames**

A parametric study was carried out to compare the effective length approach and the notional load approach for accuracy and appropriateness for cold-formed steel frame design. Pallet racks as shown in Fig. 5.27 were used as the vehicle for carrying out the parametric study. The parameters included: two load cases as shown in Fig. 5.26, three frame dimensions as shown in Fig. 5.27, two upright frame configurations as shown in Fig. 5.28, nine column sections as shown in Fig. 5.18, three material yield stresses (33, 55, and 70 ksi), six beam to column connection stiffnesses as given Table 5.4, and braces and shelf beams as shown in Fig. 5.29. Combinations of these parameters yielded a total of 972 pallet rack configurations for each load case. The first loading condition is the gravity load case on a frame with initial out-of plumbness of 0.5 inches in 10 feet, the second loading condition is the seismic load case on a frame with initial out-of plumbness of 0.5 inches in 10 feet, where the seismic base shear was assumed to be 12% of total gravity load on the frame.

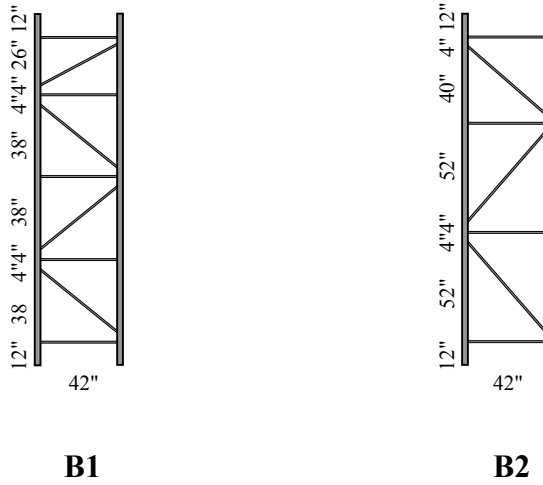
The finite element method, which considers both geometric and material nonlinearities, was used as the basis for evaluating the accuracy of the design approaches. The finite element analysis modeling assumptions included using a three-dimensional model, using open-section beam elements to model the columns and braces, using linear torsional springs to model the connection stiffness, using the



**Figure 5.26** Loading conditions in study



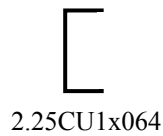
**Figure 5.27** Frame dimensions in study



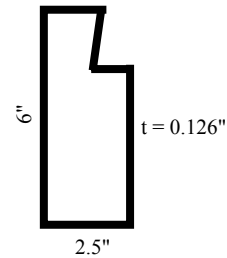
**Figure 5.28** Upright frame configurations in study

**Table 5.4** Beam to Column Connection Stiffnesses in Study

Connection	Stiffness, kip-in./rad
D1	100
D2	200
D3	300
D4	400
D5	500
D6	600



Braces



Shelf beams

**Figure 5.29** Braces and Shelf beams in Study

proposed base fixity equation given Chapter 2 to compute the base fixity, and using elastic-plastic material model.

The correlations between the different design approaches and the finite element results are summarized in Appendix E Tables E.2 and E.3 with a statistical summary of these tables given in Tables 5.5 and 5.6 where  $W_{1a}$ ,  $W_{1c}$ ,  $W_{2a}$ ,  $W_{2b}$ , and  $W_{2c}$  are the ultimate load carrying capacity per bay of the frame obtained by using the Approaches 1a, 1c, 2a, 2b, and 2c, respectively.  $W_{FEM}$  is the ultimate load carrying capacity per bay of the frame obtained by using the finite element method. In practice, the resistance factor  $\phi_c$  is equal to 0.85, and  $\phi_b$  is equal to 0.90 or 0.95; these values are, however, for research purposes in this study all assumed equal to one.

The results for load case 1, which are given in Appendix E Table E.2, are also plotted in Figs. 5.30 through 5.34 where the finite element analysis was used as the basis for evaluating the accuracy of the different design approaches. As can be seen in these figures, Approaches 1c, 2a, 2b, and 2c are conservative compared to the finite element results while Approach 1a has a few unconservative designs. The reason why these few results in Approach 1a are unconservative compared to the finite element results is because the second-order effects arising from the frame story-out-plumbness was considered in the design process.

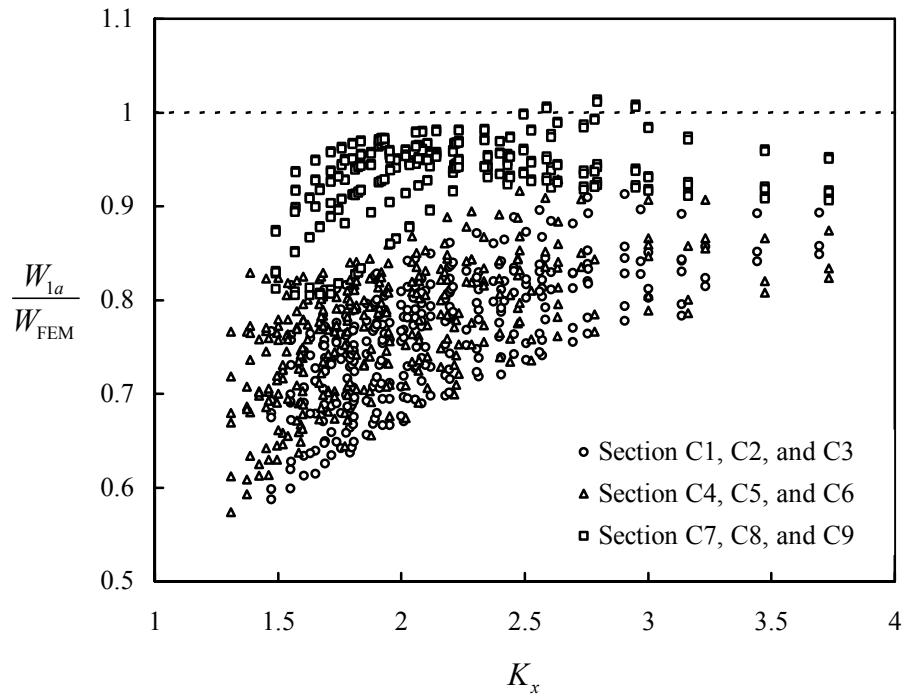
Comparison between Approach 1c and 2a for load case 1 indicates that 2a agrees better with the finite element results than 1c does. The design load obtained from the notional load approach is higher than the effective length approach because of the assumption of  $K_x$  equal to one. This is the reason why as the value of  $K_x$  increases the discrepancy between the design loads obtained from the effective length approach and the notional load approach also increases.

**Table 5.5** Load Case 1 - Statistics for the Correlation of Design Procedures with the FEM Results

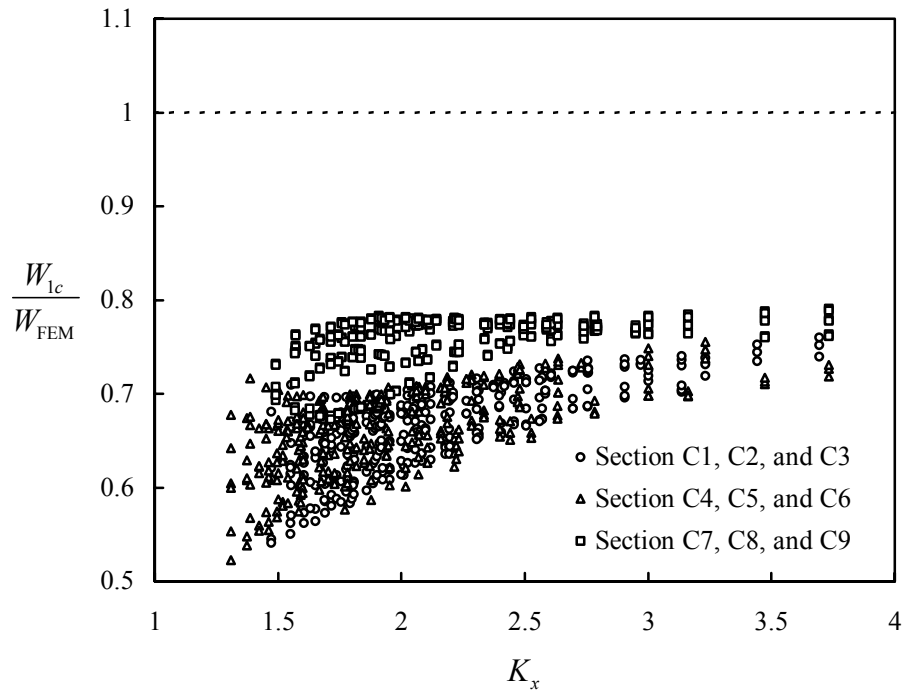
Section	Statistics	$\frac{W_{1a}}{W_{FEM}}$	$\frac{W_{1c}}{W_{FEM}}$	$\frac{W_{2a}}{W_{FEM}}$	$\frac{W_{2b}}{W_{FEM}}$	$\frac{W_{2c}}{W_{FEM}}$
C1, C2, and C3	Mean	0.763	0.666	0.873	0.875	0.827
	Max	0.913	0.760	0.999	0.999	0.904
	Min	0.587	0.541	0.633	0.656	0.628
	Standard Deviation	0.065	0.043	0.086	0.084	0.061
	Coefficient of Variation, %	8.5	6.5	9.9	9.5	7.4
C4, C5, and C6	Mean	0.768	0.663	0.834	0.843	0.796
	Max	0.928	0.755	0.993	0.993	0.900
	Min	0.574	0.522	0.589	0.626	0.584
	Standard Deviation	0.066	0.044	0.094	0.085	0.070
	Coefficient of Variation, %	8.6	6.7	11.3	10.1	8.8
C7, C8, and C9	Mean	0.933	0.757	0.936	0.939	0.873
	Max	1.014	0.790	1.000	1.000	0.904
	Min	0.805	0.673	0.772	0.785	0.762
	Standard Deviation	0.041	0.026	0.054	0.050	0.032
	Coefficient of Variation, %	4.4	3.4	5.7	5.4	3.6
All sections	Mean	0.821	0.696	0.881	0.886	0.832
	Max	1.014	0.790	1.000	1.000	0.904
	Min	0.574	0.522	0.589	0.626	0.584
	Standard Deviation	0.098	0.058	0.090	0.085	0.065
	Coefficient of Variation, %	12.0	8.4	10.3	9.5	7.8

**Table 5.6** Load Case 2 - Statistics for the Correlation of Design Procedures with the FEM Results

Section	Statistics	$\frac{W_{1c}}{W_{FEM}}$	$\frac{W_{2a}}{W_{FEM}}$	$\frac{W_{2b}}{W_{FEM}}$	$\frac{W_{2c}}{W_{FEM}}$
C1, C2, and C3	Mean	0.682	0.759	0.759	0.746
	Max	0.754	0.879	0.879	0.848
	Min	0.581	0.595	0.600	0.591
	Standard Deviation	0.029	0.054	0.054	0.050
	Coefficient of Variation, %	4.2	7.2	7.1	6.7
C4, C5, and C6	Mean	0.638	0.694	0.695	0.684
	Max	0.722	0.835	0.835	0.808
	Min	0.549	0.560	0.566	0.557
	Standard Deviation	0.034	0.058	0.057	0.054
	Coefficient of Variation, %	5.4	8.4	8.2	8.0
C7, C8, and C9	Mean	0.655	0.727	0.727	0.714
	Max	0.732	0.879	0.879	0.847
	Min	0.555	0.573	0.575	0.569
	Standard Deviation	0.045	0.078	0.078	0.073
	Coefficient of Variation, %	6.8	10.7	10.7	10.2
All sections	Mean	0.658	0.726	0.727	0.715
	Max	0.754	0.879	0.879	0.848
	Min	0.549	0.560	0.566	0.557
	Standard Deviation	0.041	0.070	0.069	0.065
	Coefficient of Variation, %	6.2	9.6	9.5	9.1

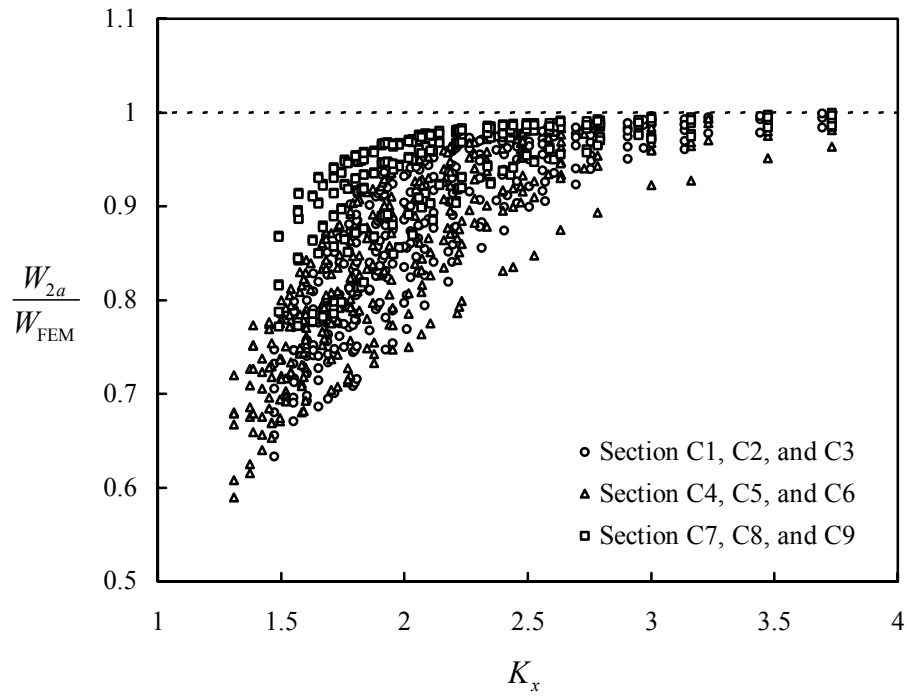


**Figure 5.30** Load Case 1 - Correlation between the Effective Length Approach (Approach 1a) and the FEM results

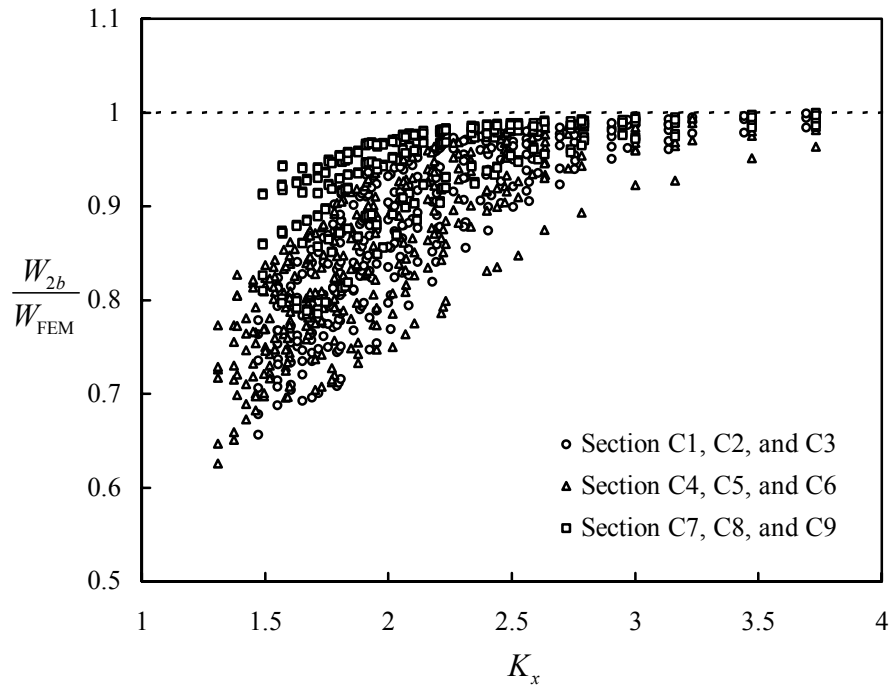


**Figure 5.31** Load Case 1 - Correlation between the Effective Length Approach (Approach 1c) and the FEM results

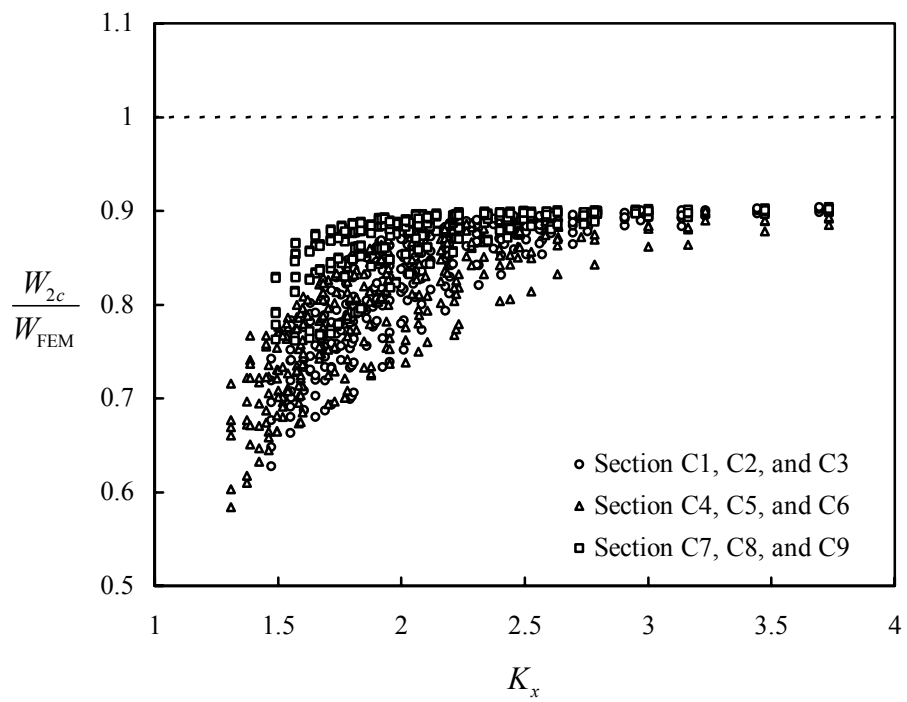




**Figure 5.32** Load Case 1 - Correlation between the Notional Load Approach (Approach 2a) and the FEM results



**Figure 5.33** Load Case 1 - Correlation between the Notional Load Approach (Approach 2b) and the FEM results



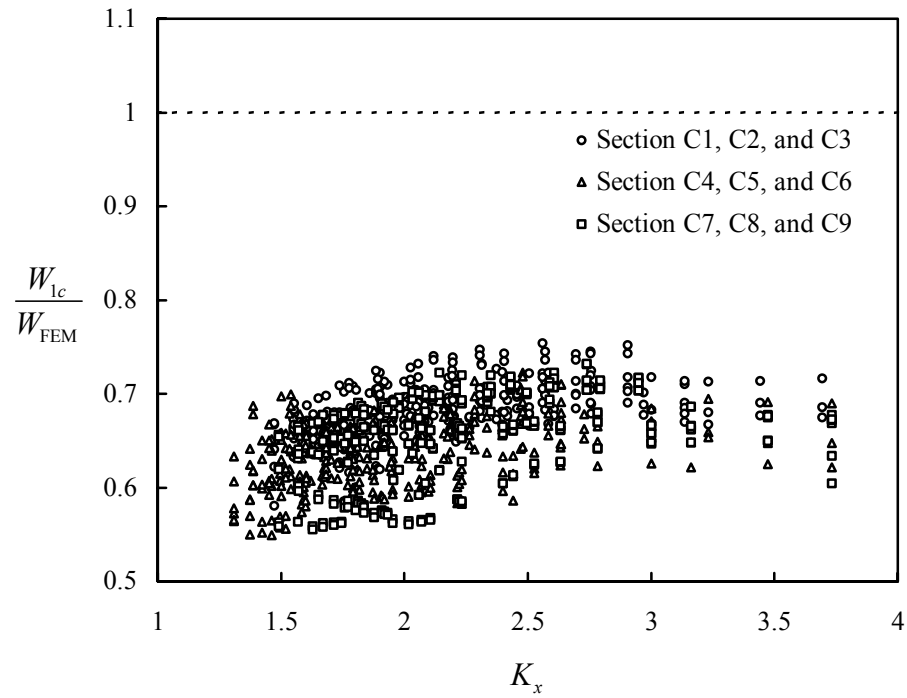
**Figure 5.34** Load Case 1 - Correlation between the Notional Load Approach (Approach 2c) and the FEM results

Comparisons among the three notional load approaches:  $2a$ ,  $2b$ , and  $2c$  for load case 1 indicate few differences between  $2a$  and  $2b$ , and  $2c$  is more conservative than  $2a$  and  $2b$ .

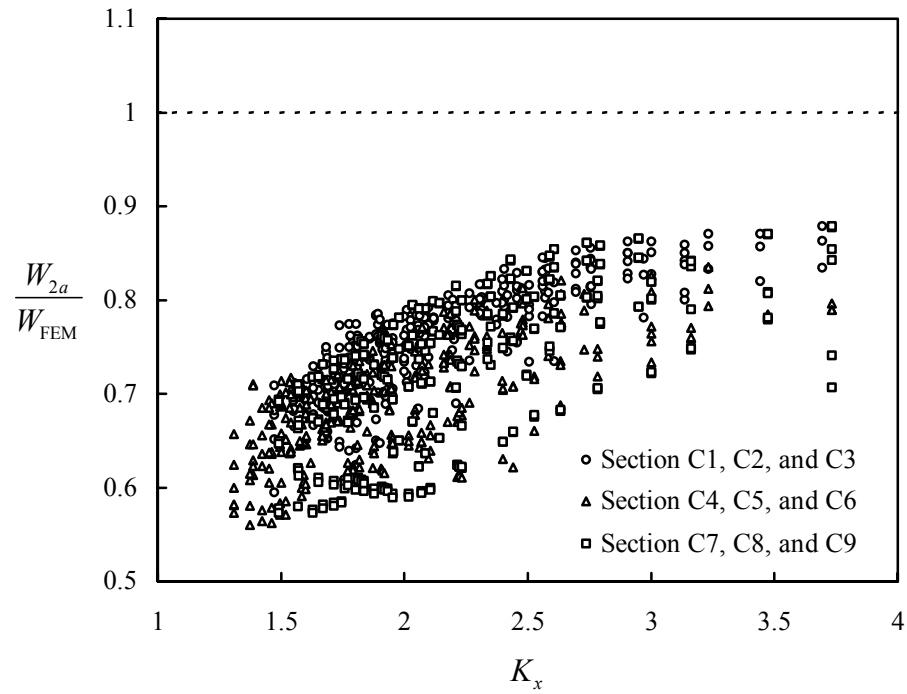
The results for load case 2, which are given in Appendix E Table E.3, are also plotted in Figs. 5.35 through 5.38 where the finite element analysis was used as the basis for evaluating the accuracy of the different design approaches. As can be seen in these figures, both the effective length approach and the notional load approach are conservative compared to the finite element results. The differences between the design loads obtained from the effective length approach and the notional load approach in this load case has decreased from the previous load case. The reason for this is because the horizontal force in this load case causes the storage rack to fail from the column flexural strength rather than axial strength. The column flexural strength used in both the effective length approach and the notional load approach is the same.

Comparisons between Approach  $2a$  and  $2b$  for load case 2 indicate few differences between these two approaches. Comparisons among the three notional load approaches:  $2a$ ,  $2b$ , and  $2c$ , indicates that  $2c$  is slightly more conservative than  $2a$  and  $2b$  because flexural stiffness reduction is made to analysis model in Approach  $2c$ .

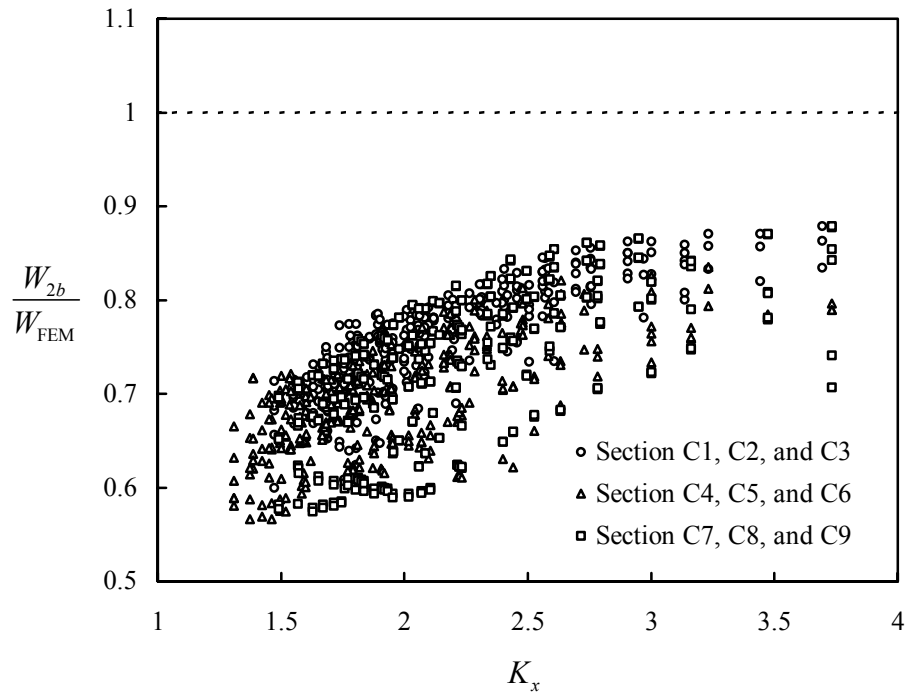
When the notional load approach is used for an earthquake load design or wind load design, applying additional notional horizontal loads are usually not necessary if the real horizontal forces coming from the earthquake loads or the wind loads are much greater, making the additive notional horizontal loads insignificant. However, if the magnitude of the real horizontal forces coming from the earthquake loads or the wind loads are comparable with the required notional horizontal loads then that notional horizontal loads must be applied as additive loads. It is recommended that the notional horizontal loads always be applied for earthquake load design or wind load design because it is more conservative with them.



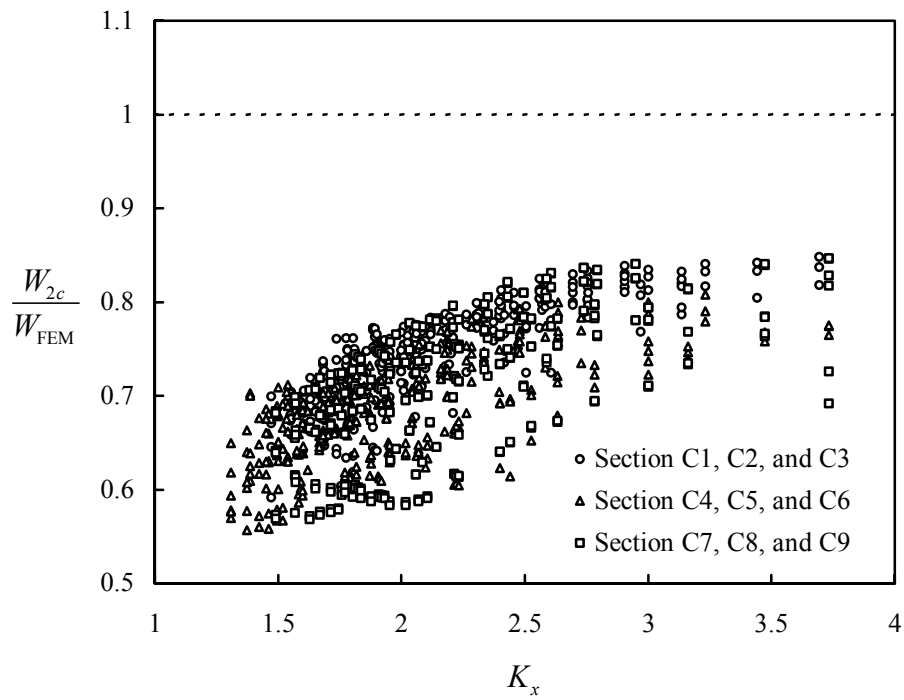
**Figure 3.35** Load Case 2 - Correlation between the Effective Length (Approach 1c) and the FEM results



**Figure 5.36** Load Case 2 - Correlation between the Notional Load Approach (Approach 2a) and the FEM results



**Figure 5.37** Load Case 2 - Correlation between the Notional Load Approach (Approach 2b) and the FEM results



**Figure 5.38** Load Case 2 - Correlation between the Notional Load Approach (Approach 2c) and the FEM results

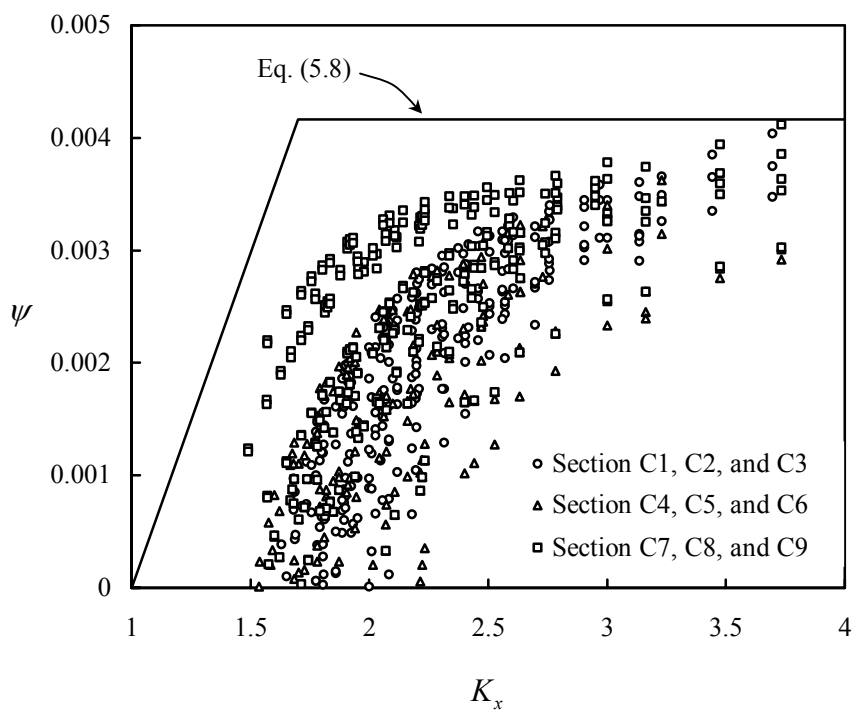
#### 5.6.4 Development of Approach 2b

As can be seen in Fig. 5.32, the notional load approach 2a is conservative compared to the finite element results, especially when the value of  $K_x$  is close to one. Attempts are made in this study to make improvements to this approach. The objective is to increase the design load so that the results will agree better with the finite element solution. This is done by decreasing the initial out-of plumbness  $\psi$  used in the second-order elastic analysis frame model. Decreasing the value of  $\psi$  is equivalent to applying less notional horizontal loads,  $\xi W_{story}$ .

The values of  $\psi$  needed to agree with finite element results were obtained by trial and error. The result was determined by linear interpolation within the tried values of  $\psi$  equal to 0.0025, 0.005, 0.001, 0.0015, 0.002, 0.0025, 0.003, 0.0035, and 0.00417. Results are shown in Fig. 5.39. As expected the obtained value of  $\psi$  decreases as the value of  $K_x$  becomes closer to one. From this obtained relationship between  $\psi$  and  $K_x$ , a new notional load approach 2b, which selects the notional horizontal load according to the column  $K_x$  value, is therefore proposed, by using the following conservative design equation

$$\psi = \begin{cases} (K_x - 1)/168, & 1 < K_x < 1.7 \\ 1/240, & K_x \geq 1.7 \end{cases} \quad (5.15)$$

When Eq. (5.15) is used the previous result, which was shown in Fig. 5.32, improves to become as shown in Fig. 5.33. As can be seen in these figures, improvements are made when this proposed equation is used.



**Figure 5.39** Load Case 1 - Frame out-of-plumb or the magnitude of the notional horizontal load required for the notional load approach

### **5.6.5 Approach 1a with $K_x = 1.7$**

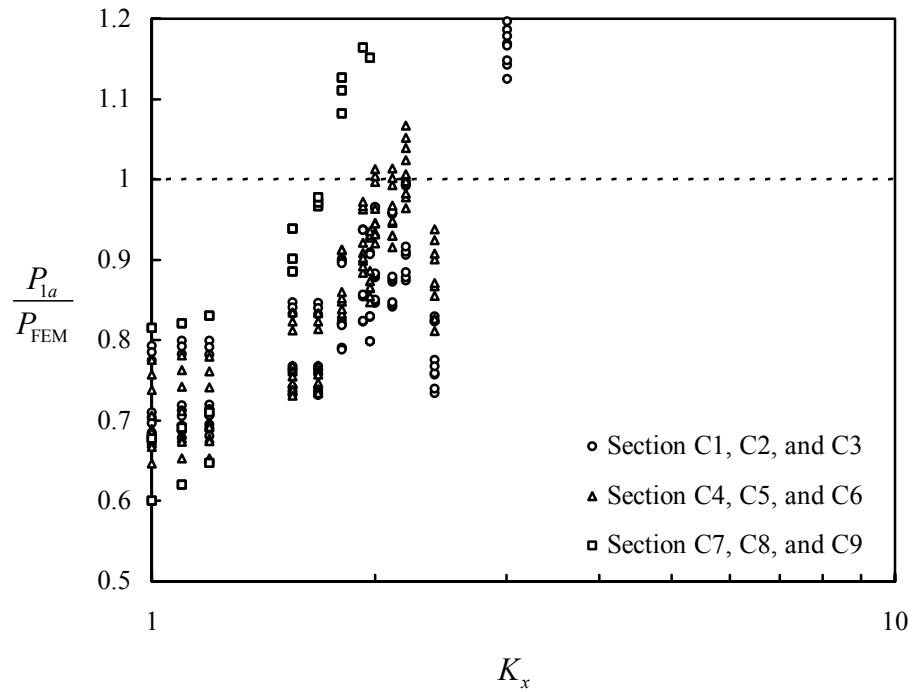
Additional parametric studies were carried out using Approach 1a with the value of  $K_x$  assumed to be 1.7. The results of this parametric study carried out for the isolated rotationally restrained sway column are given in Figs. 5.40 and 5.41. The results of this parametric study carried out for the cold-formed steel frames are given in Figs. 5.42 and 5.43.

The RMI specification allows the use of  $K_x$  equal to 1.7 as a default value. This value was chosen to give a reasonable amount of protection against sidesway for most common rack configurations. The results from this study suggested that this approach is unconservative if the real value of  $K_x$  is much higher than 1.7. However, the results also suggested that this approach when used to design open-sections is still conservative if the real value of  $K_x$  is just slightly higher than 1.7. The reason for this is because of the conservatism in the AISI torsional-flexural buckling provisions.

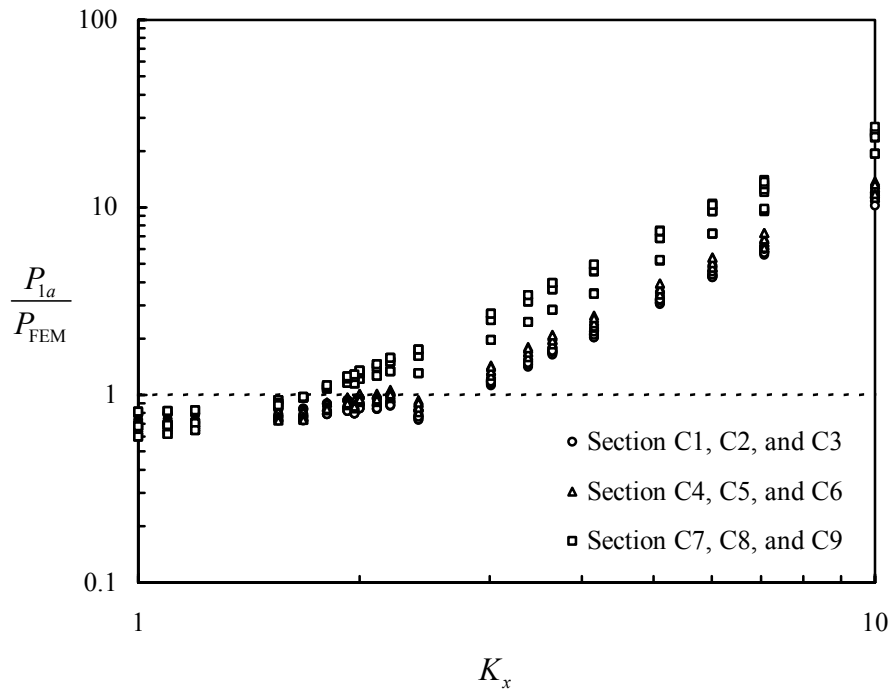
## **5.7 FINITE ELEMENT SIMULATION OF PALLET RACK TEST**

A physical test of pallet rack structures and components was conducted by Peköz (1975). A finite element simulation of the physical pallet rack test was carried out to investigate the behavior of the frame and verify finite element assumptions. A pallet rack manufactured design designated as type A-LDR was studied. Its geometry is given in Appendix G and Fig. 5.44. Two load cases were studied: the first load case had gravity loads applied on each bay equally, and the second load case had a combination of gravity and horizontal loads. Horizontal loads at 1.5% of the gravity loads at each beam level were applied to the right at each beam level of the left upright frame.

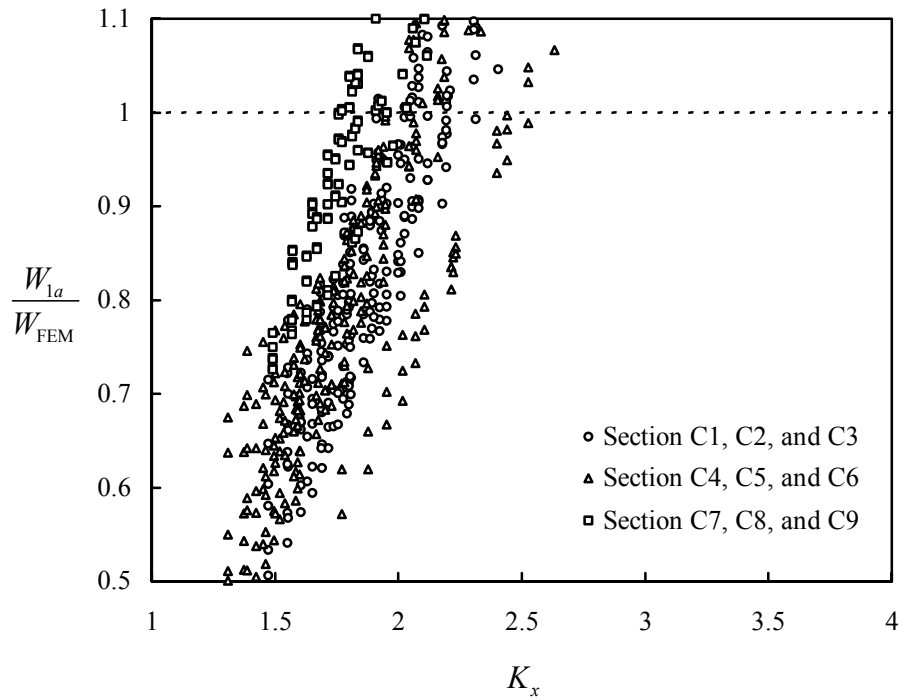




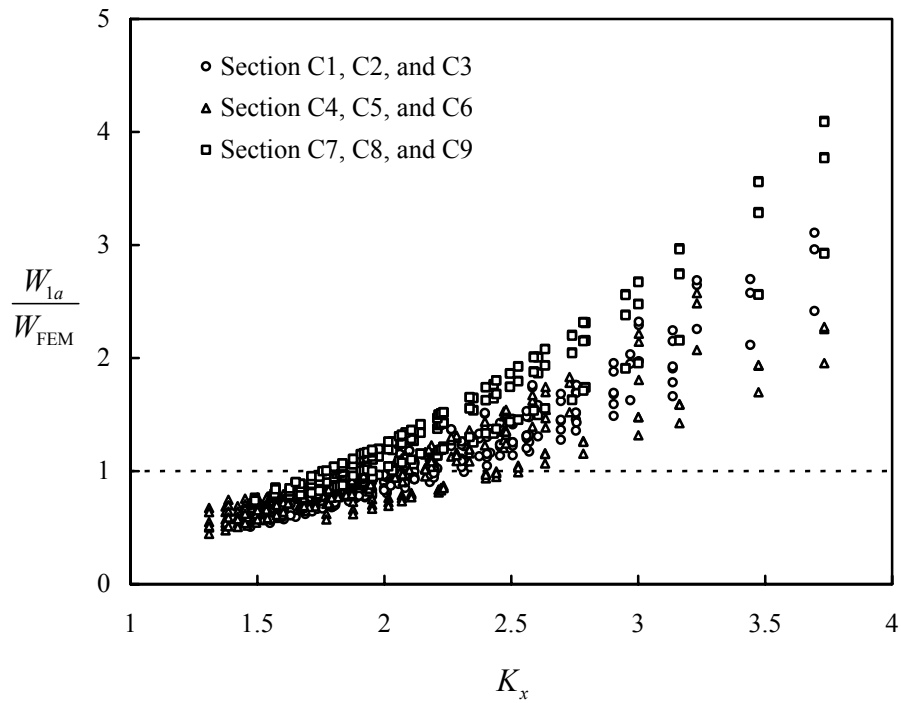
**Figure 5.40** Correlation between the Effective Length Approach (Approach 1a with  $K_x = 1.7$ ) and the FEM results



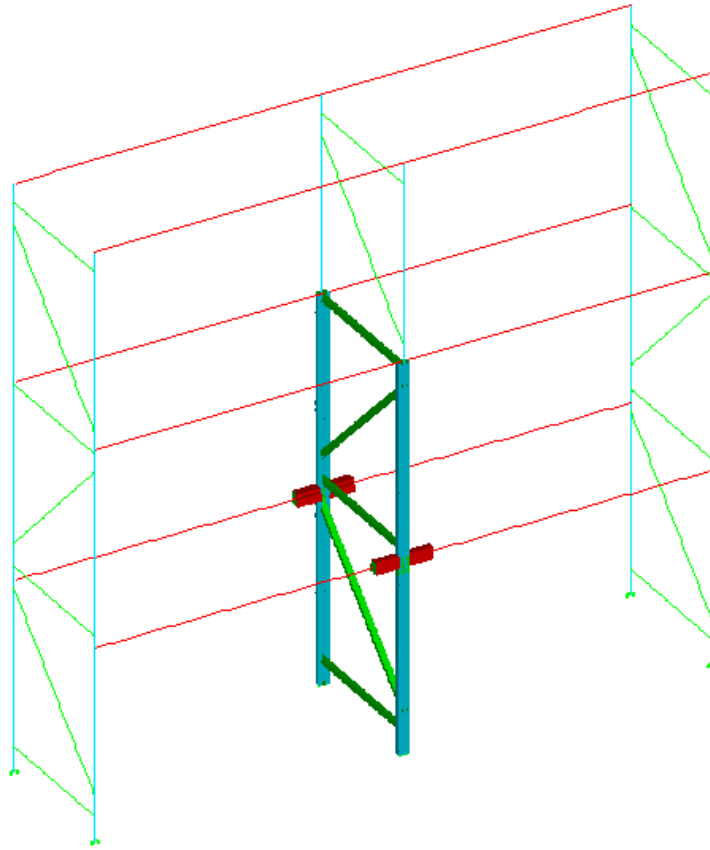
**Figure 5.41** Same plot as Figure 5.40 but with a different y-axis scale



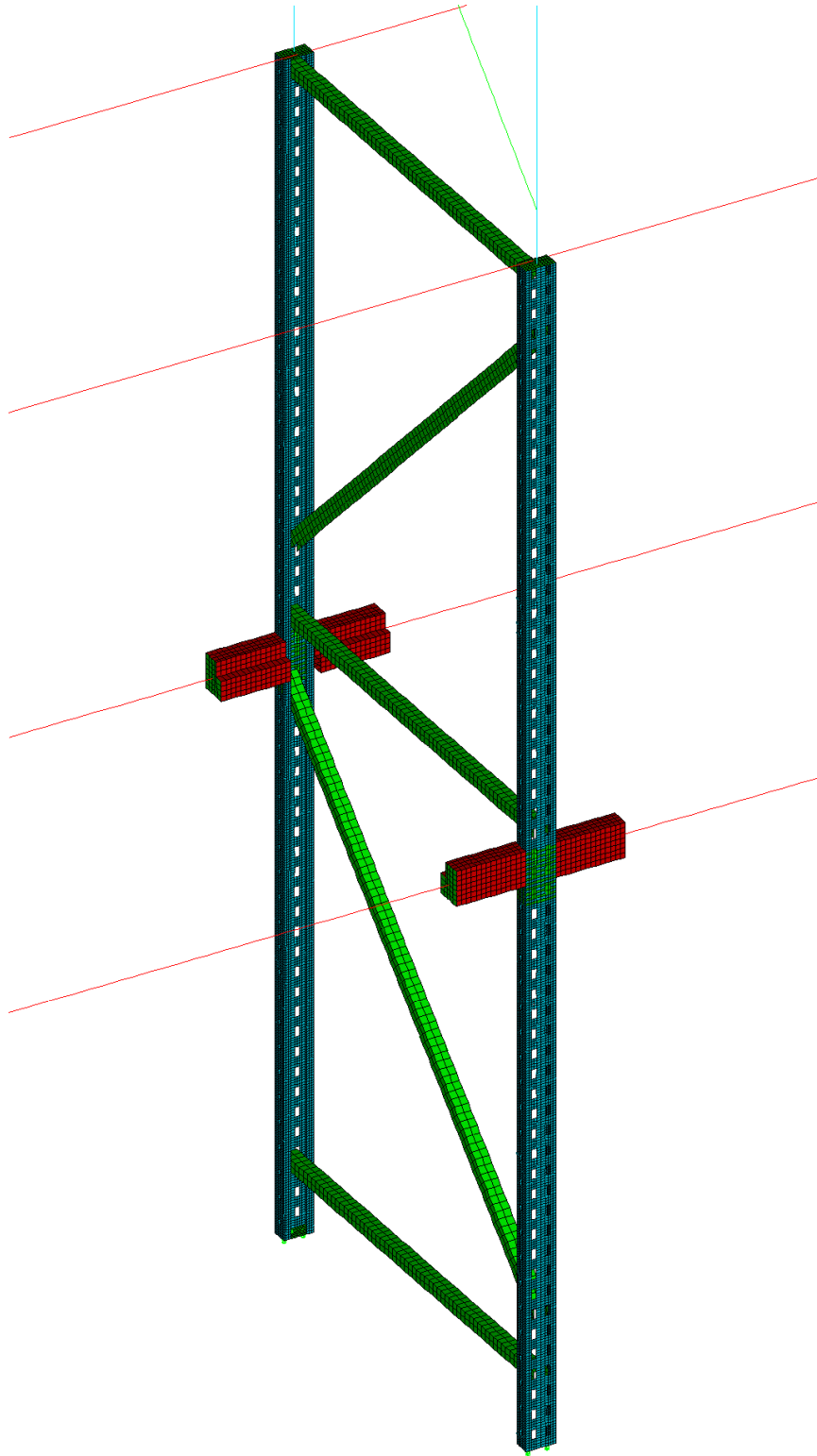
**Figure 5.42** Load Case 1 - Correlation between the Effective Length Approach (Approach 1a with  $K_x = 1.7$ ) and the FEM results



**Figure 5.43** Same plot as Figure 5.42 but with a different y-axis scale



**Figure 5.44** Combined shell and beam finite element frame model



**Figure 5.45** Middle upright frame modeled as shell elements

### 5.7.1 Beam Model

Beam elements are used to model the three-dimensional structural frame members. Available beam elements in ABAQUS that were used are the 3-node quadratic beam elements (B32) for close sections and the 3-node quadratic beam elements (B32OS) for open sections. Open section beam elements have a warping magnitude as an additional degree of freedom at each node. An idealization of the material model that is elastic-plastic with strain hardening was assumed where the yield stress and the ultimate stress were from the tensile coupon test. The material model is  $F_y = 45$  ksi,  $F_u = 59$  ksi,  $E = 29500$  ksi,  $E_{st} = E/45$ ,  $\nu = 0.3$ , and  $e_{st}$  is 15 times the maximum elastic strain for the columns, and  $F_y = 49$  ksi and  $F_u = 59$  ksi for the beams. No tensile coupon test was conducted for the braces; therefore, its material model is assumed to be the same as the columns.

A non-linear torsional spring element was used to model the beam to column connection. The moment rotation relationship used was obtained from the physical connection test as given in Chapter 3 Table 3.1. The joint connection between the braces and column are considered to be continuous except for the warping degree of freedom.

Physical tests for determining base fixity were not available; therefore, two base fixity models were considered. One is to use a linear torsional spring model at the supports as shown in Fig. 5.15a with the stiffness determined from the proposed base fixity equation given in Chapter 2. The other is to use a double axial spring model as shown in Fig. 5.15b. This model not only has the same stiffness as the first one but will also capture the upper bound limit of base fixities behavior. Further details of this base fixity model can be found in Appendix A.

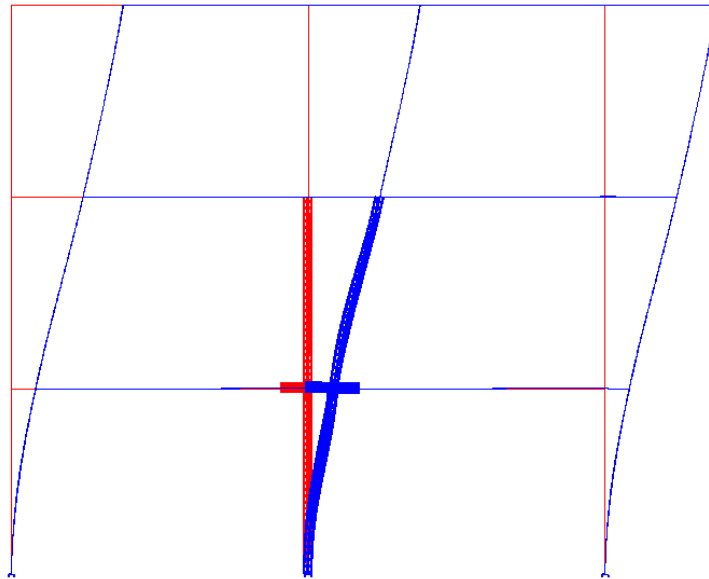
A buckling analysis was first performed for the case of gravity loads to predict its critical buckling load and the corresponding buckling mode. Maximum deflection

of the buckling mode occurred at the top end of the columns as shown in Fig. 5.46. This buckling mode shape with a plumbness of 0.5 inches in 10 feet was then used as the initial geometric imperfection shape for the non-linear analysis of this load case. No plumbness was considered for the case of the combination of gravity and horizontal loads.

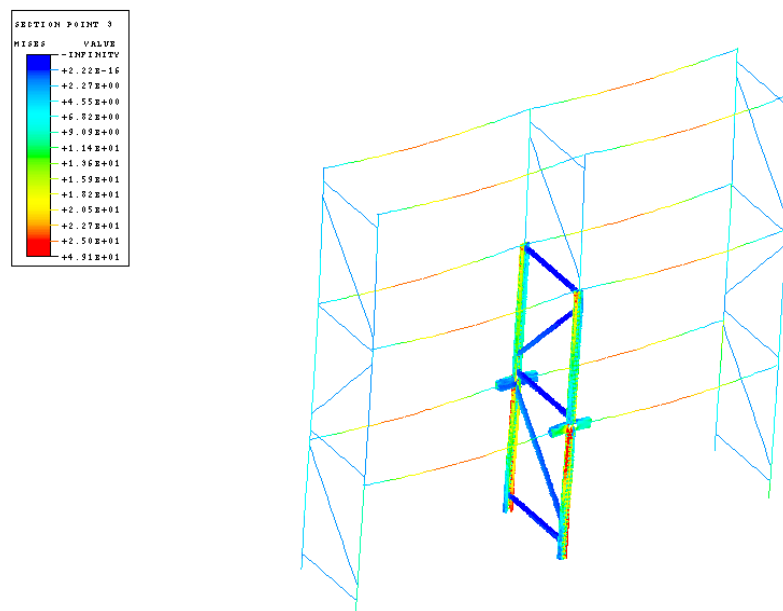
Non-linear finite element analyses were then performed and the results were compared with the physical tests as given in Figs. 5.48 and 5.49. When physical tests were conducted, deflection was measured at several different points. The lateral deflection of the frame measured at the bottom beam level along with its corresponding gravity load carried by the frame was used here to compare the results with the finite element approach. The finite element results designated as Model I is for the case of the base fixity modeled as the torsional spring, and Model II is for the case of the base fixity modeled as the double axial spring. However, they were not distinguished in the case of gravity loads because the same results were obtained.

### **5.7.2 Shell Model**

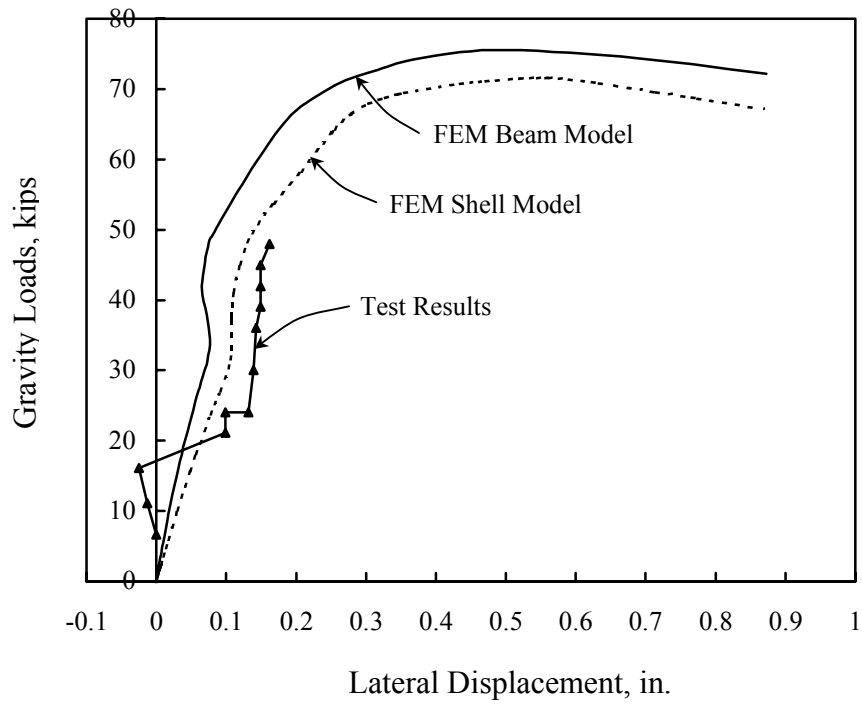
When the results in the previous study were compared to the physical tests, it was found that two cases overestimated the load carrying capacity of the rack: one is the gravity loads and the other is the combination of gravity and horizontal loads in Model I. The results might have been due to the fact that beam elements did not accurately capture the local behavior. If this was the source of the overestimation then shell elements should be used instead. However, modeling and computation effort can become very time consuming if the entire frame is modeled by shell elements. A combined shell and beam model was instead considered in this study to investigate whether section collapses had occurred.



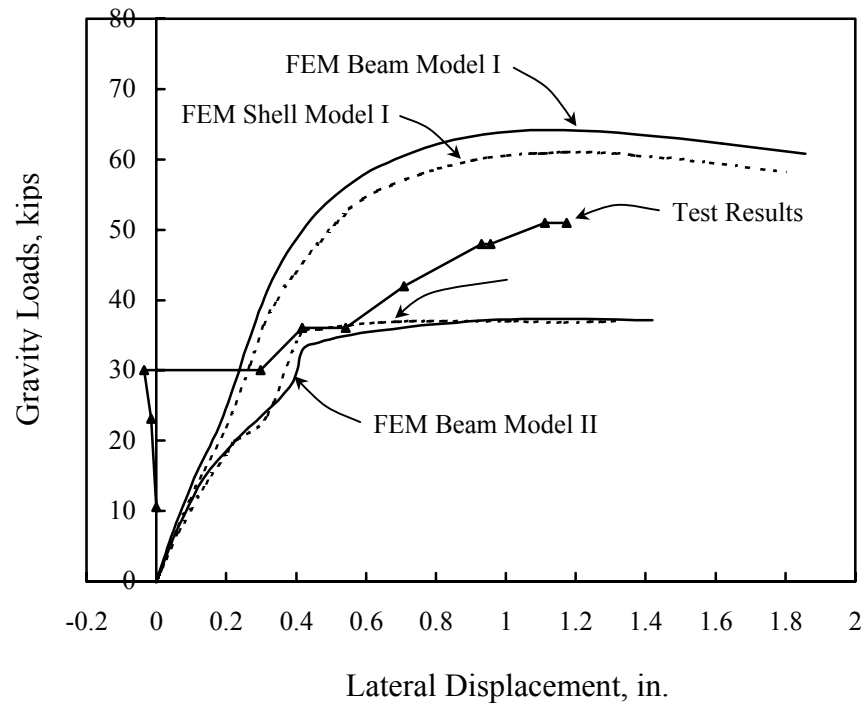
**Figure 5.46** Finite element frame model: Critical buckling mode



**Figure 5.47** Finite element shell model II Gravity + Horizontal Load Case: von Mises stress at ultimate load (5x displacement)



**Figure 5.48** Results for Gravity Loads



**Figure 5.49** Results for Gravity + Horizontal Loads



The bottom length of the middle column is normally the critical member in the assessment of the load carrying capacity of the pallet rack. The middle columns and their braces up to the second story beam level were; therefore, selected to be modeled by shell elements as shown in Figs. 5.44 and 5.45. It is also important that some initial local geometric imperfection is introduced in to these shell columns. Here this imperfection was introduced by superimposing the eigenmodes for the local and distortional buckling, with an imperfection magnitude of one tenth of the thickness for both modes. The boundary condition for the buckling analysis was a concentrically loaded compression column with full lateral supports to avoid overall buckling. Ends of the beam at the bottom level connecting the shell columns were also modeled as shell elements. Rigid plates were used for interconnections between the shell and beam elements. Modeling details of the shell element beam to column connection are the same as the finite simulation of the cantilever test in Charter 3. Other finite element assumptions and procedures are the same as the previous beam model. The non-linear analysis of the shell models was compared with the previous results in Figs. 5.48 and 5.49. Fig. 5.47 shows the displacement shape at the failure load for the case of the combined gravity and horizontal loads.

The new results of the two cases, the gravity loads and the combination of gravity and horizontal loads Model I, were still higher than the test results. This indicates that the local behavior in the columns was not critical in the assessment of the load carrying capacity of the rack. Although the results were not as anticipated, they were found to be in agreement with the frames' behavior in the actual test.

For the case of gravity loads in the physical test, the failure did not take place in the columns as assumed but instead took place in the beams by yielding and local buckling. Shell elements should have been used for modeling the shelf beams. However, further finite element analysis was not needed because the load carrying

capacity of the tested frame was consistent with the load carrying capacity of the tested simply supported shelf beam. This comparison could be made because although the beam to column connections was semi-rigid they were rather flexible. Therefore the results of the simply supported shelf beam could be used to approximate the frame capacity.

For the case of the combination of gravity and horizontal loads in the physical test, failure was due to sidesway collapse where most of the lag bolts were broken off due to the excessive rotation of the columns at the bases. This result falls in line between the finite element Model I and Model II as seen in Fig. 5.49. For finite element Model II failure took place by exceeding the upper bound limit of the base fixity, which means that the actual upper bound limit of the base fixity was slightly higher than assumed. Additional resistance from the base fixity could be due to the presence of the lag bolts.

## **5.8 CONCLUSIONS**

Numerous frame elastic buckling analyses were carried out to evaluate the alignment chart and the AISI torsional-flexural buckling provisions. It was found that the alignment chart is inaccurate when used for semi-rigid frames, and the differences between the base fixity and the connection flexibility is high, the results are unconservative when used for the bottom story column and too conservative when used for the second story column. Results showed that the elastic buckling load obtained from the AISI torsional-flexural buckling provisions is generally conservative compared the results obtained from performing frame elastic buckling analysis.

A study comparing the effective length approach and the notional load approach for cold-formed steel frame and beam-column design was also carried out. The finite element method, which considers both geometric and material nonlinearities, was used as the basis for evaluating the accuracy of these two design approaches. Results showed that, the effective length approach is more conservative than the notional load approach, and that the notional load approach agrees with the finite element results better than the effective length approach does. It is therefore recommended that the notional load approach, in particularly Approach 2c, be considered as an alternative means for cold-formed steel frame and beam-column design. In Approach 2c the notional load parameter  $\xi$  is assumed equal to 1/240 and the second-order elastic analysis is performed on a reduced flexural stiffness model. A 10% reduction in the flexural stiffness is proposed.

---

---

# Chapter 6

## Results and Conclusions

---

---

The objective of this research was to make improvements in the RMI (1997) Specification and the AISI (1996) Specification. The results have indicated that improvements in these current design procedures are possible. The following summarizes the results and conclusions. The symbol \* indicates recommendations for changes in the specifications.

\*1. It was found that the current RMI base fixity equation underestimates the stiffness of the column base. Several analytical models of the column base were studied. The base fixity was found by solving a normal load on the boundary of the half-space problem. With this approach a parametric study was carried out for a wide range of column base configurations to develop a new base fixity equation. Unless actual tests are conducted to obtain the base fixity, the proposed base fixity equation, Eq. (2.12), along with its upper bound limit of the usage of this equation, Eq. (2.17), is recommended. Finite element studies were used to verify this proposed equation. The proposed equation agrees well with the finite element results.

\*2. A new beam to column connection test was developed to be used instead of the cantilever test. The actual frames shear to moment ratio is better represented in this proposed portal test than the current cantilever test. Therefore it is recommended that in addition to current beam to column connection tests, this proposed portal test, which is given Chapter 3, should be included as a possible means of determining the moment to rotation relationship of the connection.

\*3. Numerous finite element elastic buckling analyses of perforated members were carried out. Results indicate that increasing the presence of perforations in the section will reduce the buckling strength. To take this into account, instead of using the unperforated section properties to predict the buckling strength of perforated sections, as assumed in the current design specification, it is recommend that better results can be obtained by using the weighted section, or the average section properties for torsional-flexural buckling, the average section properties for lateral buckling, and the net moment of inertia section properties for flexural buckling.

4. The torsional-flexural buckling equation used in the current design provision was evaluated by comparing the results with finite element solutions. It was found that the elastic buckling load obtained from using the buckling equation is usually conservative compared to the finite element results.

5. Effective length factors used in the current design provision were evaluated by comparing the results with finite element solutions. It was found that the recommended value of  $K_y$ , taken as one is in general conservative while  $K_t$ , taken as 0.8 is in most cases reasonable, providing that the upright frame has adequate braces and the column base is constrained against twisting.

\*6. Finite element simulations of stub-column tests were carried out to evaluate the current effective design area equation and effective section modulus equation. Modifications to these equations are suggested. The effective design area

equation of the RMI specification, Eq. (4.1), should be modified to the proposed equation, Eq. (4.5). The effective section modulus equation of the RMI specification, Eq. (4.7), should be modified to the proposed equation, Eq. (4.8).

7. Unperforated and perforated member strength capacity, under different loading conditions and for various member lengths, was computed using the finite element method and compared to those values using the RMI specification, which uses Eqs. (4.1) and (4.7), and the proposed design approach, which uses Eqs. (4.5) and (4.8). It was found that the compressive axial strength and the beam-columns strength designed according to the proposed design approach agrees better to the finite element results than the current design procedure does. Flexural strength design according to either design approach is quite conservative compared to the finite element results, if distortional buckling failure mode does not take place.

8. Finite element simulation of stub-column tests under bending moments were carried out to evaluate the current RMI procedures for determining the member flexural strength. It was found that current procedures for calculating the nominal flexural strength on the basis of initiation of yielding  $M_n$  for members not subject to lateral buckling is conservative, especially for weak axis bending. Equations for determining the nominal flexural strength on the basis of inelastic reserve capacity  $M_p$  are given in this study and have been shown to agree better with the finite element results than  $M_n$  does.

9. Equations for determining the maximum bending moments in elastic beam-columns for the case where it is simply supported with equal end eccentricities and failure is by torsional-flexural buckling are given. Determining the maximum moments for this boundary condition using the current moment magnification factor suggested by the AISI specification has been shown to give unconservative results if the member failure is by torsional-flexural.

10. Numerous frame elastic buckling analyses were carried out to evaluate the alignment chart. It was found that the alignment chart is inaccurate when used for semi-rigid frames, and the differences between the base fixity and the connection flexibility is high. The results are unconservative when used for the bottom story column and too conservative when used for the second story column.

\*11. A study comparing the effective length approach and the notional load approach for cold-formed steel frame and beam-column design was also carried out. The finite element method, which considers both geometric and material nonlinearities, was used as the basis for evaluating the accuracy of these two design approaches. Results show that, the effective length approach is more conservative than the notional load approach, and that the notional load approach agrees better with the finite element results than the effective length approach does. It is therefore recommended that the notional load approach, in particularly Approach 2c, be considered as an alternative means for cold-formed steel frame and beam-column design. The following is the recommended notional load approach design procedure:

Storage rack columns are considered to be subject to a combined compressive axial load and bending. The axial compression strength  $P_u$  and flexural strength  $M_u$  of the column is determined according to following interaction equation:

$$\frac{P_u}{\phi_c P_{n(L)}} + \frac{M_u}{\phi_b M_n} \leq 1 \quad (6.1)$$

where  $P_{n(L)}$  is the axial strength computed based on the values of  $K_x$  and  $K_y$ , both assumed equal to one, and  $K_t$  assumed equal to 0.8. The relationship between  $P_u$  and  $M_u$  is obtained by performing a second-order elastic analysis, or alternatively approximated by performing a first-order elastic analysis and using moment magnification factors. The analysis is conducted on a geometrically perfect frame subject to notional horizontal load  $\xi W_{story}$  at each story, where  $W_{story}$  is the gravity

load at that story, and  $\xi$  is the notional load parameter equal to  $1/240$ . The notional horizontal load is determined from factored design loads, and is applied as an additive force to the real horizontal forces coming from the seismic load or wind load, to cause maximum frame instability. A 10% reduced flexural stiffness analysis model is used. This can be done by using a reduced flexural stiffness  $EI^*$  for all members and connections in the analysis model

$$EI^* = 0.9EI \quad (6.2)$$

where  $E$  is the modulus of elasticity, and  $I$  is the moment of inertia about the axis of bending.



---

---

# Appendix **A**

## Column Bases

---

---

### A.1 CONCRETE SPRINGS

From Fig. 2.2 vertical displacements are related to the base rotation as

$$u_2 = -\theta x_1$$

with the spring reaction

$$\sigma_{22} = ku_2$$

the resisting moment could be found by integrating over the area of the base plate

$$M = -\int_A x_1 \sigma_{22} dA$$

$$M = \theta kb \int_{-d/2}^{d/2} x_1^2 dx_1 = \frac{\theta kb d^3}{12}$$

from this last equation the base fixity can be obtained as

$$\frac{M}{\theta} = \frac{kb d^3}{12}$$

if the stiffness of these springs are set to

$$k = \frac{E}{d}$$

where  $E$  is the modulus of elasticity of the floor. For this case and all following models the floor is assumed to be concrete,  $E = E_c$ . The base fixity is found to be the same as in Eq. (2.1).

## A.2 CONCRETE BEAM

Recall from the beam theory that the normal stress can be written as

$$\sigma_{22} = -\frac{Mx_1}{I}$$

From Hooke's law this equation gives

$$\varepsilon_{22} = -\frac{Mx_1}{EI}$$

From Fig. 2.3 the radius of curvature and the strain are related as follows:

$$\theta = \frac{\alpha}{\rho} = -\frac{\varepsilon_{22}\alpha}{x_1}$$

From these last two equations the base fixity can found as

$$\frac{M}{\theta} = \frac{EI}{\alpha}$$

where

$$I = \frac{bd^3}{12}$$

If the depth of the concrete block under the base plate is assumed to be

$$\alpha = d$$

the base fixity is found to be the same as in Eq. (2.1).

### A.3 CONCRETE BLOCK

Define the stress field in the concrete block under the base plate as

$$\sigma_{22} = -kx_1$$

$$\sigma_{ij} = 0$$

From Hooke's law the strain field can be found as

$$\varepsilon_{ij} = \frac{(1+\nu)}{E} \sigma_{ij} - \frac{\nu}{E} \sigma_{kk} \delta_{ij}$$

$$\varepsilon_{22} = -\frac{kx_1}{E}$$

$$\varepsilon_{11} = \varepsilon_{33} = \frac{\nu kx_1}{E}$$

$$\varepsilon_{12} = \varepsilon_{13} = \varepsilon_{23} = 0$$

By definition the displacement field is related to the strain field as

$$\varepsilon_{ij} = \frac{1}{2} (u_{i,j} + u_{j,i})$$

Integration of the strain field equations gives the displacement field as

$$u_1 = \frac{k}{2E} \left( (x_2 - \alpha)^2 + \nu (x_1^2 - x_3^2) \right)$$

$$u_2 = -\frac{kx_1 (x_2 - \alpha)}{E}$$

$$u_3 = \frac{\nu kx_1 x_3}{E}$$

Plot of the displacement field is shown in Fig. 2.4. The resisting moment could be found by integrating over the area of the base plate

$$M = -\int_A x_1 \sigma_{22} dA$$

$$M = kb \int_{-d/2}^{d/2} x_1^2 dx_1 = \frac{kbd^3}{12}$$

with the known vertical displacement, the rotation at the top of the concrete block  $x_2 = 0$  is

$$\theta = \frac{u_2}{x_1} = \frac{k\alpha}{E}$$

From these last two equations the base fixity can found as

$$\frac{M}{\theta} = \frac{bd^3 E}{12\alpha}$$

Similar to Model 2 by setting the depth of the concrete block under the base plate as

$$\alpha = d$$

the base fixity is found to be the same as in Eq. (2.1).

#### **A.4 TWO-DIMENSIONAL ELASTOSTATIC PROBLEM: NORMAL LOADS ON THE BOUNDARY OF HALF-SPACE**

The stress function for Fig. 2.5a where the load extends indefinitely to the left is given in Timoshenko and Goodier (1969) as follows:

$$\phi_1(p, x_1, x_2) = -\frac{p}{2\pi} \left( (x_1^2 + x_2^2) \tan^{-1} \frac{x_2}{x_1} - x_1 x_2 \right)$$

where the stress field could be found by differentiating the stress function as

$$\sigma_{11} = \phi_{1,22} \quad \sigma_{22} = \phi_{1,11} \quad \sigma_{12} = -\phi_{1,12}$$

the results of which are

$$\sigma_{11} = -\frac{p}{\pi} \left( \tan^{-1} \frac{x_2}{x_1} + \frac{x_1 x_2}{x_1^2 + x_2^2} \right)$$

$$\sigma_{22} = -\frac{p}{\pi} \left( \tan^{-1} \frac{x_2}{x_1} - \frac{x_1 x_2}{x_1^2 + x_2^2} \right)$$

$$\sigma_{12} = -\frac{p x_2^2}{\pi (x_1^2 + x_2^2)}$$

From Hooke's law and assuming the problem to be plane strain the, strain field could be obtained. By integration of the strain field the displacement field is found as

$$u_1 = -\frac{p(1+\nu)}{\pi E} \left( (1-2\nu)x_1 \tan^{-1} \frac{x_2}{x_1} + (1-\nu)x_2 \ln(x_1^2 + x_2^2) + x_2 \right)$$

$$u_2 = -\frac{p(1+\nu)}{\pi E} \left( (1-2\nu)x_2 \tan^{-1} \frac{x_2}{x_1} - (1-\nu)x_1 \ln(x_1^2 + x_2^2) \right)$$

Similar to the previous problem, the stress function for Fig. 2.5b where the linearly increasing load extending indefinitely to the left is given in Timoshenko and Goodier (1969) as follows:

$$\phi_2(p, x_1, x_2, d) = \frac{p}{6\pi d} \left( (x_1^3 + 3x_1 x_2^2) \tan^{-1} \frac{x_2}{x_1} + x_2^3 \ln(x_1^2 + x_2^2) - x_1^2 x_2 \right)$$

where the stress field could be found by differentiating the stress function as

$$\sigma_{11} = \phi_{1,22} \quad \sigma_{22} = \phi_{1,11} \quad \sigma_{12} = -\phi_{1,12}$$

the results of which are

$$\sigma_{11} = \frac{p}{\pi d} \left( x_1 \tan^{-1} \frac{x_2}{x_1} + x_2 \ln(x_1^2 + x_2^2) + \frac{5x_2}{3} \right)$$

$$\sigma_{22} = \frac{p}{\pi d} \left( x_1 \tan^{-1} \frac{x_2}{x_1} - x_2 \right)$$

$$\sigma_{12} = -\frac{px_2}{\pi d} \tan^{-1} \frac{x_2}{x_1}$$

From Hooke's law and assuming the problem to be plane strain the strain field could be obtained. By integration of the strain field the displacement field is found as

$$u_1 = \frac{p(1+\nu)}{\pi d E} \left( \left( \frac{(1-2\nu)(x_1^2 - x_2^2)}{2} - x_2^2 \right) \tan^{-1} \frac{x_2}{x_1} + (1-\nu)x_1x_2 \ln(x_1^2 + x_2^2) + \frac{(1+2\nu)x_1x_2}{6} \right)$$

$$u_2 = \frac{p(1+\nu)}{\pi d E} \left( (1-2\nu)x_1x_2 \tan^{-1} \frac{x_2}{x_1} - \frac{(x_1^2 - \nu(x_1^2 - x_2^2))}{2} \ln(x_1^2 + x_2^2) + \frac{(1-\nu)(x_1^2 - x_2^2)}{6} - \frac{x_2^2}{3} \right)$$

The stress function for the Fig. 2.5c problem may be found by superposition the stress function for Fig. 2.5a and 2.5b as

$$\phi = \phi_1(q, x_1, x_2) + \phi_1(q, x_1 + d, x_2) + \phi_2(-2q, x_1, x_2, d) + \phi_2(2q, x_1 + d, x_2, d)$$

the stress field could then be found by differentiating this new stress function or by similar superposition of the stress field of Fig. 2.5a and 2.5b. Normal stress on the boundary  $x_2 = 0$  between  $x_1 = 0$  and  $x_1 = d$  is found to be

$$\sigma_{22} = -\frac{q(2x_1 + d)}{d}$$

which is a linear bending stress under the base plate. The resisting moment could be found by integrating over the area of the base plate

$$M = -\int_A x_1 \sigma_{22} dA$$

$$M = \frac{q}{d} \int_{-d}^0 (2x_1 + d) x_1 dx_1 = \frac{qd^2}{6}$$

Displacement field could either be found from Hooke's law and assuming the problem to be plane strain or by superposition of the resulting displacement field of Fig. 2.5a and 2.5b. The vertical displacement,  $u_2(x_1, x_2)$  on the boundary  $x_2 = 0$  between  $x_1 = 0$  and  $x_1 = d$  is found and plotted in Fig. 2.6

$$u_2(x_1, 0) = \frac{q(1-\nu^2)}{d\pi E} \left( x_1(x_1 + d) \ln \left( \frac{x_1^2}{(x_1 + d)^2} \right) + \frac{d}{3}(2x_1 + d) \right)$$

at the edge of the base plate the displacement is

$$u_2(0, 0) = \frac{q(1-\nu^2)d}{3\pi E}$$

the dashed line in Fig. 2.6 is used as an approximate rotation of the base plate

$$\theta = \frac{2u_2(0, 0)}{d} = \frac{2q(1-\nu^2)}{3\pi E}$$

Dividing the resisting moment with this last equation, the base fixity equation is obtained

$$\frac{M}{\theta} = \frac{d^2\pi E}{4(1-\nu^2)}$$

## A.5 THREE-DIMENSIONAL ELASTOSTATIC PROBLEM: NORMAL LOADS ON THE BOUNDARY OF HALF-SPACE

The displacement field for the Boussinesq problem of concentrated normal force on boundary of half-space is as follows:

$$u_\alpha = \frac{P}{4\pi G} \left( \frac{x_3 x_\alpha}{r^3} - \frac{x_\alpha (1-2\nu)}{r(r+x_3)} \right)$$

$$u_3 = \frac{P}{4\pi G} \left( \frac{x_3^2}{r^3} + \frac{2(1-\nu)}{r} \right)$$

where

$$G = \frac{E}{2(1+\nu)} \quad \text{and} \quad r = \sqrt{x_1^2 + x_2^2 + x_3^2}$$

As shown in Sokolnikoff (1983) the solution can be generalized for distribution of normal loads. Let  $p(\xi, \eta)$  be the distributed normal load at coordinate  $(\xi, \eta)$  on the boundary. Inserting this in the previous equations and integrating over the boundary plane the generalized equation is obtained as

$$u_\alpha = \frac{1}{4\pi G} \left( x_3 x_\alpha \iint_A \frac{p(\xi, \eta)}{r^3} d\xi d\eta - x_\alpha (1-2\nu) \iint_A \frac{p(\xi, \eta)}{r(r+x_3)} d\xi d\eta \right)$$

$$u_3 = \frac{1}{4\pi G} \left( x_3^2 \iint_A \frac{p(\xi, \eta)}{r^3} d\xi d\eta + 2(1-\nu) \iint_A \frac{p(\xi, \eta)}{r} d\xi d\eta \right)$$

where

$$r = \sqrt{(x_1 - \xi)^2 + (x_2 - \eta)^2 + x_3^2}$$



For the case of a linear bending stress the distribution is given as

$$p(\xi, \eta) = \frac{M\xi}{I}$$

where

$$I = \frac{bd^3}{12}$$

Consider a square plate of a unit width,  $d = b = 1$  with a unit moment applied,  $M = 1$ .

The vertical displacement  $u_3(x_1, x_2, x_3)$  is found at the center edge of the plate and  $d/64$  away from the boundary to avoid singularity from the numerical integration

$$u_3\left(\frac{d}{2}, 0, \frac{d}{64}\right) = \frac{7.746}{4\pi G}$$

where it is used to find an approximate rotation of the base plate

$$\theta = \frac{2u_3\left(\frac{d}{2}, 0, \frac{d}{64}\right)}{d} = \frac{7.746(1+\nu)}{\pi E}$$

thus the base fixity can be found as

$$\frac{M}{\theta} = \frac{\pi E}{7.746(1+\nu)}$$

The result is found to be higher than Eq. (2.1) by a factor of

$$\frac{12\pi}{7.746(1+\nu)bd^2} = 4.05$$

Similar to the square plate problem, consider a rectangular plate,  $d = 2b = 1$  with a unit moment applied,  $M = 1$ . The vertical displacement  $u_3(x_1, x_2, x_3)$  is found at the center edge of the plate and  $d/64$  away from the boundary to avoid singularity from the numerical integration

$$u_2\left(\frac{d}{2}, 0, \frac{d}{64}\right) = \frac{12.253}{4\pi G}$$

where it is used to find an approximate rotation of the base plate

$$\theta = \frac{2u_2\left(\frac{d}{2}, \frac{d}{64}\right)}{d} = \frac{12.253(1+\nu)}{\pi E}$$

thus the base fixity can be found as

$$\frac{M}{\theta} = \frac{\pi E}{12.253(1+\nu)}$$

The result is found to be higher than Eq. (2.1) by a factor of

$$\frac{12\pi}{12.253(1+\nu)bd^2} = 5.128$$

## A.6 DOUBLE AXIAL SPRING

The double axial spring model shown in Fig. 5.15b is used to model the base fixity in the frame analysis. Unlike the simple torsional spring model shown in Fig. 5.15a the double axial spring model can capture the upper bound limit of base fixities behavior. The resistant moment  $M$  developed from the double axial spring model shown in Fig. 5.15c is

$$M = k_s \delta_2 \Delta$$

For small deformations, the angle of rotation  $\theta$  can be approximated as

$$\theta = \frac{2\delta_2}{\Delta}$$

The axial spring stiffness  $k_s$  can then be computed from these last two equations as

$$k_s = \frac{2M}{\Delta^2\theta}$$

Recall Eq. (2.16) the upper bound limit for the base fixity equation is given as

$$\frac{M}{P} = \frac{S}{A}$$

Let the resistant moment  $M$  and total reaction force  $P$  be from the double axial spring model shown in Fig. 5.15c then this last equation becomes

$$\frac{k_s \delta_2 \Delta}{2k_s \delta_1} = \frac{S}{A}$$

The upper bound limit is reached when the left spring is completely unloaded ( $\delta_1 = \delta_2$ ) and all the force is transferred to the right spring as shown in Fig. 5.15d. Imposing this condition the springs moment arm,  $\Delta$  can then computed from the last equation as

$$\Delta = \frac{2S}{A}$$

---

---

Appendix **B**

**Base Fixity Charts**

---

---

Chart A1

Plate Type A, ( $c = 0, t_w = 0.05$  in.)

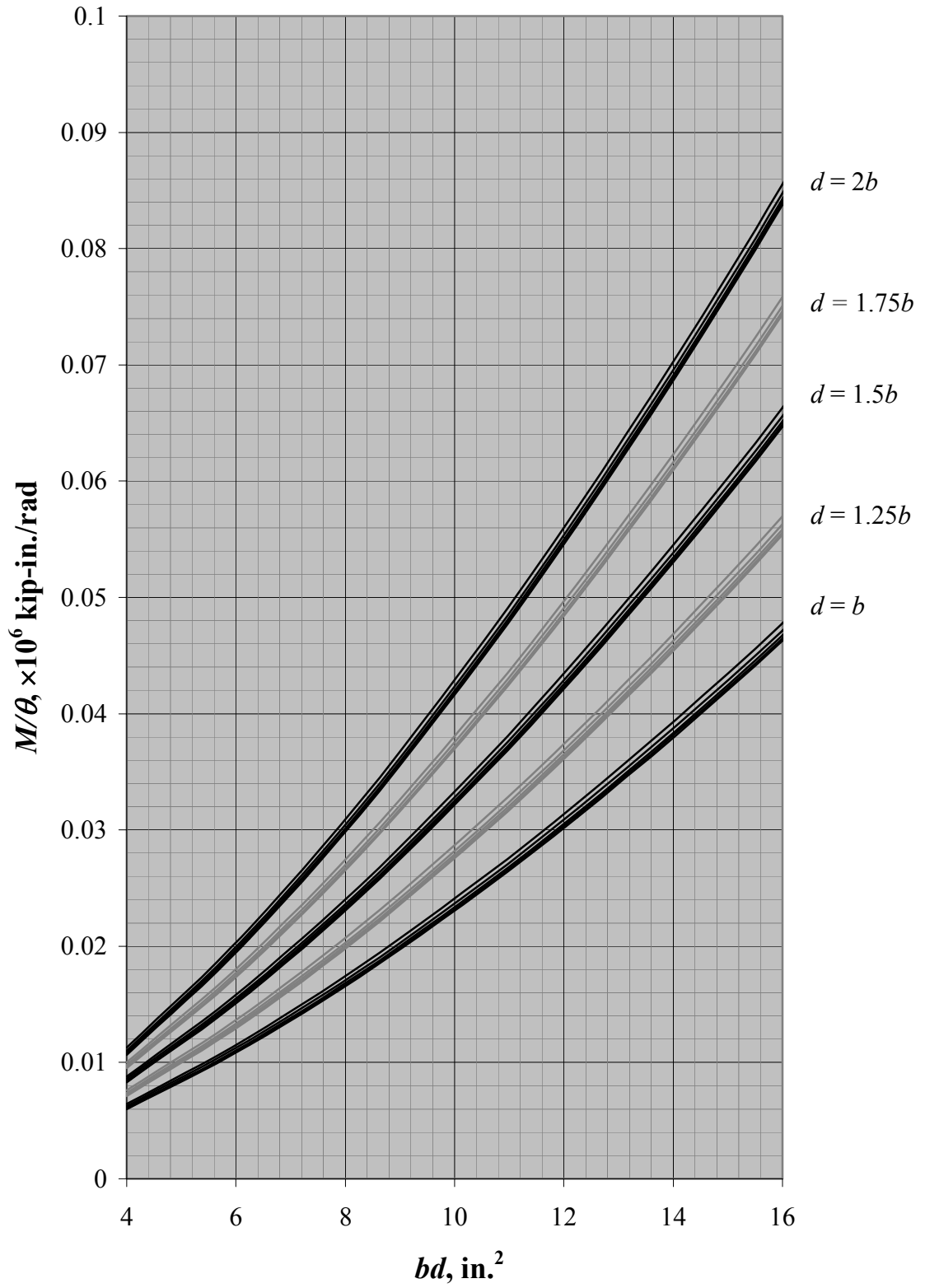


Chart A2

Plate Type A, ( $c = 0, t_w = 0.1$  in.)

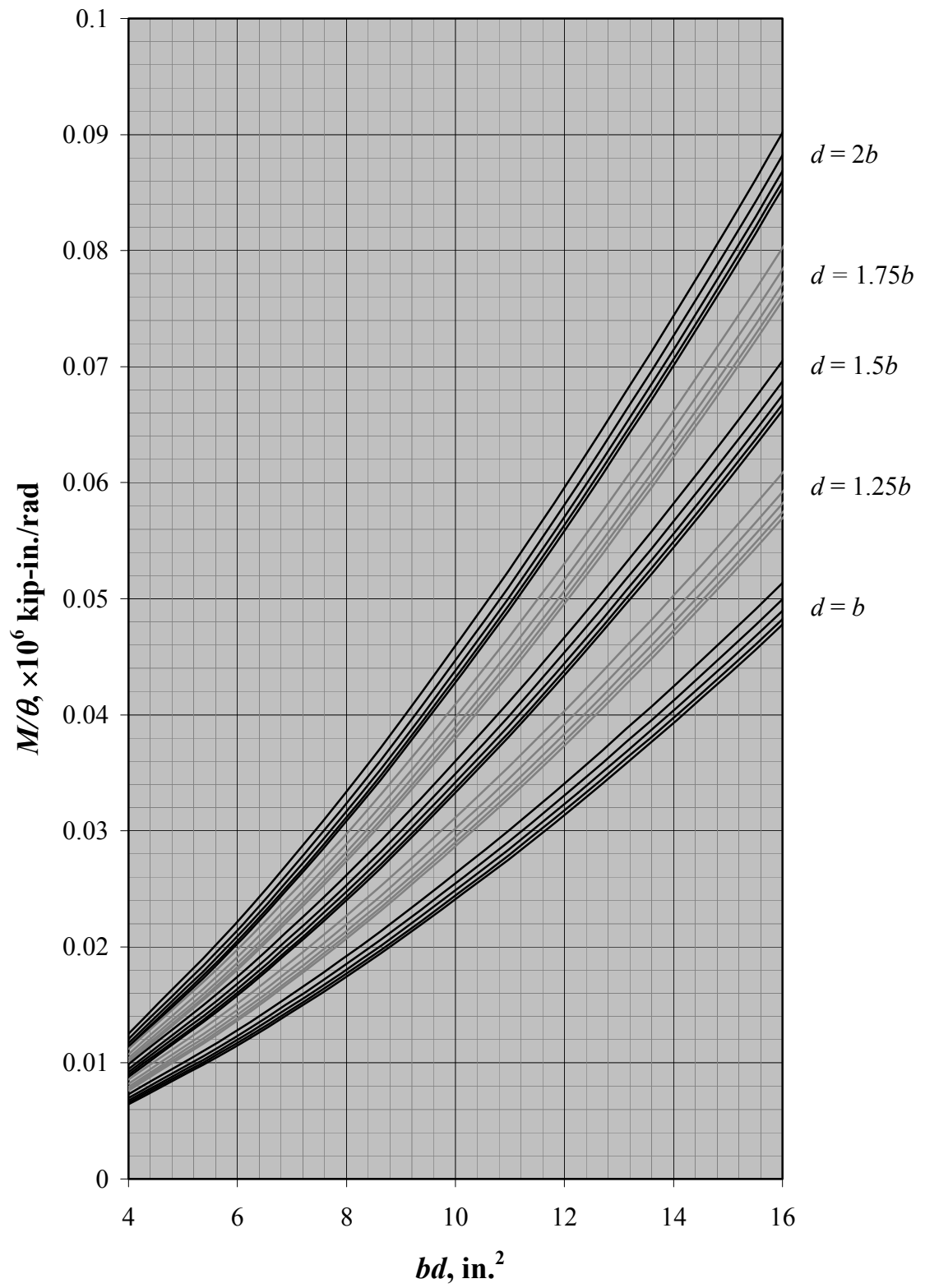


Chart B1

Plate Type B, ( $c = 0, t_w = 0.05$  in.)

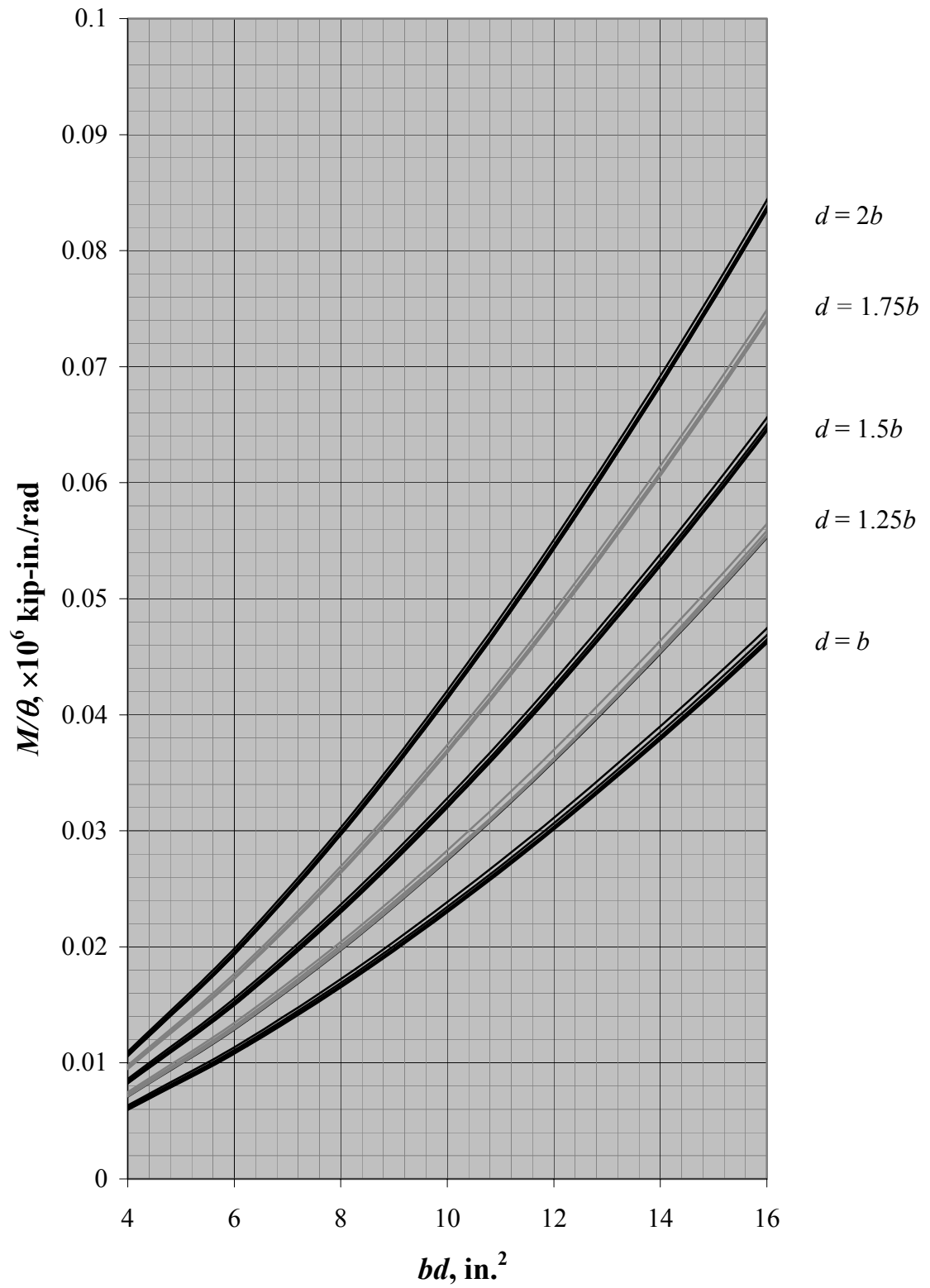


Chart B2

Plate Type B, ( $c = 0, t_w = 0.1$  in.)

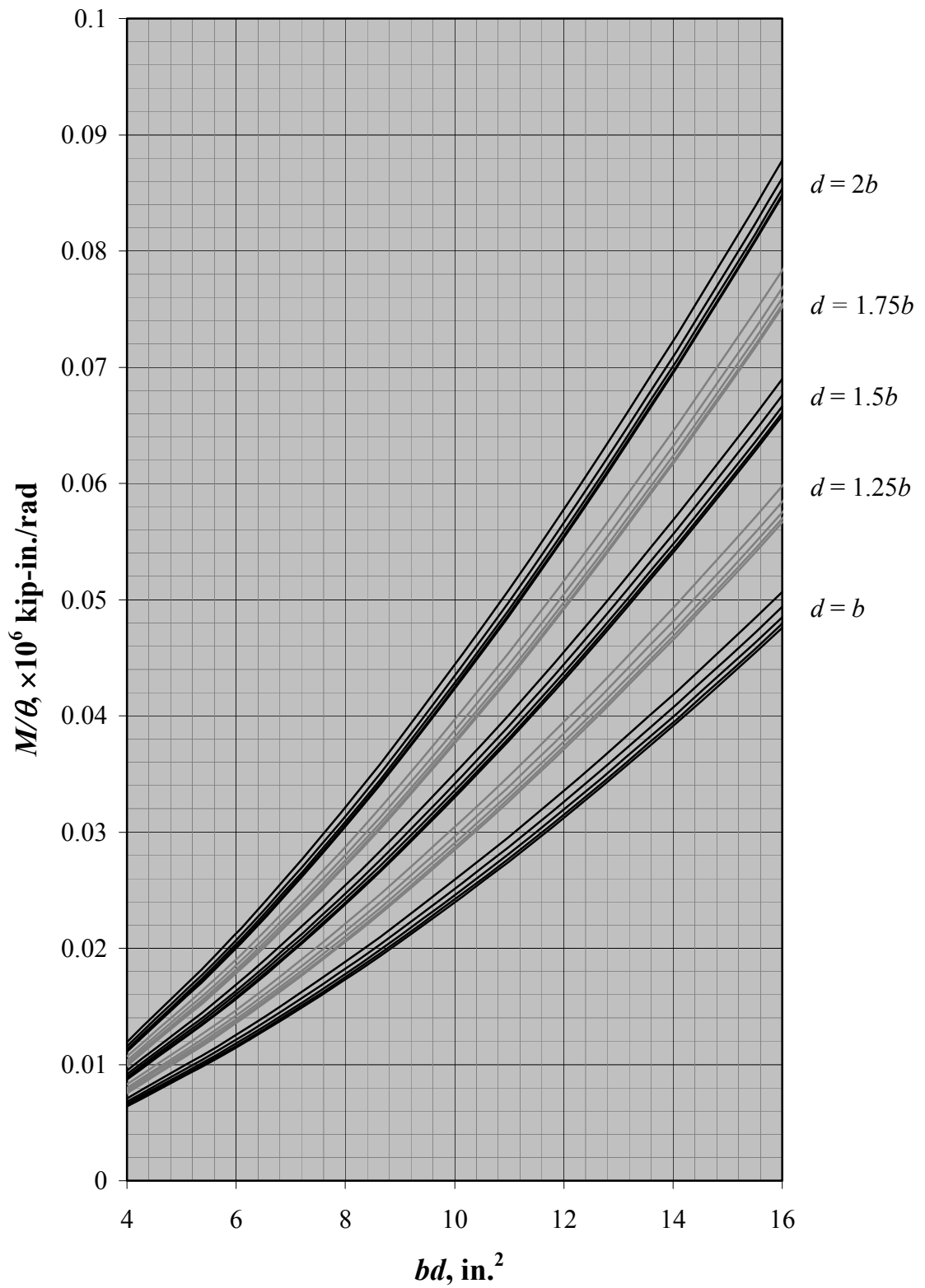




Chart C1-I

Plate Type C, ( $c = 0, t_w = 0.05$  in.)

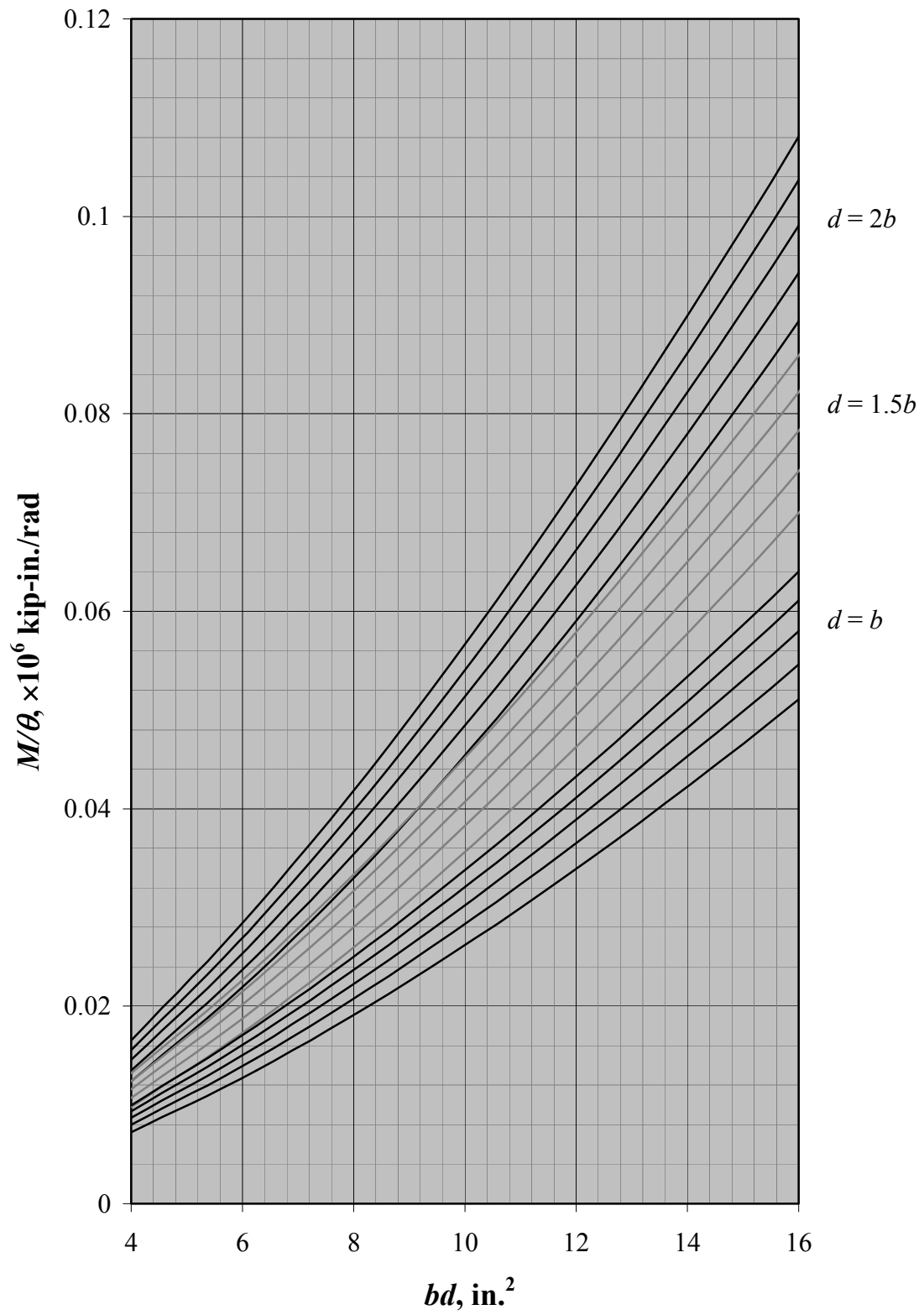


Chart C1-II

Plate Type C, ( $c = 0, t_w = 0.05$  in.)

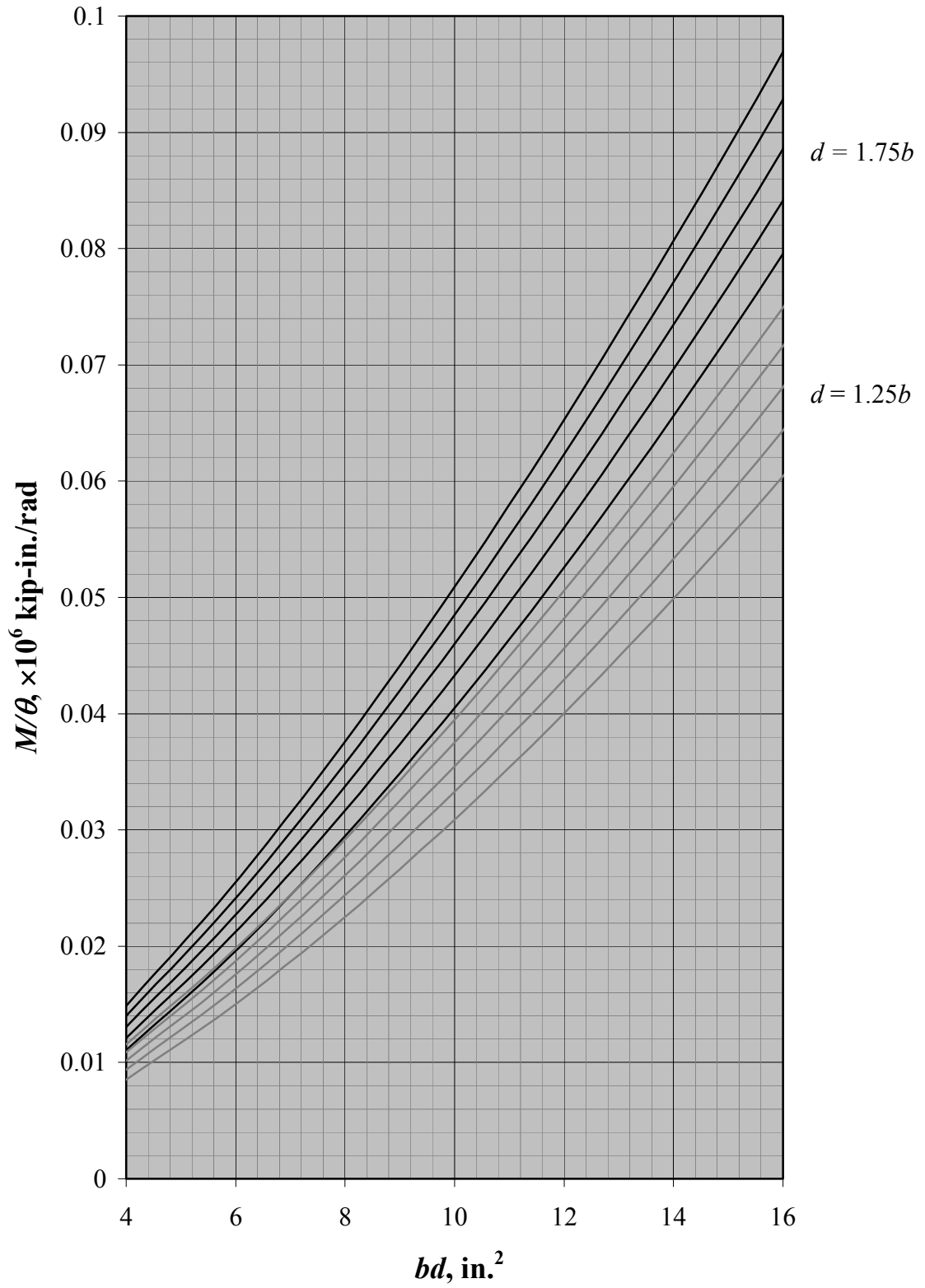


Chart C2-I

Plate Type C, ( $c = 0, t_w = 0.1$  in.)

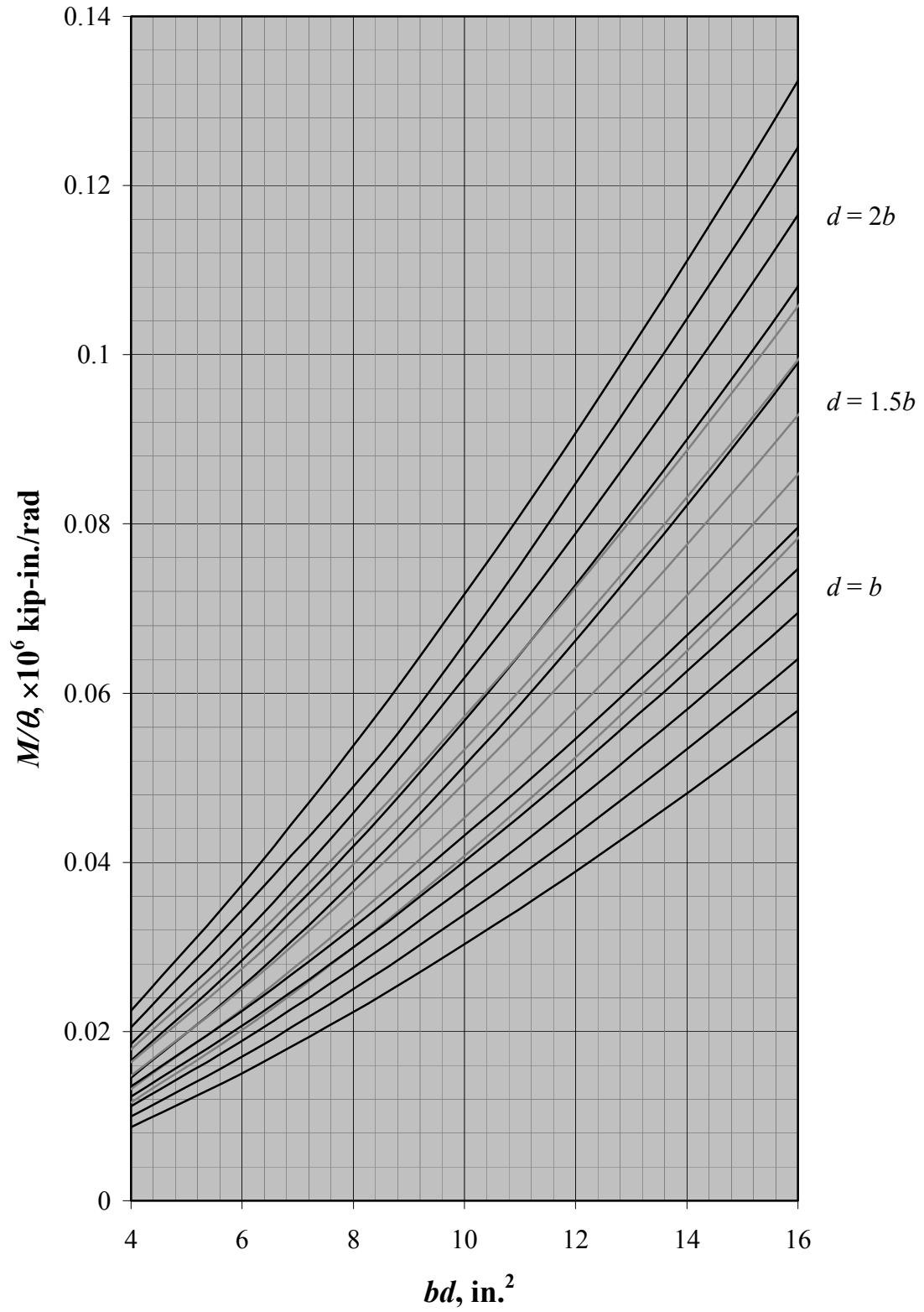


Chart C2-II

Plate Type C, ( $c = 0, t_w = 0.1$  in.)

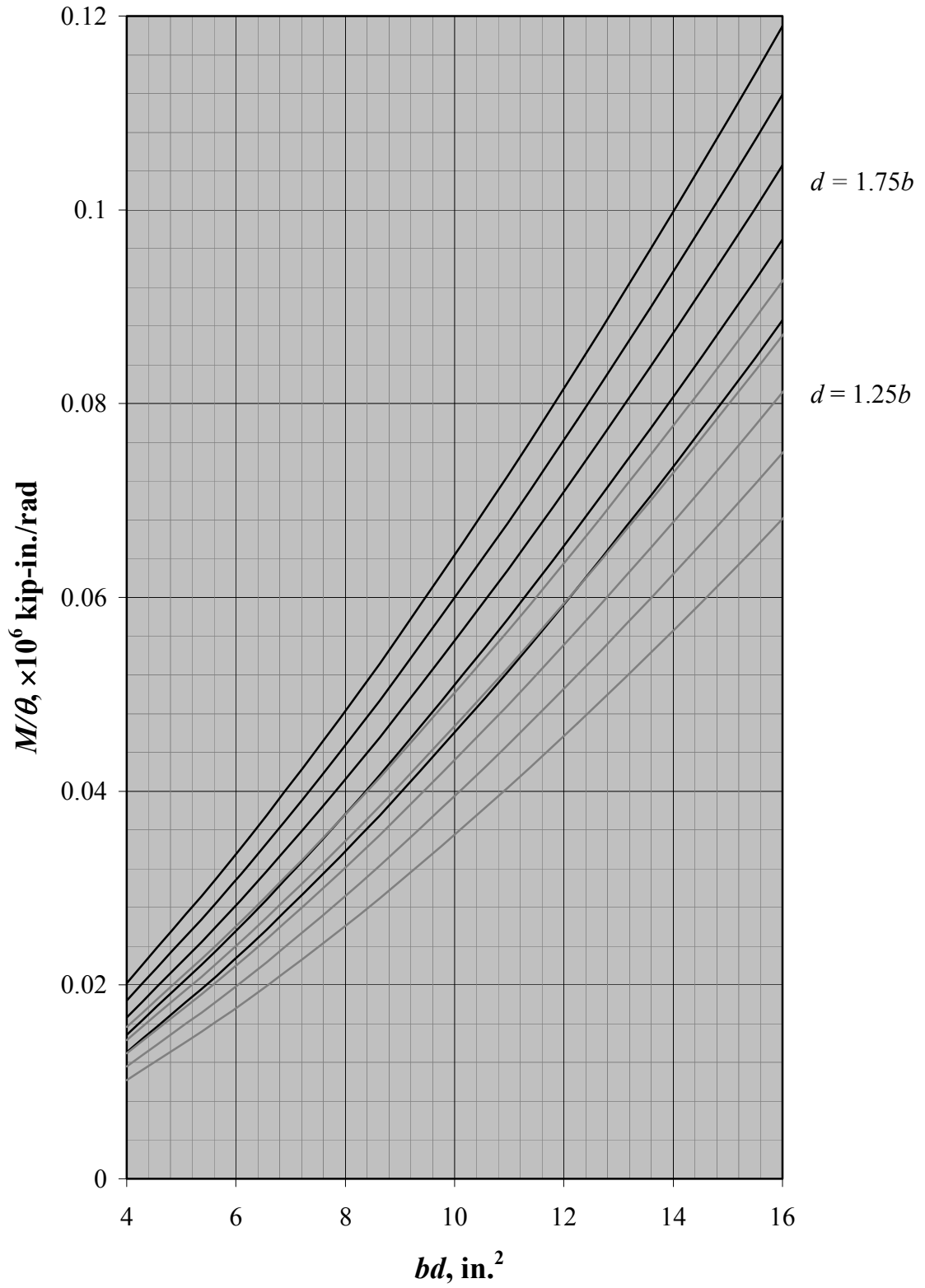
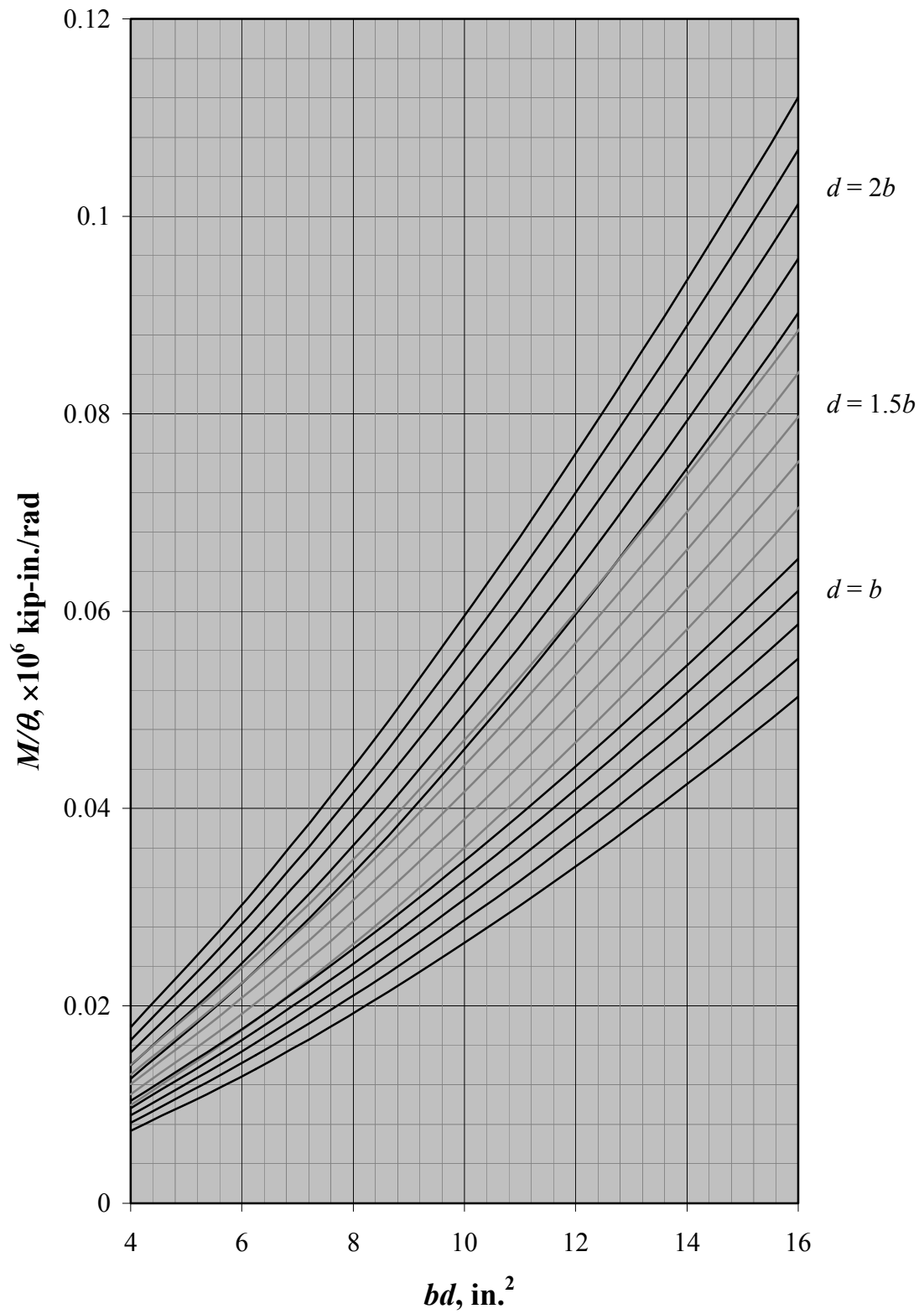


Chart D1-I

Plate Type D, ( $c = 0, t_w = 0.05$  in.)



**Chart D1-II**

**Plate Type D, ( $c = 0, t_w = 0.05$  in.)**

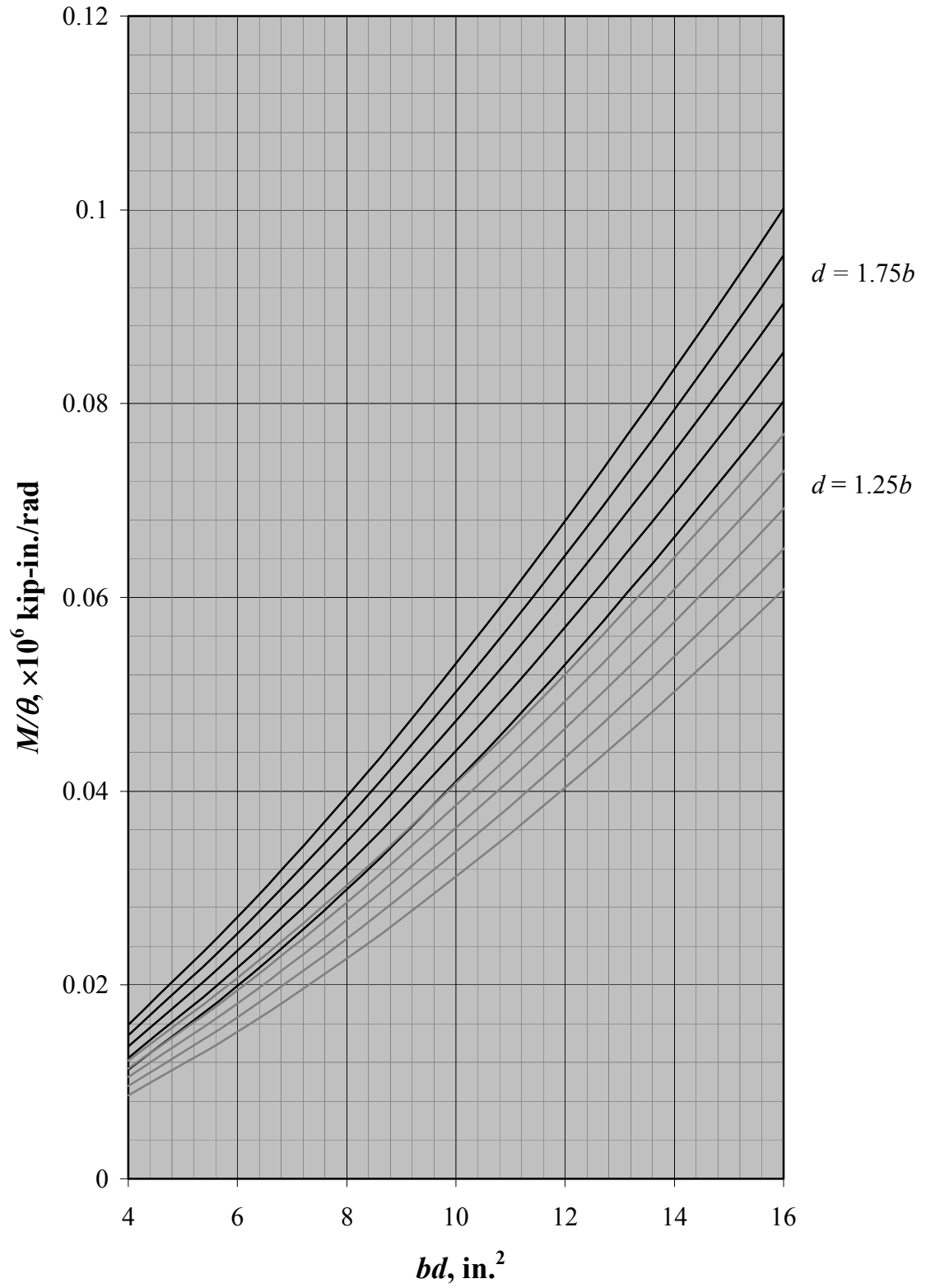
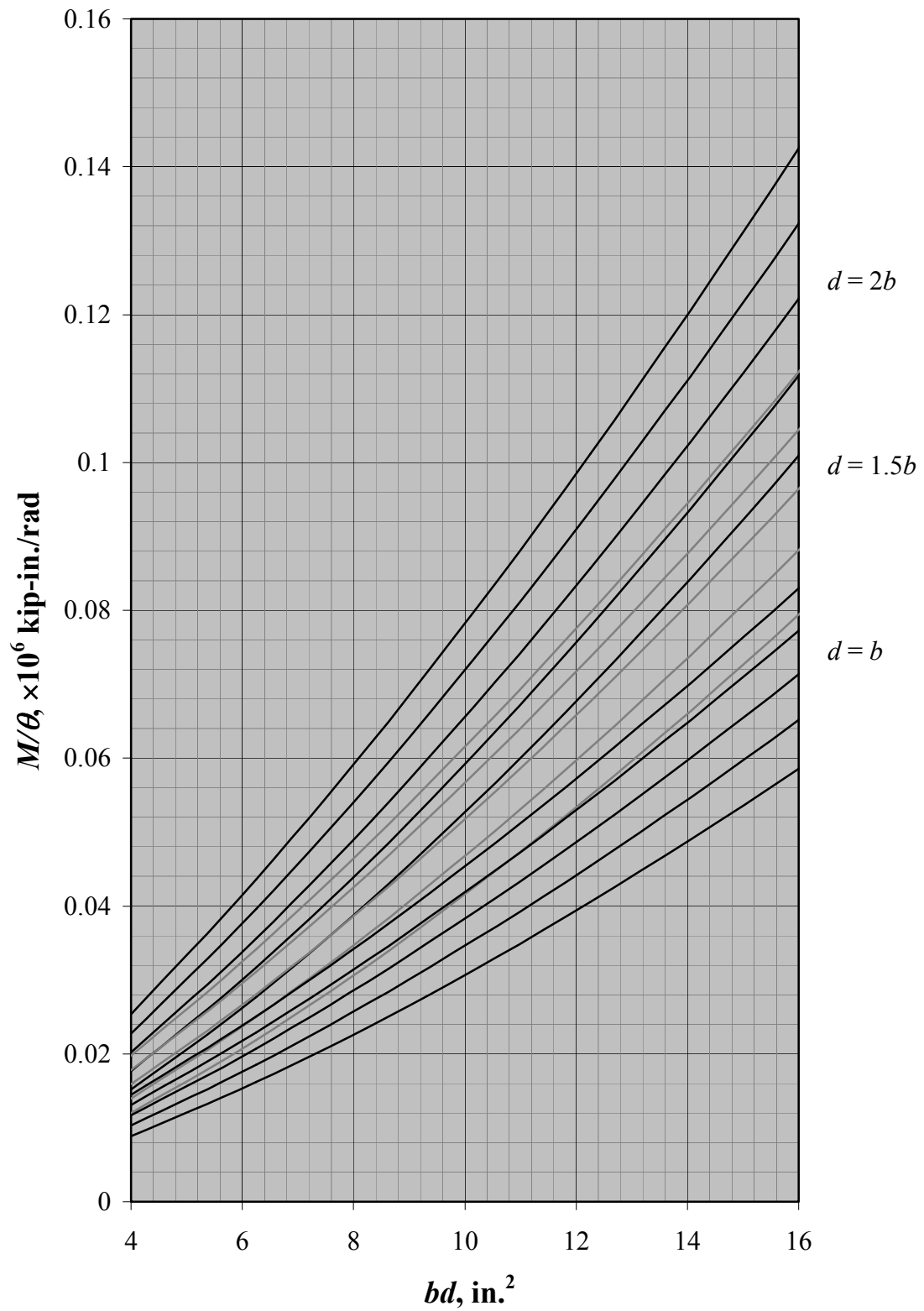


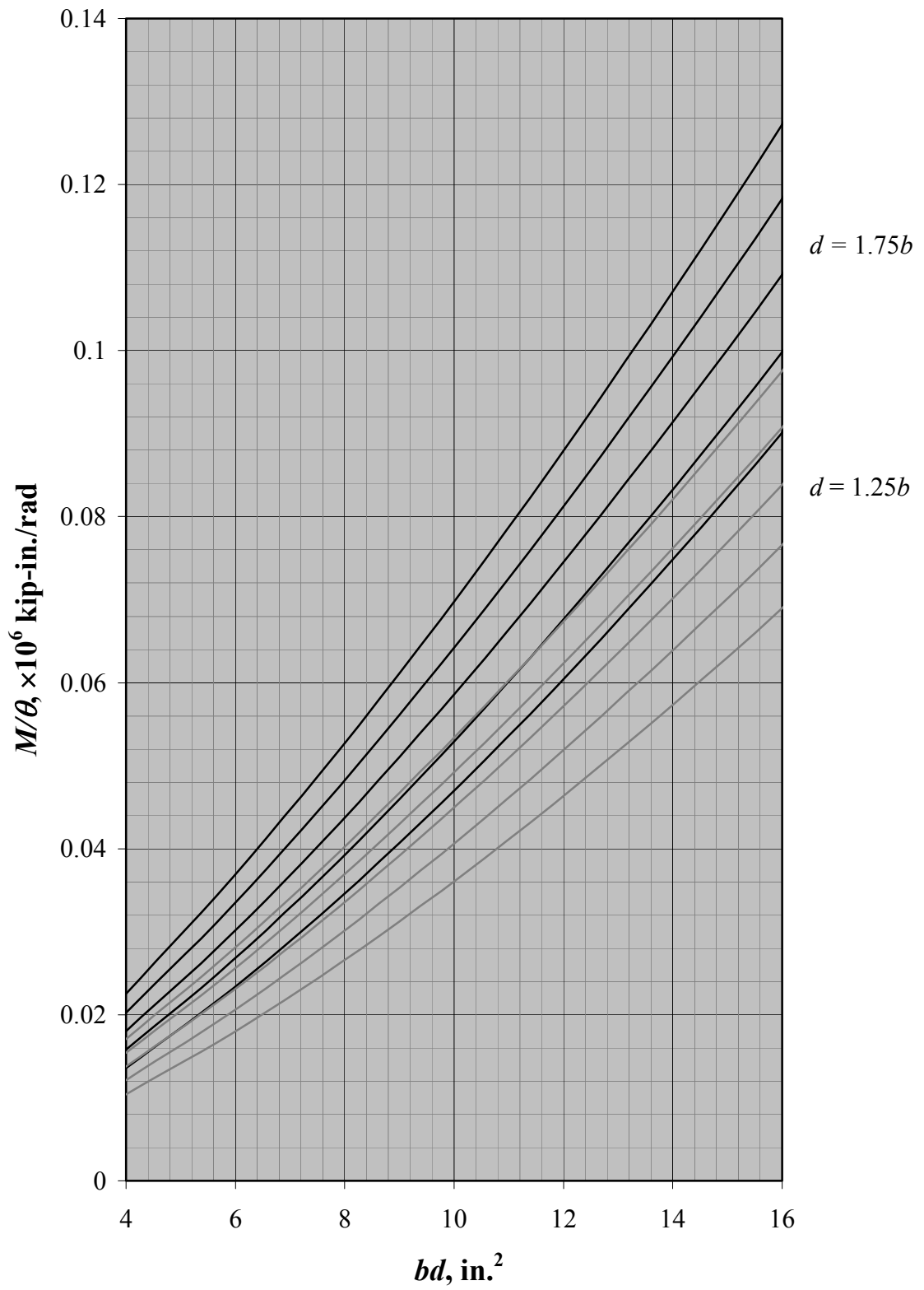
Chart D2-I

Plate Type D, ( $c = 0, t_w = 0.1$  in.)



**Chart D2-II**

**Plate Type D, ( $c = 0, t_w = 0.1$  in.)**





---

---

# Appendix C

## Thin-Walled Sections

---

---

### C.1 ELASTIC BUCKLING OF COMPRESSION MEMBERS UNDER ECCENTRIC LOAD

The elastic buckling loads can be computed by solving the following cubic equation:

$$c_1 P_e^3 + c_2 P_e^2 + c_3 P_e + c_4 = 0$$

The lowest positive elastic buckling load is the governing critical compression load.

$$P_e = \min(P_{e1}, P_{e2}, P_{e3})$$

where

$$c_1 = a_x^2 + a_y^2 - \bar{r}_o^2$$

$$c_2 = \bar{r}_o^2 (P_{ex} + P_{ey} + P_{et}) - P_{ex} a_y^2 - P_{ey} a_x^2$$

$$c_3 = -\bar{r}_o^2 (P_{ex} P_{ey} + P_{ex} P_{et} + P_{ey} P_{et})$$

$$c_4 = \bar{r}_o^2 P_{ex} P_{ey} P_{et}$$

$$P_{ex} = \frac{\pi^2 EI_x}{(K_x L_x)^2}$$

$$P_{ey} = \frac{\pi^2 EI_y}{(K_y L_y)^2}$$

$$P_{et} = \frac{1}{r_{ob}^2} \left( GJ + \frac{\pi^2 EC_w}{(K_t L_t)^2} \right)$$

$$a_x = x_o - e_x$$

$$a_y = y_o - e_y$$

$$r_o^2 = r_x^2 + r_y^2 + x_o^2 + y_o^2$$

$$\bar{r}_o^2 = r_o^2 + \beta_x e_y + \beta_y e_x$$

$$\beta_x = \frac{1}{I_x} \int_A y(x^2 + y^2) dA - 2y_o$$

$$\beta_y = \frac{1}{I_y} \int_A x(x^2 + y^2) dA - 2x_o$$

and

$P_{e1}$ ,  $P_{e2}$  and  $P_{e3}$  = roots of the cubic equation.

$E$  = Modulus of elasticity

$G$  = Shear modulus

$J$  = St. Venant torsion constant of cross section

$C_w$  = Torsional warping constant of cross section

$KL$  = Effective length of compression member

$I_x$  = Moment of inertia about the x-axis

$I_y$  = Moment of inertia about the y-axis

$r_x$  = Radius of gyration of cross section about the x-axis

$r_y$  = Radius of gyration of cross section about the y-axis

$x_o$  = x-coordinate of the shear center

$y_o$  = y-coordinate of the shear center

$e_x$  = Eccentricity about the x-axis

$e_y$  = Eccentricity about the y-axis

x- and y-axis = Centroidal principal axes

If the load acts along the shear center axis ( $e_x = x_o, e_y = y_o$ ) we have

$$P_{e1} = P_{ex}$$

$$P_{e2} = P_{ey}$$

$$P_{e3} = P_{et}$$

If the load acts along the shear center y-axis ( $e_x = x_o$ ) we have

$$P_{e1,e2} = \frac{1}{2\beta} \left( (P_{ey} + P_{et}) \pm \sqrt{(P_{ey} + P_{et})^2 - 4\beta P_{ey}P_{et}} \right)$$

$$P_{e3} = P_{ex}$$

where

$$\beta = 1 - \left( \frac{a_y}{r_o} \right)^2$$

If the load acts along the shear center x-axis ( $e_y = y_o$ ) we have

$$P_{e1,e2} = \frac{1}{2\beta} \left( (P_{ex} + P_{et}) \pm \sqrt{(P_{ex} + P_{et})^2 - 4\beta P_{ex}P_{et}} \right)$$

$$P_{e3} = P_{ey}$$

where 
$$\beta = 1 - \left( \frac{a_x}{r_o} \right)^2$$

## C.2 ELASTIC LATERAL BUCKLING OF FLEXURAL MEMBERS UNDER BIAXIAL BENDING

The elastic lateral buckling loads can be computed by solving the following equation:

$$M_{ey1,ey2} = -\frac{1}{2(c^2/P_{ey} + 1/P_{ex})} \left( (\beta_x c + \beta_y) \pm \sqrt{(\beta_x c + \beta_y)^2 + 4r_o^2 P_{et} (c^2/P_{ey} + 1/P_{ex})} \right)$$

The lowest positive lateral elastic buckling load is the governing critical load.

$$M_{ey} = \min(M_{ey1}, M_{ey2})$$

where  $c = M_{ex}/M_{ey}$  is the defined moment ratio.

## C.3 ELASTIC LATERAL BUCKLING OF FLEXURAL MEMBERS BENDING ABOUT THE $y$ -axis

The elastic lateral buckling loads can be computed by solving the following equation:

$$M_{ey1,ey2} = -\frac{P_{ex}}{2} \left( \beta_y \pm \sqrt{\beta_y^2 + 4r_o^2 (P_{et}/P_{ex})} \right)$$

The lowest positive lateral elastic buckling load is the governing critical load.

$$M_{ey} = \min(M_{ey1}, M_{ey2})$$

#### **C.4 ELASTIC LATERAL BUCKLING OF FLEXURAL MEMBERS BENDING ABOUT THE $x$ -axis**

The elastic lateral buckling loads can be computed by solving the following equation:

$$M_{ex1,ex2} = -\frac{P_{ey}}{2} \left( \beta_x \pm \sqrt{\beta_x^2 + 4r_o^2 (P_{et}/P_{ey})} \right)$$

The lowest positive lateral elastic buckling load is the governing critical load.

$$M_{ex} = \min(M_{ex1}, M_{ex2})$$

---

---

# Appendix D

## Beam-Columns

---

---

Peköz and Celebi (1969) presented an approximate analysis approach for elastic beam-columns with equal end eccentricities. For the simply supported case, the functions for deflections were assumed to satisfy the geometric boundary conditions and have the forms.

$$u = \frac{Pe_x}{2EI_y} z(z-L) + A_0 \sin \frac{\pi z}{L}$$

$$v = \frac{Pe_y}{2EI_x} z(z-L) + B_0 \sin \frac{\pi z}{L}$$

$$\phi = C_0 \sin \frac{\pi z}{L}$$

These deflection functions are then used in the elastic beam-column differential equations where the unknown coefficients  $A_0$ ,  $B_0$ , and  $C_0$  are solved by applying the Galerkin method.

$$A_0 = \frac{P^2}{\Delta P_{ey}} \left\{ Pa_x (Pe_x a_x + Pe_y e_y a_y) - e_x (P_{ex} - P) [(P_{et} - P) \bar{r}_0^2 + Pa_y^2] \right\}$$

$$B_0 = \frac{P^2}{\Delta P_{ex}} \left\{ Pa_y (Pe_y a_y + Pe_x e_x a_x) - e_y (P_{ey} - P) [(P_{et} - P) \bar{r}_0^2 + Pa_x^2] \right\}$$

$$C_0 = \frac{P^2}{\Delta} \left[ (P_{ey} - P) e_y a_x - (P_{ex} - P) e_x a_y \right]$$

where

$$\Delta = \frac{\pi}{4} \begin{vmatrix} P_{ey} - P & 0 & -Pa_y \\ 0 & P_{ex} - P & Pa_x \\ -Pa_y & Pa_x & \bar{r}_0^2 (P_{et} - P) \end{vmatrix}$$

and  $P$  is the applied eccentric load. Definitions of the other variables are given in the Appendix C. Inserting the solved deformation functions in the basic beam equations

$$M_x = EI_x \frac{d^2 v}{dz^2}$$

$$M_y = EI_y \frac{d^2 u}{dz^2}$$

$$M_t = GJ \frac{d\phi}{dz} - EC_w \frac{d^3 \phi}{dz^3}$$

The corresponding bending moments about principal axes and twisting moment in the beam-columns are obtained as follows:

$$M_x = Pe_y - B_0 P_{ex} \sin \frac{\pi z}{L}$$

$$M_y = Pe_x - A_0 P_{ey} \sin \frac{\pi z}{L}$$

$$M_t = C_0 \left( \frac{\pi GJ}{L} + \frac{\pi^3 EC_w}{L^3} \right) \cos \frac{\pi z}{L}$$

The maximum values of these moments are given in Eq. (4.13) to (4.15)



---

---

Appendix **E**

**Design Results**

---

---

**Table E.1** Correlation of Design Procedures with the FEM Results

Boundary Condition	Section	$F_y$	$P_{FEM}$	$\frac{P_{1a}}{P_{FEM}}$	$\frac{P_{1b}}{P_{FEM}}$	$\frac{P_{1c}}{P_{FEM}}$	$\frac{P_{1d}}{P_{FEM}}$	$\frac{P_{2a}}{P_{FEM}}$	$\frac{P_{2b}}{P_{FEM}}$	$\frac{P_{2c}}{P_{FEM}}$
		(ksi)	(kips)							
G1	C1	33	0.87	0.822	0.851	0.696	0.713	0.958	0.958	0.862
		55	0.94	0.762	0.789	0.649	0.666	0.897	0.897	0.807
		70	0.99	0.718	0.744	0.613	0.629	0.847	0.847	0.762
	C2	33	1.16	0.823	0.851	0.713	0.731	0.962	0.962	0.867
		55	1.23	0.776	0.803	0.677	0.694	0.919	0.919	0.828
		70	1.23	0.776	0.803	0.678	0.696	0.923	0.923	0.831
	C3	33	1.45	0.824	0.851	0.724	0.739	0.966	0.966	0.870
		55	1.48	0.805	0.832	0.713	0.728	0.959	0.959	0.864
		70	1.48	0.805	0.832	0.715	0.730	0.966	0.966	0.870
G2	C1	33	2.31	0.813	0.898	0.726	0.775	0.984	0.984	0.889
		55	2.36	0.797	0.880	0.726	0.776	0.979	0.979	0.882
		70	2.39	0.788	0.870	0.721	0.772	0.971	0.971	0.875
	C2	33	3.08	0.816	0.898	0.735	0.782	0.987	0.987	0.891
		55	3.14	0.800	0.881	0.736	0.784	0.983	0.983	0.886
		70	3.14	0.800	0.880	0.741	0.790	0.987	0.987	0.890
	C3	33	3.85	0.819	0.898	0.740	0.786	0.989	0.989	0.893
		55	3.90	0.810	0.888	0.748	0.796	0.993	0.993	0.896
		70	3.90	0.810	0.888	0.753	0.802	0.998	0.998	0.900
G3	C1	33	5.81	0.746	0.963	0.666	0.792	0.973	0.973	0.893
		55	6.08	0.714	0.921	0.662	0.798	0.982	0.982	0.894
		70	6.16	0.704	0.909	0.662	0.803	0.982	0.982	0.892
	C2	33	7.76	0.752	0.963	0.670	0.791	0.974	0.974	0.894
		55	8.11	0.719	0.921	0.666	0.799	0.983	0.983	0.895
		70	8.17	0.714	0.914	0.670	0.808	0.990	0.990	0.899
	C3	33	9.70	0.759	0.962	0.674	0.791	0.976	0.976	0.895
		55	10.14	0.726	0.921	0.671	0.799	0.985	0.985	0.896
		70	10.27	0.716	0.909	0.672	0.804	0.986	0.986	0.895
G4	C1	33	9.86	0.830	1.082	0.727	0.889	0.938	0.938	0.919
		55	11.18	0.733	1.023	0.673	0.884	0.964	0.964	0.942
		70	11.59	0.707	0.987	0.660	0.874	0.956	0.956	0.935
	C2	33	13.33	0.832	1.080	0.725	0.884	0.934	0.934	0.915
		55	15.16	0.733	1.024	0.672	0.881	0.965	0.965	0.941
		70	15.71	0.707	0.988	0.659	0.871	0.959	0.959	0.936
	C3	33	16.93	0.834	1.078	0.724	0.878	0.930	0.930	0.911
		55	19.32	0.733	1.026	0.670	0.876	0.966	0.966	0.940
		70	20.02	0.708	0.990	0.658	0.868	0.962	0.962	0.937
G5	C1	33	10.15	0.872	1.073	0.764	0.901	0.940	0.940	0.928
		55	11.53	0.775	1.023	0.712	0.900	0.967	0.967	0.953
		70	11.97	0.746	0.985	0.697	0.887	0.955	0.955	0.943
	C2	33	13.74	0.872	1.071	0.761	0.895	0.936	0.936	0.924
		55	15.67	0.774	1.025	0.710	0.898	0.968	0.968	0.954
		70	16.27	0.745	0.987	0.695	0.885	0.957	0.957	0.944
	C3	33	17.50	0.872	1.068	0.759	0.889	0.931	0.931	0.918
		55	20.05	0.774	1.028	0.707	0.895	0.969	0.969	0.953
		70	20.82	0.745	0.989	0.692	0.883	0.960	0.960	0.946

**Table E.1 (Continued)**

Boundary Condition	Section	$F_y$	$P_{FEM}$	$\frac{P_{1a}}{P_{FEM}}$	$\frac{P_{1b}}{P_{FEM}}$	$\frac{P_{1c}}{P_{FEM}}$	$\frac{P_{1d}}{P_{FEM}}$	$\frac{P_{2a}}{P_{FEM}}$	$\frac{P_{2b}}{P_{FEM}}$	$\frac{P_{2c}}{P_{FEM}}$
		(ksi)	(kips)							
G6	C1	33	1.75	0.796	0.856	0.702	0.733	0.952	0.952	0.857
		55	1.76	0.792	0.851	0.703	0.733	0.954	0.954	0.859
		70	1.76	0.792	0.851	0.704	0.735	0.956	0.956	0.860
	C2	33	2.31	0.810	0.868	0.726	0.757	0.971	0.971	0.875
		55	2.31	0.810	0.868	0.731	0.763	0.980	0.980	0.882
		70	2.31	0.810	0.868	0.733	0.765	0.982	0.982	0.884
	C3	33	2.85	0.821	0.877	0.742	0.775	0.986	0.986	0.888
		55	2.85	0.821	0.877	0.748	0.781	0.996	0.996	0.897
		70	2.85	0.821	0.877	0.750	0.783	0.999	0.999	0.899
G7	C1	33	3.21	0.784	0.899	0.716	0.787	0.983	0.983	0.888
		55	3.27	0.769	0.882	0.717	0.791	0.980	0.980	0.885
		70	3.27	0.769	0.882	0.722	0.797	0.985	0.985	0.888
	C2	33	4.28	0.787	0.899	0.723	0.792	0.986	0.986	0.891
		55	4.31	0.781	0.891	0.733	0.805	0.994	0.994	0.897
		70	4.31	0.781	0.891	0.738	0.812	0.999	0.999	0.901
	C3	33	5.35	0.791	0.899	0.728	0.796	0.987	0.987	0.893
		55	5.46	0.775	0.881	0.729	0.801	0.984	0.984	0.888
		70	5.49	0.771	0.875	0.730	0.803	0.983	0.983	0.887
G8	C1	33	6.73	0.722	0.969	0.649	0.796	0.959	0.959	0.885
		55	7.07	0.688	0.923	0.642	0.800	0.973	0.973	0.889
		70	7.17	0.678	0.911	0.640	0.804	0.974	0.974	0.888
	C2	33	8.98	0.728	0.969	0.654	0.795	0.961	0.961	0.887
		55	9.43	0.693	0.923	0.646	0.800	0.975	0.975	0.890
		70	9.56	0.684	0.910	0.645	0.804	0.976	0.976	0.890
	C3	33	11.24	0.735	0.969	0.658	0.794	0.963	0.963	0.888
		55	11.79	0.701	0.923	0.652	0.799	0.977	0.977	0.892
		70	11.96	0.691	0.910	0.651	0.804	0.979	0.979	0.891
G9	C1	33	10.23	0.830	1.069	0.731	0.890	0.925	0.925	0.910
		55	11.60	0.735	1.023	0.677	0.891	0.949	0.949	0.932
		70	12.04	0.708	0.986	0.663	0.880	0.939	0.939	0.923
	C2	33	13.84	0.831	1.066	0.729	0.884	0.920	0.920	0.905
		55	15.76	0.734	1.024	0.675	0.888	0.950	0.950	0.931
		70	16.36	0.707	0.987	0.660	0.877	0.941	0.941	0.923
	C3	33	17.61	0.832	1.064	0.726	0.877	0.916	0.916	0.900
		55	20.14	0.733	1.026	0.672	0.883	0.951	0.951	0.930
		70	20.90	0.707	0.989	0.659	0.873	0.943	0.943	0.924
G10	C1	33	10.43	0.872	1.061	0.768	0.900	0.928	0.928	0.919
		55	11.85	0.779	1.021	0.718	0.905	0.954	0.954	0.943
		70	12.31	0.750	0.984	0.702	0.891	0.940	0.940	0.931
	C2	33	14.14	0.871	1.058	0.765	0.894	0.923	0.923	0.913
		55	16.13	0.777	1.024	0.715	0.903	0.955	0.955	0.943
		70	16.76	0.748	0.986	0.699	0.889	0.942	0.942	0.931
	C3	33	18.03	0.870	1.055	0.761	0.887	0.918	0.918	0.907
		55	20.67	0.776	1.026	0.711	0.900	0.955	0.955	0.942
		70	21.48	0.747	0.988	0.696	0.887	0.944	0.944	0.932

**Table E.1 (Continued)**

Boundary Condition	Section	$F_y$	$P_{FEM}$	$\frac{P_{1a}}{P_{FEM}}$	$\frac{P_{1b}}{P_{FEM}}$	$\frac{P_{1c}}{P_{FEM}}$	$\frac{P_{1d}}{P_{FEM}}$	$\frac{P_{2a}}{P_{FEM}}$	$\frac{P_{2b}}{P_{FEM}}$	$\frac{P_{2c}}{P_{FEM}}$
		(ksi)	(kips)							
G11	C1	33	4.82	0.736	0.903	0.689	0.799	0.979	0.979	0.887
		55	4.86	0.730	0.896	0.697	0.815	0.991	0.991	0.895
		70	4.98	0.712	0.873	0.684	0.802	0.972	0.972	0.877
	C2	33	6.41	0.742	0.905	0.695	0.804	0.984	0.984	0.892
		55	6.56	0.725	0.884	0.693	0.808	0.981	0.981	0.886
		70	6.57	0.724	0.883	0.697	0.815	0.986	0.986	0.890
	C3	33	7.94	0.755	0.913	0.706	0.813	0.995	0.995	0.901
		55	8.15	0.736	0.890	0.703	0.816	0.990	0.990	0.895
		70	8.15	0.736	0.890	0.708	0.824	0.996	0.996	0.900
G12	C1	33	8.37	0.681	0.982	0.620	0.803	0.924	0.924	0.864
		55	8.87	0.644	0.928	0.606	0.802	0.948	0.948	0.873
		70	9.01	0.634	0.913	0.603	0.805	0.951	0.951	0.874
	C2	33	11.17	0.688	0.981	0.625	0.803	0.927	0.927	0.866
		55	11.83	0.650	0.928	0.611	0.802	0.952	0.952	0.876
		70	12.02	0.640	0.913	0.608	0.805	0.955	0.955	0.877
	C3	33	13.98	0.697	0.981	0.631	0.801	0.930	0.930	0.868
		55	14.80	0.658	0.927	0.617	0.801	0.956	0.956	0.879
		70	15.03	0.648	0.913	0.615	0.805	0.959	0.959	0.879
G13	C1	33	10.76	0.832	1.047	0.739	0.890	0.905	0.905	0.894
		55	12.21	0.742	1.021	0.688	0.903	0.928	0.928	0.917
		70	12.68	0.715	0.983	0.673	0.889	0.915	0.915	0.904
	C2	33	14.61	0.831	1.044	0.736	0.884	0.900	0.900	0.889
		55	16.64	0.740	1.023	0.685	0.899	0.928	0.928	0.915
		70	17.28	0.713	0.985	0.669	0.886	0.915	0.915	0.904
	C3	33	18.64	0.829	1.040	0.732	0.876	0.894	0.894	0.882
		55	21.35	0.738	1.025	0.681	0.895	0.927	0.927	0.913
		70	22.17	0.711	0.987	0.666	0.883	0.916	0.916	0.904
G14	C1	33	10.87	0.872	1.043	0.774	0.898	0.910	0.910	0.903
		55	12.34	0.787	1.019	0.729	0.913	0.934	0.934	0.926
		70	12.81	0.758	0.982	0.713	0.897	0.918	0.918	0.912
	C2	33	14.76	0.869	1.039	0.770	0.892	0.904	0.904	0.897
		55	16.83	0.785	1.021	0.725	0.911	0.934	0.934	0.926
		70	17.48	0.756	0.983	0.709	0.895	0.919	0.919	0.912
	C3	33	18.86	0.867	1.035	0.765	0.884	0.898	0.898	0.890
		55	21.62	0.783	1.024	0.721	0.908	0.933	0.933	0.924
		70	22.47	0.753	0.985	0.705	0.893	0.920	0.920	0.912
G15	C1	33	11.80	0.634	0.976	0.588	0.825	0.825	0.825	0.802
		55	13.38	0.558	0.965	0.533	0.826	0.827	0.827	0.796
		70	13.80	0.541	0.935	0.521	0.818	0.818	0.818	0.788
	C2	33	16.07	0.629	0.955	0.583	0.807	0.816	0.816	0.792
		55	18.18	0.556	0.947	0.530	0.811	0.825	0.825	0.792
		70	18.65	0.542	0.923	0.521	0.807	0.821	0.821	0.788
	C3	33	20.52	0.628	0.935	0.580	0.790	0.808	0.808	0.784
		55	22.83	0.564	0.942	0.537	0.806	0.836	0.836	0.799
		70	23.08	0.558	0.932	0.536	0.815	0.847	0.847	0.809

**Table E.1 (Continued)**

Boundary Condition	Section	$F_y$	$P_{FEM}$	$\frac{P_{1a}}{P_{FEM}}$	$\frac{P_{1b}}{P_{FEM}}$	$\frac{P_{1c}}{P_{FEM}}$	$\frac{P_{1d}}{P_{FEM}}$	$\frac{P_{2a}}{P_{FEM}}$	$\frac{P_{2b}}{P_{FEM}}$	$\frac{P_{2c}}{P_{FEM}}$
		(ksi)	(kips)							
G16	C1	33	11.57	0.853	1.016	0.772	0.897	0.882	0.885	0.877
		55	13.20	0.775	1.013	0.726	0.922	0.895	0.897	0.890
		70	13.68	0.748	0.978	0.710	0.906	0.878	0.880	0.874
	C2	33	15.79	0.846	1.008	0.764	0.888	0.873	0.876	0.868
		55	18.07	0.772	1.014	0.721	0.919	0.893	0.895	0.888
		70	18.74	0.744	0.979	0.705	0.903	0.876	0.878	0.872
	C3	33	20.31	0.838	0.999	0.755	0.875	0.862	0.865	0.856
		55	23.33	0.767	1.014	0.716	0.914	0.890	0.892	0.884
		70	24.21	0.739	0.981	0.699	0.901	0.874	0.876	0.869
G17	C1	33	11.55	0.885	1.017	0.800	0.902	0.887	0.908	0.883
		55	13.20	0.815	1.013	0.762	0.927	0.900	0.915	0.896
		70	13.67	0.787	0.978	0.745	0.910	0.882	0.895	0.879
	C2	33	15.77	0.879	1.009	0.792	0.893	0.878	0.899	0.874
		55	18.06	0.812	1.015	0.758	0.925	0.898	0.914	0.894
		70	18.73	0.783	0.979	0.741	0.909	0.881	0.893	0.877
	C3	33	20.29	0.870	1.000	0.782	0.881	0.867	0.888	0.863
		55	23.32	0.809	1.014	0.752	0.920	0.895	0.912	0.891
		70	24.21	0.779	0.981	0.735	0.907	0.878	0.892	0.875
G18	C1	33	12.25	0.907	0.991	0.846	0.917	0.875	0.920	0.873
		55	14.07	0.866	1.004	0.826	0.949	0.873	0.904	0.871
		70	14.57	0.836	0.973	0.805	0.930	0.851	0.876	0.850
	C2	33	16.76	0.899	0.982	0.837	0.907	0.865	0.911	0.863
		55	19.33	0.863	1.002	0.821	0.945	0.869	0.902	0.868
		70	20.04	0.833	0.974	0.800	0.928	0.848	0.873	0.847
	C3	33	21.62	0.888	0.971	0.825	0.895	0.853	0.900	0.851
		55	25.07	0.859	0.998	0.816	0.938	0.864	0.899	0.863
		70	26.02	0.828	0.974	0.794	0.926	0.843	0.870	0.842
G19	C1	33	12.24	0.925	0.996	0.859	0.919	0.873	0.931	0.872
		55	14.09	0.891	1.010	0.847	0.952	0.870	0.910	0.869
		70	14.61	0.860	0.979	0.825	0.933	0.848	0.879	0.847
	C2	33	16.74	0.917	0.987	0.850	0.909	0.863	0.921	0.862
		55	19.36	0.889	1.008	0.843	0.948	0.867	0.908	0.866
		70	20.09	0.857	0.979	0.821	0.932	0.844	0.876	0.843
	C3	33	21.59	0.906	0.976	0.839	0.897	0.851	0.911	0.850
		55	25.11	0.886	1.004	0.839	0.942	0.862	0.905	0.861
		70	26.09	0.853	0.980	0.816	0.931	0.840	0.873	0.839
G20	C1	33	12.34	0.933	0.994	0.872	0.924	0.872	0.933	0.871
		55	14.26	0.906	1.008	0.864	0.956	0.864	0.906	0.864
		70	14.79	0.874	0.978	0.841	0.937	0.841	0.874	0.841
	C2	33	16.90	0.924	0.984	0.862	0.914	0.862	0.923	0.861
		55	19.60	0.904	1.005	0.861	0.952	0.861	0.904	0.860
		70	20.34	0.871	0.978	0.838	0.936	0.838	0.871	0.837
	C3	33	21.80	0.913	0.972	0.850	0.901	0.850	0.912	0.849
		55	25.43	0.901	1.001	0.856	0.945	0.856	0.901	0.856
		70	26.43	0.868	0.979	0.833	0.935	0.833	0.867	0.832

**Table E.1 (Continued)**

Boundary Condition	Section	$F_y$	$P_{FEM}$	$\frac{P_{1a}}{P_{FEM}}$	$\frac{P_{1b}}{P_{FEM}}$	$\frac{P_{1c}}{P_{FEM}}$	$\frac{P_{1d}}{P_{FEM}}$	$\frac{P_{2a}}{P_{FEM}}$	$\frac{P_{2b}}{P_{FEM}}$	$\frac{P_{2c}}{P_{FEM}}$
		(ksi)	(kips)							
G1	C4	33	0.57	0.827	0.848	0.666	0.674	0.947	0.947	0.853
		55	0.62	0.761	0.780	0.615	0.622	0.877	0.877	0.789
		70	0.66	0.707	0.725	0.572	0.579	0.816	0.816	0.734
	C5	33	0.76	0.829	0.848	0.688	0.694	0.953	0.953	0.858
		55	0.82	0.762	0.780	0.635	0.641	0.883	0.883	0.795
		70	0.88	0.709	0.725	0.591	0.597	0.823	0.823	0.740
	C6	33	0.95	0.831	0.848	0.703	0.708	0.957	0.957	0.862
		55	1.03	0.764	0.780	0.650	0.655	0.889	0.889	0.801
		70	1.05	0.748	0.763	0.637	0.642	0.874	0.874	0.786
G2	C4	33	1.51	0.835	0.897	0.722	0.752	0.977	0.977	0.882
		55	1.54	0.819	0.879	0.718	0.750	0.970	0.970	0.874
		70	1.56	0.809	0.868	0.713	0.744	0.961	0.961	0.866
	C5	33	2.01	0.840	0.897	0.734	0.763	0.982	0.982	0.886
		55	2.05	0.824	0.879	0.732	0.761	0.975	0.975	0.879
		70	2.08	0.814	0.868	0.727	0.756	0.966	0.966	0.871
	C6	33	2.51	0.846	0.897	0.744	0.770	0.985	0.985	0.889
		55	2.56	0.829	0.879	0.743	0.769	0.978	0.978	0.882
		70	2.58	0.822	0.872	0.741	0.768	0.974	0.974	0.879
G3	C4	33	3.81	0.790	0.959	0.689	0.782	0.971	0.971	0.889
		55	3.97	0.760	0.922	0.687	0.785	0.974	0.974	0.886
		70	4.00	0.753	0.914	0.688	0.789	0.975	0.975	0.886
	C5	33	5.09	0.802	0.958	0.697	0.782	0.974	0.974	0.892
		55	5.30	0.771	0.921	0.695	0.785	0.978	0.978	0.889
		70	5.35	0.764	0.912	0.697	0.790	0.978	0.978	0.888
	C6	33	6.37	0.816	0.958	0.707	0.782	0.977	0.977	0.894
		55	6.63	0.784	0.921	0.706	0.786	0.981	0.981	0.891
		70	6.70	0.775	0.911	0.707	0.790	0.980	0.980	0.890
G4	C4	33	6.93	0.859	1.107	0.731	0.876	0.932	0.932	0.908
		55	7.61	0.782	1.067	0.697	0.881	0.970	0.970	0.939
		70	7.71	0.771	1.053	0.698	0.889	0.981	0.981	0.950
	C5	33	9.49	0.868	1.105	0.732	0.867	0.929	0.929	0.903
		55	10.49	0.787	1.071	0.697	0.875	0.977	0.977	0.942
		70	10.65	0.775	1.055	0.698	0.882	0.989	0.989	0.953
	C6	33	12.20	0.878	1.100	0.733	0.856	0.927	0.927	0.900
		55	13.57	0.794	1.072	0.698	0.866	0.981	0.981	0.940
		70	13.81	0.780	1.053	0.698	0.872	0.997	0.997	0.953
G5	C4	33	7.22	0.897	1.095	0.764	0.889	0.931	0.931	0.915
		55	7.97	0.819	1.066	0.730	0.900	0.972	0.972	0.952
		70	8.08	0.807	1.051	0.731	0.905	0.980	0.980	0.961
	C5	33	9.95	0.901	1.094	0.762	0.879	0.927	0.927	0.910
		55	11.06	0.822	1.075	0.729	0.897	0.980	0.980	0.957
		70	11.24	0.809	1.058	0.729	0.902	0.990	0.990	0.966
	C6	33	12.86	0.907	1.092	0.760	0.869	0.924	0.924	0.905
		55	14.43	0.828	1.085	0.728	0.892	0.985	0.985	0.957
		70	14.70	0.813	1.065	0.727	0.896	1.000	1.000	0.971

**Table E.1 (Continued)**

Boundary Condition	Section	$F_y$	$P_{FEM}$	$\frac{P_{1a}}{P_{FEM}}$	$\frac{P_{1b}}{P_{FEM}}$	$\frac{P_{1c}}{P_{FEM}}$	$\frac{P_{1d}}{P_{FEM}}$	$\frac{P_{2a}}{P_{FEM}}$	$\frac{P_{2b}}{P_{FEM}}$	$\frac{P_{2c}}{P_{FEM}}$
		(ksi)	(kips)							
G6	C4	33	1.15	0.810	0.852	0.679	0.700	0.941	0.941	0.847
		55	1.22	0.764	0.804	0.644	0.664	0.893	0.893	0.803
		70	1.22	0.764	0.804	0.644	0.665	0.894	0.894	0.804
	C5	33	1.53	0.813	0.852	0.696	0.716	0.948	0.948	0.853
		55	1.55	0.800	0.839	0.689	0.709	0.939	0.939	0.845
		70	1.55	0.800	0.839	0.690	0.710	0.940	0.940	0.846
	C6	33	1.90	0.821	0.856	0.713	0.733	0.957	0.957	0.861
		55	1.90	0.821	0.856	0.718	0.737	0.964	0.964	0.868
		70	1.90	0.821	0.856	0.719	0.738	0.966	0.966	0.870
G7	C4	33	2.09	0.812	0.897	0.724	0.772	0.976	0.976	0.882
		55	2.14	0.796	0.879	0.721	0.770	0.969	0.969	0.874
		70	2.16	0.786	0.869	0.716	0.765	0.961	0.961	0.866
	C5	33	2.79	0.819	0.897	0.735	0.778	0.981	0.981	0.886
		55	2.85	0.803	0.879	0.733	0.778	0.974	0.974	0.879
		70	2.86	0.800	0.877	0.736	0.780	0.975	0.975	0.880
	C6	33	3.49	0.826	0.897	0.742	0.784	0.984	0.984	0.889
		55	3.54	0.815	0.885	0.746	0.789	0.984	0.984	0.888
		70	3.54	0.815	0.885	0.750	0.794	0.988	0.988	0.891
G8	C4	33	4.43	0.768	0.964	0.676	0.784	0.959	0.959	0.882
		55	4.62	0.736	0.924	0.670	0.786	0.965	0.965	0.881
		70	4.66	0.729	0.915	0.671	0.790	0.967	0.967	0.881
	C5	33	5.91	0.782	0.963	0.685	0.784	0.964	0.964	0.885
		55	6.17	0.749	0.923	0.680	0.786	0.971	0.971	0.885
		70	6.24	0.741	0.913	0.681	0.789	0.971	0.971	0.884
	C6	33	7.40	0.797	0.962	0.695	0.784	0.968	0.968	0.888
		55	7.72	0.764	0.922	0.692	0.787	0.975	0.975	0.888
		70	7.81	0.755	0.911	0.692	0.790	0.975	0.975	0.886
G9	C4	33	7.25	0.854	1.090	0.731	0.874	0.914	0.914	0.895
		55	8.00	0.776	1.061	0.696	0.885	0.951	0.951	0.926
		70	8.13	0.764	1.045	0.694	0.889	0.957	0.957	0.933
	C5	33	9.97	0.860	1.088	0.730	0.865	0.911	0.911	0.890
		55	11.06	0.780	1.069	0.694	0.879	0.959	0.959	0.929
		70	11.26	0.767	1.050	0.693	0.884	0.966	0.966	0.937
	C6	33	12.84	0.868	1.083	0.730	0.853	0.909	0.909	0.885
		55	14.37	0.787	1.073	0.695	0.872	0.963	0.963	0.928
		70	14.65	0.771	1.053	0.693	0.876	0.976	0.976	0.940
G10	C4	33	7.48	0.891	1.078	0.764	0.884	0.915	0.915	0.902
		55	8.28	0.815	1.057	0.731	0.900	0.953	0.953	0.937
		70	8.42	0.802	1.039	0.729	0.902	0.957	0.957	0.942
	C5	33	10.33	0.894	1.077	0.761	0.875	0.911	0.911	0.896
		55	11.53	0.819	1.068	0.729	0.898	0.962	0.962	0.942
		70	11.74	0.803	1.049	0.727	0.901	0.967	0.967	0.949
	C6	33	13.39	0.898	1.074	0.758	0.865	0.906	0.906	0.890
		55	15.09	0.824	1.080	0.727	0.895	0.966	0.966	0.943
		70	15.40	0.807	1.058	0.724	0.897	0.978	0.978	0.955

**Table E.1 (Continued)**

Boundary Condition	Section	$F_y$	$P_{FEM}$	$\frac{P_{1a}}{P_{FEM}}$	$\frac{P_{1b}}{P_{FEM}}$	$\frac{P_{1c}}{P_{FEM}}$	$\frac{P_{1d}}{P_{FEM}}$	$\frac{P_{2a}}{P_{FEM}}$	$\frac{P_{2b}}{P_{FEM}}$	$\frac{P_{2c}}{P_{FEM}}$
		(ksi)	(kips)							
G11	C4	33	3.15	0.773	0.900	0.711	0.788	0.973	0.973	0.881
		55	3.21	0.758	0.883	0.709	0.789	0.970	0.970	0.876
		70	3.21	0.758	0.882	0.712	0.794	0.973	0.973	0.878
	C5	33	4.20	0.783	0.901	0.720	0.792	0.978	0.978	0.885
		55	4.24	0.775	0.891	0.726	0.802	0.984	0.984	0.889
		70	4.34	0.758	0.872	0.714	0.790	0.967	0.967	0.873
	C6	33	5.25	0.794	0.901	0.729	0.796	0.981	0.981	0.888
		55	5.26	0.792	0.898	0.742	0.812	0.995	0.995	0.899
		70	5.40	0.772	0.875	0.727	0.798	0.975	0.975	0.880
G12	C4	33	5.53	0.729	0.973	0.650	0.789	0.930	0.930	0.864
		55	5.81	0.695	0.927	0.640	0.786	0.944	0.944	0.867
		70	5.88	0.687	0.916	0.639	0.789	0.946	0.946	0.867
	C5	33	7.39	0.746	0.972	0.661	0.789	0.938	0.938	0.869
		55	7.75	0.711	0.926	0.652	0.787	0.953	0.953	0.873
		70	7.86	0.702	0.914	0.650	0.789	0.953	0.953	0.872
	C6	33	9.25	0.765	0.971	0.674	0.789	0.945	0.945	0.874
		55	9.70	0.728	0.925	0.665	0.787	0.960	0.960	0.878
		70	9.84	0.719	0.913	0.664	0.790	0.961	0.961	0.877
G13	C4	33	7.76	0.845	1.058	0.732	0.868	0.887	0.887	0.873
		55	8.61	0.770	1.046	0.695	0.887	0.919	0.919	0.902
		70	8.78	0.754	1.025	0.690	0.886	0.919	0.919	0.903
	C5	33	10.73	0.847	1.055	0.728	0.858	0.882	0.882	0.866
		55	11.99	0.772	1.058	0.692	0.884	0.926	0.926	0.905
		70	12.25	0.755	1.035	0.687	0.884	0.927	0.927	0.908
	C6	33	13.91	0.850	1.050	0.724	0.846	0.876	0.876	0.859
		55	15.68	0.776	1.069	0.690	0.879	0.930	0.930	0.905
		70	16.06	0.758	1.045	0.685	0.879	0.938	0.938	0.913
G14	C4	33	7.89	0.882	1.049	0.764	0.877	0.891	0.891	0.882
		55	8.77	0.811	1.040	0.732	0.897	0.923	0.923	0.912
		70	8.96	0.794	1.018	0.726	0.895	0.921	0.921	0.911
	C5	33	10.95	0.881	1.045	0.758	0.866	0.884	0.884	0.873
		55	12.28	0.813	1.053	0.728	0.898	0.930	0.930	0.917
		70	12.56	0.795	1.030	0.723	0.896	0.930	0.930	0.917
	C6	33	14.27	0.881	1.041	0.752	0.854	0.877	0.877	0.865
		55	16.17	0.817	1.066	0.726	0.895	0.934	0.934	0.917
		70	16.57	0.797	1.043	0.720	0.895	0.940	0.940	0.924
G15	C4	33	8.30	0.650	0.948	0.592	0.782	0.816	0.816	0.784
		55	9.00	0.599	0.937	0.561	0.788	0.836	0.836	0.794
		70	9.17	0.588	0.921	0.556	0.786	0.835	0.835	0.792
	C5	33	11.09	0.671	0.947	0.609	0.782	0.833	0.833	0.798
		55	12.02	0.619	0.936	0.578	0.788	0.863	0.863	0.813
		70	12.25	0.608	0.919	0.573	0.787	0.862	0.862	0.812
	C6	33	13.87	0.697	0.946	0.628	0.781	0.852	0.852	0.813
		55	15.03	0.643	0.936	0.598	0.789	0.887	0.887	0.830
		70	15.32	0.631	0.918	0.592	0.788	0.890	0.890	0.830



**Table E.1 (Continued)**

Boundary Condition	Section	$F_y$	$P_{FEM}$	$\frac{P_{1a}}{P_{FEM}}$	$\frac{P_{1b}}{P_{FEM}}$	$\frac{P_{1c}}{P_{FEM}}$	$\frac{P_{1d}}{P_{FEM}}$	$\frac{P_{2a}}{P_{FEM}}$	$\frac{P_{2b}}{P_{FEM}}$	$\frac{P_{2c}}{P_{FEM}}$
		(ksi)	(kips)							
G16	C4	33	8.63	0.840	0.997	0.744	0.857	0.846	0.849	0.839
		55	9.68	0.777	1.005	0.712	0.886	0.865	0.868	0.858
		70	9.97	0.754	0.977	0.700	0.875	0.854	0.857	0.847
	C5	33	12.13	0.830	0.985	0.731	0.840	0.831	0.834	0.824
		55	13.74	0.771	1.012	0.702	0.881	0.864	0.867	0.855
		70	14.16	0.748	0.985	0.690	0.872	0.853	0.856	0.845
	C6	33	15.99	0.821	0.974	0.718	0.824	0.816	0.820	0.808
		55	18.36	0.766	1.016	0.692	0.871	0.858	0.861	0.847
		70	18.94	0.743	0.999	0.681	0.872	0.855	0.858	0.845
G17	C4	33	8.63	0.872	0.997	0.772	0.863	0.852	0.875	0.847
		55	9.69	0.817	1.005	0.747	0.893	0.872	0.891	0.867
		70	9.97	0.793	0.976	0.734	0.881	0.860	0.876	0.855
	C5	33	12.13	0.862	0.985	0.758	0.847	0.837	0.861	0.831
		55	13.76	0.813	1.011	0.738	0.889	0.871	0.892	0.865
		70	14.19	0.788	0.984	0.725	0.880	0.859	0.877	0.854
	C6	33	16.02	0.851	0.973	0.744	0.830	0.822	0.846	0.816
		55	18.42	0.810	1.014	0.730	0.881	0.865	0.888	0.858
		70	19.02	0.785	0.997	0.718	0.880	0.862	0.882	0.855
G18	C4	33	9.23	0.886	0.962	0.815	0.878	0.840	0.893	0.839
		55	10.44	0.857	0.984	0.804	0.913	0.846	0.888	0.845
		70	10.75	0.832	0.958	0.788	0.898	0.830	0.865	0.828
	C5	33	13.11	0.867	0.943	0.795	0.856	0.820	0.874	0.818
		55	15.04	0.850	0.979	0.794	0.902	0.838	0.883	0.836
		70	15.53	0.823	0.959	0.776	0.894	0.821	0.858	0.819
	C6	33	17.56	0.846	0.921	0.772	0.832	0.797	0.852	0.795
		55	20.52	0.840	0.967	0.780	0.885	0.822	0.870	0.820
		70	21.28	0.812	0.962	0.763	0.889	0.810	0.851	0.808
G19	C4	33	9.22	0.903	0.967	0.828	0.880	0.839	0.905	0.838
		55	10.45	0.882	0.990	0.824	0.917	0.845	0.896	0.843
		70	10.77	0.856	0.964	0.807	0.901	0.828	0.871	0.827
	C5	33	13.09	0.884	0.948	0.807	0.858	0.818	0.886	0.817
		55	15.04	0.877	0.985	0.815	0.906	0.837	0.892	0.835
		70	15.55	0.849	0.966	0.797	0.898	0.819	0.865	0.818
	C6	33	17.53	0.863	0.926	0.784	0.834	0.796	0.865	0.794
		55	20.52	0.867	0.974	0.801	0.890	0.821	0.880	0.820
		70	21.30	0.841	0.970	0.786	0.895	0.809	0.859	0.808
G20	C4	33	9.28	0.911	0.965	0.841	0.886	0.841	0.911	0.840
		55	10.54	0.898	0.991	0.844	0.925	0.844	0.897	0.843
		70	10.86	0.872	0.965	0.826	0.909	0.826	0.871	0.825
	C5	33	13.18	0.893	0.946	0.821	0.865	0.821	0.892	0.820
		55	15.18	0.894	0.985	0.836	0.914	0.836	0.894	0.835
		70	15.68	0.866	0.968	0.818	0.907	0.818	0.866	0.817
	C6	33	17.64	0.872	0.925	0.799	0.842	0.799	0.872	0.798
		55	20.71	0.882	0.973	0.821	0.898	0.821	0.882	0.820
		70	21.49	0.860	0.973	0.808	0.905	0.808	0.859	0.807

**Table E.1 (Continued)**

Boundary Condition	Section	$F_y$	$P_{FEM}$	$\frac{P_{1a}}{P_{FEM}}$	$\frac{P_{1b}}{P_{FEM}}$	$\frac{P_{1c}}{P_{FEM}}$	$\frac{P_{1d}}{P_{FEM}}$	$\frac{P_{2a}}{P_{FEM}}$	$\frac{P_{2b}}{P_{FEM}}$	$\frac{P_{2c}}{P_{FEM}}$
		(ksi)	(kips)							
G1	C7	33	0.89	0.849	0.849	0.705	0.705	0.962	0.962	0.867
		55	0.97	0.776	0.776	0.649	0.649	0.904	0.904	0.815
		70	1.01	0.746	0.746	0.625	0.625	0.890	0.890	0.804
	C8	33	1.18	0.849	0.849	0.722	0.722	0.966	0.966	0.871
		55	1.25	0.805	0.805	0.689	0.689	0.946	0.946	0.855
		70	1.25	0.805	0.805	0.691	0.691	0.974	0.974	0.884
	C9	33	1.48	0.849	0.849	0.733	0.733	0.969	0.969	0.874
		55	1.50	0.834	0.834	0.725	0.725	0.987	0.987	0.894
		70	1.76	0.711	0.711	0.620	0.620	0.871	0.871	0.793
G2	C7	33	2.35	0.898	0.898	0.772	0.772	0.990	0.990	0.894
		55	2.40	0.880	0.880	0.773	0.773	0.988	0.988	0.891
		70	2.43	0.870	0.870	0.770	0.770	0.985	0.985	0.889
	C8	33	3.14	0.898	0.898	0.779	0.779	0.992	0.992	0.896
		55	3.20	0.882	0.882	0.782	0.782	0.991	0.991	0.895
		70	3.20	0.882	0.882	0.788	0.788	1.000	1.000	0.902
	C9	33	3.92	0.898	0.898	0.785	0.785	0.993	0.993	0.897
		55	4.00	0.881	0.881	0.788	0.788	0.991	0.991	0.895
		70	4.05	0.870	0.870	0.785	0.785	0.988	0.988	0.892
G3	C7	33	5.99	0.959	0.959	0.785	0.785	0.996	0.996	0.906
		55	6.24	0.921	0.921	0.794	0.794	0.998	0.998	0.904
		70	6.32	0.909	0.909	0.800	0.800	0.998	0.998	0.903
	C8	33	7.99	0.959	0.959	0.785	0.785	0.995	0.995	0.906
		55	8.32	0.921	0.921	0.795	0.795	0.998	0.998	0.904
		70	8.43	0.909	0.909	0.801	0.801	0.998	0.998	0.903
	C9	33	9.99	0.959	0.959	0.784	0.784	0.995	0.995	0.906
		55	10.41	0.921	0.921	0.795	0.795	0.998	0.998	0.904
		70	10.54	0.909	0.909	0.801	0.801	0.998	0.998	0.903
G4	C7	33	12.77	1.074	1.074	0.812	0.812	0.986	0.986	0.935
		55	15.18	1.043	1.043	0.808	0.808	0.998	0.998	0.922
		70	15.92	0.996	0.996	0.799	0.799	1.000	1.000	0.917
	C8	33	17.03	1.074	1.074	0.812	0.812	0.984	0.984	0.933
		55	20.24	1.043	1.043	0.807	0.807	0.997	0.997	0.921
		70	21.22	0.996	0.996	0.798	0.798	1.000	1.000	0.916
	C9	33	21.28	1.074	1.074	0.811	0.811	0.983	0.983	0.932
		55	25.30	1.043	1.043	0.806	0.806	0.996	0.996	0.920
		70	26.53	0.996	0.996	0.798	0.798	0.999	0.999	0.916
G5	C7	33	14.03	1.074	1.074	0.821	0.821	0.980	0.980	0.941
		55	17.49	1.060	1.060	0.814	0.814	0.996	0.996	0.928
		70	18.61	1.029	1.029	0.809	0.809	1.000	1.000	0.922
	C8	33	18.70	1.074	1.074	0.820	0.820	0.979	0.979	0.940
		55	23.32	1.060	1.060	0.814	0.814	0.994	0.994	0.927
		70	24.82	1.029	1.029	0.808	0.808	0.999	0.999	0.921
	C9	33	23.38	1.074	1.074	0.819	0.819	0.978	0.978	0.939
		55	29.15	1.060	1.060	0.813	0.813	0.993	0.993	0.926
		70	31.03	1.029	1.029	0.808	0.808	0.998	0.998	0.921

**Table E.1 (Continued)**

Boundary Condition	Section	$F_y$	$P_{FEM}$	$\frac{P_{1a}}{P_{FEM}}$	$\frac{P_{1b}}{P_{FEM}}$	$\frac{P_{1c}}{P_{FEM}}$	$\frac{P_{1d}}{P_{FEM}}$	$\frac{P_{2a}}{P_{FEM}}$	$\frac{P_{2b}}{P_{FEM}}$	$\frac{P_{2c}}{P_{FEM}}$
		(ksi)	(kips)							
G6	C7	33	1.79	0.852	0.852	0.726	0.726	0.958	0.958	0.862
		55	1.79	0.852	0.852	0.731	0.731	0.975	0.975	0.878
		70	1.79	0.852	0.852	0.732	0.732	0.988	0.988	0.890
	C8	33	2.34	0.869	0.869	0.755	0.755	0.980	0.980	0.883
		55	2.52	0.807	0.807	0.706	0.706	0.931	0.931	0.839
		70	2.52	0.807	0.807	0.708	0.708	0.947	0.947	0.855
	C9	33	2.90	0.878	0.878	0.773	0.773	0.994	0.994	0.896
		55	3.05	0.835	0.835	0.741	0.741	0.969	0.969	0.875
		70	3.05	0.835	0.835	0.743	0.743	0.991	0.991	0.896
G7	C7	33	3.27	0.899	0.899	0.785	0.785	0.990	0.990	0.894
		55	3.33	0.883	0.883	0.790	0.790	0.991	0.991	0.894
		70	3.33	0.883	0.883	0.796	0.796	0.999	0.999	0.902
	C8	33	4.36	0.899	0.899	0.790	0.790	0.991	0.991	0.895
		55	4.45	0.881	0.881	0.794	0.794	0.990	0.990	0.893
		70	4.50	0.870	0.870	0.792	0.792	0.986	0.986	0.891
	C9	33	5.44	0.900	0.900	0.794	0.794	0.993	0.993	0.897
		55	5.56	0.881	0.881	0.798	0.798	0.991	0.991	0.894
		70	5.59	0.876	0.876	0.802	0.802	0.994	0.994	0.898
G8	C7	33	6.96	0.964	0.964	0.787	0.787	0.993	0.993	0.905
		55	7.27	0.923	0.923	0.795	0.795	0.997	0.997	0.903
		70	7.37	0.911	0.911	0.801	0.801	0.998	0.998	0.902
	C8	33	9.28	0.964	0.964	0.787	0.787	0.993	0.993	0.905
		55	9.69	0.923	0.923	0.795	0.795	0.997	0.997	0.903
		70	9.82	0.911	0.911	0.801	0.801	0.998	0.998	0.902
	C9	33	11.60	0.964	0.964	0.787	0.787	0.992	0.992	0.905
		55	12.12	0.923	0.923	0.796	0.796	0.997	0.997	0.903
		70	12.28	0.911	0.911	0.802	0.802	0.998	0.998	0.902
G9	C7	33	13.54	1.058	1.058	0.810	0.810	0.977	0.977	0.931
		55	16.33	1.044	1.044	0.809	0.809	0.994	0.994	0.920
		70	17.19	1.003	1.003	0.802	0.802	0.997	0.997	0.916
	C8	33	18.06	1.058	1.058	0.809	0.809	0.976	0.976	0.930
		55	21.77	1.044	1.044	0.808	0.808	0.993	0.993	0.920
		70	22.92	1.003	1.003	0.801	0.801	0.997	0.997	0.915
	C9	33	22.57	1.058	1.058	0.808	0.808	0.974	0.974	0.929
		55	27.22	1.044	1.044	0.808	0.808	0.992	0.992	0.919
		70	28.65	1.003	1.003	0.800	0.800	0.996	0.996	0.915
G10	C7	33	14.69	1.061	1.061	0.819	0.819	0.971	0.971	0.936
		55	18.61	1.054	1.054	0.813	0.813	0.989	0.989	0.926
		70	19.91	1.035	1.035	0.812	0.812	0.995	0.995	0.921
	C8	33	19.59	1.061	1.061	0.819	0.819	0.970	0.970	0.935
		55	24.82	1.054	1.054	0.813	0.813	0.988	0.988	0.925
		70	26.55	1.035	1.035	0.811	0.811	0.994	0.994	0.920
	C9	33	24.49	1.061	1.061	0.818	0.818	0.968	0.968	0.934
		55	31.02	1.054	1.054	0.812	0.812	0.987	0.987	0.924
		70	33.19	1.035	1.035	0.810	0.810	0.994	0.994	0.919

**Table E.1 (Continued)**

Boundary Condition	Section	$F_y$	$P_{FEM}$	$\frac{P_{1a}}{P_{FEM}}$	$\frac{P_{1b}}{P_{FEM}}$	$\frac{P_{1c}}{P_{FEM}}$	$\frac{P_{1d}}{P_{FEM}}$	$\frac{P_{2a}}{P_{FEM}}$	$\frac{P_{2b}}{P_{FEM}}$	$\frac{P_{2c}}{P_{FEM}}$
		(ksi)	(kips)							
G11	C7	33	4.92	0.902	0.902	0.797	0.797	0.989	0.989	0.894
		55	5.03	0.882	0.882	0.801	0.801	0.989	0.989	0.892
		70	5.08	0.873	0.873	0.801	0.801	0.987	0.987	0.891
	C8	33	6.53	0.906	0.906	0.803	0.803	0.995	0.995	0.899
		55	6.69	0.884	0.884	0.807	0.807	0.992	0.992	0.895
		70	6.78	0.872	0.872	0.804	0.804	0.987	0.987	0.891
	C9	33	8.20	0.902	0.902	0.801	0.801	0.991	0.991	0.896
		55	8.31	0.890	0.890	0.814	0.814	0.999	0.999	0.903
		70	8.43	0.877	0.877	0.810	0.810	0.993	0.993	0.897
G12	C7	33	8.70	0.973	0.973	0.791	0.791	0.986	0.986	0.902
		55	9.14	0.926	0.926	0.796	0.796	0.995	0.995	0.902
		70	9.27	0.913	0.913	0.802	0.802	0.996	0.996	0.902
	C8	33	11.60	0.973	0.973	0.791	0.791	0.985	0.985	0.902
		55	12.18	0.926	0.926	0.796	0.796	0.995	0.995	0.902
		70	12.36	0.913	0.913	0.802	0.802	0.996	0.996	0.902
	C9	33	14.50	0.973	0.973	0.791	0.791	0.985	0.985	0.901
		55	15.23	0.926	0.926	0.797	0.797	0.994	0.994	0.902
		70	15.45	0.913	0.913	0.802	0.802	0.996	0.996	0.902
G13	C7	33	14.85	1.031	1.031	0.805	0.805	0.959	0.959	0.922
		55	18.38	1.035	1.035	0.807	0.807	0.983	0.983	0.917
		70	19.50	1.017	1.017	0.807	0.807	0.990	0.990	0.914
	C8	33	19.80	1.031	1.031	0.804	0.804	0.958	0.958	0.921
		55	24.51	1.035	1.035	0.807	0.807	0.982	0.982	0.916
		70	26.00	1.017	1.017	0.806	0.806	0.990	0.990	0.913
	C9	33	24.75	1.031	1.031	0.803	0.803	0.957	0.957	0.920
		55	30.64	1.035	1.035	0.806	0.806	0.981	0.981	0.915
		70	32.50	1.017	1.017	0.806	0.806	0.989	0.989	0.912
G14	C7	33	15.80	1.038	1.038	0.816	0.816	0.953	0.953	0.926
		55	20.59	1.037	1.037	0.810	0.810	0.976	0.976	0.921
		70	22.26	1.032	1.032	0.812	0.812	0.985	0.985	0.917
	C8	33	21.07	1.038	1.038	0.816	0.816	0.952	0.952	0.925
		55	27.46	1.037	1.037	0.809	0.809	0.975	0.975	0.920
		70	29.68	1.032	1.032	0.811	0.811	0.985	0.985	0.916
	C9	33	26.34	1.038	1.038	0.815	0.815	0.951	0.951	0.924
		55	34.32	1.037	1.037	0.808	0.808	0.974	0.974	0.919
		70	37.10	1.032	1.032	0.810	0.810	0.984	0.984	0.915
G15	C7	33	13.06	0.942	0.942	0.782	0.782	0.963	0.963	0.894
		55	14.12	0.939	0.939	0.800	0.800	0.986	0.986	0.898
		70	14.39	0.921	0.921	0.803	0.803	0.990	0.990	0.898
	C8	33	17.41	0.942	0.942	0.781	0.781	0.963	0.963	0.894
		55	18.82	0.939	0.939	0.801	0.801	0.986	0.986	0.898
		70	19.18	0.922	0.922	0.804	0.804	0.991	0.991	0.899
	C9	33	21.77	0.942	0.942	0.781	0.781	0.962	0.962	0.894
		55	23.53	0.939	0.939	0.800	0.800	0.986	0.986	0.898
		70	23.98	0.921	0.921	0.803	0.803	0.990	0.990	0.899

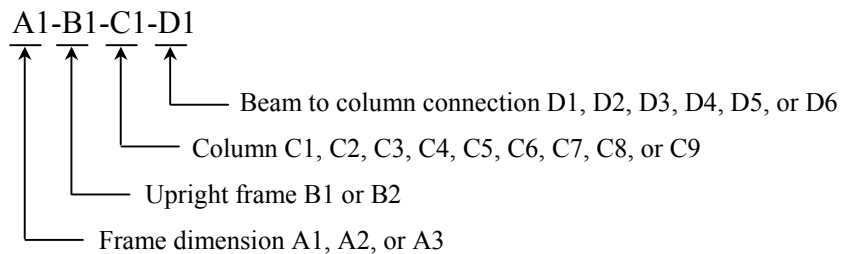
**Table E.1 (Continued)**

Boundary Condition	Section	$F_y$	$P_{FEM}$	$\frac{P_{1a}}{P_{FEM}}$	$\frac{P_{1b}}{P_{FEM}}$	$\frac{P_{1c}}{P_{FEM}}$	$\frac{P_{1d}}{P_{FEM}}$	$\frac{P_{2a}}{P_{FEM}}$	$\frac{P_{2b}}{P_{FEM}}$	$\frac{P_{2c}}{P_{FEM}}$
		(ksi)	(kips)							
G16	C7	33	17.69	0.976	0.976	0.795	0.795	0.911	0.917	0.891
		55	23.55	0.987	0.987	0.792	0.792	0.943	0.949	0.897
		70	25.64	0.998	0.998	0.800	0.800	0.960	0.965	0.900
	C8	33	23.59	0.976	0.976	0.794	0.794	0.910	0.916	0.890
		55	31.40	0.987	0.987	0.792	0.792	0.942	0.947	0.896
		70	34.18	0.998	0.998	0.800	0.800	0.959	0.964	0.899
	C9	33	29.49	0.976	0.976	0.793	0.793	0.909	0.915	0.889
		55	39.25	0.987	0.987	0.791	0.791	0.941	0.946	0.895
		70	42.73	0.998	0.998	0.799	0.799	0.958	0.963	0.898
G17	C7	33	18.22	0.993	0.993	0.811	0.811	0.907	0.946	0.893
		55	25.38	0.990	0.990	0.798	0.798	0.931	0.971	0.896
		70	28.33	0.997	0.997	0.800	0.800	0.946	0.984	0.898
	C8	33	24.29	0.993	0.993	0.810	0.810	0.906	0.945	0.892
		55	33.84	0.990	0.990	0.797	0.797	0.929	0.970	0.895
		70	37.77	0.997	0.997	0.799	0.799	0.945	0.983	0.897
	C9	33	30.36	0.993	0.993	0.809	0.809	0.905	0.944	0.891
		55	42.31	0.990	0.990	0.796	0.796	0.928	0.969	0.894
		70	47.21	0.997	0.997	0.799	0.799	0.944	0.982	0.896
G18	C7	33	20.58	0.981	0.981	0.854	0.854	0.889	0.984	0.884
		55	32.22	0.937	0.937	0.806	0.806	0.858	0.961	0.847
		70	38.73	0.921	0.921	0.786	0.786	0.847	0.956	0.831
	C8	33	27.44	0.981	0.981	0.854	0.854	0.889	0.984	0.883
		55	42.97	0.937	0.937	0.805	0.805	0.857	0.960	0.846
		70	51.64	0.921	0.921	0.785	0.785	0.847	0.956	0.831
	C9	33	34.30	0.981	0.981	0.853	0.853	0.888	0.983	0.883
		55	53.71	0.937	0.937	0.804	0.804	0.856	0.960	0.845
		70	64.55	0.921	0.921	0.785	0.785	0.846	0.956	0.830
G19	C7	33	20.82	0.995	0.995	0.863	0.863	0.879	0.994	0.875
		55	33.12	0.951	0.951	0.817	0.817	0.843	0.963	0.836
		70	40.43	0.932	0.932	0.796	0.796	0.827	0.950	0.816
	C8	33	27.76	0.995	0.995	0.862	0.862	0.878	0.994	0.875
		55	44.16	0.951	0.951	0.817	0.817	0.842	0.963	0.835
		70	53.91	0.932	0.932	0.795	0.795	0.826	0.950	0.816
	C9	33	34.71	0.995	0.995	0.861	0.861	0.878	0.994	0.874
		55	55.19	0.951	0.951	0.816	0.816	0.842	0.962	0.834
		70	67.38	0.932	0.932	0.795	0.795	0.825	0.950	0.815
G20	C7	33	20.97	1.011	1.011	0.888	0.888	0.888	1.010	0.885
		55	33.76	0.970	0.970	0.846	0.846	0.846	0.969	0.841
		70	41.79	0.947	0.947	0.822	0.822	0.822	0.946	0.815
	C8	33	27.96	1.011	1.011	0.887	0.887	0.887	1.010	0.884
		55	45.01	0.970	0.970	0.845	0.845	0.845	0.969	0.840
		70	55.73	0.947	0.947	0.821	0.821	0.821	0.946	0.814
	C9	33	34.95	1.011	1.011	0.886	0.886	0.886	1.010	0.884
		55	56.26	0.970	0.970	0.845	0.845	0.845	0.969	0.840
		70	69.66	0.947	0.947	0.820	0.820	0.820	0.946	0.814

**Table E.2** Load Case 1 - Correlation of Design Procedures with the FEM Results

Frame*	$K_x$	$F_y$	$W_{FEM}$	$\frac{W_{1a}}{W_{FEM}}$	$\frac{W_{1c}}{W_{FEM}}$	$\frac{W_{2a}}{W_{FEM}}$	$\frac{W_{2b}}{W_{FEM}}$	$\frac{W_{2c}}{W_{FEM}}$
		(ksi)	(kips)					
A1-B1-C1-D1	2.404	33	8.25	0.841	0.701	0.899	0.899	0.853
		55	9.08	0.811	0.707	0.960	0.960	0.884
		70	9.31	0.791	0.706	0.974	0.974	0.890
A1-B1-C1-D2	2.010	33	10.76	0.768	0.656	0.805	0.805	0.784
		55	12.48	0.782	0.682	0.901	0.901	0.850
		70	12.96	0.760	0.678	0.934	0.934	0.869
A1-B1-C1-D3	1.793	33	12.32	0.729	0.632	0.744	0.744	0.733
		55	15.05	0.744	0.654	0.833	0.833	0.802
		70	15.85	0.738	0.659	0.877	0.877	0.833
A1-B1-C1-D4	1.651	33	12.95	0.727	0.637	0.727	0.735	0.720
		55	16.99	0.714	0.632	0.775	0.783	0.757
		70	18.15	0.713	0.639	0.819	0.828	0.792
A1-B1-C1-D5	1.550	33	12.83	0.757	0.669	0.746	0.768	0.740
		55	18.51	0.691	0.615	0.732	0.754	0.719
		70	20.01	0.692	0.622	0.771	0.793	0.752
A1-B1-C1-D6	1.473	33	12.96	0.767	0.681	0.747	0.778	0.742
		55	19.54	0.679	0.608	0.705	0.735	0.696
		70	21.54	0.675	0.608	0.732	0.763	0.719
A1-B1-C2-D1	2.571	33	9.84	0.867	0.716	0.926	0.926	0.868
		55	10.68	0.822	0.716	0.972	0.972	0.891
		70	10.91	0.804	0.717	0.981	0.981	0.894
A1-B1-C2-D2	2.179	33	12.80	0.803	0.678	0.851	0.851	0.820
		55	14.44	0.801	0.697	0.936	0.936	0.871
		70	14.88	0.777	0.693	0.959	0.959	0.883
A1-B1-C2-D3	1.952	33	14.89	0.758	0.650	0.789	0.789	0.770
		55	17.46	0.776	0.678	0.887	0.887	0.841
		70	18.18	0.757	0.675	0.924	0.924	0.863
A1-B1-C2-D4	1.800	33	16.35	0.731	0.633	0.747	0.747	0.735
		55	19.90	0.748	0.657	0.837	0.837	0.806
		70	20.95	0.742	0.661	0.881	0.881	0.836
A1-B1-C2-D5	1.689	33	16.81	0.738	0.645	0.742	0.744	0.733
		55	21.89	0.725	0.640	0.793	0.795	0.771
		70	23.28	0.724	0.647	0.838	0.840	0.806
A1-B1-C2-D6	1.604	33	17.11	0.745	0.655	0.740	0.754	0.733
		55	23.52	0.706	0.626	0.757	0.772	0.742
		70	25.26	0.707	0.633	0.800	0.815	0.776

\*Frames are name as:



**Table E.2 (Continued)**

Frame	$K_x$	$F_y$	$W_{FEM}$	$\frac{W_{1a}}{W_{FEM}}$	$\frac{W_{1c}}{W_{FEM}}$	$\frac{W_{2a}}{W_{FEM}}$	$\frac{W_{2b}}{W_{FEM}}$	$\frac{W_{2c}}{W_{FEM}}$
		(ksi)	(kips)					
A1-B1-C3-D1	2.696	33	11.33	0.882	0.724	0.940	0.940	0.877
		55	12.20	0.829	0.722	0.977	0.977	0.893
		70	12.45	0.812	0.724	0.984	0.984	0.896
A1-B1-C3-D2	2.314	33	14.59	0.830	0.694	0.883	0.883	0.842
		55	16.18	0.811	0.706	0.954	0.954	0.882
		70	16.62	0.790	0.704	0.971	0.971	0.889
A1-B1-C3-D3	2.082	33	17.07	0.786	0.667	0.827	0.827	0.801
		55	19.53	0.796	0.692	0.919	0.919	0.862
		70	20.20	0.771	0.687	0.948	0.948	0.877
A1-B1-C3-D4	1.924	33	18.94	0.754	0.647	0.781	0.781	0.764
		55	22.33	0.774	0.675	0.880	0.880	0.836
		70	23.30	0.757	0.674	0.918	0.918	0.860
A1-B1-C3-D5	1.807	33	20.29	0.735	0.636	0.751	0.751	0.738
		55	24.69	0.752	0.659	0.840	0.840	0.809
		70	25.98	0.745	0.664	0.884	0.884	0.838
A1-B1-C3-D6	1.716	33	20.89	0.737	0.642	0.743	0.743	0.733
		55	26.70	0.733	0.646	0.805	0.805	0.782
		70	28.32	0.731	0.653	0.851	0.851	0.815
A1-B1-C4-D1	2.161	33	6.54	0.833	0.690	0.864	0.864	0.825
		55	7.27	0.821	0.707	0.939	0.939	0.870
		70	7.46	0.800	0.706	0.959	0.959	0.881
A1-B1-C4-D2	1.780	33	8.57	0.753	0.641	0.757	0.757	0.741
		55	10.17	0.778	0.672	0.852	0.852	0.813
		70	10.63	0.766	0.675	0.892	0.892	0.840
A1-B1-C4-D3	1.585	33	9.55	0.727	0.628	0.711	0.729	0.702
		55	12.18	0.733	0.640	0.773	0.792	0.753
		70	12.96	0.735	0.649	0.816	0.836	0.786
A1-B1-C4-D4	1.461	33	9.52	0.760	0.663	0.729	0.766	0.723
		55	13.61	0.702	0.618	0.718	0.754	0.705
		70	14.72	0.706	0.627	0.754	0.792	0.736
A1-B1-C4-D5	1.374	33	9.68	0.766	0.674	0.727	0.773	0.722
		55	14.54	0.686	0.608	0.686	0.730	0.677
		70	16.06	0.684	0.610	0.709	0.755	0.697
A1-B1-C4-D6	1.309	33	9.86	0.766	0.678	0.720	0.773	0.716
		55	15.14	0.680	0.605	0.667	0.717	0.660
		70	17.04	0.670	0.600	0.679	0.729	0.670

**Table E.2 (Continued)**

Frame	$K_x$	$F_y$	$W_{FEM}$	$\frac{W_{1a}}{W_{FEM}}$	$\frac{W_{1c}}{W_{FEM}}$	$\frac{W_{2a}}{W_{FEM}}$	$\frac{W_{2b}}{W_{FEM}}$	$\frac{W_{2c}}{W_{FEM}}$
		(ksi)	(kips)					
A1-B1-C5-D1	2.335	33	7.70	0.867	0.710	0.900	0.900	0.851
		55	8.40	0.834	0.718	0.958	0.958	0.881
		70	8.59	0.815	0.719	0.972	0.972	0.888
A1-B1-C5-D2	1.940	33	10.23	0.790	0.663	0.806	0.806	0.782
		55	11.73	0.809	0.695	0.900	0.900	0.847
		70	12.14	0.787	0.692	0.933	0.933	0.865
A1-B1-C5-D3	1.728	33	11.83	0.744	0.636	0.742	0.742	0.729
		55	14.21	0.771	0.667	0.835	0.835	0.802
		70	14.92	0.766	0.674	0.877	0.877	0.830
A1-B1-C5-D4	1.592	33	12.40	0.746	0.645	0.730	0.748	0.721
		55	16.12	0.739	0.644	0.778	0.797	0.757
		70	17.13	0.742	0.654	0.822	0.841	0.791
A1-B1-C5-D5	1.495	33	12.49	0.765	0.666	0.738	0.770	0.731
		55	17.58	0.715	0.627	0.736	0.769	0.721
		70	18.92	0.719	0.637	0.775	0.809	0.754
A1-B1-C5-D6	1.422	33	12.90	0.758	0.663	0.723	0.764	0.717
		55	18.70	0.698	0.615	0.706	0.747	0.695
		70	20.37	0.701	0.623	0.738	0.781	0.722
A1-B1-C6-D1	2.471	33	8.75	0.888	0.721	0.921	0.921	0.862
		55	9.44	0.843	0.726	0.968	0.968	0.886
		70	9.63	0.826	0.728	0.978	0.978	0.891
A1-B1-C6-D2	2.072	33	11.63	0.820	0.681	0.844	0.844	0.811
		55	13.05	0.826	0.707	0.929	0.929	0.865
		70	13.43	0.802	0.705	0.953	0.953	0.877
A1-B1-C6-D3	1.849	33	13.63	0.772	0.652	0.780	0.780	0.761
		55	15.89	0.799	0.687	0.878	0.878	0.832
		70	16.53	0.784	0.688	0.915	0.915	0.855
A1-B1-C6-D4	1.704	33	15.01	0.742	0.634	0.737	0.737	0.724
		55	18.16	0.770	0.666	0.828	0.828	0.796
		70	19.09	0.768	0.674	0.871	0.871	0.826
A1-B1-C6-D5	1.599	33	15.67	0.738	0.637	0.723	0.739	0.713
		55	19.99	0.745	0.648	0.785	0.803	0.762
		70	21.22	0.749	0.659	0.829	0.847	0.796
A1-B1-C6-D6	1.520	33	16.36	0.727	0.631	0.703	0.730	0.696
		55	21.47	0.725	0.634	0.750	0.780	0.734
		70	23.03	0.731	0.645	0.792	0.823	0.767



**Table E.2 (Continued)**

Frame	$K_x$	$F_y$	$W_{FEM}$	$\frac{W_{1a}}{W_{FEM}}$	$\frac{W_{1c}}{W_{FEM}}$	$\frac{W_{2a}}{W_{FEM}}$	$\frac{W_{2b}}{W_{FEM}}$	$\frac{W_{2c}}{W_{FEM}}$
		(ksi)	(kips)					
A1-B1-C7-D1	2.431	33	8.54	0.956	0.750	0.936	0.936	0.874
		55	9.25	0.948	0.774	0.978	0.978	0.894
		70	9.45	0.928	0.779	0.986	0.986	0.896
A1-B1-C7-D2	2.032	33	11.33	0.879	0.712	0.871	0.871	0.834
		55	12.84	0.949	0.768	0.952	0.952	0.880
		70	13.24	0.947	0.780	0.972	0.972	0.890
A1-B1-C7-D3	1.813	33	13.23	0.828	0.684	0.813	0.813	0.791
		55	15.63	0.913	0.748	0.917	0.917	0.862
		70	16.31	0.941	0.773	0.949	0.949	0.879
A1-B1-C7-D4	1.670	33	14.34	0.808	0.678	0.784	0.790	0.769
		55	17.82	0.879	0.728	0.879	0.886	0.838
		70	18.82	0.919	0.759	0.924	0.929	0.864
A1-B1-C7-D5	1.568	33	14.85	0.809	0.686	0.777	0.802	0.766
		55	19.56	0.852	0.712	0.846	0.874	0.814
		70	20.89	0.896	0.745	0.896	0.923	0.848
A1-B1-C7-D6	1.490	33	14.89	0.829	0.707	0.787	0.826	0.778
		55	20.97	0.831	0.700	0.816	0.860	0.792
		70	22.63	0.875	0.732	0.869	0.914	0.830
A1-B1-C8-D1	2.606	33	10.13	0.977	0.759	0.953	0.953	0.883
		55	10.87	0.942	0.771	0.983	0.983	0.896
		70	11.08	0.924	0.778	0.989	0.989	0.898
A1-B1-C8-D2	2.209	33	13.35	0.917	0.730	0.905	0.905	0.857
		55	14.77	0.960	0.775	0.968	0.968	0.889
		70	15.16	0.938	0.778	0.981	0.981	0.895
A1-B1-C8-D3	1.978	33	15.75	0.866	0.704	0.856	0.856	0.824
		55	18.01	0.943	0.763	0.945	0.945	0.877
		70	18.61	0.951	0.779	0.968	0.968	0.889
A1-B1-C8-D4	1.824	33	17.55	0.830	0.684	0.815	0.815	0.792
		55	20.67	0.916	0.747	0.919	0.919	0.863
		70	21.57	0.943	0.772	0.950	0.950	0.880
A1-B1-C8-D5	1.713	33	18.75	0.811	0.677	0.790	0.790	0.773
		55	22.90	0.890	0.733	0.891	0.891	0.845
		70	24.10	0.927	0.762	0.932	0.932	0.869
A1-B1-C8-D6	1.627	33	19.50	0.805	0.678	0.777	0.791	0.764
		55	24.78	0.868	0.719	0.864	0.880	0.828
		70	26.29	0.910	0.751	0.912	0.926	0.858

**Table E.2 (Continued)**

Frame	$K_x$	$F_y$	$W_{FEM}$	$\frac{W_{1a}}{W_{FEM}}$	$\frac{W_{1c}}{W_{FEM}}$	$\frac{W_{2a}}{W_{FEM}}$	$\frac{W_{2b}}{W_{FEM}}$	$\frac{W_{2c}}{W_{FEM}}$
		(ksi)	(kips)					
A1-B1-C9-D1	2.739	33	11.63	0.987	0.762	0.961	0.961	0.889
		55	12.41	0.938	0.769	0.986	0.986	0.898
		70	12.63	0.921	0.775	0.991	0.991	0.899
A1-B1-C9-D2	2.351	33	15.14	0.943	0.741	0.926	0.926	0.869
		55	16.52	0.955	0.772	0.975	0.975	0.893
		70	16.90	0.933	0.776	0.986	0.986	0.897
A1-B1-C9-D3	2.115	33	17.90	0.896	0.718	0.886	0.886	0.844
		55	20.05	0.957	0.770	0.960	0.960	0.885
		70	20.61	0.944	0.776	0.977	0.977	0.893
A1-B1-C9-D4	1.954	33	20.06	0.860	0.700	0.849	0.849	0.819
		55	23.06	0.939	0.759	0.940	0.940	0.875
		70	23.87	0.952	0.777	0.965	0.965	0.887
A1-B1-C9-D5	1.836	33	21.75	0.834	0.686	0.819	0.819	0.796
		55	25.65	0.918	0.747	0.920	0.920	0.863
		70	26.75	0.945	0.771	0.951	0.951	0.880
A1-B1-C9-D6	1.744	33	23.00	0.818	0.679	0.798	0.798	0.780
		55	27.89	0.897	0.735	0.898	0.898	0.850
		70	29.28	0.933	0.763	0.937	0.937	0.872
A1-B2-C1-D1	2.404	33	8.26	0.787	0.669	0.874	0.874	0.832
		55	9.09	0.739	0.659	0.939	0.939	0.869
		70	9.33	0.720	0.656	0.955	0.955	0.878
A1-B2-C1-D2	2.010	33	10.73	0.719	0.624	0.769	0.769	0.752
		55	12.48	0.697	0.623	0.856	0.856	0.816
		70	12.96	0.671	0.613	0.890	0.890	0.839
A1-B2-C1-D3	1.793	33	12.24	0.684	0.601	0.708	0.708	0.699
		55	15.01	0.664	0.597	0.773	0.773	0.753
		70	15.83	0.637	0.583	0.808	0.808	0.780
A1-B2-C1-D4	1.651	33	12.92	0.679	0.602	0.687	0.693	0.681
		55	16.86	0.639	0.577	0.714	0.721	0.702
		70	18.09	0.615	0.564	0.740	0.747	0.725
A1-B2-C1-D5	1.550	33	12.93	0.699	0.624	0.696	0.714	0.691
		55	18.32	0.619	0.562	0.671	0.688	0.663
		70	19.86	0.599	0.551	0.691	0.707	0.680
A1-B2-C1-D6	1.473	33	13.35	0.693	0.621	0.681	0.706	0.677
		55	19.66	0.598	0.545	0.633	0.656	0.628
		70	21.22	0.587	0.541	0.656	0.678	0.648

**Table E.2 (Continued)**

Frame	$K_x$	$F_y$	$W_{FEM}$	$\frac{W_{1a}}{W_{FEM}}$	$\frac{W_{1c}}{W_{FEM}}$	$\frac{W_{2a}}{W_{FEM}}$	$\frac{W_{2b}}{W_{FEM}}$	$\frac{W_{2c}}{W_{FEM}}$
		(ksi)	(kips)					
A1-B2-C2-D1	2.571	33	9.85	0.813	0.685	0.905	0.905	0.854
		55	10.70	0.757	0.673	0.956	0.956	0.880
		70	10.94	0.741	0.673	0.967	0.967	0.884
A1-B2-C2-D2	2.179	33	12.79	0.753	0.646	0.820	0.820	0.793
		55	14.44	0.720	0.642	0.905	0.905	0.850
		70	14.90	0.698	0.636	0.931	0.931	0.865
A1-B2-C2-D3	1.952	33	14.84	0.711	0.618	0.754	0.754	0.739
		55	17.45	0.694	0.621	0.839	0.839	0.805
		70	18.18	0.666	0.609	0.875	0.875	0.829
A1-B2-C2-D4	1.800	33	16.24	0.687	0.603	0.712	0.712	0.702
		55	19.85	0.669	0.601	0.780	0.780	0.758
		70	20.93	0.643	0.588	0.815	0.815	0.786
A1-B2-C2-D5	1.689	33	16.97	0.683	0.604	0.694	0.696	0.687
		55	21.77	0.650	0.585	0.733	0.735	0.719
		70	23.22	0.625	0.573	0.763	0.765	0.744
A1-B2-C2-D6	1.604	33	17.24	0.690	0.613	0.692	0.704	0.687
		55	23.32	0.634	0.573	0.698	0.710	0.688
		70	25.13	0.613	0.562	0.722	0.733	0.708
A1-B2-C3-D1	2.696	33	11.34	0.829	0.695	0.923	0.923	0.865
		55	12.23	0.771	0.684	0.965	0.965	0.884
		70	12.48	0.755	0.685	0.974	0.974	0.888
A1-B2-C3-D2	2.314	33	14.59	0.779	0.663	0.856	0.856	0.821
		55	16.19	0.738	0.657	0.931	0.931	0.866
		70	16.64	0.718	0.653	0.951	0.951	0.876
A1-B2-C3-D3	2.082	33	17.03	0.738	0.636	0.794	0.794	0.773
		55	19.53	0.714	0.637	0.882	0.882	0.836
		70	20.20	0.690	0.628	0.914	0.914	0.855
A1-B2-C3-D4	1.924	33	18.87	0.709	0.617	0.747	0.747	0.733
		55	22.31	0.695	0.621	0.831	0.831	0.799
		70	23.29	0.667	0.609	0.868	0.868	0.825
A1-B2-C3-D5	1.807	33	20.19	0.692	0.606	0.716	0.716	0.706
		55	24.64	0.675	0.605	0.786	0.786	0.764
		70	25.95	0.649	0.593	0.822	0.822	0.791
A1-B2-C3-D6	1.716	33	20.96	0.687	0.606	0.701	0.701	0.693
		55	26.58	0.659	0.592	0.748	0.748	0.732
		70	28.26	0.635	0.581	0.781	0.781	0.759

**Table E.2 (Continued)**

Frame	$K_x$	$F_y$	$W_{FEM}$	$\frac{W_{1a}}{W_{FEM}}$	$\frac{W_{1c}}{W_{FEM}}$	$\frac{W_{2a}}{W_{FEM}}$	$\frac{W_{2b}}{W_{FEM}}$	$\frac{W_{2c}}{W_{FEM}}$
		(ksi)	(kips)					
A1-B2-C4-D1	2.161	33	6.54	0.785	0.660	0.835	0.835	0.802
		55	7.28	0.749	0.657	0.907	0.907	0.848
		70	7.48	0.728	0.652	0.926	0.926	0.858
A1-B2-C4-D2	1.780	33	8.54	0.708	0.611	0.720	0.720	0.708
		55	10.17	0.698	0.616	0.792	0.792	0.766
		70	10.63	0.672	0.604	0.823	0.823	0.788
A1-B2-C4-D3	1.585	33	9.40	0.690	0.604	0.680	0.696	0.673
		55	12.11	0.659	0.586	0.709	0.725	0.695
		70	12.94	0.637	0.575	0.731	0.747	0.714
A1-B2-C4-D4	1.461	33	9.74	0.692	0.611	0.670	0.700	0.665
		55	13.51	0.630	0.564	0.653	0.682	0.645
		70	14.61	0.613	0.555	0.668	0.697	0.658
A1-B2-C4-D5	1.374	33	9.77	0.707	0.629	0.676	0.715	0.672
		55	14.56	0.609	0.548	0.616	0.651	0.610
		70	15.92	0.593	0.538	0.625	0.659	0.618
A1-B2-C4-D6	1.309	33	9.78	0.719	0.642	0.680	0.726	0.677
		55	14.90	0.612	0.553	0.608	0.647	0.603
		70	17.06	0.574	0.522	0.589	0.626	0.584
A1-B2-C5-D1	2.335	33	7.71	0.820	0.682	0.878	0.878	0.832
		55	8.41	0.773	0.677	0.937	0.937	0.867
		70	8.61	0.755	0.675	0.949	0.949	0.871
A1-B2-C5-D2	1.940	33	10.21	0.746	0.635	0.773	0.773	0.754
		55	11.73	0.733	0.643	0.858	0.858	0.815
		70	12.14	0.708	0.634	0.887	0.887	0.833
A1-B2-C5-D3	1.728	33	11.79	0.703	0.608	0.707	0.707	0.697
		55	14.20	0.697	0.615	0.778	0.778	0.754
		70	14.91	0.673	0.604	0.809	0.809	0.778
A1-B2-C5-D4	1.592	33	12.57	0.691	0.604	0.681	0.697	0.674
		55	16.06	0.667	0.592	0.718	0.734	0.704
		70	17.11	0.649	0.584	0.743	0.759	0.724
A1-B2-C5-D5	1.495	33	12.98	0.690	0.608	0.671	0.698	0.665
		55	17.51	0.644	0.575	0.674	0.701	0.664
		70	18.84	0.630	0.568	0.694	0.721	0.682
A1-B2-C5-D6	1.422	33	13.02	0.703	0.622	0.675	0.710	0.671
		55	18.72	0.625	0.560	0.640	0.673	0.633
		70	20.28	0.613	0.554	0.656	0.689	0.647

**Table E.2 (Continued)**

Frame	$K_x$	$F_y$	$W_{FEM}$	$\frac{W_{1a}}{W_{FEM}}$	$\frac{W_{1c}}{W_{FEM}}$	$\frac{W_{2a}}{W_{FEM}}$	$\frac{W_{2b}}{W_{FEM}}$	$\frac{W_{2c}}{W_{FEM}}$
		(ksi)	(kips)					
A1-B2-C6-D1	2.471	33	8.75	0.844	0.697	0.904	0.904	0.850
		55	9.46	0.792	0.691	0.952	0.952	0.875
		70	9.66	0.775	0.691	0.961	0.961	0.879
A1-B2-C6-D2	2.072	33	11.62	0.779	0.656	0.816	0.816	0.788
		55	13.05	0.757	0.662	0.899	0.899	0.844
		70	13.44	0.735	0.656	0.922	0.922	0.856
A1-B2-C6-D3	1.849	33	13.60	0.732	0.627	0.748	0.748	0.733
		55	15.89	0.730	0.640	0.833	0.833	0.798
		70	16.53	0.704	0.630	0.866	0.866	0.819
A1-B2-C6-D4	1.704	33	14.97	0.703	0.608	0.704	0.704	0.694
		55	18.14	0.702	0.618	0.775	0.775	0.752
		70	19.09	0.681	0.609	0.808	0.808	0.777
A1-B2-C6-D5	1.599	33	15.54	0.703	0.613	0.693	0.707	0.685
		55	19.96	0.678	0.600	0.728	0.744	0.713
		70	21.21	0.663	0.594	0.757	0.773	0.736
A1-B2-C6-D6	1.520	33	15.64	0.716	0.628	0.698	0.723	0.691
		55	21.46	0.658	0.585	0.692	0.716	0.680
		70	22.99	0.646	0.581	0.717	0.742	0.701
A1-B2-C7-D1	2.431	33	8.57	0.953	0.748	0.933	0.933	0.871
		55	9.30	0.943	0.771	0.973	0.973	0.890
		70	9.50	0.923	0.775	0.981	0.981	0.892
A1-B2-C7-D2	2.032	33	11.35	0.878	0.711	0.869	0.869	0.833
		55	12.88	0.946	0.766	0.949	0.949	0.878
		70	13.28	0.944	0.778	0.968	0.968	0.888
A1-B2-C7-D3	1.813	33	13.24	0.827	0.684	0.813	0.813	0.791
		55	15.66	0.912	0.746	0.915	0.915	0.860
		70	16.36	0.939	0.771	0.947	0.947	0.877
A1-B2-C7-D4	1.670	33	14.37	0.806	0.676	0.782	0.788	0.767
		55	17.86	0.877	0.726	0.878	0.884	0.836
		70	18.86	0.917	0.757	0.922	0.927	0.862
A1-B2-C7-D5	1.568	33	14.93	0.805	0.682	0.772	0.797	0.762
		55	19.59	0.851	0.711	0.844	0.872	0.813
		70	20.94	0.894	0.743	0.894	0.921	0.846
A1-B2-C7-D6	1.490	33	15.20	0.812	0.693	0.772	0.810	0.763
		55	21.00	0.829	0.699	0.815	0.859	0.791
		70	22.68	0.873	0.731	0.867	0.912	0.828

**Table E.2 (Continued)**

Frame	$K_x$	$F_y$	$W_{FEM}$	$\frac{W_{1a}}{W_{FEM}}$	$\frac{W_{1c}}{W_{FEM}}$	$\frac{W_{2a}}{W_{FEM}}$	$\frac{W_{2b}}{W_{FEM}}$	$\frac{W_{2c}}{W_{FEM}}$
		(ksi)	(kips)					
A1-B2-C8-D1	2.606	33	10.17	0.974	0.756	0.950	0.950	0.880
		55	10.91	0.938	0.768	0.979	0.979	0.893
		70	11.13	0.920	0.774	0.985	0.985	0.894
A1-B2-C8-D2	2.209	33	13.38	0.915	0.729	0.904	0.904	0.855
		55	14.81	0.958	0.773	0.965	0.965	0.887
		70	15.20	0.936	0.776	0.978	0.978	0.893
A1-B2-C8-D3	1.978	33	15.77	0.865	0.703	0.855	0.855	0.823
		55	18.04	0.941	0.762	0.943	0.943	0.875
		70	18.66	0.949	0.778	0.965	0.965	0.887
A1-B2-C8-D4	1.824	33	17.56	0.829	0.684	0.814	0.814	0.792
		55	20.71	0.914	0.746	0.917	0.917	0.861
		70	21.61	0.941	0.771	0.949	0.949	0.878
A1-B2-C8-D5	1.713	33	18.87	0.806	0.673	0.785	0.785	0.769
		55	22.94	0.888	0.731	0.889	0.889	0.844
		70	24.14	0.926	0.761	0.930	0.930	0.868
A1-B2-C8-D6	1.627	33	19.31	0.813	0.684	0.785	0.799	0.772
		55	24.81	0.866	0.719	0.863	0.879	0.827
		70	26.33	0.908	0.750	0.910	0.925	0.856
A1-B2-C9-D1	2.739	33	11.67	0.984	0.759	0.958	0.958	0.885
		55	12.45	0.935	0.766	0.982	0.982	0.895
		70	12.68	0.918	0.772	0.987	0.987	0.896
A1-B2-C9-D2	2.351	33	15.17	0.942	0.740	0.924	0.924	0.868
		55	16.56	0.952	0.770	0.973	0.973	0.891
		70	16.94	0.931	0.774	0.983	0.983	0.895
A1-B2-C9-D3	2.115	33	17.92	0.895	0.717	0.885	0.885	0.843
		55	20.08	0.955	0.769	0.958	0.958	0.883
		70	20.65	0.942	0.775	0.975	0.975	0.892
A1-B2-C9-D4	1.954	33	20.07	0.860	0.699	0.849	0.849	0.818
		55	23.10	0.938	0.758	0.939	0.939	0.874
		70	23.91	0.950	0.776	0.963	0.963	0.886
A1-B2-C9-D5	1.836	33	21.76	0.834	0.686	0.819	0.819	0.796
		55	25.68	0.917	0.746	0.918	0.918	0.862
		70	26.79	0.943	0.770	0.950	0.950	0.879
A1-B2-C9-D6	1.744	33	23.01	0.818	0.679	0.797	0.797	0.779
		55	27.92	0.896	0.734	0.897	0.897	0.849
		70	29.33	0.931	0.762	0.936	0.936	0.871

**Table E.2 (Continued)**

Frame	$K_x$	$F_y$	$W_{FEM}$	$\frac{W_{1a}}{W_{FEM}}$	$\frac{W_{1c}}{W_{FEM}}$	$\frac{W_{2a}}{W_{FEM}}$	$\frac{W_{2b}}{W_{FEM}}$	$\frac{W_{2c}}{W_{FEM}}$
		(ksi)	(kips)					
A2-B1-C1-D1	2.561	33	7.17	0.896	0.728	0.938	0.938	0.882
		55	7.97	0.830	0.715	0.972	0.972	0.893
		70	8.18	0.809	0.714	0.980	0.980	0.894
A2-B1-C1-D2	2.119	33	9.30	0.850	0.707	0.877	0.877	0.848
		55	11.09	0.817	0.701	0.931	0.931	0.873
		70	11.57	0.783	0.689	0.952	0.952	0.881
A2-B1-C1-D3	1.885	33	10.53	0.824	0.697	0.832	0.832	0.815
		55	13.32	0.794	0.685	0.881	0.881	0.842
		70	14.15	0.767	0.675	0.910	0.910	0.858
A2-B1-C1-D4	1.736	33	11.27	0.812	0.696	0.806	0.806	0.794
		55	14.90	0.776	0.673	0.840	0.840	0.814
		70	16.15	0.755	0.665	0.867	0.867	0.829
A2-B1-C1-D5	1.631	33	11.73	0.808	0.697	0.790	0.802	0.782
		55	16.03	0.764	0.667	0.809	0.822	0.790
		70	17.71	0.741	0.655	0.829	0.841	0.801
A2-B1-C1-D6	1.552	33	11.90	0.816	0.709	0.790	0.815	0.783
		55	16.86	0.758	0.664	0.787	0.813	0.773
		70	18.93	0.731	0.648	0.798	0.824	0.778
A2-B1-C2-D1	2.755	33	8.49	0.910	0.735	0.955	0.955	0.890
		55	9.28	0.839	0.723	0.979	0.979	0.896
		70	9.48	0.820	0.725	0.986	0.986	0.897
A2-B1-C2-D2	2.305	33	11.15	0.871	0.716	0.907	0.907	0.866
		55	12.80	0.824	0.707	0.955	0.955	0.885
		70	13.24	0.797	0.702	0.970	0.970	0.890
A2-B1-C2-D3	2.056	33	12.83	0.844	0.705	0.866	0.866	0.840
		55	15.52	0.814	0.698	0.921	0.921	0.867
		70	16.25	0.781	0.687	0.944	0.944	0.877
A2-B1-C2-D4	1.893	33	13.97	0.826	0.699	0.834	0.834	0.817
		55	17.63	0.797	0.687	0.884	0.884	0.844
		70	18.71	0.770	0.678	0.914	0.914	0.860
A2-B1-C2-D5	1.777	33	14.75	0.816	0.697	0.813	0.813	0.800
		55	19.27	0.783	0.678	0.852	0.852	0.823
		70	20.75	0.762	0.670	0.881	0.881	0.839
A2-B1-C2-D6	1.688	33	15.31	0.811	0.697	0.799	0.801	0.789
		55	20.54	0.773	0.672	0.827	0.829	0.804
		70	22.44	0.751	0.662	0.851	0.853	0.818

**Table E.2 (Continued)**

Frame	$K_x$	$F_y$	$W_{FEM}$	$\frac{W_{1a}}{W_{FEM}}$	$\frac{W_{1c}}{W_{FEM}}$	$\frac{W_{2a}}{W_{FEM}}$	$\frac{W_{2b}}{W_{FEM}}$	$\frac{W_{2c}}{W_{FEM}}$
		(ksi)	(kips)					
A2-B1-C3-D1	2.904	33	9.72	0.913	0.737	0.963	0.963	0.893
		55	10.50	0.845	0.728	0.983	0.983	0.897
		70	10.72	0.828	0.732	0.988	0.988	0.898
A2-B1-C3-D2	2.456	33	12.73	0.888	0.724	0.927	0.927	0.876
		55	14.29	0.831	0.714	0.967	0.967	0.891
		70	14.70	0.808	0.712	0.978	0.978	0.894
A2-B1-C3-D3	2.198	33	14.82	0.861	0.712	0.890	0.890	0.856
		55	17.35	0.823	0.705	0.944	0.944	0.879
		70	18.02	0.793	0.697	0.962	0.962	0.887
A2-B1-C3-D4	2.026	33	16.30	0.842	0.704	0.860	0.860	0.836
		55	19.85	0.814	0.698	0.915	0.915	0.864
		70	20.83	0.782	0.687	0.941	0.941	0.876
A2-B1-C3-D5	1.901	33	17.39	0.828	0.699	0.836	0.836	0.818
		55	21.89	0.801	0.688	0.887	0.887	0.846
		70	23.21	0.774	0.680	0.916	0.916	0.862
A2-B1-C3-D6	1.805	33	18.20	0.820	0.698	0.819	0.819	0.805
		55	23.56	0.789	0.681	0.861	0.861	0.829
		70	25.26	0.768	0.674	0.891	0.891	0.846
A2-B1-C4-D1	2.285	33	5.73	0.894	0.721	0.908	0.908	0.860
		55	6.44	0.844	0.716	0.956	0.956	0.882
		70	6.63	0.819	0.714	0.968	0.968	0.887
A2-B1-C4-D2	1.872	33	7.36	0.844	0.700	0.836	0.836	0.815
		55	9.03	0.823	0.696	0.891	0.891	0.844
		70	9.50	0.793	0.689	0.918	0.918	0.860
A2-B1-C4-D3	1.667	33	8.20	0.822	0.693	0.795	0.802	0.782
		55	10.69	0.795	0.679	0.833	0.840	0.805
		70	11.52	0.776	0.674	0.860	0.867	0.822
A2-B1-C4-D4	1.539	33	8.61	0.818	0.698	0.779	0.808	0.770
		55	11.75	0.779	0.671	0.794	0.825	0.776
		70	12.98	0.758	0.661	0.812	0.842	0.786
A2-B1-C4-D5	1.451	33	8.81	0.823	0.707	0.774	0.818	0.767
		55	12.47	0.770	0.668	0.769	0.814	0.755
		70	14.03	0.745	0.652	0.777	0.821	0.758
A2-B1-C4-D6	1.386	33	8.92	0.829	0.716	0.773	0.827	0.767
		55	12.97	0.765	0.666	0.752	0.805	0.741
		70	14.81	0.736	0.647	0.752	0.804	0.737



**Table E.2 (Continued)**

Frame	$K_x$	$F_y$	$W_{FEM}$	$\frac{W_{1a}}{W_{FEM}}$	$\frac{W_{1c}}{W_{FEM}}$	$\frac{W_{2a}}{W_{FEM}}$	$\frac{W_{2b}}{W_{FEM}}$	$\frac{W_{2c}}{W_{FEM}}$
		(ksi)	(kips)					
A2-B1-C5-D1	2.479	33	6.73	0.916	0.732	0.933	0.933	0.875
		55	7.39	0.853	0.725	0.969	0.969	0.890
		70	7.58	0.832	0.726	0.978	0.978	0.892
A2-B1-C5-D2	2.043	33	8.88	0.868	0.709	0.870	0.870	0.838
		55	10.43	0.841	0.710	0.927	0.927	0.867
		70	10.85	0.809	0.702	0.948	0.948	0.877
A2-B1-C5-D3	1.817	33	10.11	0.841	0.699	0.826	0.826	0.807
		55	12.60	0.820	0.694	0.879	0.879	0.837
		70	13.32	0.795	0.688	0.907	0.907	0.853
A2-B1-C5-D4	1.675	33	10.88	0.825	0.695	0.798	0.803	0.785
		55	14.14	0.801	0.683	0.838	0.843	0.809
		70	15.23	0.783	0.678	0.866	0.870	0.825
A2-B1-C5-D5	1.575	33	11.33	0.821	0.697	0.784	0.808	0.774
		55	15.26	0.788	0.676	0.808	0.833	0.787
		70	16.72	0.769	0.668	0.829	0.854	0.799
A2-B1-C5-D6	1.501	33	11.59	0.823	0.704	0.779	0.815	0.771
		55	16.09	0.779	0.672	0.786	0.823	0.769
		70	17.90	0.757	0.660	0.800	0.837	0.777
A2-B1-C6-D1	2.635	33	7.60	0.928	0.738	0.947	0.947	0.883
		55	8.25	0.860	0.731	0.976	0.976	0.893
		70	8.44	0.841	0.734	0.983	0.983	0.895
A2-B1-C6-D2	2.186	33	10.16	0.888	0.718	0.895	0.895	0.854
		55	11.60	0.848	0.716	0.948	0.948	0.878
		70	11.98	0.822	0.713	0.964	0.964	0.885
A2-B1-C6-D3	1.946	33	11.75	0.859	0.706	0.853	0.853	0.827
		55	14.13	0.839	0.707	0.910	0.910	0.857
		70	14.78	0.808	0.699	0.936	0.936	0.869
A2-B1-C6-D4	1.792	33	12.81	0.840	0.699	0.823	0.823	0.805
		55	16.08	0.821	0.695	0.874	0.874	0.834
		70	17.03	0.799	0.690	0.903	0.903	0.850
A2-B1-C6-D5	1.684	33	13.54	0.829	0.697	0.802	0.805	0.788
		55	17.56	0.807	0.686	0.843	0.846	0.812
		70	18.88	0.790	0.682	0.871	0.874	0.829
A2-B1-C6-D6	1.602	33	14.02	0.825	0.699	0.790	0.809	0.779
		55	18.70	0.796	0.680	0.819	0.838	0.795
		70	20.39	0.778	0.674	0.842	0.862	0.809

**Table E.2 (Continued)**

Frame	$K_x$	$F_y$	$W_{FEM}$	$\frac{W_{1a}}{W_{FEM}}$	$\frac{W_{1c}}{W_{FEM}}$	$\frac{W_{2a}}{W_{FEM}}$	$\frac{W_{2b}}{W_{FEM}}$	$\frac{W_{2c}}{W_{FEM}}$
		(ksi)	(kips)					
A2-B1-C7-D1	2.589	33	7.41	1.007	0.770	0.963	0.963	0.895
		55	8.11	0.953	0.773	0.985	0.985	0.899
		70	8.30	0.931	0.776	0.989	0.989	0.899
A2-B1-C7-D2	2.143	33	9.87	0.958	0.752	0.924	0.924	0.879
		55	11.38	0.982	0.780	0.970	0.970	0.896
		70	11.80	0.955	0.780	0.980	0.980	0.897
A2-B1-C7-D3	1.907	33	11.37	0.926	0.743	0.890	0.890	0.860
		55	13.85	0.965	0.770	0.947	0.947	0.885
		70	14.54	0.972	0.783	0.967	0.967	0.892
A2-B1-C7-D4	1.757	33	12.33	0.908	0.739	0.865	0.865	0.844
		55	15.69	0.945	0.760	0.924	0.924	0.874
		70	16.73	0.963	0.777	0.950	0.950	0.884
A2-B1-C7-D5	1.651	33	12.97	0.900	0.741	0.850	0.861	0.834
		55	17.08	0.929	0.754	0.904	0.916	0.864
		70	18.50	0.950	0.769	0.931	0.942	0.875
A2-B1-C7-D6	1.571	33	13.36	0.899	0.747	0.843	0.872	0.830
		55	18.14	0.918	0.751	0.887	0.918	0.854
		70	19.93	0.937	0.763	0.914	0.944	0.866
A2-B1-C8-D1	2.792	33	8.72	1.014	0.771	0.973	0.973	0.900
		55	9.42	0.945	0.770	0.988	0.988	0.900
		70	9.62	0.926	0.775	0.991	0.991	0.900
A2-B1-C8-D2	2.336	33	11.67	0.983	0.759	0.944	0.944	0.888
		55	13.07	0.972	0.775	0.980	0.980	0.899
		70	13.47	0.943	0.776	0.986	0.986	0.899
A2-B1-C8-D3	2.084	33	13.69	0.949	0.748	0.915	0.915	0.874
		55	15.98	0.981	0.777	0.965	0.965	0.893
		70	16.61	0.961	0.779	0.978	0.978	0.897
A2-B1-C8-D4	1.920	33	15.09	0.927	0.742	0.891	0.891	0.861
		55	18.33	0.967	0.769	0.947	0.947	0.885
		70	19.23	0.973	0.782	0.968	0.968	0.893
A2-B1-C8-D5	1.802	33	16.09	0.913	0.739	0.872	0.872	0.849
		55	20.22	0.951	0.761	0.930	0.930	0.877
		70	21.45	0.968	0.777	0.955	0.955	0.887
A2-B1-C8-D6	1.713	33	16.84	0.904	0.738	0.857	0.857	0.839
		55	21.75	0.938	0.756	0.915	0.915	0.869
		70	23.34	0.958	0.772	0.941	0.941	0.880

**Table E.2 (Continued)**

Frame	$K_x$	$F_y$	$W_{FEM}$	$\frac{W_{1a}}{W_{FEM}}$	$\frac{W_{1c}}{W_{FEM}}$	$\frac{W_{2a}}{W_{FEM}}$	$\frac{W_{2b}}{W_{FEM}}$	$\frac{W_{2c}}{W_{FEM}}$
		(ksi)	(kips)					
A2-B1-C9-D1	2.950	33	9.94	1.009	0.766	0.978	0.978	0.901
		55	10.66	0.940	0.767	0.990	0.990	0.900
		70	10.87	0.923	0.773	0.992	0.992	0.900
A2-B1-C9-D2	2.495	33	13.22	0.999	0.763	0.956	0.956	0.892
		55	14.55	0.961	0.771	0.984	0.984	0.900
		70	14.93	0.937	0.773	0.989	0.989	0.900
A2-B1-C9-D3	2.233	33	15.63	0.969	0.753	0.932	0.932	0.882
		55	17.77	0.982	0.776	0.975	0.975	0.897
		70	18.37	0.951	0.775	0.983	0.983	0.899
A2-B1-C9-D4	2.058	33	17.43	0.945	0.745	0.909	0.909	0.871
		55	20.47	0.980	0.774	0.962	0.962	0.892
		70	21.31	0.965	0.777	0.977	0.977	0.896
A2-B1-C9-D5	1.932	33	18.76	0.929	0.741	0.891	0.891	0.861
		55	22.75	0.968	0.768	0.948	0.948	0.885
		70	23.85	0.973	0.779	0.968	0.968	0.893
A2-B1-C9-D6	1.835	33	19.79	0.917	0.739	0.876	0.876	0.852
		55	24.66	0.956	0.762	0.934	0.934	0.879
		70	26.07	0.970	0.777	0.958	0.958	0.888
A2-B2-C1-D1	2.561	33	7.18	0.838	0.696	0.916	0.916	0.865
		55	7.98	0.764	0.672	0.955	0.955	0.880
		70	8.19	0.744	0.670	0.967	0.967	0.885
A2-B2-C1-D2	2.119	33	9.30	0.794	0.673	0.841	0.841	0.816
		55	11.10	0.728	0.642	0.893	0.893	0.845
		70	11.58	0.698	0.630	0.917	0.917	0.857
A2-B2-C1-D3	1.885	33	10.53	0.769	0.661	0.790	0.790	0.777
		55	13.33	0.707	0.626	0.826	0.826	0.798
		70	14.16	0.668	0.604	0.851	0.851	0.814
A2-B2-C1-D4	1.736	33	11.27	0.757	0.657	0.761	0.761	0.752
		55	14.91	0.690	0.613	0.775	0.775	0.758
		70	16.16	0.649	0.588	0.792	0.792	0.769
A2-B2-C1-D5	1.631	33	11.62	0.759	0.664	0.752	0.762	0.745
		55	16.03	0.679	0.606	0.741	0.751	0.728
		70	17.72	0.636	0.578	0.746	0.756	0.730
A2-B2-C1-D6	1.552	33	11.86	0.763	0.671	0.746	0.768	0.741
		55	16.86	0.672	0.602	0.717	0.737	0.707
		70	18.93	0.628	0.571	0.712	0.731	0.701

**Table E.2 (Continued)**

Frame	$K_x$	$F_y$	$W_{FEM}$	$\frac{W_{1a}}{W_{FEM}}$	$\frac{W_{1c}}{W_{FEM}}$	$\frac{W_{2a}}{W_{FEM}}$	$\frac{W_{2b}}{W_{FEM}}$	$\frac{W_{2c}}{W_{FEM}}$
		(ksi)	(kips)					
A2-B2-C2-D1	2.755	33	8.50	0.853	0.705	0.939	0.939	0.878
		55	9.29	0.781	0.687	0.968	0.968	0.888
		70	9.50	0.764	0.687	0.976	0.976	0.890
A2-B2-C2-D2	2.305	33	11.15	0.816	0.684	0.878	0.878	0.842
		55	12.81	0.748	0.658	0.930	0.930	0.867
		70	13.24	0.723	0.652	0.948	0.948	0.876
A2-B2-C2-D3	2.056	33	12.83	0.790	0.671	0.829	0.829	0.808
		55	15.53	0.727	0.641	0.879	0.879	0.836
		70	16.26	0.694	0.626	0.905	0.905	0.851
A2-B2-C2-D4	1.893	33	13.98	0.772	0.663	0.794	0.794	0.780
		55	17.64	0.712	0.629	0.831	0.831	0.802
		70	18.72	0.673	0.608	0.857	0.857	0.818
A2-B2-C2-D5	1.777	33	14.76	0.762	0.659	0.771	0.771	0.760
		55	19.27	0.699	0.619	0.792	0.792	0.772
		70	20.76	0.658	0.596	0.813	0.813	0.785
A2-B2-C2-D6	1.688	33	15.30	0.757	0.659	0.756	0.758	0.748
		55	20.54	0.689	0.612	0.762	0.764	0.747
		70	22.44	0.647	0.586	0.775	0.777	0.755
A2-B2-C3-D1	2.904	33	9.73	0.857	0.707	0.951	0.951	0.884
		55	10.52	0.793	0.696	0.974	0.974	0.891
		70	10.73	0.777	0.698	0.981	0.981	0.893
A2-B2-C3-D2	2.456	33	12.73	0.834	0.694	0.904	0.904	0.859
		55	14.30	0.764	0.671	0.950	0.950	0.879
		70	14.71	0.742	0.668	0.963	0.963	0.884
A2-B2-C3-D3	2.198	33	14.82	0.808	0.680	0.859	0.859	0.830
		55	17.36	0.743	0.654	0.913	0.913	0.858
		70	18.03	0.715	0.644	0.935	0.935	0.869
A2-B2-C3-D4	2.026	33	16.29	0.789	0.671	0.824	0.824	0.804
		55	19.86	0.729	0.642	0.874	0.874	0.832
		70	20.83	0.695	0.626	0.900	0.900	0.848
A2-B2-C3-D5	1.901	33	17.39	0.776	0.665	0.797	0.797	0.783
		55	21.90	0.718	0.633	0.836	0.836	0.806
		70	23.21	0.679	0.613	0.863	0.863	0.823
A2-B2-C3-D6	1.805	33	18.20	0.767	0.662	0.778	0.778	0.767
		55	23.56	0.707	0.625	0.805	0.805	0.782
		70	25.26	0.667	0.603	0.828	0.828	0.798

**Table E.2 (Continued)**

Frame	$K_x$	$F_y$	$W_{FEM}$	$\frac{W_{1a}}{W_{FEM}}$	$\frac{W_{1c}}{W_{FEM}}$	$\frac{W_{2a}}{W_{FEM}}$	$\frac{W_{2b}}{W_{FEM}}$	$\frac{W_{2c}}{W_{FEM}}$
		(ksi)	(kips)					
A2-B2-C4-D1	2.285	33	5.73	0.843	0.693	0.882	0.882	0.842
		55	6.45	0.776	0.671	0.929	0.929	0.862
		70	6.65	0.753	0.666	0.940	0.940	0.867
A2-B2-C4-D2	1.872	33	7.36	0.793	0.667	0.797	0.797	0.780
		55	9.04	0.740	0.641	0.838	0.838	0.803
		70	9.52	0.702	0.623	0.859	0.859	0.814
A2-B2-C4-D3	1.667	33	8.20	0.769	0.658	0.752	0.758	0.742
		55	10.70	0.712	0.621	0.767	0.772	0.747
		70	11.53	0.673	0.598	0.779	0.785	0.755
A2-B2-C4-D4	1.539	33	8.62	0.764	0.660	0.734	0.760	0.727
		55	11.76	0.695	0.610	0.723	0.748	0.711
		70	12.99	0.655	0.584	0.723	0.747	0.707
A2-B2-C4-D5	1.451	33	8.81	0.767	0.668	0.728	0.766	0.723
		55	12.47	0.685	0.605	0.696	0.732	0.687
		70	14.04	0.642	0.573	0.685	0.719	0.674
A2-B2-C4-D6	1.386	33	8.92	0.772	0.676	0.726	0.773	0.722
		55	12.96	0.680	0.603	0.679	0.721	0.671
		70	14.81	0.633	0.568	0.659	0.699	0.651
A2-B2-C5-D1	2.479	33	6.73	0.868	0.706	0.916	0.916	0.861
		55	7.41	0.797	0.688	0.952	0.952	0.876
		70	7.60	0.777	0.686	0.959	0.959	0.878
A2-B2-C5-D2	2.043	33	8.88	0.820	0.681	0.838	0.838	0.811
		55	10.44	0.763	0.660	0.890	0.890	0.840
		70	10.86	0.734	0.648	0.909	0.909	0.848
A2-B2-C5-D3	1.817	33	10.11	0.791	0.668	0.789	0.789	0.773
		55	12.60	0.742	0.642	0.826	0.826	0.795
		70	13.33	0.705	0.623	0.847	0.847	0.807
A2-B2-C5-D4	1.675	33	10.88	0.776	0.662	0.758	0.763	0.748
		55	14.15	0.722	0.629	0.777	0.782	0.757
		70	15.24	0.685	0.606	0.792	0.796	0.765
A2-B2-C5-D5	1.575	33	11.33	0.771	0.663	0.743	0.764	0.735
		55	15.27	0.709	0.620	0.743	0.764	0.728
		70	16.74	0.671	0.596	0.748	0.768	0.729
A2-B2-C5-D6	1.501	33	11.59	0.772	0.669	0.737	0.769	0.730
		55	16.08	0.700	0.615	0.719	0.750	0.708
		70	17.90	0.661	0.588	0.716	0.746	0.702

**Table E.2 (Continued)**

Frame	$K_x$	$F_y$	$W_{FEM}$	$\frac{W_{1a}}{W_{FEM}}$	$\frac{W_{1c}}{W_{FEM}}$	$\frac{W_{2a}}{W_{FEM}}$	$\frac{W_{2b}}{W_{FEM}}$	$\frac{W_{2c}}{W_{FEM}}$
		(ksi)	(kips)					
A2-B2-C6-D1	2.635	33	7.61	0.883	0.715	0.934	0.934	0.872
		55	8.27	0.813	0.701	0.963	0.963	0.883
		70	8.45	0.796	0.701	0.969	0.969	0.884
A2-B2-C6-D2	2.186	33	10.16	0.844	0.693	0.870	0.870	0.834
		55	11.61	0.784	0.675	0.922	0.922	0.860
		70	12.00	0.759	0.668	0.937	0.937	0.866
A2-B2-C6-D3	1.946	33	11.76	0.814	0.679	0.821	0.821	0.799
		55	14.14	0.766	0.660	0.871	0.871	0.827
		70	14.80	0.732	0.645	0.893	0.893	0.838
A2-B2-C6-D4	1.792	33	12.81	0.795	0.671	0.788	0.788	0.773
		55	16.08	0.749	0.647	0.825	0.825	0.794
		70	17.05	0.713	0.628	0.847	0.847	0.807
A2-B2-C6-D5	1.684	33	13.54	0.783	0.667	0.765	0.768	0.754
		55	17.56	0.734	0.637	0.788	0.791	0.766
		70	18.89	0.698	0.617	0.805	0.808	0.776
A2-B2-C6-D6	1.602	33	14.02	0.779	0.668	0.752	0.769	0.744
		55	18.70	0.723	0.630	0.761	0.778	0.744
		70	20.40	0.688	0.608	0.770	0.787	0.748
A2-B2-C7-D1	2.589	33	7.43	1.004	0.768	0.961	0.961	0.893
		55	8.13	0.950	0.770	0.981	0.981	0.896
		70	8.33	0.927	0.773	0.985	0.985	0.896
A2-B2-C7-D2	2.143	33	9.88	0.957	0.751	0.922	0.922	0.878
		55	11.41	0.980	0.778	0.968	0.968	0.894
		70	11.84	0.952	0.778	0.978	0.978	0.895
A2-B2-C7-D3	1.907	33	11.38	0.925	0.742	0.889	0.889	0.860
		55	13.87	0.964	0.769	0.945	0.945	0.883
		70	14.57	0.970	0.781	0.965	0.965	0.891
A2-B2-C7-D4	1.757	33	12.34	0.908	0.739	0.865	0.865	0.844
		55	15.71	0.943	0.759	0.923	0.923	0.873
		70	16.76	0.961	0.775	0.948	0.948	0.883
A2-B2-C7-D5	1.651	33	12.98	0.899	0.740	0.849	0.860	0.833
		55	17.10	0.928	0.753	0.903	0.914	0.863
		70	18.53	0.948	0.768	0.930	0.940	0.874
A2-B2-C7-D6	1.571	33	13.38	0.898	0.746	0.842	0.871	0.829
		55	18.17	0.917	0.750	0.886	0.917	0.853
		70	19.97	0.936	0.762	0.913	0.942	0.865

**Table E.2 (Continued)**

Frame	$K_x$	$F_y$	$W_{FEM}$	$\frac{W_{1a}}{W_{FEM}}$	$\frac{W_{1c}}{W_{FEM}}$	$\frac{W_{2a}}{W_{FEM}}$	$\frac{W_{2b}}{W_{FEM}}$	$\frac{W_{2c}}{W_{FEM}}$
		(ksi)	(kips)					
A2-B2-C8-D1	2.792	33	8.74	1.011	0.769	0.971	0.971	0.897
		55	9.45	0.942	0.767	0.985	0.985	0.897
		70	9.65	0.922	0.772	0.988	0.988	0.897
A2-B2-C8-D2	2.336	33	11.69	0.982	0.758	0.942	0.942	0.887
		55	13.09	0.970	0.774	0.978	0.978	0.897
		70	13.49	0.941	0.774	0.984	0.984	0.897
A2-B2-C8-D3	2.084	33	13.70	0.949	0.747	0.914	0.914	0.874
		55	16.00	0.979	0.775	0.963	0.963	0.892
		70	16.64	0.960	0.778	0.976	0.976	0.895
A2-B2-C8-D4	1.920	33	15.09	0.927	0.741	0.890	0.890	0.860
		55	18.35	0.966	0.768	0.946	0.946	0.884
		70	19.26	0.971	0.780	0.966	0.966	0.891
A2-B2-C8-D5	1.802	33	16.10	0.913	0.739	0.871	0.871	0.848
		55	20.24	0.950	0.761	0.929	0.929	0.876
		70	21.48	0.966	0.776	0.953	0.953	0.885
A2-B2-C8-D6	1.713	33	16.85	0.903	0.738	0.857	0.857	0.838
		55	21.77	0.937	0.755	0.914	0.914	0.868
		70	23.37	0.957	0.771	0.940	0.940	0.879
A2-B2-C9-D1	2.950	33	9.96	1.006	0.764	0.976	0.976	0.899
		55	10.69	0.937	0.765	0.987	0.987	0.898
		70	10.90	0.920	0.770	0.989	0.989	0.897
A2-B2-C9-D2	2.495	33	13.24	0.998	0.762	0.954	0.954	0.891
		55	14.58	0.959	0.769	0.982	0.982	0.898
		70	14.97	0.935	0.772	0.987	0.987	0.898
A2-B2-C9-D3	2.233	33	15.65	0.969	0.752	0.931	0.931	0.882
		55	17.79	0.981	0.775	0.973	0.973	0.896
		70	18.40	0.949	0.773	0.982	0.982	0.897
A2-B2-C9-D4	2.058	33	17.44	0.945	0.745	0.909	0.909	0.870
		55	20.50	0.978	0.773	0.961	0.961	0.890
		70	21.34	0.963	0.776	0.975	0.975	0.895
A2-B2-C9-D5	1.932	33	18.77	0.928	0.740	0.891	0.891	0.860
		55	22.77	0.967	0.767	0.947	0.947	0.884
		70	23.88	0.972	0.778	0.967	0.967	0.892
A2-B2-C9-D6	1.835	33	19.80	0.917	0.739	0.876	0.876	0.851
		55	24.68	0.955	0.761	0.933	0.933	0.878
		70	26.11	0.969	0.776	0.957	0.957	0.887

**Table E.2 (Continued)**

Frame	$K_x$	$F_y$	$W_{FEM}$	$\frac{W_{1a}}{W_{FEM}}$	$\frac{W_{1c}}{W_{FEM}}$	$\frac{W_{2a}}{W_{FEM}}$	$\frac{W_{2b}}{W_{FEM}}$	$\frac{W_{2c}}{W_{FEM}}$
		(ksi)	(kips)					
A3-B1-C1-D1	3.136	33	2.59	0.892	0.730	0.970	0.970	0.893
		55	2.74	0.843	0.736	0.988	0.988	0.899
		70	2.79	0.831	0.740	0.993	0.993	0.901
A3-B1-C1-D2	2.506	33	3.79	0.873	0.716	0.921	0.921	0.870
		55	4.18	0.822	0.712	0.969	0.969	0.889
		70	4.28	0.802	0.712	0.980	0.980	0.894
A3-B1-C1-D3	2.195	33	4.58	0.835	0.697	0.875	0.875	0.842
		55	5.29	0.809	0.698	0.939	0.939	0.874
		70	5.47	0.782	0.692	0.959	0.959	0.885
A3-B1-C1-D4	1.999	33	5.13	0.809	0.684	0.835	0.835	0.813
		55	6.18	0.795	0.687	0.904	0.904	0.854
		70	6.48	0.767	0.679	0.932	0.932	0.870
A3-B1-C1-D5	1.860	33	5.50	0.796	0.680	0.810	0.810	0.794
		55	6.91	0.778	0.676	0.869	0.869	0.833
		70	7.33	0.756	0.669	0.902	0.902	0.850
A3-B1-C1-D6	1.756	33	5.75	0.790	0.680	0.793	0.793	0.781
		55	7.48	0.764	0.667	0.838	0.838	0.811
		70	8.05	0.746	0.661	0.869	0.869	0.830
A3-B1-C2-D1	3.441	33	2.92	0.892	0.735	0.978	0.978	0.897
		55	3.06	0.852	0.744	0.993	0.993	0.901
		70	3.10	0.841	0.752	0.996	0.996	0.903
A3-B1-C2-D2	2.757	33	4.32	0.893	0.727	0.948	0.948	0.883
		55	4.66	0.833	0.723	0.981	0.981	0.895
		70	4.75	0.817	0.727	0.988	0.988	0.899
A3-B1-C2-D3	2.417	33	5.33	0.864	0.711	0.912	0.912	0.865
		55	5.94	0.820	0.709	0.962	0.962	0.888
		70	6.09	0.799	0.708	0.976	0.976	0.893
A3-B1-C2-D4	2.202	33	6.08	0.837	0.698	0.877	0.877	0.842
		55	7.01	0.811	0.700	0.940	0.940	0.876
		70	7.25	0.785	0.695	0.961	0.961	0.885
A3-B1-C2-D5	2.048	33	6.65	0.817	0.688	0.846	0.846	0.822
		55	7.92	0.802	0.693	0.915	0.915	0.862
		70	8.26	0.773	0.684	0.942	0.942	0.875
A3-B1-C2-D6	1.932	33	7.07	0.804	0.683	0.824	0.824	0.805
		55	8.69	0.789	0.683	0.889	0.889	0.846
		70	9.15	0.764	0.676	0.920	0.920	0.862



**Table E.2 (Continued)**

Frame	$K_x$	$F_y$	$W_{FEM}$	$\frac{W_{1a}}{W_{FEM}}$	$\frac{W_{1c}}{W_{FEM}}$	$\frac{W_{2a}}{W_{FEM}}$	$\frac{W_{2b}}{W_{FEM}}$	$\frac{W_{2c}}{W_{FEM}}$
		(ksi)	(kips)					
A3-B1-C3-D1	3.694	33	3.20	0.893	0.739	0.984	0.984	0.898
		55	3.33	0.858	0.752	0.994	0.994	0.902
		70	3.37	0.849	0.760	0.999	0.999	0.904
A3-B1-C3-D2	2.969	33	4.76	0.896	0.732	0.962	0.962	0.889
		55	5.07	0.841	0.731	0.987	0.987	0.898
		70	5.15	0.828	0.736	0.992	0.992	0.901
A3-B1-C3-D3	2.605	33	5.93	0.885	0.722	0.935	0.935	0.876
		55	6.47	0.829	0.718	0.974	0.974	0.893
		70	6.61	0.812	0.720	0.984	0.984	0.897
A3-B1-C3-D4	2.374	33	6.84	0.861	0.710	0.906	0.906	0.860
		55	7.66	0.820	0.709	0.960	0.960	0.886
		70	7.88	0.798	0.707	0.975	0.975	0.892
A3-B1-C3-D5	2.209	33	7.56	0.840	0.699	0.878	0.878	0.843
		55	8.71	0.814	0.701	0.942	0.942	0.876
		70	9.00	0.787	0.696	0.962	0.962	0.886
A3-B1-C3-D6	2.083	33	8.14	0.823	0.691	0.854	0.854	0.827
		55	9.62	0.808	0.696	0.922	0.922	0.865
		70	10.01	0.778	0.688	0.948	0.948	0.878
A3-B1-C4-D1	2.730	33	2.19	0.908	0.730	0.940	0.940	0.872
		55	2.34	0.850	0.728	0.977	0.977	0.893
		70	2.38	0.835	0.733	0.985	0.985	0.895
A3-B1-C4-D2	2.175	33	3.15	0.860	0.702	0.876	0.876	0.836
		55	3.56	0.830	0.708	0.938	0.938	0.870
		70	3.66	0.806	0.706	0.958	0.958	0.880
A3-B1-C4-D3	1.905	33	3.73	0.822	0.684	0.826	0.826	0.803
		55	4.46	0.813	0.694	0.892	0.892	0.844
		70	4.66	0.786	0.687	0.921	0.921	0.860
A3-B1-C4-D4	1.737	33	4.08	0.803	0.678	0.792	0.792	0.777
		55	5.14	0.791	0.678	0.848	0.848	0.813
		70	5.47	0.773	0.675	0.880	0.880	0.833
A3-B1-C4-D5	1.621	33	4.28	0.800	0.682	0.776	0.791	0.766
		55	5.65	0.773	0.667	0.811	0.826	0.788
		70	6.11	0.758	0.664	0.839	0.854	0.805
A3-B1-C4-D6	1.535	33	4.38	0.805	0.691	0.772	0.801	0.763
		55	6.02	0.762	0.661	0.784	0.814	0.766
		70	6.62	0.745	0.654	0.805	0.835	0.780

**Table E.2 (Continued)**

Frame	$K_x$	$F_y$	$W_{FEM}$	$\frac{W_{1a}}{W_{FEM}}$	$\frac{W_{1c}}{W_{FEM}}$	$\frac{W_{2a}}{W_{FEM}}$	$\frac{W_{2b}}{W_{FEM}}$	$\frac{W_{2c}}{W_{FEM}}$
		(ksi)	(kips)					
A3-B1-C5-D1	3.002	33	2.46	0.906	0.731	0.961	0.961	0.884
		55	2.60	0.859	0.740	0.984	0.984	0.895
		70	2.64	0.847	0.749	0.990	0.990	0.898
A3-B1-C5-D2	2.396	33	3.62	0.891	0.719	0.916	0.916	0.860
		55	3.97	0.842	0.719	0.962	0.962	0.885
		70	4.07	0.823	0.721	0.974	0.974	0.890
A3-B1-C5-D3	2.098	33	4.40	0.853	0.699	0.866	0.866	0.830
		55	5.05	0.831	0.707	0.930	0.930	0.867
		70	5.21	0.805	0.703	0.953	0.953	0.878
A3-B1-C5-D4	1.911	33	4.95	0.826	0.687	0.828	0.828	0.806
		55	5.91	0.819	0.697	0.897	0.897	0.847
		70	6.17	0.792	0.690	0.925	0.925	0.862
A3-B1-C5-D5	1.780	33	5.32	0.810	0.681	0.801	0.801	0.785
		55	6.61	0.802	0.685	0.863	0.863	0.824
		70	6.99	0.782	0.681	0.895	0.895	0.844
A3-B1-C5-D6	1.682	33	5.57	0.804	0.681	0.786	0.789	0.773
		55	7.16	0.787	0.676	0.834	0.837	0.805
		70	7.67	0.772	0.673	0.865	0.869	0.823
A3-B1-C6-D1	3.231	33	2.69	0.907	0.738	0.971	0.971	0.890
		55	2.82	0.866	0.747	0.989	0.989	0.898
		70	2.86	0.855	0.755	0.993	0.993	0.900
A3-B1-C6-D2	2.583	33	4.00	0.909	0.728	0.934	0.934	0.874
		55	4.32	0.851	0.728	0.973	0.973	0.889
		70	4.40	0.835	0.732	0.982	0.982	0.894
A3-B1-C6-D3	2.263	33	4.94	0.878	0.712	0.896	0.896	0.852
		55	5.51	0.841	0.716	0.952	0.952	0.879
		70	5.66	0.820	0.716	0.968	0.968	0.886
A3-B1-C6-D4	2.061	33	5.64	0.850	0.698	0.861	0.861	0.827
		55	6.50	0.835	0.708	0.927	0.927	0.865
		70	6.73	0.807	0.704	0.950	0.950	0.876
A3-B1-C6-D5	1.918	33	6.16	0.830	0.689	0.831	0.831	0.808
		55	7.34	0.824	0.700	0.900	0.900	0.848
		70	7.66	0.797	0.694	0.928	0.928	0.864
A3-B1-C6-D6	1.811	33	6.55	0.816	0.684	0.809	0.809	0.791
		55	8.04	0.811	0.691	0.874	0.874	0.832
		70	8.48	0.790	0.687	0.905	0.905	0.851

**Table E.2 (Continued)**

Frame	$K_x$	$F_y$	$W_{FEM}$	$\frac{W_{1a}}{W_{FEM}}$	$\frac{W_{1c}}{W_{FEM}}$	$\frac{W_{2a}}{W_{FEM}}$	$\frac{W_{2b}}{W_{FEM}}$	$\frac{W_{2c}}{W_{FEM}}$
		(ksi)	(kips)					
A3-B1-C7-D1	3.162	33	2.64	0.974	0.767	0.977	0.977	0.896
		55	2.77	0.926	0.775	0.992	0.992	0.900
		70	2.81	0.913	0.785	0.995	0.995	0.901
A3-B1-C7-D2	2.527	33	3.92	0.982	0.762	0.949	0.949	0.885
		55	4.24	0.949	0.776	0.983	0.983	0.897
		70	4.33	0.929	0.782	0.989	0.989	0.899
A3-B1-C7-D3	2.214	33	4.82	0.944	0.745	0.919	0.919	0.871
		55	5.42	0.968	0.778	0.968	0.968	0.891
		70	5.57	0.942	0.781	0.982	0.982	0.896
A3-B1-C7-D4	2.016	33	5.47	0.914	0.733	0.892	0.892	0.855
		55	6.39	0.961	0.772	0.953	0.953	0.884
		70	6.62	0.955	0.782	0.971	0.971	0.891
A3-B1-C7-D5	1.877	33	5.95	0.894	0.726	0.868	0.868	0.841
		55	7.19	0.945	0.764	0.936	0.936	0.877
		70	7.54	0.958	0.781	0.959	0.959	0.886
A3-B1-C7-D6	1.772	33	6.30	0.882	0.724	0.851	0.851	0.830
		55	7.87	0.929	0.756	0.920	0.920	0.868
		70	8.33	0.950	0.775	0.947	0.947	0.880
A3-B1-C8-D1	3.474	33	2.96	0.961	0.762	0.986	0.986	0.899
		55	3.09	0.921	0.780	0.994	0.994	0.901
		70	3.13	0.910	0.788	0.998	0.998	0.903
A3-B1-C8-D2	2.784	33	4.43	0.994	0.768	0.966	0.966	0.890
		55	4.72	0.939	0.775	0.989	0.989	0.899
		70	4.81	0.922	0.783	0.993	0.993	0.901
A3-B1-C8-D3	2.441	33	5.53	0.974	0.757	0.942	0.942	0.882
		55	6.04	0.954	0.775	0.980	0.980	0.896
		70	6.18	0.933	0.781	0.988	0.988	0.899
A3-B1-C8-D4	2.223	33	6.39	0.946	0.745	0.920	0.920	0.871
		55	7.17	0.968	0.778	0.969	0.969	0.891
		70	7.37	0.943	0.781	0.982	0.982	0.896
A3-B1-C8-D5	2.069	33	7.07	0.922	0.735	0.899	0.899	0.859
		55	8.16	0.965	0.774	0.958	0.958	0.886
		70	8.43	0.952	0.781	0.975	0.975	0.893
A3-B1-C8-D6	1.951	33	7.60	0.905	0.729	0.880	0.880	0.848
		55	9.01	0.955	0.768	0.946	0.946	0.881
		70	9.38	0.960	0.782	0.967	0.967	0.889

**Table E.2 (Continued)**

Frame	$K_x$	$F_y$	$W_{FEM}$	$\frac{W_{1a}}{W_{FEM}}$	$\frac{W_{1c}}{W_{FEM}}$	$\frac{W_{2a}}{W_{FEM}}$	$\frac{W_{2b}}{W_{FEM}}$	$\frac{W_{2c}}{W_{FEM}}$
		(ksi)	(kips)					
A3-B1-C9-D1	3.733	33	3.24	0.952	0.763	0.988	0.988	0.900
		55	3.37	0.917	0.779	0.996	0.996	0.902
		70	3.40	0.908	0.790	1.000	1.000	0.904
A3-B1-C9-D2	3.000	33	4.85	0.985	0.765	0.974	0.974	0.896
		55	5.13	0.932	0.775	0.992	0.992	0.901
		70	5.21	0.918	0.783	0.995	0.995	0.902
A3-B1-C9-D3	2.633	33	6.11	0.990	0.763	0.956	0.956	0.887
		55	6.56	0.945	0.774	0.986	0.986	0.899
		70	6.69	0.927	0.781	0.991	0.991	0.900
A3-B1-C9-D4	2.400	33	7.12	0.970	0.754	0.938	0.938	0.880
		55	7.81	0.957	0.775	0.978	0.978	0.896
		70	7.99	0.935	0.780	0.987	0.987	0.899
A3-B1-C9-D5	2.233	33	7.95	0.947	0.745	0.920	0.920	0.871
		55	8.91	0.969	0.776	0.970	0.970	0.891
		70	9.16	0.943	0.780	0.982	0.982	0.897
A3-B1-C9-D6	2.106	33	8.64	0.928	0.737	0.903	0.903	0.861
		55	9.89	0.968	0.775	0.961	0.961	0.887
		70	10.21	0.950	0.780	0.977	0.977	0.894
A3-B2-C1-D1	3.136	33	2.60	0.842	0.702	0.961	0.961	0.884
		55	2.75	0.795	0.704	0.981	0.981	0.893
		70	2.79	0.784	0.709	0.986	0.986	0.895
A3-B2-C1-D2	2.506	33	3.79	0.817	0.684	0.900	0.900	0.854
		55	4.18	0.754	0.667	0.950	0.950	0.878
		70	4.28	0.736	0.666	0.964	0.964	0.884
A3-B2-C1-D3	2.195	33	4.58	0.780	0.663	0.840	0.840	0.812
		55	5.29	0.726	0.643	0.906	0.906	0.852
		70	5.48	0.702	0.636	0.930	0.930	0.864
A3-B2-C1-D4	1.999	33	5.13	0.756	0.649	0.797	0.797	0.780
		55	6.19	0.708	0.628	0.857	0.857	0.819
		70	6.48	0.676	0.614	0.886	0.886	0.838
A3-B2-C1-D5	1.860	33	5.50	0.743	0.643	0.768	0.768	0.756
		55	6.91	0.693	0.617	0.811	0.811	0.785
		70	7.33	0.657	0.597	0.840	0.840	0.804
A3-B2-C1-D6	1.756	33	5.75	0.737	0.644	0.750	0.750	0.741
		55	7.49	0.679	0.607	0.774	0.774	0.756
		70	8.05	0.642	0.585	0.797	0.797	0.772

**Table E.2 (Continued)**

Frame	$K_x$	$F_y$	$W_{FEM}$	$\frac{W_{1a}}{W_{FEM}}$	$\frac{W_{1c}}{W_{FEM}}$	$\frac{W_{2a}}{W_{FEM}}$	$\frac{W_{2b}}{W_{FEM}}$	$\frac{W_{2c}}{W_{FEM}}$
		(ksi)	(kips)					
A3-B2-C2-D1	3.441	33	2.93	0.851	0.714	0.971	0.971	0.892
		55	3.07	0.812	0.719	0.987	0.987	0.896
		70	3.10	0.802	0.725	0.992	0.992	0.899
A3-B2-C2-D2	2.757	33	4.32	0.838	0.698	0.933	0.933	0.871
		55	4.67	0.776	0.685	0.969	0.969	0.888
		70	4.76	0.761	0.687	0.979	0.979	0.892
A3-B2-C2-D3	2.417	33	5.33	0.810	0.680	0.887	0.887	0.844
		55	5.94	0.750	0.663	0.944	0.944	0.873
		70	6.10	0.730	0.661	0.959	0.959	0.882
A3-B2-C2-D4	2.202	33	6.08	0.784	0.665	0.844	0.844	0.815
		55	7.01	0.731	0.647	0.910	0.910	0.854
		70	7.25	0.706	0.640	0.933	0.933	0.867
A3-B2-C2-D5	2.048	33	6.64	0.765	0.654	0.810	0.810	0.790
		55	7.92	0.716	0.635	0.873	0.873	0.831
		70	8.26	0.687	0.623	0.902	0.902	0.848
A3-B2-C2-D6	1.932	33	7.07	0.752	0.648	0.784	0.784	0.770
		55	8.69	0.705	0.626	0.839	0.839	0.806
		70	9.15	0.671	0.609	0.869	0.869	0.825
A3-B2-C3-D1	3.694	33	3.21	0.857	0.719	0.978	0.978	0.894
		55	3.34	0.823	0.732	0.991	0.991	0.899
		70	3.38	0.815	0.738	0.995	0.995	0.901
A3-B2-C3-D2	2.969	33	4.76	0.844	0.703	0.950	0.950	0.883
		55	5.07	0.792	0.700	0.978	0.978	0.893
		70	5.16	0.779	0.704	0.985	0.985	0.896
A3-B2-C3-D3	2.605	33	5.93	0.831	0.693	0.916	0.916	0.862
		55	6.48	0.768	0.679	0.961	0.961	0.884
		70	6.62	0.752	0.679	0.973	0.973	0.889
A3-B2-C3-D4	2.374	33	6.84	0.808	0.679	0.879	0.879	0.840
		55	7.67	0.750	0.662	0.939	0.939	0.872
		70	7.88	0.730	0.659	0.957	0.957	0.880
A3-B2-C3-D5	2.209	33	7.56	0.788	0.667	0.847	0.847	0.818
		55	8.71	0.735	0.650	0.913	0.913	0.856
		70	9.00	0.711	0.643	0.936	0.936	0.869
A3-B2-C3-D6	2.083	33	8.14	0.772	0.658	0.819	0.819	0.797
		55	9.62	0.724	0.640	0.885	0.885	0.838
		70	10.01	0.696	0.630	0.913	0.913	0.854

**Table E.2 (Continued)**

Frame	$K_x$	$F_y$	$W_{FEM}$	$\frac{W_{1a}}{W_{FEM}}$	$\frac{W_{1c}}{W_{FEM}}$	$\frac{W_{2a}}{W_{FEM}}$	$\frac{W_{2b}}{W_{FEM}}$	$\frac{W_{2c}}{W_{FEM}}$
		(ksi)	(kips)					
A3-B2-C4-D1	2.730	33	2.19	0.858	0.703	0.927	0.927	0.864
		55	2.34	0.801	0.698	0.964	0.964	0.880
		70	2.39	0.786	0.698	0.968	0.968	0.882
A3-B2-C4-D2	2.175	33	3.15	0.810	0.673	0.847	0.847	0.814
		55	3.56	0.758	0.659	0.910	0.910	0.850
		70	3.67	0.736	0.653	0.926	0.926	0.856
A3-B2-C4-D3	1.905	33	3.73	0.771	0.652	0.786	0.786	0.767
		55	4.47	0.731	0.637	0.842	0.842	0.804
		70	4.67	0.699	0.622	0.866	0.866	0.818
A3-B2-C4-D4	1.737	33	4.09	0.752	0.644	0.750	0.750	0.738
		55	5.15	0.709	0.621	0.785	0.785	0.762
		70	5.47	0.674	0.601	0.807	0.807	0.775
A3-B2-C4-D5	1.621	33	4.28	0.748	0.647	0.733	0.733	0.725
		55	5.65	0.691	0.608	0.742	0.742	0.726
		70	6.12	0.656	0.586	0.755	0.755	0.734
A3-B2-C4-D6	1.535	33	4.38	0.752	0.654	0.727	0.727	0.721
		55	6.02	0.680	0.601	0.712	0.712	0.701
		70	6.63	0.644	0.577	0.715	0.715	0.701
A3-B2-C5-D1	3.002	33	2.47	0.866	0.710	0.951	0.951	0.878
		55	2.60	0.820	0.713	0.975	0.975	0.889
		70	2.64	0.808	0.717	0.980	0.980	0.890
A3-B2-C5-D2	2.396	33	3.62	0.844	0.692	0.893	0.893	0.843
		55	3.98	0.784	0.681	0.943	0.943	0.869
		70	4.07	0.766	0.679	0.954	0.954	0.875
A3-B2-C5-D3	2.098	33	4.41	0.805	0.671	0.835	0.835	0.806
		55	5.05	0.759	0.659	0.899	0.899	0.843
		70	5.22	0.734	0.651	0.919	0.919	0.853
A3-B2-C5-D4	1.911	33	4.95	0.779	0.657	0.793	0.793	0.773
		55	5.91	0.741	0.644	0.851	0.851	0.811
		70	6.18	0.710	0.630	0.875	0.875	0.826
A3-B2-C5-D5	1.780	33	5.33	0.762	0.650	0.763	0.763	0.750
		55	6.61	0.724	0.632	0.808	0.808	0.780
		70	6.99	0.691	0.614	0.832	0.832	0.795
A3-B2-C5-D6	1.682	33	5.57	0.756	0.649	0.747	0.747	0.737
		55	7.17	0.710	0.622	0.773	0.773	0.753
		70	7.68	0.676	0.602	0.791	0.791	0.764

**Table E.2 (Continued)**

Frame	$K_x$	$F_y$	$W_{FEM}$	$\frac{W_{1a}}{W_{FEM}}$	$\frac{W_{1c}}{W_{FEM}}$	$\frac{W_{2a}}{W_{FEM}}$	$\frac{W_{2b}}{W_{FEM}}$	$\frac{W_{2c}}{W_{FEM}}$
		(ksi)	(kips)					
A3-B2-C6-D1	3.231	33	2.70	0.874	0.719	0.963	0.963	0.885
		55	2.83	0.834	0.727	0.981	0.981	0.892
		70	2.86	0.823	0.731	0.985	0.985	0.893
A3-B2-C6-D2	2.583	33	4.00	0.866	0.706	0.922	0.922	0.862
		55	4.32	0.804	0.698	0.959	0.959	0.881
		70	4.41	0.789	0.698	0.968	0.968	0.884
A3-B2-C6-D3	2.263	33	4.94	0.835	0.687	0.875	0.875	0.832
		55	5.51	0.782	0.677	0.930	0.930	0.863
		70	5.66	0.761	0.673	0.945	0.945	0.870
A3-B2-C6-D4	2.061	33	5.64	0.806	0.672	0.831	0.831	0.803
		55	6.51	0.765	0.663	0.895	0.895	0.842
		70	6.73	0.739	0.654	0.917	0.917	0.852
A3-B2-C6-D5	1.918	33	6.16	0.786	0.662	0.799	0.799	0.779
		55	7.34	0.753	0.652	0.860	0.860	0.818
		70	7.67	0.721	0.639	0.884	0.884	0.832
A3-B2-C6-D6	1.811	33	6.54	0.773	0.656	0.775	0.775	0.760
		55	8.05	0.740	0.643	0.826	0.826	0.794
		70	8.48	0.706	0.626	0.851	0.851	0.809
A3-B2-C7-D1	3.162	33	2.65	0.971	0.764	0.974	0.974	0.893
		55	2.78	0.923	0.773	0.989	0.989	0.897
		70	2.82	0.911	0.782	0.992	0.992	0.898
A3-B2-C7-D2	2.527	33	3.92	0.980	0.761	0.947	0.947	0.884
		55	4.25	0.946	0.774	0.981	0.981	0.894
		70	4.35	0.926	0.780	0.986	0.986	0.897
A3-B2-C7-D3	2.214	33	4.82	0.943	0.745	0.918	0.918	0.870
		55	5.43	0.966	0.777	0.966	0.966	0.890
		70	5.58	0.940	0.780	0.980	0.980	0.894
A3-B2-C7-D4	2.016	33	5.48	0.913	0.733	0.891	0.891	0.854
		55	6.40	0.959	0.771	0.951	0.951	0.883
		70	6.64	0.953	0.781	0.969	0.969	0.889
A3-B2-C7-D5	1.877	33	5.96	0.893	0.726	0.867	0.867	0.841
		55	7.20	0.944	0.763	0.935	0.935	0.876
		70	7.55	0.956	0.779	0.958	0.958	0.884
A3-B2-C7-D6	1.772	33	6.30	0.881	0.724	0.851	0.851	0.830
		55	7.88	0.928	0.755	0.919	0.919	0.867
		70	8.34	0.949	0.774	0.946	0.946	0.878

**Table E.2 (Continued)**

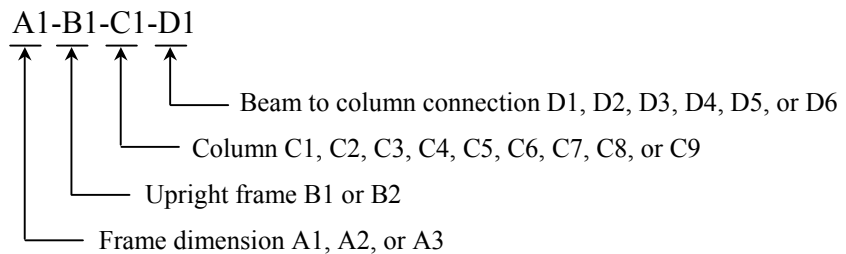
Frame	$K_x$	$F_y$	$W_{FEM}$	$\frac{W_{1a}}{W_{FEM}}$	$\frac{W_{1c}}{W_{FEM}}$	$\frac{W_{2a}}{W_{FEM}}$	$\frac{W_{2b}}{W_{FEM}}$	$\frac{W_{2c}}{W_{FEM}}$
		(ksi)	(kips)					
A3-B2-C8-D1	3.474	33	2.97	0.958	0.760	0.984	0.984	0.897
		55	3.10	0.918	0.778	0.992	0.992	0.899
		70	3.13	0.908	0.786	0.995	0.995	0.900
A3-B2-C8-D2	2.784	33	4.44	0.992	0.767	0.965	0.965	0.889
		55	4.73	0.937	0.773	0.987	0.987	0.898
		70	4.82	0.920	0.782	0.991	0.991	0.899
A3-B2-C8-D3	2.441	33	5.54	0.973	0.756	0.941	0.941	0.881
		55	6.05	0.952	0.774	0.979	0.979	0.894
		70	6.19	0.931	0.779	0.986	0.986	0.897
A3-B2-C8-D4	2.223	33	6.40	0.945	0.744	0.919	0.919	0.871
		55	7.19	0.967	0.776	0.968	0.968	0.890
		70	7.39	0.941	0.779	0.980	0.980	0.895
A3-B2-C8-D5	2.069	33	7.07	0.922	0.735	0.898	0.898	0.858
		55	8.17	0.964	0.773	0.957	0.957	0.885
		70	8.45	0.951	0.780	0.973	0.973	0.892
A3-B2-C8-D6	1.951	33	7.60	0.904	0.729	0.880	0.880	0.848
		55	9.02	0.954	0.767	0.945	0.945	0.880
		70	9.40	0.959	0.781	0.966	0.966	0.888
A3-B2-C9-D1	3.733	33	3.25	0.950	0.762	0.986	0.986	0.899
		55	3.37	0.915	0.778	0.994	0.994	0.900
		70	3.41	0.906	0.789	0.997	0.997	0.902
A3-B2-C9-D2	3.000	33	4.86	0.983	0.764	0.972	0.972	0.894
		55	5.14	0.931	0.774	0.990	0.990	0.899
		70	5.22	0.916	0.782	0.993	0.993	0.900
A3-B2-C9-D3	2.633	33	6.12	0.989	0.762	0.955	0.955	0.886
		55	6.57	0.944	0.773	0.984	0.984	0.897
		70	6.71	0.925	0.780	0.990	0.990	0.899
A3-B2-C9-D4	2.400	33	7.12	0.969	0.754	0.937	0.937	0.879
		55	7.82	0.956	0.774	0.977	0.977	0.895
		70	8.00	0.934	0.778	0.986	0.986	0.898
A3-B2-C9-D5	2.233	33	7.95	0.947	0.744	0.920	0.920	0.870
		55	8.92	0.968	0.775	0.968	0.968	0.890
		70	9.17	0.942	0.779	0.981	0.981	0.895
A3-B2-C9-D6	2.106	33	8.64	0.928	0.736	0.903	0.903	0.861
		55	9.90	0.967	0.774	0.960	0.960	0.886
		70	10.23	0.949	0.779	0.976	0.976	0.893



**Table E.3** Load Case 2 - Correlation of Design Procedures with the FEM Results

Frame*	$K_x$	$F_y$	$W_{FEM}$	$\frac{W_{1c}}{W_{FEM}}$	$\frac{W_{2a}}{W_{FEM}}$	$\frac{W_{2b}}{W_{FEM}}$	$\frac{W_{2c}}{W_{FEM}}$
		(ksi)	(kips)				
A1-B1-C1-D1	2.404	33	1.96	0.743	0.800	0.800	0.789
		55	2.90	0.714	0.820	0.820	0.804
		70	3.42	0.699	0.833	0.833	0.813
A1-B1-C1-D2	2.010	33	2.60	0.684	0.721	0.721	0.713
		55	3.76	0.697	0.767	0.767	0.755
		70	4.41	0.692	0.789	0.789	0.774
A1-B1-C1-D3	1.793	33	2.83	0.708	0.737	0.737	0.731
		55	4.39	0.681	0.733	0.733	0.723
		70	5.16	0.682	0.754	0.754	0.742
A1-B1-C1-D4	1.651	33	3.11	0.695	0.719	0.720	0.713
		55	4.88	0.669	0.710	0.711	0.701
		70	5.76	0.671	0.728	0.729	0.717
A1-B1-C1-D5	1.550	33	3.40	0.673	0.693	0.696	0.688
		55	5.16	0.673	0.708	0.711	0.700
		70	6.25	0.663	0.709	0.713	0.700
A1-B1-C1-D6	1.473	33	3.58	0.667	0.684	0.689	0.679
		55	5.62	0.649	0.678	0.682	0.671
		70	6.53	0.668	0.709	0.713	0.700
A1-B1-C2-D1	2.571	33	2.39	0.745	0.809	0.809	0.798
		55	3.51	0.714	0.832	0.832	0.814
		70	4.14	0.699	0.845	0.845	0.823
A1-B1-C2-D2	2.179	33	3.12	0.696	0.740	0.740	0.731
		55	4.45	0.708	0.794	0.794	0.780
		70	5.28	0.692	0.805	0.805	0.788
A1-B1-C2-D3	1.952	33	3.65	0.672	0.706	0.706	0.698
		55	5.21	0.694	0.759	0.759	0.747
		70	6.16	0.686	0.775	0.775	0.761
A1-B1-C2-D4	1.800	33	4.07	0.653	0.680	0.680	0.674
		55	5.85	0.678	0.731	0.731	0.721
		70	6.87	0.680	0.752	0.752	0.740
A1-B1-C2-D5	1.689	33	4.25	0.665	0.689	0.689	0.683
		55	6.35	0.669	0.713	0.713	0.704
		70	7.48	0.672	0.733	0.733	0.721
A1-B1-C2-D6	1.604	33	4.31	0.688	0.709	0.711	0.704
		55	6.77	0.661	0.699	0.701	0.690
		70	8.02	0.664	0.716	0.718	0.705

\*Frames are name as:



**Table E.3** (Continued)

Frame	$K_x$	$F_y$	$W_{FEM}$	$\frac{W_{1c}}{W_{FEM}}$	$\frac{W_{2a}}{W_{FEM}}$	$\frac{W_{2b}}{W_{FEM}}$	$\frac{W_{2c}}{W_{FEM}}$
		(ksi)	(kips)				
A1-B1-C3-D1	2.696	33	2.81	0.742	0.812	0.812	0.800
		55	4.10	0.713	0.840	0.840	0.821
		70	4.82	0.699	0.853	0.853	0.830
A1-B1-C3-D2	2.314	33	3.46	0.732	0.783	0.783	0.774
		55	5.14	0.706	0.803	0.803	0.788
		70	6.07	0.692	0.817	0.817	0.798
A1-B1-C3-D3	2.082	33	4.18	0.684	0.723	0.723	0.715
		55	5.93	0.705	0.781	0.781	0.768
		70	7.05	0.688	0.791	0.791	0.775
A1-B1-C3-D4	1.924	33	4.67	0.665	0.697	0.697	0.690
		55	6.71	0.685	0.747	0.747	0.736
		70	7.84	0.686	0.772	0.772	0.758
A1-B1-C3-D5	1.807	33	4.86	0.681	0.710	0.710	0.704
		55	7.30	0.676	0.729	0.729	0.719
		70	8.58	0.678	0.750	0.750	0.737
A1-B1-C3-D6	1.716	33	5.20	0.669	0.694	0.694	0.688
		55	7.82	0.668	0.713	0.713	0.704
		70	9.23	0.670	0.732	0.732	0.720
A1-B1-C4-D1	2.161	33	1.59	0.684	0.728	0.728	0.719
		55	2.30	0.684	0.770	0.770	0.756
		70	2.70	0.675	0.787	0.787	0.770
A1-B1-C4-D2	1.780	33	1.98	0.676	0.704	0.704	0.697
		55	3.00	0.665	0.717	0.717	0.706
		70	3.56	0.660	0.731	0.731	0.719
A1-B1-C4-D3	1.585	33	2.58	0.582	0.600	0.602	0.595
		55	3.38	0.670	0.707	0.710	0.699
		70	4.14	0.651	0.701	0.703	0.690
A1-B1-C4-D4	1.461	33	2.85	0.565	0.578	0.583	0.574
		55	3.84	0.640	0.667	0.672	0.660
		70	4.51	0.652	0.690	0.695	0.681
A1-B1-C4-D5	1.374	33	2.98	0.570	0.581	0.587	0.577
		55	4.16	0.624	0.646	0.653	0.640
		70	4.87	0.641	0.671	0.678	0.663
A1-B1-C4-D6	1.309	33	3.09	0.572	0.581	0.589	0.578
		55	4.48	0.607	0.624	0.632	0.618
		70	5.17	0.633	0.657	0.665	0.650

**Table E.3** (Continued)

Frame	$K_x$	$F_y$	$W_{FEM}$	$\frac{W_{1c}}{W_{FEM}}$	$\frac{W_{2a}}{W_{FEM}}$	$\frac{W_{2b}}{W_{FEM}}$	$\frac{W_{2c}}{W_{FEM}}$
		(ksi)	(kips)				
A1-B1-C5-D1	2.335	33	1.91	0.696	0.748	0.748	0.738
		55	2.75	0.688	0.789	0.789	0.773
		70	3.23	0.676	0.803	0.803	0.783
A1-B1-C5-D2	1.940	33	2.52	0.651	0.684	0.684	0.677
		55	3.59	0.672	0.737	0.737	0.725
		70	4.22	0.667	0.755	0.755	0.741
A1-B1-C5-D3	1.728	33	2.73	0.676	0.702	0.702	0.696
		55	4.22	0.654	0.700	0.700	0.690
		70	4.96	0.656	0.721	0.721	0.708
A1-B1-C5-D4	1.592	33	3.35	0.595	0.613	0.616	0.608
		55	4.52	0.667	0.705	0.707	0.696
		70	5.53	0.648	0.698	0.700	0.687
A1-B1-C5-D5	1.495	33	3.71	0.569	0.583	0.587	0.579
		55	4.90	0.656	0.686	0.691	0.678
		70	5.83	0.657	0.699	0.704	0.689
A1-B1-C5-D6	1.422	33	3.91	0.564	0.576	0.581	0.572
		55	5.34	0.631	0.655	0.661	0.648
		70	6.21	0.650	0.685	0.691	0.676
A1-B1-C6-D1	2.471	33	2.19	0.706	0.765	0.765	0.754
		55	3.18	0.688	0.798	0.798	0.781
		70	3.73	0.676	0.813	0.813	0.792
A1-B1-C6-D2	2.072	33	2.84	0.671	0.711	0.711	0.702
		55	4.11	0.677	0.753	0.753	0.740
		70	4.83	0.669	0.771	0.771	0.754
A1-B1-C6-D3	1.849	33	3.42	0.631	0.660	0.660	0.653
		55	4.81	0.665	0.721	0.721	0.710
		70	5.67	0.661	0.739	0.739	0.726
A1-B1-C6-D4	1.704	33	3.49	0.672	0.697	0.697	0.690
		55	5.35	0.657	0.702	0.702	0.692
		70	6.35	0.654	0.715	0.715	0.703
A1-B1-C6-D5	1.599	33	4.29	0.580	0.598	0.600	0.593
		55	5.71	0.658	0.696	0.698	0.687
		70	6.93	0.645	0.695	0.697	0.684
A1-B1-C6-D6	1.520	33	4.57	0.570	0.585	0.589	0.581
		55	6.16	0.642	0.674	0.678	0.666
		70	7.18	0.657	0.701	0.705	0.691

**Table E.3 (Continued)**

Frame	$K_x$	$F_y$	$W_{FEM}$	$\frac{W_{1c}}{W_{FEM}}$	$\frac{W_{2a}}{W_{FEM}}$	$\frac{W_{2b}}{W_{FEM}}$	$\frac{W_{2c}}{W_{FEM}}$
		(ksi)	(kips)				
A1-B1-C7-D1	2.431	33	2.14	0.704	0.758	0.758	0.748
		55	3.02	0.717	0.822	0.822	0.805
		70	3.55	0.708	0.842	0.842	0.820
A1-B1-C7-D2	2.032	33	2.92	0.636	0.670	0.670	0.663
		55	3.98	0.694	0.762	0.762	0.749
		70	4.64	0.701	0.794	0.794	0.777
A1-B1-C7-D3	1.813	33	3.58	0.586	0.611	0.611	0.605
		55	4.73	0.671	0.721	0.721	0.710
		70	5.48	0.690	0.758	0.758	0.744
A1-B1-C7-D4	1.670	33	4.04	0.562	0.582	0.582	0.577
		55	5.35	0.650	0.689	0.690	0.680
		70	6.16	0.677	0.731	0.732	0.719
A1-B1-C7-D5	1.568	33	4.00	0.603	0.620	0.623	0.616
		55	5.87	0.632	0.665	0.668	0.656
		70	6.73	0.666	0.710	0.713	0.699
A1-B1-C7-D6	1.490	33	4.48	0.563	0.577	0.582	0.573
		55	6.28	0.622	0.649	0.654	0.642
		70	7.21	0.656	0.694	0.698	0.684
A1-B1-C8-D1	2.606	33	2.55	0.722	0.785	0.785	0.774
		55	3.65	0.716	0.835	0.835	0.816
		70	4.27	0.707	0.854	0.854	0.831
A1-B1-C8-D2	2.209	33	3.40	0.664	0.706	0.706	0.698
		55	4.66	0.710	0.794	0.794	0.779
		70	5.49	0.703	0.815	0.815	0.796
A1-B1-C8-D3	1.978	33	4.13	0.619	0.650	0.650	0.643
		55	5.57	0.685	0.748	0.748	0.735
		70	6.48	0.695	0.781	0.781	0.765
A1-B1-C8-D4	1.824	33	4.77	0.583	0.609	0.609	0.603
		55	6.29	0.668	0.719	0.719	0.708
		70	7.29	0.687	0.756	0.756	0.741
A1-B1-C8-D5	1.713	33	5.26	0.563	0.584	0.584	0.579
		55	6.92	0.652	0.694	0.694	0.685
		70	7.98	0.677	0.735	0.735	0.722
A1-B1-C8-D6	1.627	33	5.57	0.558	0.577	0.578	0.572
		55	7.47	0.639	0.675	0.676	0.666
		70	8.59	0.669	0.718	0.720	0.706

**Table E.3** (Continued)

Frame	$K_x$	$F_y$	$W_{FEM}$	$\frac{W_{1c}}{W_{FEM}}$	$\frac{W_{2a}}{W_{FEM}}$	$\frac{W_{2b}}{W_{FEM}}$	$\frac{W_{2c}}{W_{FEM}}$
		(ksi)	(kips)				
A1-B1-C9-D1	2.739	33	2.94	0.731	0.802	0.802	0.790
		55	4.25	0.714	0.842	0.842	0.822
		70	4.97	0.704	0.861	0.861	0.836
A1-B1-C9-D2	2.351	33	3.85	0.681	0.730	0.730	0.721
		55	5.37	0.707	0.803	0.803	0.787
		70	6.30	0.700	0.825	0.825	0.805
A1-B1-C9-D3	2.115	33	4.63	0.642	0.679	0.679	0.672
		55	6.34	0.692	0.766	0.766	0.752
		70	7.38	0.696	0.797	0.797	0.780
A1-B1-C9-D4	1.954	33	5.33	0.608	0.638	0.638	0.632
		55	7.16	0.678	0.738	0.738	0.726
		70	8.30	0.691	0.773	0.773	0.757
A1-B1-C9-D5	1.836	33	5.95	0.581	0.607	0.607	0.601
		55	7.86	0.665	0.716	0.716	0.705
		70	9.10	0.684	0.753	0.753	0.739
A1-B1-C9-D6	1.744	33	6.47	0.563	0.585	0.585	0.580
		55	8.49	0.653	0.697	0.697	0.687
		70	9.79	0.677	0.737	0.737	0.724
A1-B2-C1-D1	2.404	33	1.95	0.735	0.793	0.793	0.783
		55	2.90	0.698	0.807	0.807	0.792
		70	3.42	0.680	0.815	0.815	0.797
A1-B2-C1-D2	2.010	33	2.60	0.675	0.713	0.713	0.705
		55	3.75	0.679	0.753	0.753	0.741
		70	4.40	0.669	0.768	0.768	0.754
A1-B2-C1-D3	1.793	33	3.06	0.645	0.673	0.673	0.667
		55	4.38	0.663	0.718	0.718	0.708
		70	5.18	0.652	0.729	0.729	0.717
A1-B2-C1-D4	1.651	33	3.19	0.667	0.691	0.692	0.685
		55	4.88	0.648	0.691	0.692	0.683
		70	5.76	0.644	0.704	0.705	0.694
A1-B2-C1-D5	1.550	33	3.39	0.665	0.684	0.688	0.680
		55	5.11	0.659	0.696	0.699	0.688
		70	6.27	0.633	0.682	0.685	0.673
A1-B2-C1-D6	1.473	33	4.05	0.581	0.595	0.600	0.591
		55	5.67	0.622	0.652	0.656	0.645
		70	6.52	0.640	0.683	0.687	0.675

**Table E.3** (Continued)

Frame	$K_x$	$F_y$	$W_{FEM}$	$\frac{W_{1c}}{W_{FEM}}$	$\frac{W_{2a}}{W_{FEM}}$	$\frac{W_{2b}}{W_{FEM}}$	$\frac{W_{2c}}{W_{FEM}}$
		(ksi)	(kips)				
A1-B2-C2-D1	2.571	33	2.39	0.736	0.802	0.802	0.791
		55	3.51	0.700	0.820	0.820	0.803
		70	4.14	0.683	0.829	0.829	0.809
A1-B2-C2-D2	2.179	33	2.99	0.717	0.764	0.764	0.755
		55	4.44	0.691	0.781	0.781	0.767
		70	5.28	0.671	0.786	0.786	0.770
A1-B2-C2-D3	1.952	33	3.64	0.664	0.698	0.698	0.691
		55	5.21	0.675	0.743	0.743	0.732
		70	6.15	0.662	0.754	0.754	0.741
A1-B2-C2-D4	1.800	33	4.02	0.652	0.680	0.680	0.674
		55	5.84	0.661	0.715	0.715	0.706
		70	6.87	0.653	0.730	0.730	0.718
A1-B2-C2-D5	1.689	33	4.24	0.657	0.681	0.681	0.675
		55	6.36	0.649	0.695	0.695	0.686
		70	7.49	0.644	0.708	0.708	0.698
A1-B2-C2-D6	1.604	33	4.34	0.672	0.693	0.695	0.688
		55	6.80	0.639	0.678	0.680	0.670
		70	8.02	0.637	0.691	0.693	0.682
A1-B2-C3-D1	2.696	33	2.80	0.736	0.808	0.808	0.797
		55	4.10	0.700	0.828	0.828	0.810
		70	4.82	0.684	0.838	0.838	0.816
A1-B2-C3-D2	2.314	33	3.42	0.731	0.784	0.784	0.775
		55	5.14	0.690	0.790	0.790	0.775
		70	6.07	0.674	0.800	0.800	0.782
A1-B2-C3-D3	2.082	33	4.16	0.677	0.717	0.717	0.710
		55	5.97	0.681	0.761	0.761	0.749
		70	7.05	0.666	0.771	0.771	0.756
A1-B2-C3-D4	1.924	33	4.67	0.656	0.689	0.689	0.682
		55	6.67	0.671	0.736	0.736	0.726
		70	7.87	0.659	0.748	0.748	0.735
A1-B2-C3-D5	1.807	33	5.09	0.642	0.669	0.669	0.664
		55	7.30	0.658	0.713	0.713	0.703
		70	8.58	0.652	0.728	0.728	0.717
A1-B2-C3-D6	1.716	33	5.04	0.681	0.707	0.707	0.701
		55	7.81	0.650	0.697	0.697	0.688
		70	9.22	0.644	0.710	0.710	0.700

**Table E.3** (Continued)

Frame	$K_x$	$F_y$	$W_{FEM}$	$\frac{W_{1c}}{W_{FEM}}$	$\frac{W_{2a}}{W_{FEM}}$	$\frac{W_{2b}}{W_{FEM}}$	$\frac{W_{2c}}{W_{FEM}}$
		(ksi)	(kips)				
A1-B2-C4-D1	2.161	33	1.56	0.689	0.733	0.733	0.725
		55	2.29	0.658	0.742	0.742	0.729
		70	2.70	0.631	0.733	0.733	0.718
A1-B2-C4-D2	1.780	33	2.03	0.653	0.680	0.680	0.674
		55	3.02	0.632	0.682	0.682	0.673
		70	3.55	0.612	0.678	0.678	0.667
A1-B2-C4-D3	1.585	33	2.58	0.574	0.591	0.593	0.586
		55	3.42	0.631	0.667	0.670	0.659
		70	4.13	0.599	0.646	0.648	0.637
A1-B2-C4-D4	1.461	33	2.89	0.549	0.562	0.567	0.558
		55	3.83	0.609	0.636	0.640	0.629
		70	4.47	0.602	0.638	0.642	0.630
A1-B2-C4-D5	1.374	33	3.04	0.550	0.560	0.566	0.557
		55	4.21	0.587	0.608	0.614	0.602
		70	4.87	0.587	0.615	0.621	0.608
A1-B2-C4-D6	1.309	33	3.08	0.564	0.573	0.580	0.569
		55	4.56	0.566	0.582	0.589	0.577
		70	5.18	0.578	0.600	0.607	0.594
A1-B2-C5-D1	2.335	33	1.88	0.698	0.751	0.751	0.741
		55	2.75	0.664	0.761	0.761	0.747
		70	3.23	0.637	0.753	0.753	0.736
A1-B2-C5-D2	1.940	33	2.50	0.649	0.682	0.682	0.675
		55	3.57	0.648	0.713	0.713	0.702
		70	4.22	0.622	0.705	0.705	0.692
A1-B2-C5-D3	1.728	33	2.74	0.664	0.690	0.690	0.684
		55	4.22	0.626	0.672	0.672	0.663
		70	4.95	0.609	0.670	0.670	0.660
A1-B2-C5-D4	1.592	33	3.35	0.588	0.606	0.608	0.601
		55	4.52	0.638	0.674	0.677	0.666
		70	5.51	0.600	0.648	0.650	0.639
A1-B2-C5-D5	1.495	33	3.74	0.557	0.571	0.575	0.567
		55	4.99	0.615	0.644	0.648	0.637
		70	5.83	0.607	0.646	0.650	0.638
A1-B2-C5-D6	1.422	33	3.94	0.552	0.564	0.569	0.560
		55	5.36	0.599	0.623	0.628	0.617
		70	6.17	0.603	0.636	0.641	0.628

**Table E.3** (Continued)

Frame	$K_x$	$F_y$	$W_{FEM}$	$\frac{W_{1c}}{W_{FEM}}$	$\frac{W_{2a}}{W_{FEM}}$	$\frac{W_{2b}}{W_{FEM}}$	$\frac{W_{2c}}{W_{FEM}}$
		(ksi)	(kips)				
A1-B2-C6-D1	2.471	33	2.17	0.704	0.764	0.764	0.754
		55	3.17	0.668	0.775	0.775	0.759
		70	3.73	0.642	0.767	0.767	0.749
A1-B2-C6-D2	2.072	33	2.81	0.672	0.712	0.712	0.704
		55	4.09	0.655	0.731	0.731	0.719
		70	4.82	0.630	0.724	0.724	0.710
A1-B2-C6-D3	1.849	33	3.15	0.678	0.709	0.709	0.702
		55	4.80	0.643	0.698	0.698	0.688
		70	5.65	0.620	0.694	0.694	0.682
A1-B2-C6-D4	1.704	33	3.49	0.664	0.688	0.688	0.682
		55	5.37	0.630	0.673	0.673	0.665
		70	6.34	0.610	0.669	0.669	0.659
A1-B2-C6-D5	1.599	33	4.20	0.586	0.604	0.606	0.599
		55	5.63	0.642	0.679	0.681	0.671
		70	6.87	0.605	0.653	0.655	0.644
A1-B2-C6-D6	1.520	33	4.63	0.556	0.571	0.574	0.567
		55	6.13	0.620	0.651	0.654	0.643
		70	7.19	0.611	0.652	0.655	0.643
A1-B2-C7-D1	2.431	33	2.13	0.706	0.760	0.760	0.750
		55	3.01	0.718	0.823	0.823	0.806
		70	3.54	0.709	0.843	0.843	0.822
A1-B2-C7-D2	2.032	33	2.92	0.636	0.671	0.671	0.663
		55	3.98	0.695	0.762	0.762	0.749
		70	4.63	0.702	0.795	0.795	0.778
A1-B2-C7-D3	1.813	33	3.59	0.583	0.608	0.608	0.602
		55	4.72	0.672	0.722	0.722	0.711
		70	5.48	0.690	0.758	0.758	0.744
A1-B2-C7-D4	1.670	33	4.07	0.558	0.578	0.578	0.573
		55	5.35	0.649	0.689	0.689	0.679
		70	6.16	0.678	0.731	0.732	0.719
A1-B2-C7-D5	1.568	33	4.28	0.563	0.580	0.583	0.575
		55	5.89	0.631	0.663	0.666	0.655
		70	6.73	0.665	0.710	0.713	0.699
A1-B2-C7-D6	1.490	33	4.52	0.559	0.573	0.577	0.569
		55	6.31	0.620	0.647	0.651	0.639
		70	7.23	0.654	0.692	0.696	0.681



**Table E.3 (Continued)**

Frame	$K_x$	$F_y$ (ksi)	$W_{FEM}$ (kips)	$\frac{W_{1c}}{W_{FEM}}$	$\frac{W_{2a}}{W_{FEM}}$	$\frac{W_{2b}}{W_{FEM}}$	$\frac{W_{2c}}{W_{FEM}}$
A1-B2-C8-D1	2.606	33	2.55	0.722	0.786	0.786	0.775
		55	3.64	0.716	0.835	0.835	0.816
		70	4.27	0.707	0.854	0.854	0.831
A1-B2-C8-D2	2.209	33	3.40	0.664	0.707	0.707	0.698
		55	4.70	0.705	0.788	0.788	0.773
		70	5.49	0.703	0.815	0.815	0.796
A1-B2-C8-D3	1.978	33	4.13	0.619	0.650	0.650	0.643
		55	5.57	0.685	0.748	0.748	0.735
		70	6.48	0.696	0.782	0.782	0.765
A1-B2-C8-D4	1.824	33	4.78	0.582	0.607	0.607	0.601
		55	6.30	0.668	0.719	0.719	0.708
		70	7.29	0.687	0.756	0.756	0.742
A1-B2-C8-D5	1.713	33	5.29	0.560	0.581	0.581	0.576
		55	6.92	0.653	0.695	0.695	0.685
		70	7.98	0.678	0.735	0.735	0.722
A1-B2-C8-D6	1.627	33	5.61	0.555	0.573	0.575	0.569
		55	7.48	0.638	0.674	0.676	0.665
		70	8.59	0.668	0.718	0.719	0.706
A1-B2-C9-D1	2.739	33	2.94	0.732	0.803	0.803	0.791
		55	4.25	0.714	0.842	0.842	0.822
		70	4.97	0.704	0.861	0.861	0.836
A1-B2-C9-D2	2.351	33	3.65	0.720	0.772	0.772	0.762
		55	5.37	0.707	0.804	0.804	0.787
		70	6.30	0.701	0.826	0.826	0.805
A1-B2-C9-D3	2.115	33	4.63	0.642	0.680	0.680	0.672
		55	6.34	0.693	0.767	0.767	0.753
		70	7.36	0.698	0.799	0.799	0.781
A1-B2-C9-D4	1.954	33	5.34	0.608	0.638	0.638	0.631
		55	7.15	0.679	0.739	0.739	0.727
		70	8.30	0.691	0.773	0.773	0.758
A1-B2-C9-D5	1.836	33	5.97	0.579	0.605	0.605	0.599
		55	7.86	0.665	0.716	0.716	0.705
		70	9.10	0.684	0.753	0.753	0.739
A1-B2-C9-D6	1.744	33	6.48	0.562	0.584	0.584	0.579
		55	8.49	0.653	0.697	0.697	0.687
		70	9.79	0.676	0.737	0.737	0.724

**Table E.3** (Continued)

Frame	$K_x$	$F_y$	$W_{FEM}$	$\frac{W_{1c}}{W_{FEM}}$	$\frac{W_{2a}}{W_{FEM}}$	$\frac{W_{2b}}{W_{FEM}}$	$\frac{W_{2c}}{W_{FEM}}$
		(ksi)	(kips)				
A2-B1-C1-D1	2.561	33	1.66	0.754	0.814	0.814	0.804
		55	2.48	0.718	0.830	0.830	0.813
		70	2.92	0.706	0.845	0.845	0.825
A2-B1-C1-D2	2.119	33	2.10	0.740	0.781	0.781	0.773
		55	3.25	0.704	0.779	0.779	0.766
		70	3.82	0.697	0.799	0.799	0.783
A2-B1-C1-D3	1.885	33	2.73	0.645	0.672	0.672	0.666
		55	3.63	0.725	0.783	0.783	0.772
		70	4.39	0.705	0.784	0.784	0.771
A2-B1-C1-D4	1.736	33	3.05	0.627	0.649	0.649	0.644
		55	4.27	0.673	0.718	0.718	0.709
		70	4.81	0.709	0.773	0.773	0.761
A2-B1-C1-D5	1.631	33	3.08	0.658	0.678	0.680	0.673
		55	4.65	0.661	0.698	0.699	0.689
		70	5.40	0.678	0.730	0.731	0.719
A2-B1-C1-D6	1.552	33	3.10	0.683	0.701	0.705	0.696
		55	4.95	0.652	0.684	0.687	0.676
		70	5.78	0.668	0.711	0.715	0.702
A2-B1-C2-D1	2.755	33	2.04	0.745	0.813	0.813	0.802
		55	2.97	0.720	0.844	0.844	0.826
		70	3.51	0.704	0.856	0.856	0.833
A2-B1-C2-D2	2.305	33	2.53	0.747	0.796	0.796	0.786
		55	3.87	0.706	0.796	0.796	0.782
		70	4.55	0.699	0.817	0.817	0.799
A2-B1-C2-D3	2.056	33	2.93	0.732	0.770	0.770	0.762
		55	4.41	0.718	0.788	0.788	0.776
		70	5.35	0.691	0.786	0.786	0.771
A2-B1-C2-D4	1.893	33	3.48	0.672	0.701	0.701	0.695
		55	4.87	0.716	0.774	0.774	0.763
		70	5.82	0.705	0.785	0.785	0.772
A2-B1-C2-D5	1.777	33	4.04	0.616	0.639	0.639	0.634
		55	5.54	0.676	0.723	0.723	0.713
		70	6.27	0.706	0.774	0.774	0.762
A2-B1-C2-D6	1.688	33	4.10	0.639	0.660	0.660	0.655
		55	5.96	0.663	0.704	0.704	0.695
		70	6.90	0.681	0.738	0.738	0.727

**Table E.3** (Continued)

Frame	$K_x$	$F_y$	$W_{FEM}$	$\frac{W_{1c}}{W_{FEM}}$	$\frac{W_{2a}}{W_{FEM}}$	$\frac{W_{2b}}{W_{FEM}}$	$\frac{W_{2c}}{W_{FEM}}$
		(ksi)	(kips)				
A2-B1-C3-D1	2.904	33	2.34	0.752	0.828	0.828	0.816
		55	3.45	0.717	0.850	0.850	0.831
		70	4.06	0.703	0.863	0.863	0.839
A2-B1-C3-D2	2.456	33	3.11	0.705	0.757	0.757	0.747
		55	4.43	0.709	0.811	0.811	0.795
		70	5.20	0.699	0.829	0.829	0.810
A2-B1-C3-D3	2.198	33	3.37	0.739	0.783	0.783	0.774
		55	5.21	0.697	0.778	0.778	0.764
		70	6.11	0.693	0.800	0.800	0.784
A2-B1-C3-D4	2.026	33	3.74	0.728	0.765	0.765	0.757
		55	5.64	0.715	0.783	0.783	0.770
		70	6.85	0.688	0.779	0.779	0.764
A2-B1-C3-D5	1.901	33	4.03	0.722	0.754	0.754	0.747
		55	6.14	0.707	0.765	0.765	0.754
		70	7.30	0.699	0.779	0.779	0.766
A2-B1-C3-D6	1.805	33	4.96	0.618	0.642	0.642	0.636
		55	6.72	0.685	0.734	0.734	0.724
		70	7.72	0.704	0.774	0.774	0.762
A2-B1-C4-D1	2.285	33	1.32	0.714	0.761	0.761	0.752
		55	1.96	0.697	0.789	0.789	0.774
		70	2.32	0.683	0.800	0.800	0.782
A2-B1-C4-D2	1.872	33	1.92	0.613	0.640	0.640	0.634
		55	2.62	0.668	0.723	0.723	0.712
		70	3.08	0.669	0.745	0.745	0.732
A2-B1-C4-D3	1.667	33	2.06	0.642	0.663	0.664	0.657
		55	3.08	0.649	0.688	0.689	0.679
		70	3.59	0.661	0.716	0.716	0.704
A2-B1-C4-D4	1.539	33	2.04	0.699	0.717	0.721	0.712
		55	3.39	0.639	0.669	0.673	0.662
		70	3.95	0.656	0.699	0.703	0.689
A2-B1-C4-D5	1.451	33	2.47	0.607	0.620	0.626	0.616
		55	3.45	0.667	0.693	0.699	0.686
		70	4.24	0.650	0.685	0.690	0.676
A2-B1-C4-D6	1.386	33	2.53	0.618	0.629	0.636	0.625
		55	3.49	0.687	0.710	0.717	0.703
		70	4.26	0.678	0.709	0.716	0.700

**Table E.3** (Continued)

Frame	$K_x$	$F_y$	$W_{FEM}$	$\frac{W_{1c}}{W_{FEM}}$	$\frac{W_{2a}}{W_{FEM}}$	$\frac{W_{2b}}{W_{FEM}}$	$\frac{W_{2c}}{W_{FEM}}$
		(ksi)	(kips)				
A2-B1-C5-D1	2.479	33	1.58	0.722	0.779	0.779	0.769
		55	2.36	0.691	0.797	0.797	0.780
		70	2.77	0.681	0.813	0.813	0.793
A2-B1-C5-D2	2.043	33	2.21	0.649	0.683	0.683	0.676
		55	3.11	0.676	0.745	0.745	0.733
		70	3.65	0.673	0.767	0.767	0.752
A2-B1-C5-D3	1.817	33	2.71	0.598	0.622	0.622	0.616
		55	3.67	0.661	0.711	0.711	0.701
		70	4.30	0.664	0.735	0.735	0.722
A2-B1-C5-D4	1.675	33	2.75	0.639	0.660	0.661	0.655
		55	4.10	0.647	0.686	0.687	0.677
		70	4.78	0.660	0.715	0.716	0.704
A2-B1-C5-D5	1.575	33	2.75	0.678	0.697	0.700	0.691
		55	4.42	0.640	0.673	0.676	0.665
		70	5.16	0.655	0.701	0.704	0.691
A2-B1-C5-D6	1.501	33	2.80	0.697	0.714	0.719	0.709
		55	4.52	0.659	0.688	0.692	0.680
		70	5.47	0.651	0.690	0.694	0.680
A2-B1-C6-D1	2.635	33	1.86	0.710	0.773	0.773	0.762
		55	2.71	0.691	0.806	0.806	0.789
		70	3.18	0.679	0.821	0.821	0.800
A2-B1-C6-D2	2.186	33	2.49	0.668	0.708	0.708	0.700
		55	3.55	0.682	0.763	0.763	0.749
		70	4.15	0.678	0.785	0.785	0.768
A2-B1-C6-D3	1.946	33	3.02	0.627	0.657	0.657	0.650
		55	4.19	0.670	0.729	0.729	0.718
		70	4.91	0.669	0.752	0.752	0.738
A2-B1-C6-D4	1.792	33	3.44	0.599	0.623	0.623	0.617
		55	4.70	0.657	0.704	0.704	0.694
		70	5.50	0.663	0.730	0.730	0.718
A2-B1-C6-D5	1.684	33	3.42	0.642	0.663	0.664	0.657
		55	5.13	0.645	0.685	0.685	0.676
		70	5.97	0.659	0.715	0.715	0.703
A2-B1-C6-D6	1.602	33	3.44	0.669	0.689	0.691	0.683
		55	5.45	0.640	0.674	0.677	0.666
		70	6.35	0.655	0.703	0.705	0.692

**Table E.3 (Continued)**

Frame	$K_x$	$F_y$	$W_{FEM}$	$\frac{W_{1c}}{W_{FEM}}$	$\frac{W_{2a}}{W_{FEM}}$	$\frac{W_{2b}}{W_{FEM}}$	$\frac{W_{2c}}{W_{FEM}}$
		(ksi)	(kips)				
A2-B1-C7-D1	2.589	33	1.87	0.690	0.746	0.746	0.736
		55	2.60	0.711	0.821	0.821	0.804
		70	3.04	0.708	0.846	0.846	0.824
A2-B1-C7-D2	2.143	33	2.62	0.618	0.653	0.653	0.646
		55	3.33	0.722	0.796	0.796	0.782
		70	4.03	0.699	0.797	0.797	0.780
A2-B1-C7-D3	1.907	33	3.19	0.576	0.601	0.601	0.595
		55	4.15	0.668	0.720	0.720	0.709
		70	4.78	0.690	0.762	0.762	0.748
A2-B1-C7-D4	1.757	33	3.42	0.583	0.604	0.604	0.599
		55	4.70	0.649	0.690	0.690	0.681
		70	5.38	0.680	0.737	0.737	0.725
A2-B1-C7-D5	1.651	33	3.58	0.592	0.611	0.612	0.606
		55	5.12	0.638	0.673	0.674	0.664
		70	5.86	0.671	0.719	0.720	0.707
A2-B1-C7-D6	1.571	33	3.70	0.601	0.618	0.621	0.613
		55	5.37	0.641	0.671	0.674	0.663
		70	6.26	0.664	0.705	0.708	0.695
A2-B1-C8-D1	2.792	33	2.20	0.708	0.775	0.775	0.763
		55	3.10	0.714	0.838	0.838	0.819
		70	3.63	0.705	0.858	0.858	0.834
A2-B1-C8-D2	2.336	33	2.77	0.708	0.754	0.754	0.745
		55	4.10	0.696	0.784	0.784	0.768
		70	4.76	0.700	0.817	0.817	0.797
A2-B1-C8-D3	2.084	33	3.69	0.605	0.637	0.637	0.630
		55	4.89	0.681	0.746	0.746	0.733
		70	5.61	0.698	0.790	0.790	0.773
A2-B1-C8-D4	1.920	33	4.24	0.574	0.600	0.600	0.594
		55	5.53	0.665	0.718	0.718	0.707
		70	6.36	0.687	0.760	0.760	0.745
A2-B1-C8-D5	1.802	33	4.49	0.580	0.602	0.602	0.597
		55	6.09	0.650	0.695	0.695	0.684
		70	6.97	0.679	0.741	0.741	0.728
A2-B1-C8-D6	1.713	33	4.67	0.587	0.607	0.607	0.602
		55	6.53	0.641	0.680	0.680	0.671
		70	7.49	0.672	0.725	0.725	0.713

**Table E.3** (Continued)

Frame	$K_x$	$F_y$	$W_{FEM}$	$\frac{W_{1c}}{W_{FEM}}$	$\frac{W_{2a}}{W_{FEM}}$	$\frac{W_{2b}}{W_{FEM}}$	$\frac{W_{2c}}{W_{FEM}}$
		(ksi)	(kips)				
A2-B1-C9-D1	2.950	33	2.52	0.717	0.793	0.793	0.781
		55	3.59	0.711	0.845	0.845	0.825
		70	4.19	0.703	0.865	0.865	0.840
A2-B1-C9-D2	2.495	33	3.37	0.670	0.721	0.721	0.711
		55	4.66	0.699	0.800	0.800	0.784
		70	5.41	0.701	0.831	0.831	0.810
A2-B1-C9-D3	2.233	33	3.59	0.720	0.764	0.764	0.755
		55	5.52	0.690	0.768	0.768	0.754
		70	6.42	0.693	0.799	0.799	0.781
A2-B1-C9-D4	2.058	33	4.78	0.592	0.623	0.623	0.616
		55	6.28	0.674	0.737	0.737	0.724
		70	7.10	0.702	0.791	0.791	0.775
A2-B1-C9-D5	1.932	33	5.29	0.573	0.599	0.599	0.593
		55	6.90	0.662	0.716	0.716	0.705
		70	7.94	0.683	0.757	0.757	0.743
A2-B1-C9-D6	1.835	33	5.55	0.577	0.600	0.600	0.594
		55	7.47	0.650	0.697	0.697	0.686
		70	8.56	0.677	0.742	0.742	0.728
A2-B2-C1-D1	2.561	33	1.71	0.722	0.782	0.782	0.772
		55	2.47	0.706	0.820	0.820	0.804
		70	2.91	0.690	0.831	0.831	0.811
A2-B2-C1-D2	2.119	33	2.09	0.736	0.778	0.778	0.770
		55	3.18	0.701	0.781	0.781	0.769
		70	3.82	0.676	0.780	0.780	0.766
A2-B2-C1-D3	1.885	33	2.79	0.623	0.650	0.650	0.644
		55	3.65	0.701	0.761	0.761	0.751
		70	4.38	0.680	0.763	0.763	0.751
A2-B2-C1-D4	1.736	33	3.03	0.621	0.643	0.643	0.638
		55	4.28	0.654	0.701	0.701	0.692
		70	4.82	0.680	0.749	0.749	0.738
A2-B2-C1-D5	1.631	33	3.09	0.647	0.667	0.668	0.662
		55	4.70	0.635	0.673	0.675	0.666
		70	5.40	0.651	0.706	0.708	0.697
A2-B2-C1-D6	1.552	33	3.02	0.690	0.709	0.712	0.704
		55	4.96	0.632	0.665	0.668	0.658
		70	5.81	0.638	0.684	0.687	0.675

**Table E.3** (Continued)

Frame	$K_x$	$F_y$	$W_{FEM}$	$\frac{W_{1c}}{W_{FEM}}$	$\frac{W_{2a}}{W_{FEM}}$	$\frac{W_{2b}}{W_{FEM}}$	$\frac{W_{2c}}{W_{FEM}}$
		(ksi)	(kips)				
A2-B2-C2-D1	2.755	33	2.02	0.743	0.815	0.815	0.803
		55	2.97	0.708	0.834	0.834	0.817
		70	3.50	0.691	0.842	0.842	0.821
A2-B2-C2-D2	2.305	33	2.52	0.741	0.791	0.791	0.782
		55	3.86	0.692	0.786	0.786	0.772
		70	4.54	0.682	0.801	0.801	0.784
A2-B2-C2-D3	2.056	33	3.26	0.649	0.684	0.684	0.677
		55	4.42	0.698	0.773	0.773	0.761
		70	5.34	0.671	0.768	0.768	0.754
A2-B2-C2-D4	1.893	33	3.72	0.620	0.648	0.648	0.642
		55	4.84	0.702	0.764	0.764	0.753
		70	5.84	0.678	0.761	0.761	0.749
A2-B2-C2-D5	1.777	33	3.45	0.711	0.739	0.739	0.733
		55	5.53	0.659	0.708	0.708	0.699
		70	6.29	0.678	0.750	0.750	0.738
A2-B2-C2-D6	1.688	33	4.09	0.630	0.652	0.652	0.647
		55	6.01	0.640	0.682	0.682	0.674
		70	6.91	0.654	0.715	0.715	0.705
A2-B2-C3-D1	2.904	33	2.34	0.743	0.823	0.823	0.810
		55	3.45	0.707	0.841	0.841	0.822
		70	4.06	0.691	0.850	0.850	0.828
A2-B2-C3-D2	2.456	33	3.09	0.701	0.755	0.755	0.745
		55	4.41	0.697	0.801	0.801	0.786
		70	5.19	0.684	0.815	0.815	0.796
A2-B2-C3-D3	2.198	33	3.36	0.733	0.778	0.778	0.770
		55	5.19	0.684	0.768	0.768	0.755
		70	6.10	0.675	0.785	0.785	0.769
A2-B2-C3-D4	2.026	33	3.79	0.711	0.748	0.748	0.740
		55	5.64	0.696	0.767	0.767	0.756
		70	6.75	0.676	0.771	0.771	0.757
A2-B2-C3-D5	1.901	33	4.64	0.619	0.647	0.647	0.641
		55	6.09	0.695	0.757	0.757	0.746
		70	7.30	0.675	0.759	0.759	0.746
A2-B2-C3-D6	1.805	33	5.04	0.600	0.624	0.624	0.619
		55	6.81	0.659	0.710	0.710	0.700
		70	7.73	0.678	0.753	0.753	0.741

**Table E.3 (Continued)**

Frame	$K_x$	$F_y$	$W_{FEM}$	$\frac{W_{1c}}{W_{FEM}}$	$\frac{W_{2a}}{W_{FEM}}$	$\frac{W_{2b}}{W_{FEM}}$	$\frac{W_{2c}}{W_{FEM}}$
		(ksi)	(kips)				
A2-B2-C4-D1	2.285	33	1.38	0.678	0.724	0.724	0.715
		55	1.96	0.670	0.759	0.759	0.745
		70	2.32	0.640	0.746	0.746	0.731
A2-B2-C4-D2	1.872	33	1.96	0.595	0.621	0.621	0.615
		55	2.63	0.638	0.691	0.691	0.682
		70	3.08	0.619	0.690	0.690	0.678
A2-B2-C4-D3	1.667	33	2.05	0.635	0.656	0.656	0.650
		55	3.11	0.612	0.650	0.651	0.642
		70	3.62	0.603	0.655	0.655	0.645
A2-B2-C4-D4	1.539	33	2.04	0.687	0.705	0.709	0.700
		55	3.38	0.612	0.641	0.645	0.634
		70	3.98	0.598	0.638	0.641	0.629
A2-B2-C4-D5	1.451	33	2.50	0.592	0.605	0.610	0.601
		55	3.41	0.642	0.667	0.673	0.661
		70	4.19	0.604	0.637	0.642	0.630
A2-B2-C4-D6	1.386	33	2.55	0.602	0.613	0.620	0.609
		55	3.79	0.603	0.623	0.629	0.617
		70	4.29	0.618	0.646	0.652	0.639
A2-B2-C5-D1	2.479	33	1.58	0.718	0.776	0.776	0.766
		55	2.35	0.671	0.773	0.773	0.758
		70	2.77	0.643	0.763	0.763	0.746
A2-B2-C5-D2	2.043	33	2.20	0.644	0.678	0.678	0.671
		55	3.11	0.651	0.719	0.719	0.708
		70	3.65	0.631	0.717	0.717	0.704
A2-B2-C5-D3	1.817	33	2.65	0.606	0.630	0.630	0.624
		55	3.68	0.632	0.681	0.681	0.672
		70	4.30	0.618	0.683	0.683	0.672
A2-B2-C5-D4	1.675	33	2.75	0.632	0.653	0.654	0.648
		55	4.10	0.621	0.660	0.660	0.651
		70	4.78	0.611	0.664	0.664	0.654
A2-B2-C5-D5	1.575	33	2.76	0.666	0.685	0.688	0.680
		55	4.42	0.613	0.645	0.648	0.638
		70	5.15	0.607	0.650	0.652	0.641
A2-B2-C5-D6	1.501	33	3.26	0.591	0.605	0.609	0.600
		55	4.52	0.630	0.658	0.662	0.651
		70	5.47	0.602	0.638	0.642	0.630



**Table E.3** (Continued)

Frame	$K_x$	$F_y$	$W_{FEM}$	$\frac{W_{1c}}{W_{FEM}}$	$\frac{W_{2a}}{W_{FEM}}$	$\frac{W_{2b}}{W_{FEM}}$	$\frac{W_{2c}}{W_{FEM}}$
		(ksi)	(kips)				
A2-B2-C6-D1	2.635	33	1.84	0.710	0.775	0.775	0.764
		55	2.70	0.673	0.785	0.785	0.769
		70	3.18	0.646	0.776	0.776	0.757
A2-B2-C6-D2	2.186	33	2.48	0.666	0.707	0.707	0.699
		55	3.53	0.662	0.742	0.742	0.729
		70	4.16	0.638	0.736	0.736	0.722
A2-B2-C6-D3	1.946	33	3.03	0.617	0.647	0.647	0.640
		55	4.18	0.647	0.707	0.707	0.696
		70	4.91	0.628	0.705	0.705	0.693
A2-B2-C6-D4	1.792	33	3.43	0.595	0.619	0.619	0.613
		55	4.72	0.631	0.678	0.678	0.668
		70	5.50	0.619	0.682	0.682	0.671
A2-B2-C6-D5	1.684	33	3.41	0.636	0.658	0.658	0.652
		55	5.13	0.621	0.660	0.660	0.651
		70	5.96	0.614	0.667	0.668	0.658
A2-B2-C6-D6	1.602	33	3.46	0.657	0.676	0.679	0.671
		55	5.48	0.613	0.646	0.648	0.638
		70	6.36	0.610	0.655	0.657	0.646
A2-B2-C7-D1	2.589	33	1.86	0.694	0.750	0.750	0.740
		55	2.60	0.712	0.822	0.822	0.805
		70	3.03	0.708	0.847	0.847	0.825
A2-B2-C7-D2	2.143	33	2.62	0.618	0.653	0.653	0.645
		55	3.47	0.692	0.763	0.763	0.750
		70	4.03	0.699	0.797	0.797	0.780
A2-B2-C7-D3	1.907	33	3.20	0.573	0.598	0.598	0.592
		55	4.15	0.668	0.720	0.720	0.709
		70	4.78	0.690	0.762	0.762	0.748
A2-B2-C7-D4	1.757	33	3.45	0.578	0.599	0.599	0.594
		55	4.71	0.647	0.688	0.688	0.679
		70	5.38	0.679	0.736	0.736	0.724
A2-B2-C7-D5	1.651	33	3.61	0.587	0.606	0.607	0.601
		55	5.14	0.635	0.670	0.671	0.661
		70	5.87	0.670	0.718	0.719	0.707
A2-B2-C7-D6	1.571	33	3.73	0.596	0.613	0.615	0.608
		55	5.40	0.636	0.666	0.669	0.658
		70	6.29	0.661	0.702	0.705	0.692

**Table E.3 (Continued)**

Frame	$K_x$	$F_y$ (ksi)	$W_{FEM}$ (kips)	$\frac{W_{1c}}{W_{FEM}}$	$\frac{W_{2a}}{W_{FEM}}$	$\frac{W_{2b}}{W_{FEM}}$	$\frac{W_{2c}}{W_{FEM}}$
A2-B2-C8-D1	2.792	33	2.20	0.710	0.776	0.776	0.765
		55	3.10	0.714	0.839	0.839	0.820
		70	3.63	0.705	0.858	0.858	0.834
A2-B2-C8-D2	2.336	33	2.83	0.691	0.737	0.737	0.728
		55	4.09	0.698	0.785	0.785	0.770
		70	4.76	0.701	0.817	0.817	0.798
A2-B2-C8-D3	2.084	33	3.69	0.604	0.636	0.636	0.629
		55	4.89	0.681	0.746	0.746	0.733
		70	5.60	0.699	0.790	0.790	0.774
A2-B2-C8-D4	1.920	33	4.26	0.572	0.597	0.597	0.592
		55	5.53	0.666	0.718	0.718	0.707
		70	6.37	0.686	0.759	0.759	0.745
A2-B2-C8-D5	1.802	33	4.52	0.576	0.598	0.598	0.592
		55	6.10	0.649	0.693	0.693	0.683
		70	6.97	0.679	0.740	0.740	0.727
A2-B2-C8-D6	1.713	33	4.70	0.583	0.603	0.603	0.598
		55	6.55	0.640	0.678	0.678	0.669
		70	7.48	0.673	0.726	0.726	0.714
A2-B2-C9-D1	2.950	33	2.52	0.717	0.793	0.793	0.780
		55	3.59	0.712	0.846	0.846	0.825
		70	4.19	0.703	0.866	0.866	0.841
A2-B2-C9-D2	2.495	33	3.38	0.668	0.719	0.719	0.709
		55	4.66	0.700	0.801	0.801	0.784
		70	5.41	0.701	0.831	0.831	0.810
A2-B2-C9-D3	2.233	33	4.12	0.628	0.666	0.666	0.658
		55	5.52	0.690	0.768	0.768	0.754
		70	6.42	0.694	0.799	0.799	0.781
A2-B2-C9-D4	2.058	33	4.78	0.592	0.622	0.622	0.616
		55	6.27	0.674	0.737	0.737	0.725
		70	7.11	0.701	0.791	0.791	0.774
A2-B2-C9-D5	1.932	33	5.31	0.571	0.597	0.597	0.591
		55	6.91	0.662	0.715	0.715	0.704
		70	7.95	0.683	0.757	0.757	0.742
A2-B2-C9-D6	1.835	33	5.58	0.573	0.596	0.596	0.591
		55	7.48	0.650	0.696	0.696	0.686
		70	8.56	0.677	0.742	0.742	0.728

**Table E.3** (Continued)

Frame	$K_x$	$F_y$	$W_{FEM}$	$\frac{W_{1c}}{W_{FEM}}$	$\frac{W_{2a}}{W_{FEM}}$	$\frac{W_{2b}}{W_{FEM}}$	$\frac{W_{2c}}{W_{FEM}}$
		(ksi)	(kips)				
A3-B1-C1-D1	3.136	33	0.70	0.710	0.800	0.800	0.787
		55	1.00	0.691	0.842	0.842	0.820
		70	1.17	0.679	0.859	0.859	0.832
A3-B1-C1-D2	2.506	33	0.99	0.679	0.734	0.734	0.725
		55	1.39	0.686	0.795	0.795	0.778
		70	1.62	0.679	0.816	0.816	0.796
A3-B1-C1-D3	2.195	33	1.08	0.726	0.771	0.771	0.762
		55	1.67	0.680	0.763	0.763	0.749
		70	1.96	0.673	0.783	0.783	0.766
A3-B1-C1-D4	1.999	33	1.22	0.713	0.750	0.750	0.742
		55	1.91	0.672	0.738	0.738	0.726
		70	2.17	0.689	0.783	0.783	0.768
A3-B1-C1-D5	1.860	33	1.37	0.682	0.712	0.712	0.706
		55	1.99	0.701	0.759	0.759	0.748
		70	2.40	0.683	0.761	0.761	0.748
A3-B1-C1-D6	1.756	33	1.41	0.702	0.729	0.729	0.723
		55	2.27	0.653	0.700	0.700	0.691
		70	2.63	0.667	0.732	0.732	0.721
A3-B1-C2-D1	3.441	33	0.82	0.713	0.820	0.820	0.804
		55	1.17	0.690	0.857	0.857	0.833
		70	1.36	0.677	0.871	0.871	0.842
A3-B1-C2-D2	2.757	33	1.09	0.725	0.795	0.795	0.784
		55	1.61	0.689	0.815	0.815	0.796
		70	1.88	0.679	0.833	0.833	0.810
A3-B1-C2-D3	2.417	33	1.35	0.693	0.745	0.745	0.736
		55	1.96	0.681	0.782	0.782	0.767
		70	2.28	0.676	0.805	0.805	0.786
A3-B1-C2-D4	2.202	33	1.46	0.716	0.760	0.760	0.752
		55	2.24	0.676	0.758	0.758	0.745
		70	2.61	0.671	0.781	0.781	0.765
A3-B1-C2-D5	2.048	33	1.63	0.692	0.730	0.730	0.723
		55	2.36	0.704	0.777	0.777	0.764
		70	2.82	0.686	0.784	0.784	0.769
A3-B1-C2-D6	1.932	33	1.69	0.710	0.744	0.744	0.737
		55	2.58	0.690	0.752	0.752	0.741
		70	3.03	0.688	0.774	0.774	0.760

**Table E.3 (Continued)**

Frame	$K_x$	$F_y$	$W_{FEM}$	$\frac{W_{1c}}{W_{FEM}}$	$\frac{W_{2a}}{W_{FEM}}$	$\frac{W_{2b}}{W_{FEM}}$	$\frac{W_{2c}}{W_{FEM}}$
		(ksi)	(kips)				
A3-B1-C3-D1	3.694	33	0.92	0.716	0.835	0.835	0.818
		55	1.32	0.686	0.863	0.863	0.837
		70	1.53	0.675	0.879	0.879	0.848
A3-B1-C3-D2	2.969	33	1.28	0.702	0.781	0.781	0.769
		55	1.81	0.688	0.827	0.827	0.807
		70	2.12	0.677	0.844	0.844	0.819
A3-B1-C3-D3	2.605	33	1.58	0.676	0.735	0.735	0.725
		55	2.20	0.684	0.798	0.798	0.781
		70	2.56	0.676	0.819	0.819	0.798
A3-B1-C3-D4	2.374	33	1.64	0.727	0.779	0.779	0.770
		55	2.52	0.678	0.774	0.774	0.759
		70	2.94	0.673	0.797	0.797	0.778
A3-B1-C3-D5	2.209	33	2.00	0.649	0.690	0.690	0.682
		55	2.69	0.701	0.786	0.786	0.772
		70	3.26	0.669	0.779	0.779	0.762
A3-B1-C3-D6	2.083	33	2.04	0.680	0.718	0.718	0.711
		55	2.91	0.697	0.771	0.771	0.758
		70	3.53	0.670	0.768	0.768	0.753
A3-B1-C4-D1	2.730	33	0.58	0.678	0.747	0.747	0.735
		55	0.83	0.663	0.789	0.789	0.770
		70	0.97	0.653	0.806	0.806	0.783
A3-B1-C4-D2	2.175	33	0.83	0.630	0.670	0.670	0.662
		55	1.15	0.659	0.742	0.742	0.728
		70	1.34	0.654	0.763	0.763	0.746
A3-B1-C4-D3	1.905	33	1.02	0.592	0.620	0.620	0.614
		55	1.39	0.643	0.701	0.701	0.690
		70	1.62	0.647	0.729	0.729	0.715
A3-B1-C4-D4	1.737	33	1.03	0.647	0.671	0.671	0.665
		55	1.59	0.626	0.671	0.671	0.662
		70	1.83	0.644	0.707	0.707	0.695
A3-B1-C4-D5	1.621	33	1.17	0.607	0.626	0.628	0.621
		55	1.68	0.636	0.674	0.676	0.665
		70	1.98	0.643	0.695	0.696	0.684
A3-B1-C4-D6	1.535	33	1.20	0.620	0.637	0.640	0.632
		55	1.67	0.679	0.712	0.716	0.704
		70	2.10	0.642	0.685	0.689	0.675

**Table E.3** (Continued)

Frame	$K_x$	$F_y$	$W_{FEM}$	$\frac{W_{1c}}{W_{FEM}}$	$\frac{W_{2a}}{W_{FEM}}$	$\frac{W_{2b}}{W_{FEM}}$	$\frac{W_{2c}}{W_{FEM}}$
		(ksi)	(kips)				
A3-B1-C5-D1	3.002	33	0.67	0.685	0.772	0.772	0.758
		55	0.96	0.665	0.809	0.809	0.788
		70	1.12	0.655	0.825	0.825	0.800
A3-B1-C5-D2	2.396	33	0.94	0.662	0.714	0.714	0.704
		55	1.33	0.664	0.765	0.765	0.749
		70	1.56	0.656	0.783	0.783	0.764
A3-B1-C5-D3	2.098	33	1.22	0.596	0.631	0.631	0.624
		55	1.62	0.656	0.731	0.731	0.718
		70	1.89	0.653	0.754	0.754	0.738
A3-B1-C5-D4	1.911	33	1.37	0.590	0.618	0.618	0.612
		55	1.85	0.644	0.702	0.702	0.691
		70	2.15	0.648	0.730	0.730	0.716
A3-B1-C5-D5	1.780	33	1.36	0.638	0.664	0.664	0.657
		55	2.05	0.633	0.680	0.680	0.671
		70	2.38	0.642	0.709	0.709	0.697
A3-B1-C5-D6	1.682	33	1.42	0.646	0.669	0.669	0.663
		55	2.19	0.628	0.669	0.670	0.660
		70	2.54	0.642	0.700	0.700	0.688
A3-B1-C6-D1	3.231	33	0.75	0.695	0.794	0.794	0.779
		55	1.09	0.659	0.812	0.812	0.790
		70	1.26	0.654	0.835	0.835	0.808
A3-B1-C6-D2	2.583	33	1.04	0.679	0.741	0.741	0.730
		55	1.50	0.666	0.780	0.780	0.763
		70	1.76	0.655	0.796	0.796	0.774
A3-B1-C6-D3	2.263	33	1.29	0.646	0.690	0.690	0.682
		55	1.81	0.662	0.752	0.752	0.737
		70	2.12	0.656	0.771	0.771	0.753
A3-B1-C6-D4	2.061	33	1.53	0.609	0.643	0.643	0.636
		55	2.08	0.655	0.726	0.726	0.714
		70	2.43	0.652	0.749	0.749	0.733
A3-B1-C6-D5	1.918	33	1.71	0.587	0.616	0.616	0.609
		55	2.31	0.644	0.703	0.703	0.692
		70	2.68	0.648	0.731	0.731	0.716
A3-B1-C6-D6	1.811	33	1.72	0.619	0.645	0.645	0.639
		55	2.51	0.634	0.684	0.684	0.673
		70	2.91	0.643	0.714	0.714	0.701

**Table E.3** (Continued)

Frame	$K_x$	$F_y$	$W_{FEM}$	$\frac{W_{1c}}{W_{FEM}}$	$\frac{W_{2a}}{W_{FEM}}$	$\frac{W_{2b}}{W_{FEM}}$	$\frac{W_{2c}}{W_{FEM}}$
		(ksi)	(kips)				
A3-B1-C7-D1	3.162	33	0.78	0.662	0.747	0.747	0.734
		55	1.04	0.686	0.836	0.836	0.813
		70	1.23	0.666	0.842	0.842	0.815
A3-B1-C7-D2	2.527	33	1.11	0.624	0.676	0.676	0.666
		55	1.49	0.666	0.769	0.769	0.752
		70	1.72	0.670	0.803	0.803	0.781
A3-B1-C7-D3	2.214	33	1.39	0.587	0.624	0.624	0.616
		55	1.82	0.658	0.734	0.734	0.720
		70	2.09	0.668	0.773	0.773	0.755
A3-B1-C7-D4	2.016	33	1.61	0.564	0.593	0.593	0.587
		55	2.09	0.647	0.707	0.707	0.695
		70	2.39	0.666	0.751	0.751	0.735
A3-B1-C7-D5	1.877	33	1.70	0.573	0.599	0.599	0.593
		55	2.32	0.635	0.686	0.686	0.675
		70	2.65	0.661	0.731	0.731	0.717
A3-B1-C7-D6	1.772	33	1.77	0.586	0.609	0.609	0.603
		55	2.51	0.628	0.671	0.671	0.661
		70	2.87	0.657	0.716	0.716	0.704
A3-B1-C8-D1	3.474	33	0.89	0.676	0.779	0.779	0.764
		55	1.27	0.650	0.808	0.808	0.785
		70	1.40	0.675	0.870	0.870	0.840
A3-B1-C8-D2	2.784	33	1.27	0.641	0.705	0.705	0.694
		55	1.70	0.678	0.802	0.802	0.782
		70	1.99	0.669	0.820	0.820	0.796
A3-B1-C8-D3	2.441	33	1.58	0.612	0.659	0.659	0.650
		55	2.11	0.660	0.756	0.756	0.740
		70	2.43	0.667	0.791	0.791	0.771
A3-B1-C8-D4	2.223	33	1.85	0.585	0.622	0.622	0.615
		55	2.42	0.655	0.732	0.732	0.718
		70	2.79	0.665	0.770	0.770	0.752
A3-B1-C8-D5	2.069	33	2.08	0.565	0.596	0.596	0.590
		55	2.70	0.647	0.711	0.711	0.699
		70	3.09	0.663	0.753	0.753	0.737
A3-B1-C8-D6	1.951	33	2.21	0.566	0.593	0.593	0.587
		55	2.94	0.639	0.694	0.694	0.683
		70	3.36	0.661	0.738	0.738	0.723

**Table E.3** (Continued)

Frame	$K_x$	$F_y$	$W_{FEM}$	$\frac{W_{1c}}{W_{FEM}}$	$\frac{W_{2a}}{W_{FEM}}$	$\frac{W_{2b}}{W_{FEM}}$	$\frac{W_{2c}}{W_{FEM}}$
		(ksi)	(kips)				
A3-B1-C9-D1	3.733	33	1.12	0.604	0.707	0.707	0.692
		55	1.37	0.678	0.854	0.854	0.828
		70	1.57	0.672	0.878	0.878	0.846
A3-B1-C9-D2	3.000	33	1.43	0.647	0.722	0.722	0.710
		55	1.94	0.666	0.801	0.801	0.780
		70	2.26	0.658	0.820	0.820	0.794
A3-B1-C9-D3	2.633	33	1.75	0.627	0.682	0.682	0.672
		55	2.36	0.661	0.771	0.771	0.754
		70	2.72	0.665	0.804	0.804	0.782
A3-B1-C9-D4	2.400	33	2.04	0.604	0.649	0.649	0.640
		55	2.72	0.657	0.749	0.749	0.733
		70	3.13	0.664	0.784	0.784	0.764
A3-B1-C9-D5	2.233	33	2.31	0.583	0.621	0.621	0.613
		55	3.03	0.652	0.729	0.729	0.715
		70	3.48	0.663	0.768	0.768	0.750
A3-B1-C9-D6	2.106	33	2.54	0.567	0.599	0.599	0.593
		55	3.30	0.646	0.713	0.713	0.700
		70	3.79	0.661	0.754	0.754	0.737
A3-B2-C1-D1	3.136	33	0.69	0.714	0.808	0.808	0.794
		55	0.99	0.685	0.838	0.838	0.817
		70	1.16	0.670	0.850	0.850	0.824
A3-B2-C1-D2	2.506	33	0.92	0.722	0.782	0.782	0.772
		55	1.38	0.677	0.790	0.790	0.774
		70	1.61	0.666	0.804	0.804	0.784
A3-B2-C1-D3	2.195	33	1.08	0.719	0.766	0.766	0.757
		55	1.68	0.660	0.746	0.746	0.733
		70	1.96	0.656	0.768	0.768	0.752
A3-B2-C1-D4	1.999	33	1.23	0.697	0.734	0.734	0.727
		55	1.90	0.655	0.724	0.724	0.713
		70	2.17	0.666	0.762	0.762	0.748
A3-B2-C1-D5	1.860	33	1.39	0.664	0.694	0.694	0.688
		55	1.99	0.679	0.739	0.739	0.729
		70	2.41	0.655	0.736	0.736	0.724
A3-B2-C1-D6	1.756	33	1.66	0.586	0.609	0.609	0.604
		55	2.14	0.675	0.726	0.726	0.717
		70	2.63	0.641	0.711	0.711	0.700

**Table E.3** (Continued)

Frame	$K_x$	$F_y$	$W_{FEM}$	$\frac{W_{1c}}{W_{FEM}}$	$\frac{W_{2a}}{W_{FEM}}$	$\frac{W_{2b}}{W_{FEM}}$	$\frac{W_{2c}}{W_{FEM}}$
		(ksi)	(kips)				
A3-B2-C2-D1	3.441	33	0.81	0.718	0.828	0.828	0.813
		55	1.16	0.683	0.851	0.851	0.827
		70	1.35	0.669	0.863	0.863	0.834
A3-B2-C2-D2	2.757	33	1.08	0.723	0.797	0.797	0.785
		55	1.60	0.681	0.809	0.809	0.791
		70	1.88	0.667	0.822	0.822	0.800
A3-B2-C2-D3	2.417	33	1.35	0.685	0.739	0.739	0.730
		55	1.95	0.670	0.774	0.774	0.759
		70	2.27	0.662	0.792	0.792	0.774
A3-B2-C2-D4	2.202	33	1.45	0.710	0.756	0.756	0.748
		55	2.23	0.661	0.747	0.747	0.734
		70	2.61	0.654	0.766	0.766	0.750
A3-B2-C2-D5	2.048	33	1.64	0.680	0.719	0.719	0.711
		55	2.35	0.685	0.762	0.762	0.750
		70	2.82	0.662	0.762	0.762	0.748
A3-B2-C2-D6	1.932	33	1.70	0.698	0.732	0.732	0.726
		55	2.55	0.678	0.744	0.744	0.734
		70	3.04	0.660	0.750	0.750	0.737
A3-B2-C3-D1	3.694	33	0.92	0.713	0.833	0.833	0.816
		55	1.32	0.680	0.858	0.858	0.833
		70	1.52	0.667	0.871	0.871	0.841
A3-B2-C3-D2	2.969	33	1.23	0.722	0.808	0.808	0.795
		55	1.81	0.681	0.821	0.821	0.801
		70	2.11	0.668	0.834	0.834	0.810
A3-B2-C3-D3	2.605	33	1.56	0.674	0.735	0.735	0.725
		55	2.18	0.675	0.792	0.792	0.775
		70	2.56	0.664	0.807	0.807	0.787
A3-B2-C3-D4	2.374	33	1.69	0.699	0.752	0.752	0.743
		55	2.51	0.665	0.764	0.764	0.750
		70	2.93	0.658	0.784	0.784	0.766
A3-B2-C3-D5	2.209	33	1.80	0.713	0.760	0.760	0.751
		55	2.79	0.657	0.743	0.743	0.731
		70	3.26	0.652	0.764	0.764	0.748
A3-B2-C3-D6	2.083	33	2.03	0.673	0.712	0.712	0.704
		55	2.89	0.683	0.762	0.762	0.750
		70	3.52	0.650	0.751	0.751	0.736



**Table E.3** (Continued)

Frame	$K_x$	$F_y$	$W_{FEM}$	$\frac{W_{1c}}{W_{FEM}}$	$\frac{W_{2a}}{W_{FEM}}$	$\frac{W_{2b}}{W_{FEM}}$	$\frac{W_{2c}}{W_{FEM}}$
		(ksi)	(kips)				
A3-B2-C4-D1	2.730	33	0.57	0.687	0.758	0.758	0.746
		55	0.82	0.648	0.770	0.770	0.753
		70	0.96	0.621	0.760	0.760	0.740
A3-B2-C4-D2	2.175	33	0.83	0.620	0.660	0.660	0.652
		55	1.14	0.637	0.719	0.719	0.706
		70	1.33	0.616	0.716	0.716	0.701
A3-B2-C4-D3	1.905	33	1.02	0.583	0.612	0.612	0.605
		55	1.40	0.613	0.670	0.670	0.660
		70	1.62	0.600	0.676	0.676	0.664
A3-B2-C4-D4	1.737	33	1.04	0.631	0.656	0.656	0.650
		55	1.58	0.601	0.645	0.645	0.636
		70	1.84	0.590	0.649	0.649	0.640
A3-B2-C4-D5	1.621	33	1.02	0.682	0.704	0.704	0.698
		55	1.68	0.608	0.644	0.644	0.637
		70	1.99	0.588	0.637	0.637	0.628
A3-B2-C4-D6	1.535	33	1.22	0.602	0.618	0.618	0.614
		55	1.68	0.641	0.673	0.673	0.666
		70	2.12	0.586	0.626	0.626	0.618
A3-B2-C5-D1	3.002	33	0.66	0.691	0.781	0.781	0.768
		55	0.96	0.647	0.785	0.785	0.765
		70	1.12	0.625	0.781	0.781	0.758
A3-B2-C5-D2	2.396	33	0.93	0.665	0.718	0.718	0.709
		55	1.32	0.649	0.748	0.748	0.733
		70	1.55	0.623	0.739	0.739	0.722
A3-B2-C5-D3	2.098	33	1.23	0.586	0.621	0.621	0.614
		55	1.61	0.634	0.708	0.708	0.696
		70	1.88	0.614	0.708	0.708	0.694
A3-B2-C5-D4	1.911	33	1.36	0.584	0.612	0.612	0.606
		55	1.86	0.616	0.673	0.673	0.663
		70	2.15	0.604	0.680	0.680	0.668
A3-B2-C5-D5	1.780	33	1.37	0.623	0.648	0.648	0.642
		55	2.06	0.603	0.649	0.649	0.640
		70	2.38	0.595	0.658	0.658	0.648
A3-B2-C5-D6	1.682	33	1.43	0.631	0.653	0.653	0.647
		55	2.21	0.597	0.637	0.637	0.629
		70	2.55	0.593	0.647	0.647	0.638

**Table E.3** (Continued)

Frame	$K_x$	$F_y$	$W_{FEM}$	$\frac{W_{1c}}{W_{FEM}}$	$\frac{W_{2a}}{W_{FEM}}$	$\frac{W_{2b}}{W_{FEM}}$	$\frac{W_{2c}}{W_{FEM}}$
		(ksi)	(kips)				
A3-B2-C6-D1	3.231	33	0.75	0.690	0.789	0.789	0.775
		55	1.09	0.647	0.797	0.797	0.775
		70	1.27	0.622	0.789	0.789	0.765
A3-B2-C6-D2	2.583	33	1.05	0.671	0.733	0.733	0.723
		55	1.49	0.653	0.764	0.764	0.748
		70	1.75	0.626	0.756	0.756	0.737
A3-B2-C6-D3	2.263	33	1.29	0.643	0.688	0.688	0.679
		55	1.80	0.647	0.735	0.735	0.721
		70	2.11	0.623	0.730	0.730	0.715
A3-B2-C6-D4	2.061	33	1.54	0.596	0.630	0.630	0.623
		55	2.07	0.633	0.704	0.704	0.692
		70	2.42	0.616	0.706	0.706	0.692
A3-B2-C6-D5	1.918	33	1.71	0.583	0.611	0.611	0.605
		55	2.31	0.619	0.677	0.677	0.667
		70	2.68	0.608	0.685	0.685	0.673
A3-B2-C6-D6	1.811	33	1.72	0.613	0.639	0.639	0.633
		55	2.53	0.607	0.656	0.656	0.647
		70	2.91	0.600	0.666	0.666	0.655
A3-B2-C7-D1	3.162	33	0.77	0.663	0.749	0.749	0.735
		55	1.10	0.648	0.790	0.790	0.769
		70	1.23	0.665	0.841	0.841	0.814
A3-B2-C7-D2	2.527	33	1.11	0.626	0.677	0.677	0.668
		55	1.49	0.666	0.769	0.769	0.752
		70	1.72	0.671	0.804	0.804	0.782
A3-B2-C7-D3	2.214	33	1.39	0.587	0.624	0.624	0.617
		55	1.82	0.659	0.735	0.735	0.721
		70	2.09	0.668	0.774	0.774	0.756
A3-B2-C7-D4	2.016	33	1.61	0.561	0.590	0.590	0.583
		55	2.09	0.647	0.707	0.707	0.695
		70	2.39	0.666	0.751	0.751	0.735
A3-B2-C7-D5	1.877	33	1.72	0.568	0.594	0.594	0.588
		55	2.32	0.635	0.685	0.685	0.674
		70	2.65	0.661	0.731	0.731	0.717
A3-B2-C7-D6	1.772	33	1.79	0.579	0.602	0.602	0.597
		55	2.52	0.626	0.669	0.669	0.659
		70	2.87	0.656	0.716	0.716	0.703

**Table E.3** (Continued)

Frame	$K_x$	$F_y$	$W_{FEM}$	$\frac{W_{1c}}{W_{FEM}}$	$\frac{W_{2a}}{W_{FEM}}$	$\frac{W_{2b}}{W_{FEM}}$	$\frac{W_{2c}}{W_{FEM}}$
		(ksi)	(kips)				
A3-B2-C8-D1	3.474	33	0.88	0.678	0.781	0.781	0.766
		55	1.27	0.650	0.807	0.807	0.784
		70	1.40	0.676	0.871	0.871	0.841
A3-B2-C8-D2	2.784	33	1.27	0.642	0.706	0.706	0.695
		55	1.69	0.680	0.804	0.804	0.785
		70	1.98	0.670	0.821	0.821	0.797
A3-B2-C8-D3	2.441	33	1.58	0.613	0.660	0.660	0.651
		55	2.11	0.661	0.757	0.757	0.741
		70	2.42	0.667	0.792	0.792	0.772
A3-B2-C8-D4	2.223	33	1.85	0.585	0.622	0.622	0.615
		55	2.42	0.655	0.732	0.732	0.718
		70	2.78	0.666	0.771	0.771	0.753
A3-B2-C8-D5	2.069	33	2.08	0.564	0.594	0.594	0.588
		55	2.70	0.647	0.711	0.711	0.699
		70	3.09	0.663	0.753	0.753	0.737
A3-B2-C8-D6	1.951	33	2.23	0.562	0.589	0.589	0.583
		55	2.94	0.639	0.694	0.694	0.682
		70	3.36	0.661	0.738	0.738	0.723
A3-B2-C9-D1	3.733	33	1.07	0.634	0.741	0.741	0.726
		55	1.39	0.668	0.843	0.843	0.817
		70	1.57	0.673	0.879	0.879	0.847
A3-B2-C9-D2	3.000	33	1.42	0.648	0.723	0.723	0.711
		55	1.93	0.667	0.802	0.802	0.781
		70	2.26	0.658	0.820	0.820	0.794
A3-B2-C9-D3	2.633	33	1.75	0.628	0.683	0.683	0.673
		55	2.36	0.662	0.771	0.771	0.754
		70	2.71	0.666	0.805	0.805	0.783
A3-B2-C9-D4	2.400	33	2.04	0.605	0.649	0.649	0.640
		55	2.71	0.658	0.749	0.749	0.734
		70	3.12	0.665	0.785	0.785	0.766
A3-B2-C9-D5	2.233	33	2.30	0.585	0.623	0.623	0.615
		55	3.03	0.653	0.730	0.730	0.716
		70	3.47	0.663	0.769	0.769	0.751
A3-B2-C9-D6	2.106	33	2.55	0.565	0.597	0.597	0.591
		55	3.30	0.647	0.713	0.713	0.700
		70	3.79	0.661	0.754	0.754	0.737

---

---

# Appendix F

## Design Examples

---

---

### DESIGN EXAMPLE - Rotationally Restrained Sway Column

*Given:*

1. Section C9 as shown in Fig 5.18. The section properties are:  $A = 1.2 \text{ in.}^2$ ,  $I_x = 1.8 \text{ in.}^4$ ,  $S_x = 1.161 \text{ in.}^4$ ,  $F_y = 55 \text{ ksi}$ , and  $Q = 1$
2. Rotationally restrained sway column as shown in Fig. 5.17a, with  $L = 60 \text{ in.}$ ,  $\psi = 1/240$ ,  $G_A = 0.6$ ,  $G_B = 20$ , and  $K_x = 1.965$
3. For research purposes assume  $\phi_c = 1$  and  $\phi_b = 1$

*Required:*

1. Determine the axial load carrying capacity of the column based on Chapter 5 Approaches 1a, 1c, 2a, 2b, and 2c
2. Compare the results with the finite element solution  $P_{\text{FEM}} = 30.64 \text{ kips}$

## APPROACH 1 - EFFECTIVE LENGTH APPROACH

### Approach 1a - Concentrically Loaded Compression Members

$$P_{ex} = \frac{\pi^2 EI_x}{(K_x L_x)^2} = \frac{\pi^2 (29500)(1.8)}{((1.965)(60))^2} = 37.7 \text{ kips}$$

$$F_e = \frac{P_{ex}}{A} = \frac{37.7}{1.2} = 31.42 \text{ ksi}$$

$$\lambda_c = \sqrt{\frac{F_y}{F_e}} = \sqrt{\frac{55}{31.42}} = 1.32 < 1.5, \text{ therefore}$$

$$F_n = (0.658^{\lambda_c^2}) F_y = (0.658^{1.32^2})(55) = 26.52 \text{ ksi}$$

$$P_n = A_e F_n = (1.2)(26.52) = 31.82 \text{ kips (Fully effective)}$$

$$P_u = \phi_c P_n = (1)(31.82) = 31.82 \text{ kips Answer}$$

### Approach 1c - Combined Compressive Axial Load and Bending

a) The objective is to solve the following interaction equation for  $P_u$

$$\frac{P_u}{\phi_c P_n} + \frac{M_u}{\phi_b M_n} = 1$$

b) Approximate  $M_u$  by modifying  $M_{1t}$ , which is the moment from first-order elastic analysis, using moment magnifier

$$M_u = \frac{C_{mx} M_{1t}}{\left(1 - \frac{P_u}{P_{ex}}\right)}$$

c) Express the relationship between  $P_u$  and  $M_{1t}$  from first-order elastic analysis as

$$M_{lt} = C_{lx} P_u$$

where

$$C_{lx} = \frac{\xi L \bar{\alpha}_A (2 + \bar{\alpha}_B)}{2(\bar{\alpha}_A + \bar{\alpha}_A \bar{\alpha}_B + \bar{\alpha}_B)}$$

$$\xi = \psi = \frac{1}{240}$$

$$\bar{\alpha}_A = \frac{6}{G_A} = \frac{6}{0.6} = 10$$

$$\bar{\alpha}_B = \frac{6}{G_B} = \frac{6}{20} = 0.3$$

therefore

$$C_{lx} = \frac{(1/240)(60)(10)(2+0.3)}{2(10+(10)(0.3)+0.3)} = 0.216$$

d) Using the equations given in (b) and (c), the interaction equation given in (a)

becomes

$$\frac{P_u}{\phi_c P_n} + \frac{C_{mx} C_{lx} P_u}{\phi_b M_n \left(1 - \frac{P_u}{P_{ex}}\right)} = 1$$

Solve for  $P_u$

$$P_u = A - \sqrt{A^2 - B}$$

where

$$A = \frac{\phi_c P_n \phi_b M_n + \phi_b M_n P_{ex} + \phi_c P_n P_{ex} C_{mx} C_{lx}}{2\phi_b M_n}$$

$$B = \phi_c P_n P_{ex}$$

$$P_n = 31.82 \text{ kips (From Approach 1a)}$$

$$P_{ex} = 37.7 \text{ kips (From Approach 1a)}$$

$$M_n = F_y S_x = (55)(1.161) = 63.85 \text{ kip-in. } (M_e \geq 2.78M_y \text{ and Fully effective})$$

$$C_{mx} = 0.85$$

therefore

$$A = \frac{(31.82)(63.85) + (63.85)(37.7) + (31.82)(37.7)(0.85)(0.216)}{2(63.85)} = 36.48 \text{ ksi}$$

$$B = (31.82)(37.7) = 1199.6 \text{ ksi}^2$$

$$P_u = 36.48 - \sqrt{36.48^2 - 1199.6} = 25.03 \text{ ksi } \mathbf{Answer}$$

## APPROACH 2 - NOTIONAL LOAD APPROACH

### Approach 2a

Solve for  $P_{n(L)}$

$$P_{ex(L)} = \frac{\pi^2 EI_x}{L_x^2} = \frac{\pi^2 (29500)(1.8)}{60^2} = 145.58 \text{ kips}$$

$$F_e = \frac{P_{ex}}{A} = \frac{145.58}{1.2} = 121.32 \text{ ksi}$$

$$\lambda_c = \sqrt{\frac{F_y}{F_e}} = \sqrt{\frac{55}{121.32}} = 0.673 < 1.5, \text{ therefore}$$

$$F_n = (0.658^{\lambda_c^2}) F_y = (0.658^{0.673^2})(55) = 45.5 \text{ ksi}$$

$$P_{n(L)} = A_e F_n = (1.2)(45.5) = 54.6 \text{ kips (Fully effective)}$$

The objective is to solve the following interaction equation for  $P_u$

$$\frac{P_u}{\phi_c P_{n(L)}} + \frac{M_u}{\phi_b M_n} \leq 1$$

Using similar procedures as Approach 1c, the interaction equation above becomes

$$\frac{P_u}{\phi_c P_{n(L)}} + \frac{C_{mx} C_{lx} P_u}{\phi_b M_n \left(1 - \frac{P_u}{P_{ex}}\right)} = 1$$

Solve for  $P_u$

$$P_u = A - \sqrt{A^2 - B}$$

where

$$A = \frac{\phi_c P_{n(L)} \phi_b M_n + \phi_b M_n P_{ex} + \phi_c P_{n(L)} P_{ex} C_{mx} C_{lx}}{2 \phi_b M_n}$$

$$B = \phi_c P_{n(L)} P_{ex}$$

$$P_{ex} = 37.7 \text{ kips (From Approach 1a)}$$

$$M_n = 63.85 \text{ kip-in. (From Approach 1c)}$$

$$C_{lx} = 0.216 \text{ (From Approach 1c)}$$

$$C_{mx} = 0.85$$

therefore

$$A = \frac{(54.6)(63.85) + (63.85)(37.7) + (54.6)(37.7)(0.85)(0.216)}{2(63.85)} = 49.11 \text{ ksi}$$

$$B = (54.6)(37.7) = 2058.4 \text{ ksi}^2$$



$$P_u = 49.11 - \sqrt{49.11^2 - 2058.4} = 30.31 \text{ ksi} \quad \text{Answer}$$

### Approach 2b

From Eq. (5.8),  $K_x > 1.7$  therefore  $\xi = 1/240$ . Since this is the same  $\xi$  value used in Approach 2a, the resulting  $P_u$  would also be the same.

### Approach 2c

The objective is to solve the following interaction equation for  $P_u$

$$\frac{P_u}{\phi_c P_{n(L)}} + \frac{M_u}{\phi_b M_n} \leq 1$$

Using the same procedures as Approach 1c, the interaction equation above becomes

$$\frac{P_u}{\phi_c P_{n(L)}} + \frac{C_{mx} C_{lx} P_u}{\phi_b M_n \left(1 - \frac{P_u}{P_{ex}^*}\right)} = 1$$

Solve for  $P_u$

$$P_u = A - \sqrt{A^2 - B}$$

where

$$A = \frac{\phi_c P_{n(L)} \phi_b M_n + \phi_b M_n P_{ex}^* + \phi_c P_{n(L)} P_{ex}^* C_{mx} C_{lx}}{2\phi_b M_n}$$

$$B = \phi_c P_{n(L)} P_{ex}^*$$

$$P_{n(L)} = 54.6 \text{ kips} \quad (\text{From Approach 2a})$$

$$M_n = 63.85 \text{ kip-in.} \quad (\text{From Approach 1c})$$

$$C_{lx} = 0.216 \quad (\text{From Approach 1c})$$

$$C_{mx} = 0.85$$

The only parameter that is effected by making the flexural stiffness reduction is  $P_{ex}^*$  used in the above equations for determining  $A$  and  $B$ . From Eq. (5.9)

$$EI_x^* = 0.9EI_x = (0.9)(29500)(1.8) = 47790 \text{ kip-in.}^2$$

$$P_{ex}^* = \frac{\pi^2 EI_x^*}{(K_x L_x)^2} = \frac{\pi^2 (47790)}{((1.965)(60))^2} = 33.93 \text{ kips}$$

therefore

$$A = \frac{(54.6)(63.85) + (63.85)(33.93) + (54.6)(33.93)(0.85)(0.216)}{2(63.85)} = 46.93 \text{ ksi}$$

$$B = (54.6)(33.93) = 1852.6 \text{ ksi}^2$$

$$P_u = 46.93 - \sqrt{46.93^2 - 1852.6} = 28.23 \text{ ksi} \quad \text{Answer}$$

### Compare the results with the finite element solution

Approach	$P_u$	$\frac{P_u - P_{FEM}}{P_{FEM}} \times 100\%$
1a	31.82	3.85% Unconservative
1c	25.03	18.31% Conservative
2a and 2b	30.31	1.08% Conservative
2c	28.23	7.87% Conservative

---

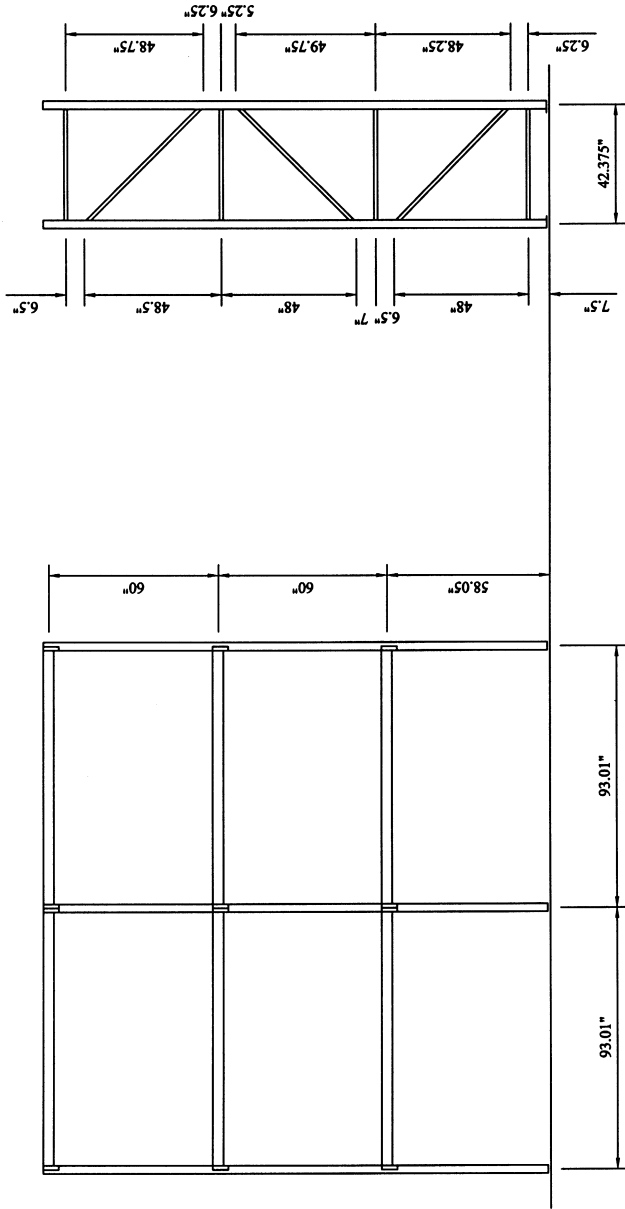
---

Appendix **G**

**Pallet Rack Drawings**

---

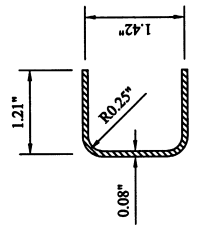
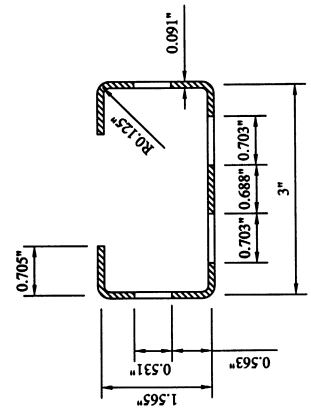
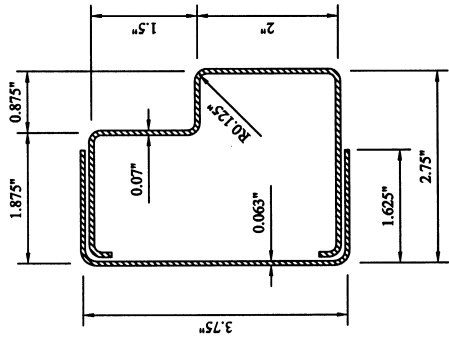
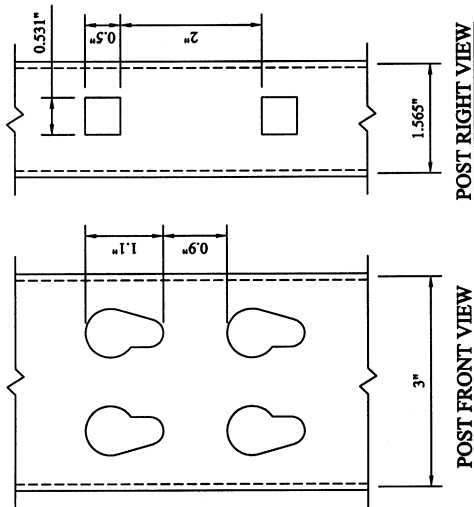
---



FRONT ELEVATION VIEW

CONFIGURATION OF UPRIGHT FRAMES

<b>CORNELL UNIVERSITY</b>			
DRAWN BY ATS	SCALE 1:50	DATE 10/29/00	
DWG. TITLE RACK TYPE A-LDR		DWG. NO. S-200	



<b>CORNELL UNIVERSITY</b>			
DRAWN BY ATS	SCALE 1:2	DATE 10/29/00	
DWG. TITLE RACK TYPE A-LDR		DWG. NO. S-201	

---

---

# Appendix H

## Computer Programs

---

---

Four computer programs have been developed to carry out the extensive parametric studies which involved the analysis and the design of cold-formed steel members and structures conducted in this research project. Description for each of these computer programs, and their User's Guide are as follows:

CUEWA Effective Width Approach: is a computer program designed to compute the nominal flexural strength  $M_n$  and the nominal axial strength  $P_n$  of cold-formed steel sections using two approaches: the AISI (1996) method, and the Intergraded Distortional Buckling method given by Schafer and Peköz (1999).

CUPBF Plate Buckling and Free Vibration: is a computer program designed to solve three types of problems involving the eigenvalue analysis: plate elastic buckling, free-vibration, and free-vibration with initial in-plane stresses. The program uses the finite element method with four-node rectangular thin plate elements. Various boundary conditions and perforations can be applied.

CUTWP Thin-Walled Section Properties: is a computer program designed to compute cross section properties and overall elastic buckling loads of thin-walled members.

CUSRF Semi-Rigid Frame Analysis: is a computer program designed to perform first-order elastic, second-order elastic, and elastic buckling analyses of two-dimensional semi-rigid frames.

---

# *CUEWA*

*Effective Width Approach*

---

*Developed by:*  
*Andrew Sarawit*  
*Prof. Teoman Peköz*

*Cold-Formed Steel Structures Research Group*  
*School of Civil and Environmental Engineering*  
*Cornell University*

*Sponsored by:*  
*The Rack Manufactures Institute*  
*The American Iron and Steel Institute*



*User's Guide*  
*Version 2003*

---



## Introduction

- CUEWA is a computer program designed to compute the nominal flexural strength,  $M_n$ , and the nominal axial strength,  $P_n$  of cold-formed steel sections using two approaches: the AISI (1996) method, and the Intergraded Distortional Buckling method given by Schafer and Peköz (1999).
- The program can be obtained at <http://ceeserver.cce.cornell.edu/tp26>, available as both a stand-alone windows application and a Matlab application.
- To run the Matlab version simply change the Matlab current directory to the installed CUEWA directory then type `cuewa` at the Matlab command line.
- Matlab version of this program should not be installed in a directory path name that contain spaces.

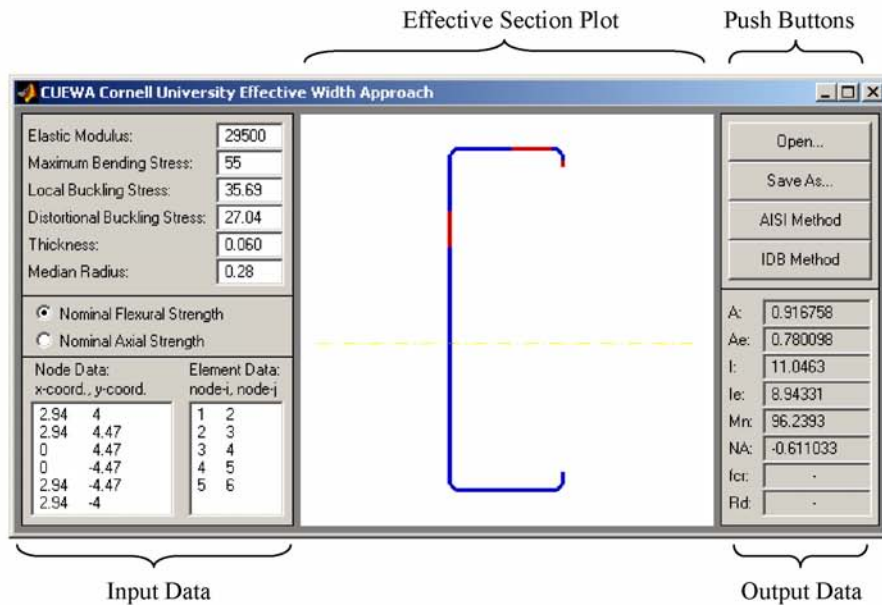
*Incorrect:* c:\Program Files\CUEWA\_MATLAB

*Correct:* c:\Program\_Files\CUEWA\_MATLAB

- The program is best viewed on a 1024×768 pixels screen resolution.

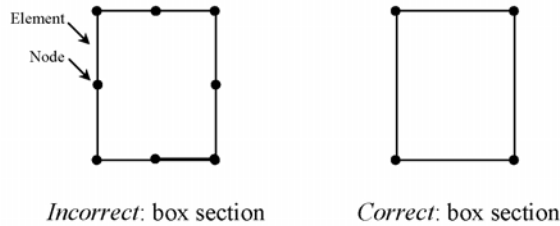
## Getting Started with CUEWA

- The following figure shows the layout of the CUEWA program, which consists of 4 components, descriptions of these components are as follows:



### Input Data:

- Define the nodal x- and y- coordinates in Noda Data. Node numbering is defined automatically as the row index number.
- Define the first and second node numbers forming the element in Element Data.
- The thin-walled section could be either an open section or a closed section.
- Elements forming the cross section should not be refined.



- Elements with intermediate stiffeners are not applicable.
- The local and distortional buckling stress could be obtained by using the Finite Strip Method program CUFSM.
- Local and distortional buckling stresses are not needed for the AISI method.
- If the section does not have a distortional buckling mode, simply provide a very high value, such that the distortional buckling mode will not be the controlling buckling stress in the IDB method.
- The inelastic flexural reserve capacity is not considered for both the AISI method and the IDB method
- A single median radius is used for all corners.
- Arithmetic operators +, -, \*, and / can be used in the edit text fields.
- The units chosen must be self-consistent.

## Output Data:

- The computed data are displayed in this area.
- When the nominal flexural strength option is selected, the location of the effective section neutral axis, NA, is computed. The value is the vertical distance of this axis from the origin.
- When the nominal axial strength option is selected, the location of the effective sections centroid is computed. The  $x_c$  and  $y_c$  are the centroid coordinates with respect to the origin.
- $f_{cr}$  is the controlling buckling stress, and  $R_d$  is the reduction factor for the distortional buckling. A detailed definition of these values can be found in Schafer, B.W., and Peköz, T.P., (1999).

## Push Buttons

- Saving the file for future use or loading an existing file is possible by use of the Save As... button or Open... button.
- A report is automatically generated when the file is saved. The created text file has the `ewa` extension.
- Use the AISI method button to compute the section strength according to the AISI (1996) Specification.
- Use the IDB method button to compute the section strength on the basis of the Intergraded Distortional Buckling method given by Schafer and Peköz (1999).
- Procedures of both methods are similar except that the IDB method integrates the distortional buckling into the unified effective width approach and an alternative approach for calculating the effective width of the web introduced by Schafer (1997) is used.
- Verification examples from the AISI (1996) are given in the example folder.

## Effective Section Plot:

- This area is used to display the effective section, which is in blue. The red color shows the region of the ineffective area of the section.
- The yellow line is the effective section neutral axis in the case of nominal flexural strength, and is the effective section centroid in the case of nominal axial strength.

## Reference

- AISC (1998): *Manual of Steel Construction, Load and Resistance Factor Design*, 2nd ed. Vol. 1 and 2, American Institute of Steel Construction.
- Schafer, B.W. (1997): "Cold-Formed Steel Behavior and Design: Analytical and Numerical Modeling of Elements and Members with Longitudinal Stiffeners," *Ph.D. Dissertation*, Cornell University.
- Schafer, B.W., and Peköz, T. (1999): "Laterally Braced Cold-Formed Steel Flexural Members with Edge Stiffened Flanges," *Journal of Structural Engineering*, 125(2), 1999.

---

# *CUPBF*

*Plate Buckling & Free-Vibration*

---

*Developed by:*

*Andrew Sarawit*

*Prof. Teoman Peköz*

*Cold-Formed Steel Structures Research Group*

*School of Civil and Environmental Engineering*

*Cornell University*

*Sponsored by:*

*The Rack Manufactures Institute*

*The American Iron and Steel Institute*



*User's Guide*

*Version 2003*

---

## Introduction

- CUPBF is a computer program designed to solve three types of problems involving the eigenvalue analysis: plate elastic buckling, free-vibration, and free-vibration with initial in-plane stresses.
- The program uses the finite element method with four-node rectangular thin plate elements. Various boundary conditions and perforations can be applied.
- The program can be obtained at <http://ceeserver.cee.cornell.edu/tp26>, available only as a Matlab application.
- To run the Matlab version simply change the Matlab current directory to the installed CUPBF directory then type `cupbf_post` at the Matlab command line.
- Matlab version of this program should not be installed in a directory path name that contain spaces

*Incorrect:* c:\Program Files\CUPBF\_MATLAB

*Correct:* c:\Program\_Files\CUPBF\_MATLAB

- The program is best viewed on a 1024×768 pixels screen resolution

## Plate Elastic Buckling

The m-file that performs the finite element elastic buckling analysis is called “cupbf.m”. This m-file requires 10 input parameters and returns 1 output. To run the analyses make the call to the m-file cupbf by:

```
APRATIOS = cupbf('filename', coord, ends, t, E, v, fixity, req_modes, cload, dload);
```

Description of the input and output parameters are as follows:

- a) Give the ‘filename’ which will be the filename.mat containing the data results from the analysis. The results may be viewed later by using the post-processor.
- b) Define coordinates [“coord”] of all nodes. Since this is a two-dimensional problem the first and second columns contain x- and y-coordinates of the nodes. Therefore, [“coord”] will be a

two-column matrix with numbers of node rows. Node numbering is defined automatically as the row index number.

- c) Give the node connectivity matrix ["ends"]. This matrix defines which nodes are connected to each other. It will be a four column matrix containing indices to the corner points, given counter clockwise order. The number of rows in this matrix is equal to the number of elements. Element numbering is defined automatically as the row index number.

The next three inputs ["t"], ["E"] and ["v"] are all vector matrixes. The size of the vector matrix is equal to the number of elements and element numbering is defined automatically as row index number.

- d) Define the element thickness in ["t"].
- e) Define the element material elastic modulus, Young's Modulus in ["E"].
- f) Define the element material Poisson's ratio in ["v"].
- g) Establish support conditions ["fixity"] by first defining transverse d.o.f.  $x$ ,  $y$ ,  $z$  and then rotation d.o.f. about  $x$ -axis,  $y$ -axis,  $z$ -axis of each node. A free degree of freedom will have a value of NaN while a supported degree of freedom will have a value of 0. ["fixity"] is a six-column matrix with numbers of node rows. Node numbering is defined automatically as the row index number.
- h) Request the maximum number of eigenvalue in ["req\_modes"].
- i) Define the in-plane concentrated load in ["cload"] where we give the numerical value of the force in  $x$  and  $y$  direction at each node. Nodes that do not have concentrated load should be defined with a value of zero. ["cload"] is a two-column matrix with numbers of node rows. Node numbering is defined automatically as the row index number.
- j) Define the in-plane distributed load in ["dload"] where we give the numerical value of the distributed stress in  $x$  and  $y$  direction at each node. Nodes that do not have distributed load should be defined with a value of NaN. The distributed stress will be linearly interpolated between the adjacent nodes. ["dload"] is a two-column matrix with numbers of node rows. Node numbering is defined automatically as the row index number.

Instead of giving these input parameters manually a preprocessor function “cupbf\_pre.m” is also provided.

```
[coord,ends,t,E,v,fixity,cload,dload,p] = cupbf_pre(wx,wy,nx,ny,t,E,v,p);
```

This function generates a default input parameter for a rectangular plate automatically by defining the width [‘wx’], length [‘wy’], the number of elements in the width [‘nx’], the number of elements in the length [‘ny’], [‘t’], [‘E’] and [‘v’], all as a scalar.

Once all the inputs are defined the output eigenvalue [“APRATIOS”] and the result file “filename.mat” can be generated by simply running the function “cupbf.m” with the input parameters in the parentheses as shown. The results of running this analysis can be viewed by running the post-processor program “cupbf\_post.m”.

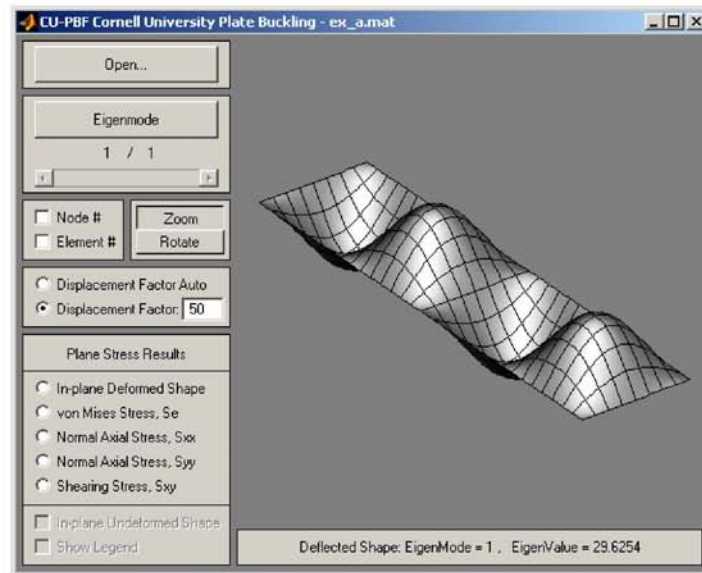


Figure 1 CUPBF Post-Processor



The following is a detailed example of how to use the elastic buckling analysis option in the CUPBF program. The objective is to verify the plate buckling coefficients for various types of boundary conditions. The theoretical elastic buckling stress for a plate may be expressed as

$$F_{cr} = k \frac{\pi^2 E}{12(1-\nu^2)(b/t)^2} \quad (1)$$

where  $E$  is the modulus of elasticity,  $\nu$  Poisson's ration,  $b/t$  the width to thickness ratio and  $k$  the plate buckling coefficient depending on type of stress, edge support conditions, and length to width ratio of the plate. Values of  $k$  for long plates and various boundary conditions are shown in Table 1 as given by AISI (1996). Consider the case (a) in Table 1 a rectangular compression plate with an idealized simply supported condition for all four edges. Dimensions of the rectangular plate in the study are 6 x 24 in. and thickness,  $t = 0.1$  in. The material model used is  $E = 29500$  ksi and  $\nu = 0.3$ .

The critical buckling stress is calculated from the obtained eigenvalue and with the critical buckling stress known the plate-buckling coefficient can be calculated from Eq. 1. The m-files for all the other different types of boundary conditions given in Table 1 are also included with the program. The buckled shape, critical stress and plate buckling coefficients are summarized and compared with the given value by AISI (1996) in Table 1. It is expected that as the length to width ratio of the plate increases the  $k$  obtained from the buckling analysis will converge to the given values for long plate.

**The complete m-file ex\_a.m is given here:**

```

% Define the plate properties
t = 0.1; E = 29500; v = 0.3; wx = 6; wy = 4*wx; nx = 8; ny = 4*nx; req_modes = 1;

% Use the preprocessor function to generate the default input parameter
[coord,ends,t,E,v,fixity,cload,dload] = cupbf_pre(wx,wy,nx,ny,t,E,v);

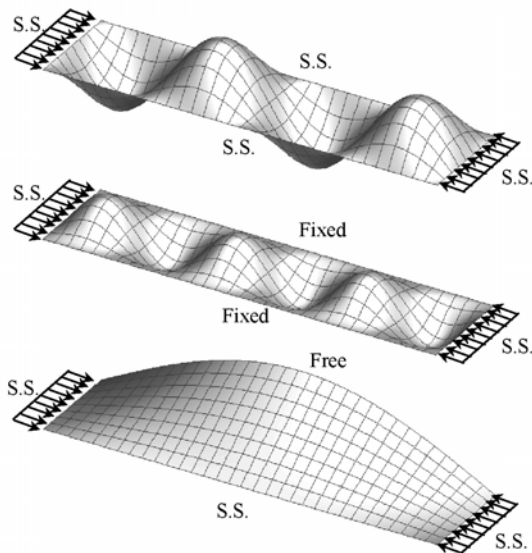
% Define the apply distributed stress and the boundary condition by modifying
% the input parameters generated from cupbf_pre.m
nnodes = size(coord,1);
for j = 1:nnodes
    if coord(j,1) == 0 | coord(j,1) == wx
        fixity(j,[3 4]) = 0;
    end
    if coord(j,2) == 0
        fixity(j,[3 5]) = 0;
        dload(j,2) = 1;
    elseif coord(j,2) == wy
        fixity(j,[3 5]) = 0;
        dload(j,2) = -1;
    end
end
fixity(149,[1 2 6]) = 0;

% Perform the Elastic buckling Analysis
APRATIOS = cupbf('ex_a',coord,ends,t,E,v,fixity,req_modes,cload,dload)

% Calculate the plate buckling coefficients
k = APRATIOS*12*(1-0.3^2)*(6/0.1)^2/(pi^2*29500)

```

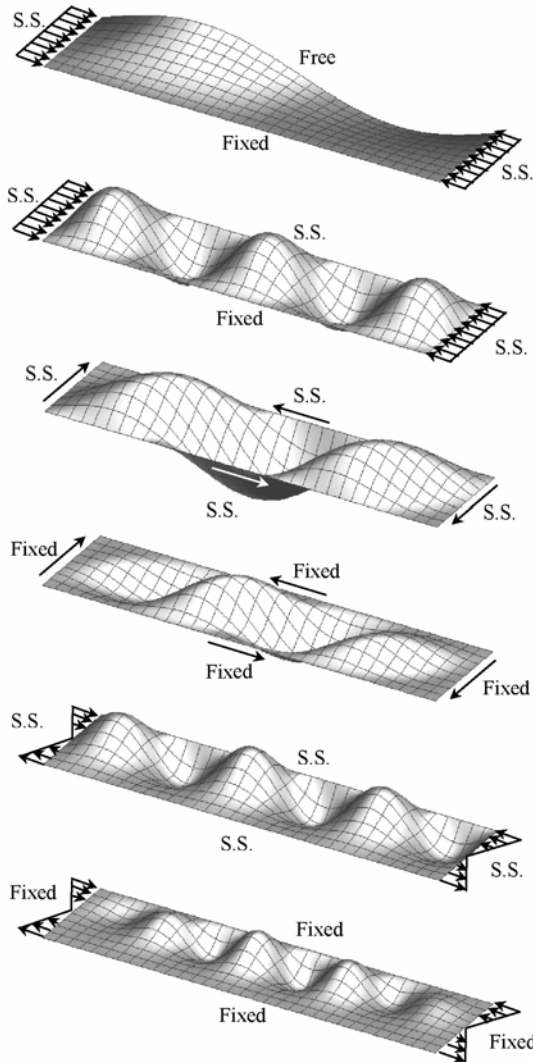
**Table 1 Values of Plate Buckling Coefficients**



Case	Type of stress	Value of k for long plate	Critical stress from CUPBF	Value of k from CUPBF
(a)	Compression	4.0	29.625	4.000
(b)	Compression	6.97	51.404	6.941
(c)	Compression	0.425	3.600	0.486

Table 1 (cont.) Values of Plate Buckling Coefficients

Case	Type of stress	Value of k for long plate	Critical stress from CUPBF	Value of k from CUPBF
(d)	Compression	1.277	9.891	1.336
(e)	Compression	5.42	40.004	5.401
(f)	Shear	5.34	41.648	5.623
(g)	Shear	8.98	68.639	9.268
(h)	Bending	23.9	180.52	24.375
(i)	Bending	41.8	298.01	40.238



## Plate Free-Vibration

The m-file that performs the finite element free-vibration analysis is called “cupbf.m”. This m-file requires 9 input parameters and returns 1 output. To run the analyses make the call to the m-file plate\_buckling by:

```
APRATIOS = cupbf('filename',coord,ends,t,E,v,fixity,req_modes,p);
```

Description of the input parameters is the same as previously given except for an additional vector matrix, the element material mass per unit volume [“p”]. The size of the vector matrix is equal to the number of elements and element numbering is defined as from first row to last row respectively. The output eigenvalue [“APRATIOS”] is the square of the natural frequency.

The following is a detailed example of how to use the free-vibration analysis option in CUPBF program. The consistent mass matrix of the four-node rectangular element is used to test a free-vibration problem of a simply supported square plate. Sixteen elements are used here to modal the plate. The results for the six fundamental natural frequencies together with the exact values are given in Table 2. It appears that this element serves as a good tool for dynamic analysis. The theoretical solution for the natural frequencies may be expressed as

$$\omega_{mn} = \pi^2 \sqrt{\frac{D}{\rho h} \left( \frac{m^2}{l_1^2} + \frac{n^2}{l_2^2} \right)} \text{ with } (m,n) \text{ being the mode number}$$

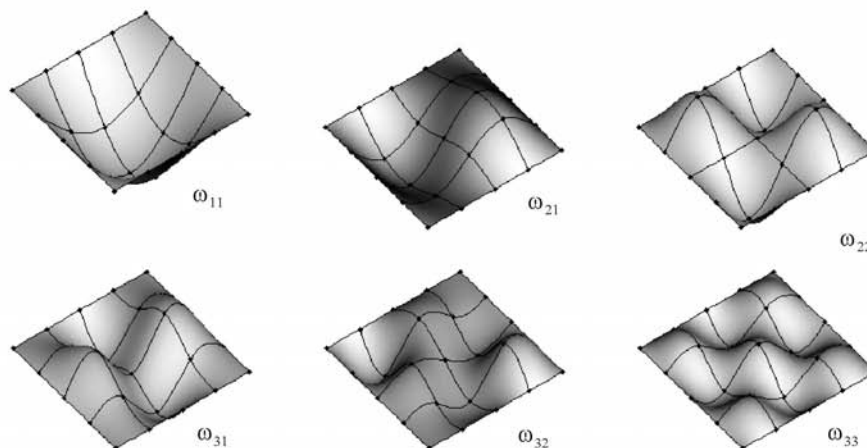


Figure 2 Simply supported square plate free-vibration mode shapes

Table 2 Natural frequencies  $\omega_{ij}$  (rad/sec) for a simply supported square plate\*

	$\omega_{11}$	$\omega_{12}$ $\omega_{21}$	$\omega_{22}$	$\omega_{13}$ $\omega_{31}$	$\omega_{23}$ $\omega_{32}$	$\omega_{33}$
FEM solution	1034.8	2593.3	4147.4	5251.2	6791.3	9409.7
Exact solution	1035	2587	4147	5251	6791	9410
error, %	-0.019	0.244	0.010	0.004	0.004	-0.003

$$l_1 = l_2 = 10 \text{ in.}; h = 0.1 \text{ in.}; E = 30 \times 10^6 \text{ psi}; \nu = 0.3; \rho = 0.001 \text{ lb-sec}^2/\text{in.}^4$$

The complete m-file `ex_free.m` is given here:

```
% Define the plate properties
t = 0.1; E = 30e6; nu = 0.3; wx = 10; wy = wx; nx = 4; ny = nx; req_modes = 6;
p = 0.001;

% Use the preprocessor function to generate the default input parameter
[coord,ends,t,E,nu,fixity,cload,dload,p] = cupbf_pre(wx,wy,nx,ny,t,E,nu,p);

% Define the the boundary condition by modifying the input parameters
% generated from cupbf_pre.m
nnodes = size(coord,1);
for j = 1:nnodes
    if coord(j,1) == 0 | coord(j,1) == 10
        fixity(j,[3 4]) = 0;
    end
    if coord(j,2) == 0 | coord(j,2) == 10
        fixity(j,[3 5]) = 0;
    end
end

% Perform the Elastic buckling Analysis
APRATIOS = cupbf('ex_free',coord,ends,t,E,nu,fixity,req_modes,cload,dload,p)
```

## Plate Free-Vibration with Initial In-plane Stress

The m-file that performs the finite element free-vibration with initial in-plane stress analysis is called “cupbf.m”. This m-file requires 11 input parameters and returns 1 output. To run the analyses make the call to the m-file cupbf by:

```
APRATIOS = cupbf('filename',coord,ends,t,E,nu,fixity,req_modes,cload,dload,p);
```

Description of the input parameters is same as previously. The output eigenvalue [“APRATIOS”] is the square of the natural frequency.

## References

- Huebner, K.H., Thornton, E.A., and Byrom, T.G. (1995): *The Finite Element Method for Engineers*, 3rd ed. John Wiley and Sons, New York.
- Yang, T.Y. (1986): *Finite Element Structure Analysis*, Prentice-Hall, New Jersey.

---

# *CUTWP*

*Thin-Walled Section Properties*

---

*Developed by:*  
*Andrew Sarawit*  
*Prof. Teoman Peköz*

*Cold-Formed Steel Structures Research Group*  
*School of Civil and Environmental Engineering*  
*Cornell University*

*Sponsored by:*  
*The Rack Manufactures Institute*  
*The American Iron and Steel Institute*



*User's Guide*  
*Version 2003*

---

## Introduction

- CUTWP is a computer program designed to compute cross section properties and overall elastic buckling loads of thin-walled members.
- The program can be obtained at <http://ceeserver.cee.cornell.edu/tp26>, available as both a stand-alone windows application and a Matlab application.
- To run the Matlab version simply change the Matlab current directory to the installed CUTWP directory then type `cutwp` at the Matlab command line.
- Matlab version of this program should not be installed in a directory path name that contain spaces.

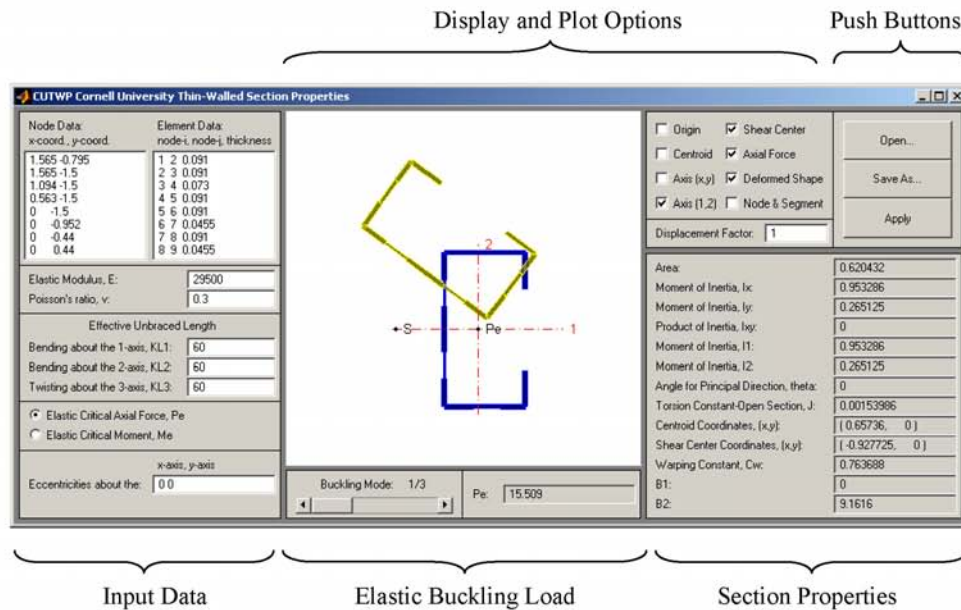
*Incorrect:* c:\Program Files\CUTWP\_MATLAB

*Correct:* c:\Program\_Files\CUTWP\_MATLAB

- The program is best viewed on a 1024×768 pixels screen resolution.

## Getting Started with CUTWP

- The following figure shows the layout of the CUTWP program, which consists of 5 components; descriptions of these components are as follows:



### **Input Data:**

- Define the nodal x- and y- coordinates in Noda Data. Node numbering is defined automatically as the row index number.
- Define the first and second node numbers forming the element and then the element thickness in Element Data. Element numbering is defined automatically as the row index number.
- The thin-walled section could be either an open section or a closed section.
- The shear center coordinates, warping constant,  $B_1$ ,  $B_2$ , and elastic buckling loads are not computed for closed sections.
- Sections with multiple closed loops or loops with additional element segment branches are not applicable.
- Definition of the effective unbraced length is as defined by AISI (1996); however, the effective unbraced lengths are  $KL_1$  and  $KL_2$  not  $KL_x$  and  $KL_y$  because the supports are defined about the principle axis.
- The (x,y) axis is used to define the cross section while the (1,2) axis is the cross sectional principal axis.
- If the elastic critical axial force,  $P_e$ , is selected, the load eccentricities from the centroid about the x-axis and the y-axis must be defined.
- If the elastic critical moment,  $M_e$ , is selected, additional options are given to define the axis of bending.
- Axis of bending is about the principal axis (1,2) not the reference axis (x,y). Generally axis (1,2) and (x,y) may not coincide; for example, a Z-section with the web defined parallel to the y-axis.
- Arithmetic operators +, -, \*, and / can be used in the edit text fields.
- The units chosen must be self-consistent.

### **Section Properties:**

- The computed cross section properties are displayed in this area.
- Moment of inertia values are computed with respect to the cross sectional centroid.
- The centroid and shear center coordinates are given with respect to the origin.



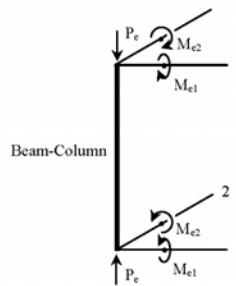
- Definition of  $B_1$  and  $B_2$  are similar to the AISI Eq. C3.1.2-14 but here it is computed with respect to the principal axis (1,2).

$$B_1 = \frac{1}{I_1} \int_A x_2 (x_1^2 + x_2^2) dA - 2x_{o2}$$

$$B_2 = \frac{1}{I_2} \int_A x_1 (x_1^2 + x_2^2) dA - 2x_{o1}$$

### Elastic Buckling Load:

- Use the slider bar to observe the different buckling modes.
- For axial force, the first buckling mode is generally the most critical.
- Negative buckling load values are possible, this simply means that the axial force is in tension or the bending moment is in the opposite direction from the positive sign convention given in the following figure:



### Push Buttons

- Saving the file for future use or loading an existing file is possible by use of the Save As... button or Open... button.
- A report is automatically generated when the file is saved. The created text file has the `twp` extension.
- Use the Apply button to compute the cross section properties.

### **Display and Plot Options:**

- This area is used to display and control the plots of the cross section.
- Judgment should be made when viewing the buckled shape. Any scalar multiple of the buckled shape (eigenvector) is also a solution to this eigenvalue buckling problem.
- Node & Segment option is useful for when defining the cross section.
- Axis (1,2) option is useful when identifying the principle axis.
- Axis (x,y) is displayed at the cross sectional centroid and is used to compute  $I_x$ ,  $I_y$ , and  $I_{xy}$ . It is not the reference axis (x,y) which is at the origin and is used to define geometry of the cross section.

### **Reference**

- AISI (1996): *Cold-Formed Steel Design Manual*, 1996 ed. American Iron and Steel Institute.
- Chen, W.F., and Atsuta, T. (1976): *Theory of Beam-Columns*, McGraw-Hill, New York.
- Timoshenko, S.P., and Gere J.M. (1961): *Theory of Elastic Stability*, 2nd ed. McGraw-Hill Book Company, New York.

---

# *CUSRF*

*Semi-Rigid Frame Analysis*

---

*Developed by:*  
*Andrew Sarawit*  
*Prof. Teoman Peköz*

*Cold-Formed Steel Structures Research Group*  
*School of Civil and Environmental Engineering*  
*Cornell University*

*Sponsored by:*  
*The Rack Manufactures Institute*  
*The American Iron and Steel Institute*



*User's Guide*  
*Version 2003*

---

## Introduction

- CUSRF is a computer program designed to perform first-order elastic, second-order elastic, and elastic buckling analyses of two-dimensional semi-rigid frames.
- The program can be obtained at <http://ceeserver.cee.cornell.edu/tp26>, available as both a stand-alone windows application and a Matlab application.
- To run the Matlab version simply change the Matlab current directory to the installed CUSRF directory then type `cusrf` at the Matlab command line.
- Matlab version of this program should not be installed in a directory path name that contain spaces.

*Incorrect:* c:\Program Files\CUSRF\_MATLAB  
*Correct:* c:\Program\_Files\CUSRF\_MATLAB

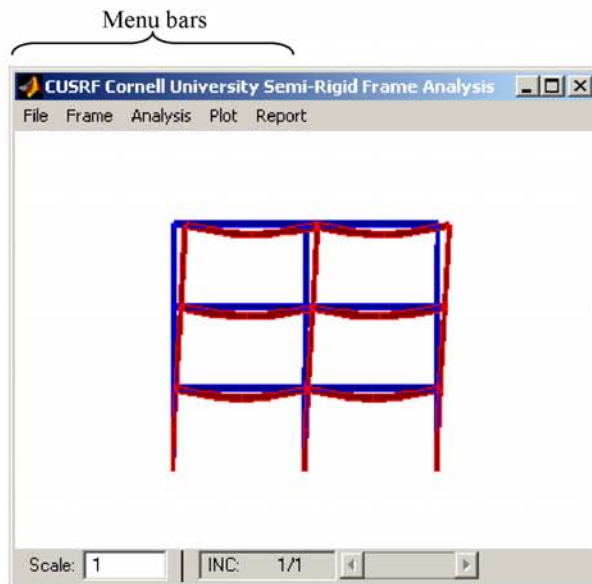
- The program is best viewed on a 1024×768 pixels screen resolution.
- If you are using Windows XP there could be some display problems. Possible workarounds that you can do is to change to the "Windows Classic Style" mode. This can be done as follows
  - 1) Choose the Control Panel from the Start Menu.
  - 2) Choose Appearance and Themes from the Control Panel.
  - 3) Choose the Display Control Panel Icon from the Appearance and Themes menu.
  - 4) Select the Appearance Tab. Then, under Windows and Buttons, change the display to Windows Classic style.

## Getting Started with CUSRF

- The figure in the following page shows the layout of the CUSRF program, which consists 5 menu bars, descriptions of these menus are as follows:

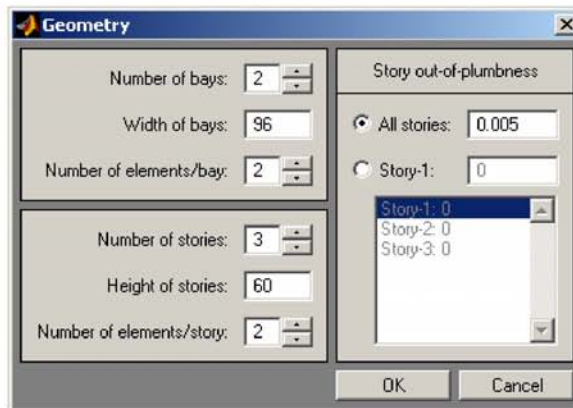
### File Menu:

- Saving the file for future use or loading an existing file is possible by use of the Save As... button or Open... button.



## Frame Menu:

### Frame > Geometry



- The geometry of the frame is simply defined by giving the dimensions of the width of bays and the height of stories.

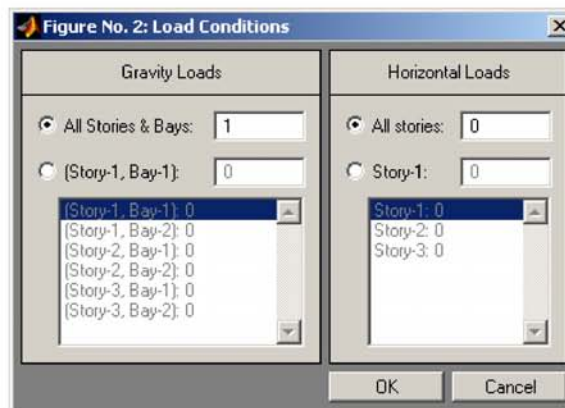
- The number of beam elements to be used in each bay and each story is defined in “Number of elements/bay” and “Number of elements/story”
- Frame geometric imperfection can be defined in “Story out-of-plumbness” (*units*: length/length) by giving the inter story out-of-plumbness for each story level. If the value is same for all stories, simply select the “All stories” option.
- Arithmetic operators +, -, \*, and / can be used in the edit text fields.
- The units chosen must be self-consistent.

### Frame > Connection Stiffness



- The connection stiffness can be defined as semi-rigid, rigid or pin.
- k is the constant connection stiffness (*units*: moment/rad)

### Frame > Load Conditions



- Uniformly distributed gravity load (*units*: force/length) applied on each bay can be defined in “Gravity Loads”. If the value is same for all bays, simply select the “All stories & Bays” option.
- Horizontal load (*units*: force) applied on each story level can be defined in “Horizontal loads”. If the value is same for all stories, simply select the “All stories” option.

### Frame > Section Properties

Column Section Properties	Beam Section Properties
A: 0.84	A: 1.337
Iz: 1.418	Iz: 5.564
As: 0.84	As: 1.337
E: 29500	E: 29500
v: 0.3	v: 0.3

- Similar to a typical pallet rack structure, a single column section and a single beam section are used for the entire frame.
- $A_s$  is the equivalent shear area used to calculate the shearing deformation. Define this value as “int” (infinity) to disregard the transverse shear deformation.

### Frame > Sidesway Uninhibited or Inhibited

- The frame can be defined either as a sidesway uninhibited frame or a sidesway inhibited frame by using the frame menu.

### Analysis Menu:

- The analysis type, which will be performed, can be selected from this menu. To execute the analysis simply press the Run button.

- Choose a node number to be monitored. The results for this node will be shown in Report > Summary data
- Define the number of buckling modes to be computed “Number of modes” when the elastic buckling analysis is selected.
- Defined initial load proportion factor “LPFin” and the acceptable equilibrium tolerance “etol” when the second-order elastic analysis is selected.
- The second-order elastic analysis is terminate when the maximum value of the load proportional factor “LPFmax” or the maximum number of increments “Number of INC” is reach.
- The constant arc length method is used in the second-order elastic analysis

### Plot Menu:

- This menu is used to control the plots options.
- Use the slider bar located at the bottom left portion of the program to observe the different increments or the different buckling modes.
- Use “Scale” located at the bottom left portion of the program to change the magnitude of the plot

### Report Menu:

- This menu is used to display the generated input data, output data and summary data.
- A report containing these data is also automatically generated when the file is saved. The created text file that contains the input data has the `in` extension, output data has the `out` extension, and summary data has the `sum` extension.

### References

- McGuire, W., Gallagher, R.H., and Ziemian, R.D. (2000): *Matrix Structural Analysis*, 2nd ed., John Wiley and Sons, New York.
- Gattass, M., and Abel, J.F. (1987): “Equilibrium Considerations of the Updated Lagrangian Formulation of Beam-Columns with Natural Concepts,” *International Journal for Numerical Methods in Engineering*, 24(11), 1987.



## REFERENCES

- AISC (1998): *Manual of Steel Construction, Load and Resistance Factor Design*, 2nd ed. Vol. 1 and 2, American Institute of Steel Construction.
- AISI (1996): *Cold-Formed Steel Design Manual*, 1996 ed. American Iron and Steel Institute.
- ASCE (1997): *Effective Length and Notional Load Approaches for Assessing Frame Stability: Implications for American Steel Design*, American Society of Civil Engineers.
- Baldassino, N., and Bernuzzi, C. (2000): "Analysis and Behaviour of Steel Storage Pallet Racks," *Thin-Walled Structures*, 37(4), 2000.
- Chen, W.F., and Atsuta, T. (1976): *Theory of Beam-Columns*, McGraw-Hill, New York.
- Cheng, P.H. (1973): "Effect of Semi-Rigid Connection to Steel Column of Cold-Formed Perforated Singly Symmetric Section," *Proceedings of the 2nd Specialty Conference of Cold-Formed Steel Structures*, University of Missouri-Rolla.
- Galambos, T.V. (1960): "Influence of Partial Base Fixity on Frame Stability," *Journal of the Structural Division*, 86(5), 1960.
- Galambos, T.V. (1988): *Guide to Stability Design Criteria for Metal Structures*, 4th ed. John Wiley and Sons, New York.
- Gattass, M., and Abel, J.F. (1987): "Equilibrium Considerations of the Updated Lagrangian Formulation of Beam-Columns with Natural Concepts," *International Journal for Numerical Methods in Engineering*, 24(11), 1987.

- Godley, M.H.R. (2002): "The Behaviour of Drive-In Storage Structures," *Proceedings of the 16th Specialty Conference of Cold-Formed Steel Structures*, University of Missouri-Rolla.
- Gotluru, B.P., (1998), "Torsion in Thin-Walled Cold-Formed Steel Beams," *M.S. Thesis*, Cornell University.
- Gurtin, M.E., (1981): *An Introduction to Continuum Mechanics*, Academic Press, San Diego.
- Hancock, G.J. (1998): *Design of Cold-Formed Steel Structures (To Australian/New Zealand Standard AS/NZA 4600: 1996)*, 3rd ed. Australian Institute of Steel Construction.
- Harris, E., and Hancock, G.J. (2002): "Sway Stability Testing of High Rise Rack: Sub-Assemblages," *Proceedings of the 16th Specialty Conference of Cold-Formed Steel Structures*, University of Missouri-Rolla.
- Huebner, K.H., Thornton, E.A., and Byrom, T.G. (1995): *The Finite Element Method for Engineers*, 3rd ed. John Wiley and Sons, New York.
- Lewis, G.M. (1991): "Stability of Rack Structures," *Thin-Walled Structures*, 12(2), 2000.
- Malvern, L.E., (1969): *Introduction to the Mechanics of a Continuous Medium*, Prentice-Hall, New Jersey.
- Markazi, F.D., Beale R.G., and Godley, M.H.R. (1997): "Experimental Analysis of Semi-Rigid Boltless Connectors," *Thin-Walled Structures*, 28(1), 1997.
- McGuire, W., Gallagher, R.H., and Ziemian, R.D. (2000): *Matrix Structural Analysis*, 2nd ed., John Wiley and Sons, New York.
- Olsson, A.M.J., Sandberg, G.E. and Austrell, P.E. (1999): "Load-Carrying Capacity of Damaged Steel Columns with Channel Sections," *Journal of Structural Engineering*, 125(3), 1999.

- Peköz, T. (1967): “Torsional-Flexural Buckling of Thin-Walled Sections under Eccentric Load,” *Ph.D. Dissertation*, Cornell University.
- Peköz, T. (1975), “Pallet Rack Tests,” *Report submitted to Rack Manufacturers Institute*, Cornell University.
- Peköz, T. (1987): “Development of a Unified Approach to the Design of Cold-Formed Steel Members,” *Report CF 87-1*.
- Peköz, T., and Celebi, N. (1969): “Torsional-Flexural Buckling of Thin-Walled Sections under Eccentric Load,” *Engineering Research Bulletin 69-1*, Cornell University.
- Peköz, T., and Winter G. (1973): “Cold-Formed Steel Rack Structures,” *Proceedings of the 2nd Specialty Conference of Cold-Formed Steel Structures*, University of Missouri-Rolla.
- Rhodes, J. (1991): *Design of Cold-Formed Steel Members*, Elsevier Applied Science, London.
- RMI (1997): *Specification for the Design, Testing and Utilization of Industrial Steel Storage Racks*, 1997 ed. Rack Manufacturers Institute.
- Salmon, C.G., and Johnson, J.E. (1996): *Steel Structures: Design and Behavior*, 4th ed. HarperCollins College Publishers, New York.
- Salmon, C.G., Schenker, L. and Johnston, B.G. (1955): “Moment Rotation Characteristics of Column Anchorages,” *Journal of the Structural Division*, 81(3), 1955.
- Salmon, M.A., Welch, R.E., and Longinow, A. (1973): “Analysis of Drive-in and Drive-Thru Storage Racks,” *Proceedings of the 2nd Specialty Conference of Cold-Formed Steel Structures*, University of Missouri-Rolla.

- Schafer, B.W. (1997): "Cold-Formed Steel Behavior and Design: Analytical and Numerical Modeling of Elements and Members with Longitudinal Stiffeners," *Ph.D. Dissertation*, Cornell University.
- Schafer, B.W., Peköz, T. (1998): "Computational Modeling of Cold-Formed Steel: Characterizing Geometric Imperfections and Residual Stresses," *Journal of Constructional Steel Research*, 47(3), 1998.
- Schafer, B.W., and Peköz, T. (1999): "Laterally Braced Cold-Formed Steel Flexural Members with Edge Stiffened Flanges," *Journal of Structural Engineering*, 125(2), 1999.
- Sokolnikoff, I.S. (1983): *Mathematical Theory of Elasticity*, Krieger Publishing Company, Florida.
- Sputo, T. (1993): "History of Steel Beam-Column Design," *Journal of Structural Engineering*, 119(2), 1993.
- Teh, L.H., Hancock, G.J., and Clarke, M.J. (2000): "Spatial Buckling Behavior of High-Rise Rack Frames," *Proceedings of the 15th Specialty Conference of Cold-Formed Steel Structures*, University of Missouri-Rolla.
- Timoshenko, S.P., and Gere J.M. (1961): *Theory of Elastic Stability*, 2nd ed. McGraw-Hill Book Company, New York.
- Timoshenko, S.P., and Goodier, J.N. (1969): *Theory of Elasticity*, 3rd ed. McGraw-Hill Book Company, New York.
- White, D.W., and Clake, M.J. (1997): "Design of Beam-Columns in Steel Frames," *Journal of Structural Engineering*, 123(12), 1997.
- Yang, T.Y. (1986): *Finite Element Structure Analysis*, Prentice-Hall, New Jersey.
- Yu, W.W. (2000): *Cold-Formed Steel Design*, 3rd ed. John Wiley and Sons, New York.



**American Iron and Steel Institute**

1140 Connecticut Avenue, NW  
Suite 705  
Washington, DC 20036

[www.steel.org](http://www.steel.org)

